The Interface of Geophysical & Geochemical Survey at Scottish Archaeological Sites

Exploring the Potential of an Integrated Approach for Archaeological Prospection

Carmen Cuenca-García
BA (Valencia), MSc (Bradford)

Submitted in fulfilment of the requirements for the degree of
Doctor of Philosophy

Archaeology

December 2012

Abstract

This thesis illustrates how geophysical and geochemical methods can be combined to study archaeological sites and obtain enhanced interpretations of the results using the complementary information they provide. Whilst these two disciplines tend to be used independently, this thesis brings them together, with a view to exploring their relationships and developing strategies that lead to non-destructive and cost-effective surveys. The investigation focuses on the correlation of geophysical and geochemical results over common archaeological features and their analysis using soil geochemistry in order to understand the factors of contrast involved in their detection.

Five case study sites in Scotland were selected, each one presenting a specific challenge to be assessed by the integrated methodology developed in this thesis. The research employed a range of geophysical (earth resistance, magnetometry, magnetic susceptibility, FDEM and GPR) and geochemical (total phosphate and multi-element analysis) techniques routinely used in archaeological prospection. The different geophysical responses obtained over targeted archaeological features were considered with respect to soil texture, organic matter content, pH, conductivity and chemical composition from archaeological deposits, topsoil and subsoil samples.

The results not only provide a nuanced understanding of the character of the archaeological features surveyed, but begin to develop a better insight of how the setting of a site may affect geophysical and geochemical datasets at Scottish archaeological sites. This thesis concludes that the detection of archaeological anomalies depends upon inter-related and site-specific contrast factors including: general site settings (e.g. the effect of highly variable glacial drift deposits), the type of features to be detected (*e.g.* cut or impervious), and the effect of soil post-depositional processes inside archaeological features and surrounding matrix. For example, at the prehistoric site at Forteviot site (Perthshire) redox processes inside archaeological ditches contribute to their negative magnetic response. Also, chemical composition related to anthropogenic organic materials may enhance the conductivity of theoretical impervious features as illustrated at the Bay of Skaill site (Orkney).

Contents

Acronyms

ALGAO	Association of Local Government Archaeological Officers
BGS	British Geological Survey
BSLAP	Birsay-Skaill Landscape Archaeology Project
CEC	Cation Exchange Capacity
DBLPS	Discover Bute Landscape Partnership Scheme
EC	Electrical Conductivity
FDEM	Frequency Domain Electromagnetic
GEF	NERC Geophysical Equipment Facility
GeoSIG	Geophysics Special Interest Group (IfA)
GPR	Ground-penetrating Radar
IfA	Institute for Archaeologists
ICP-OES	Inductively Coupled Plasma Optical Emission Spectrometry
LOI	Loss on Ignition
MAG	Gradiometer Survey
MLURI	Macaulay Land Use Research Institute
MS	Magnetic Susceptibility
Mya	Millions of years ago
NERC	Natural Environment Research Council
NMRS	The National Monuments Record of Scotland
ORS	Old Red Sandstone
PAN	Planning Advice Note
(p)OSL	(Portable) Optically Stimulated Luminescence reader
pXRF	Portable (handheld) X-ray Fluorescence spectrometer
RCAHMS	Royal Commission on the Ancient and Historical Monuments of Scotland
RES	Electrical Resistance Survey
SASAA	Scottish Analytical Services for Art and Archaeology
SASSA	Soil Analysis Support System for Archaeologists
SERF	Strathearn Environs and Royal Forteviot research project
SHARP	Solway Hinterland Archaeological Remote Sensing Project
SIFSS	Soil Indicators For Scottish Soils
Total P	Total Phosphate
TWT	Two-way Traveltime
UCVLP	Upper Clyde Valley Landscape Project

List of Figures

List of Tables

In loving memory of my grandparents
Rafael Cuenca González (1917-2009), Carmen Valle Muñoz (1922-2012),

and my dearest uncles
Manuel García Rubio (1947-2009), Jose Miguel Cuenca Valle (1960-2010)

"Mira a la derecha y a la izquierda del tiempo
y que tu corazón aprenda a estar tranquilo."

— Federico García Lorca

Acknowledgements

The completion of this thesis has been a challenging journey full of alternating peaks and troughs of excitement, joy and anguish, especially knowing, according Mayan sources, that final submission day was going to be the last day of the World. I would like to say to those lucky survivors that are about to read this thesis, that I owe 'a big thank you' to many contributors that help me during my investigation. This thesis was developed under the funding of a NERC research grant and it would not have been possible without the financial support and the fieldwork equipment facilities provided by this agency.

First of all I would like to thank my supervisors, Dr Allan J. Hall and Dr Richard E. Jones, who have patiently steered and supported me during the course of this PhD. I offer my most sincere gratitude for their guidance and advice throughout this work and for the united broad knowledge in archaeological geophysics and soil geochemistry that they provided in this cross-disciplinary PhD research. Secondly, special thanks to Dr Tessa Poller, for all the enthusiasm shared on archaeological geophysics during the surveys we carried out together.

No fieldwork no data, no data no research. Therefore, all my gratitude to all the volunteers and friends that helped me out during the surveys, especially to Peta Lucy Glew, Cathy MacGiver and Christine McPherson for their laughs and very hard work on Scalpsie Bay (Bute). I am equally indebted to the landowners that kindly allowed us to carry out fieldwork on their land: my thanks to John Dickson from Scalpsie Farm (Bute); and William McGregor and the Maxwell-Stuarts of Lamington from Chesterhall Parks Farm (Wiston). Part of the fieldwork was carried out within the framework of on-going archaeological projects, therefore my gratitude to: the Discover Bute Landscape Partnership Scheme (DBLPS) project and especially to Paul Duffy for all his help in organising the voluteers and permissions for survey; Dr David Griffiths and Jane Harrison from the Birsay-Skaill Landscape Archaeology Project (BSLAP) and their team of archaeologists for their welcome to the project, especial thanks to Åsmund Aasberg for his assistance during the surveys and the superb fresh fish breakfasts; the Strathearn Environs & Royal Forteviot (SERF) team and the Solway Hinterland Archaeological Remote Sensing Project, for providing me with invaluable

infrastructure and support. Some of the fieldwork volunteers also became part of a dedicated team of lab assistants that collaborated during the preparation of the large number of soil samples for analysis, as well as helping with analysis. Such a massive workload would not have been possible to complete without the help of Charalambos Stylianou, Zane Stepka, Sara Spiga, Jane Stewart-Bollen, Joss Durnan, Steven Watt, Sara-Pamela Andrea Bryson, Benjamin Inglis-Grant and Derrick Melan.

I am deeply grateful to Alan Hobbs, Paul Kearney and Colin Kay from the Geophysical Equipment Facility (GEF) for the excellent training provided on the differential GPS system they supplied for this project and their technical support with the GPR system. Orkney College Geophysics Unit (UHI) kindly provided their EM38 instrument during the surveys carried out on Orkney, my thanks to Amanda Brend and Mary Saunders for their help in arranging this. Logistical and technical support was provided throughout my fieldwork and lab analysis by Gert Petersen (Archaeology) and Kenny Roberts (Geography and Earth Science). I would like to thank them both for their enormous help and patience. Thanks also to the Head of Archaeology, Dr Jeremy Huggett for administrative support and help with infrastructure.

Key information and advice for this thesis also came from colleagues working on archaeological geophysics, therefore I owe to Dr Kayt Armstrong, Dr Allete Kattenberg, Dr Luiggia Nuzzo, Dr Mercedes Solla, GPR expert Erica Utsi and Dr Lieven Verdonck a big thank you for all the information they shared and all their kind advice. I also had the great advantage to be working along great geophysicists at CTBTO training meetings where, of course, I took advantage of their expertise in between training cycles. Therefore my thanks to Dr Claude Antoine, Dr Claudia Arango, Dr Lluís Gaya-Piqué, Dr Malte Ibs-von Seht and Dr Stefka Stefanova from the CPT team for their contributions in different theoretical and practical aspects of the range of geophysical techniques used in this investigation, as well as advice and second opinions on data processing and analysis.

The contributions from researchers in Earth Science have been important because of the nature of this investigation. Hence, I would like to thanks Dr Walter Geibert (SAGES) and Dr Clare Wilson (School of Natural Sciences,

University of Stirling) for their comments in digestion methods and help with ICP-OES analysis. Also, my thanks to Professor David Sanderson (SUERC) for his ideas and suggestions on OSL analysis and Professor Paul Bishop (School of Geographical and Earth Sciences) for his support and help with the OSL instrument. The James Hutton Institute (former Macaulay Land Use Research Institute) played a key role at the beginning of this project. Therefore, all my gratitude to the institute and especially to Dr Lorna Dawson and Dr Jason Owen for their welcome, help and advice on soil sampling methods, tools and analysis.

At the department, I am particularly thankful to Dr Louisa Campbell, Terence Christian and Dr Elizabeth Pierce for contributing to refine this text in detail, and to Professor Bill Hanson for the information he kindly provided from Chesterhall Parks Farm. My warmest thanks to my colleagues for providing a great work environment: Dr Dene Wright, Amanda Charland, Tom Horne, Alison Kyle, Dr Adrian Maldonado, Ryan McNutt, Morgana McCabe, Jen Novotny, and Rebecca Younger. Thanks to Dr Alicia Jiménez, Beatriz Marín-Aguilera and Dr Andrea Roppa for refreshing my memories of the Mediterranean and Spanish archaeology during many nights of good food and good wine.

More wine, laughs and roots were provided by Iraia Arabaolaza, María Calero, Carmen Cuesta, Eva Denche and Teresa Garro, thanks very much ladies for keeping me sane and merry! César Baila and Eva Granell from Boxer Graphics designed the CD cover/front-cover of this thesis. Thanks very much for such a great job at such short notice. Finally, I wish to thank my parents for their support and love and very especially to my partner and best friend Gavin, my constant source of adventures, encouragement and inspiration since I started this journey.

Author's declaration

The material presented in this thesis is entirely the result of my own independent research carried out in the Department of Archaeology at the University of Glasgow, under the supervision of Dr. Richard E. Jones and Dr. Allan J. Hall. Any published or unpublished material that is used has been given full acknowledgement in the text.

Part I: Aims & Background to the Research

Chapter 1

Introduction

1.1. Non-destructive and Ground-based Approaches in Archaeological Prospection

Geophysical and geochemical survey have been widely applied to locate and interpret evidence of past human occupation in a non-destructive manner (Clark 1990; Sarris and Jones 2000; David 2005). Geophysical survey has played a major role in the discovery and exploration of single features and sites (Hesse 1980; Wynn 1986; Scollar *et al*. 1990; Neubauer 2001) to entire archaeological landscapes (Powlesland and Lyall 1996; Becker and Fassbinder 2001; Gaffney and Gater 2003; Kvamme 2003; Campana and Piro 2009). Geochemical survey, although adopted on a smaller scale, also provides valuable information on the location of sites (Bintliff *et al.* 1990; Aston *et al.* 1998a; Schlezinger and Howes 2000; Eckel *et al.* 2002; Linderholm 2007) and has the potential of investigating activity areas (Middleton and Price 1996; Entwistle *et al.* 2000b; Terry *et al.* 2004; Wells 2004; Wilson *et al.* 2005; Oonk *et al.* 2009b; Wilson *et al.* 2009; Jones *et al.* 2010) and past land use practices (Entwistle *et al.* 1998; Entwistle *et al.* 2000a; Entwistle *et al.* 2007; Wilson *et al.* 2006).

There are different degrees of 'non-invasiveness' between these two non-destructive approaches. Geophysical techniques can detect archaeological assets remotely, or quasi remotely (e.g. earth resistance technique generally needs the insertion of probes into the ground). Geochemical surveys are slightly more intrusive since these methods require samples of soil (i.e. soil surface sampling, coring/augering or an exposed section or horizon of an archaeological feature). More traditional methods for archaeological investigation, such as test pitting or open plan excavation, are the key to documenting and investigating archaeological sites. However, they are destructive and expensive, and the consequent processing, conservation, documentation and archival of finds, increases the costs even more. The implementation of rapid, non-destructive and integrated prospecting techniques can help in focusing archaeological

excavations to reduce costs and make site exploration and discovery more efficient.

Constant technological developments of geophysical and geochemical methods contribute greatly to cultural resource management as they are able to inform about the archaeological record in a relatively non-invasive and cost-effective manner. These include affordable and portable X-ray fluorescence (pXRF) spectrometry for multi-element soil analysis (Kalnicky and Singhvi 2001; Entwistle and Wilson 2007; Cook *et al.* 2005; Oonk *et al.* 2009c) or more novel, although expensive, rapid area coverage multi-channel GPR systems (Sala and Linford 2010; Trinks *et al.* 2010).

Despite the huge developments in geochemical and geophysical instrumentation, there is still a lot to understand about the soil dynamics involved in the detection of geophysical and geochemical anomalies. This is fundamental in order to understand, for example, what the data really means or how site settings impact on the different techniques. Whilst geophysical and geochemical surveys tend to be used separately in archaeological prospection, this thesis integrates routine geophysical and geochemical methods, breaking down traditional compartmentalised approaches. The goal of this thesis is to explore the relationships, or interface, between these two disciplines and develop integrated strategies to study archaeological sites and improve the cost-effectiveness of non-destructive surveys.

1.1.1. Geophysical Survey

Near-surface geophysical methods are well-established routine techniques in cultural resource management in some countries. For example in England they are recognised by the national PPS5, Planning Policy Statement 5 (DCLG 2012). In orther countries they are increasingly being applied, such as Spain (Brito-Schimmel and Carreras 2010; Peña 2010) and Sweden (Viberg *et al.* 2011). However, the degree of implementation of the different techniques in archaeological investigation is different and, sometimes, country-specific. For example, whilst magnetometry is extensively used in the UK because of its rapid area coverage capacities, followed by slower earth resistance surveys, other

techniques such as ground-penetrating radar (GPR) and frequency domain electromagnetics (FDEM) are still demonstrating their potential.

Regardless of the range of geophysical techniques and the improvements in instrumentation, there is a gap in the development of mechanisms to assess their potential and effectiveness in order to design *ad hoc* survey strategies. Furthermore, most of the published research tends to focus on descriptive and non self-analytical surveys (Jordan 2009). These aspects constrain the overall potential of geophysical survey to answer archaeological questions.

1.1.2. Geochemical Survey

Geochemical techniques are not as routine in archaeological prospection as are geophysical techniques. This is because there are still important methodological issues to be resolved about how to distinguish anthropogenic elements in soils from modern or geological signals and also other analytical issues (e.g. standardisation of protocols or soil horizons to be sampled). These important methodological issues make geochemistry a rather immature discipline in archaeological prospection (Oonk *et al.* 2009a) if compared with geophysical survey. Moreover, some of these techniques are still relatively costly (e.g. ICP-OES analysis) and require laboratory procedures that carry safety concerns, for example digestion of soil using strong acids such as HF.

The increasing availability of less specific but affordable instruments, such as pXRF (Frahm and Doonan 2013), and the adoption of rapid microwaves, for sample digestion on ICP-OES analysis, may be the way forward to improve the cost and time-effectiveness of these techniques. However, these new instruments need first to be well-tested and the results cross-correlated in order to validate them as tools for archaeological prospection.

1.2. The Problem & Basis for an Integrated Approach

Despite the fact that geophysical and geochemical techniques are based on very different detection and analytical principles, a fundamental and common requisite for their successful application is the existence of contrast between the detectable physical properties (Hesse 1980; Scollar *et al.* 1990, 9) and the soil chemical variations or signatures (Aston *et al.* 1998b, 840; Heron 2001, 565)

caused by anthropogenic activity and remains against the surrounding environment (or background) in which they are buried. If sufficient contrast exists, these methods are able to map 'anomalous' variations of the physical properties of the ground and 'enhanced' or 'depleted' soil geochemical concentrations caused by past human activity (Figure 1-1).

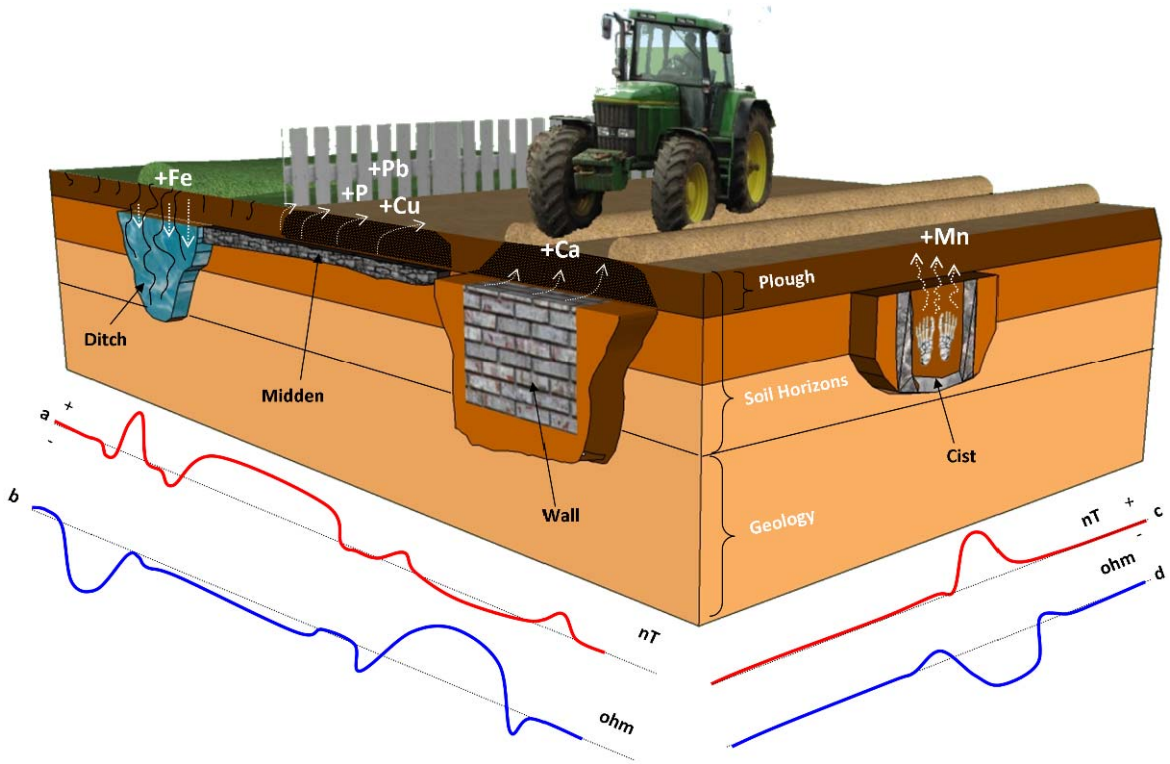

Figure 1-1: Diagram showing idealised geophysical and geochemical responses of common archaeological features. The magnetic response is shown in red and the earth resistance in blue (© C. Cuenca-García).

Factors linking soil physical, chemical and biological properties, processes and their dynamics with different types of archaeological features are fundamental in controlling the indispensable contrast to detect geophysical and geochemical 'anomalies'. For example, the higher moisture content retained inside the backfill of a ditch provides an easy path for an electrical current to flow, usually producing a low resistance anomaly during an earth resistance survey. Dry media, such as wall features (Figure 1-1b), impede the current to flow, hence usually produces a high resistance anomaly. However, these responses can be reversed by climatic conditions (e.g. temperature, rain, sunshine) (Schmidt 2009). Soil properties such as particle size, pore space and moisture content influence soil electrical resistivity (Scollar *et al.* 1990, 12). Current flows more easily in an aqueous solution where there are dissolved electrolytes in the form

of ions. Since ions in soil solution affect the passage of electrical current, whatever soluble components there are in the soil must also affect the results of earth resistance surveys (Sharpe 2004, 3).

A ditch may often be detected as a positive magnetic anomaly as a result, for example, of an enhanced magnetic susceptibility (MS) produced by magnetotactic bacteria developed in the remains of wooden palisades (Fassbinder and Stanjek 1993) or other pathways (Chapter 2) that lead to the general enhancement of MS in archaeological sites. However, the dynamics behind the genesis of negative magnetic features or the factors behind the lack of magnetic contrast in archaeological sites are still not completely understood and require both geological knowledge and further research into the geochemistry of archaeological deposits (Kattenberg and Aalbersberg 2004).

Ploughing physically alters the structure of soils. In geochemical prospecting, this can obscure patterns in element concentrations of archaeological soils. On the other hand, ploughing can enhance concentrations of elements in topsoils by bringing up deeper buried material, for example, increased values of P, Pb and Cu from archaeological midden deposits and (Figure 1-1). By sampling and analysing topsoil samples by multi-elemental analysis, the midden feature can be mapped. However, enhancements of P and Pb in the topsoil can also be derived from modern husbandry or agricultural practice (e.g. fertilisers, fuel spills). Therefore, there is a need for a better understanding of the influence of the site setting, geology and physico-chemical soil conditions on geochemical prospection (Oonk *et al.* 2009a).

In other words, there is still a lot to understand about the soil dynamics involved in the detection of geophysical and geochemical anomalies. This thesis explores the integration of routine geophysical and geochemical techniques in order to assess how site setting affects the different surveys and how archaeological anomalies reveal themselves. This will allow us to develop strategies that will help in the planning of *ad hoc* survey strategies and will allow a more meaningful interpretation of the geophysical and geochemical data.

The integration of geophysical and geochemical approaches can provide a better understanding of the causes of contrast detected as anomalies by the different

techniques. This can be explored by establishing relationships between the following:

- Measured geophysical property and the general soil physical and chemical properties.
- Detailed analysis of enhanced/depleted elements and type of geophysical response at the location of the targeted feature.

By focusing on single features and assessing their geophysical and geochemical relationships, other soil formation processes involved in the 'history' of buried archaeological features can be devised, and the reasons behind their detection, or not, better understood.

1.3. Aim & Objectives

This thesis aims to examine the responses to common archaeological features that are detected by routine geophysical and geochemical techniques by using a new integrated approach at five contrasting archaeological sites in Scotland. This is in order to improve the existing understanding about how geophysical and geochemical anomalies reveal, or do not reveal, themselves.

In so doing, the objectives are to:

- Develop an integrated survey strategy and identify the case studies and archaeological targets to carry out the surveys and soil sampling.
- Characterise the geophysical response of the targeted features using four routine techniques (Earth resistance, gradiometry, GPR and FDEM) and qualitatively assess their results in terms of speed, area coverage and degree of certainty. This is followed by sampling of the topsoil and/or excavated sections of the archaeological targets and experiment with sequential/repetitive geophysical surveys and soil sampling to evaluate the effects of the topsoil on the data.
- Correlate the geophysical and geochemical responses of archaeological features *vs*. soil matrix in terms of their physical and chemical composition in order to establish relationships and understand the factors involved in their detection. This will also allow the assessment of how site settings affect the results of the different geophysical and geochemical techniques and allow the

formulation of recommendations for future prospection in similar survey environments.

- Finally, to propose strategies that integrate soil geochemical analysis and geophysical survey in the study of archaeological sites and improve the cost-effectiveness of prospection techniques.

The work presented in this investigation focuses on the integration of methods to study specific features. Rather than extensive geophysical and geochemical surveys, the measurements were targeted in order to study particular features within the time-limits of the project. Representative sites were selected on the basis that they covered different survey environmental settings and presented specific challenges relating to archaeological prospecting.

1.4. Structure

This thesis is structured in four parts which contain the following chapters and appendices:

Part I: Introduction, Background & Methods

This part is composed of three chapters. **Chapter 1** introduces the general PhD project. It starts with a short introduction about the role of geophysical and geochemical survey in archaeological prospection. It defines the problem tackled in this thesis and describes the reasons behind the integration of geophysical and geochemical techniques to approach the stated problem. The chapter formulates the research project in terms of aims and objectives and finishes by summarising the structure of the thesis. **Chapter 2** provides the theoretical background to the thesis with an overview on general principles of soil science and geophysical and geochemical methods used in archaeological prospection taking into consideration the existing literature. It also provides an overall description of Scottish geology and soil environments to contextualise the investigation and ends by formulating the research questions to be considered in this investigation. **Chapter 3** describes the research strategy designed for this investigation and summarises the methods used. The chapter starts by describing the planning involved in the project (i.e. the selection of the case study sites and the integration of existing information obtained from different databases).

The chapter then focuses on describing the techniques used during the surveys and soil sampling strategies. The soil analysis methods used during the laboratory work are also summarised. The chapter ends with a description of how the soil data was analysed and integrated with the geophysical results.

Part II: Case Study Sites

This part is dedicated to the five case study sites (**Chapters 4 to 8**) used in order to explore the integrated strategy introduced in Chapter 3. The format of these chapters is based on the UK guidelines for reporting in geophysical survey (English Heritage 2008) with some new additions in relation to the soil geochemical analysis integrated into this investigation. The standard structure of each case study site is the following:

1. Introduction to the site (geology, soils, land use, archaeological background, and challenges to be addressed).
2. Geophysical survey (aims and objectives, methods and specific survey settings, results and conclusions).
3. Soil geochemical analysis (aims and objectives, sampling strategy and specific analyses used, results and conclusions).
4. General conclusions.

Each case study also reports on any excavation carried out to confirm the targeted archaeological features and/or other detected anomalies.

Part III: Discussion & Conclusions

The discussion and conclusions derived from this thesis are presented in a single chapter. **Chapter 9** discusses the research questions stated in Chapter 1, critically reviews several aspects of the overall research strategy and outlines the impact of this investigation. The chapter finishes with some recommendations on the use of integrated strategies to be used in archaeological prospection and suggests directions for future work.

Part IV: Appendices

All the appendices are in digital format in an attached CD:

Appendix A: Contains the raw and processed geophysical data, ArcGIS shape files and GPS measurements for each case study.

Appendix B: Contains the protocols of the pH and total phosphate analysis.

Appendix C: Lists all the MS measurements from each case study (Chapter 4-8).

Appendix D: Lists the pXRF data sheets from each case study (Chapter 4-8).

Appendix E: Lists the ICP data sheets from each case study (Chapter 5-8).

Appendix F: Lists the full correlation coefficient, scatter and matrix plots made with Minitab and used in the soil analysis of Chapter 7 (Forteviot).

Appendix G: Contains the complete set of pOSL readings of the samples analysed collected at Forteviot (Chapter 7).

Appendix H: Outlines the publications resulting from the study.

Chapter 2

Soils, Geophysical & Geochemical Prospection

2.1. Introduction

Soil is the natural medium that characterises the subsurface matrix in which archaeological features are cut and buried. Soil is also intrinsically associated with the contrast between the material properties of buried interfaces and the host materials that allows their detection as anomalies. Furthermore, this contrast can be affected by soil dynamics. For example, aeolian processes in which accumulation of deep wind-blown sands over the buried features may mask them and impede their detection.

The soil environment is extremely complex and variable in biological, chemical, physical and mineralogical properties which can be modified by soil formation processes and hence, influences the functioning of different geophysical techniques. Soil properties and processes also play a key role in the retention of anthropogenic chemical elements in archaeological soils (Middleton 2004). Therefore, it is important to understand and recognise those soil properties upon which different geophysical and geochemical techniques are based (Scollar *et al.* 1990, 9) and those soil processes which may affect their results. This chapter encapsulates the theoretical background of the thesis. It provides a review of previous research focused on the principles and interactions between a range of disciplines comprising soil science, and geophysical and geochemical prospection. The chapter finishes by stating the research questions to be considered in this investigation. The length of treatment on geophysical methods in comparison to the geochemical ones reflects the relative underuse of the latter in archaeological prospection to date (section 1.1.2).

2.2. Soil Formation, Materials & Processes

This section introduces some basic notions taken from soil science on soil formation, properties and processes, and includes some aspects of soil geochemistry and mineralogy. The information has been extracted from various

sources including: Soil Analysis Support System for Archaeology- SASSA (www.sassa.org.uk), the Macaulay Lands Used Research Institute- MLURI (www.macaulay.ac.uk), and the Natural Resource Conservation Service- NRCS (www.soils.usda.gov).

2.2.1. Soil Formation

The term 'soil' means a different thing to different disciplines but soil can be usefully defined as "the solid material on the Earth's surface that results from the interaction of weathering and biological activity on the parent material or underlying hard rock" (Macaulay Land Use Research Institute 2012). Soils develop from the interaction of parent material, climate, vegetation, organisms, geomorphology and time. They are composed of four major components: weathered minerals, organic matter, water and air (Figure 2-1). Their relative proportions define the physical properties of the soil (texture, structure and porosity). These physical properties affect the movement of air and water in a soil.

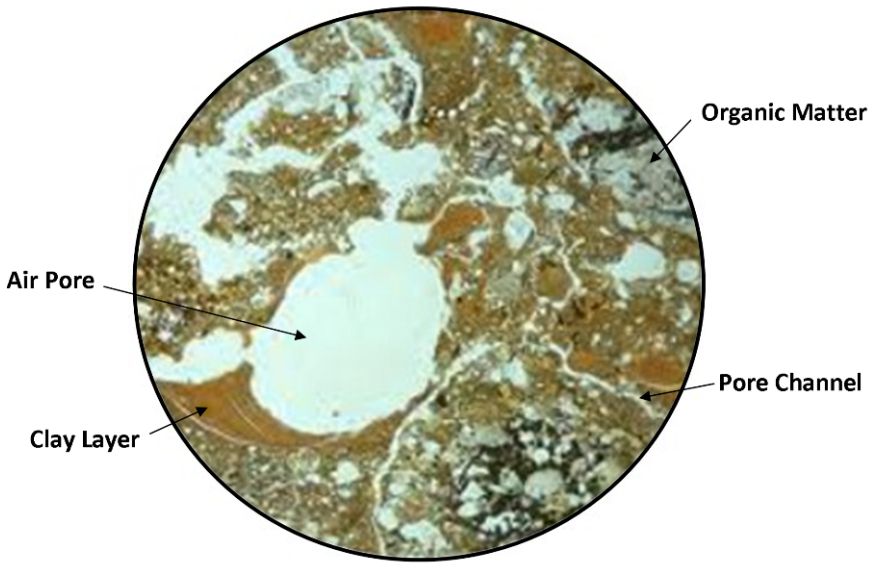

Figure 2-1: Thin section of undisturbed soil materials showing the four major components of soils: minerals (mineral particles and clay layers), organic matter, water (pore channel) and air (in voids such as pore channel) (based on Macaulay Land Use Research Institute 2012).

2.2.1.1. **Soil Weathering**

The soil inorganic component is made up of fragments of rocks and minerals derived from the igneous (e.g. granite, basalt), sedimentary (e.g. sandstone, limestone, conglomerates) or metamorphic (e.g. gneiss, schist, marble) bedrock.

The type of parent material that forms soils has an effect on its properties; for example, quartz-based granite will generally weather into a sandy (quartz-rich) soil which will have a lower capacity to retain water than a clay soil.

The weathering of bedrock provides the parent material from which soil develops. This weathering can be mechanical or chemical i.e. breakage or alteration of the parent material to form mineral particles. Mechanical weathering breaks up the rock into smaller units and may move it from its original source. It is caused by temperature changes (e.g. freezing of the water in a rock), erosion and deposition by water, ice or wind (e.g. glacial drift), or by plant or fauna action (e.g. tree roots). Chemical weathering continues the decomposition of rock fragments and mineral particles and also changes its chemical composition by forming 'secondary products'. It is caused by hydrolysis (dissociation of H_2O into H^+ and OH^- ions which chemically combine with minerals and form new compounds), hydration (chemical combination of water molecules with a mineral, leading to a change in structure), carbonation (carbon dioxide dissolved in water forms carbonic acid that attacks the rock and minerals, brings them into solution and precipitates carbonate minerals), solution (soluble rock substances removed by continuous action of water forming holes in the rock), and oxidation-reduction (redox).

Oxidation and reduction involve the transfer of electrons from one compound to another and are coupled reactions (Delaune and Reddy 2005). Oxidation is the process of conversion to oxides (e.g. carbon in organic matter becomes carbon dioxide, or iron becomes rust, hence an iron oxide) and involves the combination of oxygen (or other oxidant) with minerals. The reaction involves the removal of electrons from a compound (electron donor). Electron donors in soils are: organic matter and organic compounds; and reduced inorganic compounds (e.g. Fe^{2+}, Mn^{2+}). Oxidants (electron acceptors) are inorganic compounds (e.g. O_2 present in the atmosphere and dissolved in water). The reaction is more active in warm aerated and moist environments and results in hydrated oxides such as Fe and Mn. For example:

$$6\ Fe(OH)_2\ (\text{ferrous hydroxide}) + O_2 \rightarrow 2\ Fe_3O_4\ (\text{magnetite}) + 6\ H_2O$$

Reduction is the reverse of oxidation and, in soils, is usually the process of oxygen removal from minerals. Reduction happens by the addition of electrons

to a compound (electron acceptor or oxidant). Reduction changes the soil colour to grey, blue or green as ferric irons are converted to ferrous iron compounds. The reaction takes place under anaerobic conditions (water saturation) where no oxygen is available. An example is:

$$2Fe_2O_3 \text{ (hematite)} - O_2 \rightarrow 4FeO \text{ (ferrous oxide)}$$

The tendency of compounds to accept or donate electrons is the redox potential. This reaction is microbially driven in soils, hence there has to be an energy source (e.g. organic matter) for any redox to take place in a soil environment. A high redox potential indicates oxidising conditions, while a low redox potential indicates a reducing environment.

Chemical weathering has an effect on soil properties. In arid regions (less rainfall) there is less chemical weathering than in humid regions (high rainfall). Therefore fewer minerals will change to other minerals, and fewer soluble materials are formed or leached to deeper horizons. For this reason, many soils in arid regions are alkaline and in humid regions acidic.

2.2.1.2. **Soil Profile & Horizons**

A soil profile forms as a result of soil formation processes. Soil profiles are composed of a series of 'horizons', each with characteristic texture, structure, colour and other properties. The master horizons are defined by the capital letters: O, A, B, C and R. 'O' is the litter or organic layer above the mineral soil; 'A' is the mineral soil or topsoil, which may present also an 'E' horizon (eluviated or leached); and 'B' or subsoil is the zone of accumulation of material leached down from the 'A' horizon (e.g. clay and carbonates); 'C' is the weathered parent material which overlies 'R', which defines the bedrock or other deep geological deposits. Soil horizons vary and some may not be present, for example, a 'B' horizon may not be present in weakly developed soils. Also, other subcategories may be present (with a lower case letter) following the master horizon. For example, Ap is a ploughed topsoil.

2.2.2. Soil Materials & Properties

Soils can be characterised by their mineralogy as well as their physical, chemical and biological properties. Soil materials and properties are linked and they underpin soil formation processes.

2.2.2.1. **Soil Mineralogy**

Minerals are usually natural inorganic compounds with specific physical, chemical and crystalline properties. Soil mineral materials can be categorised as silicates or non-silicates. Most soils contain silica as their major structural component (in silicates), while non-silicates are mainly oxides, carbonates and sulphates.

Minerals are divided into native elements; sulphides; oxides and hydroxides; carbonates, nitrates and borates; sulphates, chromates and molybdates; phosphates, arsenates and vanadates; and silicates which dominate in most soils. Common silicate minerals in soils include quartz, feldspars, micas and clays (Table 2-1). Non-silicate minerals include oxides/hydroxides and salts. Table 2-2 shows a list of non-silicate minerals commonly found in soils. Soil minerals are also referred to as primary and secondary. Primary minerals are those inherited from the parent material, which have experienced little chemical or structural variation since their crystallization within igneous or metamorphic rocks or their deposition in sedimentary rocks. Secondary minerals are those that have been re-crystallized or transformed by chemical breakdown and/or alteration of primary minerals.

Silicate Structure	Mineral	Formula
Isolate	Olivine	$(Mg,Fe)_2SiO_4$
Single Chain	Pyroxene Group (e.g. Augite)	$(Ca,Na)(Mg,Fe,Al)(Al,Si)_2O_6$
Double Chain Silicate	Amphibole Group (e.g. Hornblende)	$(Ca,Na)_{2-3}(Mg,Fe,Al)_5(Al,Si)_8O_{22}(OH,F)_2$
Sheet	Mica (e.g. Muscovite) Clay (e.g. Kaolinite)	$KAl_2(AlSi_3O_{10})(F,OH)_2$ $Al_2Si_2O_5(OH)_4$
Framework	Feldspar (e.g. Andesite) Quartz	$(Ca, Na)(Al, Si)_4O_8$ SiO_2

Table 2-1: Classification of silicate minerals (based on Esu 2010).

Group	Mineral	Formula
Halides	Halite	$NaCl$
	Sylvite	KCl
Sulfates	Gypsum	$CaSO_4$-$2H_2O$
	Jarosite	$KFe\ (SO_4)_2(OH)_6$
Sulfides	Pyrite	FeS_2
Carbonates	Calcite	$CaCO_3$
	Dolomite	$CaMg(CO_3)_2$
	Trona	Na_3CO_3-$NaHCO_3$-$2H_2O$
Phosphates	Apatite	$Ca_5(PO_4)_3(F,Cl,OH)$
Oxides & Hydroxides		
Al	Gibbsite	$Al(OH)_3$
Fe	Hematite	Fe_2O_3
	Goethite	$FeOOH$
	Lepidocrocite	$FeOOH$
	Maghemite	Fe_2O_3
	Ferrihydrite	$Fe_5O_7(OH)$-$4H_2O$
	Magnetite	Fe_3O_4
Mn	Birnessite	(Na, Ca, Mn^{2+}) Mn_7O_4-$2.8H_2O$
	Lithiophorite	$LiAl_2Mn_2{}^{4+}Mn^{3+}O_6(HO)_6$
	Todorokite	$(Na,Ca,K)_{0.3\text{-}0.5}$ (Mn^{4+}, Mn^{3+})$_6O_{12}$-3.5H
Ti	Rutile	TiO_2
	Anatase	TiO_2
	Ilmenite	$Fe^{2+}TiO_3$

Table 2-2: Common non-silicate minerals (based on Dixon and Schulze 2002).

Primary minerals are usually found in the sand and silt particles of soils (section 2.2.2.2) and include silicates; oxides of Fe, Zr and Ti; and phosphates. Secondary minerals are mainly found in fine particles in the clay and fine-silt fractions (section 2.2.2.2). Typical secondary minerals in soils include alumino-silicates, oxides and hydroxides, carbonates, sulphates and amorphous minerals. The mineralogical composition of a soil is based on the nature of the parent material(s) from which they were derived and the intensity of the weathering regime.

Oxides such as Fe and Al-oxides, often referred as sesquioxides, can play an important role in soil aggregation and structural formation. The abundance of Fe-oxyhydroxides can have an important influence on the colour of soils due to their pigmentation properties. On oxidation they present brownish-yellow to bright-red colours, whist under reducing conditions they turn grey (due to Fe^{3+} to

Fe^{2+} transitions). These changes in soil colour are an indicator of soil development and wetness.

Mn-oxides and hydroxides are also very common in soils, for example, as brown/black concentric nodules and reflect periodic water saturation. Ti-oxides are found in soils but in smaller quantities, in the sand and silt fractions where they come from igneous and metamorphic rocks. They are fairly resistant to weathering. Phosphate minerals are not very common in soils and if they are weathered, they can form Al and Fe-phosphates (Karathanasis 2006).

2.2.2.2. **Soil Physical Properties**

Mineral soil particles (sand, silt and clay) are the result of the physical and chemical breakdown of rocks and minerals (section 2.2.1.1). They are distinguished by their diameter size, gravels being the largest (>2mm) and clay the finest particles (<0.002mm). Soil texture is related to the relative proportion of mineral particles in a soil (Figure 2-2).

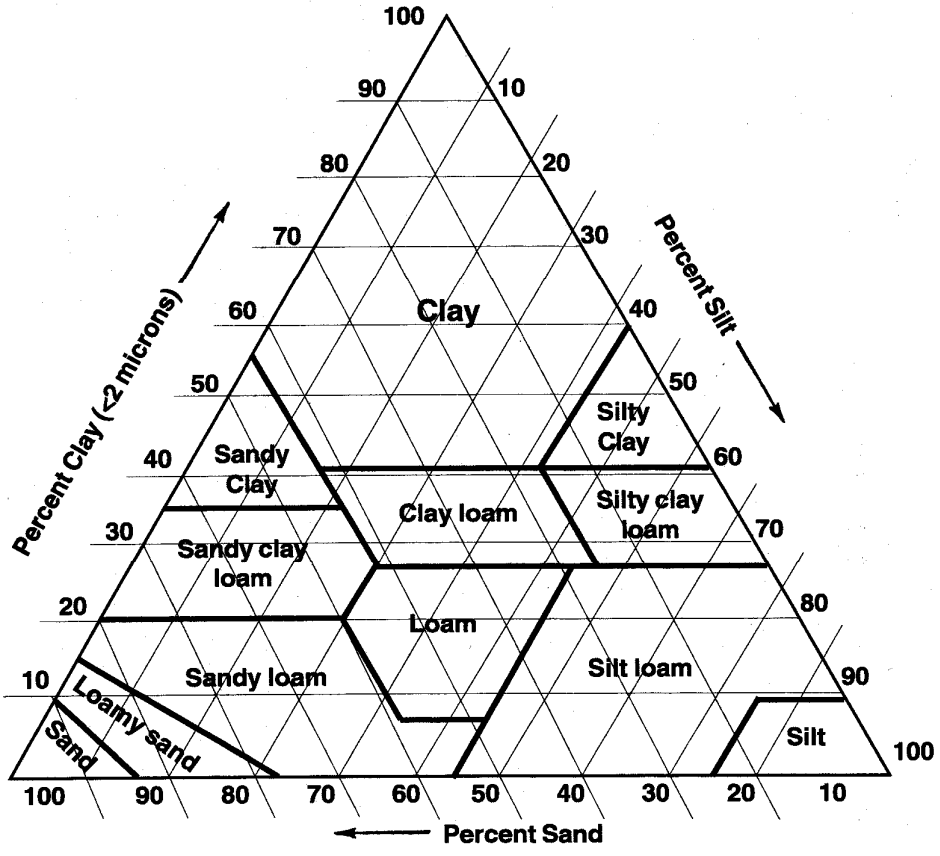

Figure 2-2: Soil textural triangle according to the proportion of sand, silt and clay content (from www.soils.usda.gov).

Soil structure arises from the arrangement of soil particles in large clusters (aggregates or peds) and is an important factor in water movement and sequestration of chemical elements in the soil. 'Granular' structures are loose peds bonded by organic particles. Large peds (plates, blocks or prisms) tend to shrink (dry or thaw) and swell (wet or freeze), as do similar adhesive substances (Gardiner and Miller 2004) such as organic substances, iron oxides, clays and carbonates. Cracks in peds are important for the circulation of water and air in soil. Finer soils normally have stronger structures due to the shrinking/swelling processes, especially clay-rich soils (e.g. smectite clay soils).

Soil porosity is the proportion of pore space (the air or water-filled spaces between particles). It is determined by soil texture and structure as they determine the size, number and interconnection of pores. Coarse soils have larger macro pores (less porosity) and fine soils have smaller pores (greater porosity). Soil physical properties directly affect the movement and retention of water. When all the soil pores are filled with water the soil is 'saturated'. Macropores allow easy movement of water and drain freely via gravity (free water). Micropores immobilise and hold water via 'capillary' forces and their amount is the 'water holding capacity' of soils (capillary water). According to Pallat and Thornley (1990) a third type of water in a porous media is bound water, the least mobile and strongly held to negatively charged clay mineral surfaces (adsorbed water). Water can also be absorbed into the mineral particles or organic matter in soil (solids). Therefore, water retention increases with increasing clay content and organic matter because of the affinities of water for those solids (Schaetz and Anderson 2005). Volumetric water content expresses the moisture content in the soil and represents the fraction of the total volume of soil that is occupied by the water.

2.2.2.3. **Soil Chemical Properties**

Soil colloids' are the finest clay and soil organic matter particles. Since smaller particles have a larger surface area than larger particles, this increases their bonding and cohesion with other colloids and the soil solute. Most chemical interactions in soil occur on colloid surfaces because their surfaces are charged (i.e. positively-charged ions or cations and/or negatively-charged ions or anions) (McCauley *et al.* 2005).

Salts are ionic compounds naturally present in soil solution. In most soils, Ca^{2+}, Mg^{2+}, K^{+} and Na^{+} ions predominate and their concentrations determines soil salinity. The main source of all salts in the soil are the primary minerals (section 2.2.2.1) released during chemical weathering processes (section2.2.1.1) which are gradually released and made soluble. The released salts are transported away from their source of origin through surface waters or groundwater. Salts can also come from irrigation water, fertilisers, compost and manure, and can be leached by filtration.

Due to the chemical makeup and larger surface area of soil colloidal particle, they have charged surfaces that are able to attract or absorb ions (charged particles) present in soil solution. Depending on the charge, size and concentration of the ions, they can be sorbed by colloids or exchanged with other ions. The ability of a soil to sorb, hold and exchange ions is the 'exchange capacity'. Despite both positive and negative charges being present on colloid surfaces they have a general negative charge. More cations are attracted to exchange sites than anions. Therefore, soils tend to have a large cation exchange capacity (CEC) (Figure 2-3). Fine textured soils generally have a greater CEC than coarse soils because of their high number of colloidal clay particles. In general, the higher the organic matter and clay content, the higher the CEC.

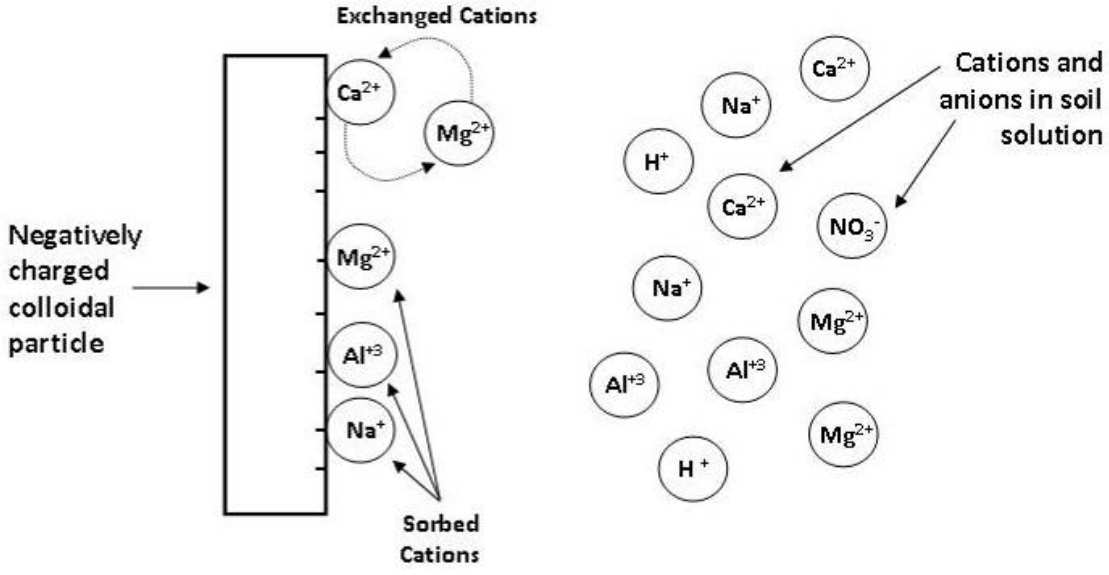

Figure 2-3: Diagram showing the cation exchange capacity (CEC) of soils (based on McCauley *et al.* 2005).

Soil pH defines the degree of alkalinity or acidity of a soil. Soil pH can affect the CEC by altering the charged colloidal surface. A higher concentration of H^+ (lower pH) will neutralise the negative charge on colloids, therefore decreasing the CEC and increasing the exchange with anions (AEC).

2.2.2.4. **Soil Biological Properties**

Soil biota (plants, fauna and microorganisms) contribute to the development of soil aggregation, structure and porosity. It is also fundamental in organic matter decomposition and mineralisation processes. Plants add organic matter to the soils via shoot and root residues and this influences the structure and porosity of soils. Root channels may remain open after the root decomposes, adding a way for air and water circulation. Fauna (e.g. earthworms) in soil initiate the early stages of: breaking down organic matter (dead plant, animal material); burrowing channels which enhance water and air circulation; and mixing of soil layers (bioturbation). Microorganisms in soils aid particle cohesion though the secretion of organic compounds (mainly sugars), which contribute to the formation of granular structures. This is typical of A horizons (section 2.2.1.2) where the microbial population is more dense. Bacteria are the smallest and more diverse of soil microbes. Bacteria contribute to organic matter decomposition, nutrient transformation and minor clay aggregation.

2.2.3. Soil Processes

Soil formation processes are determined by climate and organisms (plants and animals) operating over the local geology over time and under the influence of the geomorphology as well as human activity. These processes include additions, losses, transformations and translocations (Krzic *et al.* 2008).

2.2.3.1. **Additions**

Additions to the developing soil profile can come, for example, from leaves (organic additions) or soluble salt from ground water (mineral additions). For example, organic matter accumulation can happen when biological activity ceases due to waterlogging and cold temperatures. The result is the formation of peat, which may reach considerable thickness. Other additions may come with rainfall or deposition by wind, such as the aeolian deposits.

2.2.3.2. **Translocations**

Translocation (or transportation) of organic and inorganic material can occur from one to another horizon either up or downwards by water or organism action. Types of translocation processes include: bioturbation, clay accumulation, eluviations (downward movement of the suspended material in soil through the percolation of water) or illuviation (deposition of soil suspended material in a lower soil horizon through the process of eluviation from an upper soil horizon). Other translocation processes such as colluviation and solifluction involves the movement of sediment downhill to the bottom of a slope. Gravity and sheetwash induced by rainfall are precursors of these processes and they result in unsorted sediment of variable particle size, ranging from boulders to clay, accumulating over the existing topsoil.

2.2.3.3. **Transformations**

Transformations of soils constituents from one form to another through mineral weathering and organic matter breakdown include, for example, general redox processes (section 2.2.1.1) and gleying. Gley soils are characterised by red/yellow/grey-bluish mottling produced by waterlogging and reduction conditions. It is caused by different oxidation states of Fe and Mn. In summer when the water table drops and soil is drained, air can infiltrate into the soil, therefore any Fe that is in the soil becomes oxidised forming the red colour. In winter, the soil is saturated, resulting in anaerobic/reducing conditions and predominantely yellow or grey-bluish colours. The fluctuations in the water table create pockets of different colours, termed mottling or gleying. Waterlogging can occur by poor drainage conditions because of: a high water table (groundwater gley); or when precipitation inputs encounter an impermeable soil layer such as a clay deposit (surface-water gley).

2.2.3.4. **Loss of materials**

Loss of material from the soils can be caused by leaching processes, erosion of surface material (e.g. due to intensive ploughing) or other forms of translocation or transformation and these may produce the accumulation of material in a layer. Leaching is the process of losing soluble material from the soil profile by percolating water. This effect is more noticeable on coarse and free-draining soils and areas with high rainfall. The process leads to the acidification of

topsoils. Podzolization involves the leaching of sesquioxides (Fe and Al) downwards in the soil profile and is generally associated with acidic parent material (rock) and/or acid vegetation (e.g. coniferous woodland). The percolation of soluble organic matter from humus and its bonding with other elements (Fe, Si and Al) results in their mobilization downwards in the profile. As a consequence of the loss of organic and mineral components by leaching, a pale grey, sandy eluvial horizon develops. The mobilised metal-humus complexes are then deposited in a spodic or illuvial horizon, characterised by a dark brown or reddish colour. A thin indurate soil horizon in which iron oxide is the principal cement can develop in Podzols. This impervious horizon or 'iron-pan' may form upon periodic water stagnation in the soil and causes the re-deposition of less soluble soil cations such as Fe, Al and Mn, either at the B horizon or below it (Macaulay Land Use Research Institute 2012).

2.3. General Geological & Soil Settings in Scotland

The geology in Scotland is characterised by its diversity of rock types and landforms. Figure 2-4 shows the distribution of the different bedrock types in Scotland: metamorphic, sedimentary and igneous rocks and the location of the different sites surveyed in this study. Much of northern and central Scotland is formed on a hard crystalline core of schists (metamorphic rock) and granites. The central lowlands and the Borders are occupied by softer sedimentary rock. The Scotish landscape is defined by its ancient and intricate geology and it has been further reshaped by the more recent effect of glaciers and ice-sheets, developing a complex combination of erosional and depositional geomorphological features. Many of the superficial deposits that form the parent material of contemporary Scottish soils are fundamentally characterised by Quaternary glacial drift deposits(Figure 2-5), since very few superficial deposits in Scotland derive from direct weathering of the bedrock *in situ* (Macaulay Land Use Research Institute 2012) and locally weathered hard rock is often deeper than 12m (Fitzpatrick 1963), (Gordon *et al.* 2002; Macaulay Land Use Research Institute 2010b). These deposits are characterised by an extreme heterogeneity of components, such as mixtures of sands, gravels, silts and weathered rocks carried by glaciers and dropped as the ice sheet advanced or receded.

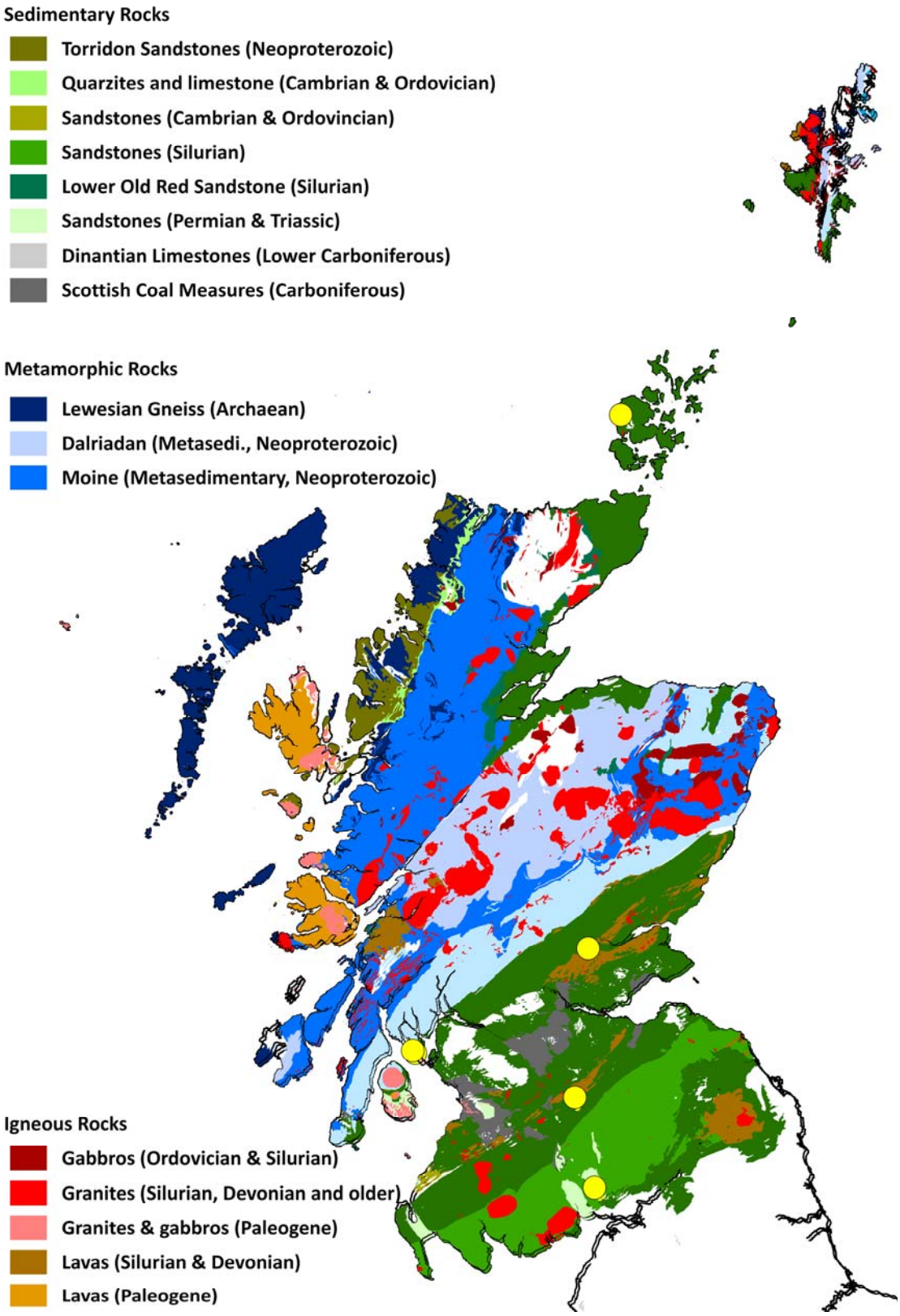

Figure 2-4: Bedrock geology in Scotland and location of the five case study sites (yellow dots) (based on © Crown Copyright/database right 2012. An Ordnance Survey/EDINA supplied).

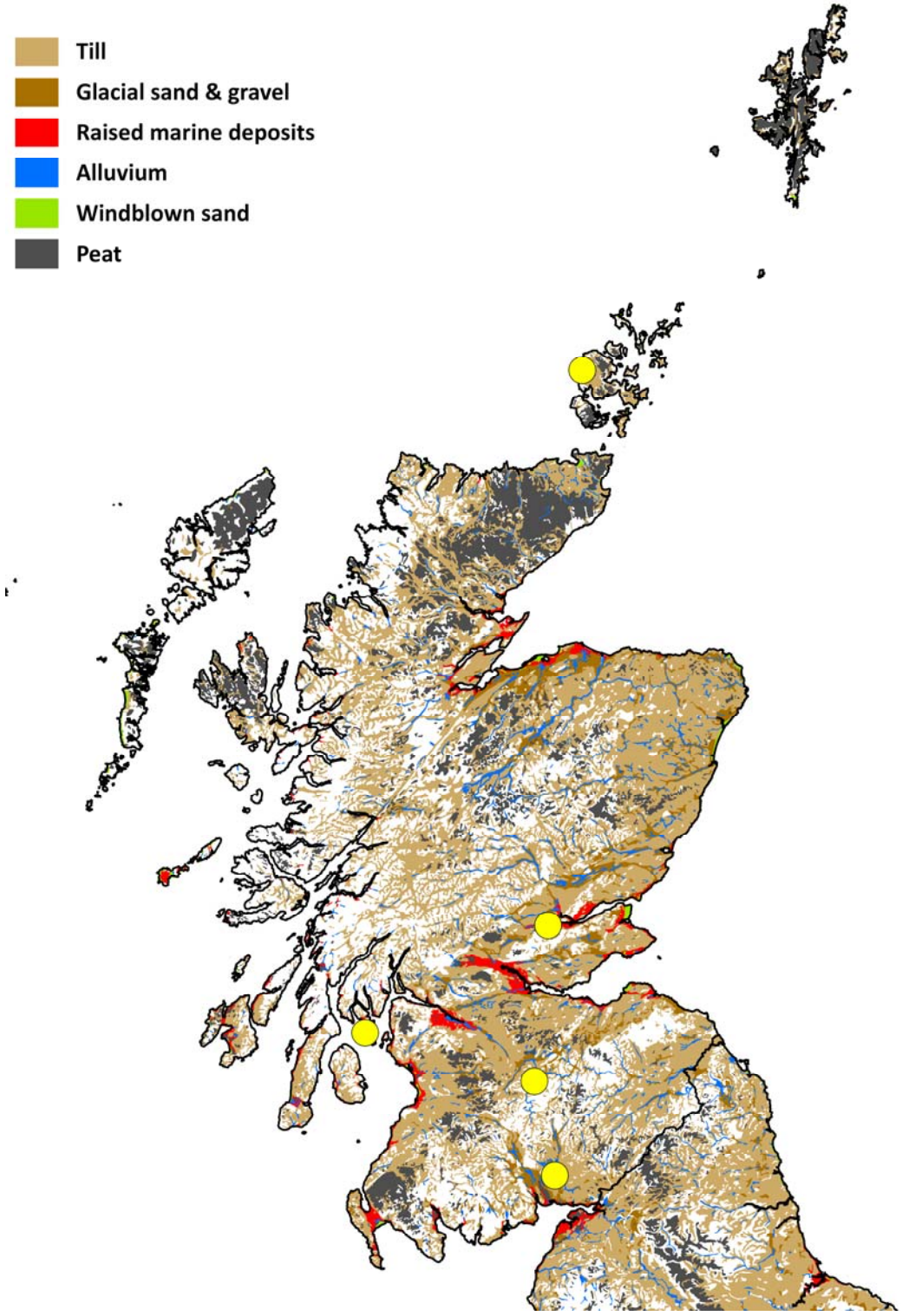

Figure 2-5: Distribution of the superficial deposits in Scotland and site locations (yellow dots). The glacial deposits are in brown scale and areas in white are unmapped zones (based on © Crown Copyright/database right 2012. An Ordnance Survey/EDINA supplied).

Scottish soils are very varied because of the wide diversity of parent materials from which the drift ultimately derives (Wilson *et al.* 1984). Also, since most of the soils in Scotland are developed from heterogeneous glacial drift deposits they are fairly young, having begun to develop *c.* 10,000 to 15,000 years ago. Figure 2-6 shows the distribution of the main soil types in Scotland and these

are: leached soils (podzols and brown soils), gleyed soils, organic soils (peat), immature soils and non-leached soils. The soil processes (*e.g.* podzolization, gleying and organic matter addition) behind the formation of these soils are discussed in section 2.2.3. Podzols (the most common soil type) and gleys are widespread throughout Scotland. Mineral soils are predominantly found in the lowlands of Scotland, with podzols associated with the more acidic areas and freely draining brown earth soils more common in the drier east. Poorly draining gleys are mainly found in the wetter west and areas in the Midland Valley and Southern Uplands, while peaty soils are most commonly found in the Highlands and Southern Uplands.

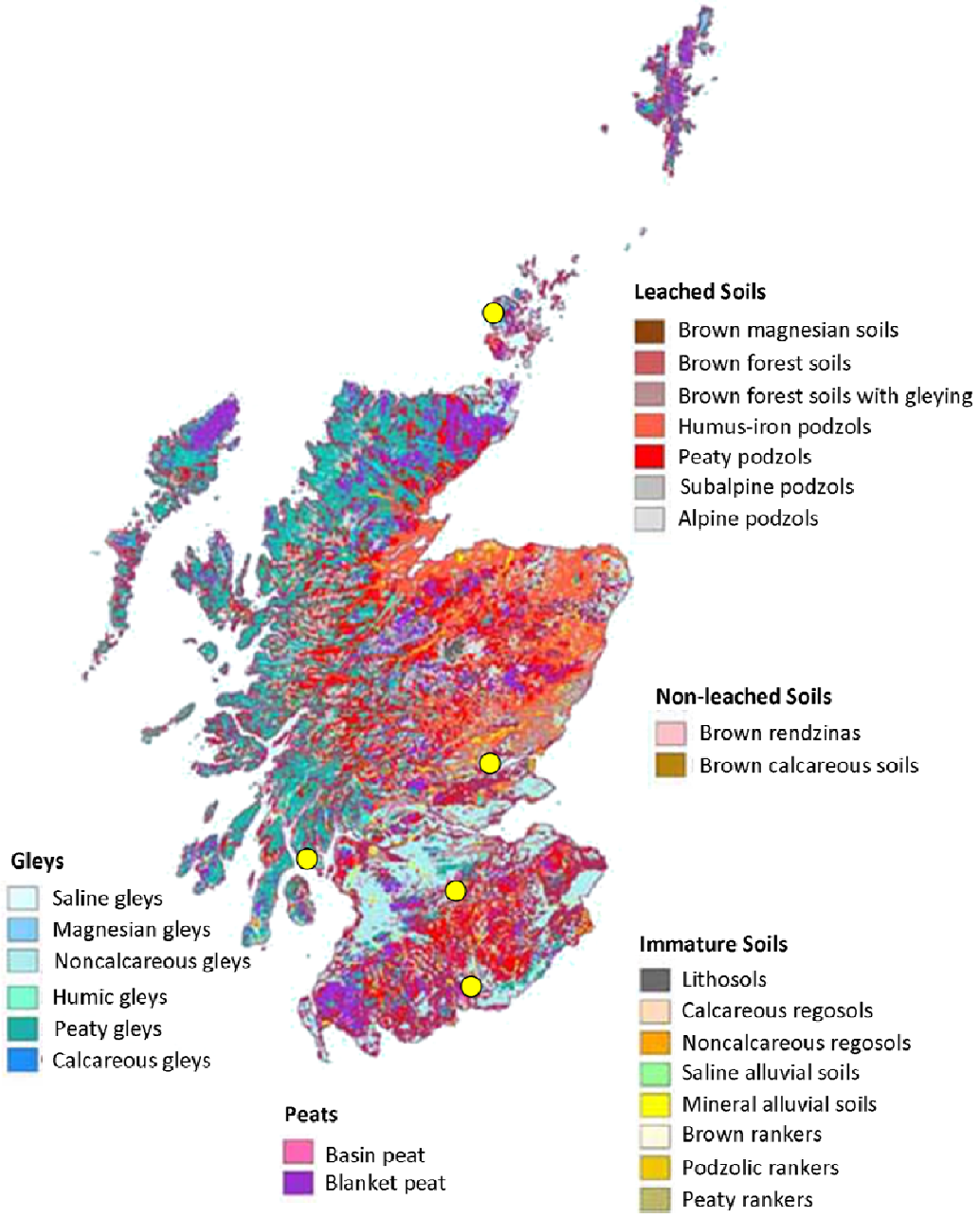

Figure 2-6: Major soil distribution in Scotland and site locations (based on The Macaulay Institute Soil Map 2010a).

2.4. Soil Properties & Geophysical Methods

Near-surface geophysical methods are able to detect and map buried archaeological features by measuring a series of physical properties and collecting data from above the Earth's surface. As dicussed in section 2.2.2, these physical properties are strongly associated with soil physico-chemical and biological soil properties and processes. Therefore, the functioning and the relative degree of success of geophysical surveys in detecting archaeological features are strongly related to the properties and dynamics of the soil environment in which they take place. This section briefly introduces the principles of geophysical methods used in archaeological prospection (i.e. electrical, magnetic and electromagnetic methods), with particular emphasis on soil properties. This section combines information synthesised from a series of manuals on the use of geophysical techniques for archaeological prospection and other applications (Clark 1990; Scollar *et al.* 1990; Conyers 2004; Gaffney and Gater 2003; Witten 2006; Aspinall *et al.* 2008; and Jol 2009).

2.4.1. Electrical Methods

2.4.1.1. **Electrical Properties of Soil**

Electrical resistivity is a property present in all materials, including soils, and defines how strongly a material opposes the flow of electric current. This property governs the relationship between the current density and the gradient of the electrical potential. Soil resistivity is a variable property which may change upon climatic conditions (temperature, rainfall). Soil factors that influence electrical resistivity include porosity, grain size distribution and water content (Samouëlian *et al.* 2005). Water allows current to be conducted, whereas its movement is impeded in dry media. Pure water is virtually non-conductive but in soil solution water forms a conductive electrolyte when it contains dissolved salts (section 2.2.2.3). When the salts dissociate in the presence of water they form moving charged particles which carry the electric current and make the solution electrically conductive. Therefore, soil resistivity is mainly governed by the water content of the ground (Schmidt 2009, 68). The relative abundance of salts and the resulting salinity of the pore-water also affect the conductivity (inverse of resistivity) and they vary between different types of soil.

Soil solutions represent a complex balance between water content, pH, and organic and inorganic components. As electrolytes in the soil solution must affect the passage of electrical current, what is dissolved or held in the soil must also affect soil resistivity (Sharpe 2004, 3). Soil composition (clay mineral and metal content) can also affect soil resistivity (Wightman *et al.* 2003). Clays and a few minerals (e.g. magnetite and other metallic sulphides) if found in sufficient concentration can increase the conductivity of soil. Although clay particles are non-conductive when dry, the conductivity of pore water is due to the ionization of clay particles (Zhdanov 2009, 416). Since clay has a huge surface area to volume ratio, it has a high exchange capacity. In clay water mixtures, the exchange ions separate from the clay mineral by desorption (a process similar to ionization), forming a mobile cloud around each clay particle (Wightman *et al.* 2003; Zhdanov 2009, 426). These ions increase the conductivity of a soil when an electric field is applied and, therefore clays can dramatically increase the conductivity of fresh water.

According to Pozdnyakov and Pozdnyakova (2002), soil chemical properties including organic matter content, CEC and soil mineral composition are related to the total amount of charges in soils, whist soil physical properties (e.g. water content and temperature) influence the mobility of electrical charges (ions) in soils.

2.4.1.2. **Earth Resistance Survey**

Electrical methods are based on the principle that the distribution of electrical potential in the ground around a current-carrying electrode depends on how strongly a material opposes the flow of an electric current (i.e. soil electrical resistivity). If a medium easily conducts a current the resistivity will be low, otherwise the resistivity will be high.

The method usually involves passing an electrical current into the ground using two electrodes (current electrodes, C1 and C2 in Figure 2-7). The current passing through the ground sets up a distribution of the electrical potential in the sub-surface (Figure 2-7). The difference in electrical potential is measured by two additional electrodes (potential electrodes, P1 and P2 in Figure 2-7) as a voltage.

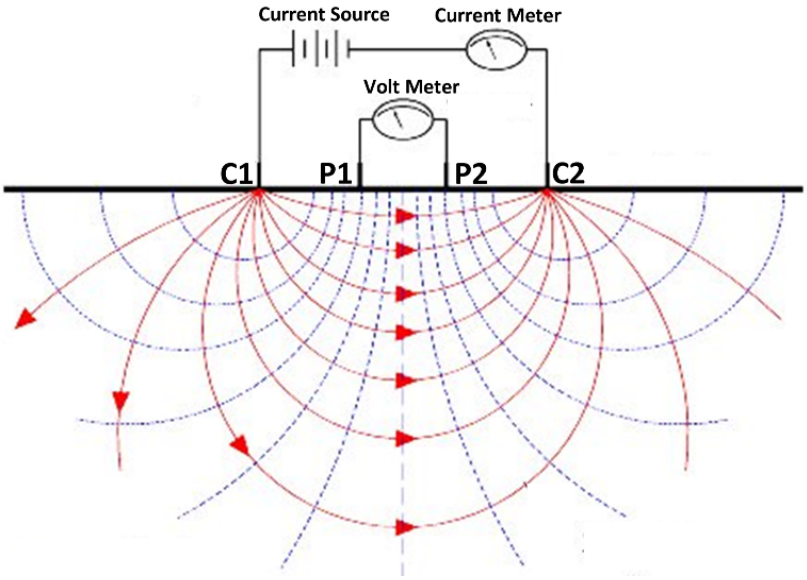

Figure 2-7: The electric field around two electrodes (C1 and C2) in terms of equipotentials (black broken lines) and current lines (in red) on a homogeneous half-space (e.g. subsurface). The equipotential lines represent contours of equal electrical potential. The current lines represent the electrical current spread in a homogeneous media (based on Muchingami *et al*. 2012).

According to Ohm's Law which states that the intensity of a current (I) is proportional to the difference in potential (V) measured through a resistive media and inversely proportional to the resistance (R) of the media. This means that if the resistance (R) increases or the potential difference (V) decreases, the current (I) drops:

$$I = \frac{V}{R}$$

Where

R = resistance of the earth in units of Ohms (Ω).
V = potential difference measured between the current electrodes in Volts (V).
I = current through the earth in units of Amperes (A).

An electrical current will spread evenly in a homogeneous ground (Figure 2-7), but obstacles to this current will lead to a difference in the electrical potential measurements taken at the surface. Using Ohm's law the potential difference (V) measured on the surface can be converted into a resistance reading for the ground between the two potential electrodes:

$$R = \frac{V}{I}$$

Lateral surface variations (or anomalies) on the ground resistance mapped with this technique may be a representation of subsurface features, including

archaeological remains. The electrical resistance (R) is calculated as the ratio of the electrical potential measured at the surface and expressed in ohms (Ω). This measurement depends on the different resistivities of the ground and the arrangement of the electrodes. The resistivity (ρ) of a buried feature or soil is the resistance per unit volume and measured in Ohm-metres (Ωm). A single value of earth resistance (R, in Ω) at the surface is an average of all the different resistivities (ρ, in Ωm). It is possible to convert the resistance measurement into the resistivity value taking into account the electrode configuration used (Schmidt 2009, 71). To do this, the concept of apparent resistivity (ρa) is used and defined as the resistivity of an electrically homogeneous half-space that would yield the measured relationship between the applied current and the potential difference for a particular spatial arrangement of electrodes.

This was the first geophysical method to be used in archaeological investigations (Atkinson 1953; Bevan 2000). Scollar *et al.* (1990) gave a comprehensive theoretical introduction using examples from surveys at archaeological sites. The most recent publication on electrical methods for archaeological applications is the forthcoming book by Schmidt (2013). This book describes traditional earth resistance area surveys and other more novel electrical techniques such as vertical imaging for 3D electrical depth investigations.

2.4.1.3. **Types of Anomalies**

Electrical methods are effective in mapping masonry and similar impervious structures buried near the surface. It can also map the backfill of buried pits and ditches and locate anomalous moisture variations associated, for example, with palaeochannels.

The types of anomalies detected in the surveys are generally described as high and low resistance anomalies. Since soil resistivity is linked to moisture content and soil porosity (section 2.4.1.1), hard dense features (*e.g.* a wall) will generally give a relatively high resistance response. Ditch-like features will give a relatively low response as they retain moisture. However, changes in the moisture content of the soil, as well as variations in temperature, can affect the form of anomalies. For example, the 'negative' resistivity contrast often

expected from a ditch feature can present a reversed and complex sequence of responses (Schmidt 2009, 70). In dry conditions, in-filled cut features may contain less moisture than the material into which the feature is cut and result in a relatively high resistance response. Other weak or broad linear anomalies of unknown cause can be described as 'trends'.

2.4.1.4. **Depth of Investigation & Resolution**

The different array configurations of the electrodes and their separation determine the depth of investigation and resolution achieved (Gaffney and Gater 2003, 28-30). In earth resistance surveys, the wider the probes are separated, the deeper the detection achieved (Gaffney and Gater 2003, 32). The twin probe array configuration (Figure 2-8) has been demonstrated to provide a good spatial resolution for archaeological investigation (Gaffney 2008). It provides the simplest type of response (single peak instead of the complicated multi-peak responses from other arrays) as well as improving the speed and ease of use. With the twin array configuration, one current (C1) and one potential (P1), the mobile electrode pair, separated by a short and fixed distance, is moved from station to station along resistance survey lines. The maximum spatial resolution is equivalent to the mobile electrodes separation distance. The second remote electrode pair, with current (C2) and potential (P2) is located at a remote distance away, at least 30 times the distance between the probe separation, to place the remote pair effectively at infinity. Therefore, in a survey grid using a 0.5m electrode separation, the remote pair of electrodes should be at least 15m away from the nearest grid point (Figure 2-8).

The twin-probe configuration focuses its detection capacities on a subsurface ground volume where the potential gradient changes rapidly near the current electrodes (Figure 2-8), ensuring that the majority of variation in the signal results from near surface variations and is measured by the closely spaced potential electrode. Therefore, the effectiveness of this array lies in the small distance between the mobile current and potential probe where the potential gradient is highest, and not in the overall spread of the probe configuration. The general depth of investigation for a 0.5m twin-probe configuration reaches *c*.0.5m - 0.75m, similar to the depth of burial of many archaeological features (typically up to 1m). This is why this array provides the best match between

penetration and detection sensitivity. Investigation depth can be increased by expanding the twin array size (the distance between the mobile electrodes). However, this usually affects the resolution, and if there are near-surface features present, narrower than the array dimensions, these will result in lateral averaging of the electrical resistivity and thus, lead to poor lateral resolution. Other array configurations are more sensitive to vertical variation and are more useful for measuring the depths of deposits.

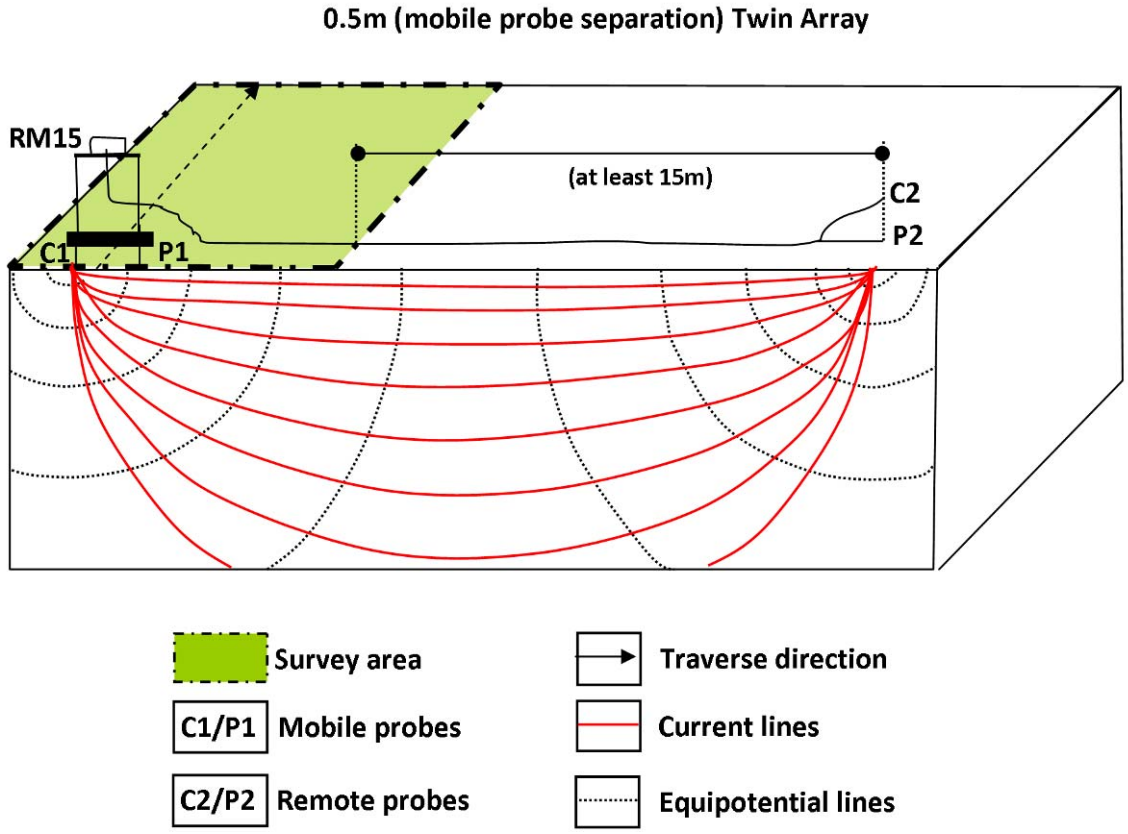

Figure 2-8: The twin probe array configuration with a 0.5m mobile probe spacing. The figure shows the potential gradient (equipotential lines) changing quickly near the current probe (C1) and closely spaced potential probe (P1). This ensures a good sensitivity of the twin-probe array for archaeological investigations.

2.4.1.5. **Factors Affecting Earth Resistance Surveys**

The earth resistance survey has some inherent limitations with regards to resolution. The value of a measurement obtained at any location represents a weighted average of the effects produced over a large volume of material, with the nearby portions to the electrodes contributing most heavily. This tends to produce smooth curves, which do not lend themselves to high resolution for interpretations if the traverse spacing is too wide (> or = 1m).

Environmental factors (such as temperature, rain, wind and sunshine) can affect the resistivity contrast of buried features and affect the responses from earth resistance surveys. These factors must be taken into account before and during surveys. Possible variations in soil moisture and resistivity contrast after days of heavy rain can modify 'expected' responses and lead to erros in data interpretation (Schimidt 2013, 24-25, 124-125). Datasets recorded during different days or seasons may present different diverse ranges and affect the display of the different data grids (Schimidt 2013, 124).

The technique requires the insertion of the probes for each measurement making the technique slightly invasive and the slowest technique in archaeological geophysics. Recent innovations with greater speed probably improve this issue. For example, the MSP40 square array cart (Geoscan Research manufacturer) allows earth resistance meters to be used with cart-based platforms on which spiked wheels replace the traditional electrodes. These platforms offer faster rates of ground coverage and it is possible to mount other instruments, such as GPS receivers or magnetometers, for simultaneous coverage.

2.4.2. Magnetic Methods

2.4.2.1. **Magnetic Properties of Soils**

Magnetism is a physical phenomenon that results in a force of attraction or repulsion between materials. Magnetic materials exhibit a magnetic field (H), a force field generated by moving electrical charges. Permanent magnets create their own persistent magnetic field, while other materials only exhibit an induced magnetic field (I) when an external field is applied. Since the origin of magnetism lies in orbits and spinning of electrons and how the electrons interact, every atom has a magnetic moment (tendency to align with a magnetic field). The magnetic susceptibility (MS) of a material is a property that describes how 'magnetisable' a material is in response to an applied magnetic field (Dearing 1999).

Materials are more or less magnetic depending on the degree of interaction between the atomic magnetic moments (Moskowitz 1991). The five types of magnetic behaviour of materials are diamagnetic, paramagnetic, ferromagnetic,

ferrimagnetic and antiferromagnetic. These magnetic classes characterise many soil minerals or other archaeological materials that may be detected by magnetic surveys.

Diamagnetism, is the weakest type of magnetic behaviour, is due to the non-cooperative behaviour of orbiting electrons under an applied magnetic field. The atoms have no net magnetic moments as all the orbital shells are filled and there are no unpaired electrons. Diamagnetism produces a negative susceptibility response when exposed to an external field and the magnetisation is zero when the field is removed. The susceptibility of these materials is temperature independent. Quartz, calcite and water are examples of diamagnetic materials (Moskowitz 1991).

Paramagnetic matter presents a net positive magnetisation, hence positive susceptibility only when a field is applied. This is caused by net magnetic moment of the atoms due to unpaired electrons in partially filled orbitals. However, there is no magnetic interaction between the individual magnetic moments, hence the magnetisation returns to zero when the external field is removed. The susceptibility of these materials depends on temperature. The susceptibility of paramagnetic materials is small at normal temperature. Paramagnetic minerals include pyrite (Fe-sulphide), siderite (Fe-carbonate) and montmorillonite (clay) (Moskowitz 1991).

Ferromagnetic materials have atomic moments that interact strongly because of electronic exchange forces that produce the parallel alignment of the atomic moments. The resulting net magnetisation is large and independent of the application an external field. Ferromagnetic elements comprise Fe, Ni, Co and many of their alloys. At the Curie temperature, the thermal energy can overcome the exchange forces in ferromagnetic materials, reducing the magnetisation field to zero. Ferromagnets can also retain the memory of an applied field once it is removed. The hysteresis loop shows the history dependent nature of the magnetisation of ferromagnetic materials. A saturated material will keep most of its magnetisation (memory) once the magnetisation field is dropped to zero. The remaining magnetisation is called remanence. In order to attain zero magnetisation, a field in the opposite direction must be applied. The amount required is the coercivity. Ferrimagnetism is similar to

ferromagnetism, hence these materials have a high MS. Ferrimagnetic minerals include magnetite and maghemite which are the most influential iron oxides in soil (Kattenberg 2008, 16).

Antiferromagnetic materials have a small positive MS. All the electron spins are aligned in two opposite directions resulting in a net magnetic moment of zero. Antiferromagnetic materials (e.g. Cr) have a small positive MS and they can become paramagnetic above the Curie temperature. 'Spin-canted' materials are characterised by a small rotation of the spin directions of the electrons, therefore the two spin directions are not to perfectly opposite (Kattenberg 2008, 15), resulting in a weak magnetic moment. Hematite is an example of such a spin-canted mineral. Table 2-3 contains a summary of the magnetic properties of some minerals and elements.

Group	Mineral	Formula	Magnetic Order	Tc(°C)	σs (Am2/kg)	χ
Oxides	Magnetite	Fe_3O_4	Ferrimagnetic	575-585	90-92	50,000
	Ulvite	Fe_2TiO_4	AFM	-153		
	Hematite	αFe_2O_3	Canted AFM	675	0.4	60
	Ilmenite	$Fe^{2+}TiO_3$	AFM	-233		200
	Maghemite	γFe_2O_3	Ferrimagnetic	~600	~80	40,000
	Jacobsite	$MnFe_2O_4$	Ferrimagnetic	300	77	
	Trevorite	$NiFe_2O_4$	Ferrimagnetic	585	51	
	Magnesioferrite	$MgFe_2O_4$	Ferrimagnetic	440	21	
Sulfides	Pyrrhotite	Fe_7S_8	Ferrimagnetic	320	~20	~5,000
	Greigite	Fe_3S_4	Ferrimagnetic	~333	~25	
	Troilite	FeS	AFM	305		
Oxyhydroxides	Goethite	αFeOOH	AFM, weak FM	~120	<1	70
	Lepidocrocite	γFeOOH	AFM/Paramagnetic	-196		70
	Feroxyhyte	δFeOOH	Ferrimagnetic	~180	<10	
Metals & Alloys	Iron	Fe	FM	770		
	Nickel	Ni	FM	358	55	
	Cobalt	Co	FM	1131	161	
Other	Quartz	SiO_3	Diamagnetic			−0.6
	Water	H_2O	Diamagnetic			-0.9

Table 2-3: Magnetic properties of minerals (especially Fe-bearing) that occur as soil constituents (based on Moskowitz 1991 and Van Dam *et al.* 2008). The abbreviations stand for ferromagnetic (FM) and antiferromagnetic (AFM) magnetic orders, Curie or Néel temperature (Tc), saturation magnetization at room-temperature (σs) and magnetic susceptibility (χ).

The magnetic properties of soils results mainly from the presence of Fe-oxides in different forms (e.g. magnetite and maghemite) and their abundance (Mullins 1977). Iron oxides can be inherited from the parent material (e.g. igneous and

metamorphic rocks) or the result of soil formation processes (section 2.2). Paramagnetic and antiferromagnetic minerals are the most abundant oxides in soils. Minerals that influence the overall soil magnetism are magnetite, maghemite and pyrrhotite as they are the most magnetic forms (ferrimagnetic) (Van Dam *et al.* 2008). Other Fe-Ti oxides and Fe-sulphides also influence the magnetism of soils. Table 2-3 shows the magnetic ordering and MS for Fe and Fe-Ti oxides, Fe-sulphides and other soil components.

Soil mineralogy can be modified by a number of processes (e.g. redox processes), including anthropogenic ones such as burning activities, land use practices, industrial areas. The altered soil mineralogy can be brought up to the topsoil by ploughing or other processes and remains in the topsoil, enhancing its MS. Therefore, areas of artificial MS enhancement derived from topsoils or shallow archaeological horizons can be mapped by magnetic and electromagnetic methods.

2.4.2.2. **Magnetometer Survey**

The Earth has a magnetic field created primarily by the movement of ions and electrons in the area between the liquid core and the solid mantle of the Earth (Figure 2-9a). The form of the field can be approximated as the dipole of a bar magnet located at the Earth's centre and aligned sub-parallel to its geographic axis (Figure 2-9b), with the south tip pointing northwards hence attracting the northern tip of compass needles (Schmidt 2009, 75).

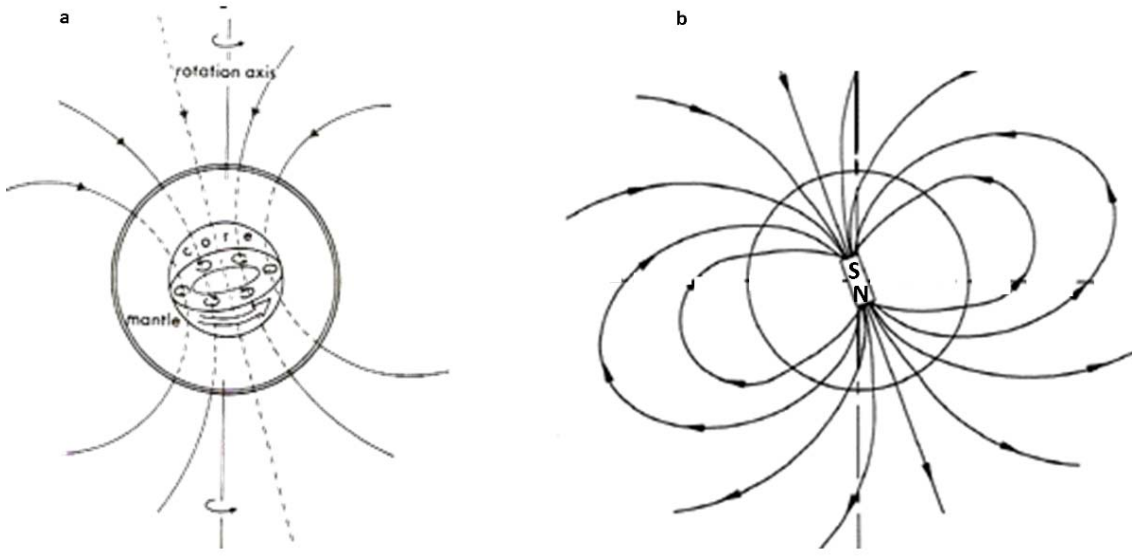

Figure 2-9: The outer core of the Earth as the source of the magnetic field (a) and magnetic dipole approximation (b) of the Earth's magnetic field (based on Sharma 1997).

Since all matter is magnetic (Moskowitz 1991), soil materials and other buried interfaces (e.g. archaeological features) present a degree of magnetisation. The individual field that these subsurface interfaces may exhibit causes perturbations in the Earth's magnetic field (anomalies) which can be detected by magnetic surveys.

Induced magnetisation occurs by the application of an external field to a material. The enhanced ambient field makes the material act as a magnet (Wightman *et al.* 2003). The elementary magnets of the material partially align with the external field and therefore increase its intensity (Schmidt 2009). The greater the alignment, the stronger the enhancement of the applied external magnetic field. The induced magnetisation (*I*) is hence the product of the volume MS (k) and the inducing field of the Earth (H_{earth}):

$$\boldsymbol{I} = \boldsymbol{k}\boldsymbol{H}_{earth}$$

The SI unit for the magnetic field strength is the 'Tesla', or more conveniently the 'nano Tesla' (1 nT = 10^{-9}T) because of the weak magnetic anomalies usually caused by archaeological anomalies.

The location of buried archaeological remains is achieved by the precise mapping of local anomalies in the Earth's magnetic field with high-resolution field magnetometers (Scollar *et al.* 1990). Buried interfaces can act as small magnets creating their own magnetic field and producing distortions (anomalies) in the earth's magnetic field (Gaffney and Gater 2003, 36). The anomalous magnetic field combined with the earth's magnetic field forms the 'total field' that can be measured at the surface with a magnetometer.

Magnetometers are sensors that measure the intensity of the total magnetic field (scalar instruments such as caesium vapour total field sensors) or its horizontal or vertical component (e.g. fluxgate sensors). Scalar magnetometers have a higher sensitivity (up to 0.001nT) in comparison to fluxgate instruments (generally 0.1nT) but they are usually less portable and more expensive. Other instruments such as the Foerster Ferex MK 26 (www.foerstergroup.de) and the Sensys Magneto MX (www.sensys.de) combine arrays of 4 or 16 fluxgate sensors respectively in a multi-channel configuration. They are mounted in a cart and

towed by operators or vehicles to provide very fast data acquisition as well as good data quality. The most updated review on the state-of-the-art of the instrumentation can be found in Aspinall *et al.* (2008).

Magnetometer survey often offers the most rapid and informative results and it has been described as the workhorse of British archaeological prospecting (Clark 1990, 69). Magnetic anomalies detected with magnetometers can be as small as 0.1nT with a range of *c.*10nT in an overall field strength of about 30,000nT-50,000nT. These intensities are often produced by an enhancement in MS of cut (or negative) archaeological features such as ditches, storage pits or postholes. Other anomalous intensities can be higher. Substantial magnetic responses may be caused by strongly magnetized pottery kilns due to thermoremanence or the ferrimagnetism of buried iron-based objects. The strength of these deviations depends on the type of magnetization of archaeological features, the depth of burial, and other soil dynamics involved in the contrast between the archaeological structure and the undisturbed subsoil. The technique is less successful in detecting structural features such as buried walls or footings unless the structural materials have a magnetic contrast with the surrounding soil (e.g. bricks carrying a thermoremanent magnetisation or the surrounding soil being more magnetically enhanced).

2.4.2.3. **Types of Anomalies**

Magnetic anomalies are approximated with the dipole model. The idealised magnetic response of a localised archaeological feature buried in northern latitudes will produce an anomaly composed of a positive peak (slightly shifted to the south of the buried feature) and negative trough (or halo) to the north of the feature (Figure 2-10).

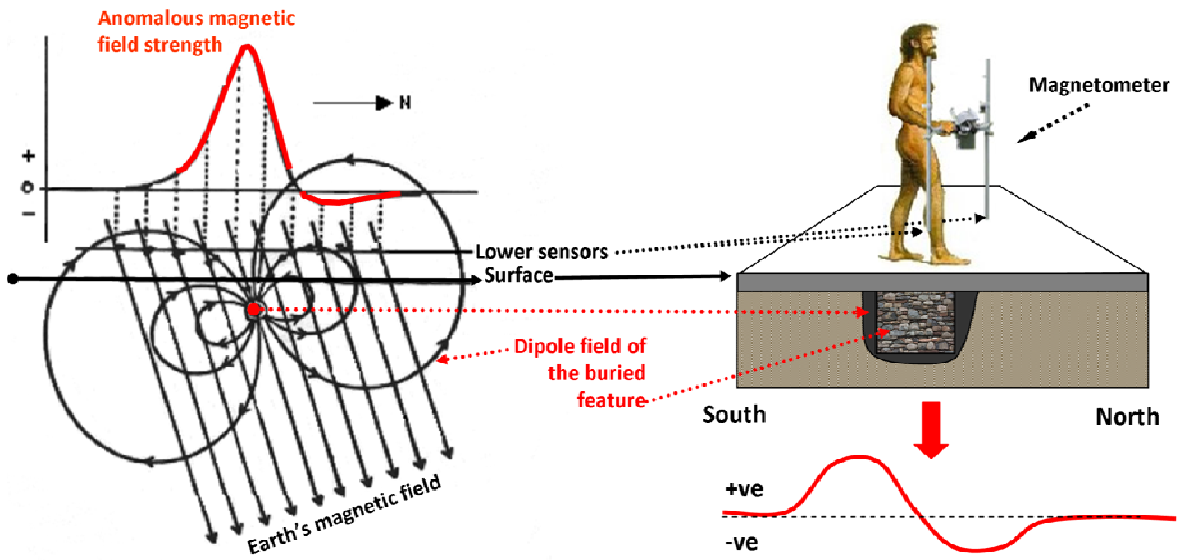

Figure 2-10: Magnetic anomaly of a buried feature measured at northern latitudes. The anomaly is characterised by a positive peak that is slightly shifted to the south of the buried feature and a negative trough to the north (based on Weymouth 1986).

There are several processes by which MS can be enhanced in soils and archaeological features. According to Kattenberg (2008, 59), the main mechanisms of MS enhancement of archaeological features are:

- Heating, by conversion of weakly magnetic iron oxides to stronger magnetic forms. For example, hematite (antiferromagnetic) can be converted to magnetite (ferrimagnetic) during burning.
- Microbially-mediated, due to the conversion of hematite to magnetite by bacteria growing in decomposing organic deposits.
- Development of magnetotactic bacteria responsible for the creation of magnetic crystals in soils (Fassbinder *et al.* 1990).
- Presence of incorporated magnetic material, such as pottery sherds or brick debris.
- Pedogenesis: Magnetic anomalies produced by iron-sulphides (greigite or pyrrhotite) at estuarine sites showing geological creek-like features. This has been reported by Kattenberg and Aalbersberg (2004). According to these authors, the anomalies were the results of changes in soil chemistry during sea water invasion of the site, through the liberation of Fe and the formation of Fe-sulphides during persistent inundation.

As can be seen from these processes, MS enhancement of soils and archaeological features may therefore be associated with soil organic matter content. Organic matter is usually more abundant in topsoil than subsoil, producing a magnetic contrast between these two soil horizons (Schmidt 2009, 76). The process of cutting archaeological features (e.g. a ditch) and backfill with magnetically enhanced soil causes a contrast in MS with the surrounding soil matrix. Soil accumulation processes of anthropic organic deposits such as in middens can also contribute to the MS enhancement of buried archaeological soils.

However, archaeological features do not always show a positive or detectable magnetic contrast. This may be caused by similar magnetic properties between archaeological features and soil matrix, or may be due to subsequent processes that have altered the iron mineralogy and thereby changed their MS (Kattenberg 2008, 60). Waterlogging of soils during a prolonged periods of time can dissolve even ferrimagnetic minerals or reduce iron oxides to iron hydroxides causing a drop in soil MS (Weston 2002). Severe leaching and gleying can cause the dissolution and movement of iron, and will usually lead to a change in soil MS (Kattenberg 2008, 29). Sharpe (2004, 222), explored the geochemical links between geophysical results (magnetic and electric methods) and cropmark responses of archaeological sites in Scotland. She postulated that pH and redox changes had an influence on the character of magnetic responses.

Magnetic anomalies are generally described as ‘positive’ or ‘negative’. Anomalies showing positive values relative to their magnetic background matrix are the general response expected from archaeological features. They often present additional negative data (halo) as explained above (Figure 2-10). When the mean magnetic background is stronger than the backfill of the anomaly, the response shows ‘negative’ values. Anomalies characterised by a faint response are described as ‘weak’ magnetic anomalies. ‘Magnetic or discrete dipoles’ are used to describe the typical dipole response showing a positive and negative peak (negative halo, not always in North). These responses are often caused by ferrous debris either on the surface or in the topsoil but also by ferrous archaeological features. They produce a ‘spiky’ trace in the data (i.e. trace plots in Geoplot). ‘Trend’ is usually a weak or broad linear anomaly of unknown cause. ‘Magnetic disturbance’ is used to describe responses caused by ferrous

objects such as fences, pylons or barbed wire fencing or buried pipes. This type of anomaly is characterised by a strong response that often can mask other responses of interest. 'Magnetic noise' relates to responses of subsurface rubble/debris, burnt material, slag waste or geology. 'Strong magnetic anomalies' refers to responses produced by buried objects characterised by a strong magnetization (e.g. a thermo-remanent feature).

2.4.2.4. **Depth of Investigation & Resolution**

The strength of a magnetic anomaly depends both on the intensity of the magnetisation contrast and, very much, on the burial depth of the feature. The strength of the anomalous magnetic fields tends to weaken with depth and create broader anomalies. Shallow features (e.g. buried archaeological remains, modern ferrous objects) produce sharper anomalies. The sensitivity limit falls off at depths greater than *c.*1m (Clark 1990, 78). The spatial resolution depends on the traverse spacing and sampling interval used. The English Heritage guidelines (2008) suggest a maximum reading and traverse spacing of 0.25m x 1.0m respectively. Closer traverse and sampling spacing can enhance the resolution capabilities of these surveys but they will increase the time of survey.

2.4.2.5. **Factors Affecting Magnetometer Surveys**

Magnetometer instruments are directionally sensitive and have to be carried out with consistency. The instrument can pick up metal objects with high susceptibility carried by the operators conducting the surveys. The sensitivity of the magnetometers does not normally allow survey in urban areas as the magnetic noise is generally too high. Other sources of noise can be produced by topographic variations or sampling imperfections such as 'heading errors' (e.g. rotational errors can produce spurious signals if the data is collected in zig-zag instead of parallel traverses). The surveys can be affected by localised distortions due to high iron-bearing rock such as in igneous geological regions. Also some deposits (such as overburden) can introduce noise in the data that masks detection of anomalies related to the buried archaeology. Finally, deep deposits (e.g. windblown sands or alluvium) can mask anomalies produced by archaeological features.

Highly magnetic soils can affect magnetic surveys and results since the strong magnetic response can obscure any contrast produced by archaeological features. On the other hand, the concentration of Fe-oxides can be influential in detecting archaeological features, since they can enhance the MS of the backfill of archaeological features. Waterlogging (and related redox processes) may produce chemical changes that can suppress soil MS measurements (English Heritage 2008).

2.4.3. Electromagnetic Methods

Electromagnetic methods include ground-penetrating radar (GPR) and frequency domain electromagnetic (FDEM). Single-coil MS instruments (section 3.4.2.6) use the same principle as do the FDEM technique. All types of electromagnetic methods use different frequencies of electromagnetic energy and the observation of the effect of this energy at a receiving point.

2.4.3.1. **Electromagnetic Properties of Soils**

Electromagnetic (EM) waves are a form of electromagnetic energy composed of co-joined oscillating electrical (E) and magnetic (H) fields. According to Maxwell's equations, a changing electric field generates a magnetic field and vice versa, and the coupling between the two fields leads to the generation and propagation of electromagnetic waves through a medium (Baker *et al.* 2007, 8). The E and H components oscillate in phase perpendicular to each other to the direction of energy and wave propagation (Figure 2-11).

Electromagnetic radiation propagates displaying a characteristic amplitude or intensity (the height from the equilibrium point to the highest point of a peak of the wave), wavelength (peak to peak measurement equal to one cycle of a wave), and frequency (number of cycles that can happen in a certain amount of time) (Figure 2-11).

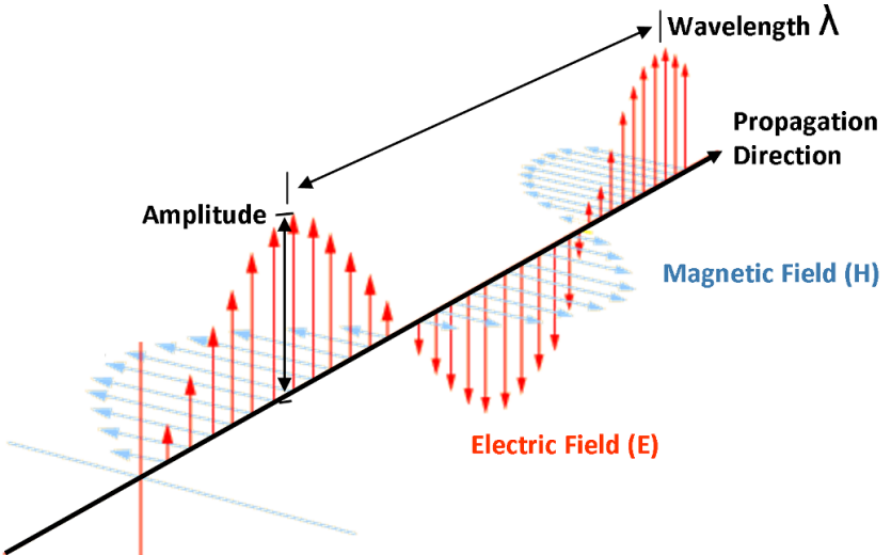

Figure 2-11: Electromagnetic wave propagation showing the transverse electric (E) and magnetic (H) fields. Wavelength is inversely proportional to frequency. Therefore, given a specific velocity of the EM waves, higher frequencies have shorter wavelengths, and lower frequencies have longer wavelengths.

The wave impedance is the ratio of the transverse E and H components (Zhang and Li 2007, 2040). For a plane wave travelling through empty space, the wave impedance is equal to the impedance of free space. EM waves propagating in air or space, unless they encounter a medium that absorbs or reflects them, will travel an infinite distance. If the EM wave is absorbed, attenuated or conducted away, the wave will lose either the E or H component (Conyers 2004, 23).

Electromagnetic waves penetrate the ground a few metres or more, depending on the frequency and if ground conditions are favourable. The electromagnetic wave propagation in soils is determined by two main parameters: the attenuation/loss of the EM signal with distance; and the velocity of the signal through the ground. These two parameters rely upon the dielectric properties (permittivity and conductivity) and magnetic permeability of sub-surface materials which affect the impedance of the medium.

The dielectric permittivity refers to the ability of a material to store and release electromagnetic energy through the separation of charges (e.g. ions, protons, electrons). It is divided between a real component or the storage of energy, and an imaginary component or loss mechanism that degrade energy storage. When is expressed in terms of its ratio to the permittivity of a vacuum, it is known as the relative dielectric permittivity (RDP) or dielectric constant. Permittivity of subsurface materials can vary drastically, especially in the presence of free

(pore space) and bound (capillary) water (section 2.2.2.2) and is the fundamental factor influencing the velocity of electromagnetic propagation in earth materials at the frequencies used by GPR. Contrasts in velocity, in turn, produce reflections of electromagnetic energy, therefore the detection of buried interfaces. The permittivity value of materials is often defined by the dielectric constant and is useful in determining the velocity of electromagnetic waves in a medium.

Conductivity is the degree to which a soil allows the passage of a current through it. Soil conductivity (section 2.2.2.2) causes a charge interaction and a consequent loss of signal and attenuation of the electromagnetic signal (Cassidy 2008b). Thus lower conductivity means less attenuation. The water content of soil (free and bound water in section 2.2.2.2) has a strong influence on propagation velocity and attenuation of electromagnetic signals (Cassidy 2009a, 67) since moisture content affects soil conductivity. The depth at which a plane electromagnetic wave will be attenuated to approximately 37% of its amplitude is called the skin depth (Cassidy 2009a, 60). This concept represents the maximum penetration of an electromagnetic method operating at a given frequency (f) in a medium of conductivity (σ). However, the actual exploration depth may well be much less than the skin depth owing to other loss factors.

Magnetic permeability measures the signal stored in the material, due to the lining up of atomic and sub-atomic particle spin directions. The magnetic effect of materials has only an effect on the propagation of electromagnetic waves in the presence of ferromagnetic materials. Ni and Fe-sulphides and Fe-oxides can affect the velocity and attenuation of the electromagnetic energy. Therefore, the concentration of magnetite, maghemite and hematite such as in Fe-rich soils (Figure 2-12) can lead to considerable loss effects and attenuation of the electromagnetic signal (Cassidy 2009a, 55).

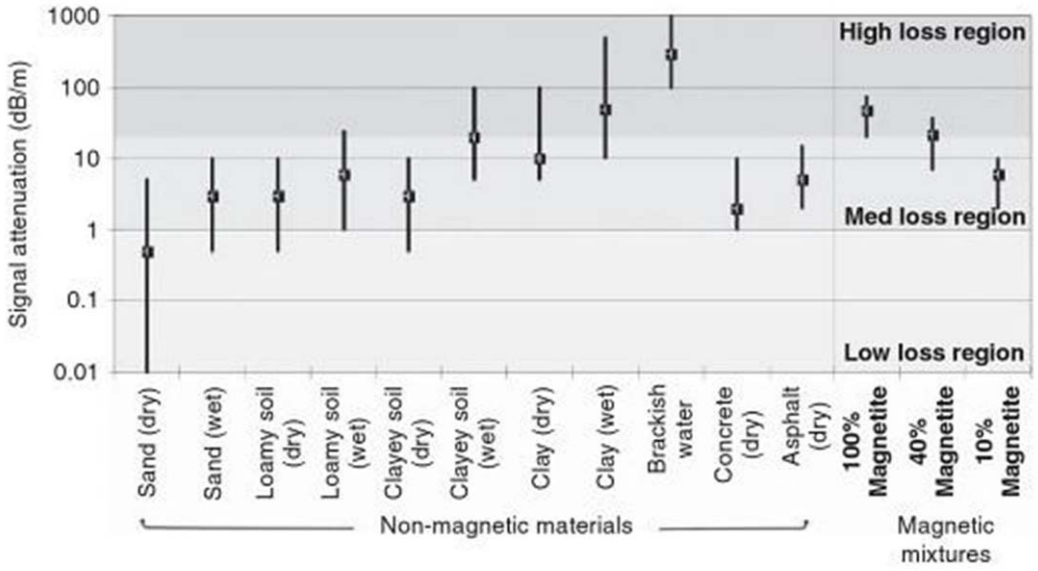

Figure 2-12: Typical material attenuation values of common subsurface materials across the frequency range of 200-1200 MHz/1.2 GHz). The vertical bars shows the full attenuation range and the square marks the average values (from Cassidy 2009a, 56).

2.4.3.2. **Ground-penetrating Radar (GPR)**

Radar (an acronym for "radio detection and ranging") uses transmission and reflection of high frequency electromagnetic waves to characterise the subsurface in 'real time'. A typical GPR system has three main components: transmitter and receiver antennae and a control unit ('timing' in Figure 2-13a).

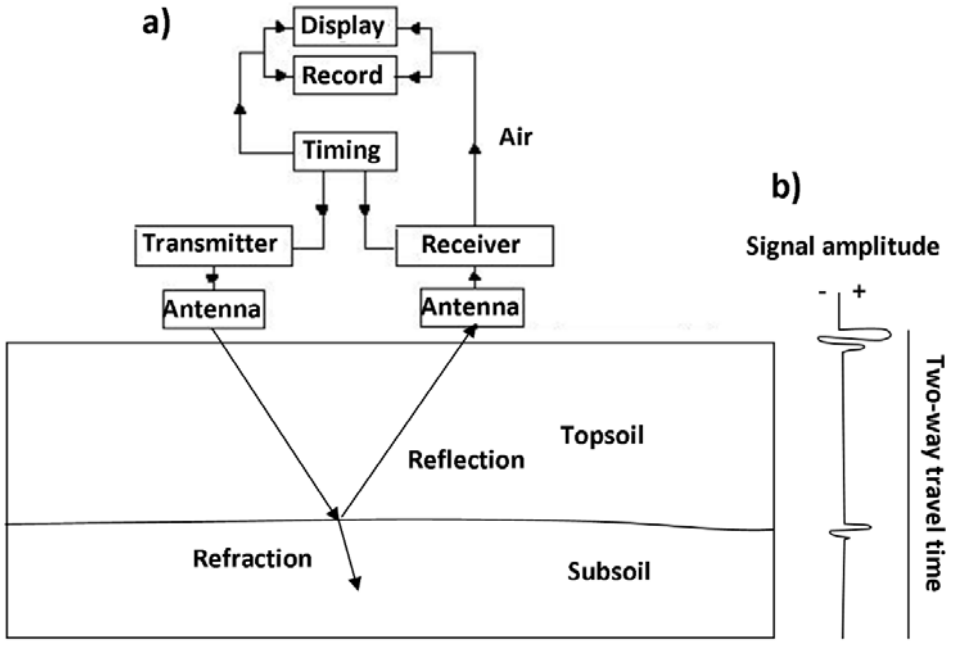

Figure 2-13: Diagram showing the main components of a GPR system (a) and schematic representation of the resulting reflection radar trace (b) (modified from Annan 2009, 18).

The transmitted energy propagates as waves into the ground where it is refracted, diffracted and reflected (Figure 2-13a), primarily when it encounters subsurface materials with different electromagnetic properties (dielectric permittivity, conductivity and magnetic permeability in section 2.4.3.1). Part of the transmitted energy is reflected back to the surface and captured by a receiving antenna. The reflected energy is displayed and recorded as a voltage signal, characterised by a positive-negative-positive wavelet (Figure 2-13b).

The time taken for this energy to be transmitted and returned back to the surface is measured (two-way travel time in Figure 2-13b) in nanoseconds (10^{-9}s) and can be used to estimate the depth of the reflectors by knowing the velocity of wave propagation in the medium. The depth estimation capacity of this technique is an obvious advantage for archaeological investigations. The reflectivity of radar energy produced by buried interfaces is proportional to the magnitude of change in the dielectric contrast, in other words, it is a function of the magnitude of velocity changes at a buried interface. The greater the change in velocity at an interface, the higher the amplitude of the reflection will be.

GPR data is conventionally acquired in reflection mode with a 'common offset' antenna configuration. The separation of the transmitting and receiving antennae is kept fixed at all sample locations. The antennae are positioned in a fixed geometry (i.e. separation and orientation) and measurements are recorded at regular intervals. Therefore, this mode allows mapping of subsurface reflectively versus spatial position to a high resolution. This mode involves dragging the antennae on the ground along parallel traverses and stacking thousands of returned wavelets and traces in a radar reflection profile (radargram) which is a two-dimensional cross-sectional view through the ground along the survey transect, showing the reflecting buried interfaces. Each GPR trace that forms a radargram is formed by a sequence of sample points that indicates the time variation of the amplitude of the recorded signal. The variations in reflection amplitude and time delay indicate changes in the radar wave velocity, attenuation of the signal and impedance. Therefore, the amplitude of the signals may give information about the character of the detected anomalies.

GPR reflection profiles also record signals that are not directly related to subsurface interfaces. The first arrival recorded in radargrams is the air-wave which travels from the transmitting antenna to the receiver. The second pulse to arrive is the ground-wave which travels through the ground between the antennae.

Closely spaced GPR traverses at regular intervals allow their transformation into time-slices. These are computer-generated two-dimensional images produced in a horizontal dimension, similar to archaeological spatial plan views which map the evolution of the detected reflections with depth. Sequential time-slices can be processed to create 3D cubes of the data and certain amplitudes rendered to produce realistic images of the subsurface, or they can be crosscut with reflection profiles to produce three-dimensional diagrams. 3D visualization techniques allow complex GPR cross-sectional data to be displayed in horizontal images which can facilitate the understanding of the 3D spatial relationship of the identified reflections. Therefore they improve the quality and efficiency of archaeological interpretation.

The high resolution of the surveys, the depth information and the 3D visualisation capacities for data presentation as well as the better understanding of its operational limits in certain excessively attenuating environments are key to the increasing use of this technique in archaeological investigations. The most up-to-date review of the current state of development of GPR applications and theory was published by Jol (2009), including a section dedicated to archaeological applications.

2.4.3.2.1. *Types of Anomalies*

Reflections are caused by a change in radar wave propagation velocity created by contrasting subsurface interfaces and, thus, electromagnetic wave impedance (Van Dam 2001, 98). For example, reflections can be generated by: electrical or magnetic properties of the rock, sediment or soil; variations in their water content; lithological changes in bulk density at stratigraphic interfaces; buried interfaces (e.g. walls, artefacts); and void spaces in the ground (e.g. tombs, tunnels). The different properties of these buried interfaces (e.g. archaeological features) will affect the velocity of propagation of the electromagnetic waves

and therefore the strength of the consequent reflected waves (Van Dam *et al.* 2002).

Iron oxides have been reported as the indirect cause of GPR reflections in sandy soils (Van Dam *et al.* 2002) because the larger moisture retention capacity of the iron oxides influences the volumetric water content and the relative permittivity leading to impedance contrast and signal reflection. In a study of the potential of geophysical methods in peat environments (Armstrong 2010, 154), the GPR reflections of a buried trackway were reported to be caused by the effect of chemical concentrations produced by the hydrological barrier that the trackway represented and not because of the specific characteristics of the preserved wood.

The types of anomalies detected by GPR are often not straightforward as the reflection patterns created by buried features can be fairly complex. The type of responses recorded in radargrams depends on many parameters (*e.*g the size, orientation, and chemical and physical properties of buried features, geological deposits, survey orientation) and as a result the interpretation of these responses can be difficult. The type of anomaly terminology used in this thesis is as follows:

- 'Linear' reflections are horizontal or sub-horizontal anomalies and are formed when the antenna repeatedly receives reflections from sections of that boundary within the antenna footprint. They are generated from any linear boundary between materials, such as a buried soil horizon, the water table, or horizontal archaeological features, such as house floors (Conyers 2004, 55-56). These reflections can be used to approximate the shape, depth, size, and orientation of subsurface layer-like boundaries and discontinuities. 'Dipping' linear reflections may indicate sloping buried interfaces.

- 'Hyperbolic' reflections are often generated by discrete point source reflectors. They are commonly generated from distinct, spatially-restricted, non-planar features ('point targets'), such as rocks, metal objects, walls, tunnels, voids, and pipes crossed at right angles (Conyers 2004, 54, 56). The form is due to the conic shape of the emitted GPR energy, as reflections and

diffractions are produced by approaching, at a right angle, a buried feature. Since the 'footprint' of the antennae is conical (section 2.3.3.2.2.), the hyperbola response is formed by the reflections produced by the antenna approaching the point source reflector, being on the top (apex) and going away from it. Only the apex of the hyperbola denotes the actual location of the feature (Cassidy 2009b, 165).

- Amplitude changes of the reflections may be due to variations in subsurface material properties. 'High amplitude' reflections are generated at boundaries between materials of highly contrasting physical and chemical properties. In contrast, 'low amplitude' reflections may come from materials of similar properties or uniform matrixes (Conyers 2004, 49 and 149). 'Areas of attenuation' may produce low amplitude reflections (Hammon III *et al.* 2000) and their increase or enhancement may provide useful information (e.g. saturation index, organic matter content) about the buried materials (Møller and Anthony 2003; Cassidy 2008b).
- 'Reverberations' (or multiples) are distinctive responses created by highly-reflective materials (such as metals) and their interaction with the GPR signal. The phenomenom is characterised by multiple stacked high-amplitude reflections imaged below the feature (Conyers 2004, 54). Metals are considered as complete reflectors and do not allow any signal to pass through. Other features beneath the reverberations caused by metal interfaces will not be detected.

There are other types of reflections that may not be produced by buried interfaces but from surface objects (e.g. trees, buildings, fences) creating background noise in the data or introducing spurious signals such as '*X marks the spot*' (Solla *et al*. 2012). These unwanted signals are more likely to be captured by unshielded antennae as a larger part of the signal can be radiated above ground and reflected back from surface features. Spurious signals generally produce high amplitude reflections and can be confused by anomalies (Conyers 2004, 77). They can sometimes be recognised from the much shallower dips of the diffraction hyperbolae, indicating a much higher wave velocity than the subsurface velocity (van der Kruk and Slob 2004). Other spurious signals can be present in the data if the survey terrain is uneven or rough, even if the survey is

carried out with shielded antennae. Such terrains may not allow a good ground coupling of the antennae, hence some energy can be lost and artifacts can be introduced in the data (English Heritage 2008).

2.4.3.2.2. *Depth of Investigation & Resolution*

Penetration depth and resolution of the GPR data depends on wavelength and frequency of the electromagnetic waves. Generally, the best results for archaeological investigations are achieved using 200MHz-500MHz antennae (English Heritage 2008). The long-wavelength radar energy generated by low-frequency antennae (e.g. *25*0 MHz) penetrates deeper into the soil but maps features with a lower spatial resolution, resolving only very large features. On the other hand, high-frequency antennae (e.g. 450 MHz) produce shorter wavelength energy which allows a greater resolution but to a shallower depth. The penetration capacities of these frequencies are also affected by the electromagnetic properties of the subsurface host media. Most important are the relative dielectric permittivity (RDP) and conductivity as these control the velocity of electromagnetic waves and their attenuation (section 2.4.3.1). The conductivity of buried materials introduces significant absorptive losses, which attenuate the radar energy and limit its penetration depth.

The vertical and horizontal resolution of subsurface features is primarily determined by the wavelength. Resolution is influenced by the frequency and the velocity of electromagnetic waves in the host material, as well as the geometry of the targets. Vertically, if two pulses are coincident in time, the amplitude will be enhanced, producing an event with larger amplitude (Annan 2001). In order for two nearby reflective interfaces to be distinguished well, they have to be separated by a distance of at least one quarter of the wavelength, therefore the vertical resolution can be estimated by:

$$\lambda = v/f$$

Where

λ= wavelength.
V= velocity of the media.
F= frequency used.

GPR systems radiate energy into the ground in a conical pattern called the Fresnel zone (Figure 2-14).

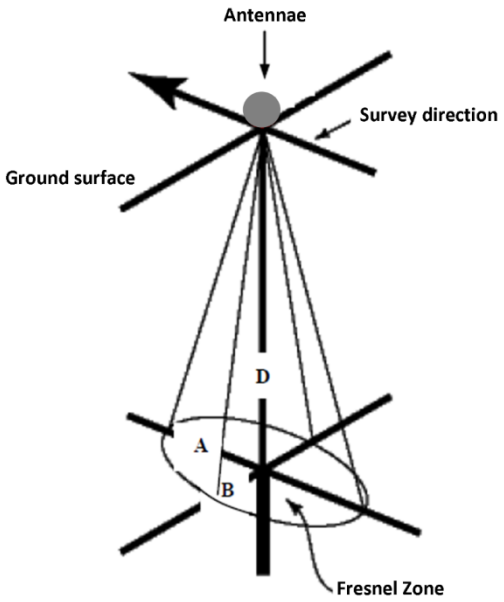

Figure 2-14: Approximate GPR-antenna footprint where A is the long dimension radius of the Fresnel zone, B is the short radius, and D the depth of the Fresnel zone. The 'footprint' increases with depth (D) reducing the effective horizontal resolution (English Heritage 2008).

The Fresnel zone can be described as the portion of the reflective surface where reflected waves will interfere constructively, i.e. waves with paths differing by less then half a wavelength (Sheriff 2001). Hence, this zone of influence determines the horizontal resolution of GPR surveys. In order to obtain a coherent reflection from a buried feature, its cross-sectional area should be approximately at least half of the area of the propagating wave's first Fresnel zone (area illuminated by the first quarter of the wavelength) at a given depth (Cassidy *et al.* 2011). The larger the wavelength, the larger the illuminated area from which the energy is reflected hence, the lower the resolution. Practice has shown that with 250-500MHz antennae, archaeological anomalies *c*.0.5m across are about the smallest that can be detected in routine survey, unless they provide a very strong contrast with the surrounding matrix or they are buried at very shallow depths.

The Fresnel zone is frequency dependent and increases with depth. This means that the horizontal resolution is reduced with depth hence limiting the capacity of the instrument to resolve certain targets and introducing reflections from other side features in the data (English Heritage 2008).

In order to ensure a good horizontal and vertical resolution for the correct mapping of buried features, the spacing of traverses (cross-line spacing) and

traces (in-line spacing) should be dense enough in order to avoid spatial aliasing in the data (an effect that causes different signals to be indistinguishable when sampled). According to the Nyquist condition, an aliased sampling occurs when the Nyquist sampling interval, which is one quarter of the wavelength transmitted in the host material (λ/4), is exceeded (Novo *et al.* 2008).

2.4.3.2.3. *Factors Affecting GPR Surveys*

Heavy rain may hamper GPR surveys and cause ground saturation. Since the systems are not fully waterproof, heavy rain may also cause failure to the GPR equipment and affect the penetration of EM energy.

There are some highly attenuating soil environments that may limit the penetration of electromagnetic energy. The EM energy must be able to propagate to, and be reflected from, the buried interfaces. Therefore, in environments where the signal rapidly attenuates (e.g. high conductivity) it may not be possible to get reflections back to the receiver antenna. There are some well-known attenuating conditions such as wet environments with saline intrusions or sandy soils with interstitial water. Saline water is a good conductor hence attenuates the GPR signal. Swelling clay (e.g. smectite) may present a problem as this type of clay can hold water in its matrix, making it a conductor, hence likely to attenuate the signal (Arcone *et al.* 2008). However, other waterlogged environments such as some type of peat areas have given good results (Clarke *et al.* 1999; Utsi 2004; Armstrong 2010).

Other causes of attenuation may arise by the selective absorption of the pulses by the ground, because of geometrical spreading and because of an alteration of the actual amplitude due to the instrument amplification (Leucci 2008). Rubble deposits and noisy topsoils may produce attenuation of the signal or to produce reflections that may complicate the interpretation of the data.

As with any other geophysical technique, a *conditio sine qua non* for detection of buried features is the existence of contrast between the targets and host material, even if a good penetration of radar energy into the ground exists. In this case, the contrast is determined by variations the subsurface RDP. The sharper the contrast, the stronger the reflection will be. Therefore, gradual changes in RDP will not be detected as no relevant reflection will be produced.

The surveys may be affected by other electromagnetic sources present in the surveys area that operates in the same bandwidth as GPR. For example, mobile phones, power lines or railroad communications can produce high-radio frequencies interferences.

2.4.3.3. **Frequency Domain Electromagnetics (FDEM)**

The technique maps variations in ground conductivity and MS, which may be related to archaeological features, by quantifying how soil materials respond to an applied electromagnetic field. A transmitter coil emits a sinusoidally alternating current at a specific frequency into the ground. In the presence of conducting body, the magnetic component of the electromagnetic field penetrating the ground induces alternating currents or eddy currents to flow in the conductor (McNeill 1997). The eddy currents generate a secondary electromagnetic field which is phase shifted from the primary field and travels to the receiver coil. The magnitude of the secondary field is measured in-phase in the receiver at 90˚ out of phase of the primary field at the receiver (Figure 2-15) (Jansen *et al.* 1992). Differences between transmitter and receiver fields reveal the presence of the conductor and provide information on its geometry.

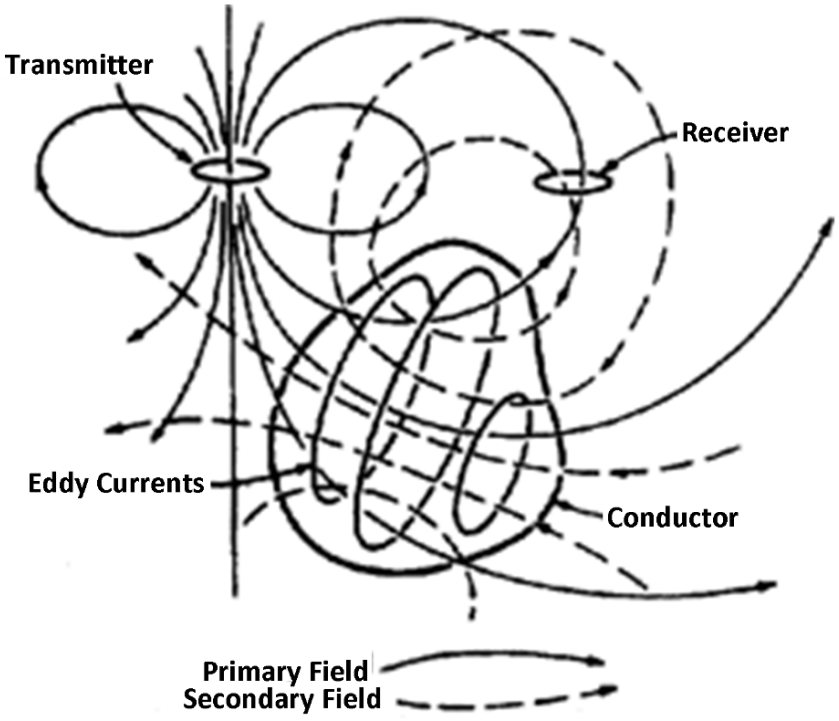

Figure 2-15: Relationship between primary and secondary electromagnetic fields: the primary field (solid lines) represents the electromagnetic field induced by the transmitter; the secondary field (dotted lines) represents the field created by the current within the ground (from Sheriff 1989).

The FDEM is based on the analysis of the two components of the secondary field: the out of phase component (quadrature) and the in-phase component. The quadrature component is related to conductivity at low frequencies for most natural soils (Jansen *et al.* 1992) whilst the in-phase component is essentially zero.The in-phase component is especially sensitive to the presence of metal and hence can be used to measure magnetic susceptibility (MS). The quadrature is measured in mS/m and the in-phase in parts per thousand (ppt). The advantage of this technique is that two types of response can be mapped with a single instrument (i.e. conductivity and MS), it can provide rapid area coverage (especially if the instrument is attached to a GPS) and thick vegetation or bushy conditions are often not a problem. The instruments used for this technique do not need to make ground contact as do the earth resistance probes or the MS single coils. FDEM survey has demonstrated its potential for archaeological prospection (Scollar 1962; Tabbagh 1986; Benech and Marmet 1999; Simpson 2009). However, the technique is not routinely used in the UK partially because the types of response can be complex to understand and interpret, by comparison with earth resistance and MS routine surveys.

2.4.3.3.1. *Types of Anomalies*

The anomalies detected by FDEM are generally described as 'conductive' or 'enhanced MS' anomalies. In this research, the terms included 'conductive trends' for the quadrature data and 'MS trends' for the in-phase data.

2.4.3.3.2. *Depth of Investigation & Resolution*

The penetration depth of this technique depend upon the coil arrangement, frequency used and ground conductivity. For example, the 1m coil separation of a Geonics EM38 with an operating frequency of 14.6 kHz provides a penetration to a maximum depth of about 1.5m (McNeill 1986). The coplanar coil separation of the instrument has a generally greater sensitivity to depth by taking measurements with the coils held vertical to the ground than by using the horizontal mode. However, the horizontal mode is very sensitive to anomalies near the surface, but it quickly decreases in sensitivity at depths of *c.* 0.4m/0.5m. The detection capacities near surface when using the vertical mode are generally low until *c.* 0.4m depth where the instrument shows its higher

sensitivity (Figure 2-16). This can be advantageous where there is a disturbed plough zone that adds noise to conventional surveys.

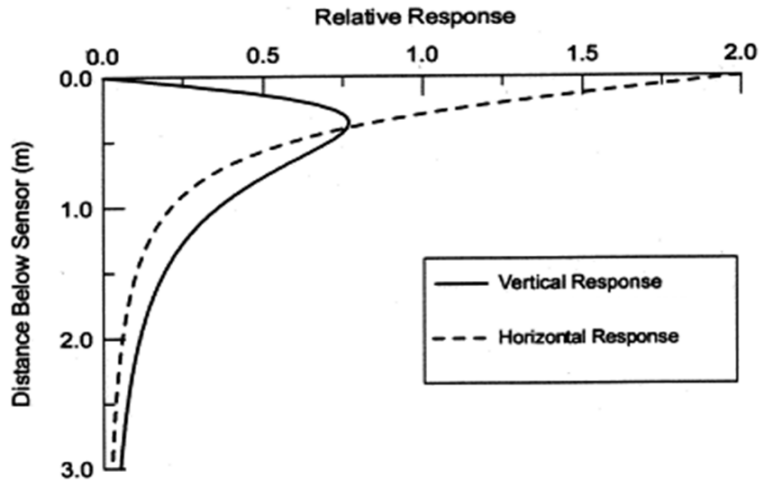

Figure 2-16: Relative response (quadrature and in-phase) of the Geonics EM38 as a function of depth (from McNeill 1980).

The responses measured with the in-phase component can be more complex as the vertical coil mode can produce a negative response to positive anomalies at depths under 0.6m (Figure 2-17). This effect can make the interpretation of the data difficult or prevent the detection of positive features at these depths.

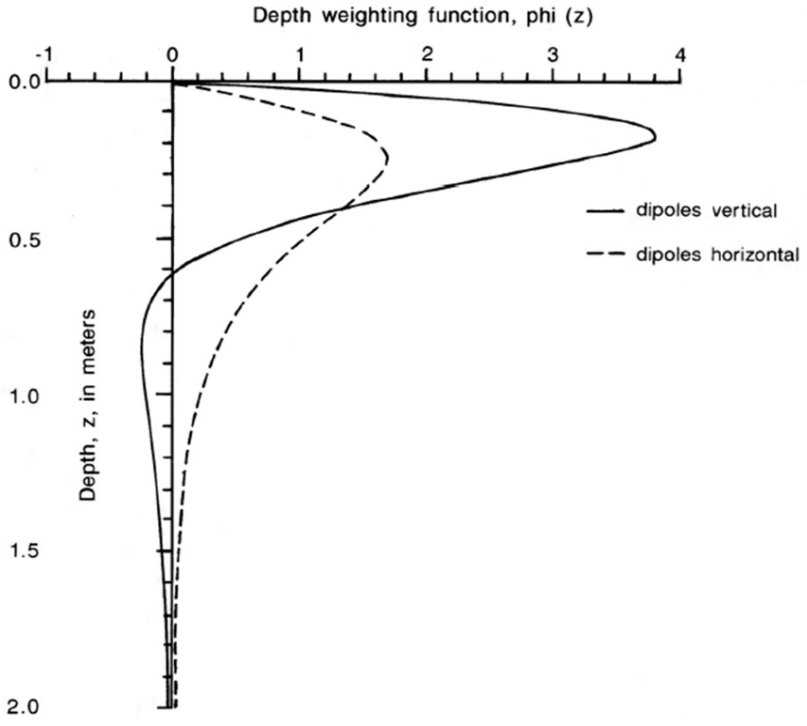

Figure 2-17: Depth response of the vertical and horizontal dipole (in-phase component) of the Geonics EM38. With the instrument on its side (dipoles horizontal), the response is always positive. With the instrument in the upright position (dipoles vertical and coplanar), the response of the instrument changes sign depending on the depth of the feature (from J.D. McNeill, Geonics Limited).

Other instruments with larger coil separation allow deeper investigations with, however, expected loss of resolution. For example the Geonics EM31 with the coils spaced at 4m and operating frequency of 9.8 kHz allows investigation to a depth of *c*.6m and has been successfully employed to locate sedimentary environments associated to past human occupation (Conyers *et al.* 2008). The most common instrument used in archaeological surveys is the Geonics EM38. Horizontal resolution for the EM38 is also related to the coil separation. According to Dalan (2006, 177), the minimum width of a feature that can be resolved is one-fourth to one-third of this coil spacing. For the EM38, with a coil spacing of 1m, horizontal resolution is approximately 0.25–0.30m.

2.4.3.3.3. *Factors Affecting FDEM Surveys*

Variations in soil moisture, organic matter content and clay content can all affect electrical conductivity measurements (Conyers *et al.* 2008). Also, properties that affect the pore spacing of the soil volume (e.g. compaction), salinity and temperature (e.g. fluid viscosity) can influence soil conductivity (Simpson *et al.* 2008).

Whilst comparative studies between the Geonics EM38 may demonstrate a good correlation with earth resistance and magnetometer surveys, there are certain responses from the EM38 instrument that may be complex and difficult to correlate with the results of other techniques. This is the case with the potential in-phase negative response of the EM38 in vertical dipole mode, to positive magnetic anomalies (Figure 2-17). The instrument tends to drift with time, especially on measuring the in-phase component. The drift may give a false image of the background values and if one is looking for small changes in susceptibility, drift can easily obscure anomalies of interest (Simpson 2009, 129). The instrument is sensitive to conductive and magnetic objects in the near-surface (e.g. metal fences, rubbish) and these may affect the surveys and complicate the interpretation of the data. Due to their high conductivity, metals may be expressed as negative values and complicate the interpretation of the data. As with any other electromagnetic instrument, the EM38 is sensitive to power lines and to atmospheric electricity (spherics) wich may cause interferences and may limit the use of the instrument.

2.5. Soil Properties & Geochemical Survey

This section describes the basics of geochemical analysis in archaeological prospection and reviews the current knowledge on soil properties and processes involved in the retention of common anthropogenic geochemical elements.

2.5.1. Soil Geochemistry

The retention and preservation of chemical elements in archaeological soils are determined and influenced by a wide range of soil processes and properties. The weathering of inorganic and organic soil materials and their translocation and accumulation in the soil profile are fundamental in understanding the nature of geochemical anomalies. The rate at which these processes lead to the fixation of chemical elements in archaeological soils is also influenced by climate, topography, vegetation, soil fauna, the nature of the parent material and time (Haslam and Tibbett 2004).The sequestration of inorganic signals involves many soil processes such as adsorption, occlusion, CEC, precipitation of elements. As an example, Figure 2-18 illustrates the inter-related dynamics involved in the retention of phosphorus (P) in contemporary soils.

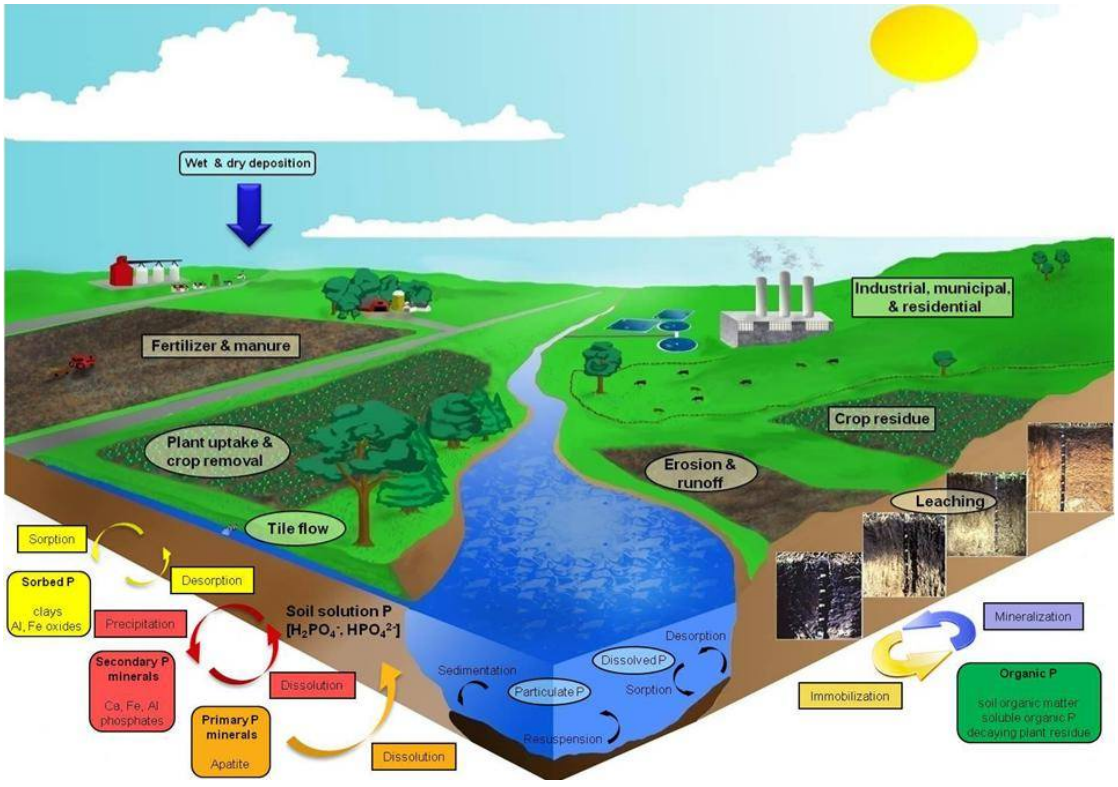

Figure 2-18: The illustration shows the phosphorus cycle. It describes the addition pathways, translocation and transformation of P in soil and water (© M. Dietz and J. Strock from Southwest Research and Outreach Center, University of Minnesota).

These processes interact with other factors such as source (e.g. manure or crop deposits in Figure 2-18) and soil composition, soil pH, soil redox conditions and soil texture (Oonk *et al*. 2009a).

2.5.2. Geochemical Survey

There is a strong link between past human habitation and its footprint left in soils. Human activity can significantly affect chemical soil composition leading to enrichments of certain chemical elements. These inputs may remain within the soil system over a long time developing a 'soil memory' that can reveal evidence about past human activities. Soils can act as a sink of anthropogenic organic matter and retain some inorganic components (Figure 2-19) as a fixed anthropogenic input over the soil chemical signal (Heron 2001, 565).

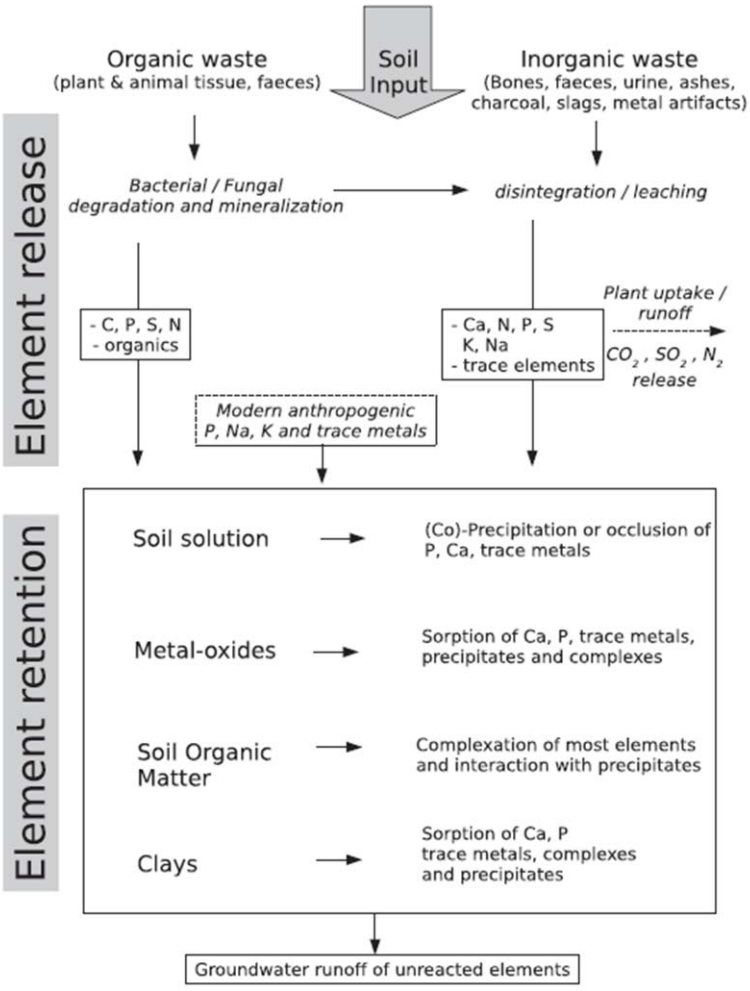

Figure 2-19: Overview of anthropogenic inputs and geochemical processes in archaeological soils (from Oonk *et al.* 2009a).

Furthermore, specific human activities can leave a geochemical input in the soil. Therefore, the spatial distribution of these differences in geochemical concentrations can determine the source and spatial extent of past human activities.

The purpose of geochemical survey in archaeology is to identify geochemical anomalies (concentrations) that differ from the surrounding natural chemical patterns by analysing soil samples. Approaches in geochemical prospection for archaeological investigations generally involve: the measurement of a single chemical attribute (e.g. phosphate content); or multi-elemental analysis of a range of elements (e.g. ICP-OES or pXRF analysis). Reviews of these geochemical analysis in archaeological prospection have been done by Aston *et al.* (1998a), Middleton (2004) and Oonk (2009). Other approaches include magnetic susceptibility analysis, a physical soil property (section 2.3.2.1.) that is closely related to soil chemical properties and the presence of various oxides (e.g. of Fe, Mn) that may be of interest in archaeological investigations (e.g. burning, metal working sites). Milek and Roberst (2012) have reported about the beneficts of integrating multi-element analysis with other geochemical analyses (pH, conductivity, LOI and soil micromorphology) and datasets (tephra deposits, artefact/bone distribution) to study the of floors sediments of a Viking Age house and identify possible activity areas.

2.5.2.1. **Geochemical Anomalies**

Soil environments are complex and one of the principal problems in interpreting the data of geochemical surveys is distinguishing geochemical anomalies from other dispersion patterns of no archaeological significance (Figure 2-18). According to Hawkes (1957, 233), the key parameters to take into account to identify and interpret geochemical anomalies are:

- The range of non-significant variations in background.
- The threshold between non-significant and anomalous values (cut-off value below which the variations represent only normal background effects and above which they have an anthropic significance, using off-site/on-site soils).
- The contrast (or ratio) between anomalous and background values.

- The homogeneity of the anomalous pattern (anomalies within which values vary erratically through a wide range within short distances may be considered relatively inhomogeneous and non-significant).

Statistical methods have been successfully applied to interpret geochemical data sets and define anomalies. Statistical approaches normally use a range of techniques to explore the nature of geochemical data before selecting anomalous values (e.g. Reimann *et al.* 2005). Since geochemical data sets seldom fit a normal distribution pattern or distribution (i.e. the data are typically spatially dependent), statistical methods need to be used cautiously (McQueen 2008). Typical multivariate statistical methods used in multi-element analysis include:

- Scatter plots: bivariate plots that compare pairs of variables.
- Correlation matrices: linear regression to test the correlation between pairs of elements.
- Cluster analysis: hierarchical grouping of elements in a data set with differing degrees of correlation of their abundance.
- Principal component/Factor analysis (ANOVA, analysis of variance): useful for grouping elements into associations.
- Discriminant analysis: method of optimising the distinction between two or more populations of samples.

Geochemical data sets are inherently multivariate because the processes that have generated the anomaly commonly have an association of elements. Therefore, multi-element approaches to anomaly detection may give a more complete view of the causes behind the formation of geochemical anomalies. Methods for determining element sources input include isotopic analysis, combined geochemical and mineralogical analysis to target particular host minerals, and multi-element analysis to detect associations of elements. Some examples of archaeological sites and features, and associated element enrichments in their soils are listed in Table 2-4.

Archaeological Site/Feature	Element	Reference
Burials/graves	P, Cu, Mn, Ca	Cook and Heizer,1965; Parsons,1962; Keeley,1981; Bethell and Smith,1989.
Hearths, middens	P, K, Mg, K	Barba *et al.,* 1996; Knudson *et al.,* 2004; Chaya*,* 1996; Fernandez *et al.,* 2002; Wells *et al.,* 2000 *and* Parnell *et al.,* 2001.
(Farm)houses	P, Ca, Mg, Fe, K, Th, Rb, Cs, Pb, Zn, Sr, Ba	Zimmerman *et al.,* 1992; Chaya, 1996; Manzanilla, 1996; Fernandez *et al.,* 2000; Entwistle *et al.,* 2000; Wells *et al.,* 2000; Parnell *et al.,* 2001 *and* Wilson *et al.,* 2005, 2006.
Painted buildings	Heavy metals	Wells *et al.,* 2000
Mining, metal smelting and production sites	Cu,Pb,Mn	Jenkins, 1989; Maskalland Thornton*,* 1998; Hong *et al.,* 1994; Pyatt *et al.,* 2002 *and* Monna *et al.,* 2004.
General archaeological sites	B, Cu, Mg, Mn, Ni, P, Se, Zn, K, Ba, Ca, Na	Cook and Heizer, 1965; Ottaway and Matthews, 1988; Bethel and Smith, 1989.

Table 2-4: List of archaeological features and associated elements (from Oonk *et al.* 2009a).

P is unique among the elements in being a sensitive and persistent indicator of human activity and an important plant nutrient. Anthropogenic additions of P to the soil come from human refuse and waste, burials, the products of animal husbandry in barns, pens, on livestock paths, or intentional enrichment from soil fertiliser. Phosphorus exists in soils in both organic and inorganic forms, usually of phosphate, PO_4^{3-}. Organic forms of P are found in humus and other organic material. Phosphorus in organic materials is released by a mineralization process involving soil organisms. Inorganic phosphorus is negatively charged in most soils. Because of its particular chemistry, phosphorus (as PO_4^{3-}) reacts readily with positively charged Fe, Al and Ca ions to form relatively insoluble substances. When this occurs, the phosphorus is considered fixed. It forms relatively stable chemical compounds of inorganic phosphate minerals and organic phosphate esters, depending on local chemical conditions (particularly pH and microbial activity). Some forms of soil P are highly resistant to normal oxidation, reduction, or leaching processes. Therefore, when humans add phosphate to soil, it often accumulates at the site of the deposition with prolonged occupation, becoming quite high in comparison to the content of natural phosphate in the soil (Holliday and Gartner 2007). K is also an anthropogenic alkaline element of interest for archaeological prospection (Oonk 2009). K occurs almost entirely within the structure of silicates and the lowest concentration values of K are associated with organic soils in Scotland (Paterson 2011). Ca is

another alkali element and a potential anthropogenic indicator. It is abundant in manure and can be released from bones and teeth (Adderley *et al.* 2004; Oonk *et al.* 2009a). The sorption of anthropogenic alkali elements is largely dependent upon the organic matter and clay content, and their release in archaeological soils is associated with the ion exchange capacity of soils. Naturally occurring alkaline elements are retained in soil minerals, such as feldspars and micas (Oonk *et al.* 2009a).

The behaviour of trace elements (generally those with an average concentration <100ppm) is complex and their retention and sequestration in soils generally depends on their oxidation state, soil pH, cation exchange capacity and the presence of clay minerals, Fe-oxides, carbonates, phosphates, sulphides and organic matter (Kumpiene *et al.* 2008; Oonk *et al*. 2009a). Mn has been reported as an anthropogenic trace element in association with burials and graves and other general archaeological sites. Furthermore, depletions of Mn have been found to be indicative of human occupation as a result of reductive dissolution of Mn oxides, due to the decomposition of organic matter (Oonk 2009). Mn is one of the most abundant trace metals in the Earth's crust and its behaviour in soils is dominated by its susceptibility to redox alteration. Cu is a promising anthropogenic indicator because it is relatively stable in soils and easily fractionates with organic matter (Paterson 2011). The stability of Cu is, however, significantly higher in acidic soils than in alkaline soils (Kumpiene *et al.* 2008). Pb enrichments have been reported as an indicator of craft production areas (Parnell *et al.* 2002), hearths and fuel sources such as peat, turf and wood (Wilson *et al.* 2008). However, other sources of anthropogenic Pb enrichment may be fairly modern and the product of contamination from atmospheric and fuel combustion (Pavageau *et al.* 2004).

According Kabata-Pendias and Mukherjee (2007, 20), the interactions between trace elements are generally multi-variate and of an either antagonistic or synergistic character. These interactions can be closely associated to soil chemical processes and are shown in Table 2-5. The concentrations of metals at any point within soil will depend upon the rate and the amount of anthropogenic activity, both archaeological and modern. Therefore, it is important that soil samples for analysis and comparison are collected from the same soil horizon (Haslam and Tibbett 2004).

Element	Associated Trace Element
Ca	B, Ba, Cd, Co, Cr, Cs, Li, Mn, Ni, Pb, Sr and Zn
P	As, Cr, Hg, Mo, Mg, Ni, Pb, Rb, Se and Zn
Mg	Cr, Mn, Zn, Ni, Co and Cu
Fe	Co, Ni, Mn, Mo, Cr and Zn
Mn	As, Cr, Co, Mo, Ni, V and Zn
Cu	Mo
Cd	Zn

Table 2-5: Major and trace elements affecting the distribution of associated trace elements in soils (based on Kabata-Pendias and Mukherjee, 2007).

2.5.2.2. **Factors Affecting Geochemical Surveys**

The presence and concentration of anthropic elements in archaeological sites depends on a variety of factors such as climate, parent material and abundance and type of source input (Oonk *et al*. 2009a). Eluviation and illuviation (e.g. podsolization in humid areas) of elements in soil profiles, as well as land management activities (e.g. ploughing) can result in intermixing of recent and archaeological inputs with the consequence of obscuring element concentrations of interest (Oonk *et al.* 2009a). Strong chemical leaching and marked depletion of most elements can also make some geochemical anomalies very subtle, and a multi-element approach may improve detection capabilities in such conditions (McQueen 2008). Geochemical anomalies in which a suite of elements lie near background levels may be also difficult to detect and many have probably not yet been found (McQueen 2008). The use of an appropiate sampling strategy (resolution), sampling depth (soil horizon) and an understanding of authochthonous soil elements (backgrounds) are vital to identify anthropogenic depostions at archaeological sites (Haslam and Tibbet 2004). However, there are still important methodological issues to be resolved such as the standardisation of protocols, soil horizons to be sampled and how to distinguish anthropogenic elements in soils from geological signals (Oonk *et al.* 2009a)

2.6. Research Questions

Given the need for further understanding of soil setting and the dynamics involved in the detection of geophysical and geochemical anomalies, this thesis tackles the following questions:

- Which soil factors have an impact on the detection of archaeological anomalies by geophysical means at the five case study sites?
- Can a geophysical anomaly be explained chemically?
- Can geophysical survey contribute to the understanding of geochemical anomalies of archaeological interest?
- What are the potential advantages of integrating geophysical and geochemical techniques?

Chapter 3

Research Strategy & Methods

3.1. Introduction

This chapter describes the research strategy as well as the methods used to collect, process and analyse all the data used in this thesis. It starts with an overview of the general method and planning involved in the research, and the criteria followed to choose the case study sites. The chapter follows with a comprehensive technical summary of the geophysical and geochemical techniques used during the field and lab stages of the project. It finishes by explaining the strategy followed to analyse and integrate all the results from such a wide range of techniques.

3.2. Overall Method

The general method used in this research combined qualitative approaches (i.e. interpretation of the geophysical data or comparison of the geochemical and geophysical results) and quantitative methods (e.g. data acquisition by geophysical surveys and geochemical analysis). The combination of approaches relates to the inductive and deductive character of this research since this project aims to explore the soil factors involved in the detection of chemical and geophysical anomalies at challenging survey environments in order to answer the research questions.

Figure 3-1 shows the different stages (phases) of the integrated research strategy and the range of methods (in red) used in this PhD project. Other resources or 'satellite' data gathered or created (in blue) and the analytical stages of the research (in brown) are also indicated. The final outcomes expected from the results obtained at the end of each analytical stage are shown in green.

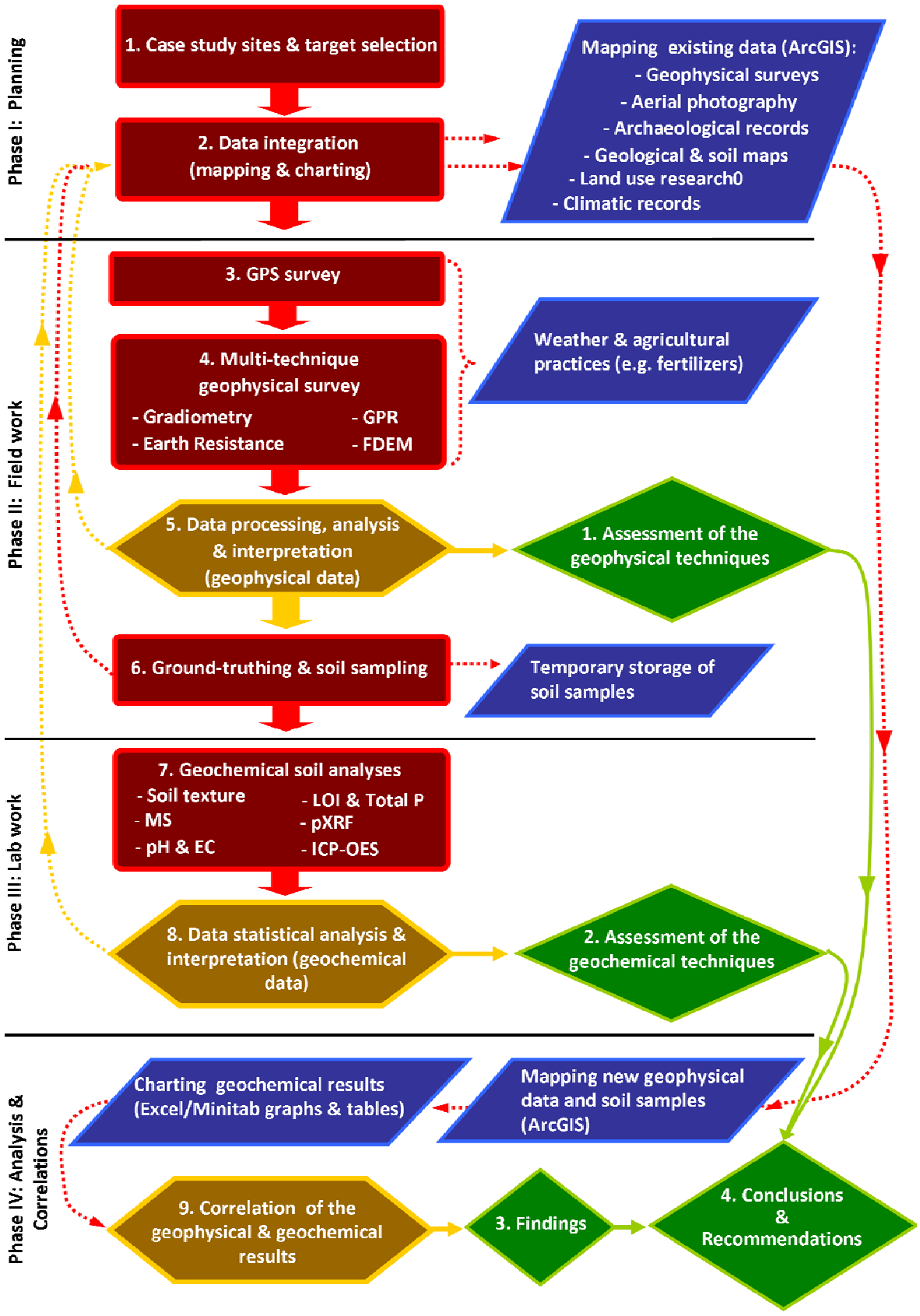

Figure 3-1: Diagram showing the integrated research strategy in four phases. The arrows show the flow of the research. Geophysical, geochemical and other methods are all in red, analytical stages are in brown, 'satellite' data collection is in blue, and the expected outcomes are in green. The acronyms in Phase II stand for global positioning system (GPS), ground-penetrating radar (GPR) and frequency domain electromagnetic (FDEM). The acronyms in Phase III stand for magnetic susceptibility (MS), loss on ignition (LOI), conductivity (EC), total phosphate (Total P), inductively coupled plasma optical emission spectrometry (ICP-OES) and portable x-ray fluorescence (pXRF).

3.3. Phase I: Planning

3.3.1. The Selection of the Study Sites

Taking into account the great diversity of combinations of geology, land use and type of archaeological features that characterise archaeological survey environments, five case study sites (Figure 3-2) lying over contrasting superficial deposits and bedrock were selected, each one presenting a specific challenge to be assessed by the integrated methodology developed in this thesis (Figure 3-1).

The criteria used in their selection were as follows:

- In order to focus the survey strategy more efficiently, and to validate and analyse the results of the multiple survey techniques used in this project, sites with known archaeological features and ancillary information (such as aerial photography archive, previous excavations and existing geophysical or geochemical surveys) were prioritised over those with no previous investigations.
- Archaeological sites that were the subjects of on-going archaeological research were also of primary importance. On-going excavation has the obvious advantage of ground-truthing the geophysical and geochemical results and provides the ideal scenario to experiment with alternative soil sampling and survey strategies.

Other considerations taken into account were the proximity of the sites in order to make more feasible repetition of the surveys or soil sampling. Relatively easy access to site was also an important consideration in site selection owing to the number of geophysical instruments as well as equipment soil sampling to be deployed. The sites, targets and challenges in relation to the survey environment are summarized in Table 3.1.

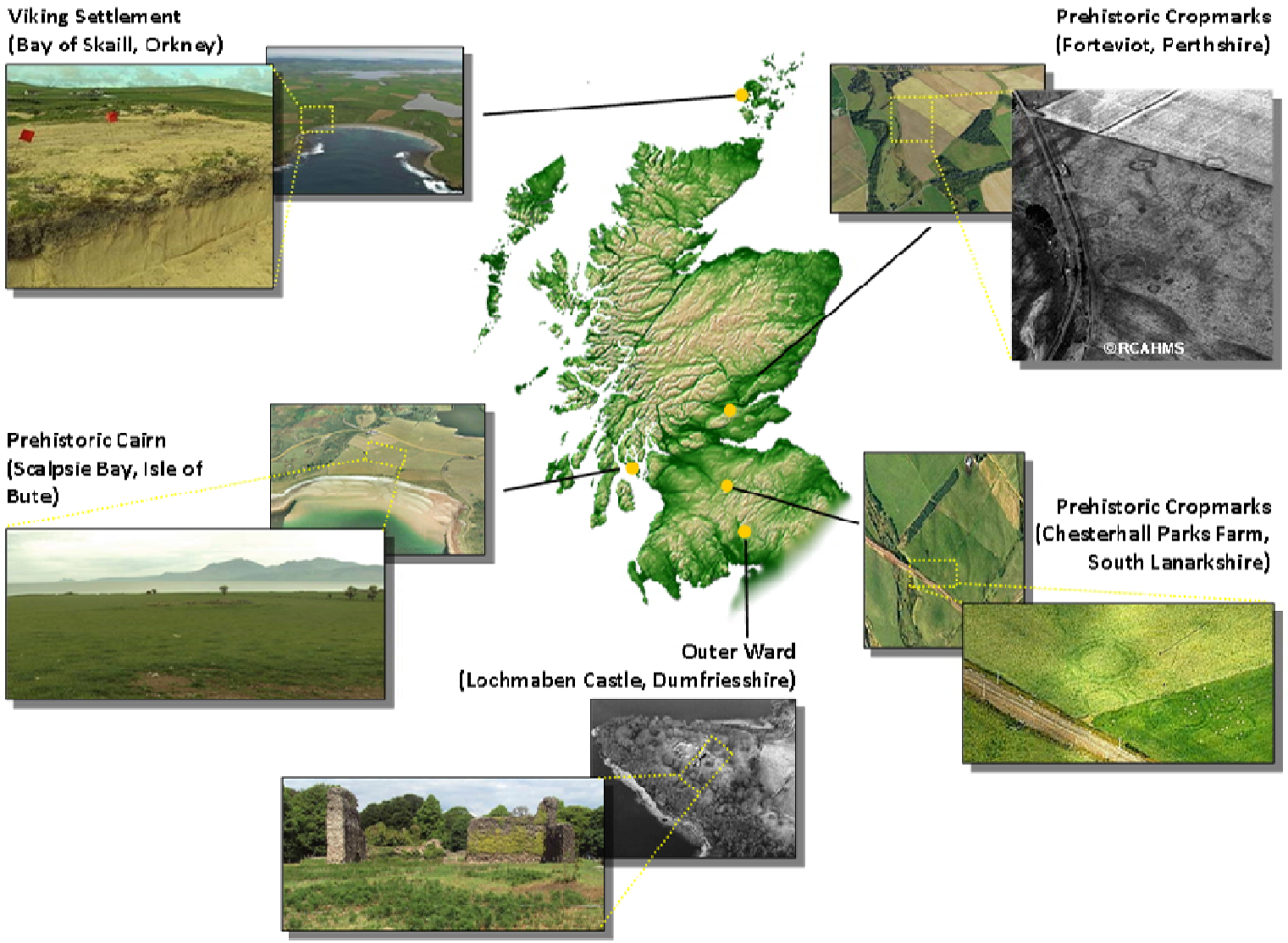

Figure 3-2: The location of the five case study sites location and general views of the survey areas (© C. Cuenca-García).

Site	Type	Previous geophysics	Challenge	Targeted Feature	Bedrock	Superficial Deposits/Soil Parent Material	Soil	Geomorphology	Land use/Ploughing Regime
Scalpsie Bay (Isle of Bute)	Burial Cairn (truncated earthwork).	No	Disturbed monument concealed in podzolic deposits (iron-pan?). Negative magnetic anomaly or a spurious anomaly?	Intriguing magnetic anomaly relating to the burial cairn.	Sedimentary (Upper ORS, conglomerates and subordinate sandstones, Stratheden Group, late Devonian) & Meta-igneous (Highland Border Ophiolite Complex, serpentinite, Cambrian).	Quaternary sands and gravels from raised marine deposits & glacial till (Corby association).	Podzol (mapped as brown earth)	Raised beach & glacial outwash	Pasture/Annual-bi-annual (silage cultivation) except around monument area.
Bay of Skaill (Orkney)	Viking Settlement (mound).	Yes	Archaeological features concealed under deep deposits of wind blown sands.	Kerbed-wall (positive archaeological feature).	Sedimentary (Middle ORS, siltstones-shales and subordinate sandstones, Caithness flagstone group, mid-Devonian).	Quaternary fine-grained windblown sands (Fraserburgh association).	Wind-blown sand	Mound (natural or anthropogenic?).	Pasture/None.
Lochmaben Castle (Dumfriesshire)	Outer Ward (cropmarks, grass).	No	Failure of the gradiometer survey in confirming circular high resistance anomalies.	High resistance anomalies showing structures (positive archaeological feature).	Sedimentary (Corncockle Sandstone Formation, Permian).	Quaternary glaciofluvial sands and gravels and alluvium (high clay content) (Crichton association).	Mixed-brown earth	Made-ground over outwash/alluvial terrace.	Recreational/Maintenance for weeds control (tilling/ploughing).
Forteviot (Perthshire)	Prehistoric ritual complex (cropmarks, barley).	Yes	Poor results from gradiometer and earth resistance surveys.	Ditched enclosure (negative archaeological feature).	Sedimentary (Lower ORS, Sandstone and subordinate conglomerates, siltstones, calcareous mudstones and pebbles of metasedimentary and volcanic rock , Arbuthnott-Garvock Group, early Devonian).	Quaternary glacio-fluvial sand and gravels deposits (Gleneagles association).	Brown earth	Outwash and river terrace.	Arable/Very intense (sometimes deep ploughing for potato crops).
Chesterhall Parks Farm (South Lanarkshire)	Prehistoric enclosure complex (cropmarks, grass)	Yes	Poor results from gradiometer and earth resistance surveys.	Ditched enclosure (negative archaeological feature).	Sedimentary (Lower ORS, volcaniclastic sandstones, Auchtitench Sandstone Formation, Larnak Group, early Devonian).	Quaternary glacio-fluvial gravels, sands and silts deposits of the Symington association.	Clay (mapped as brown earth)	Solifluction terrace.	Pasture/Seldom.

Table 3-1: General settings and challenges of the five case study sites selected for this thesis.

3.3.2. Data Integration

Before any fieldwork was carried out, all the existing datasets related to each case study site were georeferenced in order to gather, in the same GIS map, all the available information about the survey area. The software used was ESRI ArcGIS (ArcMap). As the project developed, new datasets were incorporated into the preliminary maps of each case study site. Table 3-2 shows the databases used to extract existing data relating the sites presented in this investigation.

Database Type	Name	URL	Scotland	UK
Cultural Resource Managements (CRM)	Canmore (The Royal Commission on the Ancient and Historical Monuments of Scotland-RCAHMS)	http://canmore.rcahms.gov.uk/en/search	?	no
	Scotland Places	http://www.scotlandsplaces.gov.uk	?	no
	Discovery and Excavation in Scotland (CRM)/Archaeology Data Service (ADS)	http://archaeologydataservice.ac.uk/archives/view/des/index.cfm	?	no
	National Collection of Aerial Photography	http://aerial.rcahms.gov.uk	?	?
Geophysical Surveys	Canmore Mapping (CRM) (RCAHMS)	http://canmoremapping.rcahms.gov.uk	?	?
	Discovery and Excavation in Scotland (CRM)/Archaeology Data Service (ADS)	as above	?	no
	English Heritage (Geology)	http://sdb2.eng-h.gov.uk	?	?
	GeoIndex (British Geological Survey-BGS)	http://mapapps2.bgs.ac.uk/geoindex/home.html	?	?
Geochemical Surveys	Geochemical Atlas for Scottish Topsoils (The Macaulay Land Use Research Institute-MLURI) (Soil	http://www.macaulay.ac.uk/soilquality/GeochemicalAtlas_web_aug11.pdf	?	no
	Geoindex (BGS) (Geology)	as above	?	?
Geology	GeoIndex (BGS)	as above	?	?
	Geology Digimap	http://digimap.edina.ac.uk/digimap/home	?	?
Soils	Soil Indicators For Scottish Soils (MLURY)	http://sifss.macaulay.ac.uk/	?	no
	Soil Survey of Scotland (MLURI) (Maps)	n/a	?	?
	Explore Scotland (MLURI)	http://www.macaulay.ac.uk/explorescotland/soils1.html	?	no
Land Use	Explore Scotland (MLURI)	http://www.macaulay.ac.uk/explorescotland/lcs_mapformat.html	?	no
Weather	Met Office (Historic Station Data)	http://www.metoffice.gov.uk/climate/uk/stationdata	?	?

Table 3-2: Databases used to acquire background information about the five case study sites. The table is not an exhaustive list of all the resources available in Scotland and the UK.

3.4. Phase II: Fieldwork

The fieldwork was carried out from April 2010 until September 2010 at the five case study sites. It involved topographic and geophysical survey, as well as soil sampling. During the fieldwork notes were taken about the weather conditions before and during the surveys, as well as agricultural activities and other field survey conditions observed at the sites.

3.4.1. Topographic Survey

The sites were topographically surveyed before any geophysical survey or soil sampling was undertaken.

3.4.1.1. **Differential GPS**

3.4.1.1.1. *Purpose*

A differential global positioning system (DGPS) was used to carry out the topographic surveys at the sites in order to accurately and rapidly map:

- The survey area and the location of known archaeological targets.
- The corners of the geophysical survey grids and the locations of soil sampling lines and soil controls.

The DGPS system helped in positioning the geophysical survey areas over targeted archaeological features (e.g. cropmarks at Forteviot) and locating specific sampling/ground-truthing areas of interest by extracting the OS coordinates from the data integrated in the preliminary maps. It also provided for the rapid and accurate relocation of the survey grids when the geophysical surveys were repeated over a specific area. The DGPS was also used to locate the single GPR traverses, to gather elevation data used both to correct GPR traverses and to be attached to the EM38 instrument to provide a more accurate spatial location.

3.4.1.1.2. *Instrument*

The DGPS system was borrowed from the Natural Environmental Research Council-Geophysical Equipment Facility (NERC-GEF). The instrument was a Leica GPS System 1200, a high performance military specification Global Navigation Satellite System (GNSS) receiver of sub-centimeter accuracy after data

processing. Detailed specifications can be found in Leica Geosystems (2009). The instrument has two antennae that can be used either as a base or rover in any mode from static to real-time kinematic (RTK) satellite navigation. The RTK data acquisition is similar to a total station radial survey. However, it allows for real-time surveying in the field, and more autonomy during the survey since only one operator is needed, as well as rapid and continuous surveying of features and topography. To obtain real-time coordinates at a remote point (rover) a communication link (radio modem and/or satellite) is required between the reference point (base) and the roving receiver (Figure 3-3).

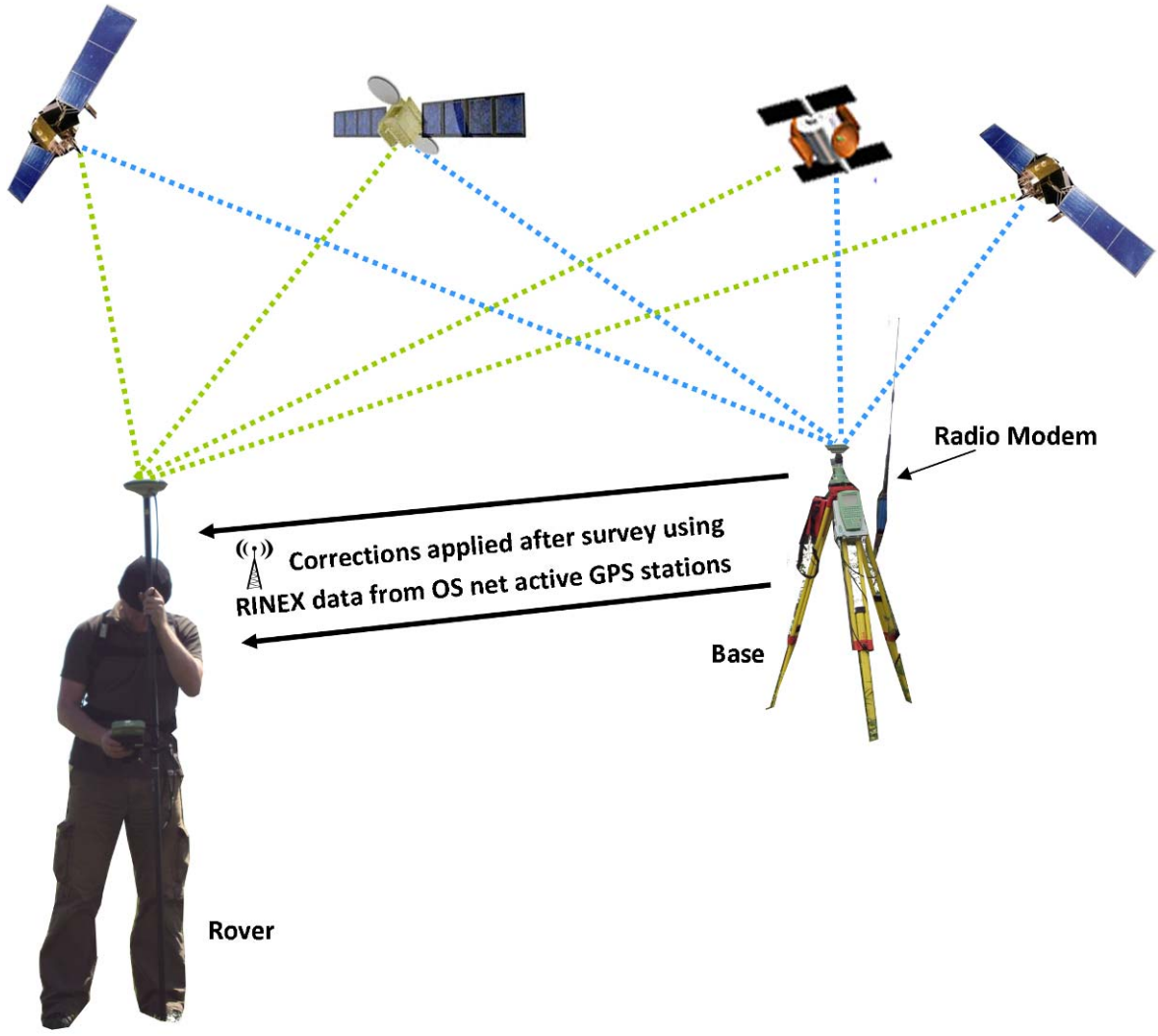

Figure 3-3: DGPS survey showing the rover attached to a lightweight carbon fibre pole (pole mode). The radio modem enables RTK corrections to be sent from the reference station (base) to the rover over a range of up to 10km (line of sight only). The 'OS net active GPS stations' are a national network of continuously operating GPS reference stations in all parts of UK (© C. Cuenca-García).

The remote/rover receiver is mounted on a range pole, similar to a prism pole for a total station. The operator performs all survey and data collection functions at the remote receiver. RTK surveying requires both the reference and remote receivers simultaneously record observations. Periodic losses of the communication link can be tolerated and/or corrected for in post-processing. The data collected from a receiver at a known stationary location (base) was used to correct the data received from a receiver at an unknown location (rover). These corrections were applied by processing the raw GPS data collected in the receiver independent exchange (RINEX) format from the nearest OS Net station. RINEX is an interchange format for raw satellite navigation system data. It allows the user to process the received data to produce a more accurate positioning.

3.4.1.1.3. *Survey Procedure*

The coverage of the nearest OS reference active station was checked and identified prior to survey at each site in order to enable correction of the raw GPS data. The GPS base station was set up on a secure and stable point and with good sky visibility. The base station recorded data in static mode for at least 2h to improve positional accuracy of the GPS survey after the processing of the raw data. This data is available at the OS Net Rinex data server for 30 days. The data was logged on a compact flash card, downloaded to a laptop and then processed. The corrected OS coordinates were introduced into the GPS base station the following day.

The real-time kinematic (RTK) survey was then carried out with the rover configuration in pole mode (Figure 3-4b). The geophysical grids and the topographic data to correct the GPR data were surveyed in this mode to ensure centimetre accuracy. The rover was attached to a backpack for the EM38 surveys. The slightly lower resolution pillar mode (Figure 3-4a) was used for the EM38 survey because this was the only possible way to attach the DGPS to the EM38 instrument and conduct the geophysical survey at the same time. The EM38 and GPS data was recorded altogether *via* a standard serial RS232 digital interface to the GPS by supporting NMEA messages.

Figure 3-4: Different GPS settings used during the fieldwork. 'a' shows the rover receiver mounted in pillar mode for the EM38 survey. The rover is set up in pole mode (in 'b') and is used to survey the topography along a GPR survey traverse to correct the elevation of the data.

3.4.1.1.4. *Data Processing*

Raw GPS data were processed with Leica GeoOffice software also provided by NERC-GEF. Raw data were downloaded into Geo Office using the compact flash card of the Leica GPS system. A project name was assigned and the data points were edited. The data collected from the static base was downloaded from the OS net RINEX data server (http://gps.ordnancesurvey.co.uk/active.asp) and imported into GeoOffice. The processing of static and kinematic GPS data were carried out in order to correct the baselines by selecting the RINEX point as the 'reference' and the reference station (base) as the 'rover'. Then the rover points were shifted to their correct position by copying the 'measured' set of coordinates of the base point and pasting them into the 'reference' point class. The corrected GPS points were exported as user-defined ASCII files into ESRI

ArchMap and these points were used to georeference all the geophysical data and to accurately locate the soil samples collected for the geochemical analyses. Further information about GPS data processing using Geo Office can be found in (Leica GeoOffice 2004).

3.4.2. Geophysical Techniques

3.4.2.1. **Purpose**

The sites were surveyed using a range of routine geophysical means in order to collect data from different techniques, assess the results, and correlate results with other data sets. Whilst the physical principles and soil dynamics involved in the measurement properties of the ground by electrical, magnetic and electromagnetic methods were reviewed in Chapter 2, this section focuses on the technical description of the geophysical techniques used in this project. Specific field survey methods are detailed with each case study site (Chapters 4 to 8). The surveys were carried out following the guidelines on the use of geophysical techniques for archaeological prospection by English Heritage (2008). The section includes information on field procedures developed for quality control during the surveys.

3.4.2.2. **Earth Resistance Survey**

3.4.2.2.1. ***Instruments***

The instrument used in the surveys was a Geoscan Research RM15-D resistance meter mounted on a PA5 frame. The frame was configured in twin array mode for all the sites surveyed in this project, using 0.5m probe spacing for most of the sites (Figure 3-5). The array configuration was sometimes modified in order to cover specific needs at some sites. The frame was sometimes extended to incorporate two parallel twin arrays with four mobile probes at 0.25m or 0.5m to increase speed in survey and test higher sampling densities (e.g. Scalpsie Bay or Lochmaben). Two simultaneous probe spacings (0.5m and 1m) were also used in order and increase the depth of penetration of the survey (e.g. the bay of Skaill). The specific configurations are detailed in the chapters dedicated to each case study site. A multiplexer module (MPX15) was attached to the RM15 in order to configure and store sequences from those surveys where simultaneous-probe spacing was used.

Since the instrument used here measures the bulk resistance and does not take into account the electrodes configuration necessary to calculate apparent resistivity (measured in Ωm) the measurement stated in the case study sites must be considered as the measurement of the resistance, hence it is given in Ω (section 2.4.1.2).

Figure 3-5: Volunteers conducting an earth resistance survey using a Geoscan RM15 at Lochmaben castle (Dumfriesshire) (© C. Cuenca-García).

Other instruments, manufactured by Campus, ABEM or TR systems, for example, are also available for earth resistance surveys. The advantage of the Geoscan RM15 system is its versatility (up to six multiplexed electrodes configuration available) and its lightweight meter for use with its mobile electrode frame.

3.4.2.2.2. *Survey Procedure*

The general survey procedures followed the standard English Heritage guidelines (2008). The dimensions of all the survey grids were 20m x 20m. The survey lines were recorded in zig-zag mode with 0.5m or 1m between lines (traverse spacing), and 0.5m or 1m in-line spacing (sampling interval).

3.4.2.2.3. *Quality Control*

The cables connecting the mobile and remote probes can sometimes affect the readings if they are twisted so care was taken to keep them untangled. The distances of the remote probes were kept as similar as possible to the mobile

probes separation at the beginning of each survey in order to maintain a 'true' twin-probe configuration (Gaffney and Gater 2003, 33).

3.4.2.2.4. *Data Processing*

Earth resistance data were processed with the Geoscan Research Geoplot (version 3.0). The software was used to create the grey scale plots and saved as bitmaps to import them into ArcMap. The general approach followed with all the geophysical data collected for this investigation was to process it minimally, in order to maintain the data as 'real' as possible. Over-processing may introduce artifacts in the data and/or obscure anomalies of interest. The data was uploaded into Geoplot, the different files merged (if required) and the raw data was initially displayed and reviewed as trace and grey scale (or shade) plots.

The general processing sequence for resistance data involved the removal of data collection defects (e.g. removal of noise spikes and edge matching of the grids), reducing the geological response (e.g. by using high pass filters), and finally data enhancing (e.g. interpolation). Table 3-3 describes the main functions used to process the earth resistance data in this thesis.

Function	Description (from Geoplot)
Clip	To limit the data to a specified maximum and minimum values for improving graphical presentation and to help in correcting the effect of noisy spikes.
Despike	To remove the effect of noise spikes caused by very high contact resistances or due to an open circuit at the potential probe at the moment of logging a data point.
Edge Match	To remove grid edge discontinuities which may be present in twin electrode resistance surveys as a result of improper placement of the remote probes.
High Pass Filter	To reduce the effect of the slowly changing geological 'background response' commonly found in resistance surveys.
Low Pass Filter	To smooth the data and to improve the visibility of weak archaeological features (e.g. wide ditches o subtle linear features).
Interpolate	To smooth the data and to improve the visibility of larger and weak archaeological features.

Table 3-3: Functions (Geoplot 3.0 software) used to process the earth resistance data.

3.4.2.3. **Magnetic Gradiometry Survey**

3.4.2.3.1. *Instruments*

Magnetometers measuring the total field need a base for correction of time-dependent variations. Variations of the Earth's magnetic field include long term 'secular' variations due to changes in the core of the earth or smoother 'diurnal' variations that result from the movement of the Earth with respect to the Moon

or the Sun. There are also variations produced by magnetic flares and storms that can affect total field instruments and tedious monitoring with a base station magnetometer and processing may be necessary. The vertical-gradient configuration of magnetometers allows the top sensor to measure the Earth's magnetic field whilst the lower sensor measures the same field but is also more affected by any localised buried field. The difference between the two sensors relates to the strength of a magnetic field created by buried features; if no field is present the difference will be close to zero as the magnetic field measured by both sensors will be the same.

The effects of potential secular or diurnal variations may be close to the variation produced by archaeological features but these are compensated for by the second vertical fluxgate sensor being located near the ground surface. Because the magnetic signal decreases by the third power of distance, the lower sensor registers a stronger signal from near-surface archaeological structures than the reference sensor above. Since gradiometers measure the rate of change between two sensors, any changes in the background field will apply to both sensors avoiding noise or the introduction of artifacts in the data. Therefore, the vertical gradient configuration is fairly effective for near-surface anomalies and its use is preferred to single sensors for archaeological investigations. A dual (or single if different sites were surveyed at the time) fluxgate gradiometer Bartington 601 instrument (Figure 3-6) was used to survey the sites presented in this investigation.

Figure 3-6: Magnetometer survey at the cropmarks at Chesterhall Parks Farm (South Lanarkshire) using a dual sensor fluxgate gradiometer Bartington 601.

This gradiometer consisting of one or two cylindrical sensors mounted vertically on a rigid carrying bar. Each sensor contains two fluxgate magnetometers with one metre vertical separation that measure the vertical component of the Earth's magnetic field at a sensitivity of 0.1nT. Fluxgate gradiometers need to be 'balanced' before starting a survey in order to remove alignment errors between the sensors of the instrument. This instrument has a simple and automated calibration set up that makes these procedures simpler and quicker than on mechanical ones (e.g. the Geoscan Research instruments).

Fluxgate sensors (Figure 3-7) generally use a pair of cores made of highly magnetic permeable material such as mu-metal (nickel-iron alloy). A primary coil (the drive) is wound around each rod, but the direction in which each coil is wrapped is reversed.

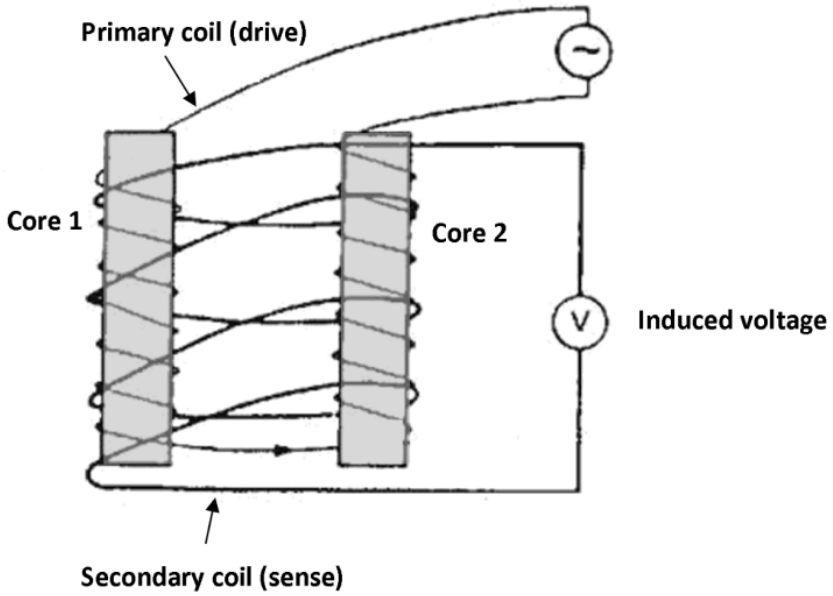

Figure 3-7: Schematic diagram of twin core fluxgate sensor.

A periodic alternating current (AC) at 50-1000 Hz is injected into the primary coil to drive the cores in and out of saturation (magnetised, unmagnetised, inversely magnetised, etc) through a magnetisation hysteresis loop. The magnetic fields induced in each rod have the same strength but in the opposite direction. A secondary coil winding is wrapped around the primary coil and cores (Figure 3-7). According to Faraday's law of induction, the change in magnetic flux induced in the cores by the primary coils produces a voltage potential in the secondary coil which is proportional to the magnetic field generated in the

cores. In the absence of an external field, the voltage detected by the secondary coil would be equal zero (Figure 3-8a). This is because the magnetic fields generated by the rods have the same strength, but opposite direction hence they cancel out. Since there is no change in the magnetic flux in the primary coil, the cores go in and out of saturation at the same time. In the presence of an external magnetic field, one of the cores comes out of saturation sooner than the core that shares direction with the external field which is reinforced (Figure 3-8b). During this time, the fields do not cancel out and there is a change in flux in the secondary coil which can be measured as an induced voltage.

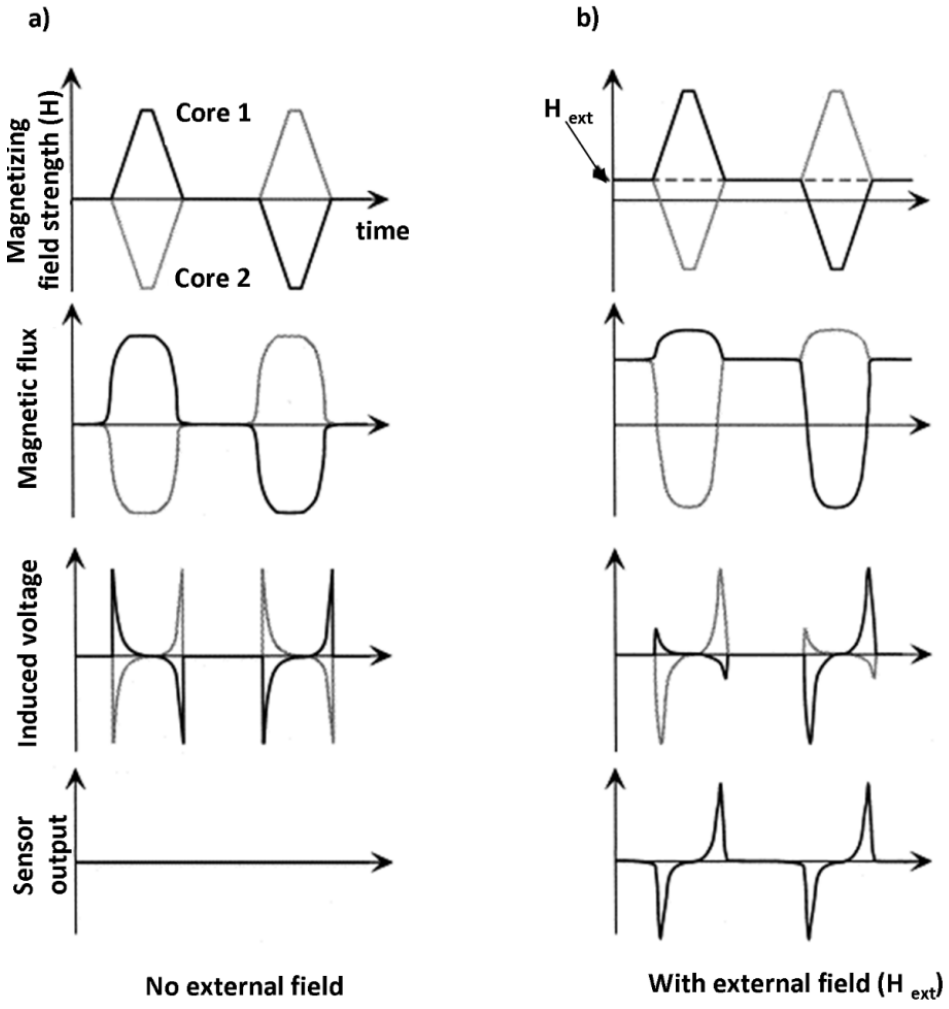

Figure 3-8: Fluxgate signal diagram showing the operating principle of the twin fluxgate sensors. The output induced signal peaks, at the frequency twice the driving current frequency, is proportional to the external field (H) strengths (based on Chiesi *et al.* 2000).

The two major manufacturers of fluxgate gradiometers are Bartington and Geoscan Research. Theoretically, the increased separation of the vertical two sensors from 0.5 (Geoscan Research FM36 and FM256) to one metre (Bartington

Grad601) has theoretically improved depth sensitivity. Archaeology at the University of Glasgow has Geoscan Research and Bartington fluxgate gradiometers, the latter being used for all the surveys presented in this project. This choice was based on the dual sensor configuration of the instrument which increases survey speed considerably as two lines can be surveyed in one traverse. Since the number of geophysical techniques and soil sampling at each site were numerous, rapid survey acquisition instruments were preferred. Nonetheless, the Geoscan Research instrumentation can be adequate in a survey environment characterised by hilly and sloping areas and terrains with denser or upstanding vegetation where a single and smaller sensor can be more portable and easier to operate. Also, when the depth of archaeological remains is expected to be fairly shallow may be another reason to select a Geoscan instead of a theoretically more depth sensitive instruments such as the Bartington.

3.4.2.3.2. *Survey Procedure*

Standard grids of 20m x 20m were surveyed using a resolution varying between 0.5m or 0.25m traverse spacing and 0.125m sampling interval. The survey mode used was parallel or zig-zag, depending on the size of the area to cover. Smaller or high resolution (0.25m traverse spacing) surveys were collected in parallel mode in order to avoid severe staggering in the data and direction-dependent heading errors (rotational errors which might produce spurious signals, and potentially masking the detection of small features of interest.

3.4.2.3.3. *Quality Control*

Before the surveys the operators and assistants were scanned to mitigate potential noise introduced in the data from metallic objects held by the surveyors. The survey lines were orientated, where possible, in N-S direction in order to ensure a greater peak to-peak magnetic anomaly at any latitude (Breiner 1999).This survey direction enhances the intensity of magnetic field caused by buried features which improves the detectability of potential anomalies of interest when the location of features is random or unknown. The instrument is always carried *c*.20cm above the ground surface as this produces the highest sensitivity to buried features whilst minimising surface noise (Bartington Instruments 1993).

3.4.2.3.4. *Data Processing*

The software used was Geoscan Research Geoplot (version 3.0). The processing sequence applied is detailed in Table 3-4. The gradiometer data processing involved the removal of data collection defects such as grid edge matching, removal of traverse stripe effects (e.g. zero mean traverse function), and removal of traverse stagger effects (i.e.destagger function).

Function	Description
Clip	To limit data to a specified maximum and minimum values for improving graphical presentation and to help in correcting the effect of random iron objects.
Despike	To remove the cluttering effect of modern and near surface iron objects.
Destagger	To remove the errors caused by bad positioning of the instrument along the zig-zag traverse. This effect is frequent when a small traverse spacing is used.
Zero Mean Grid	To remove grid edge discontinuities often found in gradiometer or similar bipolar data. It sets the background mean of each grid within a composite to zero.
Zero Mean Traverse	To neutralise the effect of major responses (e.g. geological intrusions). It also removes stripe effects, usually due to the different background level in surveys carried out in zig-zag mode or instrument tilt.
High Pass Filter	To remove strong response of an igneous anomaly in order to improve small and negative feature visibility.
Low Pass Filter	To smooth the data and improve the visibility of weak archaeological features (e.g subtle linear features).
Interpolation	To smooth the data and to improve the visibility of larger and weak archaeological features.

Table 3-4: Functions (Geoplot 3.0 software) used to process the gradiometer data.

3.4.2.4. **Ground-penetrating Radar Survey (GPR)**

3.4.2.4.1. *Instruments*

A Sensors and Software, PulseEkko 1000 GPR unit with 450 MHz or 250 MHz shielded antenna was used for all GPR surveys (Figure 3-9), on loan from GEF's instrument pool. The system has bi-static antennae with a transmitter and a receiver as separate entities, mounted in a default perpendicular-broadside configuration. The choice of both 450 MHz and 250 MHz antennae was based on the anticipated depth of investigation, likely target size, data collection time constraints and the achievable skin depth at each site. Both antennae were generally used at each case study site. An odometer (Figure 3-9) was used to trigger the PulseEKKO GPR system at defined step intervals at sites where the terrain was flat and the terrain was not slippery nor with rough vegetation.

The ‘time window’ is the length of time for which the receiving antenna will record two-way travel time data. The time window was site specific and generally required some field trials. In general, longer time windows require larger numbers of samples per trace to adequately resolve the recorded waveform (Conyers 2004, 87-88). Other instrument parameters (e.g. number of traces recorded, number of times each trace is repeated at a particular sample point or stacking) are detailed in each case study site.

Figure 3-9: Sensors & Software Pulse EKKO GPR 1000 system and odometer wheel used in the survey of the cropmarks at Forteviot (Perthshire). The red arrow shows the survey direction and the orientation of the receiver (Rx) and transmitter (Tx).

Recent innovations in multi-channel antennae configurations have significantly increased the speed of GPR surveys. These systems combine either different frequencies (allowing simultaneous mapping of near-surface and deeper targets) and/or parallel arrays (increasing the sampling densities).

3.4.2.4.2. *Survey Procedure*

The GPR reflection surveys were conducted using ‘common offset’ mode with ‘straight’ individual survey lines. The GPR system was used in its default bi-

static, coplanar, perpendicular-broadside and reflection mode (receiver leading) (Figure 3-9). The survey lines were surveyed in a uni-directional or parallel mode instead of zig-zag in order to provide a more accurate positioning of the antennae produced by offsets between alternate lines. This mode avoids extra data processing since even lines do not have to be reversed. Furthermore, since the anomaly produced can be influenced by the orientation of the targets with respect to the direction of the traverse (English Heritage 2008), a uni-directional survey was maintained in order to avoid problems related to the orientation of the non-symmetric radiation pattern of GPR antennae. The lines were orientated at right angles to the targeted features, if their orientation was known. This orientation has been shown to best resolve subsurface features (Annan 2001).

Most of the surveys were carried out in 'step' mode where the antennae were moved with fixed horizontal intervals (the 'step size'). Step-mode tends to generate more coherent and higher amplitude reflections since the antennae are stationary during data acquisition. Also, this mode allows a more consistent coupling of the antennae against the ground which is important in order to minimise signal leakage into the air and to provide a good trace stacking. Whilst this survey mode is slower during the field data collection, the processing step for distance normalization does not need to be done since the positioning of the antennae along the survey line is completely controlled by the surveyor. Alternatively, the antenna position along each survey line was controlled with an odometer wheel (Figure 3-9). The wheel has an encoder that sends a fixed number of pulses per revolution to the control unit. The control unit then uses these pulses to trigger the antenna at equal distance intervals (scan spacing). Therefore, each method has its pros and cons since some provide quicker data collection during the survey and but require more processing steps afterwards.

The cross-line spacing (traverse spacing) varied between 0.5m and 0.25m at the sites. The in-line sampling (step size) interval was kept at 0.05m for 450 MHz frequencies and 0.10m for 250 MHz. The survey resolution was designed taking into account the size of targeted features, their depth of burial and time constraints during the survey. These sampling parameters options follow the English Heritage (2008) recommendations for GPR surveys. According to Pomfret (2006), a 0.5m transect spacing is recommended to decrease data collection

time. In his study, despite a transect spacing of 0.25m resolving better the targeted features, no additional features were identified as compared to the survey taken with transect spacing 0.5m.

3.4.2.4.3. *Quality Control*

Before the survey began, the operators and survey assistants left their mobiles switched off and outside the survey area in order to avoid interferences with the GPR system. Non-metallic measuring tapes and strings were used to establish the survey grids and traverses. These were positioned with care making sure the traverses were as straight as possible as laser positioning sensors were not available. The traverses were recorded taking into account there were no cars nor other big 'mobile' metal objects nearby. The location of potential surface reflectors (e.g. trees, manholes, fences) inside or near the survey area was noted at all the sites. The odometer wheel was tested for accuracy and calibrated if required before each survey over a 50m traverse. If the wheel was used, a sole operator carried out the survey in order to ensure a constant pace was kept during the data collection as a metronome was not available. In order to increase the accuracy in antenna positioning, fiducial marks were introduced each meter along the survey line during data collection.The antennae were dragged with care and ensuring a good ground coupling. Tilts or irregularities along the traverses were marked during data collection and noted in the field survey book.

3.4.2.4.4. *Data Processing*

There are several software packages available on the market to process GPR data. Apart from the freeware packages such as MATGPR (Tzanis and Kafetsis 2004) and Seismic Unix there are other system-specific or commercial packages, including GPR-Slice and ReflexW (Sandmeier 1998). Since the University of Glasgow holds a licence for ReflexW, this was used in the GPR data processing and time-slice production.

Raw GPR data analysis can sometimes resolve basic problems such as the location of a clandestine burial for forensic purposes. However, the data generally needs some processing in order to interpret GPR anomalies correctly. The data might contain some spurious signals (artifacts) or have some other

problems generated during the data collection that need to be removed or corrected. Over-processing can also lead to the introduction of artifacts into the data. Therefore, it is important to keep the processed data real and coherent with the raw data. Whereas the degree of complexity in processing depends upon the time-cost constraints and the quality of the data, the processing flow route applied to the data must be consistent, efficient and realistic (Cassidy 2009b).

Key steps in data processing used in this investigation have been described by Annan (2001), Conyers (2004) and Cassidy (2008a, 2009b). As a minimum, some basic data processing is required in order to correct spatial inaccuracies and to meet general editing requirements (e.g. line direction, spacing, orientation, time zero correction, cut/mute/merge lines). The next steps usually involve the application of spatial and temporal filters and the assessment of time gains. Further advanced data processing can include velocity analysis, migration and time-to-depth conversion. Table 3-5 summarises and describes the specific data processing functions used in this investigation.

The final processing step involves the creation of time-slices that are maps of the amplitudes of the recorded reflections across a site at a specified time or depth. High quality time-slice production requires care both during the data acquisition and the processing stages (Nuzzo *et al.* 2002). It is particularly important to use correct temporal and spatial sampling densities during the survey. The difference between thin and finite-width time slices should be taken into account when producing time-slices. When a time slice of zero thickness (or one temporal sample) is created, the amplitude is plotted at the specified time. Therefore such a slice is generally relatively noisy since no averaging of time (smoothing) has been performed. Less noisy slices can be obtained with an averaging of the data in a time window of the same order of the pulse-width or period T=1/f, where f = is the central frequency of the antenna used (in GHz) (Dr Luigia Nuzzo *personal comment* 2008).

Function	Description
Rubberband	The data can present an un-equal number of traces between the fiducial marks inserted each metre. This occurs due to uneven pace in the antenna towing speed and/or calibration problems of the odometer wheel used. Correction of the traces to a constant step size between the fiducial marks is needed to ensure a correct horizontal scale. Since most of the data was acquired in 'step' mode in this thesis, there was in general, good positioning of traces.
Subtract-mean (dewow)	To eliminate possible low-frequencies produced by the transmitting signal. 'Wow' is caused by swamping or saturation of the signal by early arrivals and/or inductive coupling effects.This 'Wow' superimposes on the high frequency reflections of interest and must be removed. The removal of any DC level from the data can be used as an alternative or in addition to DEWOW.
Time zero Correction	Time zero in a trace is defined by the arrival time of the first wavelet. Start time must be the same in all the traces but, during the survey, do not always match correctly. This is due to down-shifting of the radar section due to the air–ground interface, instabilities or drift in radar electronics, rough surface or vegetation. A consistent time zero is fundamental in order to produce time-slices.
Background Removal	A 2D spatial filter that takes the form of an average trace removal. It works by removing all the waves that occur at the same time, leaving only those that occur more randomly. It is very effective in eliminating transmitter antenna reverberations (or ringing) in the data. Instrument noise, by operator noise or by a towing vehicle can produce horizontal bands which sometime obscure important subsurface reflections. However, this filter can also remove horizontal reflections of interest.
Gain (e.g. Manual-γ)	GPR energy is reduced when it propagates into the ground because of the different attenuation pathways of the signal (e.g.RDP, clutter, spherical spreading). The consequence is a progressive reduction in the strength of the reflected energy with depth. Hence the gain function allows the amplitude to be restored, enhancing low amplitudes in the data to make them more visible. Manual (γ) gain allows to manually define a digitalized gain curve in the γ-direction (or time axis) and to apply this gain curve to the data, equalizing the average amplitude in each time window in order to increase the visibility of the deeper parts of the image. The use of the gain function is an important processing step prior to time-slice generation in order to improve visualization (*e.g.*by avoiding the saturation of the intermediate depth slices). Nevertheless it is a delicate processing step as all gain functions amplify both noise and coherent signal, thus adding the possibility of artifact introduction.
Topographic correction & tilt of the antennae	A flat and even surface is the ideal scenario for GPR surveys. However, if significant topographic variation exists an appropriate elevation and tilt correction must be applied to the GPR data in order to avoid discrepancies in the location of the reflectors and distortion in the shape of the detected features (Goodman *et al*. 2007). This correction requires a signal velocity estimated by modelling hyperbolic responses from the radargrams (see below) as well as a digital elevation model of the survey area.
Velocity analysis (hyperbolic modelling) & Time-depth conversion	Two-way travel time scale (ns) can be converted into a depth scale (m) by determining the GPR wave velocities in a dataset. There are different methods, from assuming a constant velocity (*e.g*. using material standard velocities), to other rather more accurate measurements, such as time-domain reflectometry (TDR) laboratory measurements, wide-angle refraction and reflection (WARR) or common midpoint (CMP) measurements. Velocities can also be approximated by an interpolation along the profile using velocities given by modelling the hyperbolic responses. In materials with a high velocity (low dielectric permittivity), hyperbolas are wide and with low velocity (high dielectric) they are narrow hyperbolas. Using this principle, a quick automated velocity measurement can be done in post-processing. The function calculates the signal velocity in the medium from the shape of hyperbolic reflections. However, the accuracy of the calculated velocity will depend on: the scan spacing (smaller scan spacing produces wider hyperbolas); the radar wave velocity (higher velocity, or lower dielectric, produces wider hyperbolas and vice versa); and the orientation of scan with respect to the target (ideally perpendicular to it).
Migration (e.g. FD Migration)	Distortions caused in the reflected data by the conical (or hyperbolic) nature of the radiated GPR energy and the changes in the velocity can be resolved by migration procedures. These rely on the collapse of the hyperbola arms to their apex (downward continuation) in order to improve resolution and spatial analysis. Since migration procedures can be fairly time-consuming and their results depend upon temporal and spatial sampling quality and the homogeneity of the environment in which the survey is carried out (Cassidy 2009b), it is not always possible to apply this processing step to GPR data. Finite difference (FD) migration can handle laterally varying velocity fields and efficiently implement downward continuation.

Table 3-5: Functions (ReflexW software) used to process the GPR data.

The conversion of the data into positive values may improve the graphical presentation of the time-slices. Due to the oscillatory nature of GPR signals, with both positive and negative values, cancellation can occur when summing and consequently the amplitude decreases. Therefore, data conversion into positive values before creating the time slices allows an enhancement of the high-amplitude reflections (Dr Luigia Nuzzo *personal comment* 2008). This conversion and the time averaging (smoothing) simplifies maps and may help to delineate the main anomalies. The data is then interpolated and gridded on a regular mesh (Conyers 2004, 151). However, the production of thin-slices and preservation of wavelet polarity may be beneficial to image in detail the small and subtle features (Novo *et al*.2010; Novo *et al*. 2012; Trinks *et al*. 2010). Hence, the GPR data in this thesis was analysed using both types of visualisation (thin slices for subtle features and thick slices for main anomalies) in order to achive a full and detailed interpretation of the data.

3.4.2.5. **Frequency Domain Electromagnetic Survey (FDEM)**

3.4.2.5.1. ***Instruments***

In archaeological practice the instrument generally used is the Geonics EM38 as it offers the best resolution for the general target depth of most archaeological remains (*c*.1m). There are many model variations of the instrument: some are able to record only one component at a time; the EM38-B can simultaneously measure both components; the EM38-DD can record simultaneously vertical and horizontal coil orientation; and the EM38-MK2 is capable of measuring both components simultaneously at two coil separations (0.5m and 1m).

The instrument used in this research was the earliest version of the Geonics EM38 (only one component at a time) and it was not set up to be used in horizontal mode. The instrument was available at Archaeology at the University of Glasgow. Another EM38 instrument was borrowed from Orkney College during the fieldwork carried out at the Bay of Skaill (Chapter 5). The Geonics EM38 was used with an Allegro data logger and an attached DGPS to accurately locate the data and accelerate the surveys. The attachment of the GPS was explained in section 3.4.1.1.

3.4.2.5.2. *Survey Procedure*

The surveys were carried out over 20m x 20m grids, with survey lines spaced 1m, following the recommendation of English Heritage (2008). The instrument was set up in continuous mode and attached to the differential GPS system which allowed very fast data acquisition. The data was collected along parallel traverses in uni-directional mode with the operator conducting the data acquisition in the same the direction of travel for each traverse across the grid.

3.4.2.5.3. *Quality Control*

Prior to the start of the survey, the instrument was switched on to warm up and to adjust to air temperature for at least 1 hour. The instrument was then zeroed and calibrated, first for the conductivity survey and then for the MS survey. The operator kept similar 'magnetic hygiene' as in the magnetometer survey (i.e. non-metallic shoes and no metal from approximately the waist down). The survey lines were recorded in parallel (uni-directional) instead of zigzag mode in order to avoid grid offset problems and save time in data processing. If the operator returns to the adjacent transect going in the opposite direction, the offset may occur and features of interest may be obscured.

3.4.2.5.4. *Data Processing*

The data was downloaded from the instrument logger onto a flash card using the software DAT38 (by Geonics). The data from both the quadrature and in-phase as well as the GPS tracks were checked and converted into x,y,z ascii files. These files were imported into Excel to edit the data (e.g. removing headings, convert spaces into columns, data format).

Surfer 8 (Golder Software) was used to process the data and create the plots. The xyz files were imported into a new worksheet and the format of the data was checked. A new plot was then created applying the 'Minimum Curvature' gridding and selecting the appropriate grid geometry. The created grid-file was then plotted as 'Image' map which is similar to the shade plots created in Geoplot.

3.4.2.6. **Single-coil Magnetic Susceptibility (MS) Survey**

3.4.2.6.1. ***Instruments***

This electromagnetic technique uses and quantifies the induced magnetization of a sample in a weak magnetic field (i.e. 5–100 mT)(Dalan 2008). It measures the spread of magnetic enhancement of the topsoil in response to an applied magnetic field because of the interaction with naturally occurring iron minerals (English Heritage 2008). Further details about the soil magnetic properties and antropogenic MS topsoil enhancement were discussed in section 2.4.2.1.

The instrument used was a single coil Bartington MS2D of 185mm diameter a frequency of 0.958kHz (Figure 3-10). The sensor is placed flat on the ground surface and an alternating magnetic field of 80A/m in the coil (Gaffney and Gater 2003, 45) is induced into the soil in a shallow hemisphere below it. The difference between the frequency originally transmitted and that re-emitted is the MS of the material. The MS units from field measurements are expressed in the SI system (International System of Units) which is dimensionless (Gaffney and Gater 2003, 45).

Figure 3-10: Volunteers conducting a magnetic susceptibility survey at Scalpsie bay. The operator is zeroing the Bartington MS2D sensor before taken the soil measurement.

3.4.2.6.2. *Survey Procedure*

Areas of interest can either be mapped in detail with sampling intervals of 1 m to reveal individual archaeological features or with a wider spacing to a recommended maximum of 10m (English Heritage 2008) to obtain an overview of the MS variation over a larger area and to identify 'hotspots' that can later be investigated with higher spatial resolution. The technique only penetrates up to 10cm in field measurements (Gaffney and Gater 2003, 45). This project only carried out field measurements at one site (i.e. Scalpsie bay, Chapter 4) in order to compare the results of this technique against the results of the gradiometer survey. Whilst single-coil instruments can be sensitive to metallic noise sources, as any other electromagnetic method, they are less sensitive to interferences produced by power lines and atmospheric electricity (Dalan 2006, 177).

The grids were 20m x 20m and the data was collected in zig-zag mode. The readings were logged manually with a handheld computer. The sensor was zeroed in the air (Figure 3-10) before each reading was taken to correct the tendency of the MS2D instrument to drift (Gaffney and Gater 2003, 74) and to eliminate spurious signals derived from ferrous objects and poor sensor-ground contact.

The main disadvantage of this technique is the poor penetration of the signal, which is a function of the small diameters of the coils used. There is no-automatic data logging with the Bartington MS2D instrument hence all the measurements must be recorded by hand which makes the surveys inefficient. Masking deposits and the influence of field conditions (e.g. rough ground or thick vegetation) during the survey may reduce the contact between the field coil and the ground surface. Also, waterlogged material can suppress MS measurements by making chemical changes (English Heritage 2008). The reduction of iron oxides produced by gleying or podzolisation may also affect the surveys (Dalan 2006, 176). MS survey is considered as an indicative technique as it needs the support of additional geophysical techniques to establish the presence, or absence, of archaeological remains (English Heritage 2008).

The technique can also be used to measure soil samples taken from the topsoil of archaeological contexts. MS measurements in a laboratory environment may

provide information to assess the anthropogenic or natural cause of the soil MS enhancements and complements the results of the gradiometer results. Most of the MS measurements in this project were carried out on topsoil samples taken over targeted archaeological or from soil samples from excavated sections. The procedure for laboratory measurements is explained in section 3.5.2.2.

3.4.2.6.3. *Data Processing*

The data was processed with Geoscan Research Geoplot (version 3.0). The processing sequence applied was following Geoscan Research (2004) recommendations (Table 3-6). It involved clipping the data (i.e.to reduce the effect of iron spikes), remove any regional gradient (i.e.high pass filter), and finally enhance and present the archaeological response (e.g.interpolation). Since the survey resolution was fairly high, the high pass filter was used in the processing. However, this filter was only applied after checking that any important archaeological information was not removed.

Function	Description (from Geoplot)
Clip	To limit data to a specified maximum and minimum values for improving graphical presentation and to help in correcting the effect of random iron objects.
Despike	To remove the cluttering effect of modern and near surface iron objects.
High Pass Filter	To reduce the effect of regional gradient (background magnetic susceptibility response) and to improve small feature visibility.
Interpolation	To smooth the data and to allow a better comparison with the gradiometer data.

Table 3-6: Functions (Geoplot 3.0 software) used to process the magnetic susceptibility (MS) data.

3.4.3. 'Target' Geochemical Survey

3.4.3.1. **Purpose**

Soil samples were taken from the topsoil and excavated section from the archaeological features targeted at each case study site. The aim was to characterise their geochemical response and to assess other soil properties in the general survey environment.

A sampling strategy was designed in order to sample, densely enough, the targeted features. Most of the sampling strategies used for chemical analysis of archaeological sites are designed to cover extensive areas. Common sampling

resolution used in such extensive surveys uses a 5m x5m sampling spacing. Therefore, the general sampling resolution had to be reduced for this investigation. General information on sampling strategies for extensive geochemical surveys in archaeological investigations can be found in Haslam and Tibbett (2004).

3.4.3.2. **Soil Sampling Strategy**

3.4.3.2.1. ***Surface Sampling***

Topsoil soil samples (*c*. 300g) were collected over the targeted features along a line generally using 1m or 0.5m sampling intervals. The sampling resolution was increased over features if their exact location was known. The sampling was carried out taking topsoil bulk samples, after discharging the first *c*.0.5cm-10cm of topsoil. A trowel was generally used to collect the bulk samples but also augers or corers were tested upon the soil characteristics. The instruments were cleaned after collecting each sample in order to avoid contamination.

3.4.3.2.2. ***Section Sampling***

Bulk samples were taken for excavated sections in a similar way as described above. Prior to collecting the samples the section were cleaned in order to take un-exposed and fresh samples. The soil from archaeological deposits was collected making sure that all the visible deposits were sampled. The samples were collected from the bottom of the section upwards in order to avoid contamination.

3.4.3.2.3. ***Sample Size***

A total of 324 samples were collected from the sites presented in this investigation (Table 3-7).

Nº of Samples (n=)/Sites	Scalpsie Bay (Isle of Bute)	Bay of Skaill (Orkney)	Lochmaben Castle (Dumfriesshire)	Forteviot (Perthshire)	Chesterhall Parks Farm (South Lanarkshire)
Surface (Topsoil)	n=11	n/a	28	157	42
Section		29		28	
Controls	n=2		3		3
Other	auger 1 (n=5); auger 2 (n=6); auger 3 (n=7)			3	

Total= 324

Table 3-7: Summary numbers of samples collected at the five case study sites.

3.4.3.3. **Soil Sample Storage**

After removal of living material (e.g. worms, roots), the soil samples were sealed in air-free plastic bags with labelling, matching that of the references collected in the soil texture and site description form (Figure 3-20) and stored in a dark environment (e.g. cardboard box). The samples were transferred as quickly as possible to the refrigerator of the laboratory of archaeology (University of Glasgow) and kept at 4˚C until analysed.

3.5. Phase III: Lab work

Before the analysis, the fresh samples were subdivided into three parts: an original sub-sample retained for reference (*c.*100g); a sub-sample for pH analysis and loss on ignition analysis (*c.* 50g); and a sub-sample for geochemical analysis (*c.*150g). Part of the first original sub-sample was used for the soil texture and OSL analysis. The fresh sub-samples for pH and LOI analysis were the first to be analysed. Meanwhile, the sub-samples for geochemical analysis were air dried at room temperature and stored until analysis in order to reduce geochemical alteration of the samples. The air-dried soils were gently ground using a mortar and pestle, then sieved using a mechanical shaker for 5 minutes. A total of 242 soil samples were analysed following the strategy shown in Figure 3-11.

The 82 samples left were extra samples taken from Forteviot (Chapter 7) which were only measured for MS and as calibration samples for other analyses (e.g. pXRF and ICP-OES). The different analyses were carried out following general protocols from the Scottish Analytical Services for Art & Archaeology (SASAA) and other sources. In order process and analyse the soil samples, a team of assistants (students of Archaeology at the University of Glasgow) was organised (Figure 3-12). Their work concentrated on drying and sieving the samples before the geochemical analysis and some were also involved in the geochemical analysis.

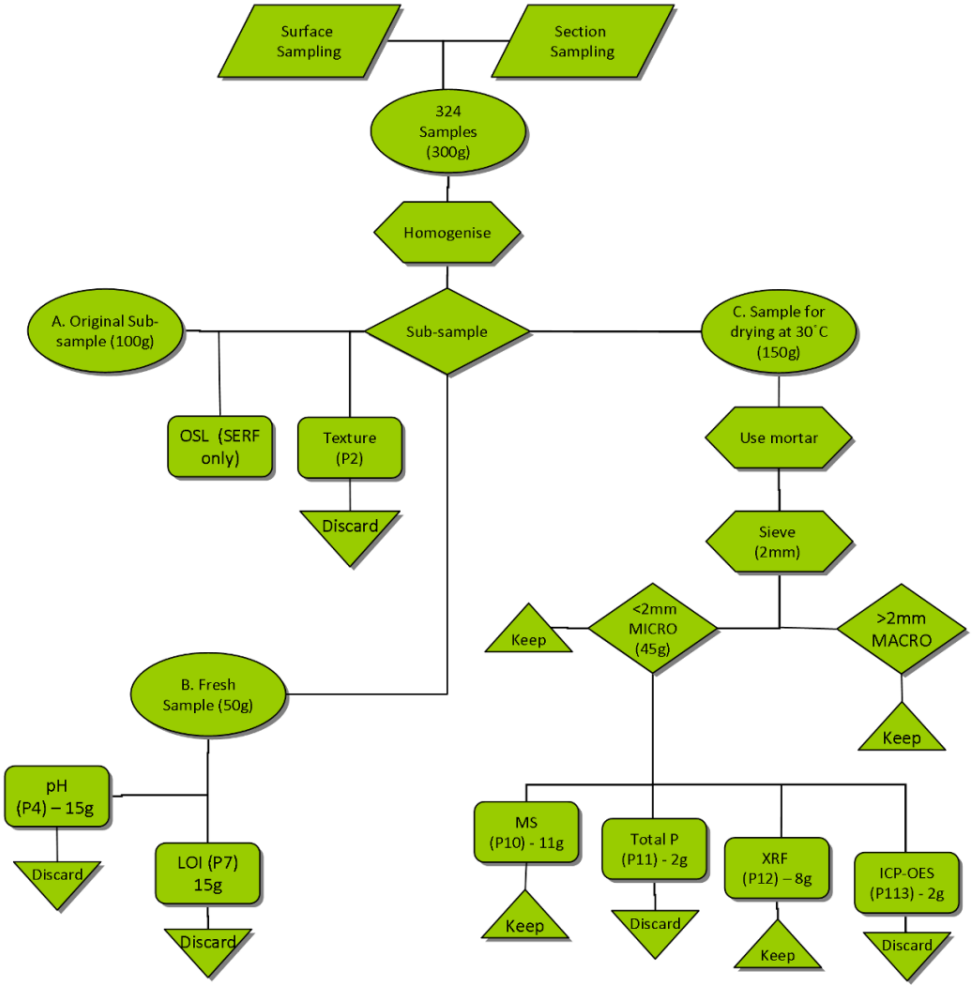

Figure 3-11: Flowchart showing the general soil analysis strategy.

Figure 3-12: Sub-sampling and sieving carried out by a team of assistants.

3.5.1. Soil Chemical Analysis

The soil samples gathered from the targeted archaeological sites were analysed by routine geochemical techniques in order to determine major (>100ppm) and trace (<100ppm) elemental concentrations and obtain the pH. The aim was to identify possible enhancement, depletions and associations, between the different elements and pH, to relate them to the geophysical responses recorded during the fieldwork stage. By establishing potential correlation between geophysical and geochemical results, potential enrichment or depletions of chemical elements associated with geophysical anomalies may help in:

- Understanding the character of the geophysical responses and increase the interpretation capabilities of geophysical results.
- Developing the understanding and current database of anthropic chemical elements for geochemical investigations since the enrichment or depletions of common or new chemical elements are in association with archaeological features and geophysical anomalies.

This section details the method followed to carry out the analysis and combines information synthesised from a series of protocols used for geochemical analysis for archaeological investigations but also from other applications in Earth Science.

3.5.1.1. **pH and Conductivity Analysis**

3.5.1.1.1. ***Purpose***

Determination of pH and related conductivity of soil samples was used to characterise the soils collected at the different sites. pH is the measure of hydrogen ions (H^+) in the soil. Acidic solutions have a higher number of hydrogen ions, while alkaline (or basic) solutions have a higher number of hydroxyl ions. Pure water has a pH very close to 7 at 25°C (neutral). Solutions with a pH less than 7 are said to be acidic and solutions with a pH greater than 7 are alkaline. The pH scale (Figure 3-13) is traceable to a set of standard solutions whose pH is established by international agreement. Soil pH is affected by the chemical, biological, and physical processes of the soil. Its determination is important to understand soil geochemistry as:

- It affects nutrient availability to plants and solubility of heavy metals (Figure 3-13).
- It determines how fast microbes in the soil break down organic matter (most bacteria like to work in a pH range of 6 to 7) and therefore pH relates to organic archaeological material survival.
- It is involved in the buffering capacities of soils (the ability of a soil to adjust to changes in the ionic composition of the soil solution) and cation exchange (between a cation in solution and another cation on the surface of any negatively charged material such a clay or organic matter). The concentration of hydrogen ions in the soil solution (pH value) is directly proportional to and in equilibrium with the hydrogen ions retained in the soil's cation exchange complex. Thus the hydrogen ions retained by clay particles replenish, or buffer, the hydrogen ions in soil water.

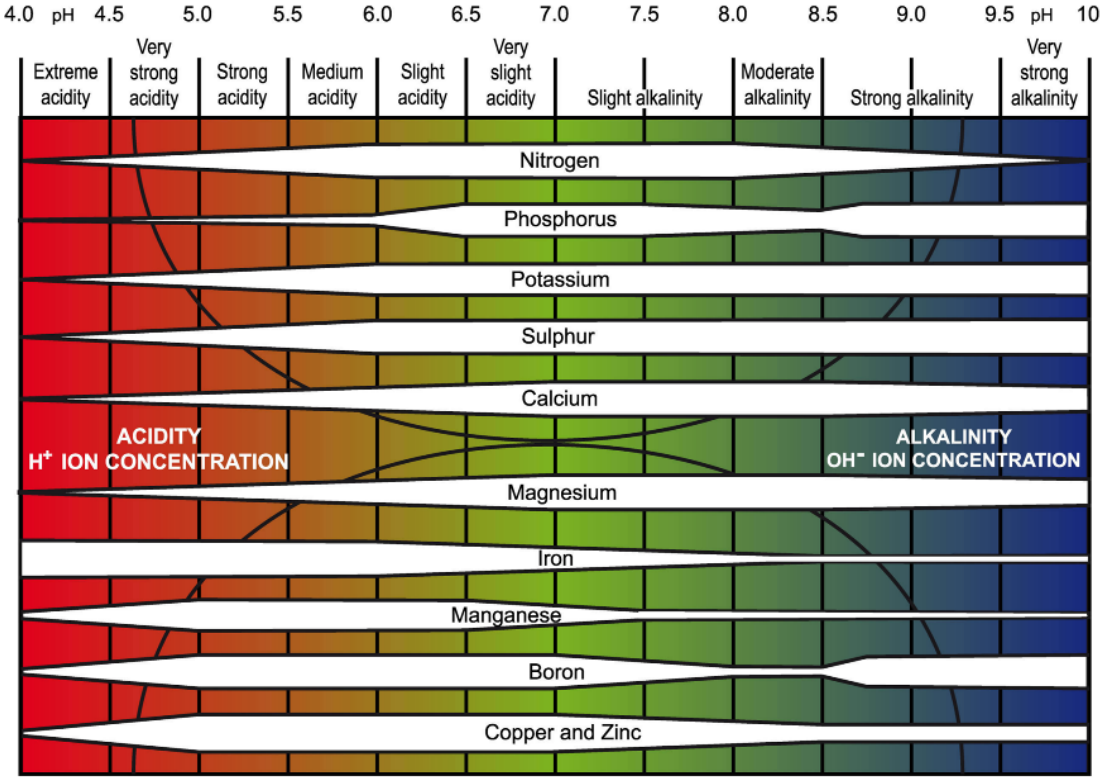

Figure 3-13: pH scale chart showing the effect of soil pH on the uptake of some chemical elements (plant nutrients and heavy metals). The availability of different nutrients at the different pH bands is indicated by the width of the white bar: the wider the bar, the more available is the nutrient (from www.pda.org.uk)

Soil pH is an important variable in the interpretation of many other soil properties (e.g. organic matter accumulation, elemental concentrations, cation exchange capacity, soil corrosivity) and hence is a routine analysis. Some

knowledge of soil pH may help in understanding the nature of soil development and soil type. pH may give clues on post-depositional processes (e.g. leaching, podzolisation) affecting soil deposits and other taphonomic processes related to archaeological features. A limitation of pH analysis is that oxidation of soil samples can result in pH values that may not reflect the *in situ* pH value. Also, the resulting pH measurement of a bulk solution tends to be higher than that of the *in situ* soil.

Electrical conductivity (EC) is a measurement of the dissolved soil material in an aqueous solution, which relates to the ability of the material to conduct an electrical current. It measures the electrolytic concentration (amount of dissolved salts), and therefore it is an approximation to salinity. EC varies not only with the concentration of salts present, but also with the chemical composition of the nutrient solution. The measurement units are micro-sieverts. Whist EC can be easily related to the electrical and electromagnetic properties of soil that also affect geophysical methods, this analysis is not used to measure these properties since the measurements were not made *in situ*. EC contributes to the geochemical characterisation of the soil samples.

3.5.1.1.2. *Instrument*

The meter used was a Hanna HI991301 Portable pH, conductivity and temperature meter.

3.5.1.1.3. *Limitations*

The suspension of the diluted soil required to carry out the measurements can be affected by samples characterised by a high content of organic matter or calcareous material (carbon dioxide is absorbed by the suspension). The lack of equilibrium in the sample may cause a rapid drifting of the readings during the measurements. Another source of error is associated with materials containing sulphidic minerals. Air-drying of such materials may speed up the oxidation rate resulting in the production of a strong acid. For such materials fresh samples should be used (CEN 2005). Since soil pH is a very variable property (e.g. rapid oxidation of off-site samples) and many variables may affect the precision of this analysis (e.g. drift of the readings), a general consistency during the analysis is fundamental to be able to compare two sets of results. Therefore, the results

from pH measurements should be viewed as 'indicative' rather than 'absolute' in this investigation.

3.5.1.1.4. *Procedure*

Fresh bulk samples from the refrigerator (c.3-4˚C) were the first to be analysed for pH. The analysis s very simple and straightforward requiring only a pH meter and basic beakers and measuring cylinders. The main steps for pH measurement were:

- Preparation of the suspension: The soil-water solutions were prepared in a 1:2.5 ratio (4g homogenised fresh soil + 10ml deionised H_2O). Samples were shaken mechanically on a vibrator mixer for 1minute in 4 pulses of 15 seconds and 5 minutes to rest.
- Calibration of pH meter: The pH-meter was calibrated as prescribed in the manufacturer's manual, using the Hanna calibration 4.01 and 7.01 buffer solutions. The calibration of conductivity used the usual 1413 micro-sieverts buffer solution.
- pH and conductivity measurement: The meter electrode was placed in the sample flask and 3 minutes equilibration time allowed before taking a pH measurement (usually estimated to +/- 0.1) and the temperature. The conductivity measurement was then taken by changing the mode button on the meter. The probe was cleaned thoroughly with deionised water after each sample.

3.5.1.1.5. *Quality Control & Analytical Error*

The pH meter was calibrated at the beginning and end of the working day in order to ensure a good accuracy. The error of the analytical method was monitored by measuring the buffer solutions between ten samples and checking the readings in order to comply with Table 3-8. If the readings were not within these margins the meter was re-calibrated and the previous five samples re-analysed. Since the measurements were carried out in the laboratory (constant temperature c.23˚C) and the meter automatically compensates for temperature compensation there was not need to correct for temperature.

pH- range	Acceptable difference
pH≤7	0,15
7<pH<7,5	0,20
7,5≤pH≥8	0,30
pH>8	0,40

Table 3-8: Acceptable limits for pH analysis (ISO/10390 2003).

3.5.1.1.6. *Reference*

The detailed protocol used in this project is in Appendix B (Protocol 1).

3.5.1.2. **Total (Inorganic) Phosphate Analysis**

3.5.1.2.1. *Purpose*

To determine total (inorganic) phosphate concentrations of the soil samples collected at the different sites. Phosphorus (P) is a strong anthropogenic indicator of human activity. Its particular chemistry and significance in archaeological prospection was explained in section 2.5.

3.5.1.2.2. *Instrument*

A Fisherbrand digital colorimeter from Archaeology (University of Glasgow) was used for the measurements.

3.5.1.2.3. *Procedure*

The analytical procedure is based on the molybdenum blue colorimetric method. Ammonium molybdate and potassium antimonyl tartrate react in acidic solution with orthophosphate (phosphoric acid) to form a heteropolyic acid (phosphomopydbic acid) which can be reduced by ascorbic acid to give an intense blue colour, the intensity of which is directly proportional to the concentration of phosphate in the soil solution.

The phosphate concentration is measured as a function of absorbance by the colorimetric technique. The amount of electromagnetic radiation in the visible region of the spectrum absorbed by a coloured solution is directly proportional to the concentration of the coloured species as defined by the Beer-Lambert

Law. The colorimetric technique involves the projection of a beam of light of a given intensity focused on a sample. The instrument measures the absorbance of particular wavelength of light by the analyte species (developed soil solution).

The samples were prepared using a standard ignition-hydrochloric acid total phosphate extraction procedure. Figure 3-14 shows the main six analytical steps of the method. The quantification of total phosphate was achieved by analysis of a series of standards and construction of a calibration curve. The samples were plotted against the calibration curve and the concentrations derived.

3.5.1.2.1. *Quality Control & Analytical Error*

Each batch was limited to 15 samples in order to ensure enough time for both sample solutions and standards to develop for exactly 30 min (after addition of the reagent), transfer into cuvettes and measure (within a total of 40 minutes after the addition of the reagent). A distilled deionised water blank was measured with every batch of samples in order to zero the colorimeter and to show that the glassware and reagents were not contaminated with phosphates. Two duplicate samples were analysed in each batch to assess the analytical error and provide quality control of the method. The estimated error was 5% based on interferences related to sample processing losses during the weighing and re-weighing of small samples after ignition and further losses during filtration of the samples after digestion.

3.5.1.2.2. *Reference*

The detailed protocol is in Appendix B (Protocol 2).

Figure 3-14: Total phosphate analysis showing six steps of the analytical procedure: a-sample weighing and ignition (to convert the organic portion to inorganic); b-digestion in 1N HCl; c-filtration; d-standards preparation; e-addition of developing solution; and f-measurement of the absorbance.

3.5.1.3. **Portable X-ray fluorescence (pXRF) Analysis**

3.5.1.3.1. ***Purpose***

To determine the concentration (enhancement and depletions) of a range of major (and some trace) elements in the soil samples. Human activity alters the concentration of some elements within soils, topsoils or archeological contexts (e.g. floor deposits). These changes can persist over long periods of time and can be determined with this technique as enrichments or depletions of a range of elements (Chapter 2). The technique also allows the determination of the major chemical composition of soil samples. pXRF analysis provides a quick determination of elemental composition of a range of elements simultaneously. The technique does not need to digest the soil samples which increases its cost-effectiveness and makes it rapid and non-destructive.

3.5.1.3.2. ***Instrument***

A Thermo Scientific Niton XL 3t Goldd+ XRF analyzer was used for the soil multi-element measurements. This energy-dispersive x-ray fluorescence (EDXRF) instrument was hired from the Scottish Analytical Services for Art and Archaeology (SASAA).

X-ray fluorescence (Figure 3-15) is the property of a material to emit x-rays, with a specific energy, upon being irradiated by x-rays.

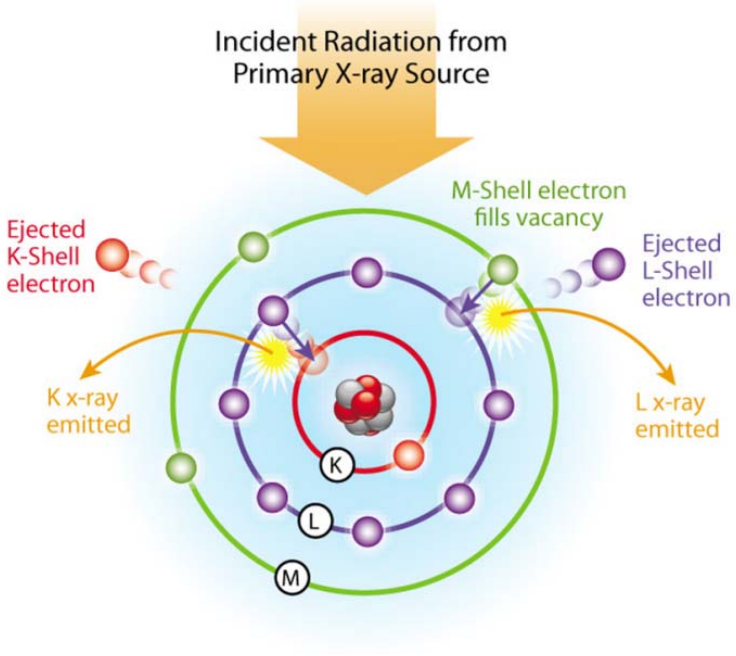

Figure 3-15: Diagram showing the X-ray fluorescence principle (courtesy of Thermo Fisher Scientific).

A fluorescent x-ray is created when a high energy x-ray hits an atom in the sample. This produces the displacement of an electron from one of the atom's inner orbital shells. By filling the vacancy left in the inner orbital shell with an electron from one of the atom's higher energy orbital shells, the atom re-stabilises. The electron drops to the lower energy state by releasing a fluorescent x-ray, whose energy is equal to the specific difference in energy between two quantum states of the electron.

Since each of the elements present in a soil sample produces a characteristic fluorescent x-ray energy spectrum, the pXRF instrument determines the elements of a sample by measuring its x-ray spectrum by irradiating x-rays. The emitted x-ray spectrum is detected simultaneously using a silicon detector (SDD) which converts the energy of each emitted x-ray into an electric current, whose strength is proportional to the energy of the x-ray. An onboard microprocessor counts how often energy is detected, assigns the energy to a particular element (the calibration being prepared by the instrument manufacturer) and reports the calculated concentration for the element to a central processor unit (CPU) where data is stored or transmitted to an external laptop (Figure 3-16).

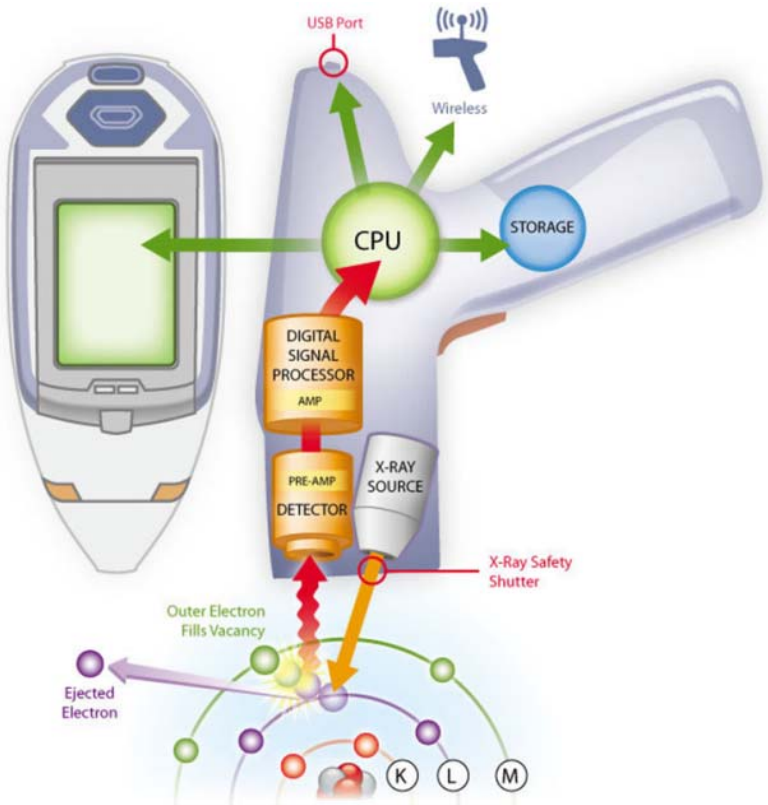

Figure 3-16: pXRF instrument diagram (courtesy of Thermo Fisher Scientific).

The pXRF instrument can therefore measure the unique set of x-rays emitted by the chemical elements in each soil sample and determine those elements present and their relative concentrations - in other words, the elemental chemistry of the sample. In general, the EDXRF instruments are more suitable for heavier elements (Figure 3-17).

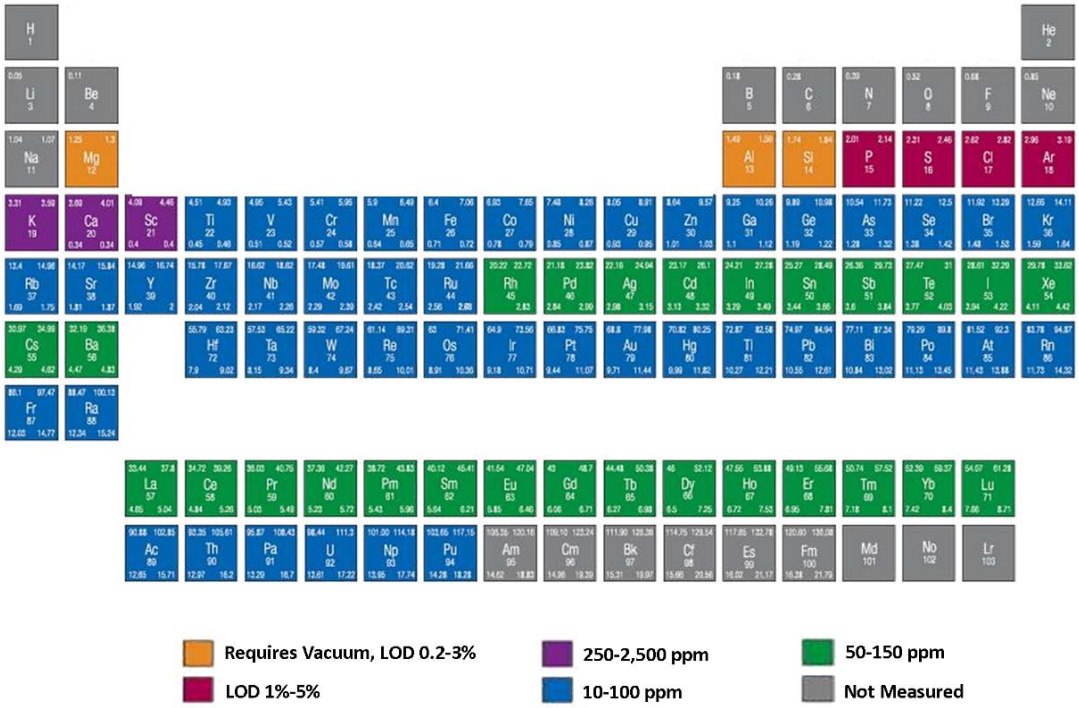

Figure 3-17: Periodic table of XRF data showing the detection limits (based on Innov-X handout).

The sensitivity of the instrument to detect lighter elements, (elements below atomic number 17 such as Mg, Al, Si, P, S, Cl) may be improved by attaching a helium purge or a vacuum pump chamber. Unfortunately, P was not a pre-determined element in the 'soil' mode of the instrument used for this investigation.

3.5.1.3.3. *Limitations*

pXRF analysis measures the total element concentration of the samples, independently of the chemical form (speciation). The detection limits are 1 to 10 ppm at best therefore, other techniques (e.g. ICP-OES) must be used to measure sub-ppm levels. The pXRF is predominantly a surface analysis technique (X-rays penetrate a few mm into sample). To obtain accurate results, the samples must be homogenised and the instrument response calibrated using standards. The total error for pXRF analysis is defined as the square root of the

sum of squares of both the instrument precision and the user- or application-related error. Generally, instrument precision is the least significant source of error in pXRF analysis. User- or application-related error is generally more significant and varies with each site and method used. Some sources of interference can be minimized or controlled by the instrument operator, but others cannot. Common sources of error are:

- Physical matrix effects that can result from variations in the physical character of the sample (particle size, uniformity, homogeneity, and surface condition). The accuracy of the analysis is strongly influenced by sample homogenization. The more homogeneous the sample (e.g. dried, sieved and measured in plastic cups), the more accurate the results. There is no control of this limitation when conducting *in situ* analysis.
- Moisture content may affect the accuracy (the higher the soil moisture in a particular matrix, the lower the recorded concentration relative to the actual concentration). This limitation may be overcome by drying the sample (e.g. in a standard laboratory oven).
- Inconsistent positioning of samples in front of the probe window (x-ray signal decreases as the distance from the x-ray source increases).
- Chemical matrix effects that result from differences in the concentrations of interfering elements. Many elements produce x-rays of similar energy and so discerning which element produced a detected x-ray is a factor of the detector's resolution and the software's ability to fit all of the data to the relative intensities produced by the various wavelengths. These effects occur as either spectral interferences (peak overlaps) or as x-ray absorption and enhancement phenomena. Both effects are common in soils contaminated with heavy metals (e.g. Fe tends to absorb Cu x-rays, reducing the intensity of the Cu measured).
- Ambient temperature changes can affect the gain of the amplifiers producing instrument drift. Gain or drift is primarily a function of the electronics (amplifier or preamplifier) and not the detector as most instrument detectors are cooled to a constant temperature. Most pXRF instruments have a built-in automatic gain control.

3.5.1.3.4. *Procedure*

Niton pXRF units utilize ionizing radiation hence a radiation safety training session was undertaken in order to comply with the ionising radiation regulations 1999 (IRR99) by the current UK legislation and internal regulations within the University of Glasgow. Also, a dosimeter was carried by the operator of the instrument in order to monitor any radiation dose acquired during the measurements.The samples were homogeonised, dried and sieved using a 2mm sieve. Each sample was kept in a clean plastic bag and transferred into a plastic cup which was covered with polypropylene X-ray film TF-240 FLUXANA. This film is *c*.6.3 μm thick and has better x-ray transmission than Mylar film. It is useful for analyzing elements from Al upwards in the periodic table. Polypropylene's weakness is that it has a poor tensile strength and breaks more easily than Mylar. The assemblage of the pXRF instrument for laboratory measurements is shown in Figure 3-18a. The 'gun' (Figure 3-18b) was positioned under a portable shielded lead box stand which provides a safe platform for analysis of small samples (Figure 3-18c). While the instrument can carry out and store the measurements, a laptop was connected to the 'gun' in order to control conveniently the software. A helium purge device was attached to the 'gun' in order to increase instrument sensitivity to lighter elements. The cup containing the sample was then loaded into the stand and over the internal probe window.

The instrument's software was set up in 'soil' mode. A total of 33 elements are available for determination in this mode in the instrument (Mo, Zr, Sr, U, Rb, Th, Pb, Se, As, Hg, Au, Zn, W, Cu, Ni, Co, Fe, Mn, Cr, V, Ti, Sc, Ca, K, S, Ba, Cs, Te, Sb, Sn, Cd, Ag, Pd). The count times for different regions of energy spectrum were set in 30 seconds at high and low energies for light elements. The analyses were carried out for *c*.2 minutes and repeated three times at different areas of the same sample. The sample was then returned to the plastic bag and the tub cleaned for the next sample. The data, in parts per million (ppm), was transferred to the instrument data visualisation software (as ntd files) and converted to excel files for data analysis. The final three measurements were averaged for each sample and the accuracy and precision estimated.

Figure 3-18: Main components of the Thermo Scientific Niton XL 3t Goldd+ pXRF instrument: a-general set up of the pXRF for laboratory measurements using an external laptop; b-the 'gun'; and c-the shielded stand mounted above the 'gun' and used to carry out safe measurements of small samples.

3.5.1.3.5. *Quality Control & Analytical Error*

The reference standard samples and two control samples (a random sample from the sampled sites and a blank sample) were run at the beginning of each working day, during the sample analyses (after each 10 samples), and at the end of each day. The blank sample was measured in order to verify that no contamination existed in the instrument or on the probe window. The calibration check was to assess the accuracy of the instrument and the stability and consistency of the analysis and was carried out with international standards (TILL-4 and NIST 2780). The precision or reproducibility of the analysis was monitored by analyzing site samples repeatedly during the analytical day.

The accuracy calculated for each element is illustrated in Table 1. Accuracy is defined here as the deviation of a single (measured) observation from the true (certified) value (Gill and Ramsey 1997) and calculated as (measured/certified) × 100%. The accuracy test gave generally good result for the majority of elements except for S, V and Rb. The general accuracy of most of the elements was *c*.100±10%. The concentrations of V and Rb were found to be slightly overestimated. Nevertheless, these two elements were retained in the discussion, except S which was completely excluded from the analysis. The precision (Table 3-9) was determined by repeating the measurements of four random samples four times and calculating the coefficient of variation (CV).

Element	Accuracy	Precision (CV)	
Fe	97.14 %	0.91 %	Excellent
K	100.13 %	1.36 %	Excellent
Ca	98.78 %	1.54 %	Excellent
Ti	94.56 %	2.53 %	Excellent
S	1962.29 %	15.81 %	Satisfactory
Mn	111.97 %	3.73 %	Excellent
Zr	114.54 %	5.22 %	Good
Sr	108.28 %	0.96 %	Excellent
Pb	108.26 %	7.10 %	Good
Cu	92.28 %	11.67 %	Moderate
V	134.17 %	4.24 %	Excellent
Zn	87.11 %	7.74 %	Good
Rb	50.03 %	1.54 %	Excellent
Cr	120.64 %	4.46 %	Excellent
As	92.31 %	15.34 %	Satisfactory

Table 3-9: pXRF accuracy and precision determined for those elements where the soil concentrations were all above the limits of detection.

For each soil, the coefficient of variation (CV) was interpreted as: 0–4.9%= Excellent; 5.0–9.9%= Good; 10–14.9%= Moderate; 15–19.9%=Satisfactory; and >20%= Unsatisfactory. The results show an acceptable precision for all elements. Since the measurements were carried out in the laboratory, the ambient air temperature was constant, hence no further re-calibration of the instrument was needed.

3.5.1.3.6. *Reference*

Further information about the use of pXRF for soil analysis can be found in EPA (2007).

3.5.1.4. **ICP- OES Analysis**

3.5.1.4.1. *Purpose*

In addition to the pXRF analysis, a series of soil sub-samples were analysed for multi-element concentration (enhancement and depletions) of a range of major and trace elements using inductively coupled plasma optical emission spectrometry (ICP-OES). Soil chemical changes produced by human activity can persist for a long time and depletions and enrichments of anthropogenic chemical elements (Chapter 2) can be determined by ICP-OES analysis of soil samples collected at archaeological sites. The aim was to compare the results with the pXRF data and to obtain further information about trace element concentration of those elements outside the limits of detection of the pXRF technique. An element of special interest was phosphorus (P) which was selected in order to compare with the Total P results.

3.5.1.4.2. *Instrument*

The technique is based on the decomposition of a liquid sample into its constituent atoms or ions using the intense heat (*c*.10,000°C) produced by inductively coupled plasma (a state of matter containing electrons and ionised atoms of Argon). The high temperature causes excitation and ionisation of the sample atoms. Once the atoms or ions are in their excited energy states, they can decay to lower energy states whilst emitting light of specific wavelengths. In OES, the intensity of the light emitted at specific wavelengths is measured and used to determine the concentrations of the elements of interest. The technique

requires calibration for quantitative analysis, which involves comparing the intensity of light emitted by solutions of known metal concentrations with that of unknown sample solutions.

The analysis was performed with an axial-view ICP-OES instrument, Varian Vista Pro at the Scottish Alliance for Geosciences, Environment and Society (SAGES) facility at the School of Geosciences at the University of Edinburgh. The instrument is a fast multi-element analyser with a dynamic linear range and moderate detection limits (~0.2-100 ppb). It can screen up to 60 elements per single sample run of less than one minute.

3.5.1.4.3. *Limitations*

Like the pXRF, this technique measures the total element concentration of the samples but it does not provide the chemical form (speciation).

The analysis of prepared soil samples by the ICP-OES is very fast and provided a good accuracy, especially for lighter (trace) elements. However, the preparation of the samples involves extracting the elements from the soil by some form of wet digestion method in order to effectively recover the total (or near total) element concentrations in that soil. This involves the use of acids, hence the destruction of the sample. This sample preparation process increases substantially the time and costs required to prepare the sample for analysis.

There are a series of problems relating to the sample preparation and the analytical method:

- Part of the sample can be lost during sample preparation (e.g. weighing the samples, digestion process).
- Spectral interference between different elements (i.e. similar wavelengths of different elements).
- Matrix effects caused by high concentrations of an element in a sample (i.e. elements easily ionisable such as Na, K, Mg or Ca). These can change the way the sample is introduced to the flame or the thermal characteristics of the plasma and lead to either an under or overestimation of concentration.

3.5.1.4.4. *Procedure*

The samples were air dried, homogenized, and sieved (2mm) before digestion. The digestion of the soil samples and the ICP-OES measurements were carried out by the author and Dr Walter Heibert (School of Geosciences, University of Edinburgh) at the trace-metal clean laboratory at the School of Geosciences (University of Edinburgh) (Figure 3-19). 50 mg soil samples were digested in a mixture of HF/HCl/HNO3 in a CEM Mars Xpress microwave digestion system (24 TFM vessels) at a temperature up to 205˚C. Samples were dried in a microwave-assisted evaporation system (XVap) connected to a vacuum pump. Finally, the samples were re-digested in 25mL of 2% nitric acid, which corresponds to a 1:500 dilution. This microwave system allows the digestion of samples in a closed environment, allowing the evaporation of acids after digestion in a safe and rapid manner without the risk of contaminating or oxidising the analytes, as is often the case in hotplate evaporation. The choice of a strong acid (HF) digestion method was based on the need to break down the more resistant soil minerals to ensure an effective recovery of all or near all elements in the soil samples in order to understand the nature of the fraction that is recovered.

Weak acid digestions are only limited to recovering the plant available fraction and are unable to break down the geological fraction. Further information on extraction can be found in Middleton (2004), Wells (2004) and Wilson *et al.* (2005, 2006).

The ICP-OES analysis measured 18 elements; Al, Fe, Na, K, Ca, Mg, Ti, P, Mn, Ba, Sr, Pb, Cu, Zn, Cr, Ni, Li, and Co. The first four batches of 20 samples (+2 blanks, +2 reference materials) were evaluated using an external calibration, batches five and six were evaluated using scandium as an internal standard. The certified reference material MESS-3 was used to monitor the quality of the entire analytical process in each batch of digestions. With each batch of samples, two procedural blanks were run to control blank levels and variability.

Figure 3-19: ICP-OES analysis: a-trace/metal clean laboratory (School of Geosciences, University of Edinburgh); b-strong acid sample digestion; c-personal protective gear; d-CEM Mars Xpress microwave digestion system with evaporation system (XVap) and attached vacuum pump; and e-Varian Vista Pro instrument.

3.5.1.4.5. *Quality Control & Analytical Error*

The measurement accuracy and the quality of the entire analytical process in each batch of digestions were assessed by using the certified reference material MESS-3. Accuracy was calculated as in the pXRF analisis and gave a general good result for the all the elements. The external reproducibility and data quality were evaluated using six repeated measurements of two samples of the standard reference material (MESS-3). For each soil sample, the coefficient of variation (CV) was calculated and interpreted as: 0–4.9%= Excellent; 5.0–9.9%= Good; 10–14.9%= Moderate; 15–19.9%= Satisfactory; and >20%= Unsatisfactory. This assessment showed a general excellent precision for all elements (Table 3-10).

Element	Accuracy	Precision (CV)	
Al	94.34 %	0.80 %	Excellent
Fe	98.63 %	1.19 %	Excellent
Na	91.60 %	1.73 %	Excellent
K	98.06 %	5.93 %	Good
Ca	93.91 %	0.89 %	Excellent
Mg	103.78 %	0.69 %	Excellent
Ti	98.92 %	0.73 %	Excellent
P	95.58 %	1.11 %	Excellent
Mn	86.80 %	1.30 %	Excellent
Ba	108.81 %	1.72 %	Excellent
Sr	98.86 %	0.54 %	Excellent
Pb	93.00 %	3.12 %	Excellent
Cu	100.86 %	0.55 %	Excellent
Zn	92.22 %	2.49 %	Excellent
Cr	100.57 %	1.19 %	Excellent
Ni	102.81 %	1.87 %	Excellent
Li	91.83 %	0.66 %	Excellent
Co	111.56 %	7.83 %	Good

Table 3-10: ICP-OES accuracy and precision.

External reproducibility for many elements was around 2-5% and mainly controlled by inhomogeneities in the samples, the uncertainties associated with weighing very small samples, and error propagation with the dilution steps during the digestion stage. There were no values for Zn available for the samples from the Bay of Skaill (Chapter 5) as the external calibration failed.

3.5.1.4.6. *Reference*

Further information about ICP-OES analysis can be found in www.sassa.org.uk.

3.5.2. Other Soil Analyses

The sub-samples collected at the archaeological sites were also analysed for soil texture and MS. The aim was to obtain additional information about the macroscopic physical and magnetic properties of the soil samples which may contribute to the understanding of potential correlations between the archaeological features and their respective geophysical and geochemical anomalies. They may also contribute to understand soil physical and mechanical properties that affect the results of the geophysical or geochemical techniques. As a pilot study, optically stimulated luminescence (OSL, a technique generally used in sediment dating) was used to characterise the dose rate of the samples collected at Forteviot (Chapter 7). The aim was to correlate potential signal intensities and depletion rates with the location of the targeted archaeological features and any possible association with the geophysical and geochemical anomalies.

3.5.2.1. **Soil texture analysis**

3.5.2.1.1. *Purpose*

To characterise the general macroscopic physical properties of the soil samples by describing the different soil organic and mineral horizons.

3.5.2.1.2. *Limitations*

The analysis was carried during the soil sampling and revised during the laboratory phase of the project. Therefore, the descriptions may not reflect soil conditions present during the geophysical surveys. Nevertheless changes in soil moisture due to rainfall and other observations were noted during the surveys and taken into account in the discussion of the results of each case study site.

3.5.2.1.3. *Procedure*

Soil texture descriptions were carried out in the field during soil sampling at each site using a standardised form (Figure 3-20). The samples were re-assessed at the laboratory phase of the project. The sites where only topsoil samples

were sampled were not systematically analysed. The procedure and terminology used in site and soil texture description are based on the National Soil Inventory of Scotland (NSIS_1) protocols (Lilly *et al.* 2010).

3.5.2.1.4. *Reference*

Further details and the full protocol used during the texture analysis can be found at www.macaulay.ac.uk/issues/NSIS1_protocols.pdf.

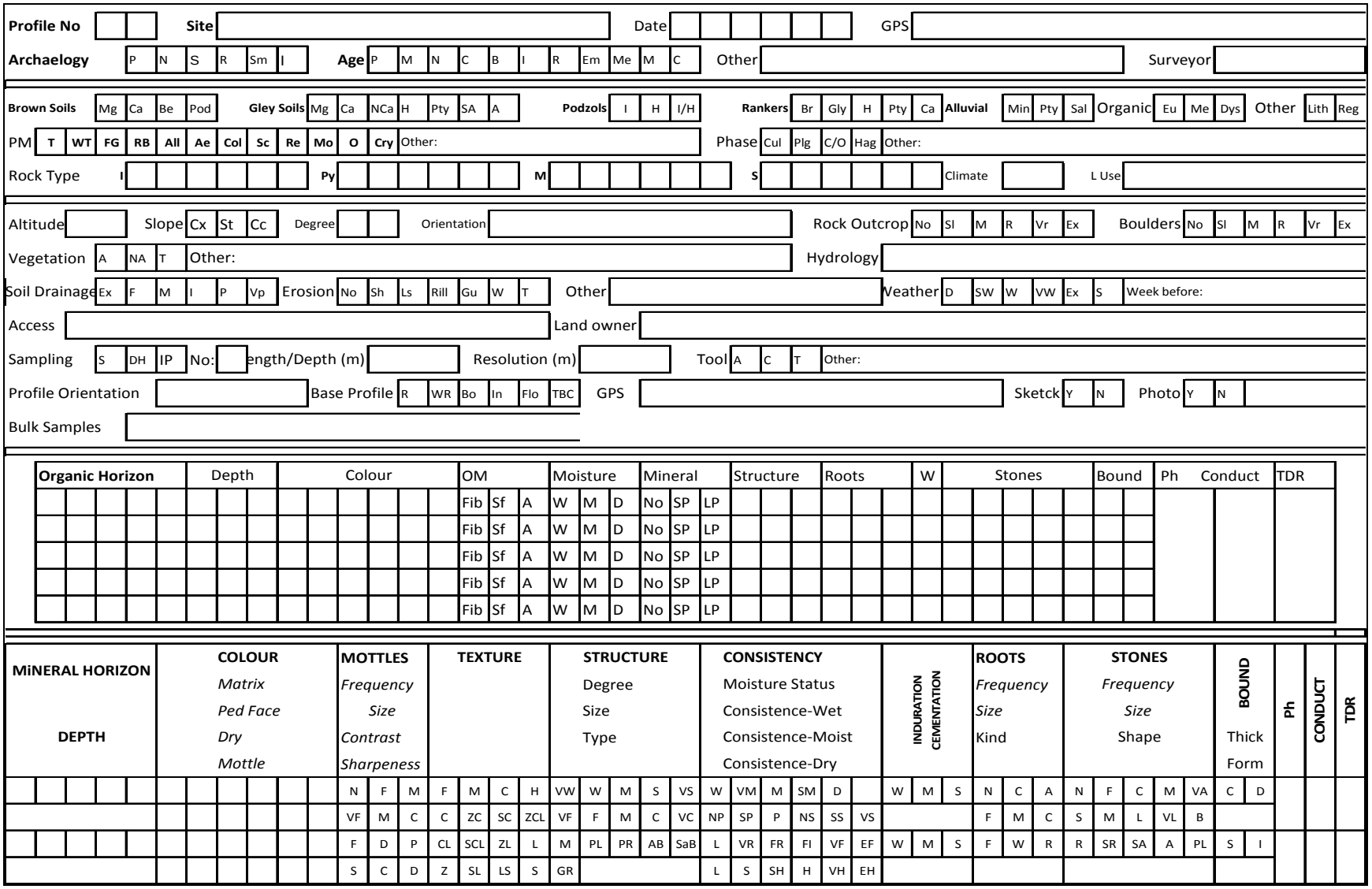

Figure 3-20: Soil texture and site description form (modified from Lilly *et al.* 2010)

3.5.2.2. **Soil Magnetic Susceptibility Analysis**

3.5.2.2.1. ***Purpose***

Topsoil samples taken over the targeted archaeological features or from excavated sections at the different sites were measured at the laboratory to determine their MS. The magnetic properties of soil, including MS, are explained in section 2.4.2.1 and the single-coil magnetic susceptibility field instrument is detailed in section 3.4.2.6. MS of soil samples is generally expressed as volume specific (κ) or mass specific (χ). The latter takes into account potential differences in sample density which improves the comparison of measurements. The units for mass specific susceptibility are expressed in $10^{-8}m^3kg^{-1}$. The sample preparation for MS analysis is minimal and the measurements are simple, safe, fast and non-destructive. Most of the laboratory soil MS analysis for archaeological investigations uses dual frequency Bartington sensors. Low frequencies (0.46 kHz) analysis is used in standard measurements of archaeological samples (Dearing 1999). High values of χ_{lf} may indicate enhancement in susceptibility due to anthropogenic activity, such as occupation, industrial ativity and/or heat-affected areas.

By measuring the magnetic susceptibilities also at high frequencies (4.6 kHz) (χ_{hf}) it is possible to establish the presence of ultrafine (<0.03μm) superparamagnetic (SP) ferromagnetic minerals. These SP grains occur as crystals and are produced by biochemical processes in soil which may be indicative of anthropogenic activity (Clark 1990, 103). If ultrafine minerals are present in samples the measurement will produce slightly lower values at a high frequency than at low frequency; samples without the minerals will show identical values at the two frequencies because the delayed response of SP grains to a magnetic field induced at higher frequency, produces a decrease in susceptibility (Dalan 2006, 164). Therefore, the difference in the χ_{lf} and χ_{hf} of the two measurements at different frequencies (frequency-dependent susceptibility, χ_{fd}) may indicate the presence and amount of SP grains hence, an artificial enhancement of the soil susceptibility. There is a debate about the precise physical basis for frequency dependence as crystals smaller than ~0.03μm may show reduced susceptibility values at the high frequency measurement. χ_{fd} is generally expressed as a percentage (%) of the original low frequency value. Maximum values for soils in

England and Wales are 12-14 %. Values over 14% are rare and may indicate an erroneous measurement, or contamination. The following values give an indication of χ_{fd} percentage (Dearing 1999):

- Low values are <2% and indicate natural soils without SP grains.
- Medium values between 2-10 % suggest a mixture of SP and coarser non-SP grains, or SP grains <0.005 μm
- High values of 10-14 % point towards >75 % of SP grains present in the soil sample.

Generally speaking, an increase in χ_{fd} suggests an increase in SP grains, and a high χ_{lf} and high χ_{fd} is potentially indicative of a developed or enhanced soil related to human activity.

The aim of the laboratory soil analysis in this project was to asses the bulk MS of the samples in order:

- To provide additional information about the factors contributing to the soil contrast detected by geophysical means (e.g. gradiometer survey). The anomalies detected by gradiometer surveys are the result of the contrast produced by a net effect of any induced and/or remanent magnetization. Therefore, MS measurements can complement the gradiometer results by distinguishing features or soil samples resulting from susceptibility contrast, from those carrying a magnetic remanence (Dalan 2008).
- To determine the MS of the topsoil and subsoil in order to further characterise the survey soil environment at the different sites. MS can provide with information about the mineralogy and geochemistry of the environment in which the soil samples were collected. From mineralogy, additional information about the samples can be deduced such as its origin or the chemistry of its environment (Dearing 1999).
- In association with chemical concentrations, to characterise the magnetic status of potential enrichment or depletion of major heavy metals such as Fe (e.g. potential Fe/Mn reduction processes) from samples collected inside features.

- To contribute to establish the natural or anthropogenic origin of elemental concentrations by assessing the χ_{fd} values of the soil samples.

The results of this analysis are presented with each case study site (Chapters 4 to 8). Only the standard χ_{lf} values are shown in the figures and tables of the chapters in order to simplify data presentation. The complete list of the χ_{lf} , χ_{hf} and χ_{fd} results is given in Appendix C.

3.5.2.2.2. *Instrument*

Bench soil MS measurements were carried out using a Bartington MS2 Susceptibility System (Figure 3-21). The system consists of a meter attached to a sensor. The meter expresses MS in either cgs (centimetre, gram, second) or SI (standard international) units (used in this project). A Bartington MS2B laboratory sensor in Archaeology (University of Glasgow) was used for the measurements. This is a dual frequency coil that analyses a single 10cm^3 sample.

Figure 3-21: Bartington MS2B sample sensor and meter.

3.5.2.2.3. *Limitations*

The instrument sensor is sensitive to some external factors such as changes in temperature, presence of magnetic materials and electromagnetic fields. These factors may affect the stability of the sensors (e.g. irregular or noisy drift) and hence the accuracy of the measurements.

3.5.2.2.4. *Procedure*

- Sample preparation: The samples were dried at room temperature, ground using a mortar and pestle and sieved (500μm).The samples were put into pre-weight 10cm^3 plastic cups, making sure the container was completelly full in order to avoid errors in volume calculations. The samples were then weighed in order to calculate mass-specific (χ) MS.

- Instrument stabilization: Before the measurements, the instrument was left to stabilise for at least two hours. The instrument was checked periodically for about 10 minutes to ensure it was stable, by logging air readings (measurements without a sample). A constant zero indicated that the instrument was ready to start.

- Analysis: Samples were measured at low frequency (χ^{lf} = 0.46kHz) and at high frequency (χ^{hf} = 4.6kHz). These measurements were used to calculate frencuency dependent mass susceptibitly (χ^{fd}) in %. The software MultiSus (by Bartington) was used to take the measurements. The program prompts the user to perform the measurement step by step, and corrects for the weight of the container before automatically recording the mass-specific readings for each sample. For each sample, high and low frequency averaged readings are automatically calculated for frequency-dependence. All the readings and statistics are recorded in an Excel-compatible spreadsheet.

3.5.2.2.5. *Quality Control & Analytical Error*

Since the instrument is fairly sensitive, the sensor was always positioned in a quiet and stable surface, away from magnetic material, electromagnetic fields and changes in temperature. The users removed rings, jewellery and other metal personal objects that could affect measurements and avoided touching the sensor. The instrument calibration was assessed and monitored by measuring two standard samples, ST1 (ferrimagnetic) and H_2O (diamagnetic). The accuracy of the measurements was partly controlled by calibration which allows comparisons with the two known references.

The samples were measured at low frequency mode first and, after re-zeroing, they were re-measured in high frequency mode by placing the samples in the

exact centre of the holder and in the same orientation as position can affect measurement of the sample. The tab on the sample was used as a reference point. This procedure was followed in order to make the measurements more systematic and avoid errors introduced by small directional variations in susceptibility (Dearing 1999).

The equipment precision is high at <1% (Dearing 1999) and the repeatability of measurements as defined by the manufacturer is in the order of 1%, based on operating conditions are often not ideal (e.g. with thermal effects and vibrations that can significantly alter the theoretical precision of the equipment and produce drift). In order to control the effect of these external factors, each sample was measured 5 times and a standard deviation and mean was automatically calculated and saved by the software MultiSus. The readings with a standard deviation >~2 were cancelled and repeated.

3.5.2.2.6. *Reference*

The MS analisis was carried out following the operation manual (Bartington Instruments 2008).

3.5.2.3. **Optically Stimulated Luminescence (OSL) Analysis**

3.5.2.3.1. *Purpose*

Soil samples collected at Forteviot (Chapter 7) were analysed using an optically stimulated luminescence (OSL) reader. Whilst the OSL technique is generally used for dating, this was not the aim of this analysis. The aim here was to test the capacities of the instrument to detect variations in luminescence signals in topsoil samples collected across a targeted ditch enclosure and from its excavated sections which may be indicative of the presence of the targeted ditch.

The technique is based on sample stimulation by light in the blue (BLSL) and infrared (IRSL) wavelengths using an OSL reader. The instrument can determine the luminescence signal that is stored (paleodose) in the crystal lattices of sediment grains from soil samples by counting the photons emitted after the grains are stimulated since they were last exposed (bleached). The intensity of the signal stored in the soil samples is a product of the deposition, burial or

sedimentation and subsequent exposure to ionizing radiation from natural radioactive elements in the surrounding sediment. These natural radioisotopes are uranium (238U, 235U), thorium (232Th) and potassium (40K) (Aitken 1998, 39) and, in minor amounts, cosmic rays (Prescott and Clay 2000) also contribute to the radiation dose. This radiation can excite electrons in sediment grains' crystal lattices from their stable orbits to more energetic ones. When sunlight or heat provides the energy for the electrons to return to their stable orbits, photons may be emitted (Muñoz-Salinas *et al.* 2011). The amount of luminescence emitted is proportional to the accumulated dose since the minerals were last exposed to heat, (e.g. by pot firing) or light (e.g. to day-light during sediment transport). A sample whose mineral grains have all been exposed to daylight can be bleached of luminescence and not emit any photons. The older the sample is, the more intense the signal is. Both quartz and many feldspar minerals act as dosimeters recording their exposure to this ionizing radiation. Quartz is excited by blue or green light and measures the near ultra-violet emission. For feldspar or silt-sized grains, the technique uses infra-red excitation and measures the violet emission.

For dating analysis two parameters are needed; the equivalent dose (i.e. the luminescence signal stored in the grains since the last resetting event), and the dose rate (i.e. the ionizing energy from from α, ß and γ radiation emitted by naturally occurring radioisotopes in the deposit, plus the effects of cosmic radiation). The naturally occurring α, ß and γ dose rates are counted using α, ß and γ-ray spectrometers, adding the cosmic ray dose (Prescott and Hutton 1994). The sediment age is calculated by dividing the palaeodose (in grays) by the dose-rate (in grays per year) (Aitken 1998). In this investigation, only the luminescence equivalent dose was used.

OSL analysis has been demonstrated to be useful to provide valuable insights into complex depositional systems. Sanderson and Murphy (2010) have described situations in connection with tsunami deposits and archaeological ditch-fills where useful information could be obtained using simple, uncalibrated measurements. Muñoz-Salinas *et al.* (2011) demonstrated that total photon counts from a portable OSL reader can also provide valuable data for interpretation of fluvial sedimentological processes in geomorphological studies. High readings may be either associated with old deposits buried for a long time

or with the inheritance of unbleached OSL signals in modern deposits (Muñoz-Salinas *et al.* 2011).

3.5.2.3.2. *Instrument*

A portable OSL system (Figure 3-22), designed and built by the Scottish Universities Environmental Research Centre (SUERC), was used for recording luminescence signals that are related to the equivalent dose. The portable configuration, make this instrument available during fieldwork for simple measurements of luminescence intensities from bulk sediments.

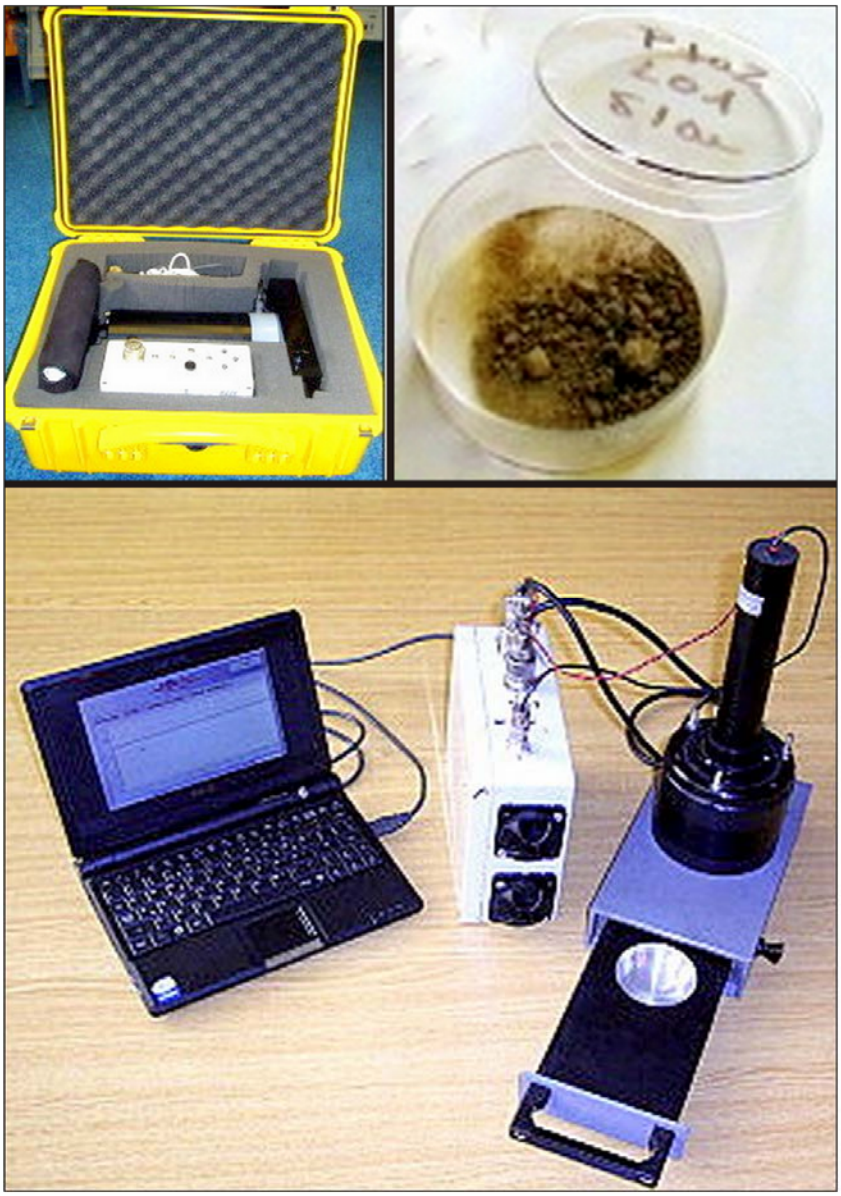

Figure 3-22: SUERC portable OSL reader system packed in a 5 kg compact field-case (top-left), Petri dishes used for the measurements (top-right) and the instrument ready for analysis (bottom) (modified from Sanderson and Murphy 2010).

The OSL reader comprises a single photon counting photomultiplier and a light-tight sample chamber where samples are stimulated with photons from arrays of light-emitting diodes in the blue and infrared portions of the electromagnetic spectrum (Sanderson and Murphy 2010). The portable OSL reader can be powered by batteries or by 'mains' power supply so that it can be used during fieldwork or in the laboratory. The main advantages of the instrument are that the reader is easy, quick to use and cheap in comparison with other techniques.

3.5.2.3.3. *Limitations*

Since samples can be optically bleached if they are exposed to sunlight, the sampling should be carried out at night or during the day using a dark cloth to cover the area. Samples can be taken using opaque containers from cleaned section profiles and sealed against the light immediately the sample is extracted. However, for this PhD research, the analysis was planned after the samples were collected and the safe light conditions mentioned above were not followed. Since the samples were kept in a dark environment a preliminary test analysis confirmed the samples were not heavily bleached and further samples were measured. Water content saturation of the sediment has an attenuating effect on the intensity of the natural radiation dose rate (Aitken 1998, 43), decreasing the signal in deposits and therefore introducing a component of uncertainty. Grain size can also influence the luminescence signal by mechanisms that are not yet completely understood (Muñoz-Salinas *et al.* 2011).

3.5.2.3.4. *Procedure*

Fresh samples were placed in disposable 5 cm diameter plastic Petri dishes (Figure 3-22) and introduced to the measurement drawer in a dark environment. The portable OSL readings were performed using the following sequence: 15 seconds of dark counts; 30 seconds of stimulation in the blue stimulation light (BLSL); 30 seconds in the BLSL (repetition); 15 seconds of dark counts. The 60 seconds sequence was repeated for the infra-red band (IRSL). The data was imported to Excel for editing, to calculate the analytical error (estimation of the standard deviation at >2 error level) and to plot the results. For the purposes of this experimental analysis, only the results of the BLSL are shown in the results (Chapter 7).

3.5.2.3.5. *Quality Control*

Approximately the same volume of material of each sample was dispensed into each Petri dish in order to standardize the results and avoid empty spaces. If grains are overlapping, the luminescence signals will come only from the surface grains. With the sample chamber empty a blank reading was repeated each 10 samples and at the end of the analytical day in order to check there was no contamination in the sample chamber.

3.5.2.3.6. *Reference*

Further information about the portable OSL reader can be found in Sanderson and Murphy (2010).

3.5.2.4. **Data Analysis & Correlations**

The evaluation of the results from the different soil analysis was done by the use of elementary statistics. The results were presented in tables and diagrams built with Excel and Minitab. From the geochemical data, relevant enhancements and depletions were established by assessing their particular concentrations in the samples taken inside and over (topsoil) the features. The results were compared to off-site controls and general backgrounds found in the literature and other databases. Bivariate correlations were calculated using Pearson and Spearman coefficients between the different elements and other soil analysis (total phosphate, MS, LOI, pH and conductivity) in order to determine the strength in association between two variables. The correlation coefficients were calculated using Minitab and the results presented in scatter plots and matrix plots. The correlations were significant at the 0.05, 0.01 and 0.001 level (2-tailed). Since most of the soil analysis data was not normally distributed owing to the nature of some of the relationship between the different variants not being linear, the non-parametric Spearman correlation was finally used.

The responses obtained from the geophysical data were compared to relevant enhancements and/or depletions from the chemical data and other associations established from the various soil analysis. The aim was to identify associations between the results from the different datasets of each case study site in order to explain the nature of the geophysical and geochemical anomalies detected and to assess the general survey environment.

Part II: Case Study Sites

Chapter 4

Surveying over Podzolic Soils: the Burial Cairn at Scalpsie Bay (Isle of Bute)

4.1. Introduction

Scalpsie Bay is not only a beautiful spot to visit on the Isle of Bute, it also contains an interesting concentration of geological features and prehistoric sites. A grassy pasture field located over raised marine deposits contains two examples of monuments associated with prehistoric burial and ritual: a Bronze Age barrow and an undated burial cairn. The Bronze Age barrow was excavated at the beginning of the 20th century and a cremation burial cist was found. The excavation was published and the document includes drawings of the cairn, cist and finds (Bryce 1904). However, little is known about the adjacent burial cairn apart from the discovery of a cist during its partial demolition to cultivate the land (NMRS N^{o} NS05NE9).

The archaeological significance of Scalpsie Bay along with the lack of knowledge regarding the current structure and preservation status of the burial cairn made the case to investigate this area, hence attracting the interests of the Discover Bute Landscape Partnership Scheme (DBLPS) project. The DBLPS aimed to preserve the distinctive landscape features of the isle of Bute, to boost tourism and to raise awareness and appreciation of the natural and historic environment of Bute (DBLPS 2011). One of their major objectives was the survey and assessment of the archaeology of Bute.

The DBLPS had in mind to carry out an excavation at the barrow (east cairn). Since intrusive archaeological investigation within the field with the two cairns was limited and focused on the re-assessment of the barrow, only non-intrusive techniques, such us geophysical survey, were deemed to be used in order to further investigate the overall site. Therefore, the DBLPS supported this PhD project.

4.1.1. Research Problem

The site lies in a varied lithological setting characterised by podzolic sands, glacial drift materials and meta-igneous geology. Spurious geophysical signals caused by iron-pans, developed in podzolic soils, like the humus-iron podzol present at the survey area, have been reported (Barton *et al*. 2009). Also, electromagnetically noisy unsorted and heterogeneous glacial till deposits (Jordan 2009; Viberg *et al*. 2011) may affect the detection of archaeological features by geophysical techniques. These podzols are characterised by heavy leaching which also may affect geochemistry (Oonk *et al*. 2009a). These challenging soil settings for archaeological prospection along with the archaeological potential of the area offered a good opportunity to use this site as a case study. Also, the confident location of targets relating to the burial cairn and the prospects for soil sampling and ground-truthing within the Discover Bute Landscape Partnership Scheme (DBLPS) project framework contributed to this.

This case study focuses on the results of the geophysical survey and the geochemical soil analysis over the burial cairn and its environs. The study aimed to assess the detection potential of a range of geophysical techniques and geochemical soil analysis in a site characterised by podzolic and varied soils and promising coastal archaeology. The investigation also aimed to contribute to the general archaeological enhancement of the burial cairn and its environs in order to contribute to the aims of the DBLPS project.

4.1.2. Location

Scalpsie Bay is located on North Bute parish (Argyll & Bute district), in the west coast of the isle (Figure 4-1). It is situated at the extreme south of a valley that runs about 6.7km south-westwards from Rothesay.

The site area (NRG NS 05815 58641 centred) is *c*.400m north of Scalpsie beach and *c*.520m south-east of Loch Quien. It lies in a flat pasture field just above the 10m OD contour and slopes steadily southwards towards the sea in the form of terraces. Quien burn and a small drain run along the east and west margin of the site respectively. The A844 road passes by the north-east of the site area.

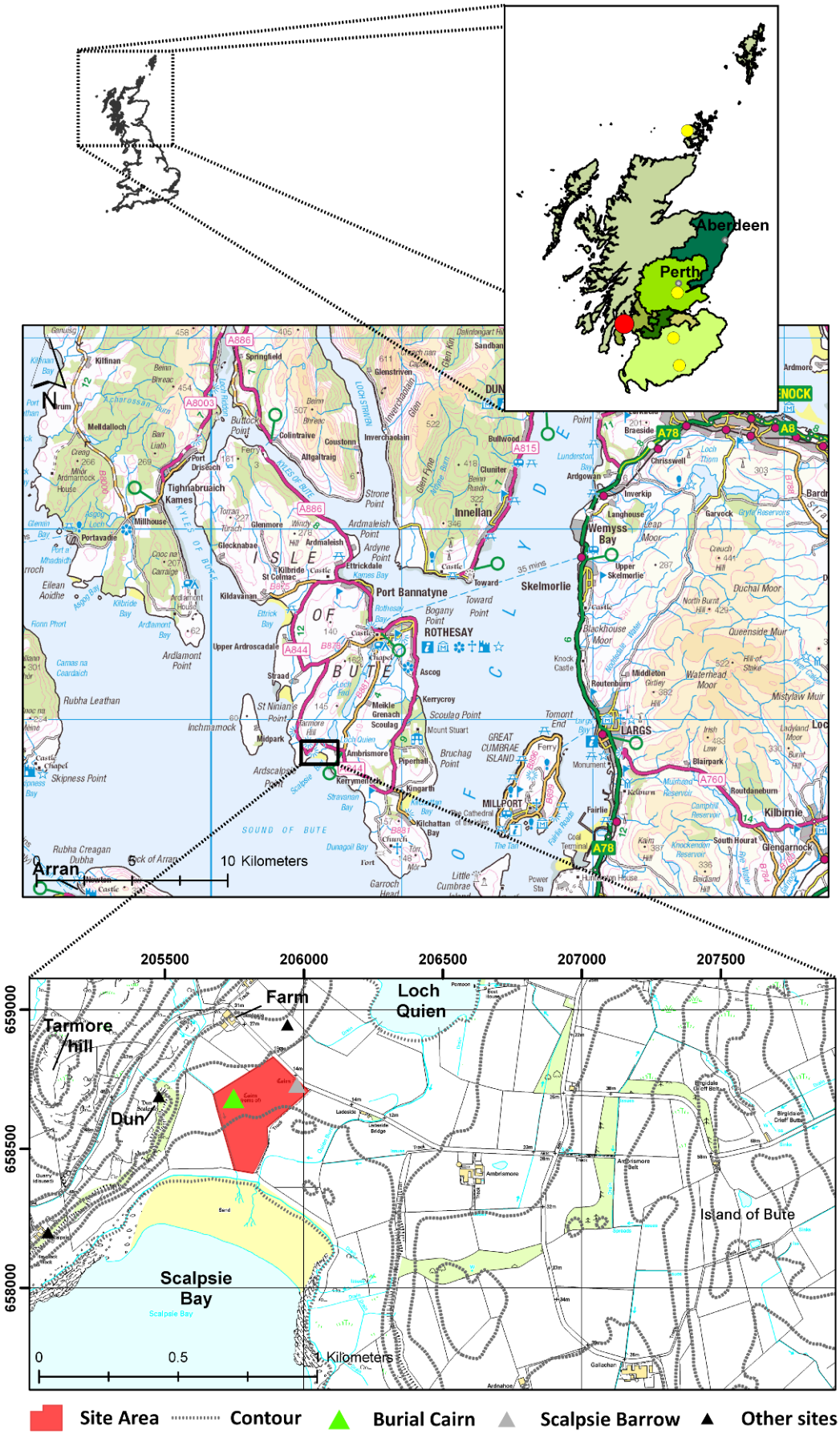

Figure 4-1: Location map (top figure) of Scalpsie Bay (red dot) in Argyll & Bute district (Strathclyde region) and in relation to the other case study sites (yellow dots). In bottom map, the pasture field that comprises the site area is delimited in red, showing the location of the burial cairn, the barrow and other prehistoric sites (based on © Crown Copyright/database right 2012. An Ordnance Survey/EDINA supplied).

The burial cairn (NRG NS 05747 58672) is located approximately 200m westwards from the barrow, in a pasture field owned by John Dickson from Scalpsie Farm. The farm is *c.*300m north of the site area and immediately north of the farm, the land rises abruptly to 80m above sea level at Tarmore hill.

4.1.3. Geology, Soils & Land Cover

4.1.3.1. **Bedrock & Superficial Deposits**

The underlying bedrock at the site is mainly formed of sedimentary rocks with a small meta-igneous area in the north-west, where the burial cairn is located (Figure 4-2). This latter area is linked with the presence of the Highland Boundary fault close to the west of the site area.

The geological formation present in most of the site area is the Upper Old Red Sandstone of late Devonian age (*c.*370-354 mya). The lithological classification corresponds to the Bute Conglomerates Formation of the Stratheden Group (Figure 4-2). This formation comprises mainly conglomerates with subordinate red pebbly sandstone and it is between 1000-1500m thick (Browne *et al*. 2002). The meta-igneous area corresponds to serpentinite rocks of early Cambrian-Arenig age (545-470 mya), related to the Highland Border Ophiolite complex (Bluck 2010).

Three types of superficial deposits are present in the site area (Figure 4-3). Sands and gravels of raised marine deposits of Flandrian age (Interglacial 10,000 BP) area present in most of the site area, including the burial cairn. These deposits are variable in lithology, including gravel (shingle), sand, silt and clay. They also are commonly charged with organic debris (plant and shell). These marine deposits are now above the level of the present shoreline as a result of the glacio-isostatic crustal uplift in response to the unloading of the ice sheet over Britain (Lambeck 1991). Superficial deposits change reaching the NE of the site. They consist of variable glacial till. Their lithology is variable but is usually sandy, silty clay with pebbles. They can contain gravel-rich or laminated sand layers. These deposits underlie the area where the barrow is located (Figure 4-3). Aeolian deposits of wind blown sands occur in the south of the site area.

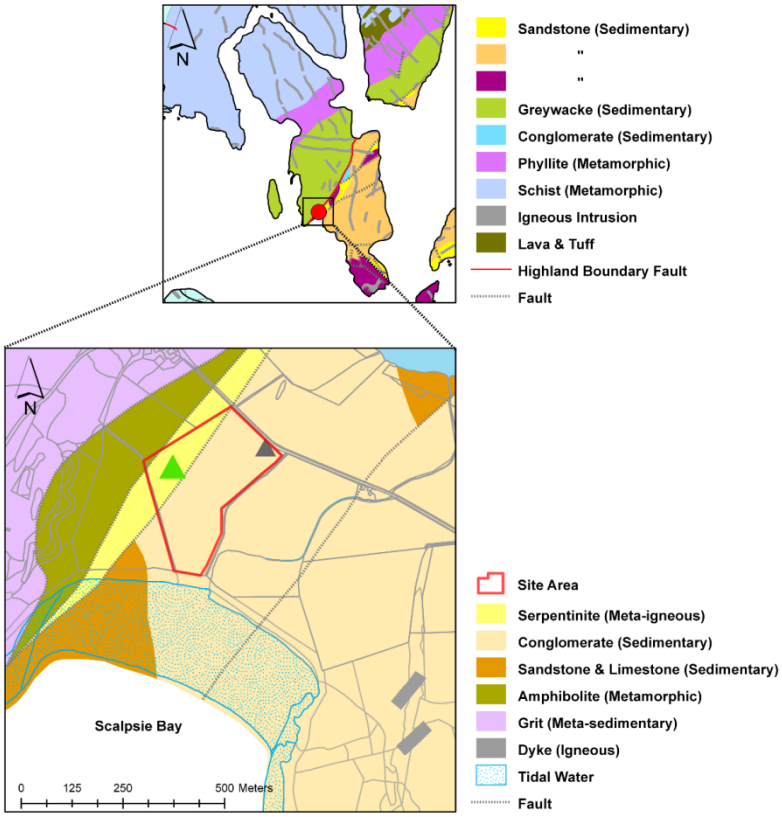

Figure 4-2: The underlying solid geology of Bute and Scalpsie Bay. The green and grey triangles show the location of the burial cairn and barrow in meta-igneous and sedimentary areas respectively (based on Geological Map Data © NERC 2012).

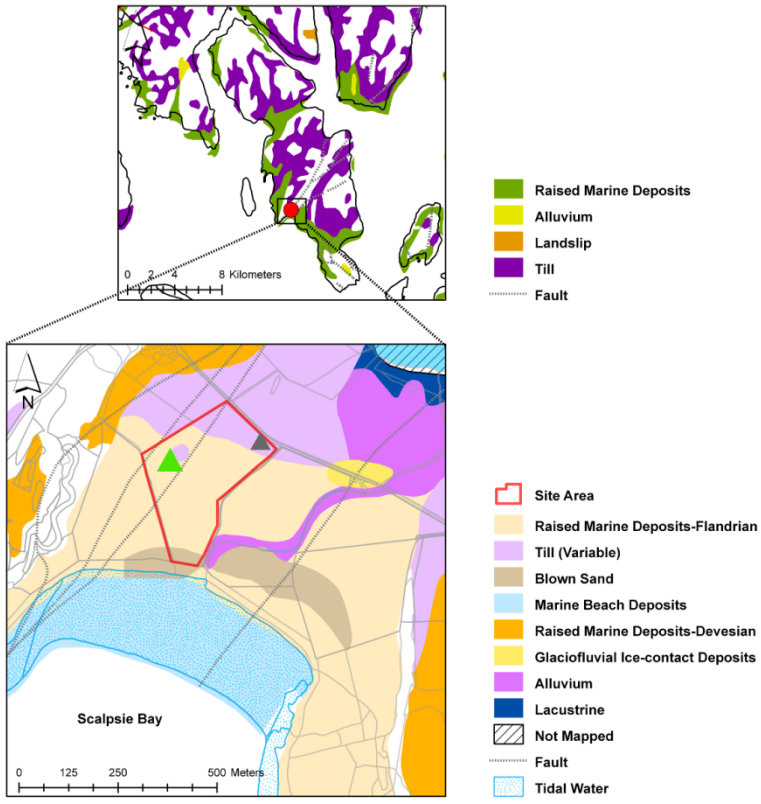

Figure 4-3: Superficial deposits at Scalpsie Bay. The green and grey triangles show the location of the burial cairn and barrow in the raised marine deposits and till areas respectively (based on Geological Map Data © NERC 2012).

4.1.3.2. **Soils**

The preliminary classification of the soils at Scalpsie Bay was slightly difficult since the information from the Soil Survey of Scotland (maps) and the SIFSS did not correlate. Therefore, some exploration (augering) was needed in order to determine the type of soils. The soils of Scalspie Bay correspond to the Corby/Boyndie/Dinnet association (Bibby 1984) and they are a mixture of humus-iron podzols, humic gleys and alluvial soils (Macaulay Land Use Research Institute 2010a). These soils developed from the raised marine, fluvioglacial and morainic sands and gravels which were mainly derived from acidic rocks.

The general soil profile recorded on the area by the web interface 'Soil Indicators for Scottish Soils' (SIFSS) of the Macaulay Landscape Research Institute is shown on Figure 4-4.

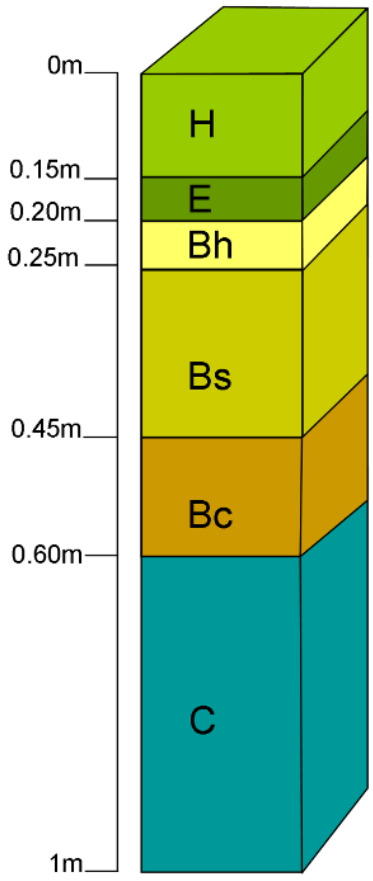

Figure 4-4: Soil horizons and depths of humus-iron podzols at the site area described by the Soil Indicators for Scottish Soils (SIFSS) database (Macaulay Land Use Research Institute 2011).

These soils are characterised by a humus layer (H) followed by an ash-grey eluvial horizon (E), which is structureless and rich in silica, and then by a humus (Bh) and/or Fe/Al (Bs) enriched illuvial horizon. Their formation is based on the leaching of soluble metal-humus complexes (Fe and Al) out of the surface to greater depth which creates a grey, silica-rich horizon (E) and their accumulation in the subsoil (B) which may contein (Bc) presence of mineral concretions (*e.g.* of Fe or Al). The eluvial horizon (E) represents all that remains of the original parent material after it has undergone extreme chemical weathering by humic acids produced by the decay of the vegetation.

The texture of these soils is generally loamy sand (Figure 4-5) with abundant gravel rounded or sub-rounded. These are free-draining soils of pale brown to greyish colour in the E horizon, whilst the Bh/Bs horizon presents generally strong brown colours. Iron-pans may form in such podzols due to periodic water stagnation (see section 2.2.3).

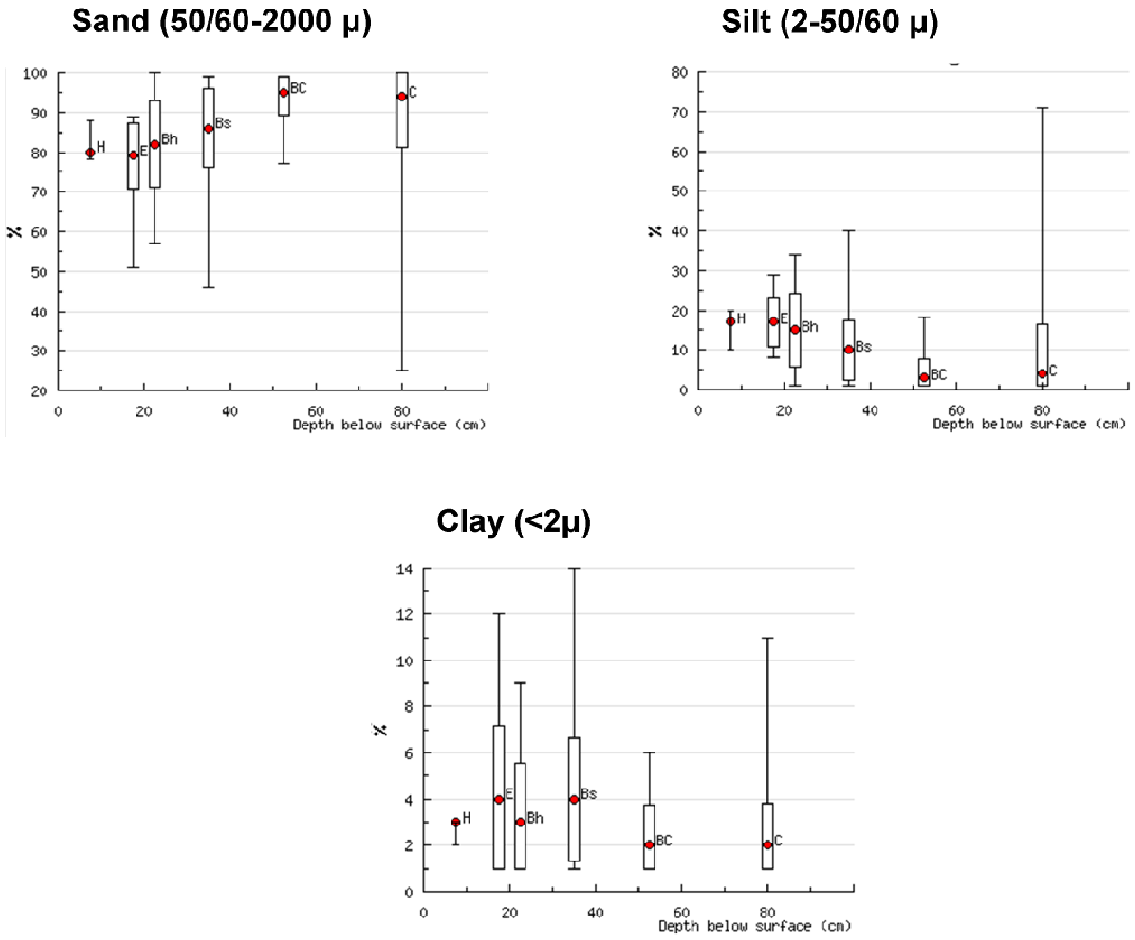

Figure 4-5 Particle size distribution of Corby soil series from the Soil Indicators for Scottish Soils (SIFSS) database (Macaulay Land Use Research Institute 2011).

Podzols are inherently acid because of the nature of the parent material and the breakdown of organic matter. Figure 4-6 (a) shows the high percentage of organic matter contained in the H horizon of the Corby soil series. Accordingly, pH (Figure 4-6, b) shows the highest level of acidity in the H horizon (pH 4), decreasing with depth to more neutral values (pH 5.3) for the C horizon.

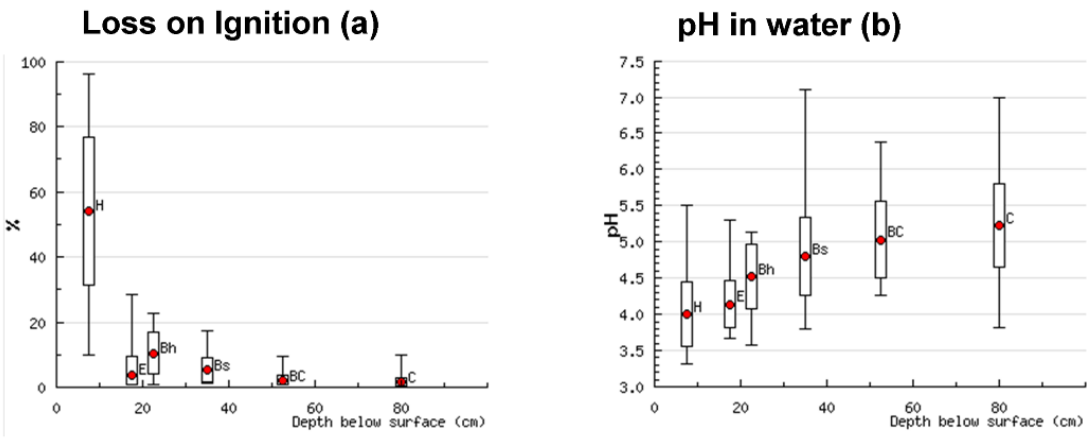

Figure 4-6: Loss on ignition and pH results of Corby semi-natural soil series from the Soil Indicators for Scottish Soils (SIFSS) database (Macaulay Land Use Research Institute 2011). The graphic shows a correlation between the highest percentage of organic matter content on the H horizon and the most acidic value on the pH results. Both, acidity and organic content therefore decrease with depth.

The cation exchange capacity of these soils is generally low, except for the H horizon (Figure 4-7), as expected for sandy soils as they are not charged. The background concentration of the elemental macronutrients at the site is generally low as a consequence of the high degree of leaching.

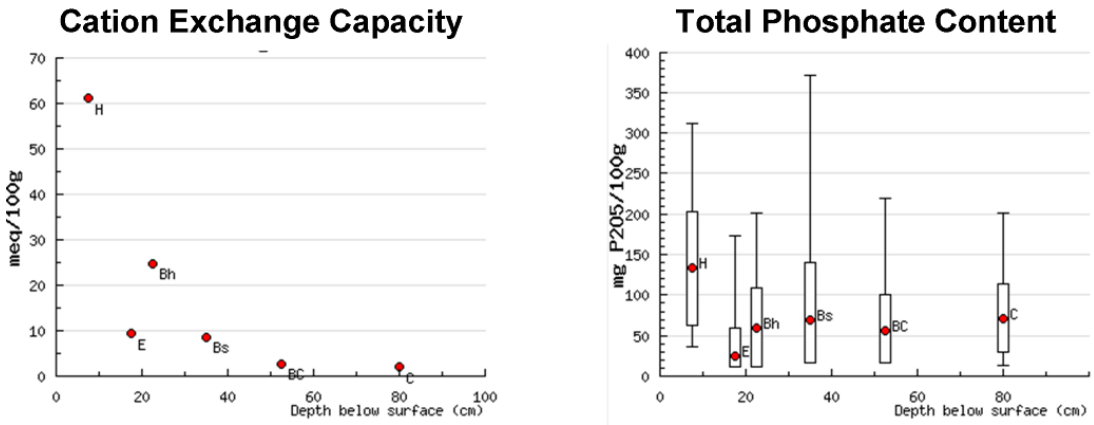

Figure 4-7: Cation exchange capacity and total phosphate content of Corby semi-natural soil series from the Soil Indicators for Scottish Soils (SIFSS) database (Macaulay Land Use Research Institute 2011). The highest value of phosphate is in the H horizon, showing an increased concentration value in the B and C horizons.

This may have an effect on the general element concentrations of the soils at Scalpsie Bay. The H horizon shows higher concentration of these macronutrients as this is where the cycling elements are released upon the breakdown of organic matter (Figure 4-6). However, phosphate might accumulate in the B horizon as Fe or Al phosphates (Figure 4-7).

Despite the classification by the SIFSS database, field visits identified areas with slight variations in the general podzolic character of the soils. An area between the two cairns appeared intermittently waterlogged giving a potential zone of stronger gleying. Also, the SE extreme of the survey area showed eroded zones of wind-blown sands (regosols) going over the limits shown in the geological map (Figure 4-3).

4.1.3.3. **Land Cover**

The site area is currently used as a pasture field for rotational grazing. However, the field has been ploughed and used to cultivate silage. There are some areas where gorse (*Ulex*) has developed showing the nature of the acid, low nutrient soils and mostly free-draining sands where the podzols develop (Rotherham 2007).

4.1.4. Archaeological Background

Scalpsie barrow (NMRS N^{o} NS05NE10) is semi-circular, approximately 15m in diameter and about 1.5m high and it was covered by gorse bushes (Figure 4-8b). During Bryce's excavation, a cist containing an inverted cremation urn with associated grave goods was found (Bryce 1904, 52-57). Bryce recorded that the outer part of the barrow was of earth, containing a few large stones, while the core was of large boulders (Figure 4-8a). This barrow was excavated again in August-September 2010 by DBLPS, tackling the same area that Bryce explored.

Figure 4-8: Plan of the barrow drawn during Bryce's excavation (1904: 53) (a). View of the barrow covered in gorse (b) the barrow after clearing in preparation for the 2010 excavation by DBLPS (c) (© C. Cuenca-García).

The burial cairn (NMRS N^{o} NS05NE9) is located approximately 200m west of the barrow. It is an irregularly-shaped stony area, *c*. 46m by 32m in diameter (Figure 4-9c). The cairn has been extensively robbed and its original nature is not completely understood. Some NMRS records point towards it being of modern origin and a product of field clearance. Other NMRS records suggest an archaeological origin as they report the cairn may contain a disturbed cist. This may be the cist described in a document in 1863 (Ordnance Survey 1893) which also reports that the large stone cairn was removed *c*. 1813 to clear the area to cultivate the land, but when the cist was found the demolition stopped. The NMRS records state that a large hollow of *c*. 8m across at the SW of the cairn may be the remains of a building (Figure 4-9). The cairns do not appear on Roy's Military Map but a series of farming structures are depicted within the site area (Figure 4-9a). Patches of possible unenclosed rig systems are depicted surrounding the site showing the character of Scalpsie Bay during the pre-Improvement period. However, the burial cairn appears on May's estate map of Scalpsie and Quien farms (1781) as an irregularly-shaped uncultivated patch of

grass surrounded by arable fields. Both cairns appear on the 1st edition of the Ordnance Survey (OS) map (Figure 4-9b) where they are depicted in two different field enclosures.

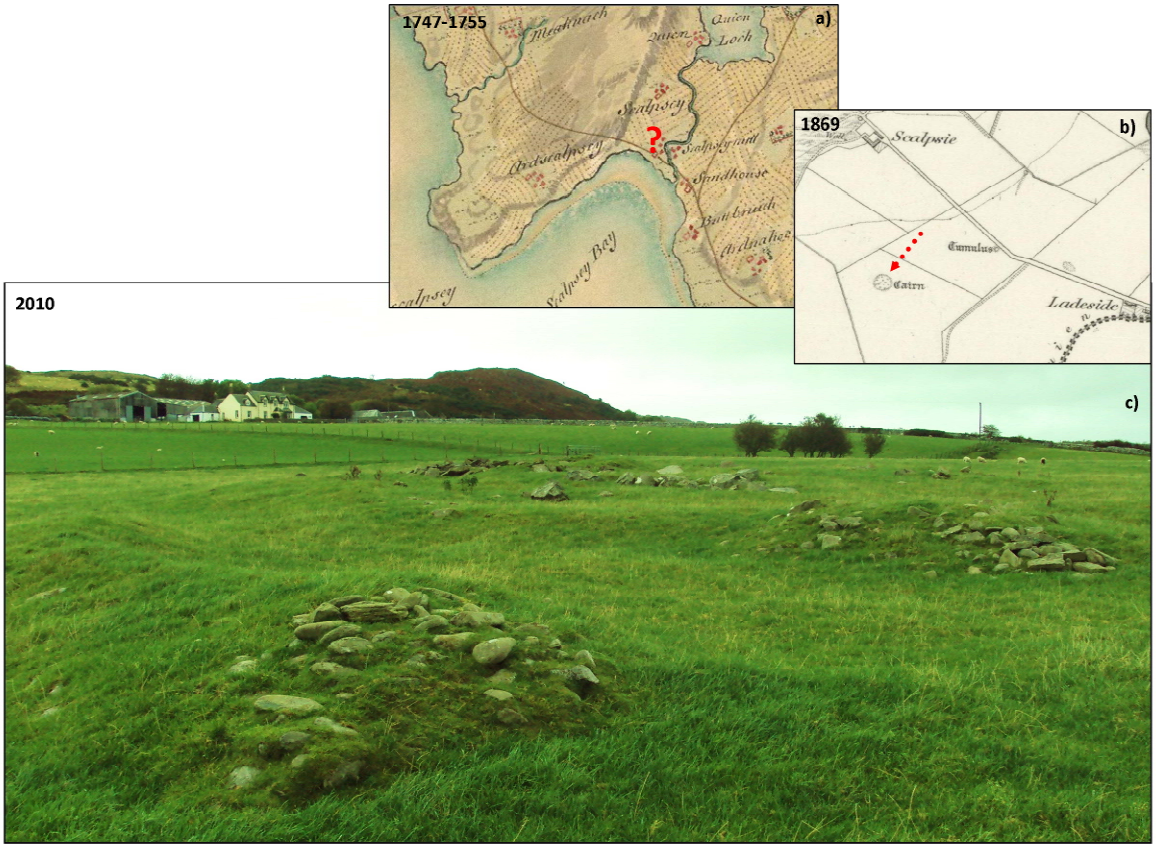

Figure 4-9: The illustration shows an extract from Roy's map (1747-1755) showing the Scalpsie Bay area during the pre-Improvement period (a) (from the National Library of Scotland). The map details the location of some buildings, a road and in area of cultivated land at the area where the burial cairn should have been mapped.The cairns are depicted on the 1st edition of the OS 6-inch map (b), Buteshire 1869, sheet CCXV (the burial cairn in red) (from OS). SW facing view of the burial cairn (c) (© C. Cuenca-García).

Despite the severe impact of the agricultural practices on the site, especially since the Improvement period, both cairns have managed to survive the transformations in the landscape, history and economy. The high concentration of prehistoric sites in the area and its environs, especially those pertaining to the Bronze- Iron Age period denotes the archaeological potential of Scalpsie Bay. The sheltered bay location and the sandy raised beach where the two cairns are located resemble many other prehistoric sites of the Argyll and Bute coastline (Cook *et al.* 1999; Marshall and Taylor 1971; Ritchie 1997). Hence, there is a high probability of occurrence of further archaeological features related to ritual, burial or other type of prehistoric activity (Dr Nyree Finlay, *personal comment* 2010). Furthermore, other landscape features related to the more

recent historic environs of Scalpsie Bay may also occur. The archaeological significance of Scalpsie Bay along with the lack of knowledge regarding the current structure (archaeological or field clearance) and preservation status of the burial cairn made the case to investigate this area.

4.2. The Burial Cairn and its Environs

Since there was no previous geophysical data, an initial gradiometer survey was carried out over the site. This extensive survey intended to create the first data set for this case study and to find potential targets to implement the other geophysical techniques and soil sampling. Exploratory soil analysis was also undertaken to confirm and describe the soil type present in the survey area.

4.2.1. Geophysical Survey

4.2.1.1. **Aims**

The gradiometer survey aimed to reveal the current extent of the burial cairn and any other related internal or external features of interest to contribute to the enhancement the archaeological record of the monument.

4.2.1.2. **Survey Area & Data Collection**

The survey grids were set out within the site area using tapes and tied in to the OS map using a GPS Leica 1200 system. A total of 89 grids of 20m x 20m were recorded during the extensive gradiometer survey covering an area of 3.56ha (Figure 4-10). The southernmost edge of the site area was not covered due to time constraints. However, the area measured was enough to satisfy the particular objectives of this PhD project.

The survey was carried out during 5 days (6^{th} - 10^{th} June 2010) with a team of 8 volunteers (students from the University of Glasgow and local volunteers) who assisted during different days. The general weather conditions during the survey were variable, usual for the Scottish climate. Day 2 and 4 were very wet and cold. The mean minimum/maximum temperature for June 2010 recorded at the Paisley weather station was of 11.2 to 20.2 °C respectively and the total rainfall was 29.7mm (Met Office 2012).

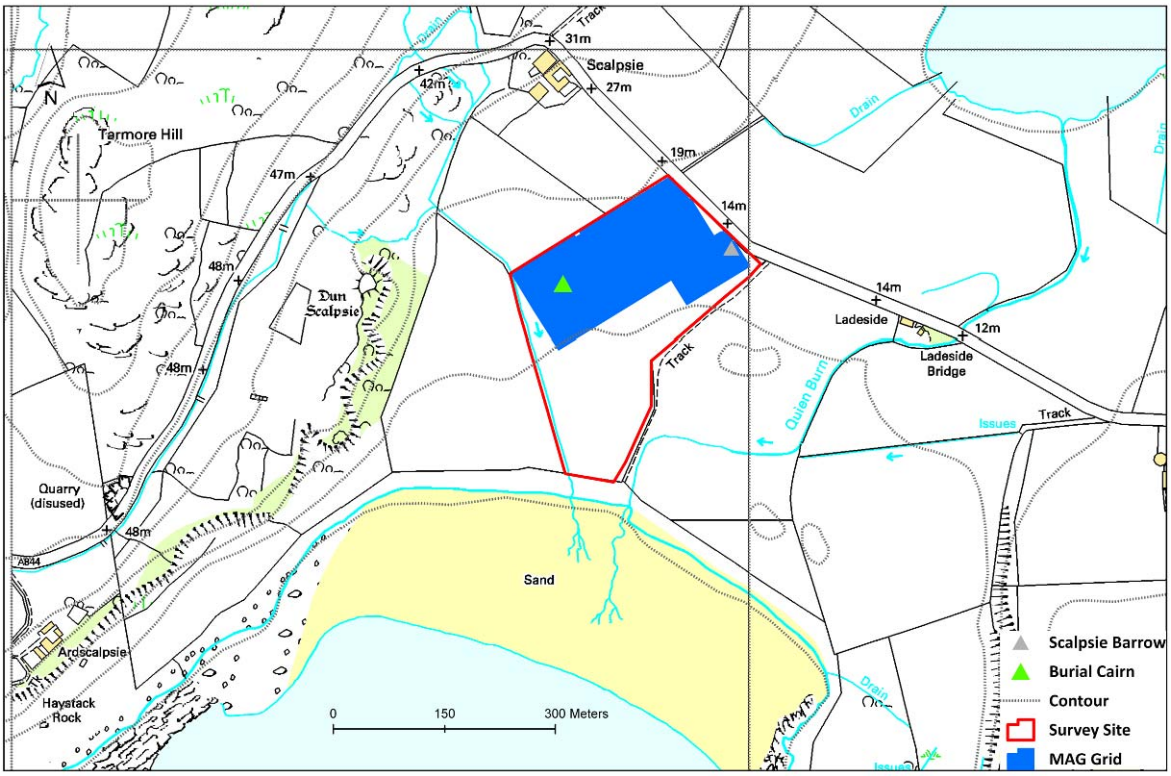

Figure 4-10: Grid location of the gradiometer (MAG) survey carried out at Scalpsie Bay.

The data was recorded in a zig-zag mode by two experienced operators to allow rapid ground coverage. The survey was carried out with single and dual Bartington 601 instruments. Other survey parameters are detailed in Table 4-1.

Technique	Instrument	Traverse Spacing	Sampling Interval	Survey Mode	Notes
Gradiometry	Bartington Grad 601-2 &1	0.5m	0.125m	Zig-zag	Lower sensor c. 20cm above the surface & 0.03nT/m (resolution)

Table 4-1: Instrument settings used during the gradiometer survey at Scalpsie Bay.

4.2.1.3. **Gradiometry Results**

The raw and processed data results of the gradiometer survey are plotted in Figure 4-11 and Figure 4-12 respectively. The range of the unclipped raw data varied from 3000 to -3000nT. This huge range was caused by spurious values introduced by ferrous superficial objects and other metal interferences. The raw data showed a longitudinal band of magnetic enhancement with a NE-SW direction. A second band of magnetic enhancement also appeared at the south of the surveyed area with a u-shaped form. These areas coincide with the

approximate location of two faults and the meta-igneous serpentinite rocks (Figure 4-2 and Figure 4-3). A large area was affected by magnetic interference in the NE of the survey area. A considerable distance was left between the end of the survey grid and the metal fence present here, and which may have caused the interference, as did the presence of the meta-igneous intrusion mentioned. A second and small area of disturbance in the E was caused by the gate used to access the field. The NNE of the survey area was magnetically noisy. The field presented a pronounced slope upwards here and some rock outcropping was seen toward the NE corner of the survey area.

A standard processing flow (Table 4-2) was applied in order to correct the effect of the spurious superficial objects and metal fences as well as to filter out the effects of the geology and enhance weaker anomalies of interest. The general gradient range was reduced to -18 to 26nT (Table 4-3). The raw data also presented some staggered traverses and banding effects which were easily removed.

The results of the gradiometer survey are characterised by the strong magnetic response of the burial cairn (west) and the barrow (east). These anomalies contrasted very clearly with the generally very low background readings. The results relating to the burial cairn are characterised by an internal ring-like anomaly and other weak positive anomalies. Other linear positive anomalies with a NNE-SSW and NWN-SES orientation were detected. Some more subtle and wider linear anomalies running with a general E-W direction were detected as well as an area of magnetic noise at the NNE of the survey area.

Function	Parameters
Clip	Min -20, Max 20
Despike	2 (X/Y Radii), 2.5 (Threshold), Mean (Replacement)
Zero Mean Traverse	All (Grid), On (Less Mean Fit), Not applied (Threshold)
Destager	87 (Grid), 6 (Shift), 27-29-31 (Line)
Low Pass Filter	2 (X & Y), Gaussian (Weighting)
Interpolate	X & Y (Direction), Expand, SinX/X

Table 4-2: Data processing (Geoplot 3.0 software) applied to the gradiometer (MAG) data acquired at Scalpsie Bay.

Gradient	Raw	Processed
Mean	-1.1nT	0.1nT
Min/Max	3000nT to -3000 nT	-18nT to 26nT

Table 4-3: Range of the dataset of the gradiometer survey at Scalpsie Bay.

4.2.1.4. **Gradiometry Interpretation**

The gradiometer survey mapped the burial cairn, the barrow and their immediate environs. The two monuments showed up as two well-defined and sub-circular areas of magnetic 'noise', a product of the concentration of dipolar magnetic anomalies. This type of response may be caused by the stony infill of the cairns and some stones scattered on the surface contrasting with the surrounding sandy loam matrix.

4.2.1.4.1. ***The Burial Cairn***

The extent of the current remains of the monument measures 37m E-W, 33m N-S and 48m NE-SW. Despite the magnetic 'noise', a slightly weaker ring-like magnetic anomaly (1 in Figure 4-13) was detected within the cairn. This anomaly was visible also as a low resistance area in the electrical data and as areas of low amplitudes in the GPR data. The anomaly may represent a primary phase of the monument, revealing its former perimeter or some other type of internal feature. However, this anomaly could also be due to modern disturbance related to the partial removal of the cairn in *c*.1813, or some other intrusive work (*e.g* a robbing trench) mentioned in the NMRS records.

To the south of the monument, an irregular and magnetically weaker area (2 in Figure 4-13) may indicate the location of a possible entrance or passage to the cairn. The negative magnetic anomaly on the edge of the cairn (3 in Figure 4-13) is more difficult to interpret as it might be of archaeological (e.g. truncated bank or ditch), modern origin, or just an effect of magnetic halos in the data.

The magnetic results showed that the elongated curvilinear anomaly (4 in Figure 4-13) is connected to the cairn main structure. Part of this anomaly is visible on the surface in the SW as an unstructured stone heap. This anomaly could be a product of either the disturbance of the cairn/field clearance or archaeological.

The survey did not provide any evidence to suggest the presence of a building as mentioned in the NMRS records. The secondary slightly noisy area, surrounding the ring-like anomaly (1 in Figure 4-13), stops abruptly in the NNE (5 in Figure 4-13). This may be suggestive of further disturbance if this secondary area was originally part of the cairn.

4.2.1.4.2. *The Environs*

Discrete dipolar anomalies outwith the monument (6 in Figure 4-13) may indicate thermo-remanent magnetic features (e.g. a hearth) but could also be irrelevant superficial ferrous objects. The high magnitude anomaly (7 in Figure 4-13) may be produced by a ferrous object. Other weaker dipoles (8 in Figure 4-13) may be of archaeological significance (e.g. a cremation).

Finally, the gradiometer survey detected landscape features related to more recent periods such as the old field boundary (9 in Figure 4-13), a track (10 in Figure 4-13) and evidence of cultivation practices (plough marks) which may have disturbed the cairn and other archaeological features at the site. Other longitudinal magnetic anomalies outside the burial cairn (11 in Figure 4-13) may represent the remains of fossil shorelines as they correlate with the gentle terraces of raised marine deposits present in the field.

4.2.1.5. **Discussion**

The gradiometer survey revealed a negative magnetic anomaly (3 in Figure 4-13) relating to the burial cairn. This anomaly could be just the halo effect of the magnetic dipoles at the area, or could also be a 'real' anomaly produced by disturbance activity relating to an archaeological feature (e.g. the remains of a truncated earthen bank or ditch) or modern disturbance. Hence, this anomaly was selected to be targeted with the multi-technique surveying order to clarify its character. The irregular and magnetically weaker area (2 in Figure 4-13) indicating a possible entrance or passage to the cairn was also selected as a target for the multi-technique survey.

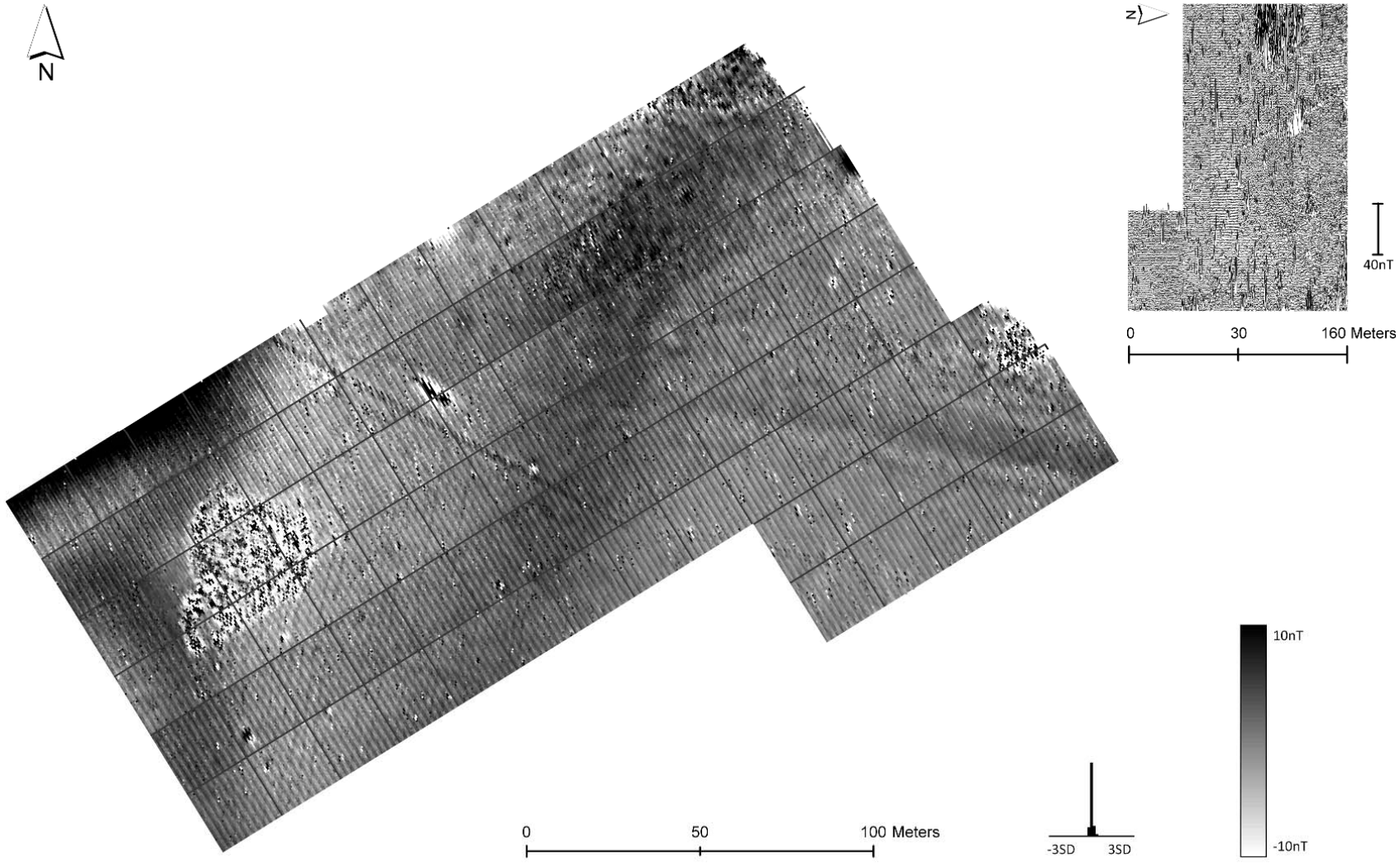

Figure 4-11: Shade (left) and trace plot (right) of the raw gradiometer data results at Scalpsie Bay. The data was plotted at -10/10 Absolute units, contrast 1 and using the Geoplot grey99 palette.

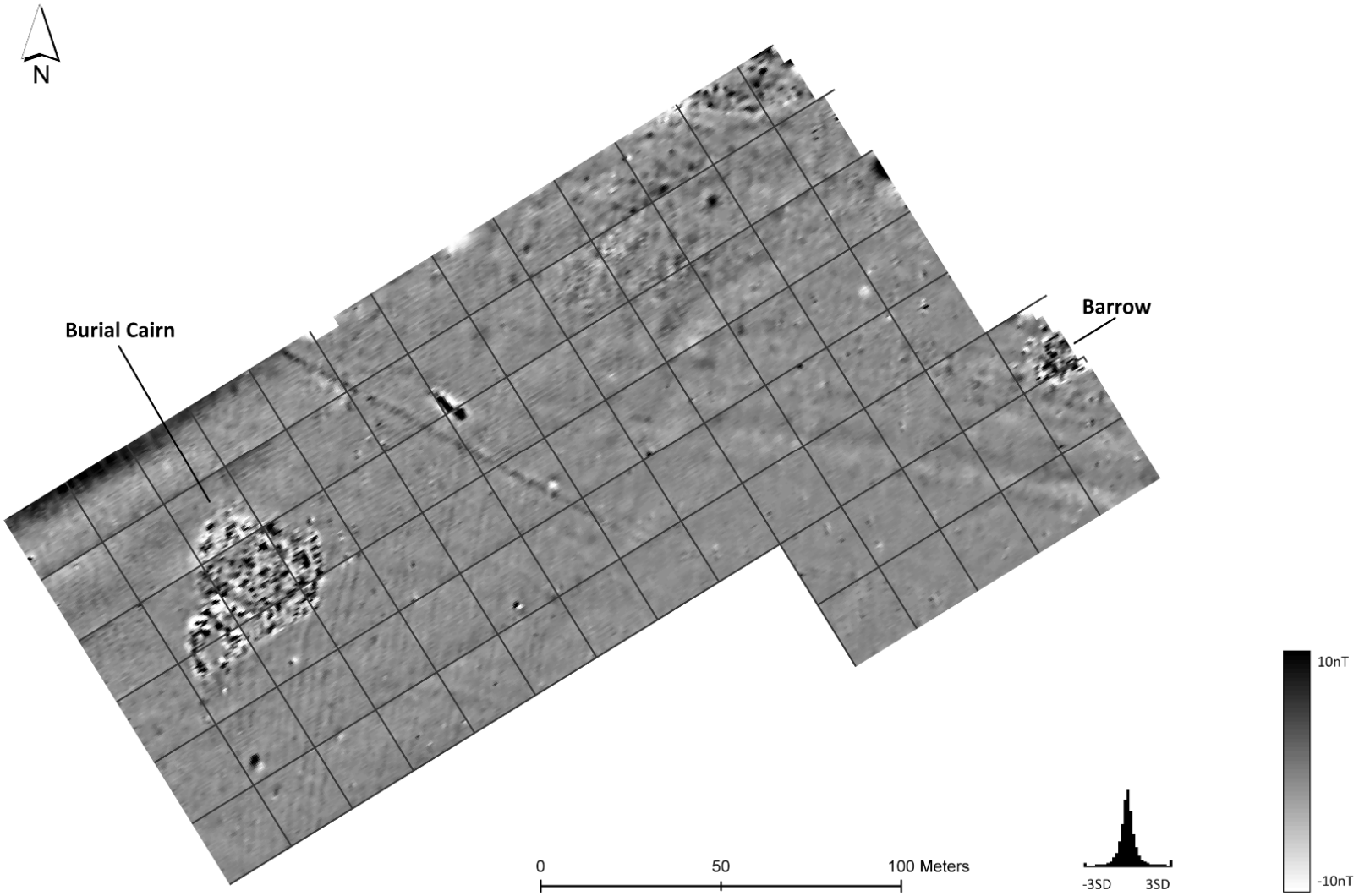

Figure 4-12: Shade plot of the processed gradiometer data results at Scalpsie Bay. The data was plotted at -10/10 Absolute units, contrast 1 and using the Geoplot grey99 palette.

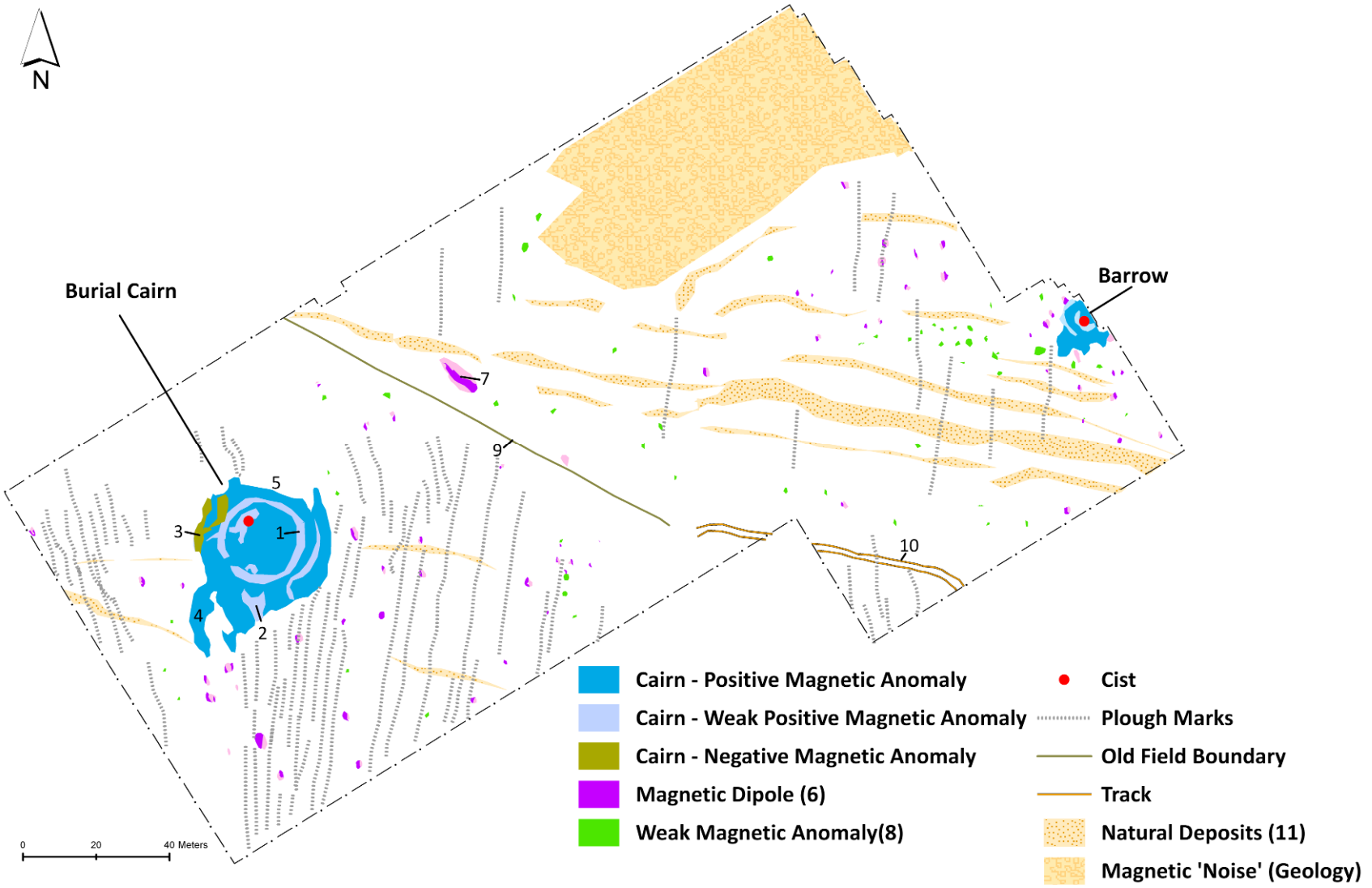

Figure 4-13: Anomaly extraction and interpretation plot of the gradiometer results at Scalpsie Bay. The numbers (1-11) mark the anomalies discussed in the main text.

4.2.2. Soil Analysis

4.2.2.1. **Aim**

The aim was to provide an independent assessment of the texture and bulk chemical characterisation (pXRF analysis) of the soil within the survey area and to correlate with the soil map classification and SIFSS database.

4.2.2.2. **Sampling Strategy**

The hand augering was carried out after the gradiometer survey and during the excavation of the barrow by the DBLPS. Soil was down-hole sampled to approximately 1m depth at three different sites within the survey area but well away from the scheduled monuments (Figure 4-14). Two control samples were also collected for the pXRF analysis. An Edelman Dutch auger (Ø 6cm) was used to sample the soil.

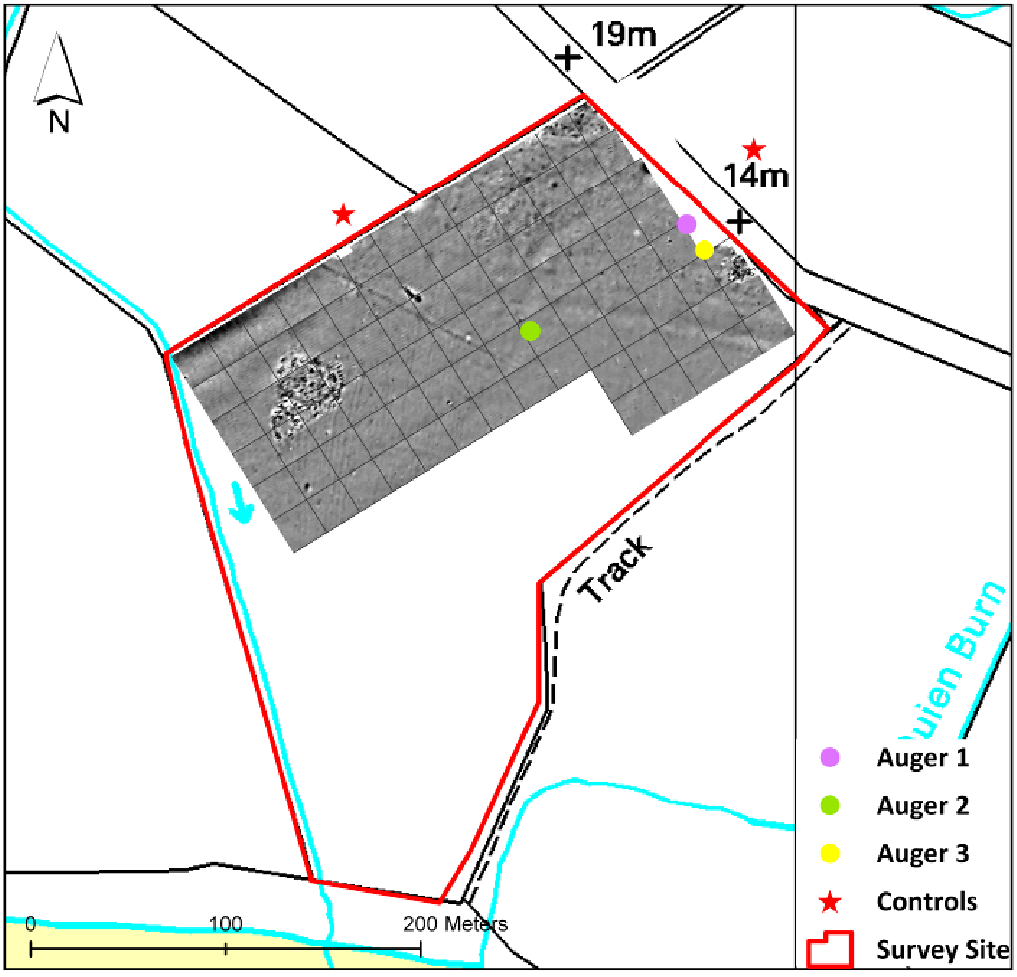

Figure 4-14: Auger & soil controls (Control 1= west, Control 2= east) locations at Scalpsie Bay.

4.2.2.3. **Soil Texture Results & Discussion**

The texture analysis identified four soil horizons in the three augers. A detailed description of the soil samples is summarized in Table 4-4.The comparison between the 3 augers and the general SIFSS profile is shown in Figure 4-15.

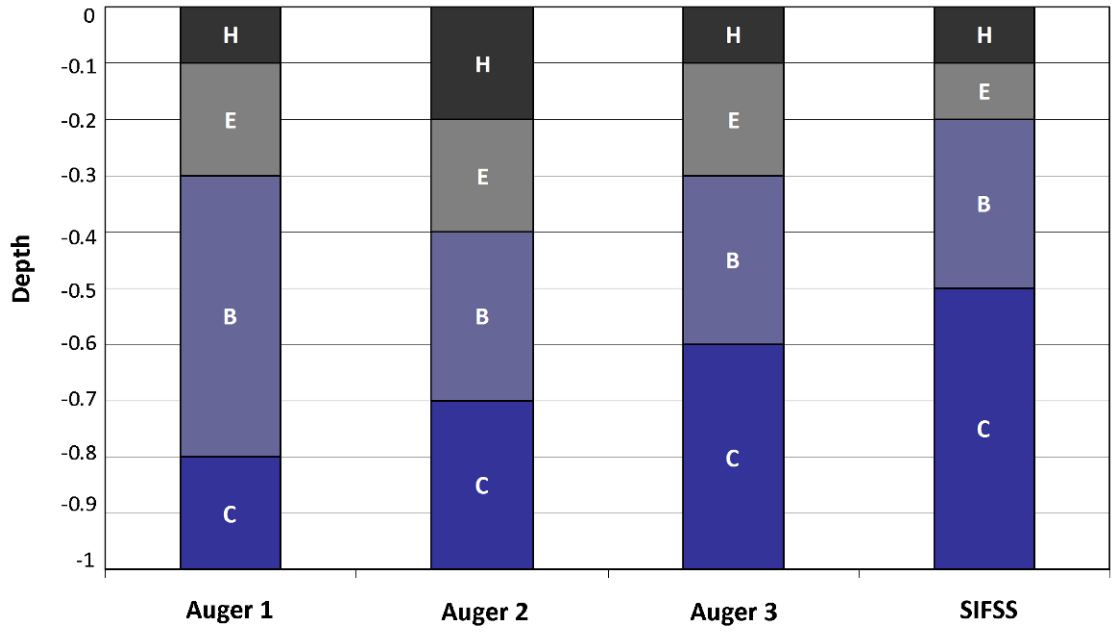

Figure 4-15: Diagram showing the four major soil horizons identified by augering and the general SIFSS profile at Scalpsie Bay.

Firstly, an organic horizon (H) with some sandy peat content was identified with a variable depth (between 5- to 10-15cm). This horizon also contained some gravels and small angular stones. Mixed dark yellowish brown and light greyish-grey loamy sand was recorded to a depth of *c.* 20cm. This greyish brown deposit was described as a mixed eluvial horizon (E). In Auger 3 some fragments of charcoal and bone were observed in horizon E. Horizon B which varied from medium to coarse sand or loamy sand was generally recorded to 30-40cm. The deposit (B) was dark yellowish brown but slightly lighter and reddish when dried. Red and dark soil colours were observed in Auger 3 showing the metal and organic compound leached though the eluvial horizon. This soil contained much gravel and sporadic small angular stones (sedimentary rock). The final horizon (C) consisted of light reddish yellow sands and gravels with some sporadic and small angular stones (of meta-sedimentary rock).

Auger	Depth (m)	H	Colour	Munsell	Texture	Structure	Consistency	Stoniness	Bioturbation	Other
1	0	H	Dark	2.5Y_2.5/1	Humic with some sandy peat mineral content	Moderate and sub-angular blocky	Moist, plastic and sticky	Common mall to medium subrounded (gravels) and few small angular stones (sedimentary rock)	Many and fine fibrous roots	Iron objects seen on surface
	0.25	E	Medium brown (some light greyish areas)	10YR_3/6	Medium to coarse loamy sand	Weak to moderate medium size to coarse granular	Moist, slightly plastic and slightly sticky when wet. Very friable when moist and loose when dry	Common, small and sub-angular (gravels)	Common, fine an fibrous roots	
	0.4	B	Light brown slightly reddish with some light greyish areas	10YR_4/4	Medium to coarse loamy sand, slightly more clayey	Moderate, medium size and granular		Common, small and sub-angular (gravels) and few small angular stones (sedimentary rock)	Few fine fibrous roots	
	0.6				Medium to coarse loamy sand	Weak, medium size and granular	Moist, not plastic and slightly sticky. Very friable when moist and loose when dry			
	0.92	C	Light brownish orange slightly reddish	7.5YR_6/8	Coarse		Moist, not plastic or sticky. Very friable when moist and loose when dry	Many small subrounded (gravels) and few small angular stones (sedimentary rock)	None	
	1.07									
2	0	H	Dark	2.5Y_2.5/1	Humic with some sandy peat mineral content	Moderate and sub-angular blocky	Moist, plastic and sticky	Common small to medium subrounded (gravels) and few angular stones (sedimentary rock)	Many and fine fibrous roots	Iron objects seen on surface
	0.35	E	Light brown slightly reddish (some light greyish areas)	10YR_4/4	Medium loamy sand	Weak to moderate, coarse and granular	Moist, slightly plastic and slightly sticky when wet. Very friable when moist and soft when dry	Common, small and sub-angular (gravels)	Common, fine an fibrous roots	
	0.5	B	Light yellowish brown slightly reddish	5YR_4/4	Coarse loamy sand	Moderate medium size to coarse granular		Common, small and sub-angular (gravels) and few small angular stones (sedimentary rock)	Few fine fibrous roots	
	0.67				Coarse loamy sand and sand	Weak coarse and granular	Moist, not plastic or sticky. Very friable when moist and loose when dry	Common, small and sub-angular (gravels) and few small angular stones (sedimentary rock)		
	0.82	C	Light yellowish brown slightly reddish	7.5YR_6/8					None	
	1.22				Coarse sand					
3	0	H	Dark	2.5Y_2.5/1	Humic with some sandy peat mineral content	Moderate and sub-angular blocky	Moist, plastic and sticky	Common small to medium subrounded (gravels) and few angular stones (sedimentary rock)	Many and fine fibrous roots	Iron objects seen on surface
	20	E	Medium Brown with greyish patches	10YR_4/2	Coarse loamy sand	Weak, coarse and granular	Moist, not plastic and slightly sticky. Very friable when moist and loose when dry	Many small subangular (graves)	Common, fine an fibrous roots	Bits of charcoal and 1 bone fragment
	0.4	B	Light brown slightly reddish	10YR_5/4	Coarse sand				None	Reddish stagnation and some charcoal
	0.6		Light reddish brown	7.5YR_5/4						
	0.7						Moist, not plastic and slightly sticky. Loose when moist and dry	Many small subangular (graves) and few small to medium angular stones (sedimentary rock)		
	1	C	Light yellowish brown slightly reddish	7.5YR_6/8		Very weak, coarse and granular				
	1.1									

Table 4-4: Full description of the major soil horizons recorded in the three augers sampled at Scalpsie Bay.

The Dutch auger worked well and held the sandy and gravely deposits sampled. The material was easily removed from the auger but the profiles were slightly mixed due to the downward thrust. To obtain an undisturbed profile a gouge auger was tested but failed as the whole deposit of uncemented sands and gravels collapsed when the gouge was removed. In spite of the slight disturbance of the deposit sampled, all the main horizons and features of the podzols were observed with the Dutch auger. This verified the acidic and free-drained sandy Podzolic soils of the survey area since the low-resolution and statistically based nature of soil maps and geochemical databases (Paterson 2011) do not always correlate with the 'real' occurrence of a particular soil in a mapped area.

During the excavation of the barrow, no hardpan was identified in the test pits dug around the barrow. These test-pits were dug to ground-truth a series of weak magnetic anomalies (8 in Figure 4-13). The augering also confirmed the varying depths of the H and E horizons. This helped the implementation of the second phase of soil sampling (horizontal surface sampling) that was carried out after the multi-technique geophysical survey as it helped in identifying the optimal depth to sample for the horizontal (superficial) soil analysis. Other areas were not augered due to time constraints but visual observation of an eroded section to the south of the site revealed wind-blown sands. During the survey, an area to the NW was intermittently waterlogged indicating the potential presence of some gleying and clay content.

4.2.2.4. **pXRF Results & Discussion**

The results of the pXRF measurements are summarized in Table 4-5. The elements showing higher concentrations were Fe, K, and Ti ('a' in Figure 4-16 and 4-21). They showed a concentration enhancement in the organic horizon (0m), followed by a general depletion at c. 0.2m (eluvial horizon), a distinctive concentration peak at 0.6-0.7m and a general depletion to a greater depth. The coherent peak shown in the results of the three augers may be showing the accumulation horizon (B in Figure 4-4) of leached soluble metal-humus complexes from the surface, through the eluviation horizon. This confirmed the podzolic character of this soil environment.

These results correlated with the general horizons characterised by soil texture (Figure 4-15). Nonetheless, the results of the pXRF analysis of Auger 3 ('a' in Figure 4-17) show a peak at a higher depth in comparison to the soil texture results. In spite of this mismatch, the general enhancement of these elements seems coherent, demonstrating the effect of the leaching of these elements from the E horizon and their concentration at *c*.0.6-0.7m (B horizon). Since the depth of the B horizon is within the range of detection of most of the geophysical techniques used in archaeological prospection, the general concentration levels of these elements may have an effect on the geophysical techniques.

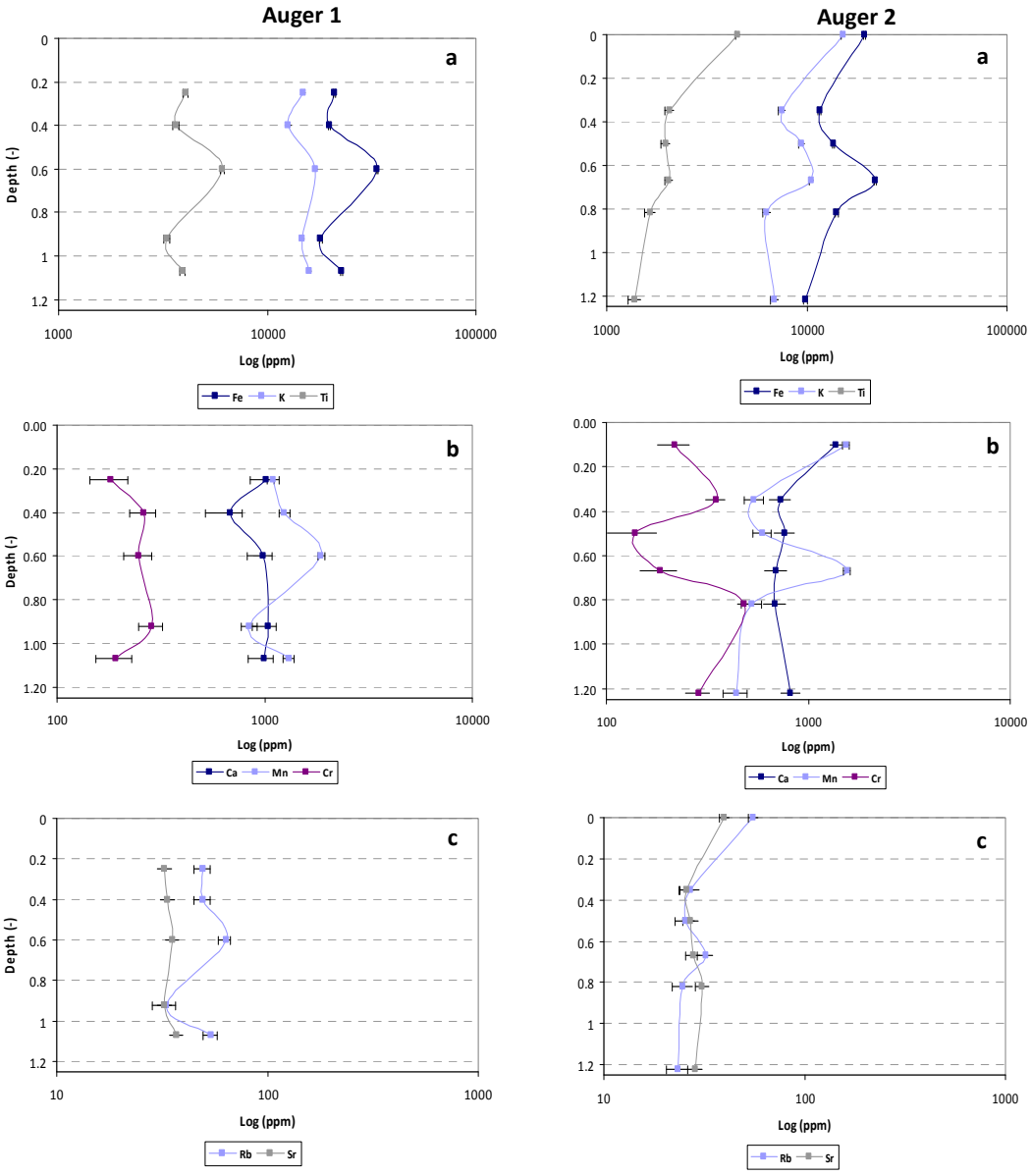

Figure 4-16: pXRF results of the soil samples collected in Auger 1 & 2 at Scalpsie Bay.

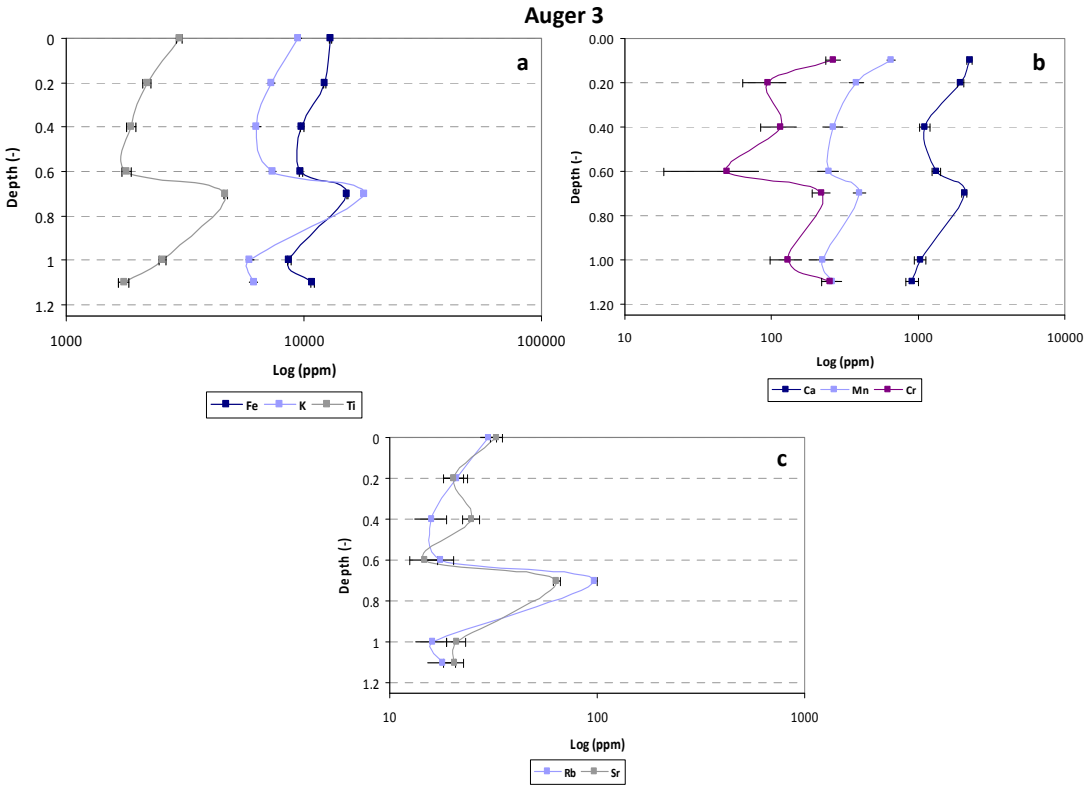

Figure 4-17: pXRF results of the soil samples collected in Auger 3 at Scalpsie Bay.

Auger	Depth (m)	Fe	K	Ti	Ca	Mn	Cr	Rb	Sr
Auger 1_a	0.25	20943	14800	4061	1014	1104	182	50	33
Auger 1_b	0.40	19779	12638	3657	685	1246	261	50	34
Auger 1_c	0.60	33699	16969	6095	985	1873	248	64	35
Auger 1_e	0.92	18037	14633	3295	1035	842	286	33	33
Auger 1_d	1.07	22646	15957	3932	998	1307	191	54	37
Auger 2_a	0.10	19390	15127	4521	1375	1540	218	55	40
Auger 2_b	0.35	11586	7484	2058	731	540	350	27	26
Auger 2_c	0.50	13630	9420	1973	768	594	140	26	27
Auger 2_d	0.67	22004	10506	2040	694	1560	185	32	28
Auger 2_e	0.82	14119	6303	1649	688	525	482	25	31
Auger 2_f	1.22	9820	6888	1381	819	439	286	23	29
Auger 3_a	0.10	13008	9489	2993	2252	653	265	30	33
Auger 3_b	0.20	12283	7328	2196	1952	381	95	21	20
Auger 3_c	0.40	9801	6333	1878	1113	264	116	16	25
Auger 3_d	0.60	9702	7387	1798	1327	247	50	18	15
Auger 3_e	0.70	15227	17849	4675	2065	402	220	97	64
Auger 3_f	1.00	8671	5923	2554	1034	222	128	16	21
Auger 3_g	1.10	10865	6151	1744	918	260	252	18	20
Control 1	0.10	28189	19830	6506	3436	1067	218	94	85
Control 2	0.15	24203	14267	5432	7651	1091	313	61	82

Table 4-5: pXRF measurements of the Scalpsie Bay soil samples. The element concentrations are expressed in mg/kg (=ppm). The location of the two control samples (Control 1 and Control 2) is shown in Figure 4-14.

4.3. Targeting the Burial Cairn

After the extensive preliminary gradiometer survey, a multi-technique geophysical survey was carried out over targeted areas of the burial cairn. Surface soil sampling for geochemical analysis was also undertaken over a negative magnetic anomaly (3 in Figure 4-13) detected by the preliminary gradiometer survey.

4.3.1. Geophysical Survey

4.3.1.1. **Aims & Objectives**

This survey aimed to map any features of interest over the burial cairn using earth resistance, magnetic susceptibility (MS) and GPR and to confirm and complement the results of the gradiometer survey. The objectives were:

- To implement earth resistance and MS surveys over the overall burial cairn to detect the magnetic anomalies 1, 2, 3 and 4 (Figure 4-13).
- To carry out targeted GPR surveys over two areas of the burial cairn to detect the magnetic anomalies 1 and 2 (Figure 4-13) targeted with two single GPR lines and anomaly 3 (Figure 4-13) covered with GPR area 1 and GPR area 2.
- To further explore the southern area of the burial cairn (GPR area 3) and the stone heap anomaly 4 in Figure 4-13 (GPR area 4) with the GPR technique.

4.3.1.2. **Survey Area & Data Collection**

The earth resistance and MS survey grids were repositioned over the previous grids of the gradiometer survey using a GPS Leica 1200 system (Figure 4-18). The earth resistance survey covered six 20m x 20m, only two grids of 20m x 20m were recorded with the MS meter because the instrument failed during the measurement of the third grid due to the bad the contact between the coil and the slighter rougher stony surface towards the centre of the cairn.

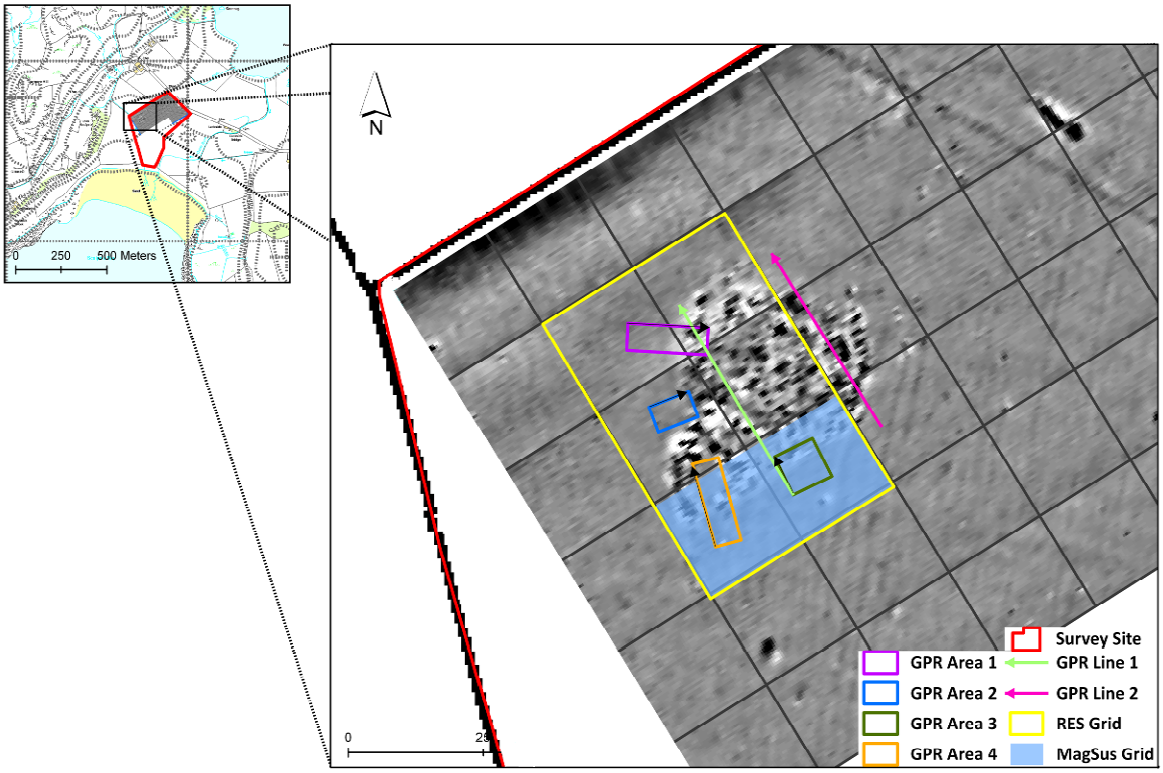

Figure 4-18: Grid location of the multi-technique geophysical survey carried out over the burial cairn at Scalpsie Bay. The black arrows indicate the origin and direction of the GPR survey transects.

The GPR surveys focussed on four areas of the burial cairn to target the four magnetic anomalies of interest. The high and low frequency antennae were tested in GPR area 1 and the low frequency was used to survey the other areas and the two single GPR lines. These two single GPR transects were collected covering the whole diameter of the monument. A total of 77 GPR traverses were recorded at the site. The GPS system was also used here to collect the data to correct the GPR data for topography (GPR area 3 in Figure 4-18) and to accurately interpret the single traverses collected across the overall monument. Further details about the survey parameters are summarised in Table 4-6. The survey was carried out over two 2 days (11th and 12th June 2010) with a team of five volunteers (students from the University of Glasgow and local volunteers). The general weather conditions during the survey were sunny and dry.

Technique	Instrument	Traverse Spacing	Sampling Interval	Survey Mode	Other
Earth Resistance	Geoscan RM15 & (MPX15)	0.5m	0.5m	Zig-zag	Twin probe separations (0.5m & 1m) & 0.5ohm resolution.
Magnetic Susceptibility	Bartington MS2D	1m	1m	Zig-zag	x1 range (sensitibity range)
GPR-450 MHz	Sensors & Software PulseEKKO 1000	0.5m	0.05m	Step Mode & Parallel Lines	Time Window=110ns, Stacks=16, Samples=200ps, Average Velocity= 0.06m/ns.
GPR-225 MHz		0.5m	0.10m		Time Window=160ns, Stacks=16, Samples=200ps, Average Velocity=0.06m/ns.
GPR Single Lines-225MHz		n/a		Step Mode	

Table 4-6: Instrument settings used during the multi-technique geophysical survey at Scalpsie Bay.

4.3.1.3. **Magnetic Susceptibility Results**

In general, the MS results were very limited as the instrument failed after the second grid because of bad contact of the field coil against the ground. The raw and processed data (Figure 4-19) showed a linear enhanced area running NE-SW, while the data collected over the burial cairn presented lower values. A very high MS value (149 SI) was recorded in the middle of the south end of the MS grid. Another two small areas of low MS were measured at the east end of the grid. Table 4-7 summarises the processing applied to the data set.

Function	Parameters
Clip	Min 2, Max 100
Despike	1 (X/Y Radii), 3 (Threshold), Mean (Replacement)
Low Pass Filter	2 (X & Y), Gaussian (Weighting)
Interpolate	X & Y (Direction), Expand, SinX/X

Table 4-7: Data processing (Geoplot 3.0 software) applied to the MS data acquired at Scalpsie Bay.

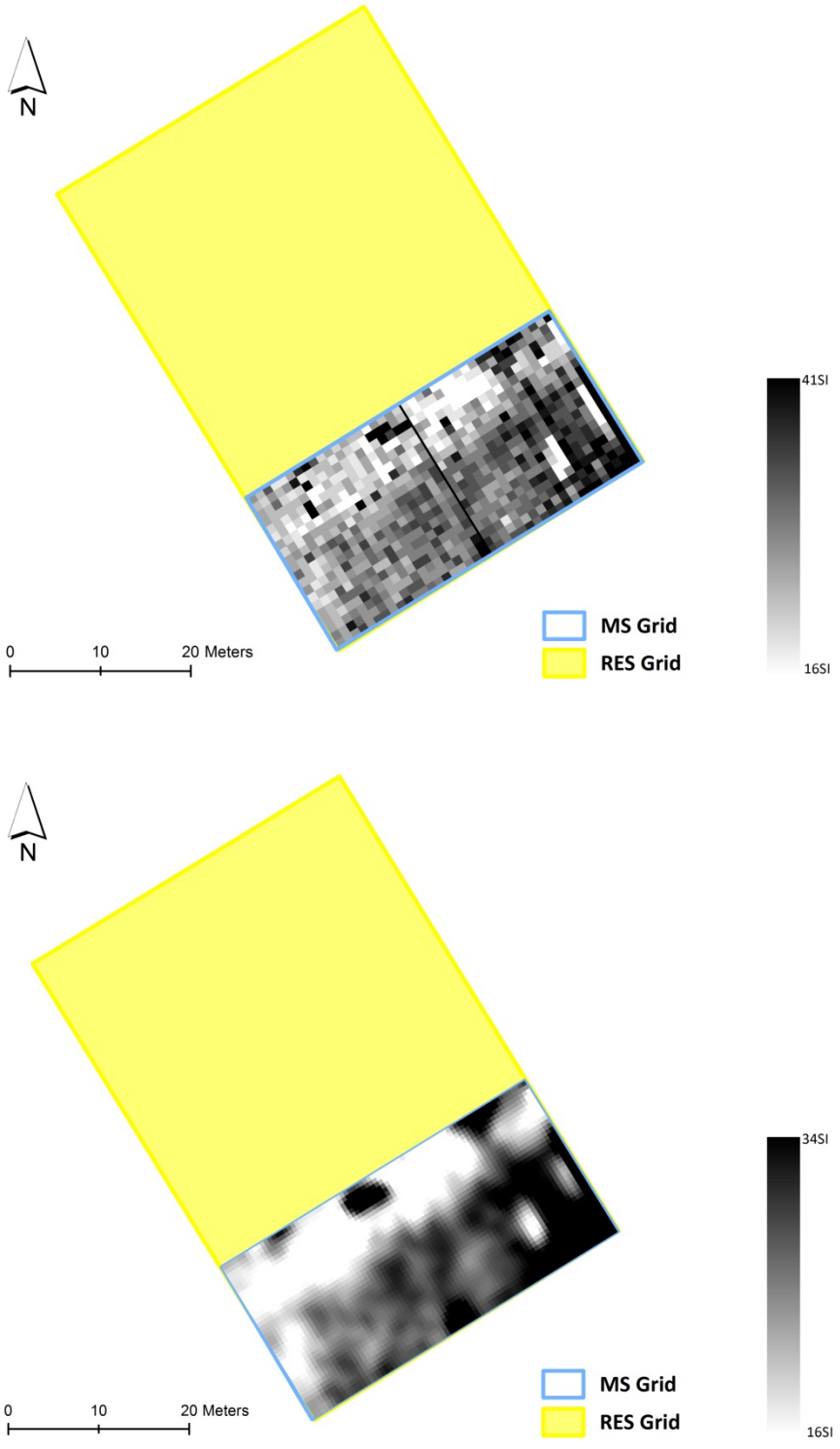

Figure 4-19: Shade plot of the raw (top) and processed (bottom) data results of the MS survey over the burial cairn Scalpsie Bay. The data was plotted at -1/1 SD units, contrast 1 and using the Geoplot grey99 palette.

4.3.1.4. **Earth Resistance Results**

The results of the two probe separations were almost identical apart from some small differences in the shapes of high resistance anomalies, hence only the results of the 0.5m probe separation are shown (Figure 4-20). Some readings were dummied owing to the presence of stones on the surface which produced high resistance contacts of the mobile probes with the soil. The data processing sequence is shown in Table 4-8 and involved the correction of the noisy spikes caused by high contacts in the area covered by the burial cairn which caused a high range (890 ohm in Table 4-9) in the raw data. The results were characterised by the strong positive response of the cairn caused by its stony content. Areas of low resistance were detected surrounding the monument in the S and NW areas. A curvilinear and weaker high resistance anomaly was detected outside the current extent of the burial cairn.

Function	**Parameters**
Clip	Min -700, Max 2000
Despike	2 (X/Y Radii), 2 (Threshold), Mean (Replacement)
Edge Match	1R, 4R & 3B
High Pass Filter	10 (X & Y), Uniform (Weighting)
Low Pass Filter	2 (X & Y), Gaussian (Weighting)
Interpolate	X & Y (Direction), Expand, SinX/X

Table 4-8: Data processing (Geoplot 3.0 software) applied to the earth resistance data acquired at Scalpsie Bay.

Gradient	**Raw**	**Processed**
Mean	890 Ω	0.7 Ω
Min/Max	-2047 Ω / 2047 Ω	-1606 Ω / 1113 Ω

Table 4-9: Range of the dataset of the earth resistance survey at t Scalpsie Bay.

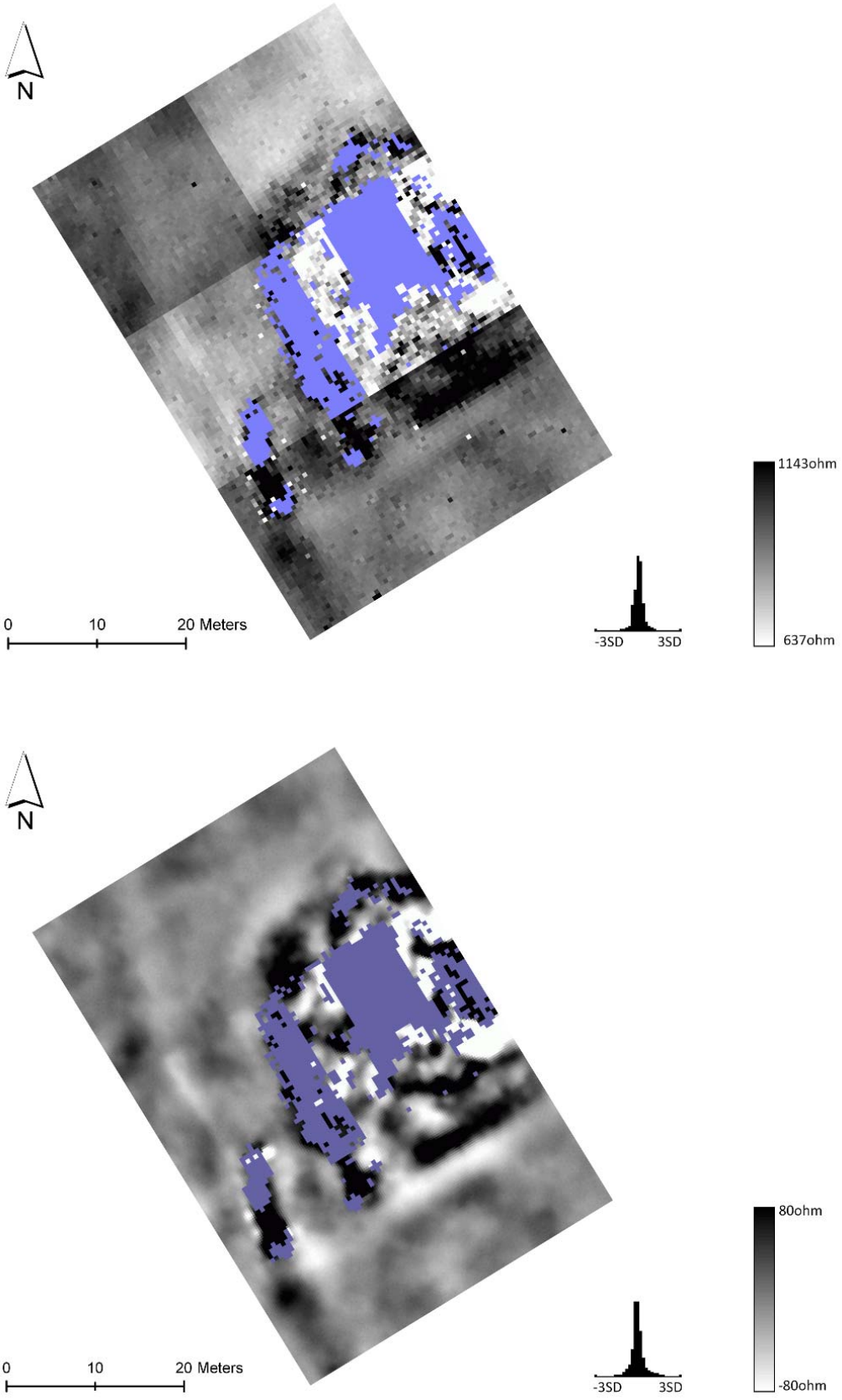

Figure 4-20: Shade plot of the raw (top) and processed (bottom) data results of the earth resistance (RES) survey (0.5m probe separation) over the burial cairn Scalpsie Bay. The data was plotted at -1/1 SD units, contrast 1 and using the Geoplot grey99 palette. The blue colour indicates dummied readings.

4.3.1.5. **GPR Results**

In general the results provided with the low frequency survey (225MHz) were more informative than the data from the high frequency survey (450MHz), especially in the results obtained from the time-slices. The penetration of the GPR signal was good and reached the first 60ns (*c*. 2.5m) with the 450MHz frequency. The lower frequency survey reached the first 90ns (*c*. 3.40m). A general velocity of 0.08m/ns was estimated by hyperbola adaptation from diffraction hyperbolae located at *c*.1 m depth and 0.03m/ns from deeper reflectors.

The results of the GPR survey are presented in the form of radargrams and time-slices. The velocity used to estimate the time window of each time-slice was 0.08m/ns ('t', top-left in each time-slice). The processing applied to the GPR data is detailed in Table 4-10.

Function	Description
Subtract-mean (dewow)	To eliminate possible low-frequencies. 'Wow' is caused by swamping or saturation of the resorded signal by early arrivals and/or inductive coupling effects.
Time zero Correction	To adjust to a time zero position to correct the down-shifting of the radar section due to the air–ground interface.
Manual gain (y)	To amplify the received signal by emphasizing y direction (time) in order to increase the visibility of the deeper parts of the image.
Background Removal	To eliminate background noise and to remove 'ringing' in the data. It also suppresses horizontally coherent energy and it can emphasize signals which vary laterally (e.g. diffractions).
Topographic Correction (velocity=0.08m/ns)	To position the data in its correct spacial context (if the surveyed surface is not flat). This is important as it place the GPR data in their correct stratigrafical context, hence ensuring that the interpretations are realistic.
Migration (Diffraction Stack)	To trace back the reflection and diffraction energy to their "source". This is useful to get the original position of the reflected signal or the target point source.

Table 4-10: Data processing (ReflexW v.5.6 software) applied to the GPR data acquired with the 225 and 450 MHz shielded antennae at Scalpsie Bay.

The two-way traveltime (twt) shown in the y-axis of the time-slices that were corrected for topography (GPR area 1, 2 and 3) should be considered much shallower as their time zero was modified by the static correction. The approximate depths detailed here were taken from the non-topographic corrected results.

4.3.1.5.1. *Single Lines (Radargrams)*

The results obtained from the single lines 1 and 2 (Figure 4-21 and Figure 4-22 respectively) are characterized by an area of high amplitudes of linear reflectors with some small diffraction hyperbolae (*c.* 20ns twt/0.60-0.80m depth). The data showed distinctive areas of signal attenuation within the first meter in association with the small diffraction hyperbolae. The amplitudes of the GPR data generally changed at *c*. 70ns twt (2-2.40m depth) and some stronger and larger hyperbolic diffractions were detected. The main differences between the two single GPR lines were the presence of deeper strong amplitudes (between 20-30 meters) along line 1 and shallow lower amplitudes (from 30.3 meters) along line 2.

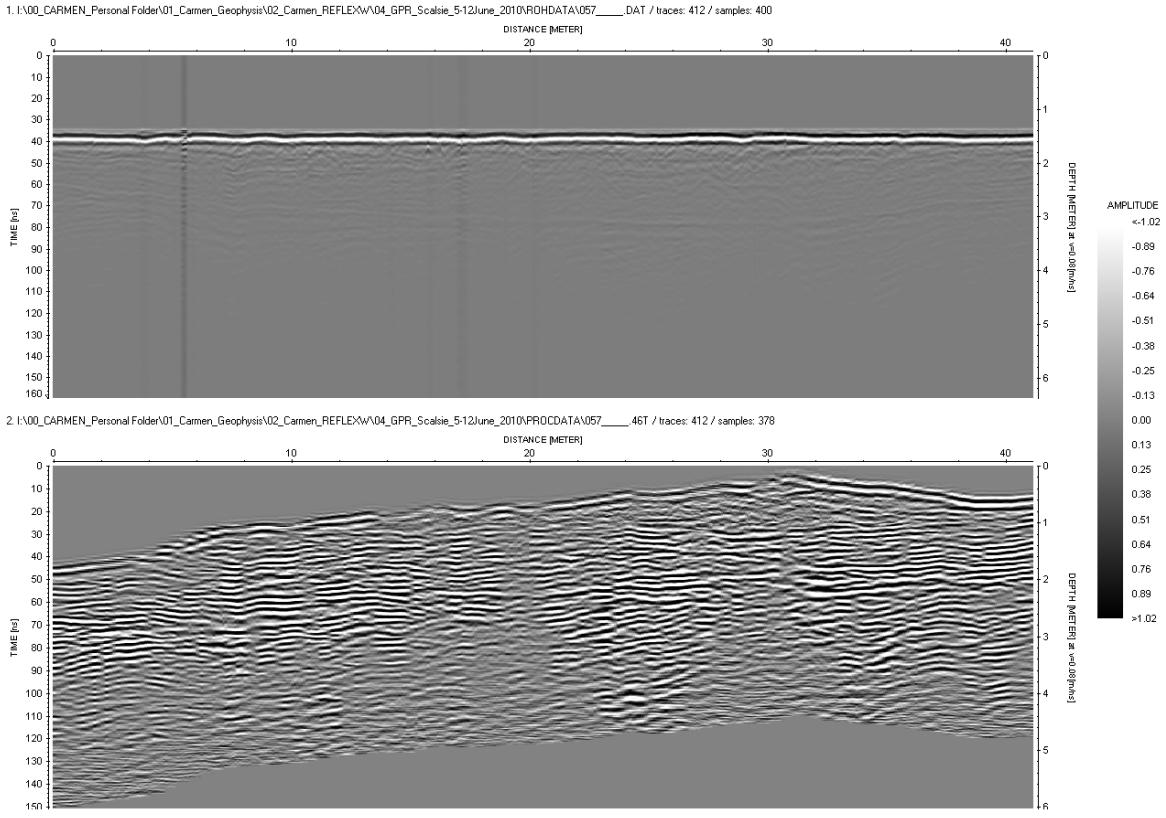

Figure 4-21: Radargram from the 225MHz survey at Scalpsie Bay showing the raw (top) and processed (bottom) results of the single line 1 (Figure 4-18).

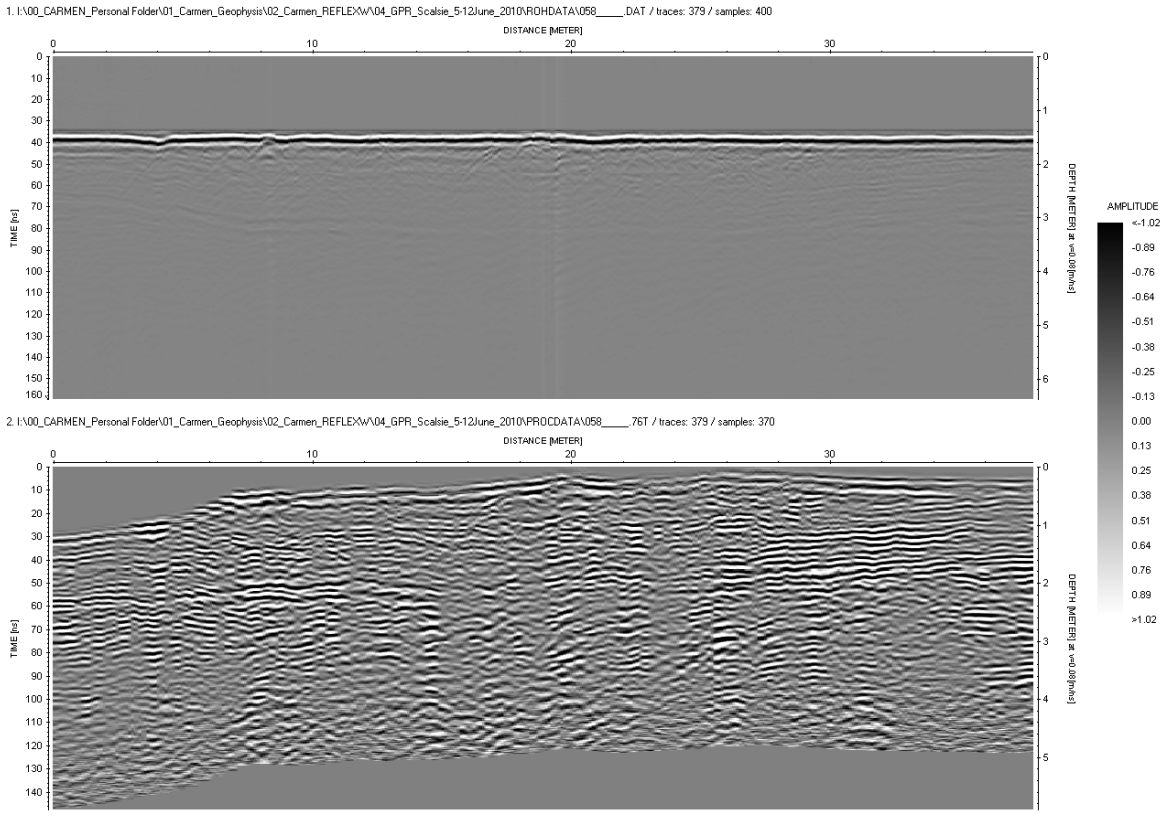

Figure 4-22: Radargram from the 225MHz survey at Scalpsie Bay showing the raw (top) and processed (bottom) results of the single line 2 (Figure 4-18).

4.3.1.5.2. *Targeted GPR Areas (Time-slices)*

Area 1

The results obtained from the 450 MHz survey (Figure 4-23) were less informative than those obtained with the 225 MHz antenna (Figure 4-24). The first time-slices were characterised by the presence of thin linear reflections with a general N-S orientation which might be due to plough marks (1 in Figure 4-24). A wider anomaly of successive high and low amplitudes was detected near the area of the burial cairn (2 in Figure 4-24). Other linear high and low amplitude reflectors were detected along the time-slice sequence which may be of archaeological interest. At a greater depth, the last time-slices showed two linear reflectors running NNW-SSE limited to the west edge of the GPR grid.

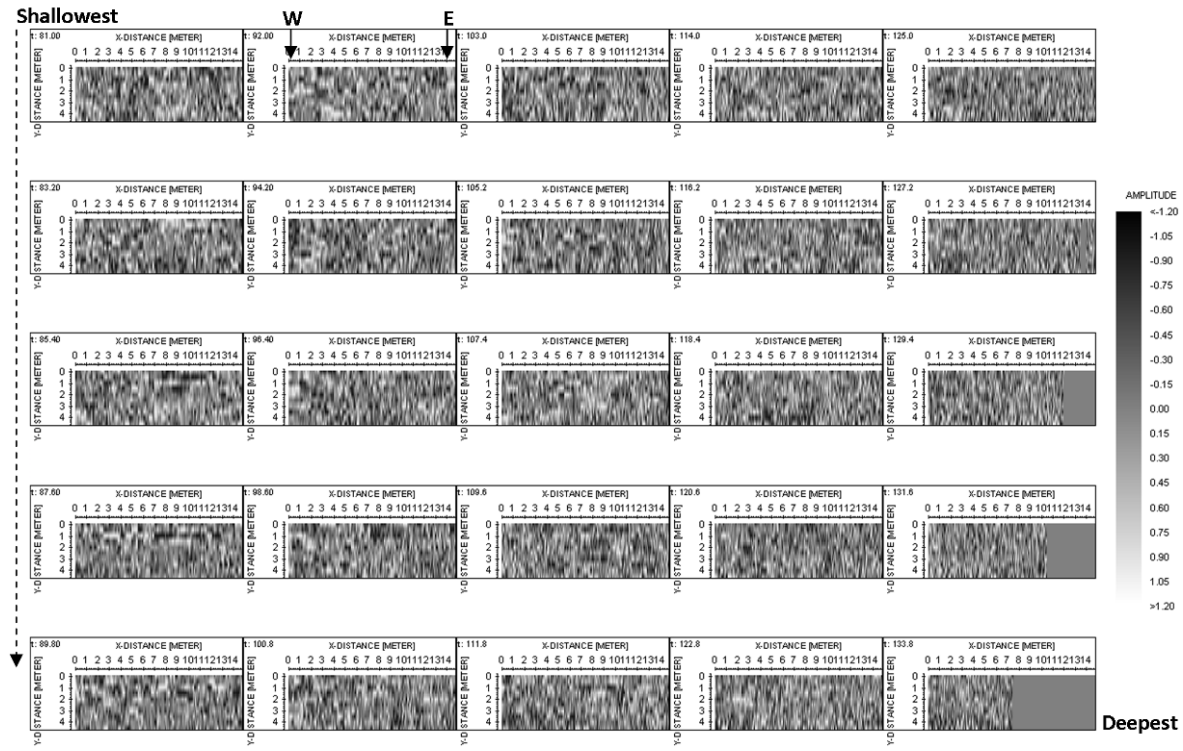

Figure 4-23: Time slices showing the results of the GPR survey (450 MHz) in Area 1 (Figure 4-18) over the burial cairn at Scalpsie Bay.

Figure 4-24: Time slices showing the results of the GPR survey (225 MHz) in Area 1 (Figure 4-18) over the burial cairn at Scalpsie Bay. The two time-slices outlined in red mark the examples described in the main text.

Area 2

The results of the 225 MHz survey (Figure 4-26) are dominated by a linear reflector with approximate E-W orientation crossing the grid. The anomaly starts at *c*. 27ns twt or 1m depth (in red in Figure 4-26) until 35.6ns twt (*c*.1.5m deph). The depth of the anomaly is thought to suggest a geological origin rather than an archaeological one.

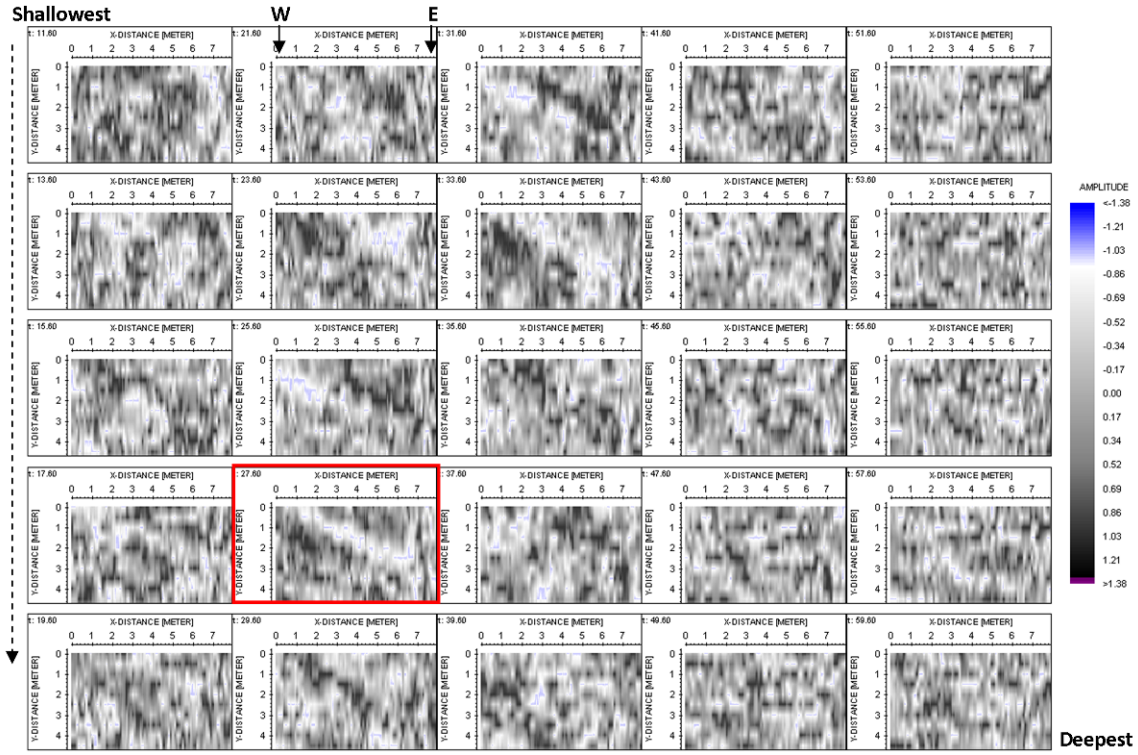

Figure 4-25: Time slices showing the results of the GPR survey (225 MHz) in Area 2 (Figure 4-18) over the burial cairn at Scalpsie Bay. The time-slice outlined in red mark the examples described in the main text.

Area 3

The first time-slices of the 225MHz data (Figure 4-26) show a linear band of high amplitudes following an E-W direction (1 in Figure 4-26). Also, thinner high-amplitude linear reflections were detected with a general NNW-SSE orientation (2 in Figure 4-26).

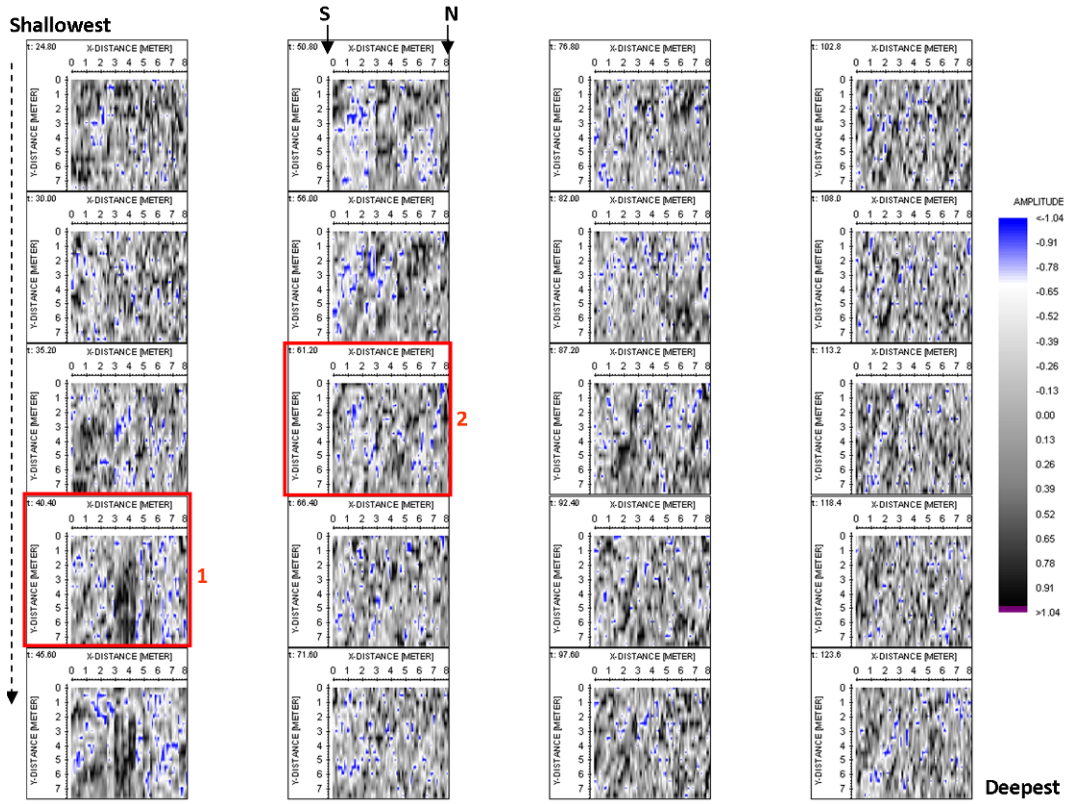

Figure 4-26: Time slices showing the results of the GPR survey (225 MHz) in Area 3 (Figure 4-18) over the burial cairn at Scalpsie Bay. The two time-slices outlined in red mark the examples described in the main text.

Area 4

The results of the 225 MHz survey show some linear reflections with a general W-E orientation (e.g. time-slice marked in red, Figure 4-27).

Figure 4-27: Time slices showing the results of the GPR survey (225 MHz) in Area 4 (Figure 4-18) over the burial cairn at Scalpsie Bay. The time-slice outlined in red mark the examples described in the main text.

4.3.1.6. **Magnetic Susceptibility Interpretation**

4.3.1.6.1. *Targeted Anomalies*

Enhanced MS values (Figure 4-28) were recorded in areas of the burial cairn and stone heap (anomaly 4 in Figure 4-13). Superficial meta-igneous stones or other debris (i.e. iron superficial objects) might be the source of the high readings. However, surrounding areas located over the current extent of the burial cairn produced lower MS readings. These areas correlate with the locations of the magnetic anomaly (2) from Figure 4-13. Since magnetic anomalies (1) and (3) from Figure 4-13 were not measured due to instrument failure after grid 2, the overall results of this survey must be considered cautiously.

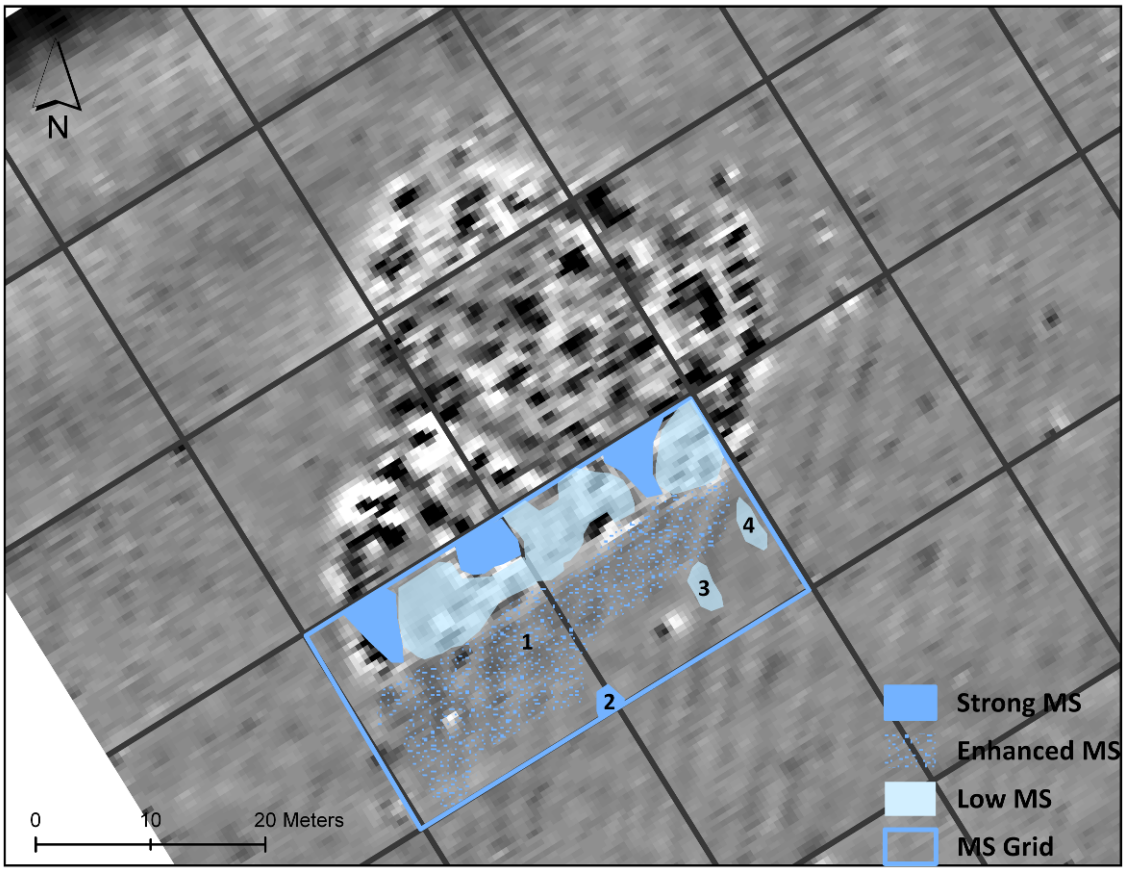

Figure 4-28: Anomaly extraction and interpretation plot of the magnetic susceptibility (MS) results at Scalpsie Bay. The MS results overly the gradiometer data. The numbers (1-4) mark the anomalies discussed in the main text.

4.3.1.6.2. *Other Anomalies*

Outside the current extent of the burial cairn, the enhanced MS area (1 in Figure 4-28) might be caused by the indirect magnetic enrichment of the topsoil due to

its organic content. Unfortunately, the limited extent of the survey did not allow a more solid interpretation of this enhancement.

The enhanced MS anomaly (2 in Figure 4-28), with readings reaching 149 SI in the raw MS data, correlates with the approximate location of a positive magnetic anomaly seen in the magnetic raw data (Figure 4-11). This response might be produced by a fairly shallow buried object. Other elongated and pit-like low MS anomalies, (3) and (4) in Figure 4-28, did not show any correlation with the gradiometer results. These anomalies might be caused by a depression or change in thickness of topsoil but a possible archaeological cause should not be disregarded.

4.3.1.7. **Earth Resistance Interpretation**

4.3.1.7.1. ***Targeted Anomalies***

The high resistance anomaly 1 (Figure 4-29) seems to correspond to a structure – a primary phase of the burial cairn - because of its coherent circular form and correlation with the ring-like magnetic anomaly (1 in Figure 4-13). The low resistance anomaly 2 (Figure 4-29) also correlating with the targeted magnetic anomaly 2 (Figure 4-13), shows an area of low resistance at the SE of the monument between two coherent areas of high resistance which reinforces its interpretation as structural, probably a chamber entrance.

In the WNW of the monument, a curvilinear low resistance anomaly 3 (Figure 4-29) was detected approximately in the area of the negative magnetic anomaly (3 in Figure 4-13). The exact position of the magnetic anomaly (3) correlates with a low resistance trend that connects two coherent low resistance anomalies (3 in Figure 4-29). The anomaly might be caused by a potential negative feature (i.e. a ditch) but also might be produced by the effect of ploughing around the monument. Regarding the targeted magnetic anomaly 4 (in Figure 4-13), the earth resistance data showed high values in the area occupied by the stone heap (4 in Figure 4-29).

To the south, a high resistance area as a prolongation of (4) may be caused by ploughing. Towards the E of anomaly 4 (Figure 4-29), another slightly weaker high resistance area was detected. Although it is difficult to interpret these

anomalies, their distance and shape point toward a link with disturbance of the monuments, for example a heap of stones remaining after the cairn was dismantled.

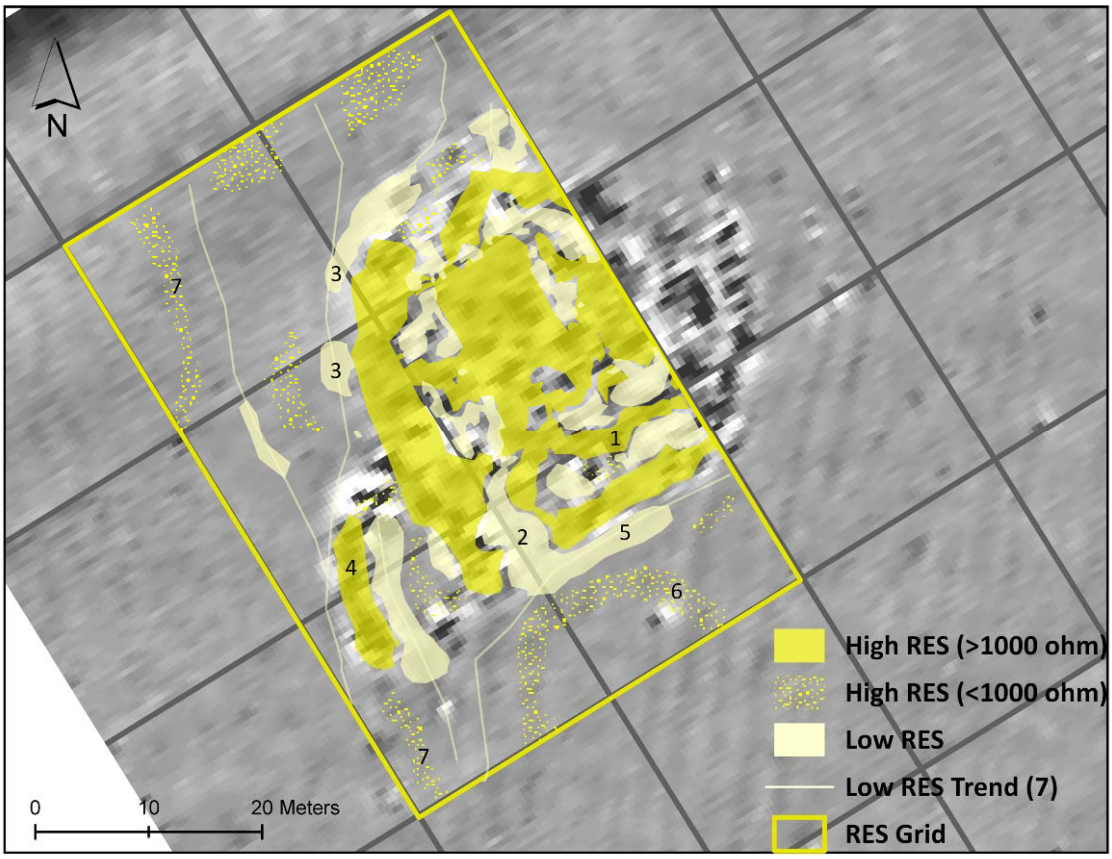

Figure 4-29: Anomaly extraction plot of the earth resistance results (0.5m probe separation) at Scalpsie Bay. The results overly the gradiometer data. The numbers (1-7) mark the anomalies discussed and interpreted in the main text.

4.3.1.7.2. *Other Anomalies*

A low resistance anomaly (5 in Figure 4-29) was detected surrounding the burial cairn on its southern edge, at the base of the slight slope of a bank (*c.*10˚) where the monument lies. This anomaly was not detected with the gradiometer and its potential archaeological or natural origin is difficult to discern because of the small scale of the survey.

The curvilinear and weak high resistance anomaly 6 (Figure 4-29) is likewise difficult to interpret. Other longitudinal anomalies (7 in Figure 4-29) with a general N-S direction correlate in location and orientation to the plough marks detected with the gradiometer survey.

4.3.1.8. **GPR Interpretation**

4.3.1.8.1. ***Targeted Anomalies***

The two subtle attenuated areas with small diffraction hyperbolae (Anomaly 1 in Figure 4-30 and Figure 4-31) correlated with the location of the ring-like magnetic anomaly (1 in Figure 4-13). Despite the problems of estimating the depths in the GPR data corrected for topography, the base of these anomalies appears to be *c.*60-80cm deep. The response produced by these anomalies suggest that they might be caused by GPR energy-absorbing materials such us fine-grained silt and clays (Bristow and Jol 2003), or small strong (point) reflectors. These anomalies possibly represent the infill of a former structure related to the burial cairn (i.e. the ring-like magnetic anomaly). Another area presenting lower amplitudes and dipping linear anomalies (anomaly 2 in Figure 4-30) was detected in the same location as the magnetic anomaly 2 (Figure 4-13). The dipping reflectors might mark the location of a slightly sloping or tilted structure (i.e. an entrance or a chamber). The negative magnetic anomaly 3 (Figure 4-13) correlated with a coherent and wide area of successive low and high amplitudes in the GPR area 1 (1 in Figure 4-32). The results of the GPR area 2, at the same time window, did not show any response of relevance (Figure 4-32).

4.3.1.8.2. ***Other Anomalies***

The wide linear band of high amplitudes (2 in Figure 4-32) was detected in the same location as the low resistance anomaly 5 (Figure 4-29). The results over the stone heap area (anomaly 4 in Figure 4-13) provided a sub-rectangular anomaly of interest (GPR area 4 in Figure 4-32). However, the interpretation of these results is difficult and inconclusive because of the small surveyed area. In Figure 4-31, anomaly 2 shows an area of general attenuation of the signal which corresponds to the area of the burial cairn that might have been disturbed. The GPR results detected a series of linear and high amplitude reflections that provide evidence of the agricultural activities (i.e. ploughing) carried out all around the monument.

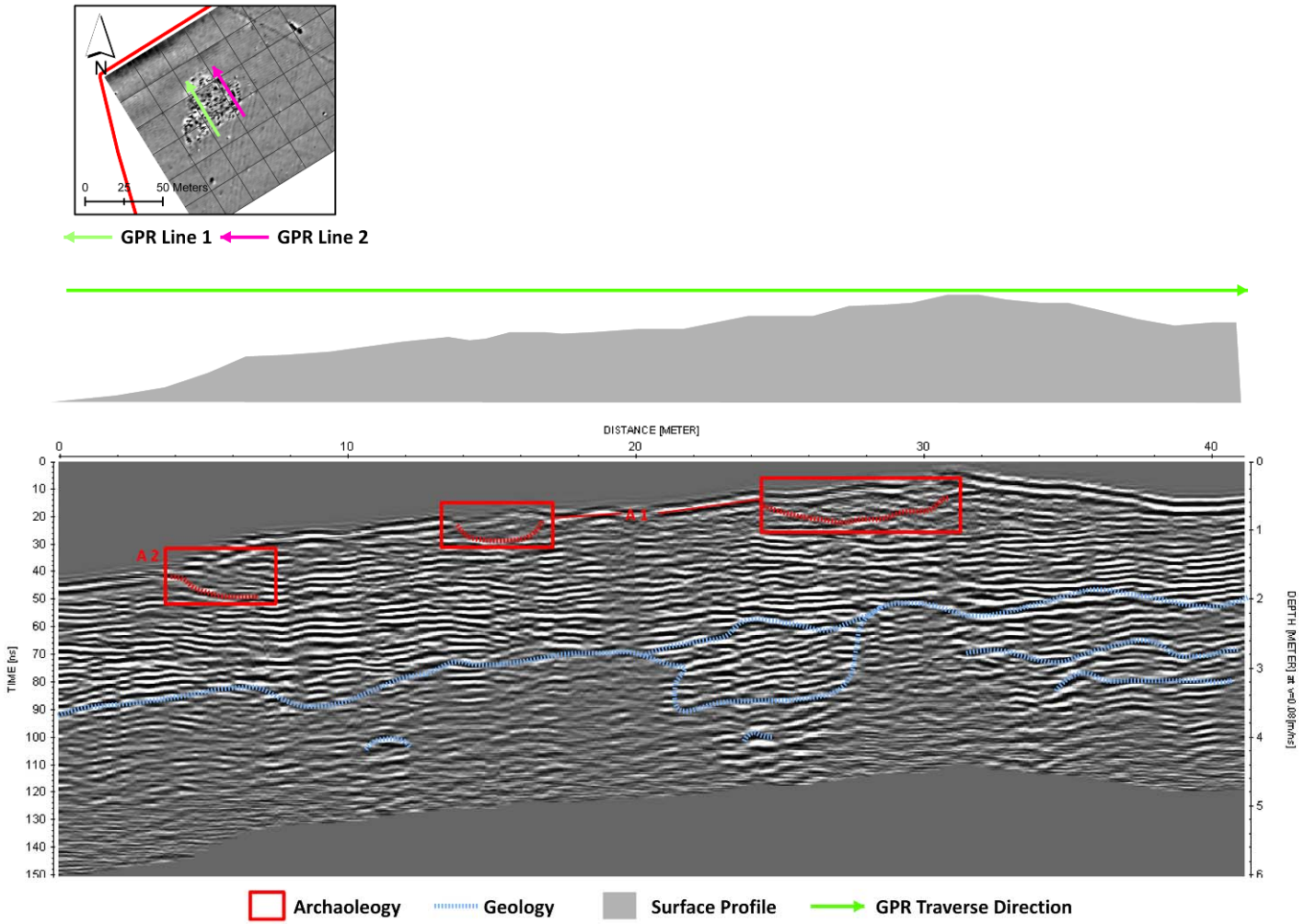

Figure 4-30: Radargram showing the results and interpretation of the GPR single line 1 (225 MHz frequency survey) over the burial cairn at Scalpsie Bay. The numbers (A1 and A2) mark the anomalies discussed in the main text.

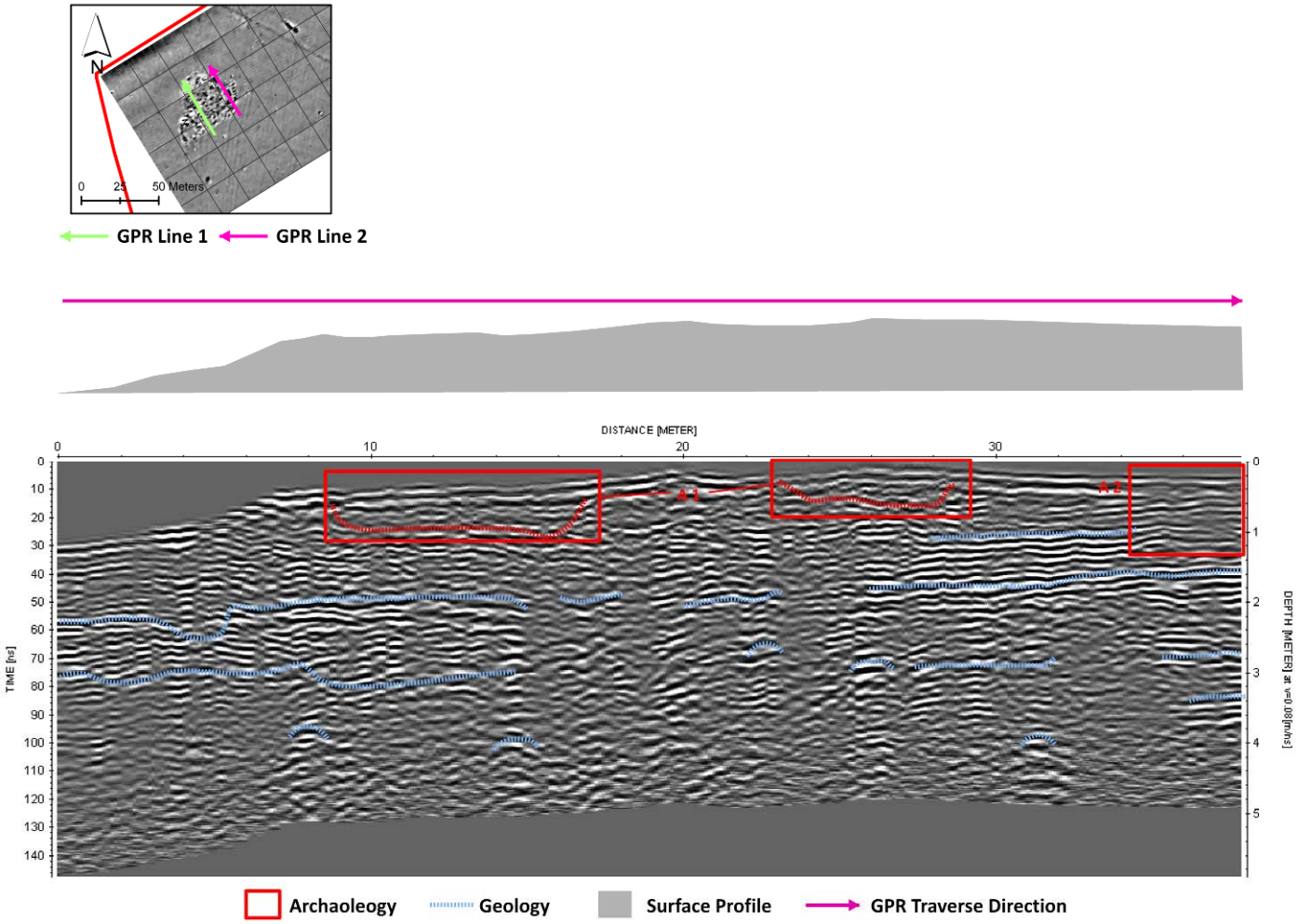

Figure 4-31: Radargram showing the results and interpretation of the GPR single line 2 (225 MHz frequency survey) over the burial cairn at Scalpsie Bay. The numbers (A1 and A2) mark the anomalies discussed in the main text.

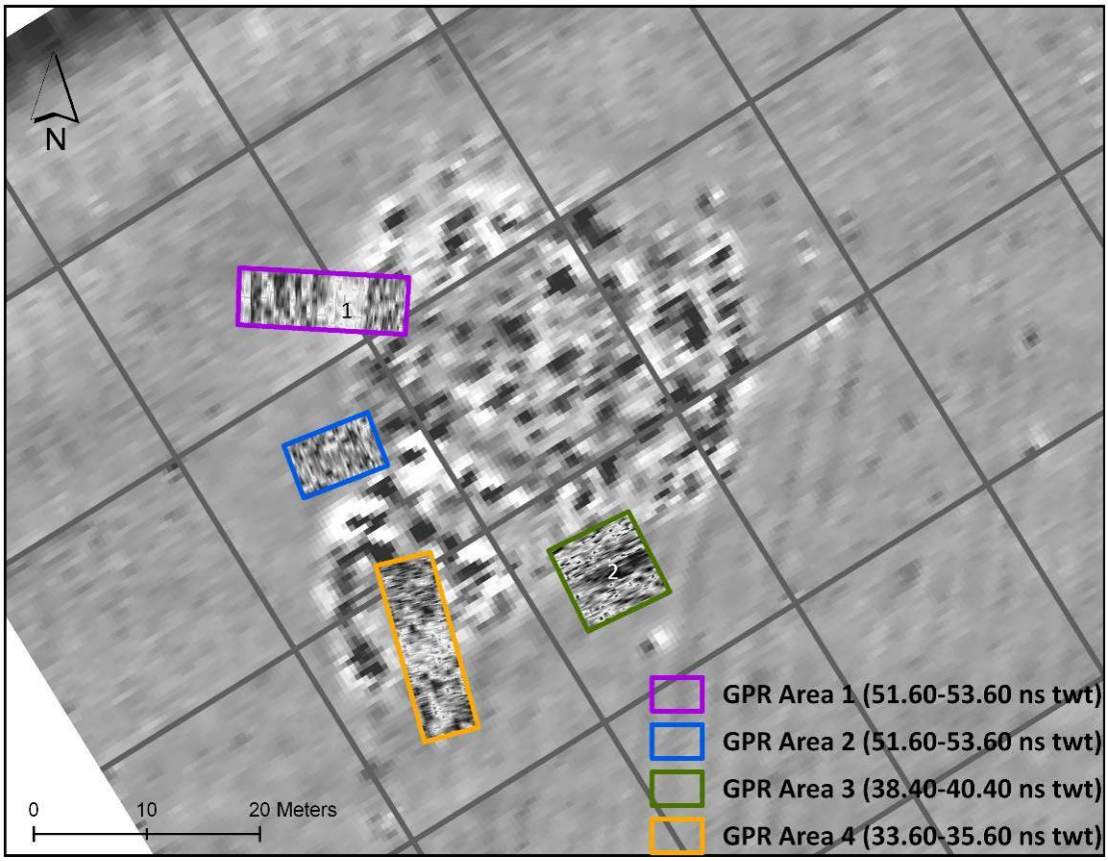

Figure 4-32: Selected time-slices showing the results of the targeted GPR surveys at Scalpsie Bay. The time-slices are overlying the gradiometer data. The GPR data shows high amplitudes in black and low amplitudes in white. The numbers (1 and 2) mark the anomalies discussed in the main text.

4.3.1.9. **Discussion**

In general, earth resistance and GPR techniques produced responses to the soil conditions on the site that are informative as most of the detected anomalies correlate with the magnetic results (Figure 4-33). This reinforces the view that the detection of these anomalies is related to soil contrast and not to errors in data collection or processing. The results of the earth resistance survey were fairly similar to the gradiometer data. However, the characterization of internal features (i.e. anomaly 1 in Figure 4-13) was resolved to a lesser extent in comparison to the gradiometer data, despite the fine traverse interval used. The constant need to dummy readings due to the presence of stones on the surface was not only time consuming but also a main factor for the low resolution, especially because of the concentration of surface stones towards the centre of the monument. Nonetheless, the earth resistance survey revealed anomalies of interest in areas around the monument which were not detected by the gradiometer (e.g. anomalies 5 and 6 in Figure 4-29).

The results of the single GPR traverses using 225 MHz frequency were of particular interest as they permitted characterization of the response and depth estimation of the ring-like anomaly (Figure 4-30 and Figure 4-31). Both the earth resistance and the GPR surveys detected an anomaly to the south of the monument which was not detected by the gradiometer survey. The archaeological or agricultural origin of this anomaly was difficult to discern because of the small scale of the survey.

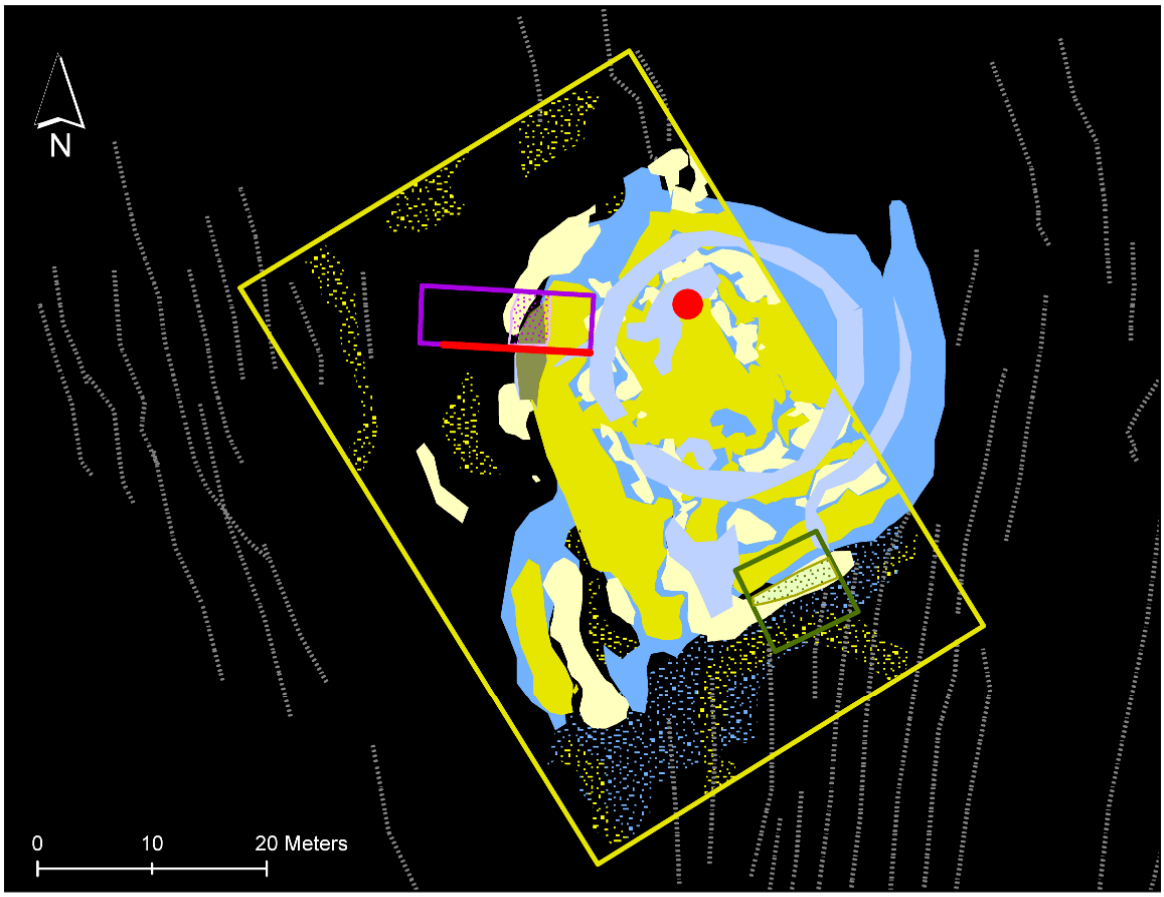

Surface Soil Sampling
GPR Area 1
GPR Area 3
RES Grid
Plough Marks
Cist
Low Amplitude Anomaly (1)
Low Resistance Anomaly (3)
Negative Magnetic Anomaly (3)
Weak Positive Magnetic Anomaly
High Amplitude Anomaly
High Resistance Anomaly (>1000 ohm)
High Resistance Anomaly (<1000 ohm)
Positive Magnetic Anomaly
Enhanced MS

Figure 4-33: Integrated anomaly extractions from all the geophysical surveys and location of the surface soil samples over the negative magnetic anomaly 3 in Figure 4-13, 3 in Figure 4-29 and 1 in Figure 4-32.

Earth resistance and GPR also detected the negative magnetic anomaly 3 (Figure 4-13). The results of the three techniques points towards this anomaly being created by the contrast in soil conditions and not by an effect of the dipolar halos. However, interpretation of anomaly 3 (Figure 4-13) as a feature of archaeological significance is difficult since intense ploughing and disturbance of the monement (i.e. stone robbing) has modified its shape. In order to verify the nature and the interpretation of anomaly 3, ground-truthing and geochemical characterization were initially planned as part of the DBLS project in Scalpsie Bay. However, the main fieldwork was focused on the east cairn and the rules related to scheduled monuments made the ground-truthing of the burial-cairn unfeasible. Nevertheless, soil analysis of surface samples was deemed to be of interest for studying potential correlations between the geochemical and geophysical results in order to aid the interpretation of anomaly 3 (Figure 4-13).

4.3.2. Soil Analysis

4.3.2.1. **Aim**

The aim was to characterise the soil surface response of an intriguing negative magnetic anomaly detected by the gradiometer survey (3 in Figure 4-13) in terms of its physical and chemical composition in order to help with the interpretation of the anomaly by establishing an archaeological, natural or other origin. Also, the analysis aimed to assess the effectiveness of pXRF, MS and phosphate analysis in detecting the targeted anomaly and/or the monument.

4.3.2.2. **Sampling Strategy**

Soil samples were collected at 1m intervals along a line in GPR area 1 (Figure 4-33). The soil was collected to an approximate depth of 0.10m in order to reach the first horizon of interest established by previous auger soil characterisation. The location of the controls is shown in Figure 4-14.

4.3.2.3. **Physical and Chemical Results & Discussion**

The general results of the different geochemical analysis are shown in Table 4-11, Figure 4-34, and Figure 4-35 to Figure 4-37 (pXRF data). The MS results showed variable values in the first metres with a gradual decrease in values from samples 5 to 9 (Figure 4-34). The lowest susceptibility value (68.2 $\chi 10^{-8} m^3 kg^{-1}$ in

Table 11) corresponds to sample 7 whose position correlates with the centre of the anomaly (Figure 4-34). The results from this point onwards showed a general and gradual increase in susceptibility along the area where the monument is situated. Therefore, the MS depletion observed in the area where the targeted anomaly was detected correlates with the geophysical results.

The results of the loss of ignition analysis showed a general decrease of the organic matter content of the samples as the burial cairn was approached (Figure 4-34). However, the total phosphate concentrations showed the reverse response, with a general increase as the samples reached the monument. Neither the loss on ignition results nor the phosphate values showed any variation in the samples located over the anomaly. The lack of correlation with the loss of ignition (LOI) results might be explained by the effect of loss of inorganic materials (Christensen and Malmros 2012).

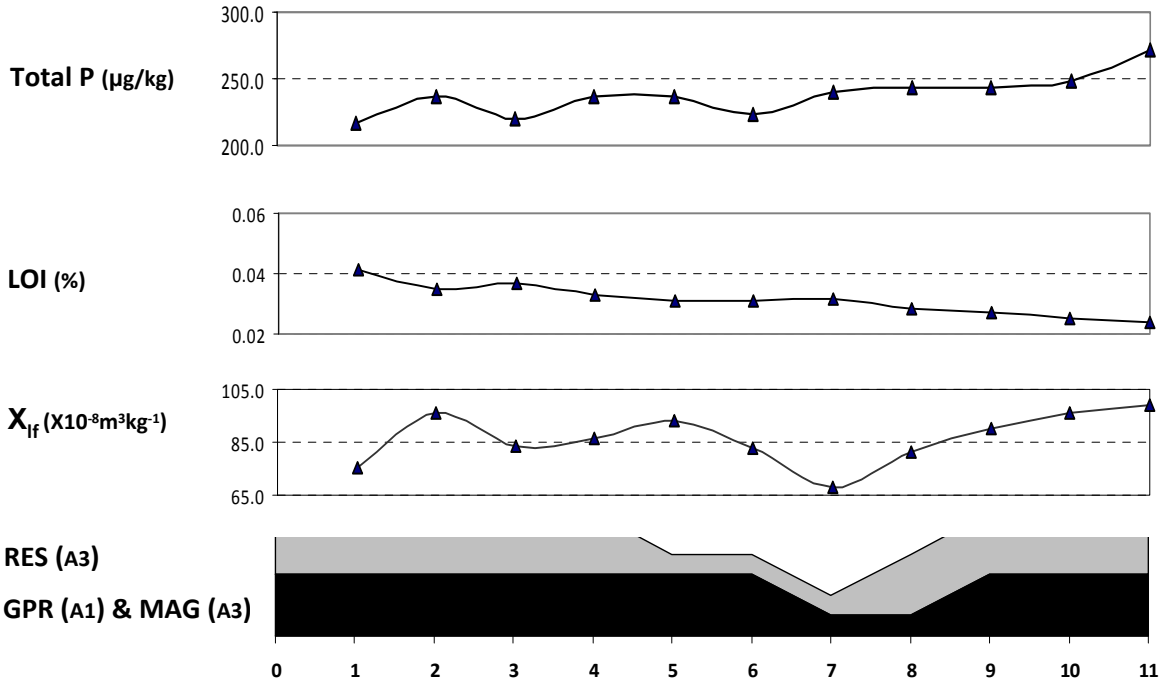

Figure 4-34: Surface distribution of magnetic susceptibility (χ_{lf}), total phosphate (P) and loss on ignition (LOI) of the samples collected over the location of a negative magnetic anomaly in GPR area 1 (Figure 4-33) at Scalpsie Bay. The black and white area graph denotes the position of the targeted anomaly in relation to the soil samples. A1 and A3 specify the anomaly number assigned in the interpretation of the results for each technique.

The pXRF results did not show distinctive enrichments or depletions in the two most abundant elements measured in the samples, Fe and K along the traverse (Figure 4-35). However, both elements presented slight depletions over the

targeted anomaly. In the case of iron, a higher sampling resolution would be necessary to validate the depletion. Since the availability for sorption of K, another common anthropogenic element , is also largely controlled by the type and content of organic matter and clay (Oonk 2009), the low values of K in sample 7 (Table 4-11) could be related to an increase of organic matter in the area where the targeted anomaly was detected.

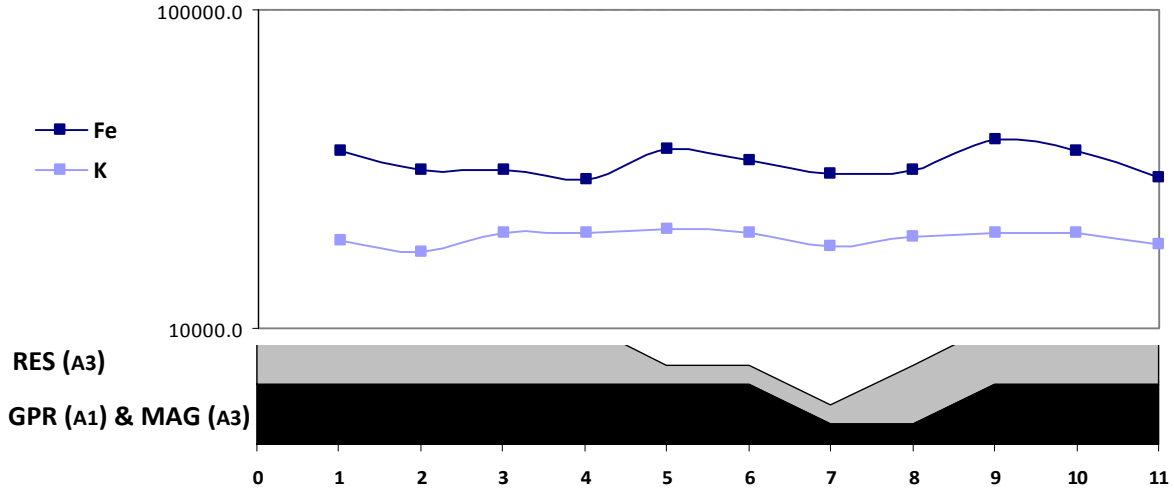

Figure 4-35: pXRF results of the samples collected over the location of a negative magnetic anomaly in GPR area 1 (Figure 4-33) at Scalpsie Bay. The element concentrations are expressed in mg/kg (=ppm).

The concentration of Ca and Mn (Figure 4-36) was low in the first samples and showed an increase in samples in closer proximity to the monument. Taking into account the stony content of the burial cairn, Ca enrichment may be due to the mineral content of the monument as Ca is an important constituent of many rock-forming minerals. An example is Ca-rich amphibole, expected in the area of Scalpsie Bay, produced on metamorphism of the meta-igneous augite (Ca-bearing rock-forming silicate).

More distinctive was the Mn depletion of the concentration of Mn in the samples located over the anomaly (Figure 4-36) which strongly suggests that the targeted negative magnetic anomaly was caused by contrast in soil conditions and not by an effect of negative magnetic halos. The depletion of Mn values may have been due to the reductive dissolution of Mn oxides as a result of decomposing organic matter (Oonk 2009) which may have implications in a potential archaeological interpretation. According to Oonk *et al*. (2009a), Mn has been found in association with burials and graves. In especific, depletions of Mn have been

found indicative of human occupation as a result of reductive dissolution of Mn oxides due to the decomposition of organic matter (Oonk 2009).

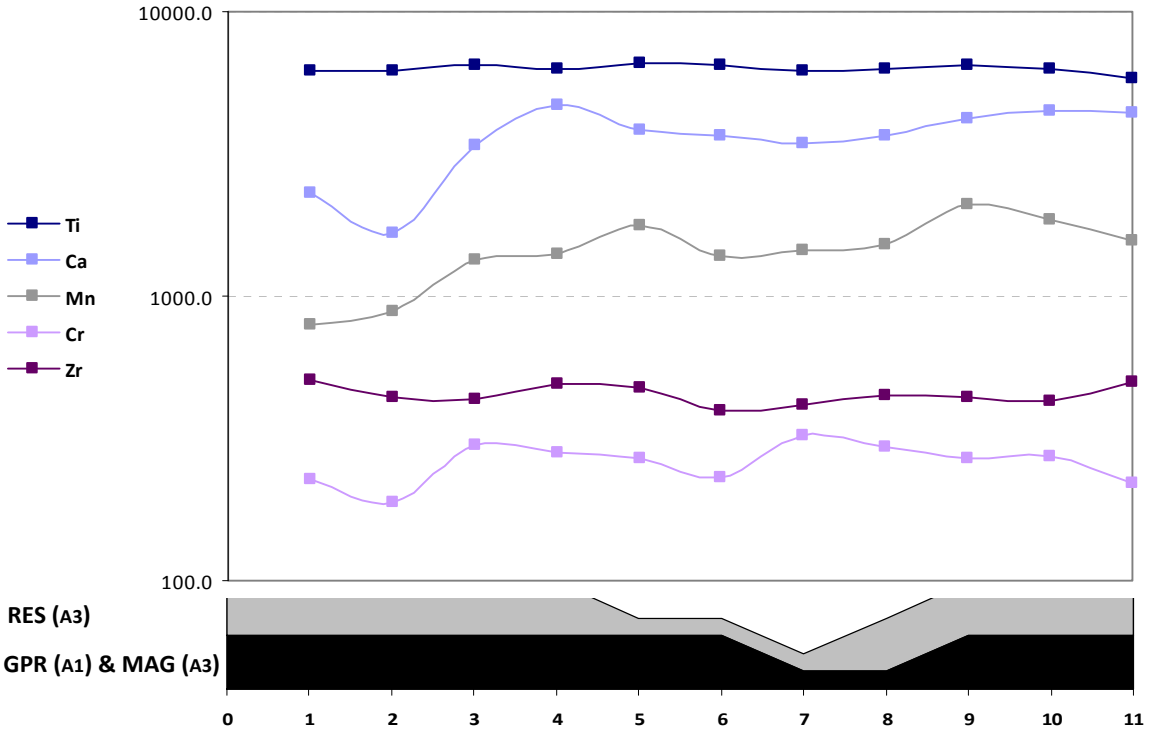

Figure 4-36: pXRF results of the samples collected over the location of a negative magnetic anomaly in GPR area 1 (Figure 4-33) at Scalpsie Bay. The element concentrations are expressed in mg/kg (=ppm).

Distance (m)	Xlf	LOI (%)	Total P µg/kg	Fe	K	Ti	Ca	Mn	Zr	Cr	Rb	Sr	Pb	Cu
1	75	0.041	217	36226	18982	6189	2286	789	508	227	106	73	49	54
2	96	0.035	236	31545	17453	6183	1663	889	441	188	91	64	33	35
3	84	0.037	220	31233	19934	6471	3392	1339	432	300	95	71	16	35
4	86	0.033	236	29337	19808	6308	4656	1412	493	283	86	68	17	34
5	94	0.031	236	36676	20525	6616	3822	1776	474	267	105	78	25	31
6	83	0.031	223	33514	19992	6457	3641	1393	394	231	92	68	27	27
7	68	0.032	239	30645	18154	6241	3450	1440	417	322	91	69	21	39
8	81	0.028	243	31608	19293	6249	3680	1515	448	295	85	67	20	28
9	90	0.027	243	38992	19859	6468	4226	2091	443	269	107	80	35	43
10	96	0.025	249	36072	19822	6319	4509	1852	428	272	102	76	23	37
11	99	0.024	271	29905	18409	5820	4381	1567	498	220	81	80	22	40
Mean	87	0.031	238	33250	19294	6302	3610	1460	452	261	95	72	26	37
S.D	10	0.005	15	3234	940	211	924	383	36	40	9	6	10	8
C.V	11	16	6	10	5	3	26	26	8	15	10	8	36	21

Table 4-11: Magnetic susceptibility (χ_{lf}), loss on ignition (LOI), total phosphate (Total P) and pXRF results of the surface soil samples collected at GPR area 1 (Figure 4-33) at Scalpsie Bay. The element concentrations are expressed in mg/kg (=ppm). The green colour (samples 6, 7 and 8) marks the soil samples that were collected over the targeted anomaly.

The concentrations of Cu were variable (Figure 4-37). However, sample 7 (Table 4-11) showed a distinctive peak over the targeted anomaly. Cu is a promising anthropogenic indicator because it is relatively stable in soils, it easily fractionates with organic matter (Paterson 2011) and correlates with the depletions of Mn and K. Therefore, this peak may be indicative of an increase in organic matter in the area where the targeted anomaly was detected. Finally, Pb shows a general depletion as the samples approach the monument. This may indicate the relationship between Pb enrichment and areas influenced by contamination from fuel combustion of agricultural machinery surrounding the monument.

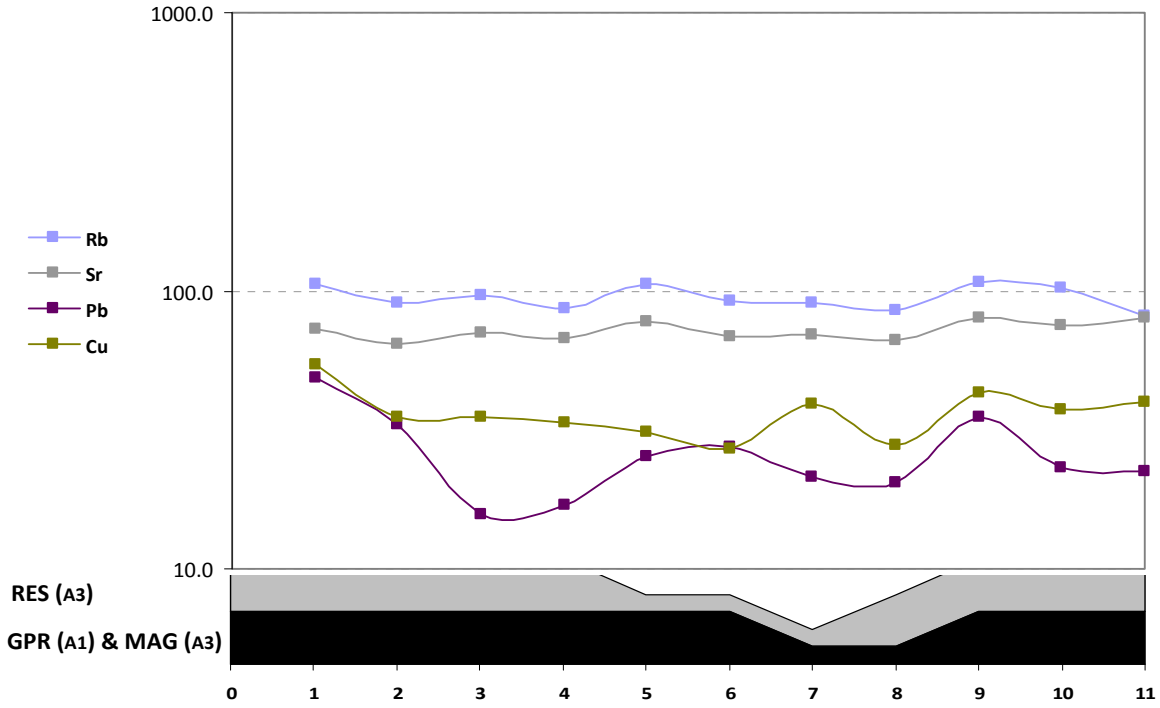

Figure 4-37: pXRF results of the samples collected over the location of a negative magnetic anomaly in GPR area 1 (Figure 4-33) at Scalpsie Bay. The element concentrations are expressed in mg/kg (=ppm).

The gradual increase in susceptibility and total phosphate content in the area occupied by the burial cairn suggest that these techniques would successfully detect the monument in the case of a more extensive survey. In this sense, the general enrichment in the concentrations of Ca and Mn may be related to the presence of the monument.

The depletion of Mn and K, along with the enrichment of Cu over the targeted anomaly may suggest that the level of retention of these elements in the soil is

due to decomposition of organic matter in the backfill of the feature detected by geophysical means. The increase in organic matter in this area at the burial cairn seecould be related to: the presence of a structure related to the cairn (e.g. the remains of a truncated bank or ditch surrounding the monument), or to a more recent event, such us the burial of an animal or garbage produced by agrico-pastoral activities. Nevertheless, the correlation of the results of the chemical analysis (Mn, K and Cu) with the results of other geophysical techniques confirms this anomaly to be a product of the contrast of soil properties and not a spurious magnetic anomaly.

4.4. General Discussion

The gradiometer survey detected anomalies which provide information of interest and enhanced the archaeological record of the burial cairn and environs. The burial cairn was detected well due to the good contrast between the sandy soil and the monument. This technique also revealed some interesting features within the monument despite its noisy character. The technique proved to be very efficient and provided a quick preliminary dataset and targets on which to base other surveys.

Despite the GPR, earth resistance and MS techniques being used only in the area of the burial cairn, and not providing quick coverage, these techniques have proven successful by confirming and complementing the magnetic anomalies. The single GPR traverses across the monument were very effective and provided depth information. Further and more extensive geophysical surveys at the site should continue to contribute to the archaeological record of this monument and its environs.

The auger soil analysis characterised the podzols in the survey area by establishing the different soil horizons, texture and chemical composition as well as confirming the lack of presence of a hard-pan. The low elemental concentration in the upper horizons and the effect of the eluvial horizon seen in the SIFSS data could have contributed to the low background readings of the gradiometer data. Also, the concentration of the leached elements in the B horizon along with the plough activity detected by geophysical means could be responsible for the detection of weak magnetic anomalies with no archaeological

significance. This effect was confirmed by ground-truthing a magnetic anomaly in a test pit dug during the excavation of the barrow (east cairn). No archaeological feature was found, only an area of red and black stagnation was observed, providing evidence of the leaching of chemical compounds.

There was no distinctive enhancement of Fe over the burial cairn. However, increased values of P (mainly inorganic), Mn and Ca were measured over the monument. Whist high levels of these elements at burial sites have been reported in literature in association with bone and teeth sources (Oonk 2009), the enhanced concentrations at this site seem more related to the mineralogical weathering of the stony monument.

The gradiometer results revealed an intriguing negative magnetic anomaly (3 in Figure 4-13) which was further studied. The anomaly could have been produced by an area of disturbance at the monument; alternatively it could be archaeological, for example a truncated ditch or bank; or spurious resulting from halos caused by the dipolar character of magnetic anomalies. The correlation of this anomaly with the results of other geophysical techniques (earth resistance and GPR) and soil sample analysis (MS and chemical analysis) indicates that this anomaly is 'real' and the result of contrasting magnetic properties caused by a buried feature. Furthermore, the K and Mn depletion and Cu enrichment in the samples gathered over the anomaly suggests that these were caused by the decomposition of organic matter. This may have contributed toward the contrast between the infill of the feature detected by geophysics and the soil matrix, although other processes such as soil compaction, temporary moisture content and soil temperature may have also contributed to the contrast. The chemical results also indicated a possible archaeological interpretation of the targeted anomaly. If the backfill of the feature contained organic matter, this could be indicative of the remains of a truncated structure related to the primary phase of the burial cairn. Turf banks and ditches are structural features associated with other burial cairns, hence the chemical analysis could support an archaeological interpretation of the anomaly. Nonetheless, a more recent event could be behind the origin of the anomaly, such as burial of dead cattle or rubbish produced by agro-pastoral activities.

The investigation succeeded in enhancing the archaeological record of the burial cairn. The survey revealed the extent and depth of the cairn, uncovered evidence of internal and external anomalies of archaeological potential as well as areas of disturbance and landscape features. The study provided a better understanding of a complex monument, the current extent of which may have been the result of many years of ancient and modern alteration.

Chapter 5

Surveying over Wind-blown Sands: the Kerbed-wall of the Viking Settlement at the 'East Mound' of the Bay of Skaill (Orkney)

5.1. Introduction

The windblown sands of the 'East Mound' at the Bay of Skaill concealed a recently discovered and remarkably well-preserved Viking/Norse longhouse. The site is located north of the Orkney World Heritage Area, which includes the well-known Neolithic settlement of Skara Brae on the south side of the bay (Childe 1931a, 1931b; Clarke 2003; Richards 1990).

Like many other archaeological sites buried under aeolian deposits, Skara Brae was concealed within a sandy mound and its exceptional remains were exposed after an erosive event, a great sea storm in 1850 (Petrie 1867). Erosive processes are intrinsically related to the discovery and the destruction of this type of coastal archaeological site. Since current climate change dynamics predict further rise in sea level, there is an urgent need to develop strategies in archaeological prospection in order to detect, preserve and protect such types of site before further destruction. Following this general aim, the Birsay-Skaill Landscape Archaeology Project (BSLAP) was responsible for the discovery of the Viking site at the 'East Mound' of the Bay of Skaill (Griffiths and Ashmore 2011; Griffiths and Harrison 2011).

BSLAP began in 2003, coordinated by Dr David Griffiths (University of Oxford) and assisted later by Jane Harrison as assistant director. Their goal was to investigate a series of coastal erosive sandy landforms in the hinterland of three archaeologically-rich bays on the West Mainland of Orkney: Birsay, Marwick and Skaill, using geophysical techniques and targeted excavation (Griffiths and Ashmore 2011; Griffiths and Harrison 2011). The work at the Bay of Skaill focussed on a series of un-studied sandy mounds at the north of the bay. Orkney

College Geophysics Unit carried out gradiometer surveys over the targeted mounds in partnership with the BSLAP in 2004 (Griffiths and Ashmore 2011) and they revealed the mounds as clusters of strong magnetic anomalies that contrasted with a magnetically 'quiet' background. Several of these magnetically 'noisy' areas were targeted with small-scale excavations and they resulted in the discovery of a longhouse in 2005. In spite of the massive stone structure uncovered, the geophysical survey did not reveal any anomaly indicative of this structure, probably because of the noisy character of the mound deposits and the masking nature of the deep windblown sands. Hence the question arose: are other geophysical techniques able to resolve structures under these types of aeolian mounds?

5.1.1. Research Problem

This site was used as a case study for this PhD project because of the challenges in geophysical prospection to survey over deep wind-blown sands. The possibility of targeting known structures and the prospects for ground-truthing and soil sampling also contributed to its selection.

This case study focuses on the results of a multi-technique geophysical survey and soil geochemical analysis over a known kerbed stone structure, adjacent to the Viking longhouse and interpreted as a boundary wall (Griffiths 2007). The study aimed to assess the detection potential of a range of techniques and soil geochemical analysis in an aeolian environment.

5.1.2. Location

The site is located in the bay of Skaill, a coastal opening in the West Mainland of Orkney (Figure 5-1). The bay is characterised by higher ground to the north and south and a central low-lying area with extensive windblown sand deposits and freshwater sources that have attracted past human settlement (Griffiths and Ashmore 2011).

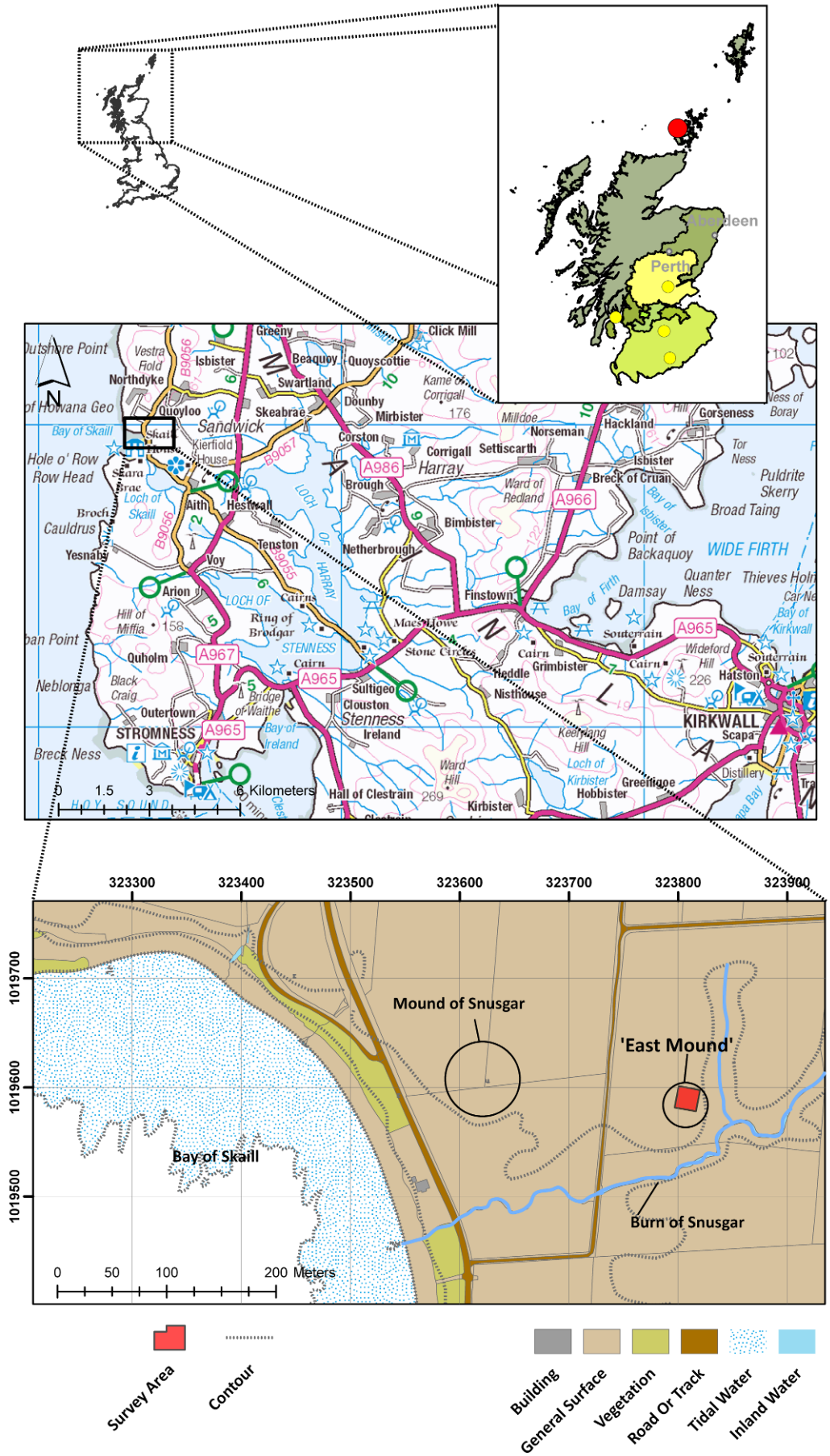

Figure 5-1: Location map of the Bay of Skaill (red dot) in Orkney Islands and in relation to the other case study sites (yellow dots). In the bottom map the survey area is delimited in red and located on the summit of the 'East Mound' (based on © Crown Copyright/database right 2012. An Ordnance Survey/EDINA supplied).

The Viking site was discovered on the summit of the 'East Mound' (NGR HY 2378 1957), situated *c*.190m east from the other important focus of Viking activity, the mound of Snusgar (Griffiths 2006). A slightly higher second summit at the NE of the 'East Mound' was the area where the kerbed-wall was found (NGR HY 2380 1959), only 12m away from the NE end of the longhouse. The mound drops steeply eastwards towards a N-S running branch of the Burn of Snusgar. The mound slopes steadily westward towards the sea.

5.1.3. Geology, Soils & Land Cover

5.1.3.1. **General Bedrock & Drift Deposits**

The underlying geology at the site is the Lower Stromness Flagstone formation (Figure 5-2) of the Caithness Flagstone group (Devonian age Old Red Sandstone super-group) laid down in the lacustrine Orcadian basin. The lithology is formed of laminated, carbonate-rich siltstones and shales with subordinate fine-grained, thinly bedded sandstones, c. 250m thick. The area also is characterised by the presence of igneous dyke swarms (camptonites and some monchiquites) that cut across the Devonian strata (Brown 1975).

The superficial deposits in the area are aeolian deposits of pale brown and fine-grained windblown sands of Quaternary age (Figure 5-3). These sands were derived from large quantities of sand and gravels swept into the sea by Quaternary glaciers. During the rise in sea level in the Holocene, the comminuted sands were mobilised onshore and mixed with shell debris forming beaches. Blown events mobilised the shell-sand beyond the water mark during windstorms, thus forming, developing and modifying sand dunes and mounds.

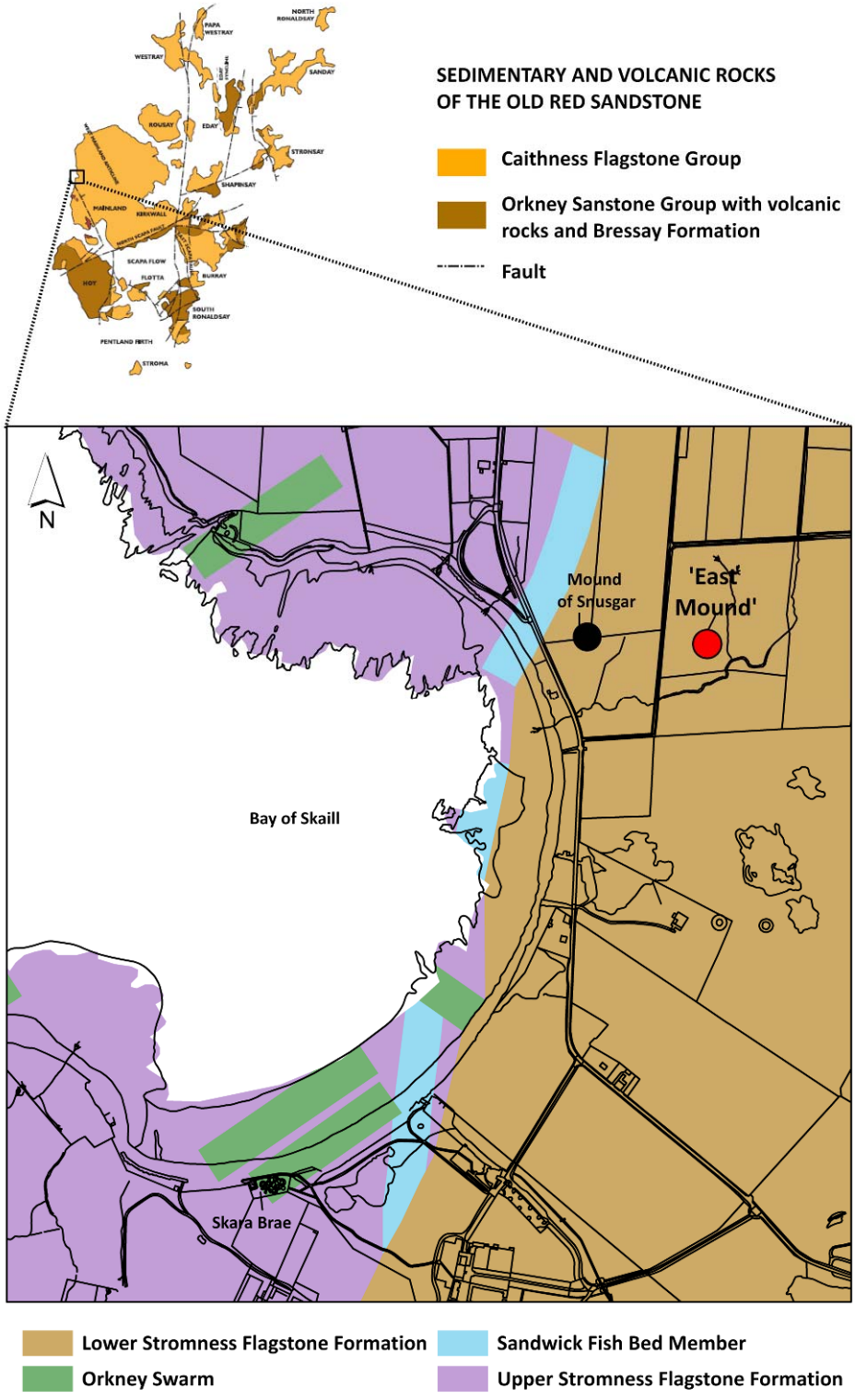

Figure 5-2: The underlying solid geology at the Bay of Skaill (based on Geological Map Data ©NERC 2012).

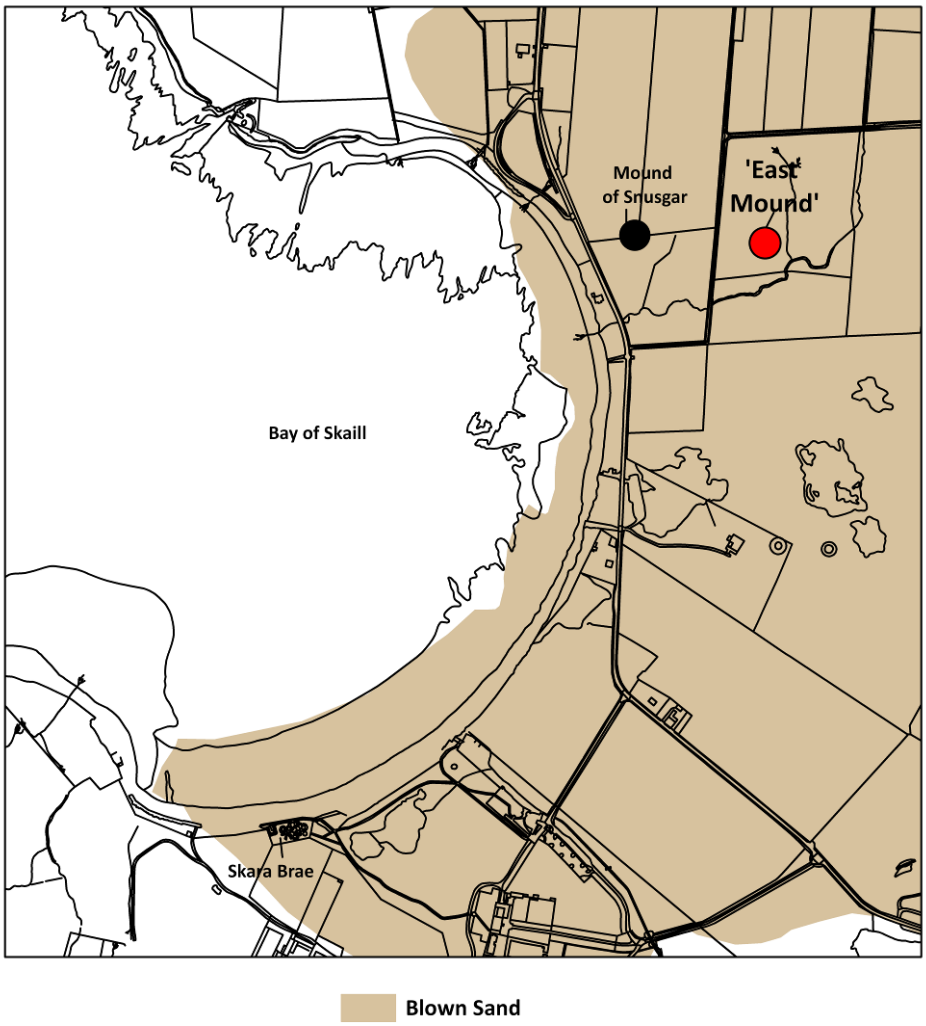

Figure 5-3: The superficial deposits at the Bay of Skaill (based on Geological Map Data ©NERC 2012).

5.1.3.2. **Soils**

Following the Scottish Soils classification of Macaulay Institute, the soils at the 'East Mound' consist of calcareous regosols (windblown sands) of the Fraserburgh series. They are well drained dune sands presenting two general soil horizons: an organic topsoil (A or H) and a thick C horizon starting at *c*.0.20m deep. These aeolian deposits can be fairly substantial and they have a high pH *c*.8 (Macaulay Land Use Research Institute 2011).

5.1.3.3. **Land Cover**

The site is currently used as a pasture area. The grassed sand deposits characterise the *machair* landscape of the coastal plain of the Bay of Skaill where the 'East Mound' is located.

5.1.4. Archaeological Background

After the gradiometer survey was carried out by Orkney College in partnership with the BSLAP in 2004, a small trench was dug in 2005 at the 'East Mound' to test a cluster of strong magnetic responses (Figure 5-4) (Griffiths 2007). The survey did not reveal any structural anomaly suggesting the longhouse and there was not a high expectation of finding any archaeological remains of relevance. After a few days of digging the corner of an unexpected stone structure was exposed in a magnetically quiet area (Figure 5-4), accompanied by midden layers rich in Viking finds. Further excavation in 2006-2007 exposed the plan of the longhouse (Figure 5-4), a large rectangular building with an E-W orientation.

In 2007 another trench was opened at the second and slightly higher summit on the NE side of the mound (in blue in Figure 5-4). The aim was to explore the causes of the strong magnetic anomalies of the 2004 gradiometer survey. Under *c.*1m of windblown sand, a section of the stone foundations of a kerbed structure was revealed, with a N-S direction and *c.*1m wide. A series of midden-type deposits and organic layers were found at the SW corner of the trench. The excavators interpreted the kerbed-structure as a relatively late or sub-recent boundary wall 'built to contain or protect what was to the west' (Griffiths 2007, 31).

Figure 5-4: Location and results of the gradiometer survey (middle) carried out by the BSLAP in 2004, over the 'East Mound' and other sites studied. The shade plots show positive magnetic anomalies in back and negative anomalies in white. A Viking longhouse (bottom) was found in a magnetically quiet area (in red). The foundations of a kerbed-wall were found in a small evaluation trench opened in a magnetically noisy area (in blue).

5.2. The Geophysical Survey

5.2.1. Aim

The aim of the survey for this thesis was to detect the kerbed-wall structure buried under *c*.1m of windblown sand using gradiometry, earth resistance, GPR and EM 38 to assess the capacities of these four techniques to detect the feature.

5.2.2. Survey Area & Data Collection

The geophysical surveys were carried out over a fairly flat area located on the top of the second and highest summit of the 'East Mound' (Figure 5-5 and 5-6).

Figure 5-5: South-facing view of the survey area with the easternmost edge of the excavation trench in the foreground. The red arrow shows the location of the kerbed-wall structure. The orange arrow shows a second wall structure visible in a north-facing section of the excavation trench (© C.Cuenca-García).

The land slightly slopes down at *c*.17m from the easternmost edge of the survey area. The slope drops abruptly *c*.1m out of the survey area towards the burn running N-S. The survey area gently slopes southwards, from *c*.16m from the northernmost edge, towards the excavation trench. Outside the survey area and at its northernmost edge, the mound gently slopes northward.

The survey area presented a high degree of rabbit burrowing (Figure 5-6), especially in the area with the gentle slope towards the burn. There were also many superficial stones and a heap of large stones left after the excavation of the trench in 2007 and from the backfill of the adjacent excavation of the longhouse. These stones and other superficial debris were systematically cleared before the survey started.

The location of the trench excavated in 2007 was pointed out by the BSLAP director and was distinguishable on the grassy surface as a slight rectangular depression *c*. 3m x 8m (Griffiths 2007). A survey grid of 20mx20m was set up around the location of this trench using tapes and tied in to the OS map using a GPS Leica 1200 system. Visible rabbit burrows, superficial big stones and the depression produced by the trench were surveyed with the GPS. The area was generally flat except for a slight rise in the middle of the survey area. Since this rise was fairly subtle and partially disturbed by the excavation of the 2007 trench, no topographic survey for GPR height correction was necessary. However, this superficial gentle rise was taken into account on the interpretation of the GPR data.

The surveys were carried out at the time of the longhouse excavation (2010 season), during four days (1-4 August 2010). The survey parameters and other instrument settings are shown in Table 5-1**.** The general weather conditions during the survey were sunny and dry with very sporadic and light morning rain showers.

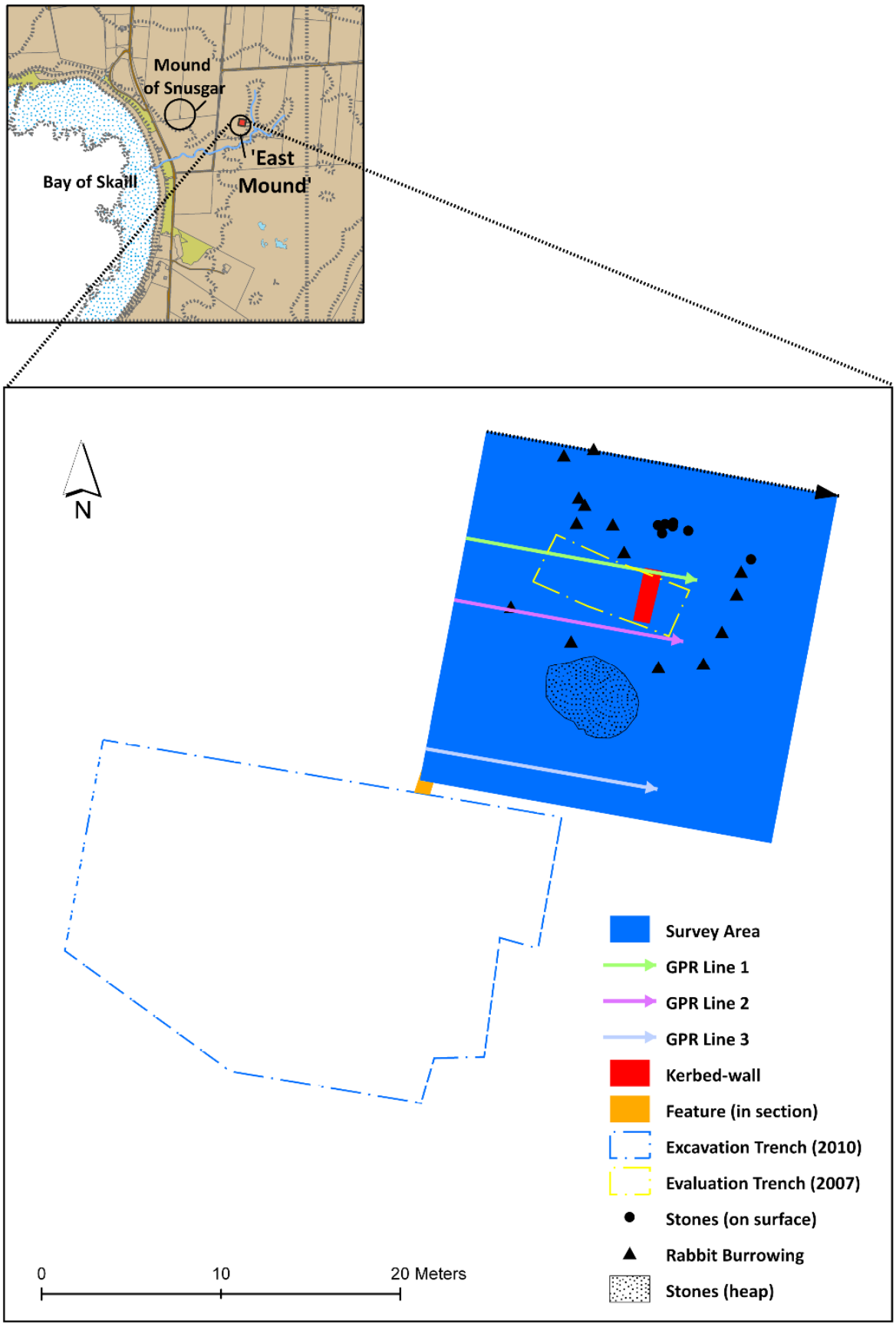

Figure 5-6: Grid location of the multi-technique geophysical survey carried out as part of this research over the kerbed-wall at the 'East Mound' (Bay of Skaill). The black arrows indicate the origin and direction of the surveys (gradiometry, FDEM, earth resistance and GPR).

Technique	Date	Instrument	Traverse Spacing	Sampling Interval	Survey Mode	Other
Gradiometry	01/08/2010	Bartington Grad 601-2	0.5m	0.125m	Parallel traverses.	Lower sensor c. 20cm above the surface & 0.03nT/m (resolution).
EM38	02/08/2010	Geonics EM 38	1m	n.a.	Parallel traverses, vertical mode & inphase and quadrature components logged.	The intrument was connected to a GPS (RTK).
Earth Resistance	03/08/2010	Geoscan RM15 & (MPX15)	0.5m	0.5m	Zig-zag traverses.	x1 range (sensitivity range).
GPR-450 MHz	03/08/2010	Sensors & Software PulseEKKO 1000	Single traverses	0.05m	Continuous mode, time window=80ns, stacks=16, samples=200ps.	An average velocity used during collection for real-time data visualisation= 0.12m/ns.
GPR-225 MHz	03/08/2010			0.10m	Parallel traverses, continuous mode, time window=120ns, stacks=16, samples=400ps.	

Table 5-1: Instrument settings used during the multi-technique geophysical survey at the Bay of Skaill.

The 0.5m traverse spacing was chosen in order to enhance the sampling resolution used during the gradiometer survey carried out in 2004 which used a 1m traverse interval. The earth resistance survey was fairly slow as the instrument gave a constant open-circuit error messages caused by a problem in the cabling of the probe array. The GPR traverses were collected across the survey area and perpendicular to the targeted feature (Figure 5-6) using high and low frequency antennae. The sands provided a good surface for antennae ground coupling and a steady dragging of the GPR system. GPR Line 1 was recorded partially over the trench excavated in 2007 whilst GPR Lines 2 and 3 were surveyed over a non-disturbed area.

5.2.3. Gradiometry Results

The raw and processed data results of the gradiometer survey are plotted in Figure 5-7 and 5-8 respectively. A standard processing flow (Table 5-2) was applied in order to improve the cluttering effect of the general noise in the dataset (Table 5-3). Despite the time spent cleaning the area of surface stones and other debris, the results were affected by the strong response of superficial ferrous objects, stones and the noise produced by rabbit burrowing. As

expected, any coherent anomaly confirmed the presence of the targeted kerbed-wall because of the masking effect of the windblown sands and noisy character of superficial mound deposits. However, there were some weak and fragmented magnetic trends running parallel and at right angles to each other.

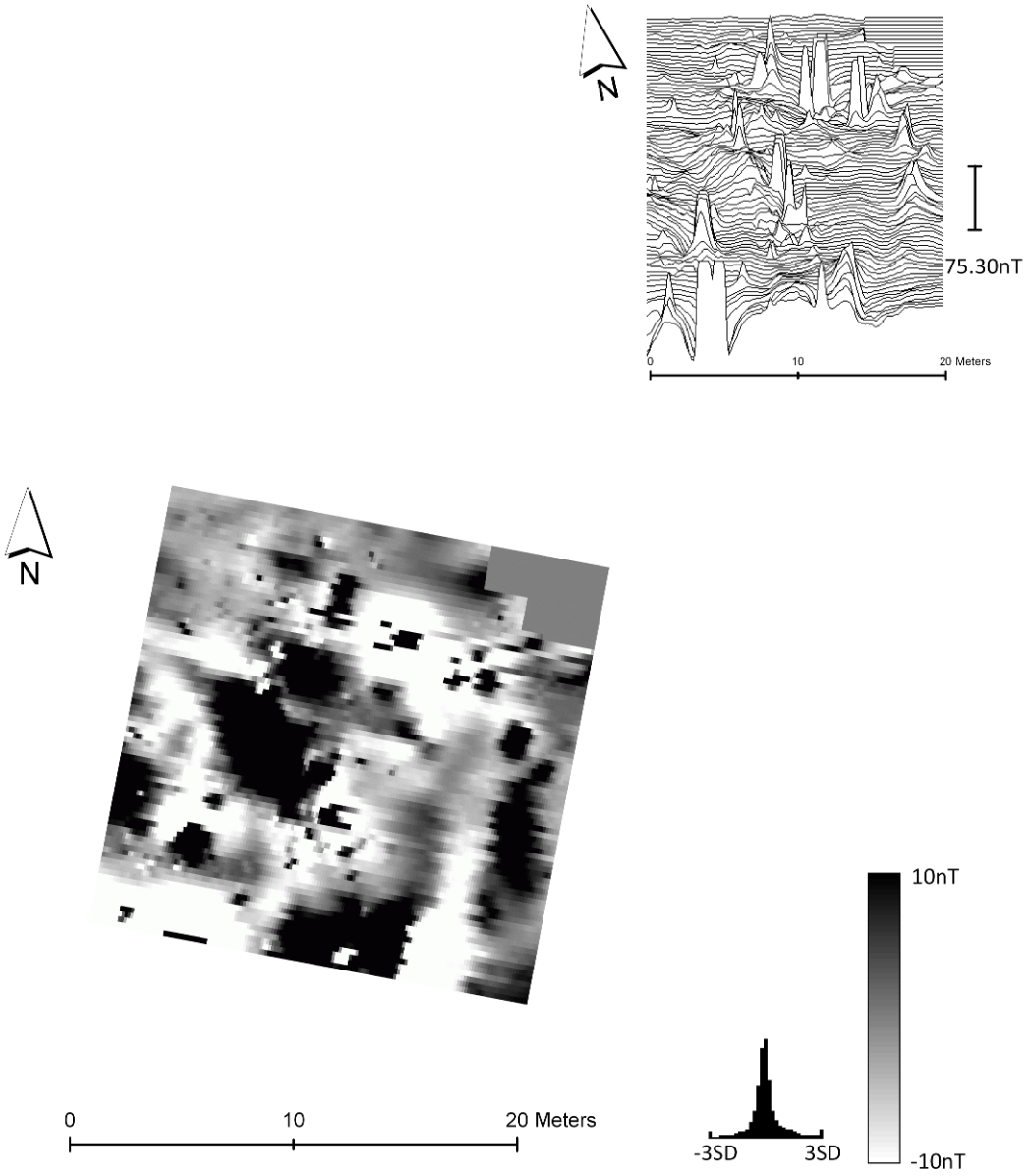

Figure 5-7: Shade (lower left) and trace plot (upper right) of the raw data results of the gradiometer survey over the kerbed-wall at the Bay of Skaill. The data was plotted at -10/10 Absolute units, contrast 1 and using the Geoplot grey99 palette.

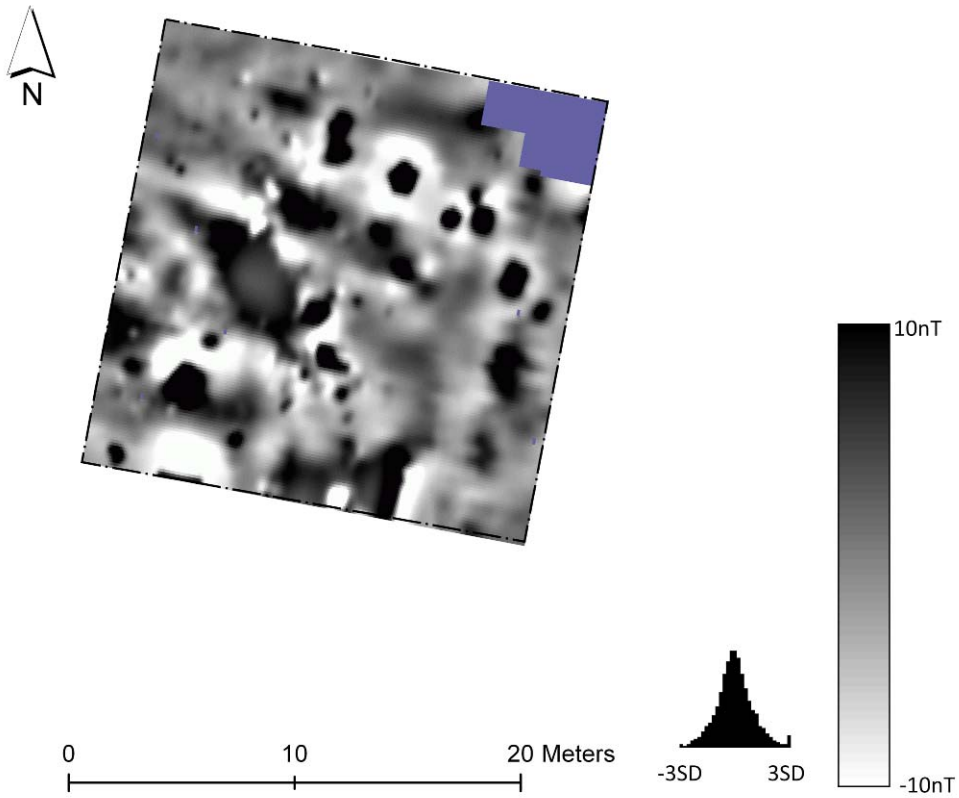

Figure 5-8: Shade plot of the processed data results of the gradiometer survey over the kerbed-wall at the Bay of Skaill. The data was plotted at -10/10 Absolute units, contrast 1 and using the Geoplot grey99 palette. The blue colour indicates dummied readings.

Function	Parameters
Clip	Min -20, Max 21
Despike	1 (X/Y Radii), 3 (Threshold), Mean (Replacement)
High Pass Filter	11 (X & Y), Uniform (Weighting)
Low Pass Filter	2 (X & Y), Gaussian (Weighting)
Interpolate	X & Y (Direction), Expand, SinX/X

Table 5-2: Data processing (Geoplot 3.0 software) applied to the data acquired during the gradiometer survey over the kerbed wall at the Bay of Skaill. The functions are described in Chapter 3.

Gradient	Raw	Processed
Mean	100nT to -100 nT	+/-31nT
Background	-6nT to 9 nT	-2nT to +4nT

Table 5-3: Range of the dataset of the gradiometer survey at the Bay of Skaill before and after processing.

5.2.4. Earth Resistance Results

The earth resistance survey provided poor results and a striping pattern in the data caused by instrument failure. The survey only detected a high resistance area related to compacted soil underlying the stone heap that was cleared before the surveys. A general gradient in soil resistance was distinctive in the results. The westernmost area showed lower resistance values probably indicating a higher degree of moisture content due to deeper topsoil and sand deposits. Towards the east, the soil resistance values progressively increased because of the shallower depth of the topsoil as the slope of the mound was approached.

The raw and processed data are plotted in Figure 5-9 and 5-10 respectively. The processing flow applied to this set of data (Table 5-4) did not reveal any other anomaly of interest. The high resistance maximum in the raw data (935 ohms in Table 5-5) may have been caused by the contact of the probes over superficial buried stones or other type of debris.

Function	Parameters
Despike	1 (X/Y Radii),3 (Threshold), Mean (Replacement)
High Pass Filter	10 (X & Y), Uniform (Weighting)
Low Pass Filter	1 (X & Y), Gaussian (Weighting)
Interpolate	X & Y (Direction), Expand, SinX/X

Table 5-4: Data processing (Geoplot 3.0 software) applied to the data acquired during the earth resistance (RES) survey over the kerbed wall at the Bay of Skaill. The functions are described in Chapter 3.

Gradient	Raw	Processed
Mean	170 Ω	9 Ω
Min/Max	4 Ω / 935 Ω	-126.94 Ω / 142 Ω

Table 5-5: Range of the dataset of the earth resistance survey at the Bay of Skaill before and after processing.

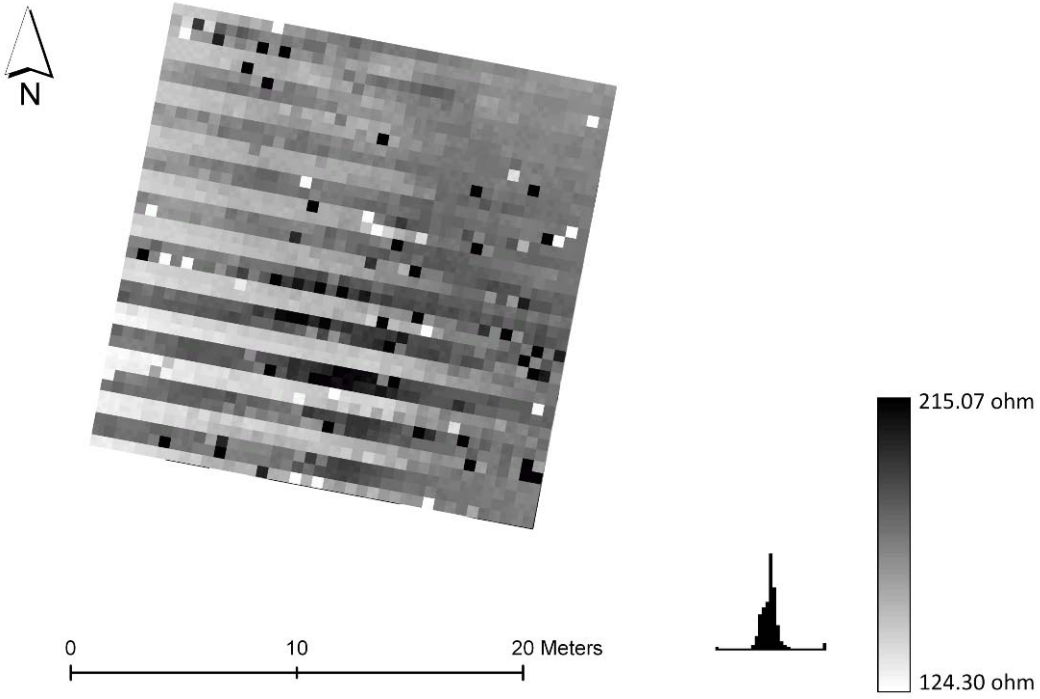

Figure 5-9: Shade plot of the raw data results of the earth resistance survey over the kerbed-wall at the Bay of Skaill. The data was plotted at -1/1 SD units, contrast 1 and using the Geoplot grey99 palette.

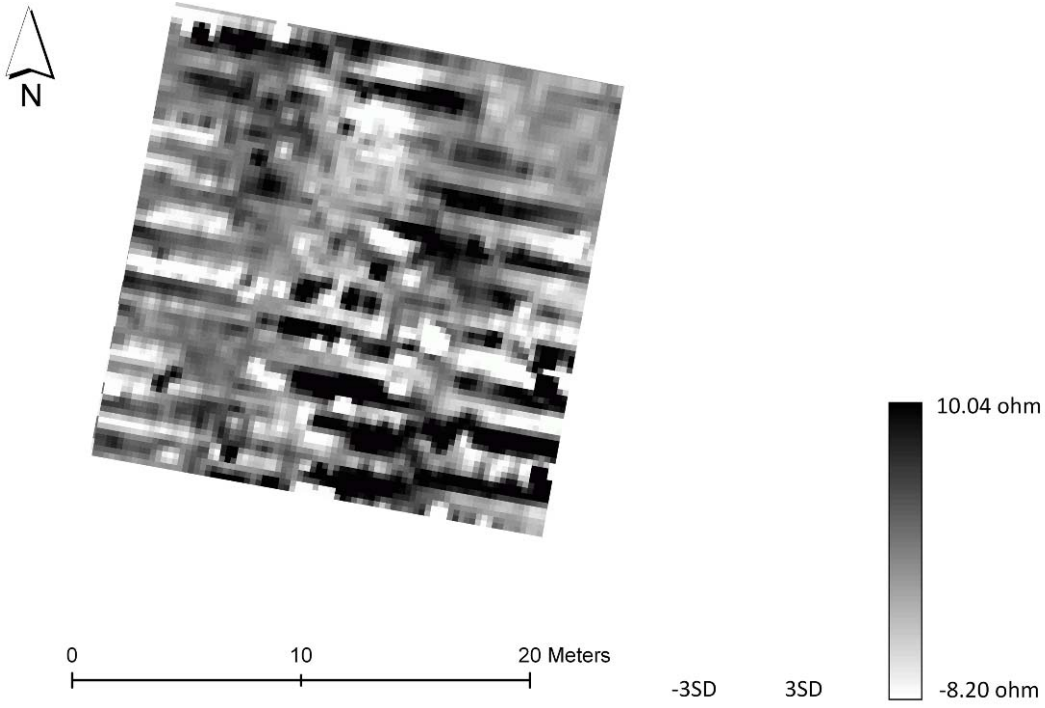

Figure 5-10: Shade plot of the processed data results of the earth resistance survey over the kerbed-wall at the Bay of Skaill. The data was plotted at -1/1 SD units, contrast 1 and using the Geoplot grey99 palette.

5.2.5. FDEM Results

Figure 5-11and Figure 5-12 shows the raw results of the vertical quadrature and in-phase of the EM38 survey. The dataset showed some stripping in traverse orientation both in the quadrature and in-phase responses. Both components had a wide range of readings, 7.85 to -19.42 mS/m for the former and 57.75 to -9.75 ppm for the latter. However, the quadrature response produced the most informative results, showing a series of longitudinal conductive anomalies running across the survey area.

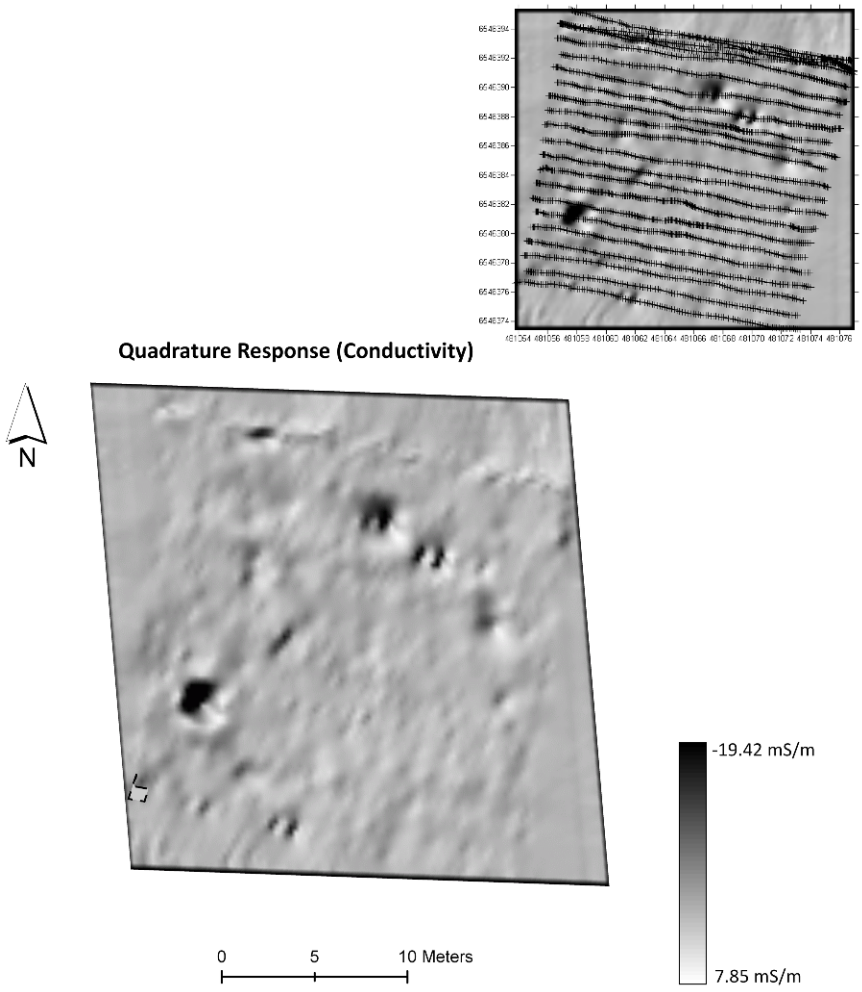

Figure 5-11: Shaded plot of the raw data results of the vertical quadrature of the FDEM survey over the kerbed-wall at the Bay of Skaill. The data was plotted using Surfer 8 software.

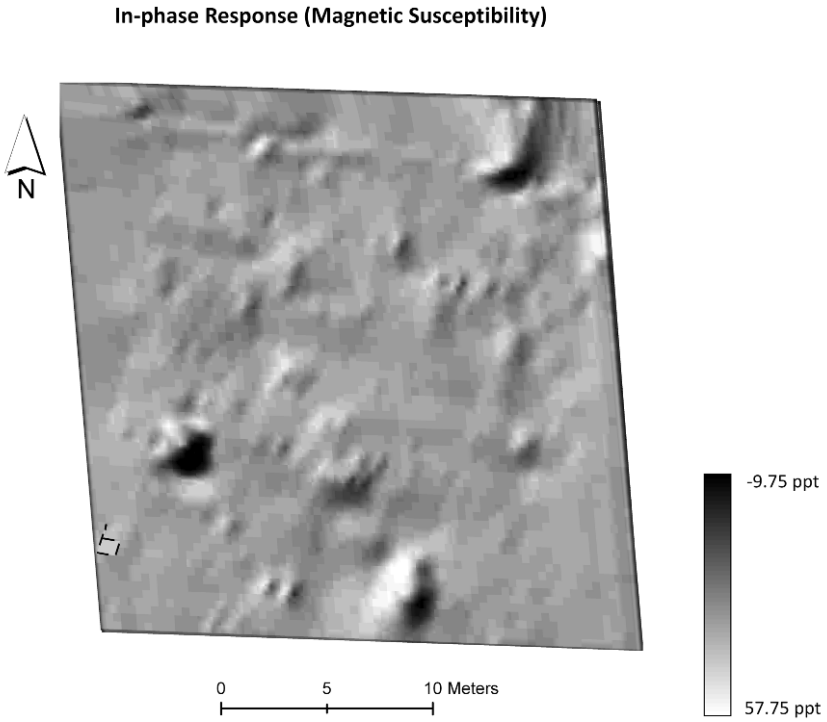

Figure 5-12: Shaded plot of the raw data results of the vertical in-phase of the FDEM survey over the kerbed-wall at the Bay of Skaill. The data was plotted using Surfer 8 software.

5.2.6. GPR Results

The results of the GPR survey are presented in the form of radargrams and time-slices. Figure 5-13 shows the results of the processing flow applied to the GPR data and Table 5-6 shows the processing sequence. A general velocity of 0.12 m/ns was estimated by hyperbola adaptation from good diffraction hyperbolae present on the dataset. After the basic processing of the GPR data, a velocity model was created and applied in the migration and time-to depth conversion of the data.

Function
Subtract-mean (dewow)
Time zero correction
Background removal
Energy decay gain
Velocity analysis (hyperbolic velocity analysis)
Migration (FD migration)

Table 5-6: Data processing flow (ReflexW v.5.6 software) applied to the GPR data acquired with the 225 and 450 MHz shielded antennas at the Bay of Skaill. The functions are described in Chapter 3.

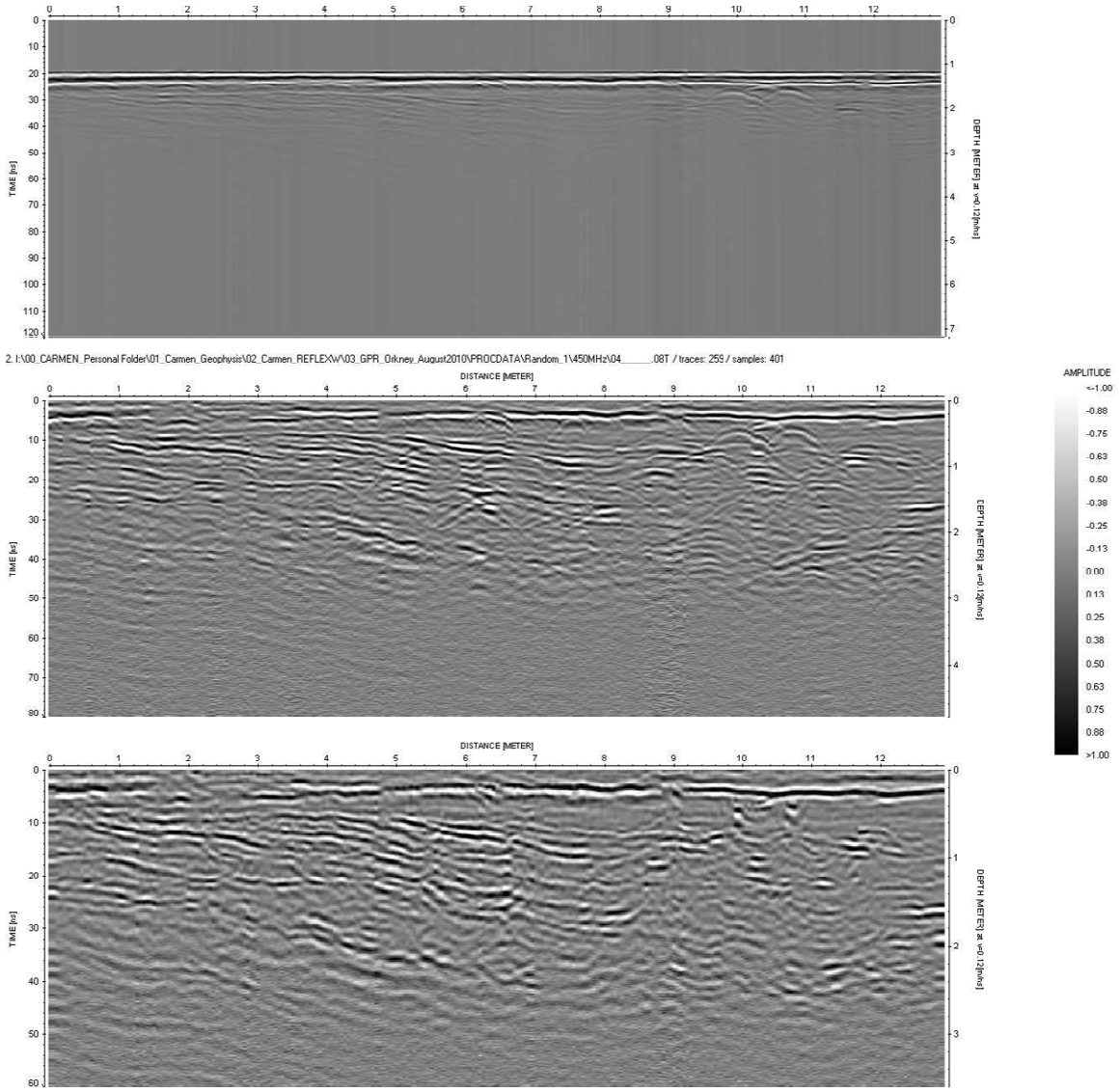

Figure 5-13: Radargrams from the 450 MHz survey over the kerbed-wall at the Bay of Skaill. The image shows the raw (top), basic processed (middle) and migrated (bottom) results of the GPR 1 (Figure 5-6).

The signal penetration was good reaching fairly deep into the windblown sands to *c*. 2.40m (44ns) with the high frequency survey (450MHz) and *c*.5m with the low frequency survey (225MHz). The results of the high frequency survey were better defined than the low frequency survey and the radar signal penetrated well despite *c*.1 m of cover sands.

Figure 5-14 toFigure 5-16 show the results of the high and low frequency antennae of the single lines GPR1, GPR 2 and GPR 3, respectively. In general, the data was characterised by a succession of well-defined linear high and low amplitude reflections. The upper reflections were parallel to the ground surface, whilst the deeper ones were dipping slightly and generally eastwards (Figure 5-14). Some of these linear reflections presented sudden breaks followed by an

area of attenuation. The low frequency survey recorded the linear reflections to *c*.3m deep (Figure 5-14 and Figure 5-15). The low frequency survey results of GPR Line 3 (bottom in Figure 5-16) were affected by a strong signal 'reverberation'. Since this line was beside the excavation trench of the longhouse, possible superficial metal objects such as pegs, nails or other tools buried by the sands may have caused this effect.

A series of hyperbolic reflections were present in the data, most of them very shallow and concentrated in the easternmost part of GPR Line 1 (Figure 5-14). These hyperbolae often indicate the presence of 'point source' buried reflectors; however, these hyperbolae may well have been produced by rabbit-burrow voids. Other more discrete high amplitude reflections were recorded in the area where the kerbed-wall was expected to be detected. Finally, areas of attenuation of the GPR signal were also noticeable, especially in the results of the high frequency survey of GPR Line 1 (Figure 5-14).

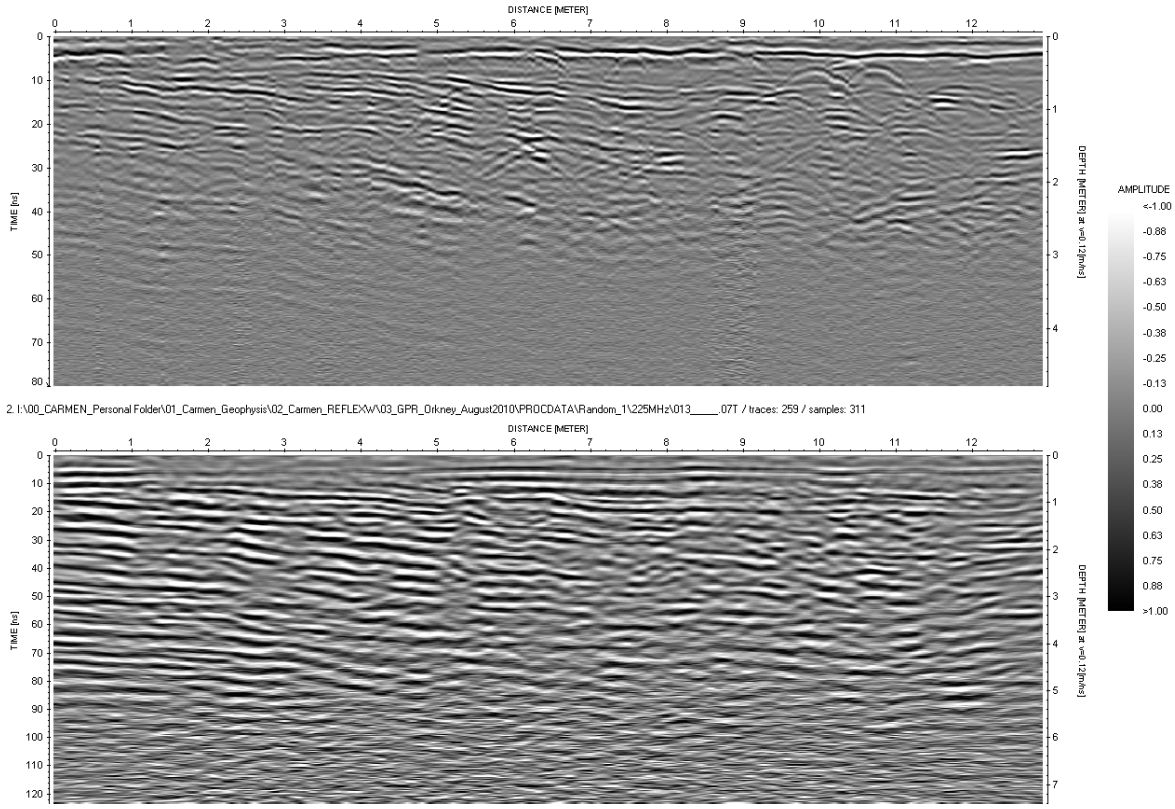

Figure 5-14: Results of GPR Line 1 (Figure 5-6) from the 450MHz (top) and 225MHz (bottom) survey over the kerbed-wall at the Bay of Skaill.

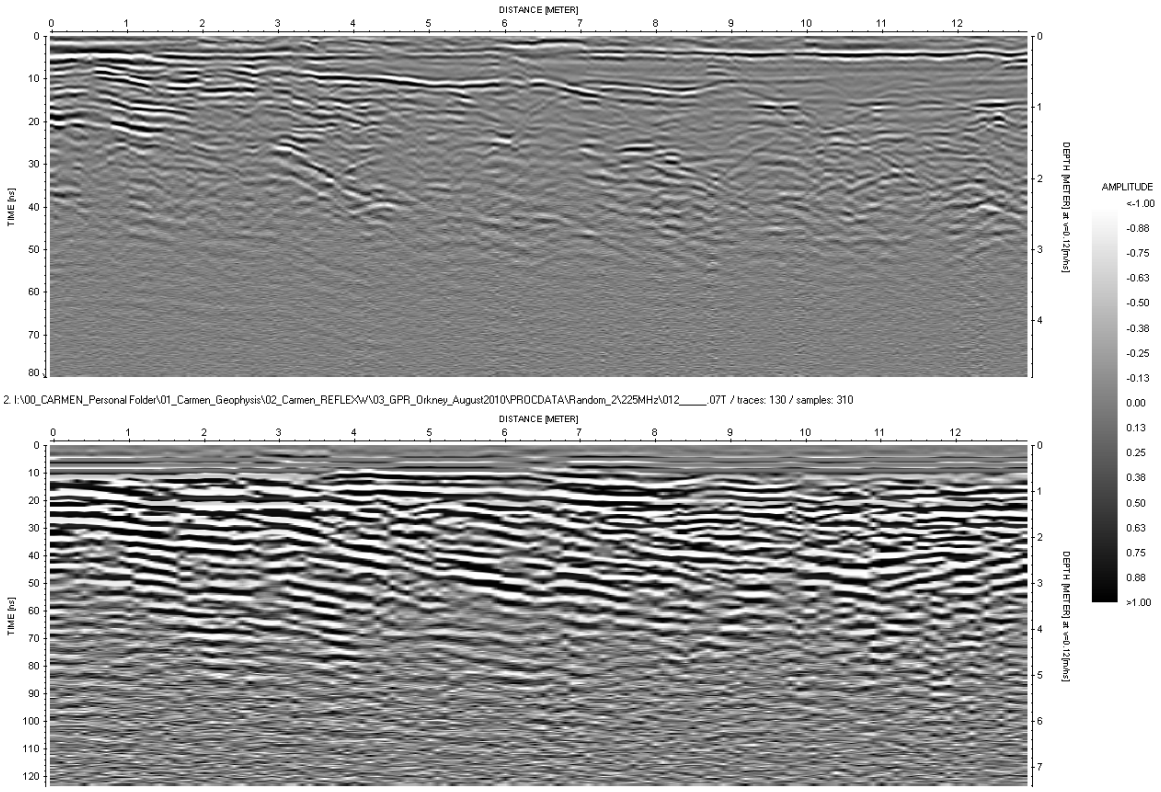

Figure 5-15: Results of GPR Line 2 (Figure 5-6) from the 450MHz (top) and 225MHz (bottom) survey over the kerbed-wall at the Bay of Skaill.

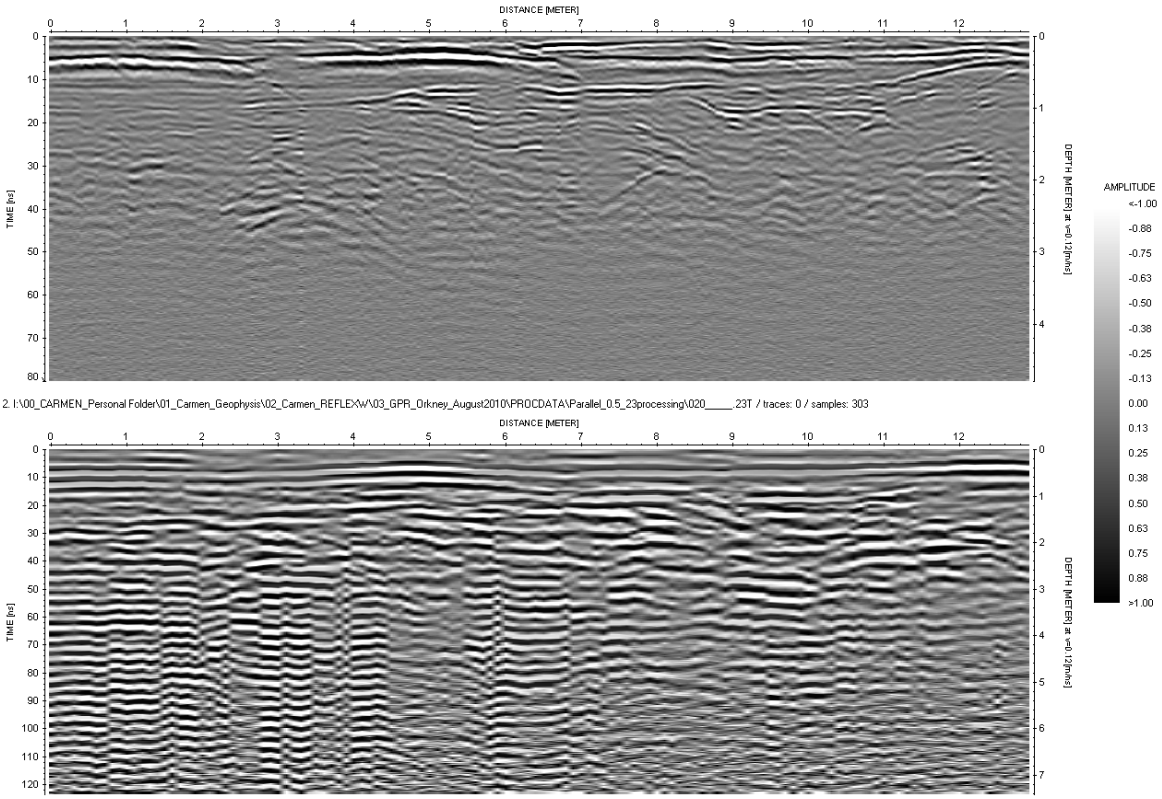

Figure 5-16: Results of GPR Line 3 (Figure 5-6) from the 450MHz (top) and 225MHz (bottom) survey over the kerbed-wall at the Bay of Skaill.

5.2.7. Gradiometry Interpretation

The interpretation of the gradiometer survey is shown in Figure 5-17. This survey did not succeed in identifying any coherent anomaly related to the targeted feature. Only a weak magnetic trend (1 in Figure 5-17) might indicate the presence of the kerbed-wall as the trend here seems to match with the southward course of the targeted feature. Other magnetic trends running parallel and at right angles to anomaly 1 (Figure 5-17) may indicate the location of other structures of archaeological interest. However, these anomalies may be the product of rabbit activity. The easternmost trends seemed to be an effect both of the slope and rabbit damage (dotted blue in Figure 5-17).

Strong magnetic anomalies were detected in the area of the 2007 trench (2 in Figure 5-17) as well as other magnetically enhanced areas (3 in Figure 5-17) which showed a similar response as in the 2004 initial gradiometer survey (Figure 5-4). After the excavation of the evaluation trench in 2007, these anomalies were thought to be generated by 'a complex series of midden-type deposits and organic layers' (Griffiths 2007, 31).

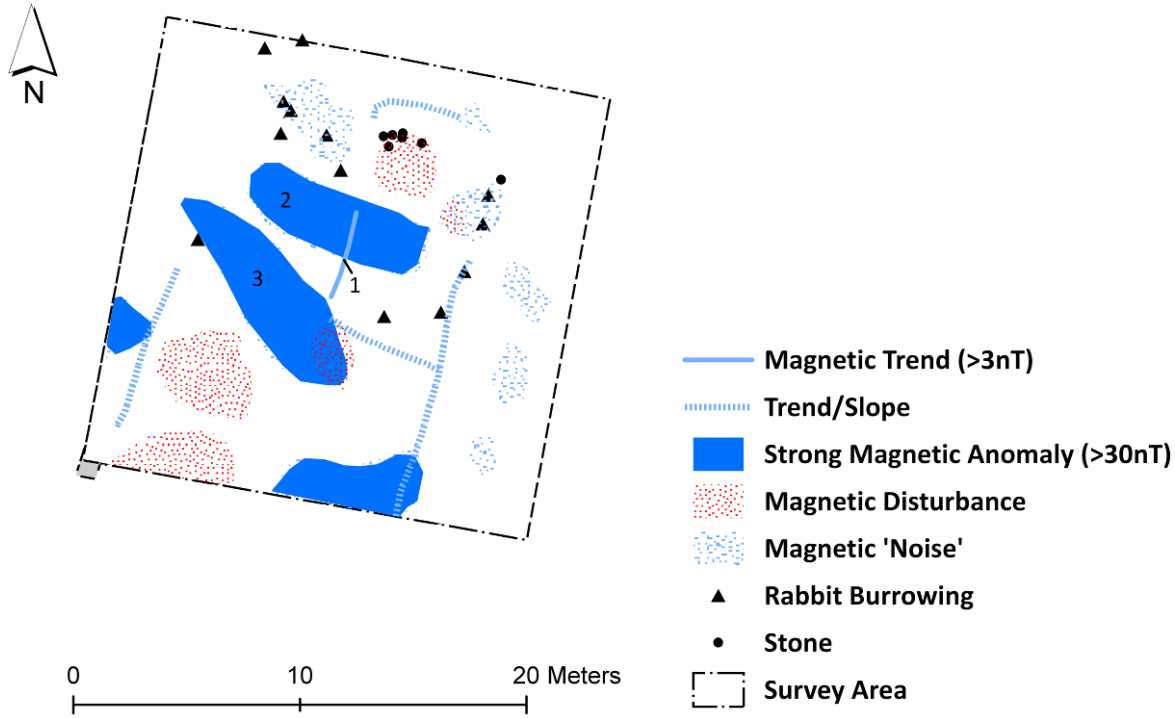

Figure 5-17: Anomaly extraction and interpretation plot of the gradiometer survey results over the kerbed-wall at the Bay of Skaill.

5.2.8. FDEM Interpretation

The interpretation of the EM38 results is based on the vertical quadrature response and shown in Figure 5-18**.** A fairly weak linear and fragmented anomaly with a general N-S orientation seems to correlate with the targeted structure (1 in Figure 5-18). The detection of the target structure was striking since generally a wall structure is not a conductive anomaly. Also a linear anomaly (2 in Figure 5-18) appeared to follow the same direction as anomaly 1 (Figure 5-18) which could be either another structure related to the targeted feature or a drain. Since the linear anomalies detected with the EM38 seemed to run from the top of the mound, they could indicate that they were taking advantage of the general slope to drain the area occupied by the sequence of midden-type deposits in order to stabilise the area. Otherwise, they could be internal wall divisions of the area dedicated to a croft garden, to hold the cattle for manure or to store midden deposits. These anomalies suddenly stop in the southern half of the survey grid perhaps due to a potential shallow depth of the windblown sand deposits here. Future surveys using the instrument in horizontal mode may be able to resolve the potential continuation of these anomalies to the W and S toward the longhouse.

A linear conductive anomaly (3 in Figure 5-18) was detected running diagonally in the survey area with a NE-SW orientation. The different trajectory of this anomaly in relation to anomalies 1 and 2 (Figure 5-18) suggests that they may not be contemporary structures; instead anomaly 3 may be related to a superficial metal wiring pit found during excavation. A sub-rectangular area (4 in Figure 5-18) was detected showing an area of disturbance. This may show the location of the first archaeological trench excavated in 2006. Finally, other conductive anomalies were revealed in areas that correlated with the location of magnetic disturbance anomalies.

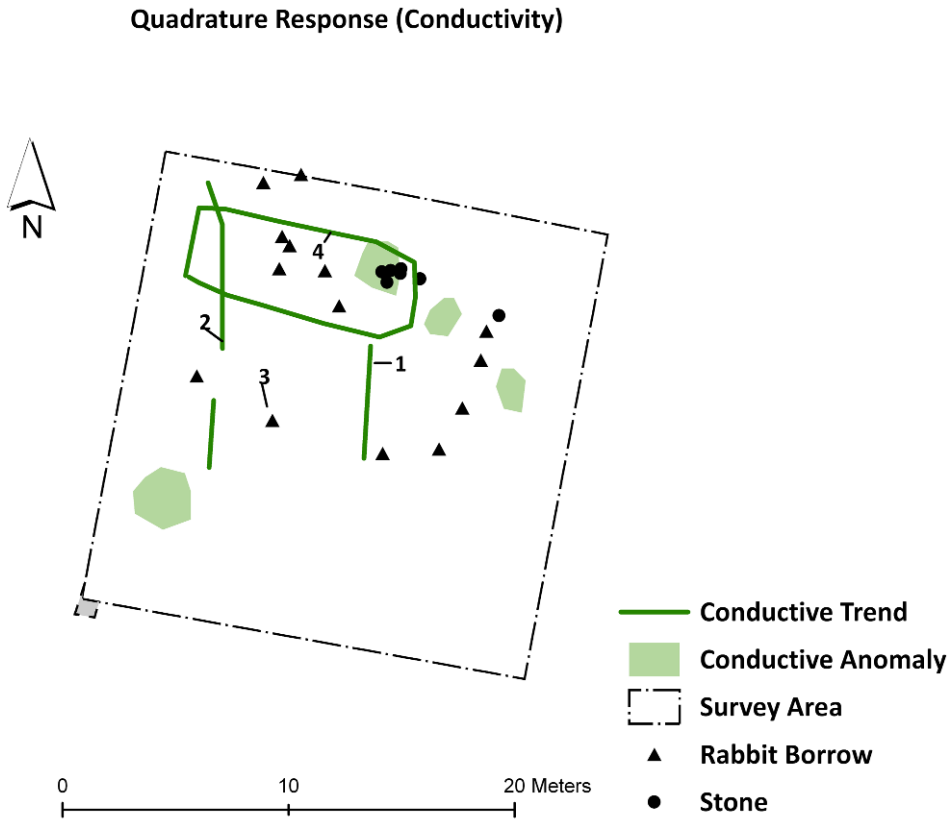

Figure 5-18: Anomaly extraction and interpretation of the vertical quadrature response of the FDEM survey over the kerbed-wall at the Bay of Skaill.

5.2.9. GPR Interpretation

The targeted kerbed-wall was successfully detected in GPR Line 1 (anomaly 1 in Figure 5-19, top) as two discrete high amplitude reflections showing the position of the upright kerbed stones. This transect was partially surveyed over the trench excavated in 2007 (Figure 5-6) and most of the reflections detected in the middle area of the radargram were produced by the backfill and packing of the trench after excavation. Since this area was fairly disturbed by excavation, no further interpretation was attempted. The targeted feature was also detected in GPR Line 2 (anomaly 1 in Figure 5-19, middle) and produced similar reflections to those in GPR Line 1. However, the space between the two upright kerb stones was slightly wider. Between the two high amplitude reflections of the upright kerb stones, a third reflection may indicate the stone lining of the kerbed-wall.

The high amplitude linear anomaly 2 (Figure 5-19, middle) correlates with the strong magnetic anomaly of NW-SE orientation (3 in Figure 5-17) which may represent a buried soil or midden deposit related to the targeted wall. There was a reflection-free area underlying anomaly 2 which may indicate the presence of attenuating materials within the sands. Reflection-free area 3 (Figure 5-19) appears to be cutting a series of undulating layered deposits (4 in Figure 5-19). It is difficult to interpret these deposits (4 in Figure 5-19) as the sequence of low and high amplitude signals could represent either sedimentary windblown sands or midden spread organic material. Further undulating high and low amplitudes were detected westward (5 in Figure 5-19) following a slightly different depositional direction and indicating a midden spread layer or a windblown sand event. Therefore, these deposits show a succession of overlying natural and midden deposits that seem to have been somehow disturbed in order to accommodate a later midden spread (2 in Figure 5-19, middle). This midden deposit may be responsible for the strong magnetic anomaly detected in the gradiometer survey (3 in Figure 5-17) and both anomalies correlate very well. The stratigraphic sequence suggests that the kerbed-wall detected may be related to this deposit, perhaps as a boundary wall of an enclosure, as suggested by the excavators (Griffiths 2007). The succession of these midden deposits and/or the barrier produced by the presence of the wall-enclosure would have led to the build-up of windblown sands, hence contributing to the formation of the mound.

The dipping reflectors (6 in Figure 5-19) may indicate an erosive bounding surface showing the depositional breaks and sand erosion of an earlier mound's slipface. Since the mound slopes steeply eastward towards the N-S burn (Figure 5-1) and there was a gentle slope southward towards the excavation area, these reflections may show the general stratigraphy of the windblown sands. The reflection-free area (7 in Figure 5-19) may be related to zones of homogeneous sand (Bristow 2009) or fine-grained silt or clayey beds within the sand sequence (Baker and Jol 2007, 146) following erosive and sloping pathways, thereby confirming the origin of the dipping reflections mentioned before.

Two anomalies were detected in GPR Line 3 (Figure 5-19, bottom) suggesting the presence of two structures. It is difficult to establish if anomaly 1 and 2 (Figure 5-19, bottom) are a continuation of the targeted wall (1 in Figure 5-19, middle).

The character of the reflections produced by these anomalies is slightly different from the anomalies in GPR Line 2. These anomalies presented the characteristic double high amplitude reflections but they also had an underlying and concave linear reflection that may indicate the wall base. The detection of these concave reflections could be explained by the shallower depth of burial of these features. Since the depth of windblown sands here was less than at the northernmost edge of the survey area, the shallower burial of the structures and the contrasting dielectric values of the stone lining and other infill deposits in the sand would have led to stronger reflections back to the GPR receiver. In order to determine the continuation and distribution of these walls or drain structures and to confirm their potential relationship with the Viking long house, an extensive, high resolution 3D GPR survey would be required.

Finally, GPR Line 3 did not detect the stratigraphic sequence of cut and deposition of midden deposit. This may indicate that this activity only happened around the northern half of the survey grid. Also, dipping linear reflections and other more hyperbolic-type reflections were detected deeper in the radargram showing the depositional sand breaks and erosion of the mound gently slipping southward (blue in Figure 5-19, bottom).

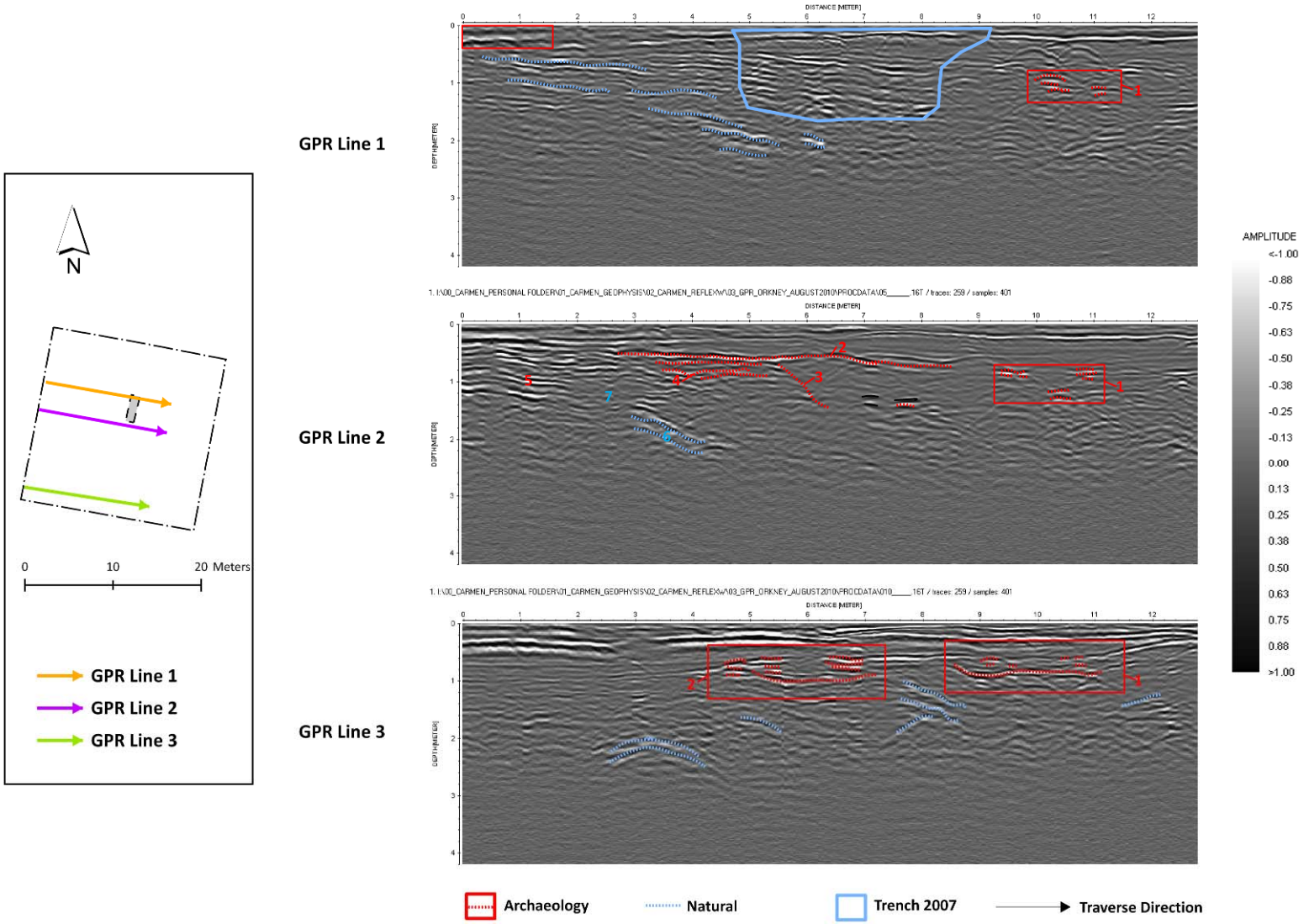

Figure 5-19: Radargrams showing the interpretation of GPR lines 1, 2 and 3 (450 MHz frequency survey) over the kerbed-wall at the Bay of Skaill. The numbers mark the anomalies discussed in the main text.

5.2.10. Conclusions

The single GPR traverse surveys provided rapid data collection and gave the most informative results since it confirmed the location of the kerbed-wall and provided a neat view of the underlying stratigraphic sequence of windblown sands and successive midden deposits. Despite the greater depth reached by the 225 MHz survey, the results of the high frequency survey (450MHz) resolved better the reflections of the wall. The radargrams (450MHz) show the targeted kerbed-wall as two high amplitude reflections, presenting a third middle reflection caused by the stone lining or infill deposits. An extensive 3D GPR survey, ideally using high frequency antennae which have been proven to reach deep enough to map the target feature, should confirm the extent and distribution of these linear anomalies and their relationship with the Viking long-house.

The EM38 survey allowed rapid area coverage and detected linear anomalies with a general NS orientation. Their slight mismatch in relation to the magnetic anomalies could be either a reflection of the nature of the anomaly that each technique gives or an error introduced at the time of geo-referencing the EM38 plots onto ArcGIS. Anomaly 2 (Figure 5-20) correlates well with the targeted wall. Since 1m traverse spacing was used in this survey, use of a lower resolution would enhance the resolution of the anomalies detected with this technique. Running parallel to anomaly 2 (Figure 5-20) are other conductive anomalies whose general disposition suggests they could be structurally related to the kerbed-wall or be the drainage systems.

The earth resistance survey failed to detect the targeted kerbed-wall or to reveal any other anomaly of archaeological interest. The poor results were affected by an instrument fault that introduced severe striping.

The gradiometer survey did not succeed in detecting the kerbed-wall owing to the masking effect of *c*.1m of windblown sand deposited at this location and the general magnetic noise of the midden deposits within the survey area. Nonetheless, the reduction of the traverse spacing to 0.5m did allow identification of some magnetic trends that may be revealing a series of structures running N-S across the survey area. Trend 1 (Figure 5-20) correlates

with the approximate location of the targeted wall structure, but since the survey area showed a high degree of rabbit action, the interpretation of these trends (especially the easternmost ones) as structures may be arguable. The gradiometer survey was informative because of the detection of the extent of the midden deposits.

Since the land slopes down towards the burn to the E of the kerbed-wall, and taking into account the series of organic/midden-type deposits to the west, three interpretations regarding the function of the detected kerbed-wall and other potential structures are offered:

- The kerbed-wall may have been a retaining structure used to stabilise the ground at this point and aided by the addition of organic/midden-type deposits.

- The kerbed-wall could be enclosing an area containing a plaggen-type manuring system (Simpson *et al.* 1998; Guttmann *et al.* 2006). The enclosed area could have been dedicated to cultivation by applying manured strips of turf and midden deposits over the infertile calcareous sands (Simpson *et al.* 2005). The other linear structures could be former retaining walls covered by the successive windblown events.

- The kerbed-wall may have been the easternmost boundary of an enclosed area with internal sub-divisions used to fold the cattle and sheep for manure, to keep midden deposits and/or dedicated to garden-size cultivation.

Some questions arising from this multi-technique survey still have to be answered: Why has only the foundation of the wall been preserved? Is this structure a robbed dry-stone wall? And why can a stone-based feature be detected as a conductive anomaly?

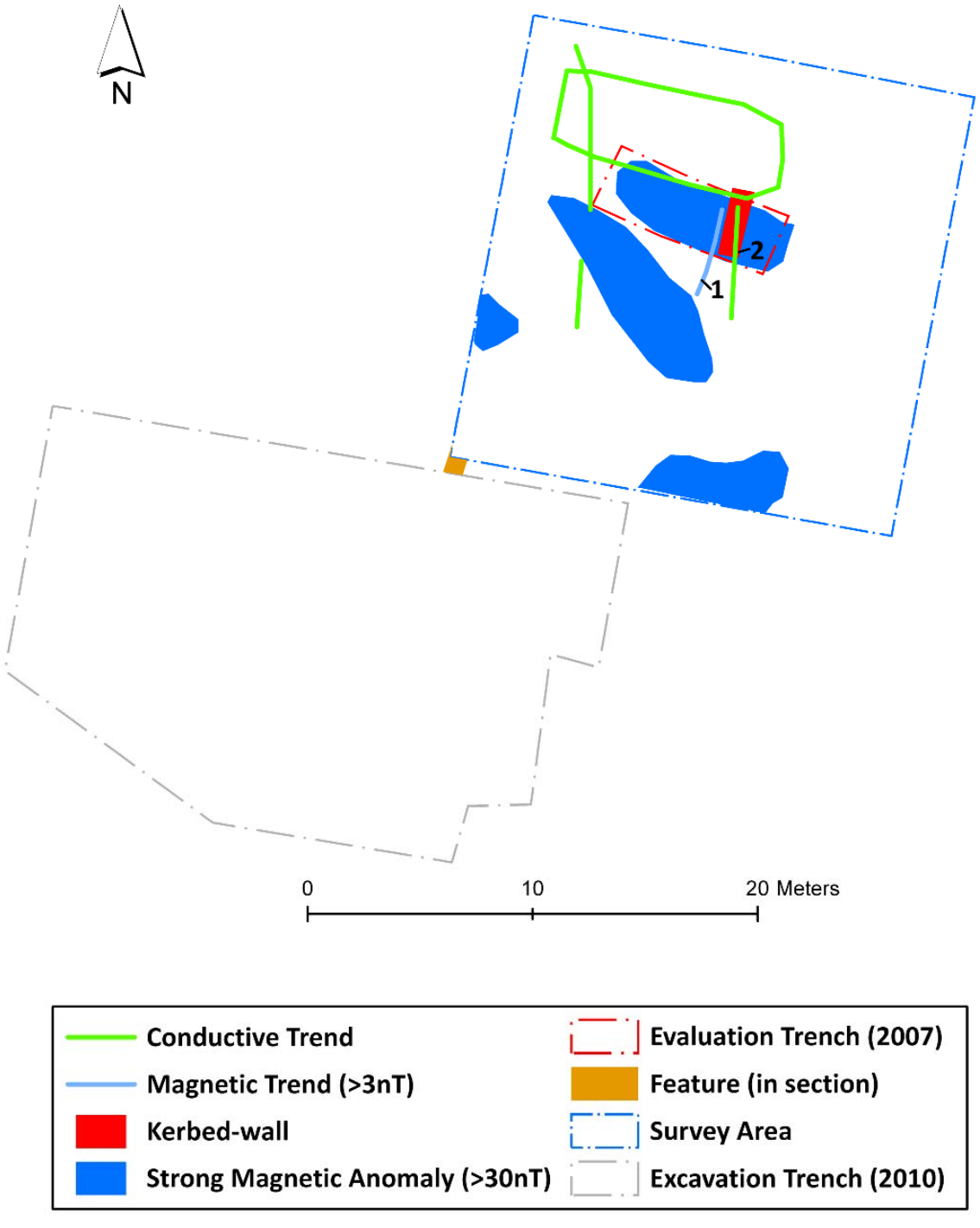

Figure 5-20: Integrated anomaly extraction and interpretation from all the geophysical techniques used over the kerbed-wall at the Bay of Skaill.

5.3. Soil Analysis

5.3.1. Aims

The aim was to characterise the vertical and horizontal response of the targeted kerbed-wall and surrounding deposits in terms of its physical and chemical composition in order to contribute towards its interpretation.

5.3.2. Ground-truthing & Sampling Strategy

A trench c.3m x 1m was dug over the area where the kerbed-wall was found in 2007 (Figure 5-21). The upright lateral kerbed stones were found 0.85m deep and the base of the wall at 1.10m deep. The wall was slightly wider at its southern end, confirming the GPR results of Line 2 (anomaly 2 in Figure 5-19) where the separation between the reflections produced by the kerbed-stones was slightly larger. A few base stones were lifted to check the underlying deposits, and the excavation was stopped at 1.36m.

After confirming the structure, the north-facing section of the trench was further extended in order to expose undisturbed soil deposits for soil sampling. A total of 29 soil samples (Table 5-7) were collected along three horizontal and one vertical sampling line (Figure 5-22). This sampling strategy simulated the sampling of an auger or corer but with the advantage of knowing the exact position of the samples in relation to the target wall. The sampling resolution, depths and locations are described in Table 5-7. Sample number 2 was lost during the drying of the soil before analysis. However, this sample was basically a repetition of sample number 1 (inside the targeted kerbed-wall).

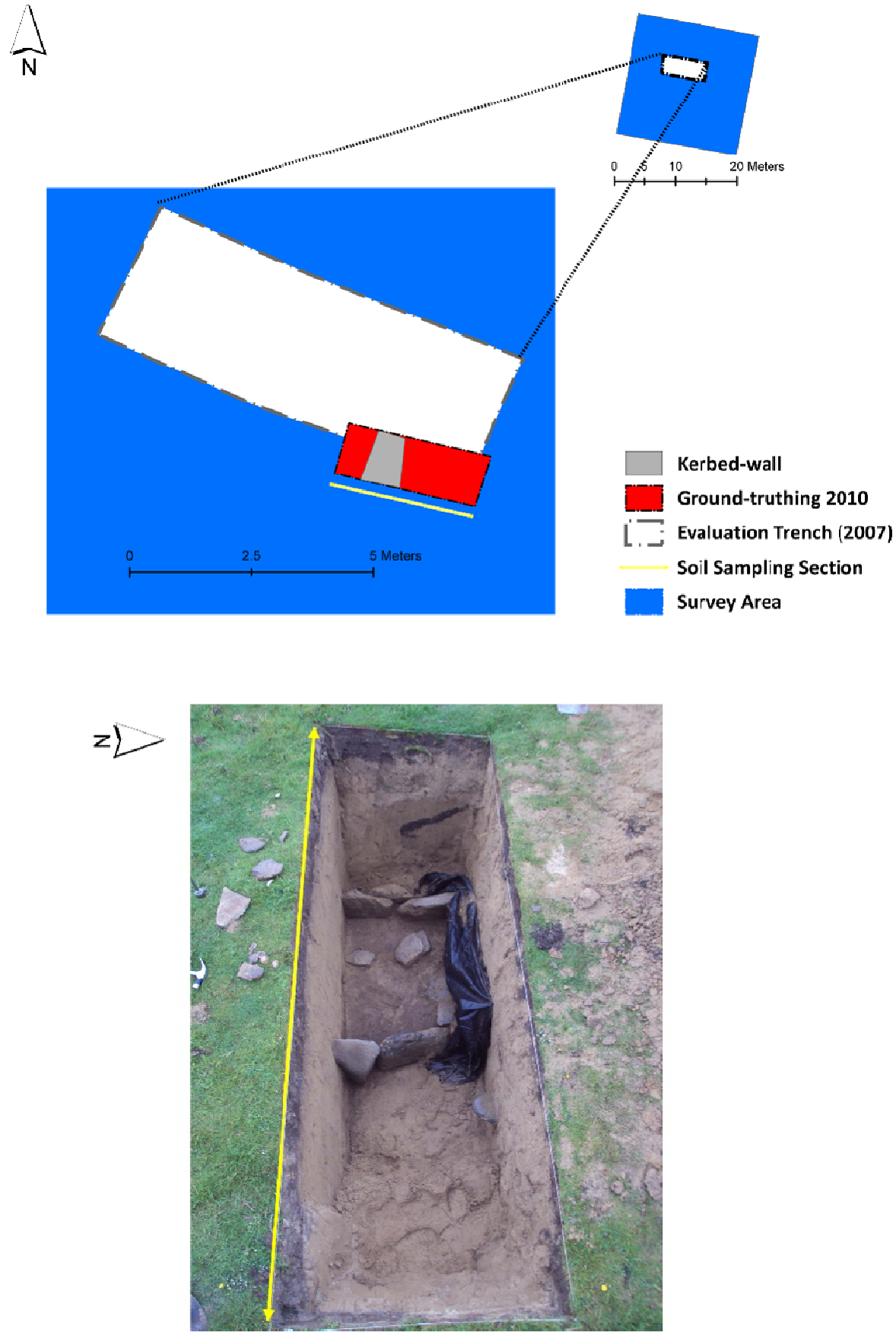

Figure 5-21: Location of the excavation trench for the ground-truth of the kerbed-wall (red) in relation to the 2007 trench (white) and general survey area (blue). The section where the soil samples were collected is marked with the double headed arrow (yellow).

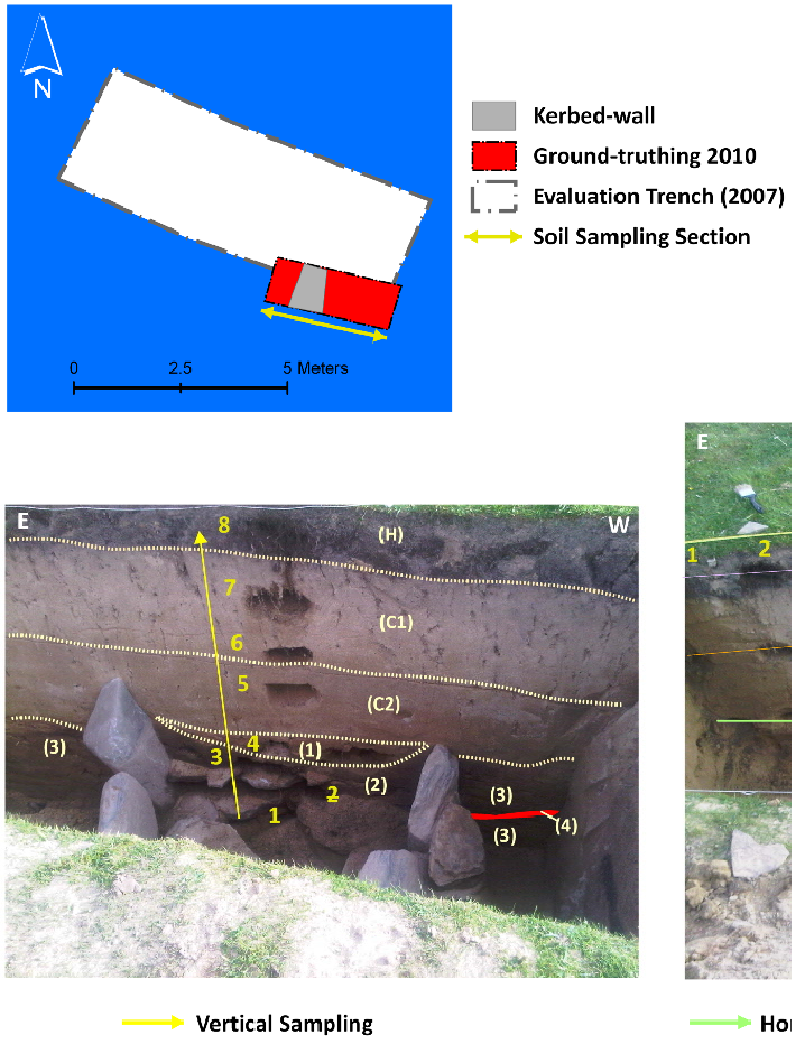

Figure 5-22: Vertical and horizontal soil sampling carried out after the confirmation of the kerbed-wall by excavation at the Bay of Skaill. The numbers indicate the location of the soil samples and the letters (bottom-left) the different soil horizons. The arrows show the orientation in which the samples were collected.

Sample	Orientation	Sample spacing	Length/Depth		N°	Notes
Vertical	N facing section (bottom-top)	*c* .0.20m	1.3m deep	8= 0.05 7= 0.35 6= 0.55 5= 0.70 4= 0.90 3= 1.00 ~~2= 1.29~~ 1= 1.30	8	Vertical samples collected during the excavation of the kerbed-wall (over and inside the feature). Sample number 2 was lost during the drying of the soil for chemical analysis.
Horizontal A	N facing section (E-W)	*c.* 0.5m	3m long	1= 0 2= 0.5	7	Horizontal samples collected during the excavation of the kerbed-wall (c.0.95m deep).
Horizontal B			3m long	3= 1 4= 1.5	7	Horizontal samples collected during the excavation of the kerbed-wall (c.0.50/0.55m deep).
Horizontal C			3m long	5= 2 6= 2.5 7= 3	7	Horizontal samples collected during the excavation of the kerbed-wall (c.0.10-0.15m deep).
Total					**29**	

Table 5-7: Summary of the soil samples collected over and inside the kerbed-wall at the Bay of Skaill.

5.3.3. Physical & Chemical Results & Discussion

5.3.3.1. **Soil Texture Analysis**

The results of the soil texture analysis are described in Figure 5-23 and Table 5-8. Under c.0.10-0.15m of turf (H), two soil horizons (C1 and C2) of windblown sands were overlying the kerbed-wall. The deposit of fine-grained and pale yellow sand (C1) contained some fragments of shells and drained very quickly. Deposit C2 differed from the former only in the colour of the soil. These sands were slightly darker, indicating possible leaching and concentration of Fe/Mn and organic compounds from the overlying deposits. These changes may have decreased the drainage capacity of the sands and increased the conductivity of this deposit. In the case of wet survey conditions, this deposit may be a potential source of attenuation of the GPR signal.

Two fill deposits relating to the kerbed-wall were identified, (1) and (2) in Table 5-8. These sandy deposits were characterised by their clay and silt content, dark

colour and presence of charcoal fleck. These suggest a high organic matter content, hence a higher water retention capacity and higher conductivity within the wall. This may have been the cause of the conductive anomaly detected by the EM38 survey. Deposit (3) was observed at the sides of the targeted structure and was characterised by some thin layered sands including a weakly cemented iron-pan deposit (4) at the west of the structure Figure 5-23. This deposit may have been the fill and packing of the trench cut for the kerbed-wall construction. In general, the deposits west of the structure were darker in colour and with higher clay content.

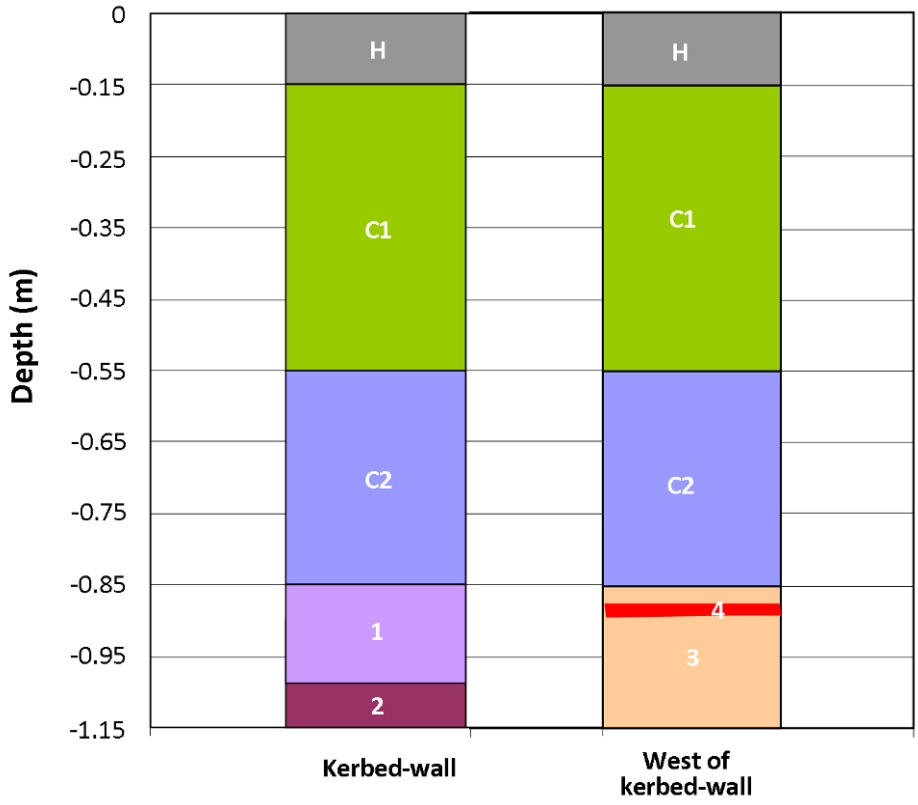

Figure 5-23: Diagram showing the main soil horizons and deposits identified during the excavation of the kerbed-wall at the Bay of Skaill. The numbers 1-4/C1-C2 are explained in the main text.

Depth (m)	H	Colour Munsell	Texture	Structure	Consistency	Stoniness	Bioturb.	Notes
0 to 0.15	H	2.5Y_2.5/1	Medium loamy sand.	Massive & coarse.	Moist.	None.	Many fibrous to semi-fibrous roots.	Topsoil
0.15 to 0.55	C_1	2.5Y_8/3	Fine sand.	Weak (single grain), fine & granular.	Slightly moist, very friable when moist & loose when dry.	None.	Common, fine and fibrous roots.	Wind-blown sand. Some fragments of shell
0.55 to 0.85	C_2	2.5Y_7/2	Fine sand.	Weak (single grain), fine & granular.	Slightly moist, very friable when moist & loose when dry.	None.		Wind-blown sand. Some fragments of shell and slightly darker than A_1, showing some leaching.
0.85 to 1	1	2.5Y_7/6	Fine sand slightly silty and clayey	Moderate, coarse & granular.	Slightly moist, slightly sticky, very friable when moist & loose when dry.	None.		Kerbed-wall fill deposit.
1.10 to 1.30	2	2.5Y_4/2				Few fragments of small to medium sub-angular stones (flagstone).		Kerbed-wall fill deposit. Some fragments of shell, charcoal flecks. Th e soil was augured untill 1.66m and further organic sand was observed.
0.85 to 1.30	3	2.5Y_7/2	Medium silt sand.	Moderate, coarse & granular.	Slightly moist, slightly sticky, very friable when moist & loose when dry.	None.		Wall packing deposit containing some organic matter.
1.1	4	2.5YR_4/6		Strong, coarse & granular.	Slightly cemented.	None.		Potential iron pan/layered sand within deposit (3) Only visible to the west of the kerbed-wall.

Table 5-8: Description of the major soil horizons and deposits recorded during the excavation of the kerbed-wall at the Bay of Skaill.

5.3.3.2. **MS, Total P, OSL, LOI, EC and pH**

The results of the magnetic susceptibility (MS), total phosphate (Total P), loss on ignition (LOI), conductivity (EC) and pH analysis are summarised in Table 5-9 and graphically represented in Figure 5-24 and Figure 5-25.

	Distance (m)	χ_{lf}	Total P µg/kg	LOI (%)	EC µs	pH
Vertical	0.05	8	145	0.010	130	9
	0.35	4	88	0.010	62	9
	0.55	4	79	0.009	58	9
	0.70	4	70	0.007	66	9
	0.90	16	199	0.010	62	9
	1.00	89	224	0.012	88	9
	1.30	27	121	0.058	96	9
	Mean	22	132	0.016	80	9
	S.D	31	61	0.018	26	0
	C.V	142	46	111	33	3
Horizontal C	0.0	6	136	0.060	102	8
	0.5	6	130	0.060	*	*
	1.0	7	130	0.058	100	8
	1.5	7	145	0.065	*	*
	2.0	8	139	0.064	*	*
	2.5	7	142	0.067	*	*
	3.0	9	258	0.054	*	*
	Mean	7	155	0.061	*	*
	S.D	1	46	0.005	*	*
	C.V	13	30	7	*	*
Horizontal B	0.0	4	58	0.009	54	9
	0.5	4	52	0.009	*	*
	1.0	4	58	0.010	*	*
	1.5	3	52	0.010	*	*
	2.0	4	73	0.012	*	*
	2.5	3	64	0.011	*	*
	3.0	4	64	0.001	*	*
	Mean	4	60	0.009	*	*
	S.D	0	8	0.004	*	*
	C.V	10	13	42	*	*
Horizontal A	0.0	8	55	0.006	*	*
	0.5	6	55	0.007	*	*
	1.0	57	148	0.011	71	9
	1.5	45	155	0.012	*	*
	2.0	26	203	0.012	*	*
	2.5	61	118	0.010	*	*
	3.0	8	185	0.009	*	*
	Mean	30	131	0.010	*	*
	S.D	24	59	0.003	*	*
	C.V	80	45	27	*	*

Inside the kerbed-wall

Over the kerbed-wall

* **Not analysed**

Table 5-9: Magnetic susceptibility (χ_{lf}), total phosphate (Total P), loss on ignition (LOI), conductivity (EC) and pH results of the soil samples over the kerbed-wall at the Bay of Skaill. The green and pale green colours mark the samples collected inside and over the kerbed-wall respectively. The Table also gives statistics for each set of samples: mean, standard deviation (S.D.), and coefficient of variation (C.V.).

5.3.3.2.1. *Magnetic Susceptibility Analysis*

The MS results did not show any variation along the horizontal lines (B and C in Figure 5-25). However, there was a higher variation (C.V. = 80% in Table 5-9) in the results of the samples collected across the kerbed-wall (Horizontal A in Figure 5-25), showing a general increase in the MS on reaching the area containing the feature. Also, the samples collected in vertical profile over the kerbed-wall showed a dramatic increase in MS (Figure 5-24) showing a great variation (C.V. =142% in Table 5-9) and reaching a maximum value of $8910^{-8}m^{-3}kg^{-1}$ (Table 5-9). These high values may have been caused by the higher organic and metal content of the clayey and silty sand recorded inside the feature in the texture analysis.

5.3.3.2.2. *Total Phosphate Analysis*

The results of the total phosphate analysis are similar to those of MS analysis. The uppermost horizontal sampling line (Horizontal C in Figure 5-25) shows high values (mean= 155 µg/kg in Table 5-9) probably due to the concentration of phosphate as a product of animal grazing and its retention by the rich organic topsoil. The phosphate concentration of the samples from the Horizontal B sampling line (Figure 5-25) was generally lower and there was not a variation along the line. The lowermost sampling line (Horizontal A in Figure 5-25) showed a general increase approaching the targeted structure and it showed the highest value in the westernmost sample collected inside the structure. The high value in the last sample indicates the continuation of high phosphate westward towards the area containing the midden deposits. The vertical samples (Figure 5-24) also show a high variation in phosphate among the samples collected inside the structure. Since the addition of organic-rich material and dung residues are sources of soil P enrichment (Holliday and Gartner 2007) it is possible that the high concentration of phosphate inside the wall reflects the material used in its construction and/or that the structure was concealing a higher organic matter content of materials westward. The results of the samples collected east of the wall were significantly lower.

5.3.3.2.3. *Loss on Ignition, Conductivity and pH*

The loss on ignition results showed the rich organic content of the topsoil (mean=0.061% in Table 5-9) in relation to the underlying deposits (mean=0.009%

in Horizontal B and mean=0.010% in Horizontal A in Table 5-9). The horizontal sampling line A (Figure 5-25) gave a slight increase of organic matter inside the kerbed-wall. More informative were the vertical samples (Figure 5-24) showing a general decrease of organic matter with depth and a strong peak inside the feature, confirming the high organic matter content of the fill deposits of the structure suggested by the previous analysis.

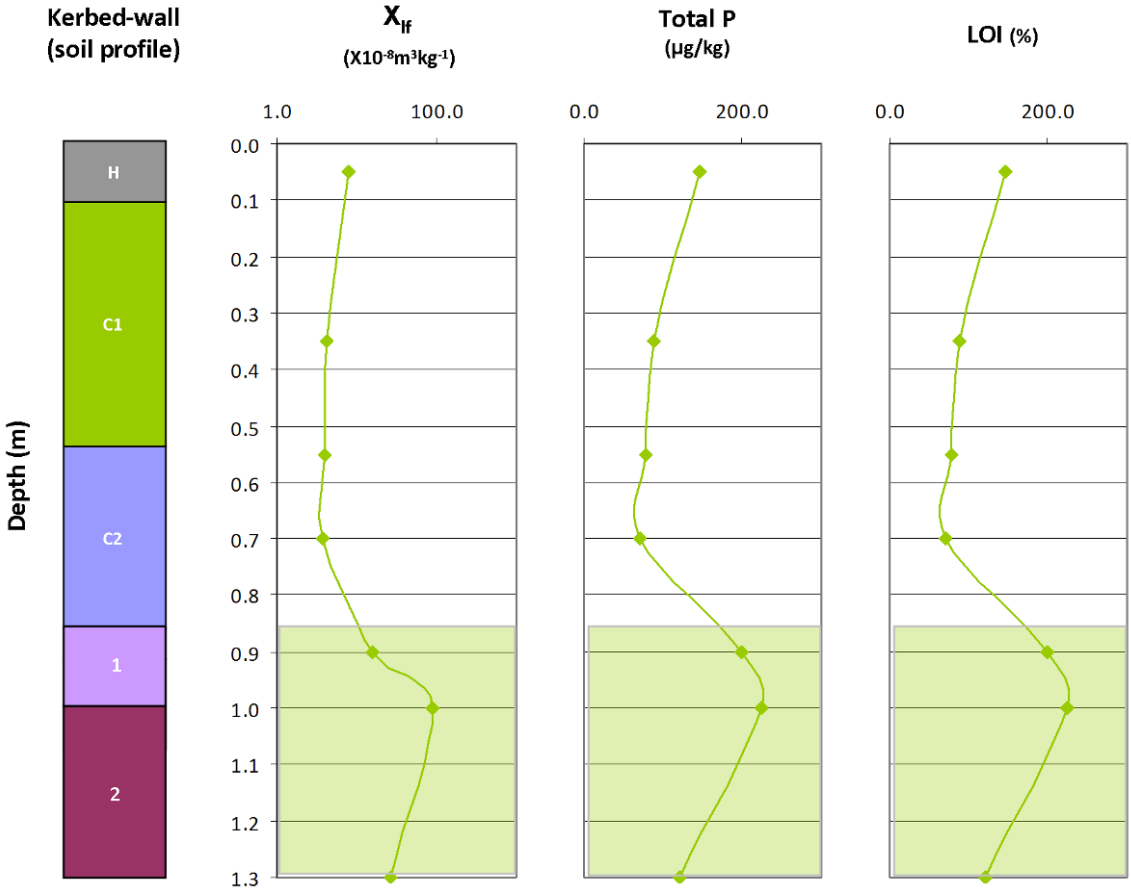

Figure 5-24: Soil profile, magnetic susceptibility (χ_{lf}), total phosphate (Total P) and loss on ignition (LOI) versus depth for the samples collected during the excavation of the kerbed-wall at the Bay of Skaill. The green colour marks the soil samples collected inside the kerbed-wall. Table 5-8 describes the major soil horizons and deposits identified in the soil texture analysis.

In regards to electrical conductivity, the topsoil samples were significantly more conductive, decreasing in conductivity with depth along with the samples collected in the two windblown sand deposits (C_1 and C_2). The samples collected inside the structures showed higher conductivity values, hence reinforcing the explanation of the detection of a conductive anomaly in the EM38 survey. The mean pH result of the vertical samples was 9 (Table 5-9) showing the basic/strongly alkaline character of the windblown sands due to the high calcium content. There was a slight increase in the pH of the samples collected from the

two windblown sand deposits (C_1 and C_2), correlating with the lower electrical conductivity values.

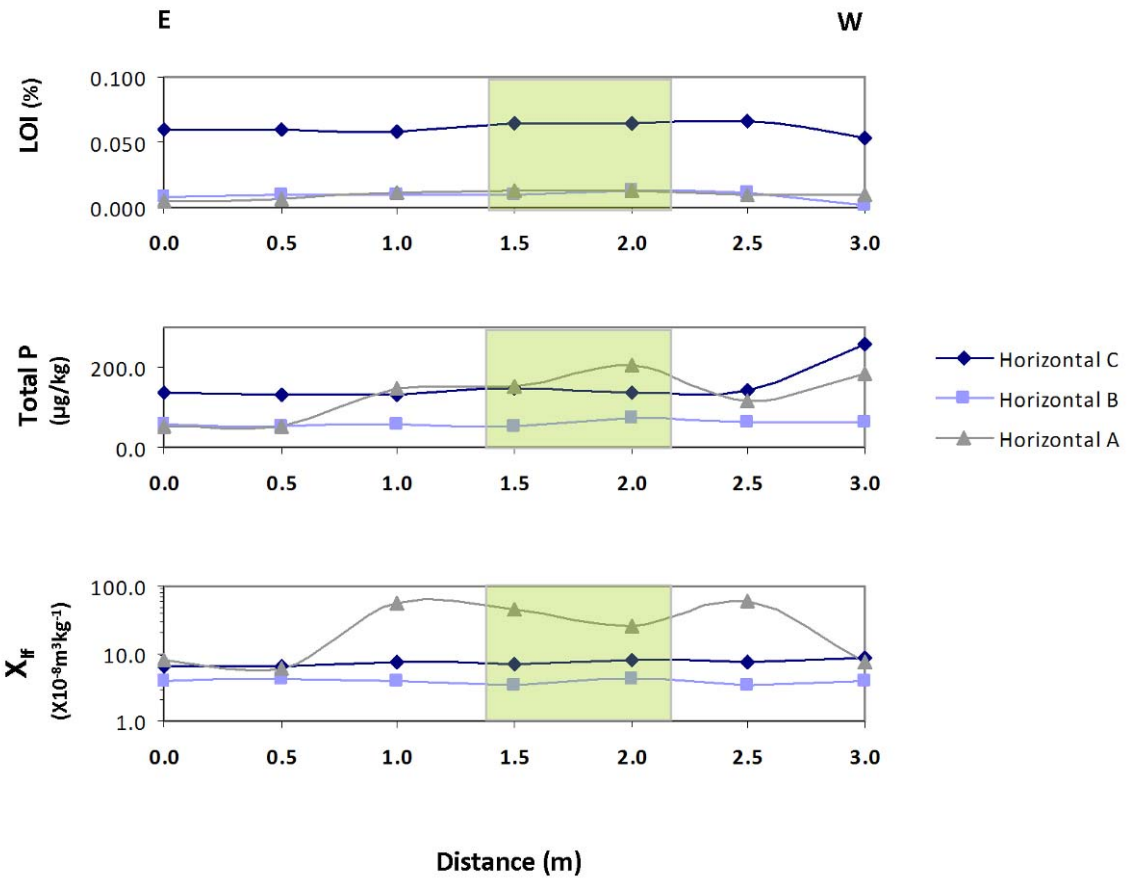

Figure 5-25: Horizontal distribution of magnetic susceptibility (χ_{lf}), total phosphate (Total P) and loss on ignition (LOI) of the samples collected over the kerbed-wall at the Bay of Skaill. The green colour marks the soil samples collected inside the kerbed-wall.

5.3.3.3. **pXRF Analysis**

The results of the pXRF measurements are summarized in Table 5-10 and Figure 5-26 and Figure 5-27. The major elements Ca, K, Fe and Ti were found in high concentration (Table 5-10). The high Ca concentration in all the sampling lines was due to the calcium-rich windblown shell-sands. The vertical samples collected inside the kerbed-wall showed a strong Ca depletion that indicates the change of chemical composition of the deposits filling the targeted structure (Figure 5-26). Sr, another alkaline earth metal, had a similar response versus depth. Like Ca, Sr has a moderate mobility in soils and sediments (Watts and Howe 2010) and a similar geochemistry, hence a slightly higher concentration of both elements in C2 (Figure 5-26) which may indicate their release and later accumulation by weathering of the uppermost sands (e.g. leaching). Therefore,

Ca/Sr enhancement and depletion here are related to natural soil processes associated with the distribution of the shell material.

K, Fe and Ti showed a positive correlation with depth and this may be linked to the leaching of oxides from the organic topsoil. There was also a general increase of these elements towards the west among the horizontal samples (Figure 5-27). This finding is more likely the result of anthropogenic activity (i.e. clay, peat and other materials used for walling) rather than be caused by natural soil processes.

There was Mn and Rb enrichment inside the kerbed-wall in both the horizontal and vertical results (Figure 5-26 and Figure 5-27). Since Mn and Rb have been reported as anthropogenic indicators as discussed in Chapter 3, this association may be related to the presence of the targeted wall structure. Also, Pb showed a positive correlation with distance and an increase inside the kerbed-wall (Figure 5-26 and Figure 5-27). Wilson *et al.* (2007) found enhanced concentrations of Pb to be product of fuel materials at the abandoned croft, and associated with the midden, byre and garden (Wilson *et al.* 2008).

	Distance (m)	Ca	K	Fe	Ti	Sr	Mn	Zr	Cu	Rb	Pb
Vertical	0.05	149099	14388	11381	1566	675	289	148	81	69	19
	0.35	108243	19395	17186	2135	683	414	275	77	74	12
	0.55	96317	19201	15267	2115	623	426	269	136	73	14
	0.7	112399	18916	14860	2002	667	423	277	49	67	11
	0.9	76768	21109	17058	2723	529	570	244	51	84	15
	1	50259	21742	17303	3584	392	609	242	34	98	17
	1.3	31358	23095	22498	3439	302	600	235	42	93	16
	Mean	89206	19692	16508	2509	553	476	241	67	80	15
	S.D	39908	2794	3362	764	152	120	45	35	12	3
	C.V	45	14	20	30	28	25	19	53	15	20
Horizontal C	0	145339	14355	12027	1486	671	298	111	40	69	21
	0.5	144420	13711	12562	1463	665	295	106	41	68	18
	1	151089	13180	11917	1392	683	293	115	72	69	20
	1.5	158129	14199	11568	1476	682	295	93	41	69	19
	2	145882	13815	12399	1463	707	321	99	65	73	17
	2.5	150367	14415	11649	1430	690	322	100	41	70	18
	3	142964	14008	11410	1480	681	328	98	58	67	20
	Mean	148313	13955	11933	1456	683	308	103	51	69	19
	S.D	5272	431	430	33	14	16	8	13	2	1
	C.V	4	3	4	2	2	5	7	26	3	7
Horizontal A	0	89837	18205	14062	2213	688	254	340	233	73	8
	0.5	94731	18532	13003	2217	658	298	334	280	66	11
	1	34380	22217	17052	3832	357	329	251	45	90	14
	1.5	50815	21640	16043	3345	402	553	241	190	97	14
	2	71285	21178	17094	2923	483	626	226	61	89	14
	2.5	32573	20196	15324	3234	305	360	248	295	84	17
	3	48197	20359	17785	2689	377	507	249	115	80	14
	Mean	60260	20333	15766	2922	467	418	270	174	83	13
	S.D	25350	1515	1747	600	151	143	47	102	11	3
	C.V	42	7	11	21	32	34	17	58	13	20

Inside the kerbed-wall **Over the kerbed-wall**

Table 5-10: pXRF results of the soil samples over the kerbed-wall at the Bay of Skaill. The element concentrations are expressed in mg/kg (=ppm). The green and pale green colours mark the samples collected inside and over the kerbed-wall respectively. The table gives statistics for each set of samples: mean, standard deviation (S.D) and coefficient of variation (C.V).

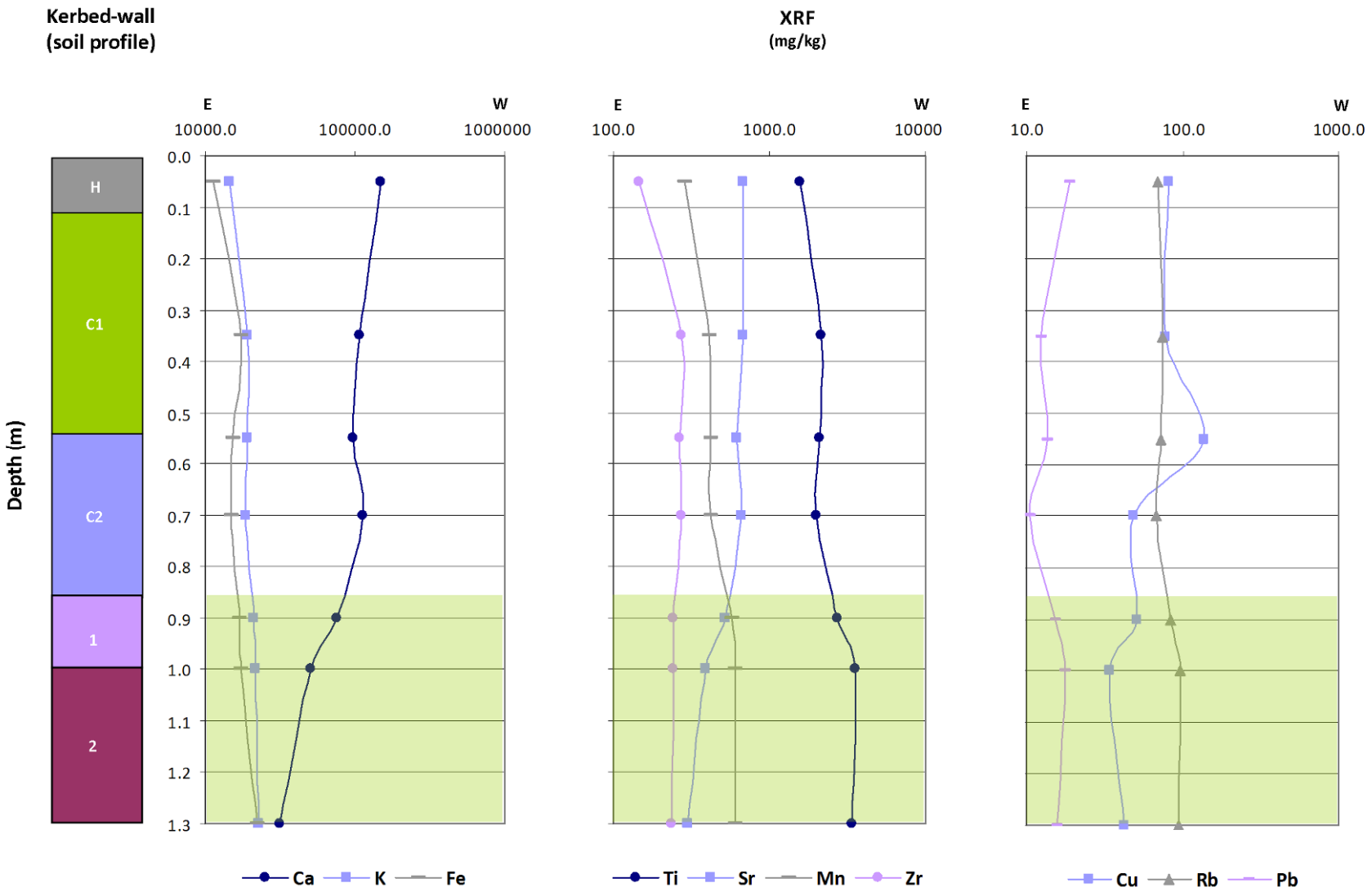

Figure 5-26: Soil profile and distribution of element concentrations (pXRF data) versus depth for the samples collected during the excavation of the kerbed-wall at the Bay of Skaill. The green colour marks the soil samples collected inside the kerbed-wall. Table 5-8 describes the major soil horizons and deposits identified in the soil texture analysis.

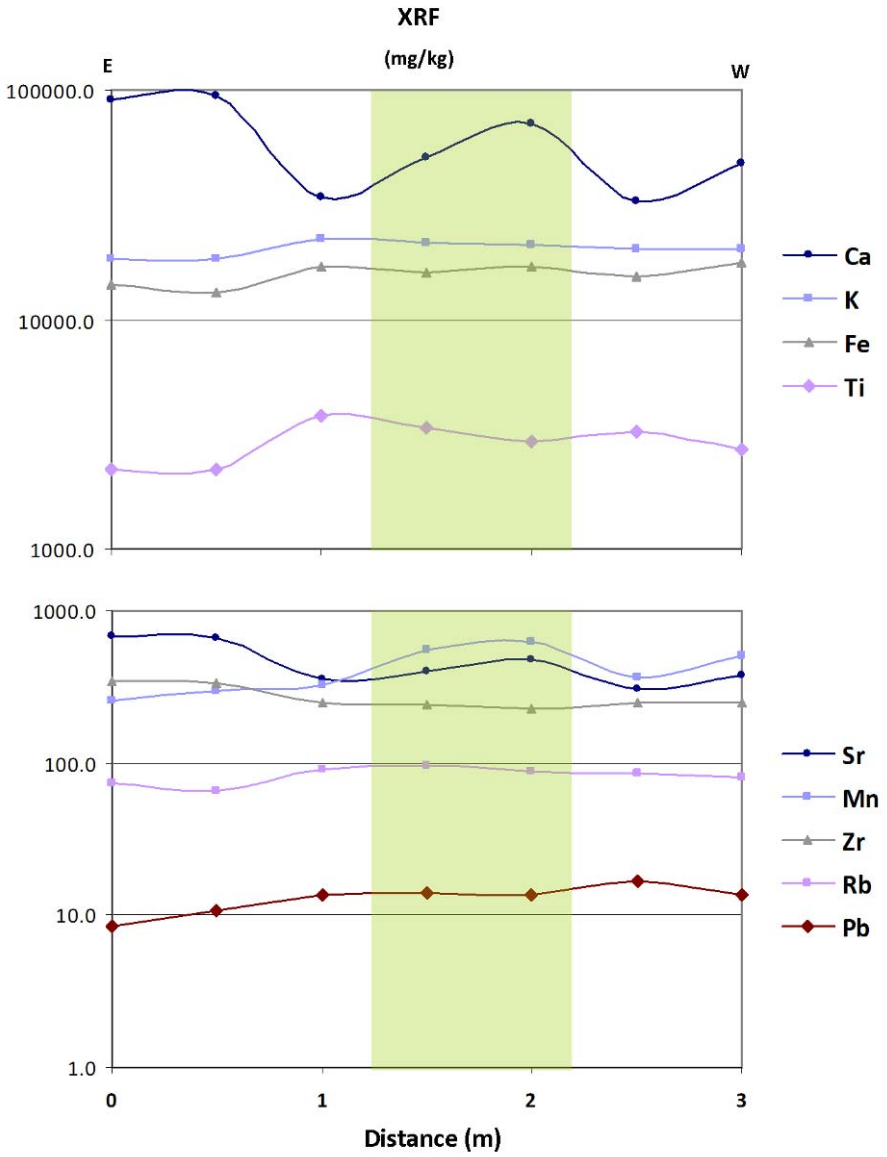

Figure 5-27: Horizontal distribution of soil element concentrations (pXRF data) at the kerbed-wall at the Bay of Skaill (Horizontal A in Figure 5-22). The green colour marks the soil samples collected inside the kerbed-wall.

5.3.3.4. **ICP-OES Analysis**

The results of the ICP-OES analysis are shown in Table 5-11 and Figure 5-28 and Figure 5-29. The results of the ICP-OES presented the same pattern to those from pXRF, and there was a good correlation between common elements except for Pb. The hierarchy of major element concentrations was Ca, Al, Fe K, Mg and Ti. The associations were similar to those in the pXRF results: Ca and Sr decreasing with depth and a steady increase of Al, Fe, K, Na and Ti with depth.

P, Mn, Ba, Cr and Li were enriched inside the kerbed-wall. P showed the same type of response as the total phosphate results. Ba showed a strong positive

relationship with depth as well as Li, and to a lesser extent Mn. Mn, Ba, Cr and Li also demonstrated a strong association. High concentrations of these elements and P have been reported in association with organic waste disposal (Holliday and Gartner 2007; Wilson *et al.* 2007). The high concentration of P within the kerbed-wall could be due to a high concentration of dung added to the turf used for walling. Mn and Ba could be present in fuel sources (turf and peat) and if so would have been concentrated by combustion. Another element with enhanced concentration in fuel (Wilson *et al*. 2007) is Pb, which showed enrichment with distance from E to W.

	Distance (m)	Ca	Al	Fe	K	Na	Mg	Ti	P	Sr	Mn	Ba	Cu	Cr	Li	Ni	Pb	Co
Vertical	0.05	92814	25516	13855	10107	9528	7581	1446	1806	616	287	212	70	39	19	14	21	4
	0.35	80122	42449	20233	17368	16320	11626	2295	949	602	365	322	68	54	28	20	10	3
	0.55	75232	44976	20013	18194	17601	11101	2433	895	594	385	341	116	66	28	22	9	4
	0.7	85145	44393	19481	18090	17729	11423	2392	805	600	355	339	45	52	27	20	9	4
	0.9	63717	49829	22179	19630	18432	10297	3015	2230	505	546	381	53	59	30	25	10	6
	1	43610	54941	22162	20210	19515	7085	3800	2684	383	629	421	45	70	35	20	10	4
	1.3	25988	58510	28597	21118	20862	7209	3522	1527	287	591	432	29	73	37	24	13	7
	Mean	66661	45802	20932	17816	17141	9474	2701	1557	512	451	350	61	59	29	21	12	5
	S.D	24065	10698	4385	3646	3659	2089	805	725	130	134	74	28	12	6	4	4	1
	C.V	36	23	21	20	21	22	30	47	25	30	21	46	20	21	17	38	27
Horizontal C	0	94730	26425	13958	10601	10277	7794	1498	1611	621	282	212	43	38	19	14	18	3
	0.5	92177	25110	13865	10107	9427	7385	1418	1702	606	280	203	39	36	18	14	19	2
	1	99258	25866	12505	10339	10673	7208	1447	1576	643	258	212	93	35	17	13	19	3
	1.5	96477	25355	13207	10262	10031	7439	1414	1727	637	274	209	33	35	18	13	18	3
	2	96736	26187	13209	10612	10476	7513	1441	1690	635	276	217	59	35	18	14	17	4
	2.5	95443	25145	13335	10431	9735	7331	1411	1761	633	285	214	39	33	18	14	17	2
	3	94110	27285	13237	11017	10902	7352	1535	1616	626	292	242	70	36	18	14	20	2
	Mean	95561	25910	13331	10481	10217	7432	1452	1669	629	278	216	54	35	18	14	19	3
	S.D	2242	792	483	297	522	186	47	68	12	10	13	22	2	0	1	1	1
	C.V	2	3	4	3	5	2	3	4	2	4	6	40	5	2	4	6	20
Horizontal A	0	62806	40110	13339	15296	17298	7956	2031	627	500	242	305	159	40	21	14	7	1
	0.5	73906	43616	15558	17370	18583	9530	2332	706	582	285	339	238	48	24	17	8	3
	1	31115	57215	22060	21525	21843	7113	3981	1919	345	326	422	73	67	27	17	9	3
	1.5	45893	54251	19773	20422	20407	7489	3535	1973	390	527	415	242	67	29	23	10	4
	2.5	28595	55258	19278	20050	21617	5933	3432	1423	290	368	411	293	62	29	16	12	4
	3	40599	51742	22161	19592	19852	7564	2902	900	361	486	387	133	69	29	22	11	5
	Mean	47152	50365	18695	19042	19933	7597	3036	1258	411	372	380	190	59	26	18	9	4
	S.D	17927	6908	3560	2290	1759	1173	751	601	109	113	48	82	12	4	4	2	2
	C.V	38	14	19	12	9	15	25	48	26	30	13	43	21	13	19	19	43

Inside the kerbed-wall **Over the kerbed-wall**

Table 5-11: ICP-OES results of the soil samples at the kerbed-wall at the Bay of Skaill. The element concentrations are expressed in ppm (=mg/kg). The green and pale green colours mark the samples collected inside and over the kerbed-wall respectively. The table gives statistics for each set of samples: mean, standard deviation (S.D), and coefficient of variation (C.V).

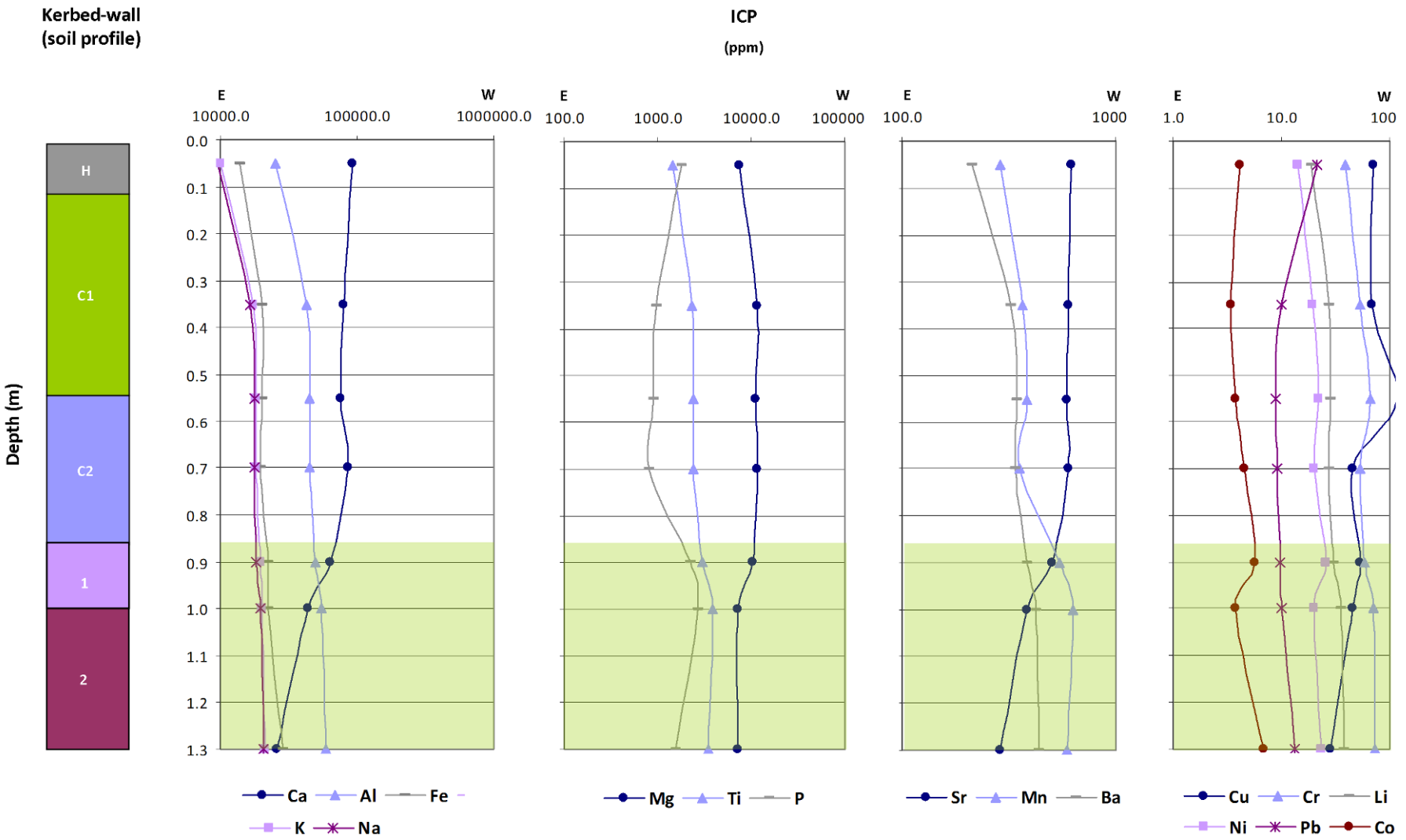

Figure 5-28: Soil profile and distribution of element concentrations (ICP-OES data) versus depth for the samples collected during the excavation of the kerbed-wall at the Bay of Skaill. The green colour marks the soil samples collected inside the kerbed-wall. Table 5-8 describes the major soil horizons and deposits identified in the soil texture analysis.

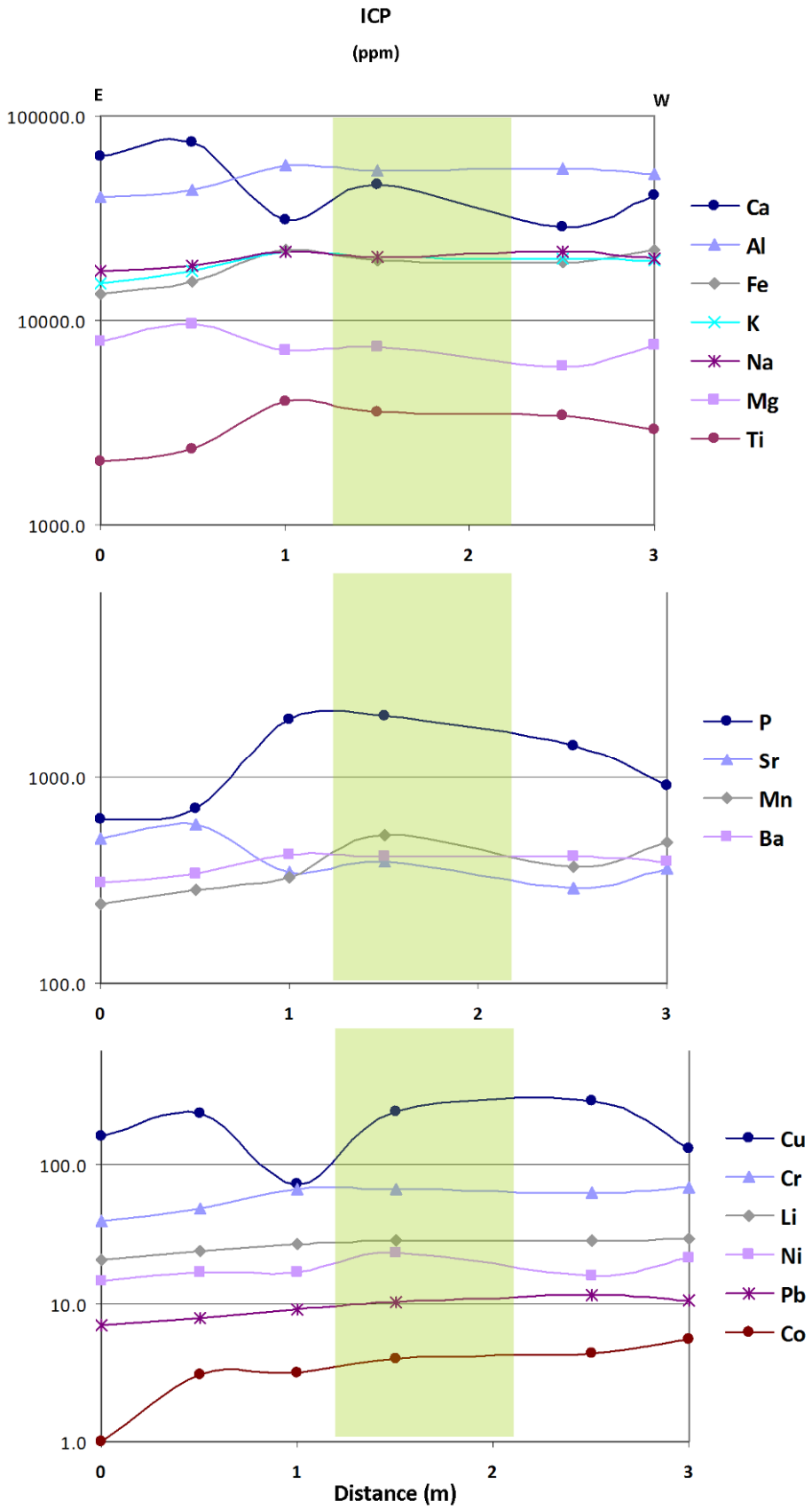

Figure 5-29: Horizontal distribution of soil element concentrations (ICP-OES data) at the kerbed-wall at the Bay of Skaill (Horizontal A in Figure 5-22). The green colour marks the soil samples collected inside the kerbed-wall.

5.3.3.5. **Conclusions**

The geochemical response of the kerbed-wall was characterised by a general increase in MS and total phosphate values, as well as more electrically conductive deposits and a higher organic matter content. These enhancements were associated with clayey, silty and organic sand deposits observed during the excavation of the kerbed-wall.

pXRF shows enrichment of Mn and Rb inside the wall, and a general enrichment from E to W of Pb. ICP shows enhancement of P and Mn, as well as Ba, Cr, Li. This suite of elements has been reported as anthropogenic indicators relating to organic waste and fuel source burning. The general increase in K, Fe and Ti concentrations within the kerbed-wall may be related to this wall's higher clay mineral content. The organic waste and fuel ash materials may have been part of the turf used for the construction of the enclosure whose kerbed stone foundations would have insulated the wall and increased drainage to avoid turf rotting. The decomposition of this turf structure would have resulted in the increase in MS (mainly from the peat) and total phosphate (organic waste and/or animal dung) as well as the elements just mentioned, all concentrated in the clayey and silty sand deposits found within the kerbed-stone foundations of the former turf enclosure. The enhancements observed in all techniques shows the potential of these to characterise the wall. However, these techniques failed to detect the presence of the wall on the surface, mainly because of the depth of the overlying windblown sands. Hence, systematic auguring could be useful to detect the extensions of the wall and characterise its interior at several points using these analysis.

5.4. General Discussion

As expected, the gradiometer results were inconclusive in locating the targeted kerbed-wall. The data was affected by general magnetic noise and the target masked by the depth of the overlying windblown sands. However, the gradiometer survey mapped the extent of the midden deposits that initially suggested the presence of past human habitation. Hence, this type of strong magnetic response may be indicative of settlement at Orcadian aeolian sites.

The GPR and EM38 surveys confirmed the location of the kerbed-wall, showing that these techniques can successfully be applied to detect relatively small targets at similar aeolian environments. Whist the effectiveness of GPR surveys carried out over wind-blown sands is known (Bristow 2009), the positive results from the EM38 were somehow unexpected since the impervious feature was a non-conductive target in principle. The results of the geochemical analysis were key in understanding the detection of the kerbed-wall as a conductive anomaly.

Geochemical techniques successfully characterised the kerbed-wall. The feature showed a general increases in MS, total phosphate and enrichment of K, Fe, Ti (clay minerals) and Mn, P Rb, Ba, Cr, Li, Pb (organic waste and fuel source burning) related to the turf used for the construction of the enclosure with kerbed stone foundations (Holliday and Gartner 2007; Wilson *et al.* 2007, 2008). The decomposition of the ephemeral turf structure resulted in the concentration of organic clayey and silty sand deposits associated with higher water retention/cation exchange capacities, hence higher conductivity. This would have caused the conductive anomaly detected by the EM38 survey. The surviving kerbed-stone foundations also contributed to the creation of contrasting point source reflections.

The targeted wall may have been a boundary turf enclosure around an area characterised by organic/midden-type deposits. These deposits could either have been used to stabilise the ground surface in relation to the longhouse or dedicated to cultivation or manuring practices. Parallel potential structures may indicate former retaining/boundary walls, internal partition enclosures or drainage systems associated to the organic/midden-type deposits.

This case study not only allowed testing of the detection capabilities of the geophysical techniques, it also enhanced the archaeological interpretation of the targeted feature and overall area. The series of structures and sequence of midden deposits and windblown sands detected by geophysical means appear to have been the product of land management practices perhaps related to agricultural strategies that have been applied for a long time in the Northern Isles (Simpson *et al.* 1998).

The limited extent of these surveys and the focused objectives of this investigation did not allow resolution of the potential relationship of these structures and the geochemical nature of the organic/midden-type deposits with the neighbouring Viking longhouse. Further extensive surveys using a combination of GPR and EM38 surveys and systematic augering for geochemical analysis may resolve these questions since they have proved their potential in this environment.

Chapter 6

Surveying over Mixed Fluvioglacial Deposits: the Outer Ward of Lochmaben Castle (Dumfries & Galloway)

6.1. Introduction

Lochmaben Castle has been an important defensive position controlling access northwards and westwards into Galloway. Originally, the castle was a 'peel' structure built of earth and timber by Edward I of England in 1298-9. The stone castle was founded in the mid-14th century, but maintained the timber peel (Macdonald and Laing 1977). The extensive remains of earthworks around the later masonry castle were contemporary with the timber 'peel' structure (Historic Scotland 2012). In 1445 it became a royal castle and James IV carried out extensive repairs, including the construction of the great hall. In 1542 James V used the castle as a base for mustering forces prior to his English campaign. The castle fell out of use in the 17th century after the Union of the Crowns.

Apart from some accounts and a small excavation carried out in 1977 (Macdonald and Laing 1977) which suggest a possible occupation of the outer ward, little is known about the environs of the earlier timber structure. In 2009, the southern area of the timber 'peel' site attracted the attention of the Solway Hinterland Archaeological Remote Sensing Project (SHARP). This research project, run by the Archaeology Department of Glasgow University, aims to place medieval fortified centres in the region within a larger landscape by using geophysical survey techniques (Jones *et al.* 2009).

A preliminary geophysical survey was carried out in summer 2009 to explore the environs of the timber peel at Lochmaben castle in two areas: the outer ward (enclosed courtyard or bailey) and a field to the south of the castle. Eventually, only the latter area was surveyed using gradiometry and earth resistance

techniques because the dense vegetation present in the outer ward prevented its exploration (Jones *et al.* 2009). The results obtained in the field to the south of the castle were fairly poor and variable: whilst the data was characterised as magnetically very quiet in the area of alluvium, the results were very noisy in the sand and gravel deposits. Nonetheless, the gradiometer survey revealed weak traces of possible ditches and other structures which required further investigation (Jones *et al.* 2009).

6.1.1. Research Problem

Following the findings of the preliminary survey and the necessity of surveying the outer ward, further investigation and implementation of other survey techniques were necessary. Given the variability and generally poor results obtained from the gradiometer surveys, the site was selected as a case study for this PhD project.

This chapter focuses on the results of a multi-technique geophysical survey and soil chemical analysis study at the outer ward of Lochmaben Castle. The study aimed to assess the detection potential of a range of geophysical techniques in a mixed soil environment characterised by fluvioglacial sands and gravels and alluvial deposits, and to analyse the results using soil geochemical analysis.

6.1.2. Location

Lochmaben castle is centred at OS NGR NY 0883 8115 (Figure 6-1). The castle is a property of Historic Scotland, located within the Castle Loch Natural Reserve. The site (NMRS NY08SE 8) lies approximately 2 km south of the town of Lochmaben, in Dumfriesshire. It is located on the top of a raised peninsula on the south shore of Castle Loch (Figure 6-2). This case study focused on the outer ward area of the castle.

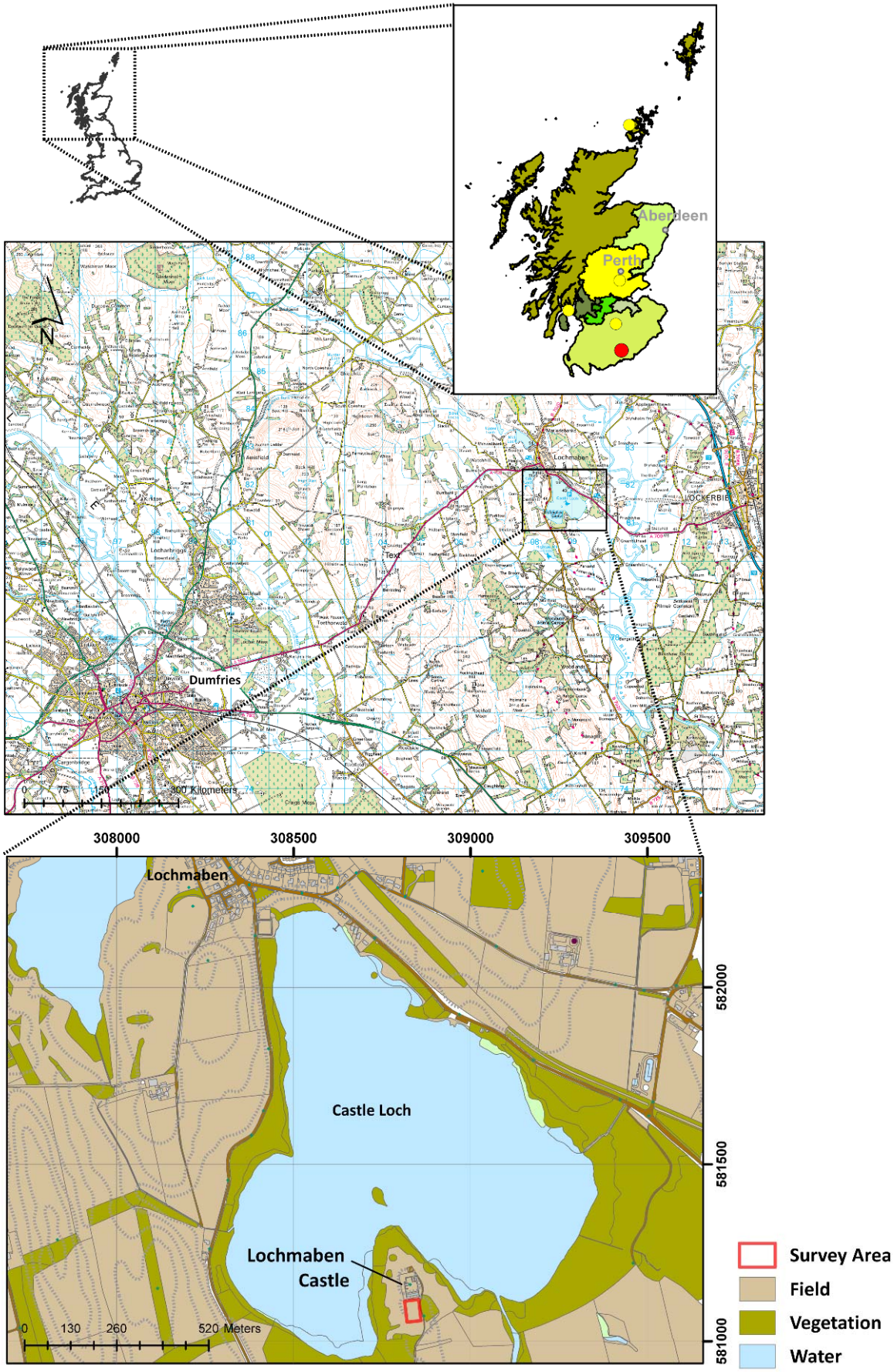

Figure 6-1: Location map (top) of the town of Lochmaben in Dumfries and Galloway (red dot) and in relation to the other case study sites (yellow dots). The middle map shows the location of Castle Loch about 10 km NE of Dumfries. In the bottom map the position of Lochmaben Castle and the survey area at the Outer Ward is indicted in red (based on © Crown Copyright/database right 2012. An Ordnance Survey/EDINA supplied).

Figure 6-2: East-facing aerial view showing the promontory on which Lochmaben Castle was built overlooking Castle Loch. Note the Outer Ward delimited in red and inside, two dark patches of vegetation (© RCAHMS).

6.1.3. Geology, Soils & Land Cover

6.1.3.1. **General Bedrock & Drift Deposits**

The solid geology consists of the Corncockle Sandstone Formation (Figure 6-3) of early Permian age (299.0 ± 0.8 - 270.6 ± 0.7 mya). It is over *c.*900m of red fine- to medium-grained, well sorted, red quartz sandstone with large-scale aeolian cross-bedding (British Geological Survey 2012a). Sands and gravels of the Kilblane Formation at the survey site (Figure 6-3) are glaciofluvial 'sheet' (terraced) superficial deposits *c.*3-10m thick (British Geological Survey 2012b). They contain cobbles and pebbles of Permo-Triasic sandstone and Lower Paleozoic sedimentary and volcanic rocks in a matrix of medium to coarse grained pale yellow to reddish brown sand. These deposits also contain greywacke and granitic clasts and their upper surface has laminated and rippled sandy silt and clays indicating the presence of temporary glacial lochs.

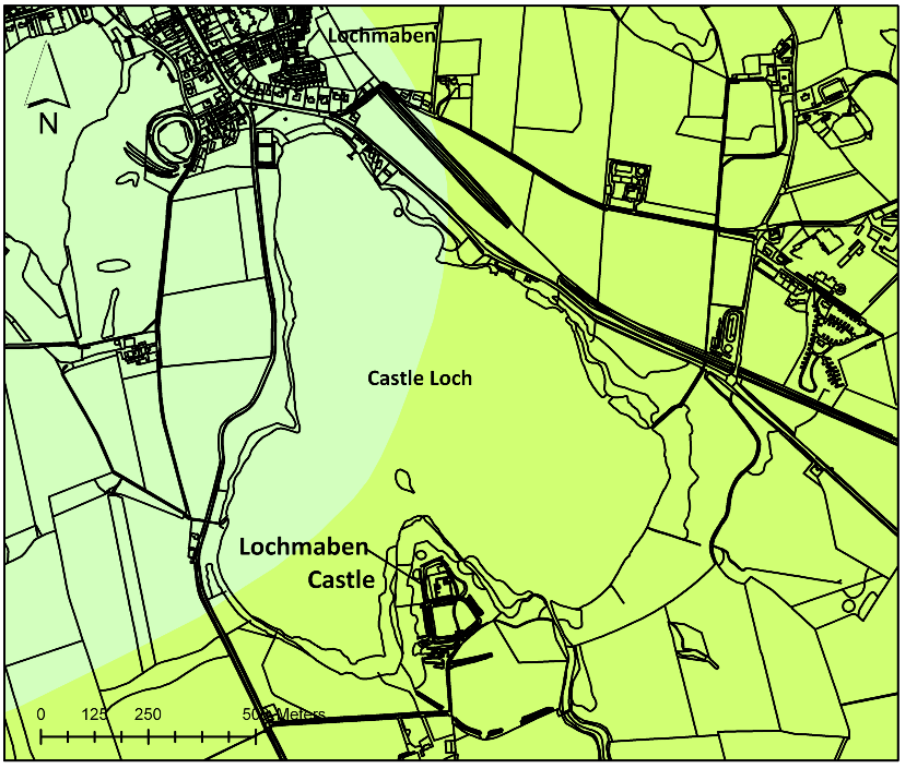

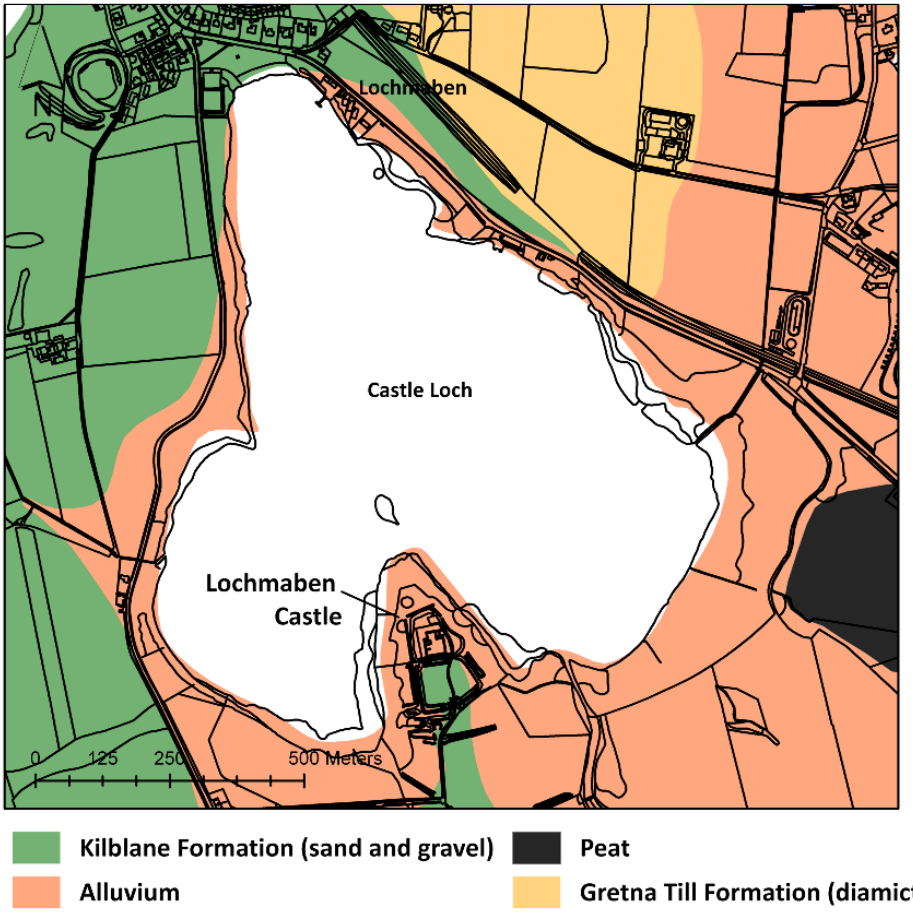

Figure 6-3: The underlying solid geology and superficial deposits at Lochmaben Castle (based on Geological Map Data ©NERC 2012).

The sands and gravels are overlain by the alluvium of the River Annan (Figure 6-3) and they surround the study area and the 'kettle hole' now occupied by Castle Loch. These fluvial deposits are normally soft to firm consolidated and compressible silty clay, and they can contain layers of silt, sand, peat and basal gravel (McMillan *et al.* 2011).

6.1.3.2. **Soils**

The soils at the site are classified as brown earths of the Crichton Series (Macaulay Land Use Research Institute 2011). These soils are free draining, have a litter rich in nutrients with intense biological activity (i.e. earthworms) which provide rapid decomposition hence, a fertile soil. Generally they present an 'Ah' topsoil which is dark coloured and enriched with humus of variable depth, and a 'B' subsoil with distinctive brown-red colours that progressively lighten as organic matter/iron content decreases with depth.

6.1.3.3. **Land Cover**

The site is a grassed and landscaped recreational area (Figure 6-4).

Figure 6-4: North view of the outer ward and entrance to Lochmaben Castle. The image shows the colony of nettles and rosebay willow herb present during the surveys undertaken for this research (© C. Cuenca-García).

The outer ward was partially colonized by patches of nettles and rosebay willow herb when the surveys started. The area is maintained by the Dumfries and Galloway Council Ranger Services and occasionally cleared of vegetation to control weed propagation.

6.1.4. Archaeological Background

MacDonald and Laing (1977) carried out archaeological excavations at several areas of the castle including the SW angle of the Outer Ward or 'bailey' (B in Figure 6-5, left). The aims were to examine the palisade or retaining wall at the edges of the Outer Ward (delimited by ditches A and B in Figure 6-5, right), and to determine the make-up of the deposits above natural in the outer ward.

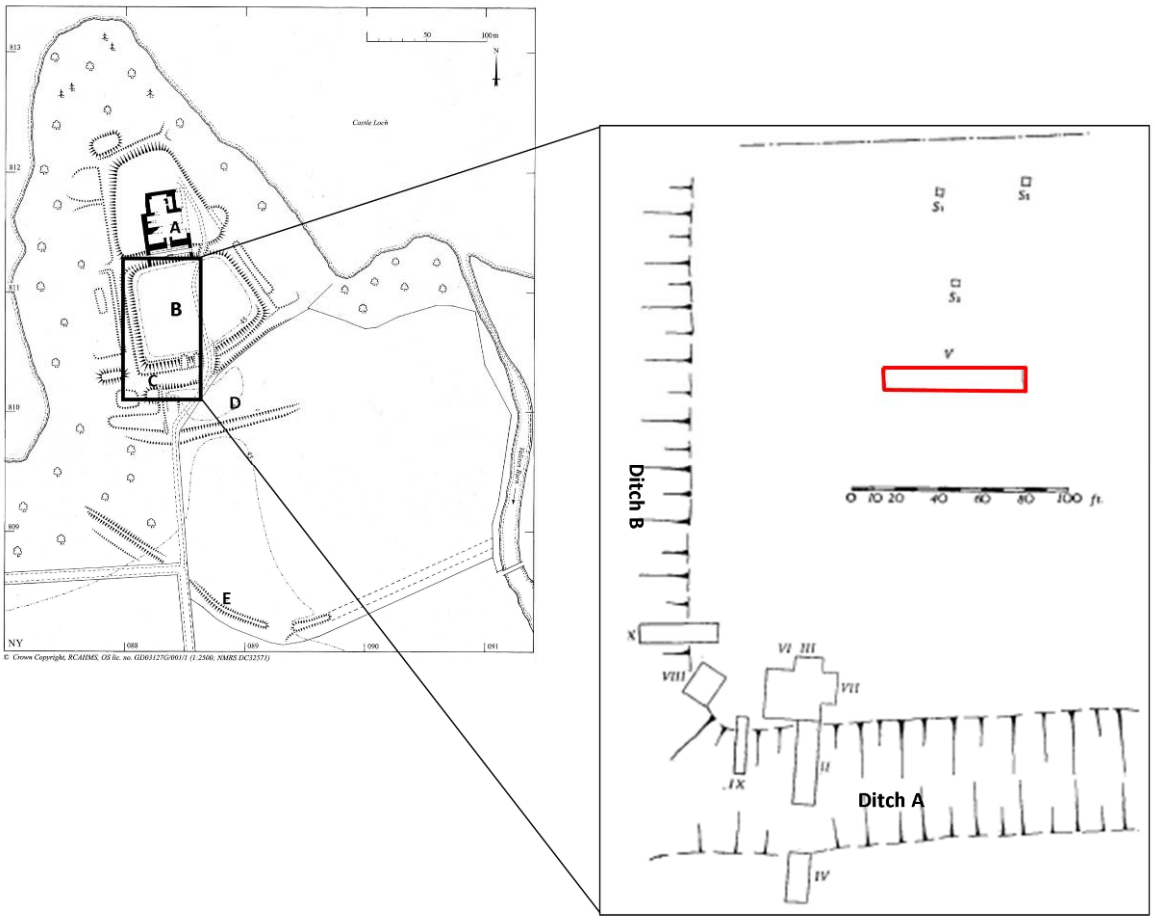

Figure 6-5: Plan of Lochmaben Castle and its immediate environs (left) where A is the Inner Ward, B is the Outer Ward (or 'bailey') where this investigation was focused, and C-D-E are potential defence ditches. The figure also shows the plan of the excavated areas by MacDonald and Laing in 1977 (right) and the location of the trench (in red) excavated within the outer ward.

In their interpretation, MacDonald and Laing (1977, 144) state,

> "*From the excavation it is apparent that the whole of the platform which now composes the 'bailey' was built up artificially with pink clay, which could have been found locally, to a height of over 1.25 m. This overlies silts. For some reason the extreme SW corner was built up to the height of the rest of the platform with a mixture of earth, clay and stones*".

The finds and structural features found in the brown earths overlying the pink clay were associated with a 'work camp' for the builders of the stone castle in the 14th century for which,

> "*The gullies and ditch can be interpreted as water carrying channels for metalworking. The lead smelting hearths could have been for roof lead, and quantities of iron slag were also found. The presence of pot wasters in Ditch B might suggest nearby pottery kilns, … and the considerable quantity of ironwork recovered is in keeping with the existence of a nearby forge. The hearths, post-holes and stake-holes probably represent the remains of buildings used by the castle builders.*" (Macdonald and Laing, 1977, 144).

Cutting V (Figure 6-5) revealed "*a band of cobbles 7 m wide lay immediately beneath the topsoil at a depth of 0.5 m, running N-S*" (Macdonald and Laing 1977, 144) that was interpreted as a cobbled approach road built to the castle across the bailey of an unknown date but "*probably late in the occupation of the castle*" (Macdonald and Laing 1977, 144). The authors suggested that the S sector of the bailey could have been abandoned and cobbled over to form a yard after the stone castle was built.

6.2. The Geophysical Survey

6.2.1. Aims & Objectives

Given the variable magnetic response and weak anomalies detected by the gradiometer in the areas surrounding the Outer Ward, the aims of the geophysical survey for this thesis were to detect potential structural features relating the timber 'peel' or evidence of occupation within the outer ward using gradiometry, earth resistance and GPR in order to assess their performance and their respective results.

6.2.2. Survey Area & Data Collection

The fieldwork started before the massive summer growth of vegetation that prevented the first survey. Hence, the surveys were carried out during four days in May (5 and 22-25 May 2010). However, patches of nettles and rosebay willow herb were already present (Figure 6-4) and the area required some clearing of vegetation prior to survey. Six 20x20 m grids were positioned over most of the outer ward (Figure 6-6) which was fairly flat.

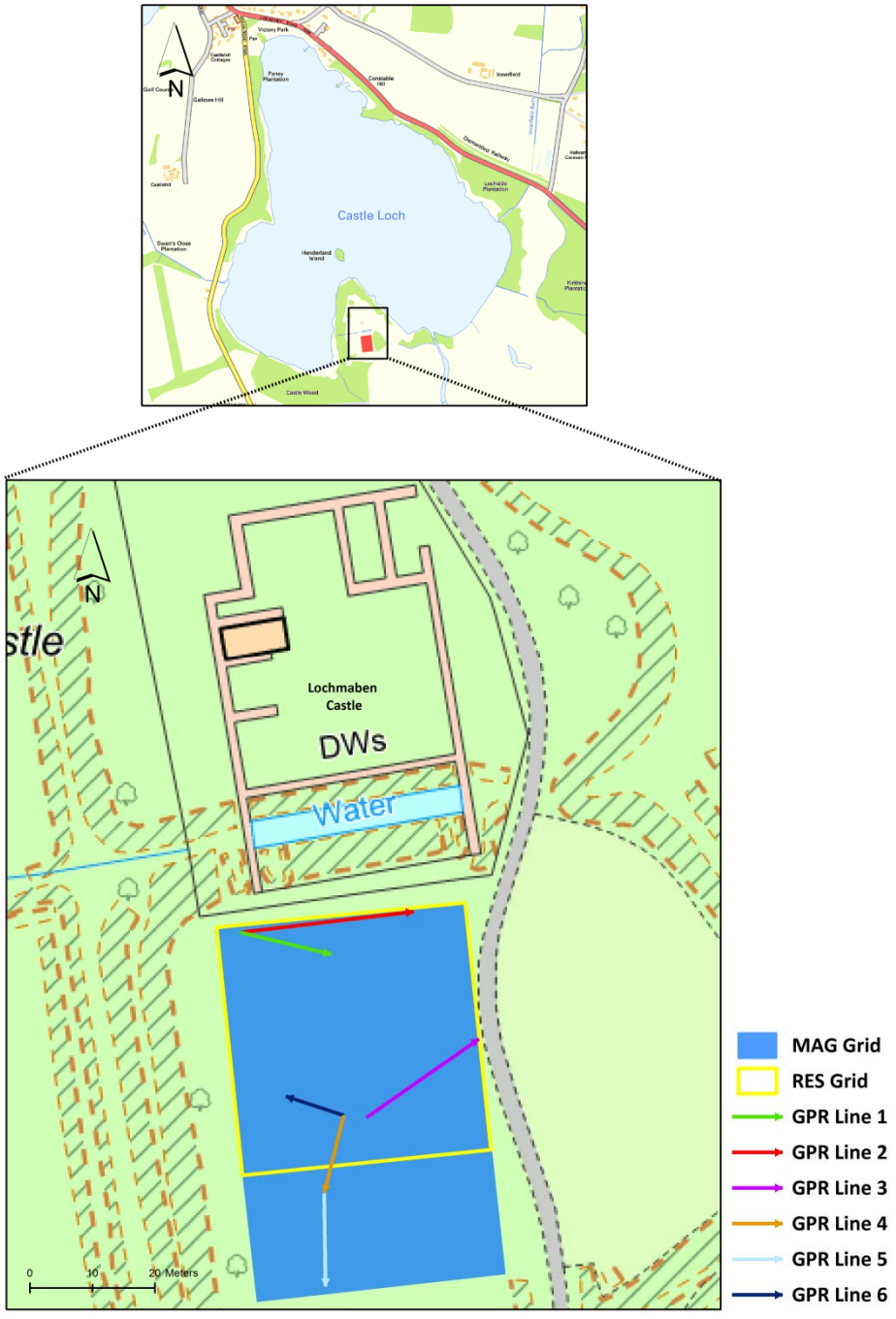

Figure 6-6: Grid location of the multi-technique geophysical survey carried out over the Outer Ward at Lochmaben Castle. The arrows indicate the origin and direction of the GPR survey traverses (based on © Crown Copyright/database right 2012. An Ordnance Survey/EDINA supplied).

The grids were set out within the site area using tapes and tied in to the OS map using a GPS Leica 1200 system. The surveys were carried out by two experienced operators assisted by students from the University of Glasgow. The weather conditions during the survey were dry and sunny. The survey dates and parameters are shown in Table 6-1.

The resolution of the gradiometer survey was increased with respect to the previous survey at the site (i.e. from 1m to 0.5m traverse spacing) and the survey lines were recorded in parallel instead of the zigzag mode. A slightly higher resolution (0.5m traverse spacing instead of the common 1m traverse spacing) was also used with the earth resistance survey.

The gradiometer surveys were carried out over the six grids and the earth resistance survey covered the northernmost four grids. Finally, several single GPR lines were recorded, focussing in particular on anomalies that were identified in the results of the previous surveys. For the purposes of this chapter, only the results from GPR line 1 and 2 are discussed.

Technique	Date	Instrument	Traverse Spacing	Sampling Interval	Survey Mode	Other
Gradiometry	05/05/2010	Bartington Grad 601-2	0.5m	0.125m	Parallel traverses.	Lower sensor *c* . 20cm above the surface & 0.03nT/m (resolution).
Earth Resistance	22 and 24/05/2010	Geoscan RM15 & (MPX15)	0.5m	0.5m	Zig-zag traverses.	0.5m and 1m probe spacing / x1 range (sensitivity range).
GPR-450 MHz	23/05/2010	Sensors & Software PulseEKKO 1000	Single traverses	0.05m	Continuous mode, time window=80ns, stacks=16, samples=200ps.	An average velocity used during collection for real-time data visualisation= 0.1m/ns.
GPR-225 MHz	24/05/2010			0.10m	Continuous mode, time window=120ns, stacks=16, samples=400ps.	

Table 6-1: Instrument settings used during the multi-technique geophysical survey at Lochmaben Castle.

6.2.3. Gradiometry Results

The raw and processed data results of the gradiometer survey are plotted in Figure 6-7 and Figure 6-8 respectively. The range of the unclipped raw data varied from 100 to -100nT. This high range was caused by an area of magnetic noise at the north edge of the grid and other strong responses scattered in the survey area. A standard processing flow Table 6-2 and the general gradient range was reduced to -12nT to 9nT (Table 6-3). The results were characterised by the noisy area at the northern end of the grid and the scattered strong magnetic dipoles, possibly a product of superficial ferrous objects. The rest of the data set did not reveal any other coherent anomaly. However, a closer look of the data revealed some very weak magnetic linear and sub-circular trends in the centre of the grid.

Function	Parameters
Clip	Min -10, Max 10
Despike	2 (X/Y Radii), 3 (Threshold), Mean (Replacement)
Zero Mean Grid	2 (Threshold)
Zero Mean Traverse	All (Grid), On (Less Mean Fit), Not applied (Threshold)
Destager	3 (Grid)/ -2 (Shift), 1(Grid)/3 (Shift)/13-14(Line), 4 (Grid)/3 (Shift)/32 (Line), 5-6 (Grid)/3(Shift)
Low Pass Filter	2 (X & Y), Gaussian (Weighting)
Interpolate	X & Y (Direction), Expand, SinX/X

Table 6-2: Data processing (Geoplot 3.0 software) applied to the data acquired during the gradiometer at Lochmaben Castle.

Gradient	Raw	Processed
Mean	2nT	0.1nT
Min/Max	100nT to -100 nT	-12nT to 9nT

Table 6-3: Range of the dataset of the gradiometer survey at Lochmaben Castle before and after processing.

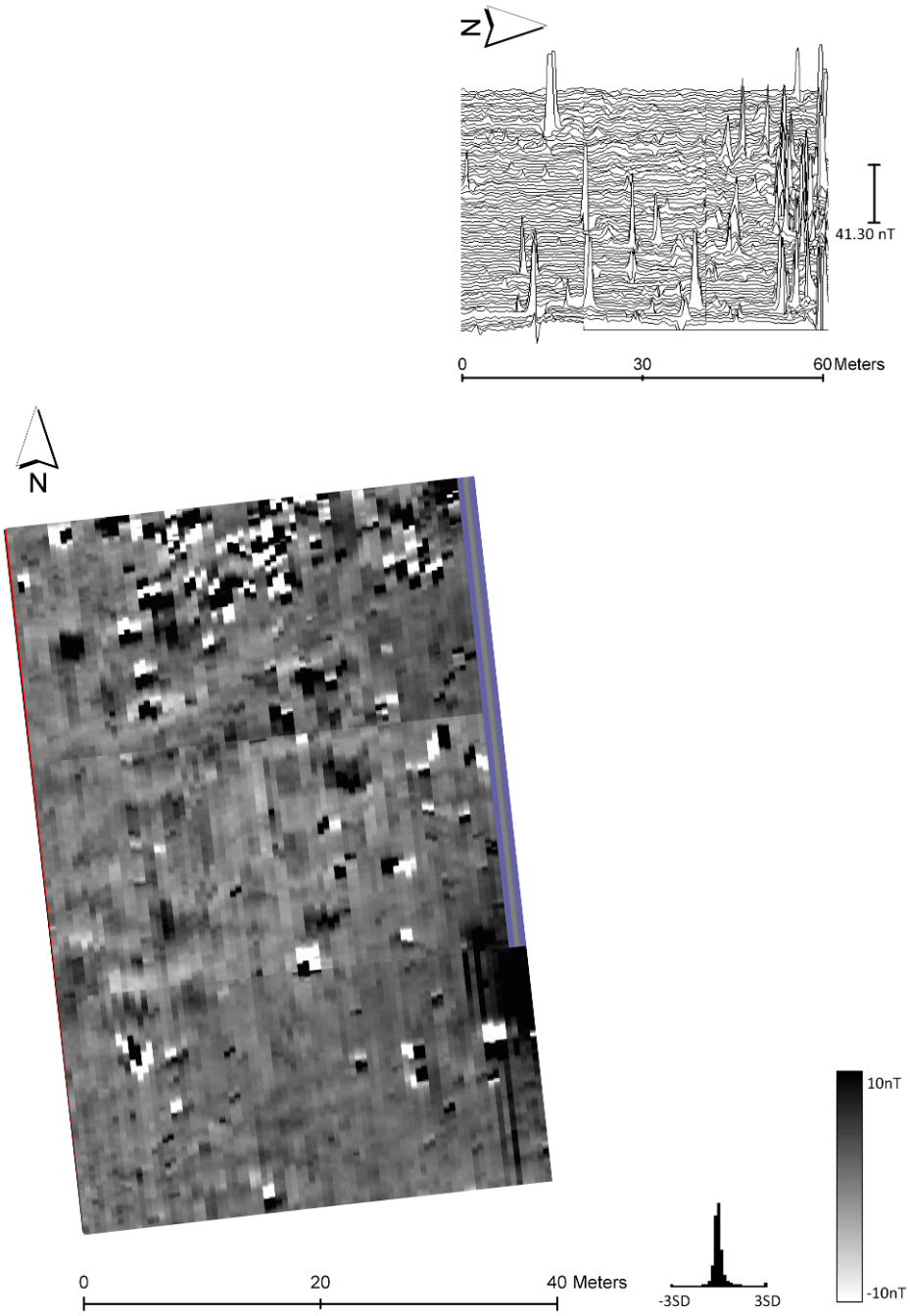

Figure 6-7: Trace (top) and shade (bottom) of the raw data results of the gradiometer survey over the Outer Ward at Lochmaben Castle. The data was plotted at -10/10 Absolute units, contrast 1 and using the Geoplot grey99 palette.

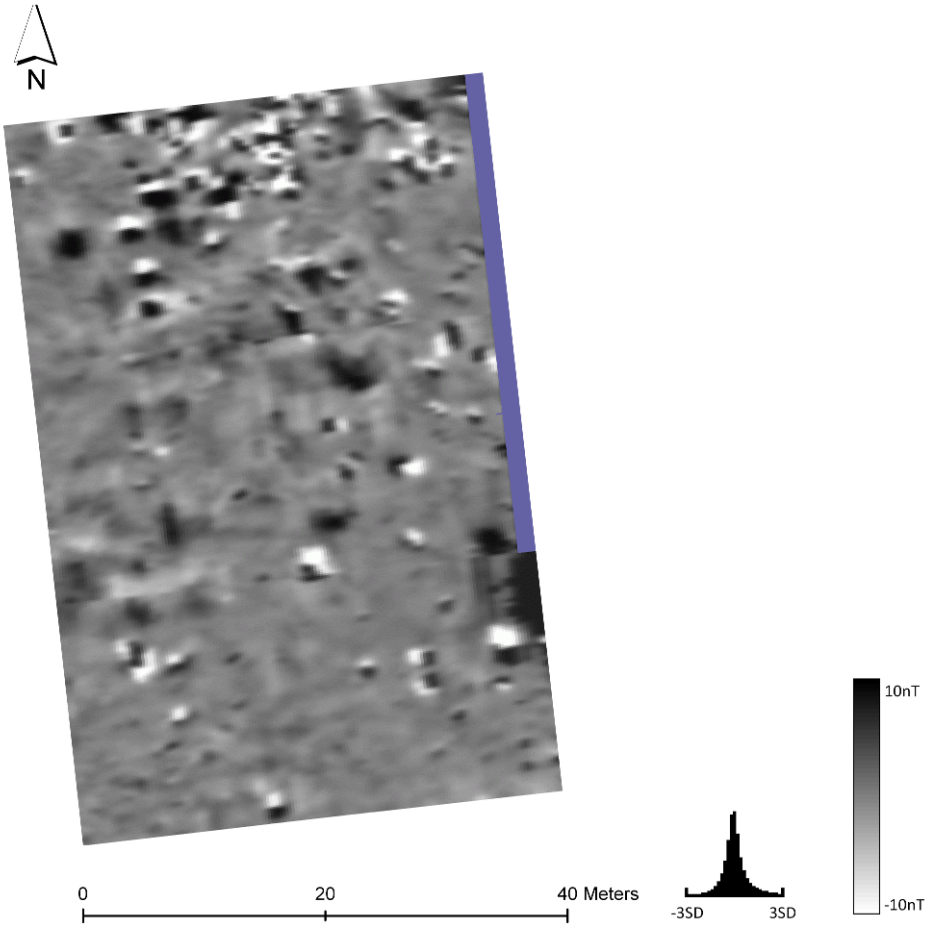

Figure 6-8: Shade plot of the processed data results of the gradiometer survey over the Outer Ward at Lochmaben Castle. The data was plotted at -10/10 Absolute units, contrast 1 and using the Geoplot grey99 palette.

6.2.4. Earth Resistance Results

The raw and processed data results of the earth resistance survey are plotted in Figure 6-9 and Figure 6-10. The processing flow applied to this set of data is summarised in Table 6-4. The results from the 0.5m probe separation resulted in better defined anomalies.

The results of the earth resistance survey provided richer and more coherent responses than those obtained from the gradiometer survey. The dataset was characterised by a high resistance linear response (>20 ohm) with N-S orientation and running parallel to the present-day track to the east of the survey grid. The anomaly seems to project SW in the S of the survey area. Two sub-circular anomalies of lower high resistance (<20 ohm) were detected at the centre of the grid, the interior of these anomalies being characterised by low resistance. The results of the 0.5m electrode spacing provided better results and revealed some smaller anomalies.

Function	Parameters
Despike	2 (X/Y Radii), 2 (Threshold), Mean (Replacement)
Edge Match	1R & 3B
High Pass Filter	10 (X & Y), Uniform (Weighting)
Low Pass Filter	2 (X & Y), Gaussian (Weighting)
Interpolate	X & Y (Direction), Expand, SinX/X

Table 6-4: Data processing (Geoplot 3.0 software) applied to the data acquired during the earth resistance survey at Lochmaben Castle.

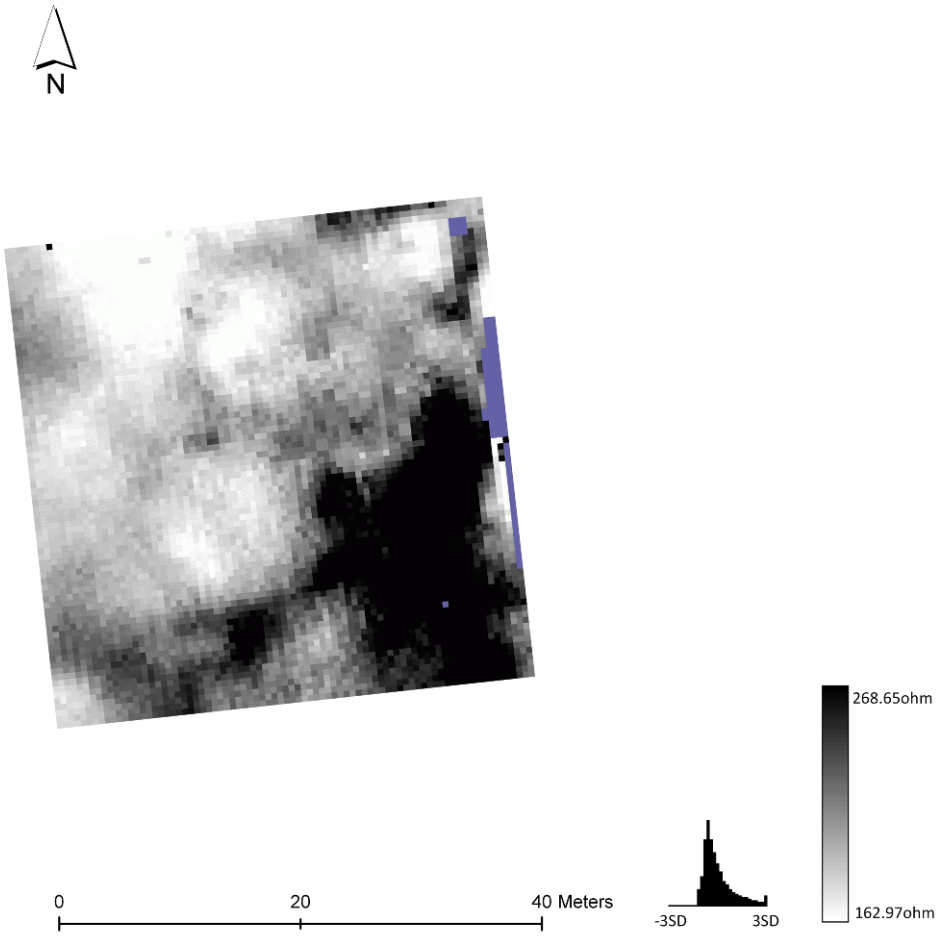

Figure 6-9: Shade plot of the raw data results of the earth resistance (RES) survey (0.5m probe separation) over the Outer Ward at Lochmaben Castle. The data was plotted at -1/1 SD units, contrast 1 and using the Geoplot grey99 palette. The blue colour indicates dummied readings.

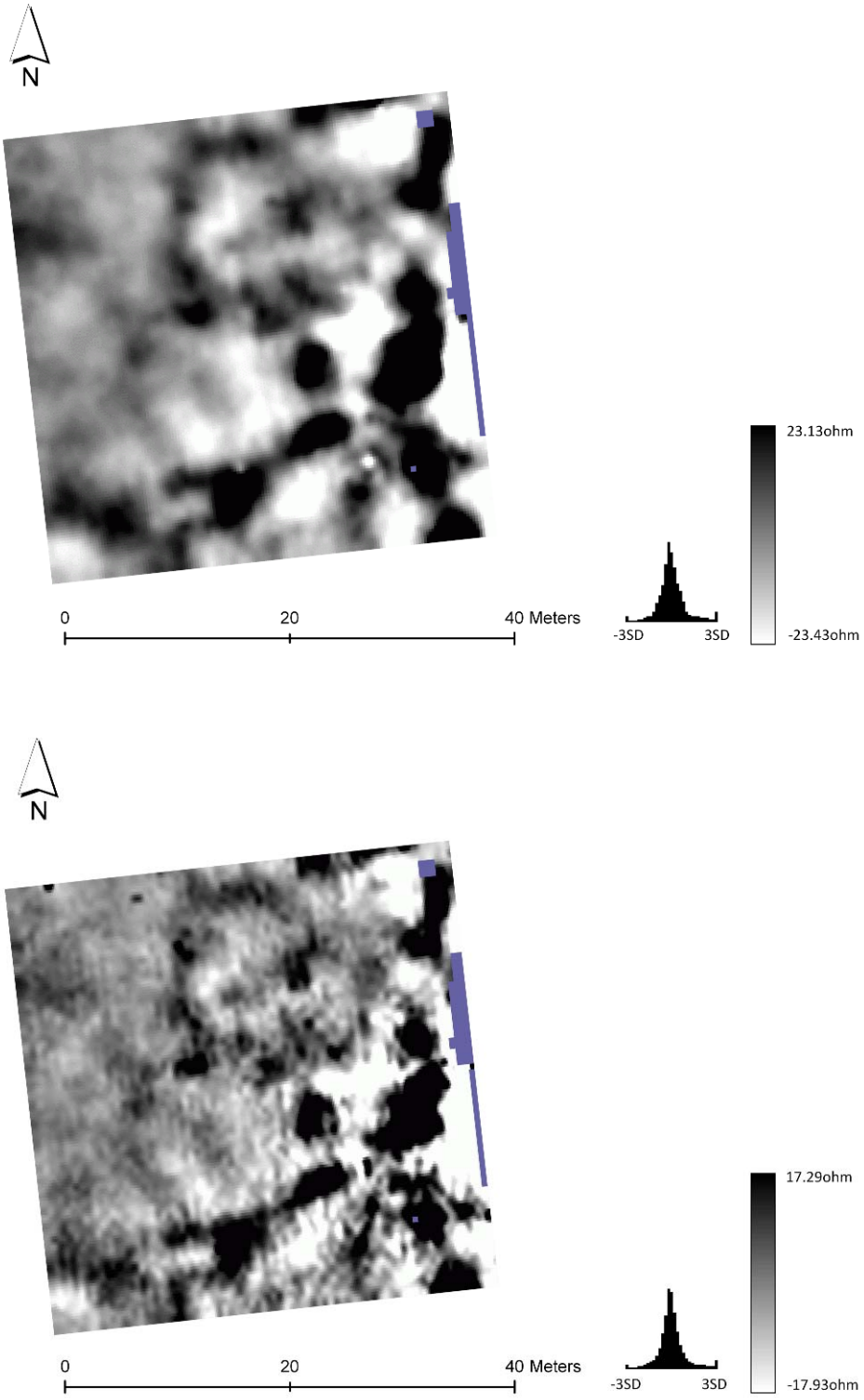

Figure 6-10: Shade plot of the processed data results of the 1m probe separation (top) and 0.5m probe separation (bottom) earth resistance survey over the Outer Ward at Lochmaben Castle. The data was plotted at -1/1 SD units, contrast 1 and using the Geoplot grey99 palette. The blue colour indicates dummied readings.

6.2.5. GPR Results

Figure 6-11 shows the raw data and the results of the processing steps applied (Table 6-5). Figure 6-12 and Figure 6-13 shows the results of the single GPR traverses collected over the area where the sub-circular high resistance anomalies were detected.

In general, the penetration of the GPR signal was affected by attenuation probably caused by lossy dielectric materials such as the pink clay which the excavators claim was used to build the made-ground that now composes the Outer Ward. The signal attenuation is visible in Figure 6-12 *c*.0.6m to *c*.1.2m, overlaying stronger reflectors *c*.1.4m and reaching a maximum of 1.6m depth. The signal attenuates to a shallower depth (*c*.1m) in line GPR 2 (Figure 6-13). The penetration achieved with the lower frequency survey was higher, as expected, and reached *c*.2.5m in lines GPR 1 and 2. The reflections seen at *c*.1.4m with the high frequency survey in line GPR 1 (Figure 6-12) were better defined when mapped with the lower frequency survey as the attenuation produced by the lossy materials (e.g. clay deposits) was overcome.

Whist the higher frequency results where characterised by shallow hyperbolic reflections, the datasets presented a series of dipping and planar (linear) reflections at a greater depth that were better defined in the low frequency results.

Function
Subtract-mean (dewow)
Time zero Correction
Background Removal
Manual gain (y)
Time cut
Migration (FD Migration)
Velocity analysis (hyperbolic velocity analysis)
Time-depth conversion

Table 6-5: Data processing (ReflexW v.5.6 software) applied to the data acquired during the GPR survey at Lochmaben Castle.

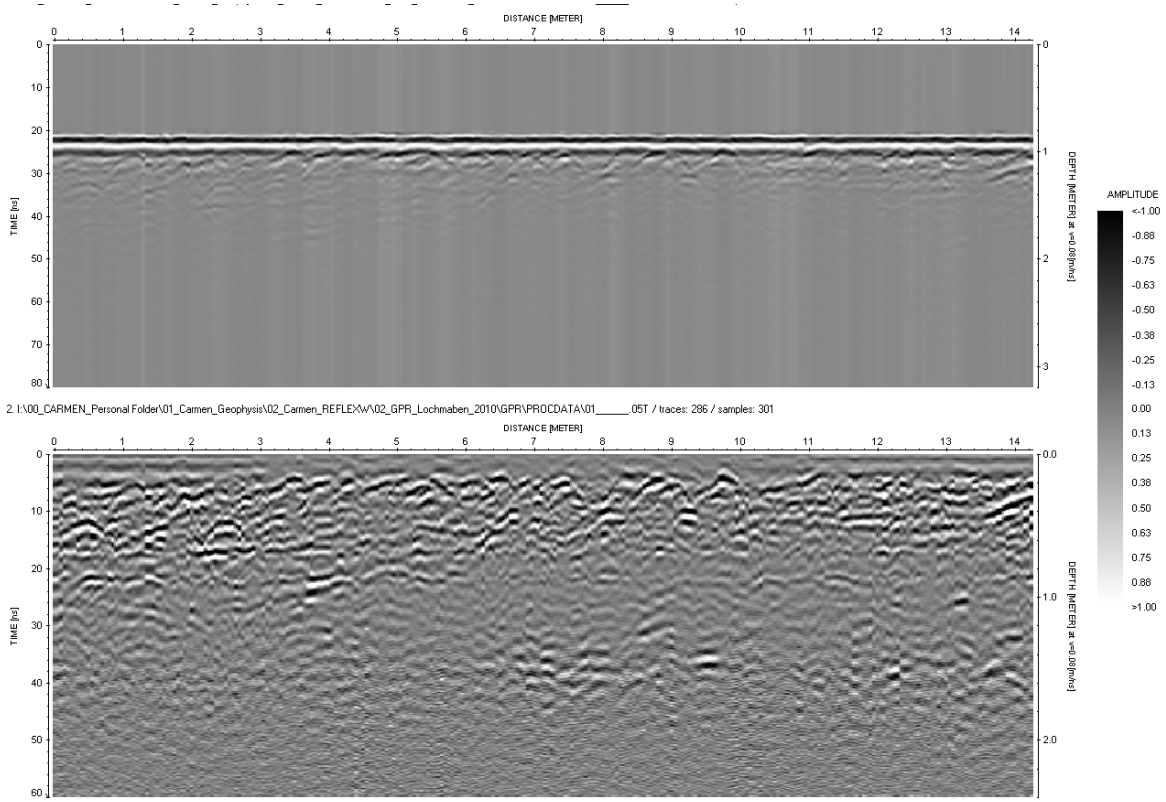

Figure 6-11: Radargram from the 450MHz survey over the Outer Ward at Lochmaben Castle showing the raw (top) and processed (bottom) results of GPR Line 1 (Figure 6-6).

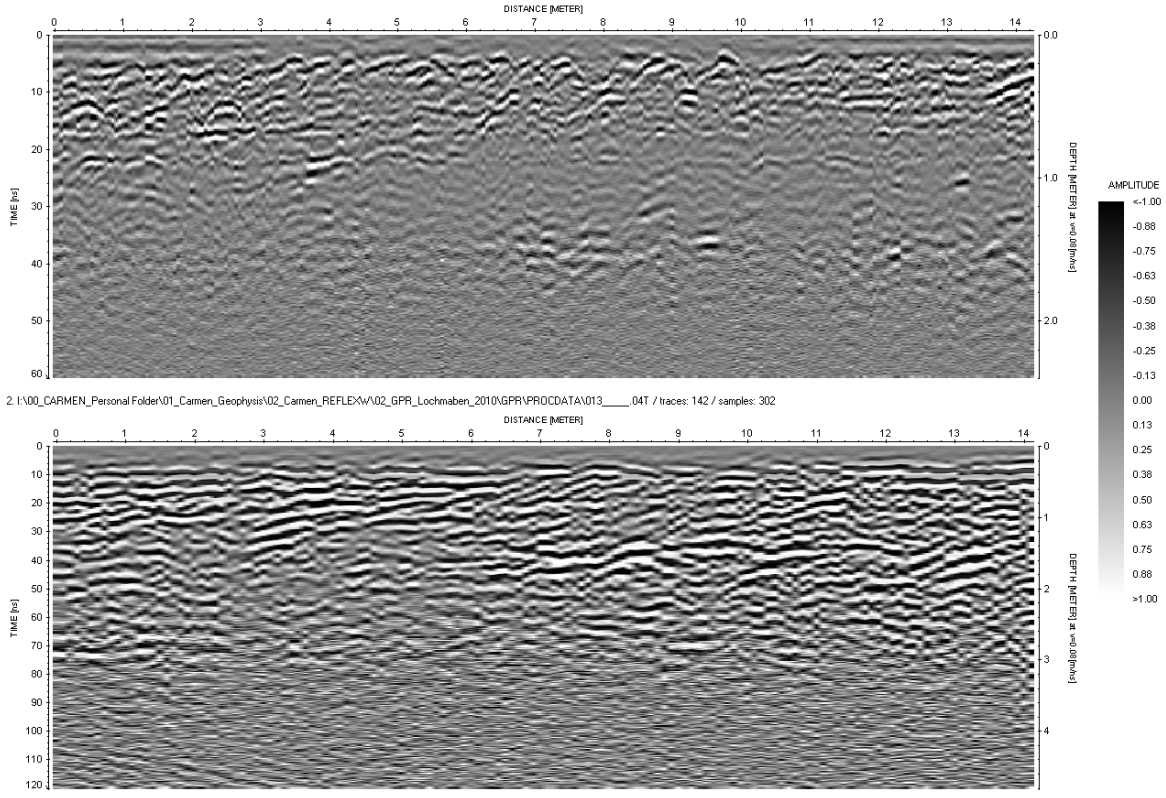

Figure 6-12: Radargram showing the results of the 450MHz (top) and 225 MHz (bottom) survey along line GPR Line 1 at the Outer Ward at Lochmaben Castle (Figure 6-6).

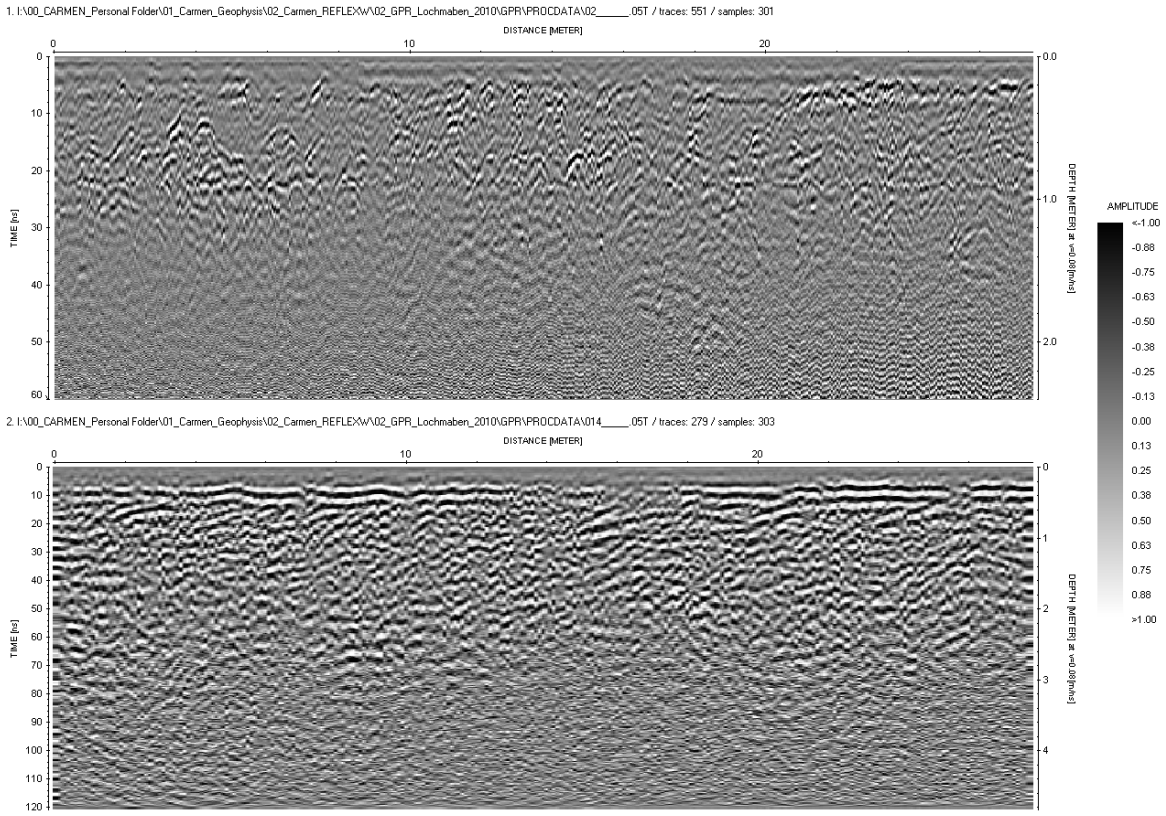

Figure 6-13: Radargram showing the results of the 450MHz (top) and 225 MHz (bottom) survey along line GPR Line 2 at the Outer Ward at Lochmaben Castle (Figure 6-6).

6.2.6. Gradiometry Interpretation

The interpretation of the gradiometer survey results is shown in Figure 6-14. The magnetically noisy area detected in the northernmost edge of the grid may be associated with the debris from the construction of the drawbridge belonging to the last of MacDonald and Laing's three phases of construction at the castle's southern front (Macdonald and Laing 1977). According to their account, part of that northern area may also represent iron-working debris.

In general, the dataset was magnetically quiet and only after careful analysis of the images a few weak magnetic trends were observed. Two linear trends (1 in Figure 6-14) suggested the presence of a possible structure. Surrounding these anomalies, a very weak sub-circular trend (2 in Figure 6-14) could be enclosing the possible structure. Another very weak linear trend (3 in Figure 6-14) seen to continue at a right-angle eastwards may be the line of a (modern) fence.

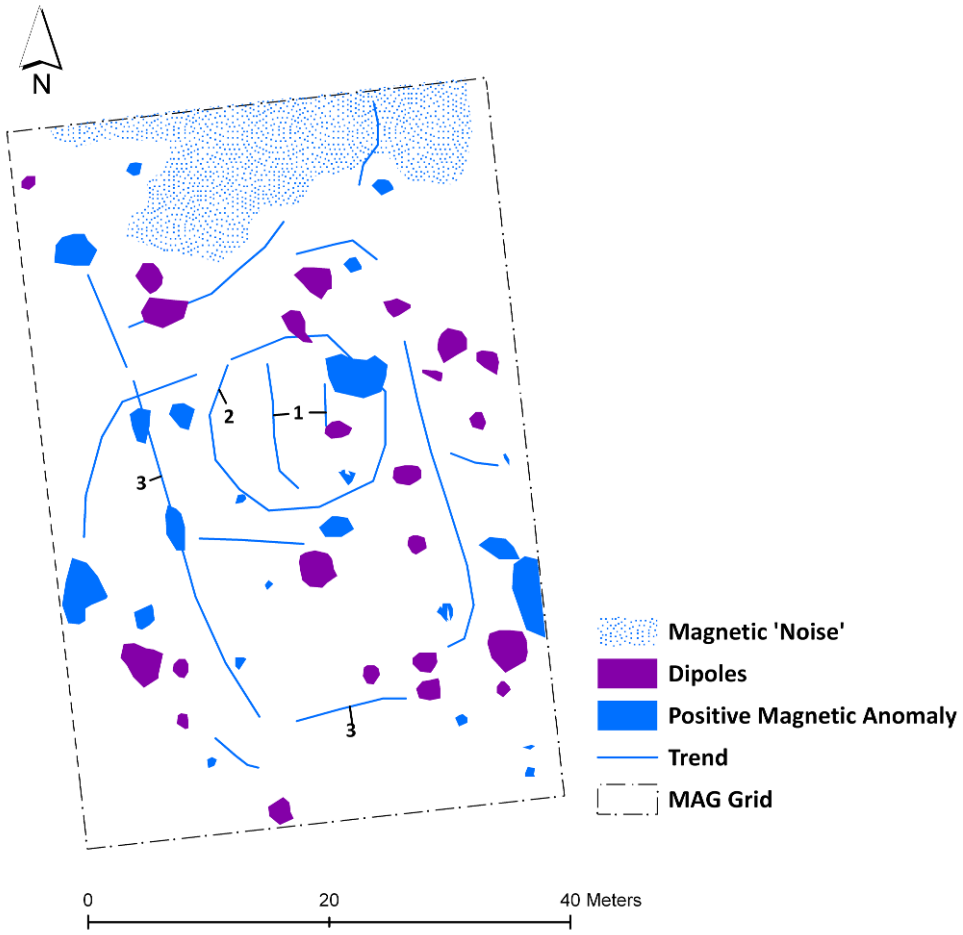

Figure 6-14: Anomaly extraction and interpretation plot of the gradiometer survey results over the Outer Ward at Lochmaben Castle. The numbers (1-3) mark the anomalies discussed in the main text.

6.2.7. Earth Resistance Interpretation

The interpretation of the earth resistance results is shown in Figure 6-15. Anomaly 1 (Figure 6-15) appears to correspond to magnetic anomaly 2 (Figure 6-14). The anomaly closest to the Inner Ward at the north of the survey area (2 in Figure 6-15) corresponds to an area of softer and less compacted raised ground noticed during the clearing of the vegetation. These two anomalies (1 and 2 in Figure 6-15) may be remains of structures.

The linear high resistance anomaly (3 in Figure 6-15) reveals the possible cobbled approach road that MacDonald and Laing (1977, 144) found in cutting V (Figure 6-5). Furthermore, the approximate geo-referencing of the excavation plan to the geophysical data showed that the location of the trench correlates with a low resistance area just over part of anomaly 3 running N-S (Figure 6-16).

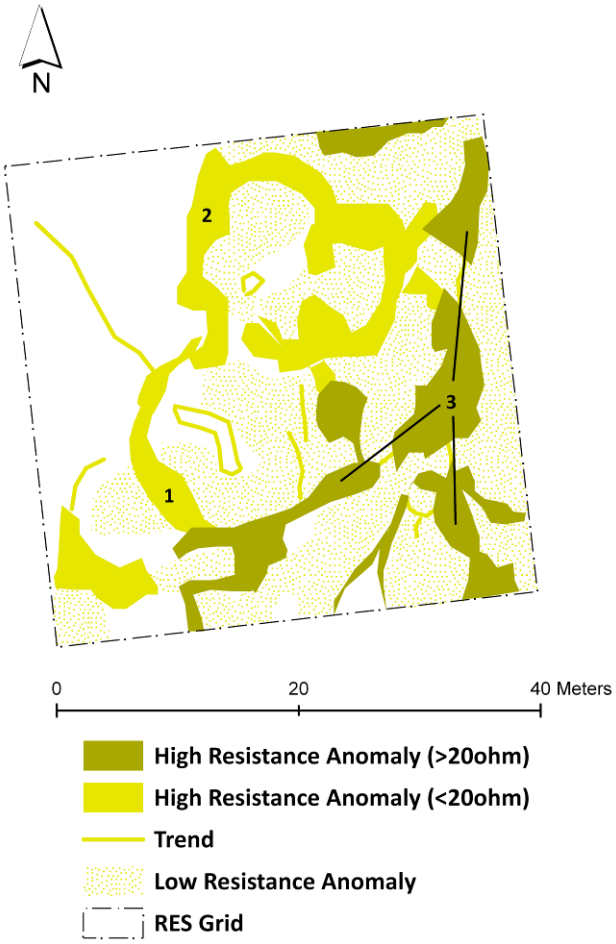

Figure 6-15: Anomaly extraction and interpretation plot of the earth resistance (RES) results (0.5m probe separation) over the Outer Ward at Lochmaben Castle. The numbers (1-3) mark the anomalies discussed in the main text.

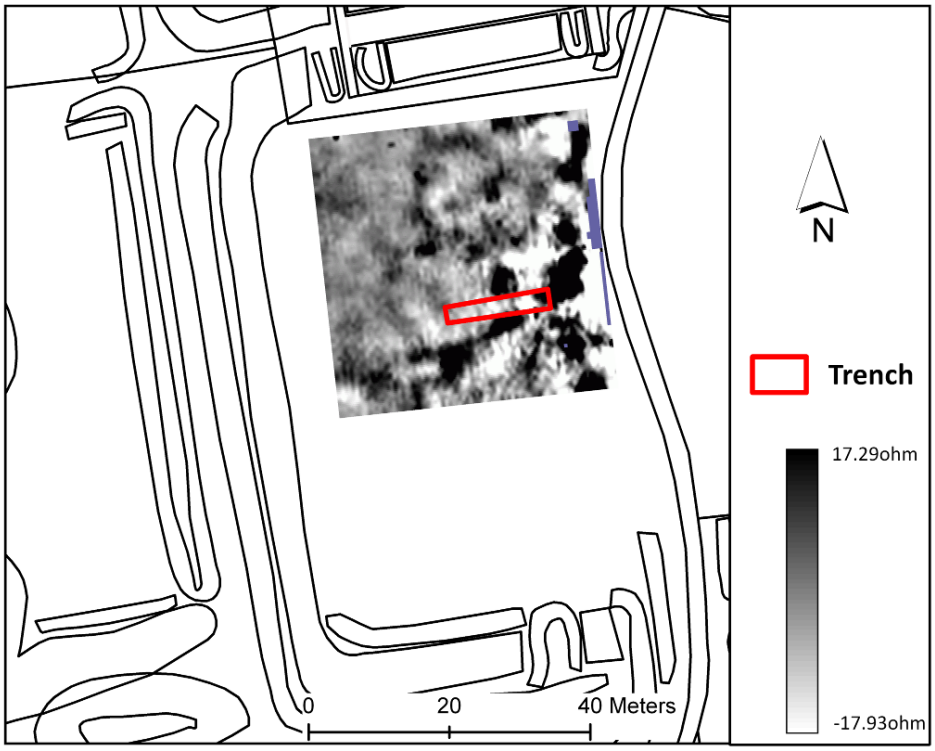

Figure 6-16: Location of the archaeological trench (in red) excavated by MacDonald and Laing (1977) on the earth resistance results.

6.2.8. GPR Interpretation

GPR line 1 was collected over the area with the sub-circular high resistance anomaly 2 (Figure 6-17) in its last 3m (i.e. from12m to 14m).

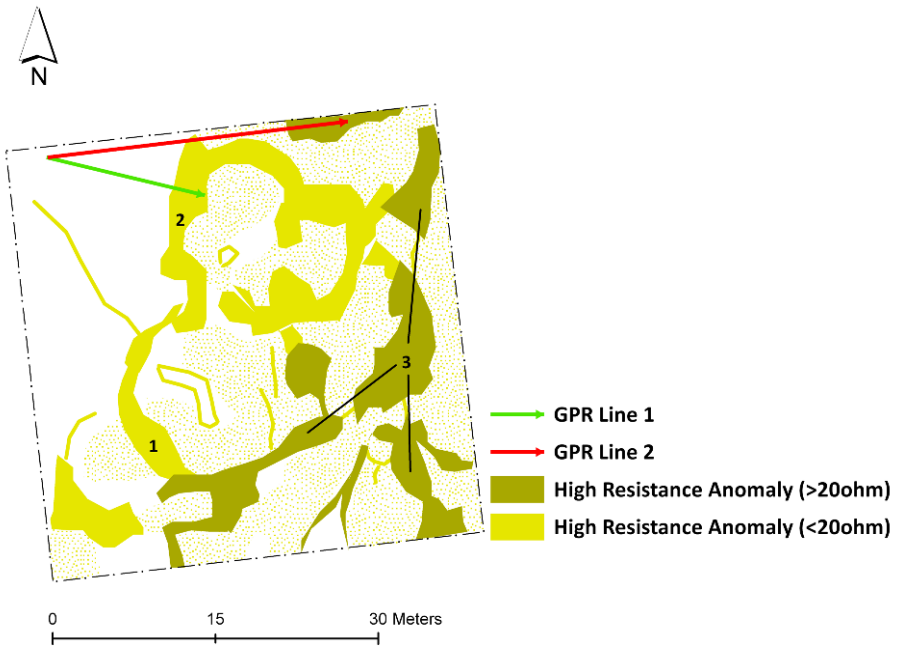

Figure 6-17: Location of the GPR lines 1 and 2 in relation to the results of the earth resistance survey.

There were a series of shallow dipping reflections *c*.0.4m deep at 14m (A1 in Figure 5-18) which were not mirrored in the low frequency survey due to its intrinsic lower resolution to shallower depths. Deeper in the radargram, other reflections were observed (A2 in that may be related to the high resistance anomaly 2 (Figure 6-17). Therefore, A1 and A2 (Figure 5-18) may be related to the same buried structure. Between 7m and 11m and to a *c*.1.4m depth a series of distinctive linear and hyperbolic reflections was observed (A3 in Figure 5-18).

The results from GPR line 2 (Figure 6-17) showed a series of reflections (A1 in Figure 6-19) that may correspond to the high resistance anomaly 2 (Figure 6-15). The result from the low frequency antennae (bottom in Figure 6-19) shows a break in the superficial linear reflection and strong dipping reflection (as A 1 in Figure 5-18 but to a greater depth). A2 (Figure 6-19) shows strong dipping and linear reflections which correlate with the high resistance anomalies in Figure 6-17.

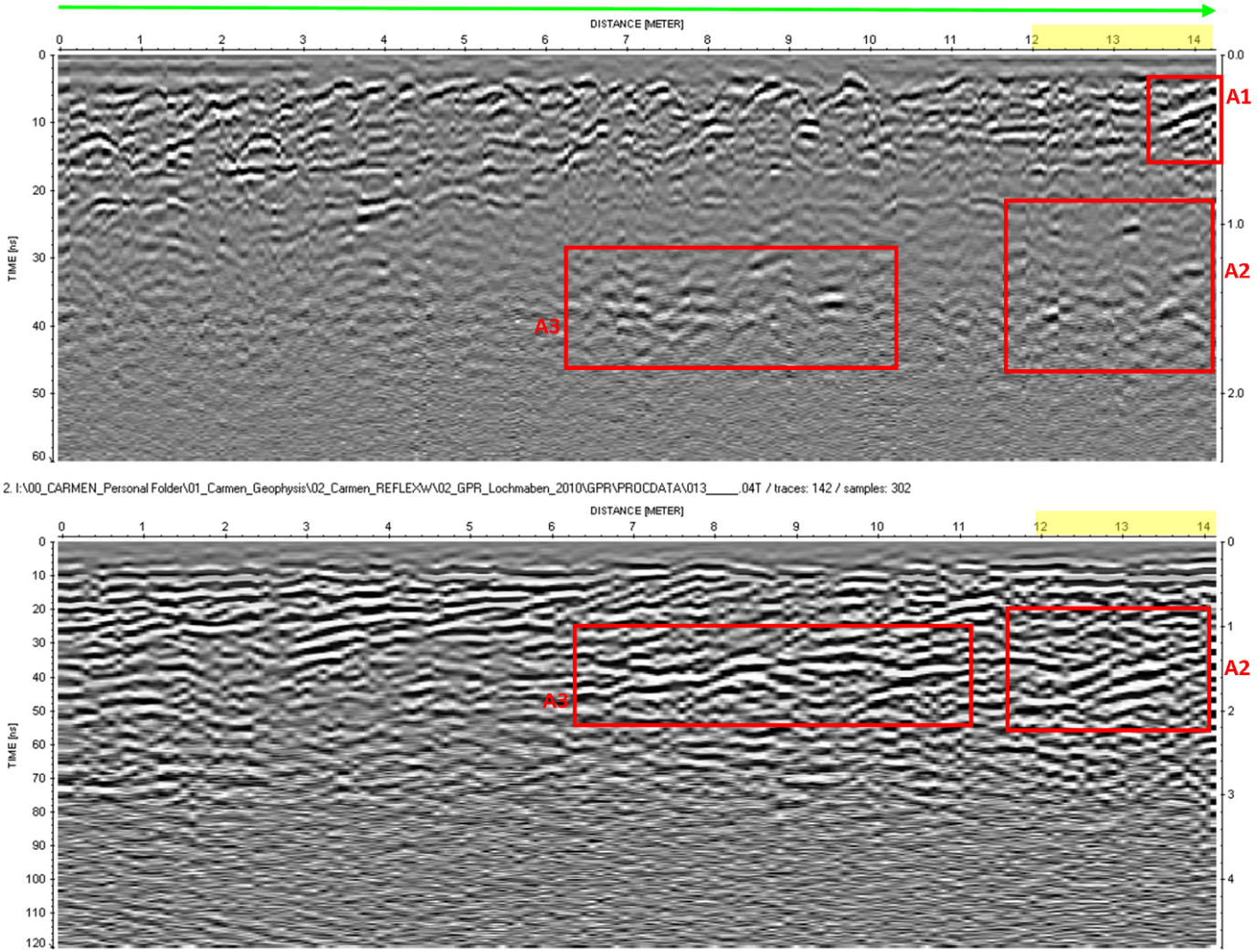

Figure 6-18: Radargram showing the results and interpretation of the GPR single line 1 (450 MHz -top- and 225MHz-bottom- frequency survey) over the Outer Ward at Lochmaben Castle. The numbers (A1 to A3) mark the anomalies discussed in the main text. The yellow bar shows the approximate location of the high resistance anomaly 2 (Figure 6-15). Note that the scale is the same as in Figure 6-12.

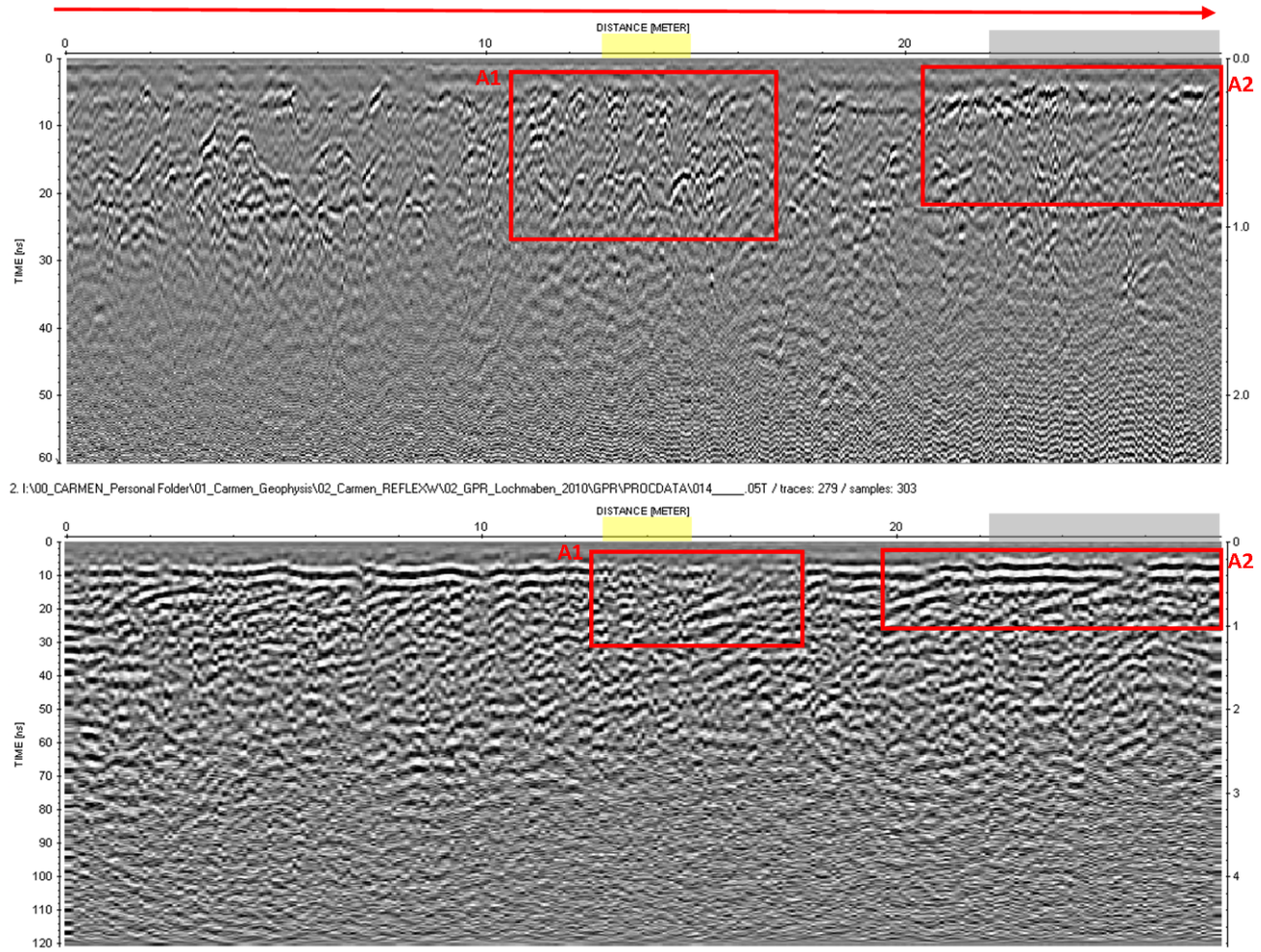

Figure 6-19: Radargram showing the results and interpretation of the GPR single line 2 (450 MHz -top, and 225MHz- bottom frequency survey) over the Outer Ward at Lochmaben Castle. The numbers (A1 and A2) mark the anomalies discussed in the main text. The yellow bar shows the approximate location of the high resistance anomaly 2 (Figure 6-15) and the grey bar another high resistance anomaly (Figure 6-15). Note that the scale is the same as in Figure 6-12.

6.2.9. Conclusions

The earth resistance survey provided the most informative datasets. It was striking how little correspondence there is between gradiometer and earth resistance results, although, carefull observation of the weak magnetic trends detected allowed their correlation with some earth resistance anomalies. However, interpretations of such weak magnetic trends would not have been possible without the good data obtained from the electrical survey.

Reducing the traverse spacing and collecting the gradiometer data in parallel mode may have helped to improve the definition of the weak magnetic trends. However, taking into consideration the time required to collect parallel traverses each 0.25m, the weak character of the magnetic contrast at the site and the results obtained from the earth resistance survey, further investigations at higher resolution were considered unnecessary.

The GPR survey detected some reflections that seem to correlate with some of the high resistance anomalies. However, the attenuation of the signal affected the signal penetration of the high frequency antennae. The lower frequency data provided more coherent reflections and allowed deeper penetration of the signal.

6.3. Soil Analysis

6.3.1. Aims

The aims were to characterise the horizontal response over the high resistance anomaly (2 in Figure 6-15) in terms of its physical and chemical composition using pXRF, MS and phosphate analysis in order to identify chemical elements related to the targeted structure.

6.3.2. Sampling Strategy

A line along GPR Line 1 and the high resistance anomaly 2 (Figure 6-17) were sampled, collecting every 0.5m and 0.10cm below topsoil (Figure 6-20). Three control samples were also taken outside the survey area and at different locations.

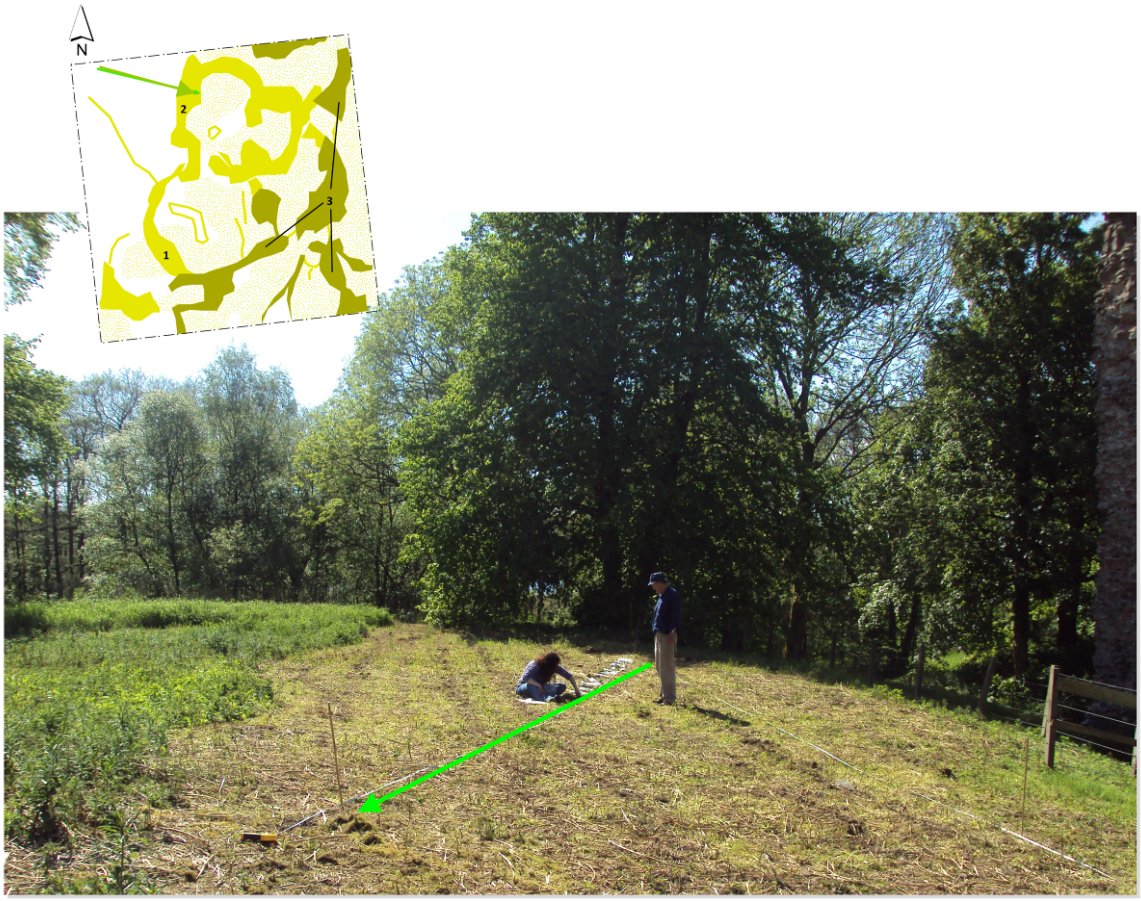

Figure 6-20: Surface soil sampling carried out over GPR Line 1 and high resistance anomaly 2 (**Figure 6-17**) at the Outer Ward (Lochmaben Castle)**. The green arrow shows the direction of the soil sampling.**

6.3.3. Physical & Chemical Results & Discussion

6.3.3.1. **MS, Total P, LOI, EC and pH**

The results of the MS, total phosphate, loss on ignition (LOI), conductivity and pH in the area of resistance anomaly 2 (Figure 6-17) are summarised in Table 6-6 and graphically represented in Figure 6-21. There was a general increase of the MS, total phosphate and organic matter content (or LOI) measurements from 12m onwards (Figure 6-21).

In particular, the increase in organic matter (LOI) was fairly dramatic, with values of 0.200 and 0.025 respectively for the samples taken over the targeted anomaly and outside. The MS values over the feature and outside were 101 and 56. The total phosphate results also increased from 13m onwards (Figure 6-21) but to a lesser extent. The general increase in organic matter content may be associated with an increase in biomass produced by the patches of nettles and rosebay willow herb which appear to be associated with the sub-circular

anomaly detected by the earth resistance surveys. These patches were visible in aerial photographic records (Figure 6-2) and during the surveys (Figure 6-4). The MS enhancement seems to coincide to the mineral content of the organic layer rather than produced directly by buried features. Only a few samples were analysed for pH and the values oscillated between 4 and 5 which correspond to acidic conditions (Table 6-6).

Distance (m)	χ_{lf}	Total P µg/kg	LOI (%)	EC µs	pH
0.05	51	270	0.025	*	*
1.00	65	294	0.024	149	5
1.50	52	270	0.023	*	*
2.00	56	291	0.027	*	*
2.50	59	264	0.025	*	*
3.00	54	285	0.028	141	5
3.50	62	273	0.025	*	*
4.00	61	276	0.026	*	*
4.50	52	252	0.025	*	*
5.00	55	258	0.022	*	*
5.50	54	252	0.024	*	*
6.00	68	309	0.024	*	*
6.50	57	306	0.027	*	*
7.00	55	280	0.023	107	6
7.50	53	292	0.025	*	*
8.00	55	289	0.025	*	*
8.50	52	295	0.023	*	*
9.00	57	295	0.028	*	*
9.50	51	274	0.027	*	*
10.00	52	271	0.026	*	*
10.50	50	292	0.025	*	*
11.00	54	286	0.028	92	6
11.50	55	305	0.028	*	*
12.00	81	308	0.200	*	*
12.50	91	288	0.200	*	*
13.00	92	340	0.201	*	*
13.50	127	392	0.200	*	*
14.00	115	347	0.200	102	4
Mean	**64**	**291**	**0.057**	**118**	**5**
S.D	**20**	**30**	**0.068**	**25**	**1**
C.V	**31**	**10**	**121**	**21**	**15**
Control 1	25	282	0.027	132	4
Control 2	94	282	0.172	85	4
Control 3	46	297	0.027	*	*

Targeted anomaly

* **Not analysed**

Table 6-6: Magnetic susceptibility (χlf), total phosphate (Total P), loss on ignition (LOI), conductivity (EC) and pH results of the surface soil samples collected over GPR Line 1 and the high resistance anomaly 2 (Figure 6-20) at Lochmaben Castle.

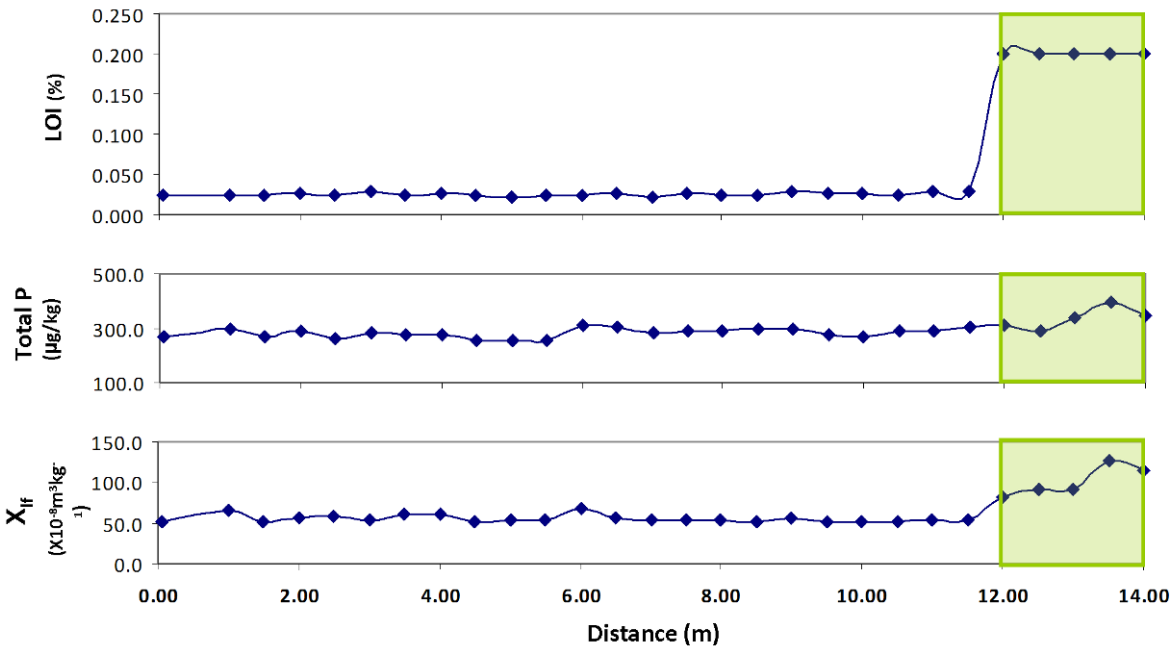

Figure 6-21: Surface distribution of magnetic susceptibility (χ_{lf}), total phosphate (Total P) and loss on ignition (LOI) of the samples collected over GPR Line 1 (Figure 6-20) at the Outer Ward (Lochmaben Castle). The green colour marks the location of the targeted anomaly (2 in Figure 6-20).

6.3.3.2. **pXRF Results**

The results of the pXRF analysis are summarized in Figure 6-22 and Table 6-7. Fe and Ti showed a weak enrichment towards the end of the sample line to the interior of anomaly 2 (Figure 6-20). This enrichment follows the increase in organic matter content and MS over the target feature (Figure 6-21).

The results were characterised by a distinctive peak in Ca towards *c.*10m with a maximum of 29857 mg/kg in sample 12 located at 10m (Table 6-7), followed by strong depletion (and corresponding but weaker depletion of Sr) until the end of the sampled line. The peak and general area showing Ca enrichment (between 6.5m and 11m) is located outside the targeted feature (anomaly 2 in Figure 6-20) and over an area of general low resistance (Figure 6-9 and Figure 6-10). The enrichment, which also correlates with the strong reflections (A2 in Figure 6-18) detected with the GPR survey, may be explained by a possible structure related to the 'work camp' suggested by MacDonald and Laing (1977), an accumulation of alkaline material (e.g. lime or mortar) that was not detected by the gradiometer or earth resistance surveys.

The area over the target anomaly also shows a Pb enrichment. Since organic matter plays a key role in the retention of Pb in soils (Oonk 2009), the increase

in organic matter content may explain the Pb retention. Pb enrichment has been reported at craft production sites, and this may support the interpretation of the targeted feature as being related to Macdonald and Laing (1977)'s 'work-camp'.

There was also a Mn depletion towards the end of the sampled line correlating with the area of the targeted anomaly 2 (Figure 6-15). This parallels what has been found elsewhere (i.e. accumulation of organic matter) and will be discussed in Chapter 9.

Distance (m)	Fe	K	Ca	Ti	Mn	Zr	Pb	Sr	Rb	V	Cu	Cr
0.5	16131	15575	5656	3941	1404	516	124	108	87	74	67	62
1.5	17034	15852	5584	3906	1416	533	135	109	88	93	71	77
2.5	17052	15174	5438	3980	1202	521	132	105	84	84	75	53
3.5	16651	14809	4553	3745	1222	512	116	103	83	76	62	49
4	15899	14925	4627	3795	1125	574	115	104	82	73	49	71
4.5	15799	15025	4726	3785	1155	584	112	105	82	72	48	78
5.5	16310	15517	4733	3643	1181	522	115	105	81	65	85	74
6.5	16024	14972	4873	3822	1097	632	121	108	82	80	43	61
7	16475	15489	5843	3733	1250	572	124	103	79	88	46	46
8	15836	15186	7361	3647	1061	642	115	108	81	76	69	46
9	15781	14870	19078	3493	1021	595	107	107	82	70	80	51
10	16054	14593	29857	3458	941	562	118	106	79	77	65	63
10.5	15966	15215	17654	3703	872	586	110	105	77	70	78	61
11	16766	15784	6581	3834	887	643	113	104	81	86	102	62
11.5	16789	15217	3878	3714	844	602	111	97	76	80	84	68
12	18209	15536	2826	4142	891	581	122	100	80	84	78	76
12.5	18019	15004	3217	3985	849	578	123	94	78	84	77	104
13	16565	14330	2244	3859	764	612	128	90	77	81	50	64
13.5	18411	14853	2445	4336	775	648	137	91	85	87	97	90
14	18593	14142	2098	4157	682	570	156	88	81	82	68	70
Mean	**16718**	**15103**	**7164**	**3834**	**1032**	**579**	**122**	**102**	**81**	**79**	**70**	**66**
S.D	**911**	**450**	**6976**	**217**	**212**	**43**	**12**	**6**	**3**	**7**	**16**	**15**
C.V	**5**	**3**	**97**	**6**	**21**	**7**	**9**	**6**	**4**	**9**	**24**	**22**
Control 1	15257	14971	1536	3851	354	551	117	91	82	80	46	58
Control 2	18492	14573	1528	4236	652	500	127	88	75	90	70	65
Control 3	15774	15587	4376	3868	1198	539	104	105	90	79	76	75

Targeted anomaly *** Not analysed**

Table 6-7: pXRF results of the surface soil samples collected along GPR Line 1 (Figure 6-20) over the high resistance anomaly 2 (Figure 6-15) at Lochmaben Castle. The element concentrations are expressed in mg/kg (=ppm). The green colour marks the approximate location of the targeted anomaly.

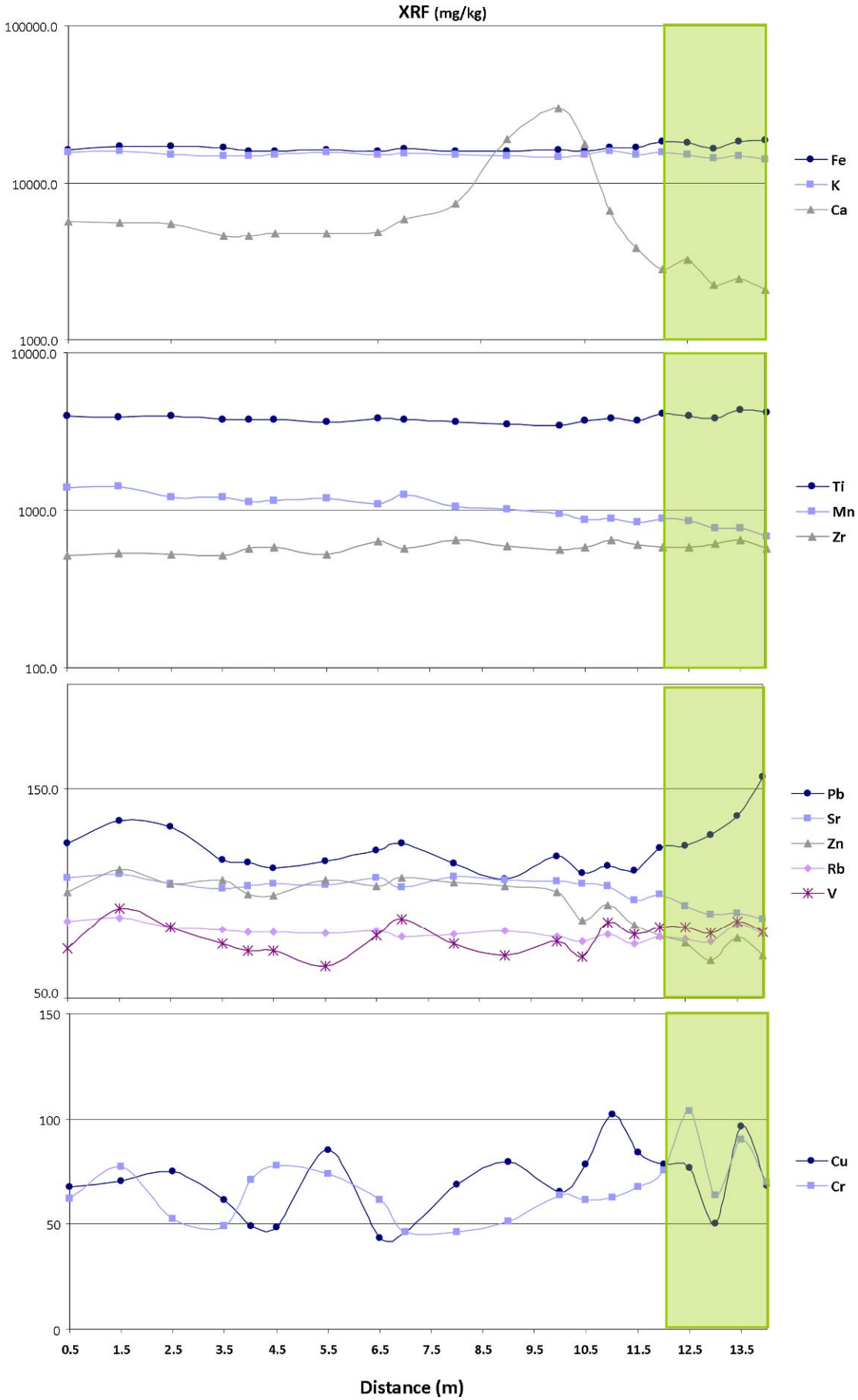

Figure 6-22: Surface distribution of the soil major element concentrations (pXRF data) along GPR Line 1 (Figure 6-20) at the outer ward of Lochmaben Castle. The green colour marks the location of the targeted anomaly (2 in Figure 6-15).

6.3.3.3. **ICP_OES**

The ICP-OES analysis (Figure 6-23 and Table 6-8) gave similar results to those of pXRF and also in the case of total phosphate analysis. The only difference was a more homogeneous and coherent Cu and Cr enrichment over the targeted anomaly (2 in Figure 6-20). These elements are generally not affected by site lithology (Oonk *et al.* 2009a) and they correlated with Pb enhancement as noted in the XRF section. The ICP-OES results provided a clearer pattern in the data averages and plotted data.

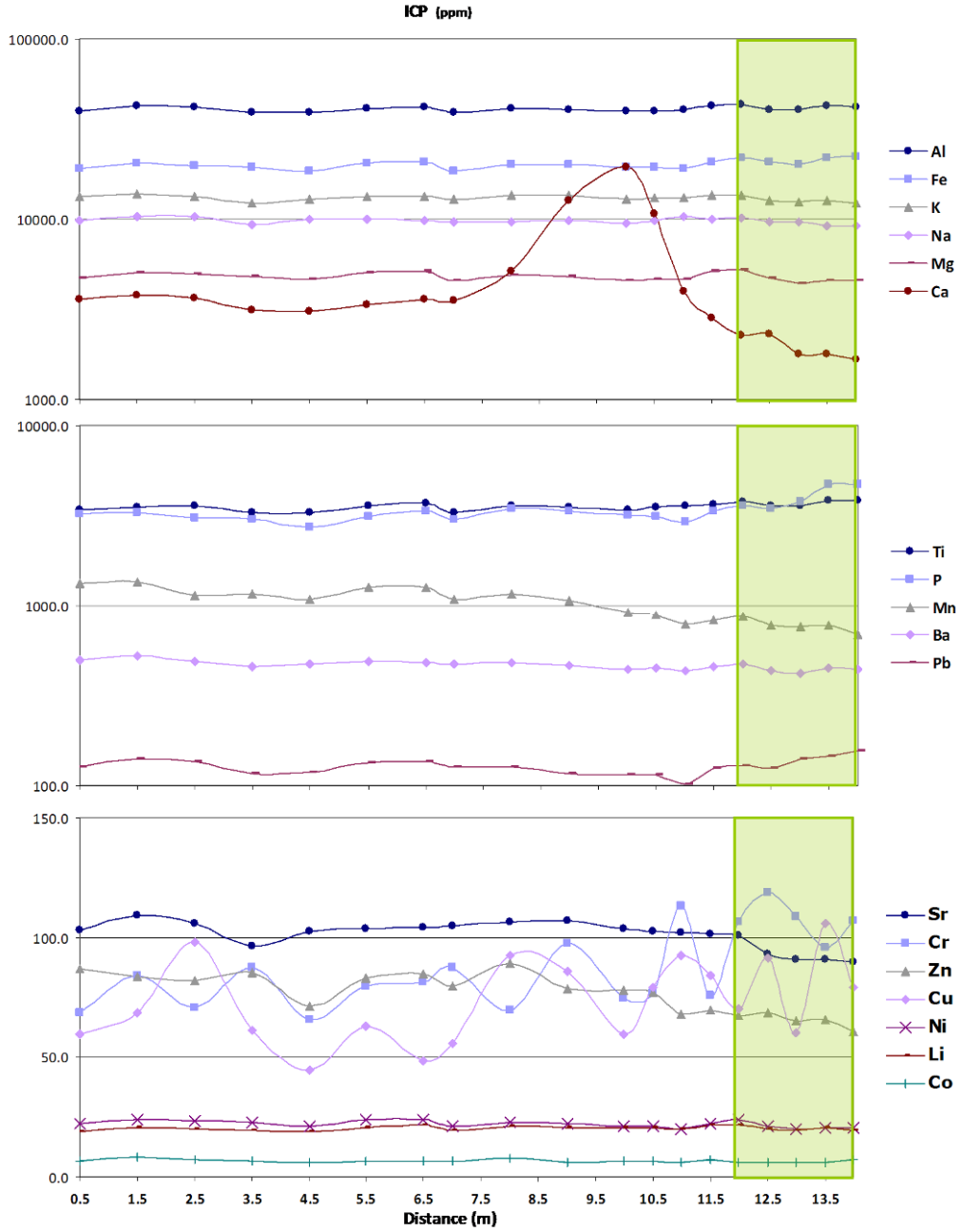

Figure 6-23: Surface distribution of soil element concentrations (ICP-OES data) along GPR Line 1 (Figure 6-20) at the outer ward of Lochmaben Castle. The green colour marks the location of the targeted anomaly (2 in Figure 6-15).

Distance (m)	Al	Fe	K	Na	Mg	Ca	Ti	P	Mn	Ba	Pb	Sr	Cr	Zn	Cu	Ni	Li	Co
0.5	40014	19138	13272	9896	4732	3624	3407	3232	1341	496	128	103	69	87	59	22	19	7
1.5	42369	20424	13888	10342	5024	3771	3557	3308	1359	519	140	109	84	84	69	24	21	8
2.5	41656	19818	13449	10378	4986	3652	3624	3062	1145	488	136	106	71	82	98	24	20	7
3.5	39029	19353	12313	9344	4815	3117	3293	3026	1165	457	116	96	88	85	61	23	19	7
4.5	39136	18416	13012	9934	4630	3093	3279	2716	1080	470	118	103	66	72	45	21	19	6
5.5	41355	20398	13450	9963	5091	3361	3573	3133	1265	492	133	104	80	83	63	24	21	7
6.5	42191	20989	13255	9892	5162	3619	3707	3356	1265	483	135	104	81	85	49	24	22	7
7	39267	18547	12974	9707	4554	3513	3291	3032	1090	471	126	105	87	80	56	21	20	7
8	41181	20243	13628	9683	4884	5186	3576	3463	1167	484	127	107	69	89	92	23	21	8
9	40612	20145	13493	9855	4803	12636	3551	3366	1071	460	117	107	98	78	86	22	21	6
10	39546	19289	12909	9558	4593	19349	3408	3199	922	441	114	104	75	78	60	21	21	7
10.5	40043	19318	13192	9764	4647	10797	3543	3129	884	448	115	102	77	77	79	21	20	6
11	40740	18965	13133	10323	4619	3976	3567	2915	782	435	101	102	113	68	93	20	20	6
11.5	42906	20961	13569	9978	5133	2809	3673	3349	834	456	124	102	76	69	84	22	22	7
12	43402	22039	13629	10187	5213	2275	3763	3594	875	469	129	101	106	67	71	24	22	6
12.5	40825	20773	12789	9624	4721	2315	3607	3459	777	431	124	93	119	68	91	21	20	6
13	40508	20153	12391	9620	4442	1796	3605	3773	758	422	140	91	109	65	60	20	20	6
13.5	42462	21842	12637	9221	4550	1783	3818	4682	779	451	145	91	96	66	106	21	21	6
14	41595	22121	12323	9240	4544	1678	3834	4710	681	438	157	90	107	61	79	20	20	7
Mean	**40991**	**20154**	**13121**	**9816**	**4797**	**4861**	**3562**	**3395**	**1013**	**464**	**128**	**101**	**88**	**76**	**74**	**22**	**20**	**7**
S.D	**1305**	**1115**	**468**	**345**	**241**	**4527**	**166**	**520**	**217**	**26**	**13**	**6**	**17**	**9**	**18**	**1**	**1**	**1**
C.V	**3**	**6**	**4**	**4**	**5**	**93**	**5**	**15**	**21**	**6**	**10**	**6**	**19**	**11**	**24**	**6**	**4**	**10**
Control 1	39976	18607	13209	9955	4468	1321	3693	3384	350	421	118	92	90	41	46	18	17	4

Targeted anomaly *** Not analysed**

Table 6-8: ICP-OES results of surface soil samples collected along GPR Line 1 (Figure 6-20**) over the high resistance anomaly 2 (**Figure 6-15**) at Lochmaben Castle. The element concentrations are expressed in ppm (=mg/kg). The green colour marks the approximate location of the targeted anomaly.**

6.3.3.4. **Conclusions**

There were general increases in total phosphate, MS and organic matter content (LOI) over the targeted feature. The strong increase in organic matter content is possibly associated with the increase in biomass related to vegetation patches (rosebay willow herb) developed over the sub-circular high resistance anomaly. The enhancement in MS seems to be related to the increase in organic matter content rather than to be directly derived from the buried feature. There was also Pb enrichment over the targeted feature. Whilst Pb enrichment may have been caused by modern fuel contamination, its correlation with Cu and Cr may be related to the work-camp/craft activities carried out in the Outer Ward during the 14th century and where the targeted structure is located.

There was a depletion of Mn over the targeted feature, possibly related to the accumulation of organic matter. Further depletion in Ca and Sr may be caused by plant uptake due to the exacerbated growth of vegetation over the buried targeted feature. The distinctive enrichment of Ca in the area outside the targeted anomaly may indicate a direct source of anthropogenic Ca, perhaps related to the work camp (e.g. mortar/lime accumulation). This geochemical anomaly correlated with strong GPR reflections and an area of low resistance. In general the common elements measured by the ICP-OES and pXRF correlated fairly well, showing the same concentration pattern (Figure 6-24 and Figure 6-25).

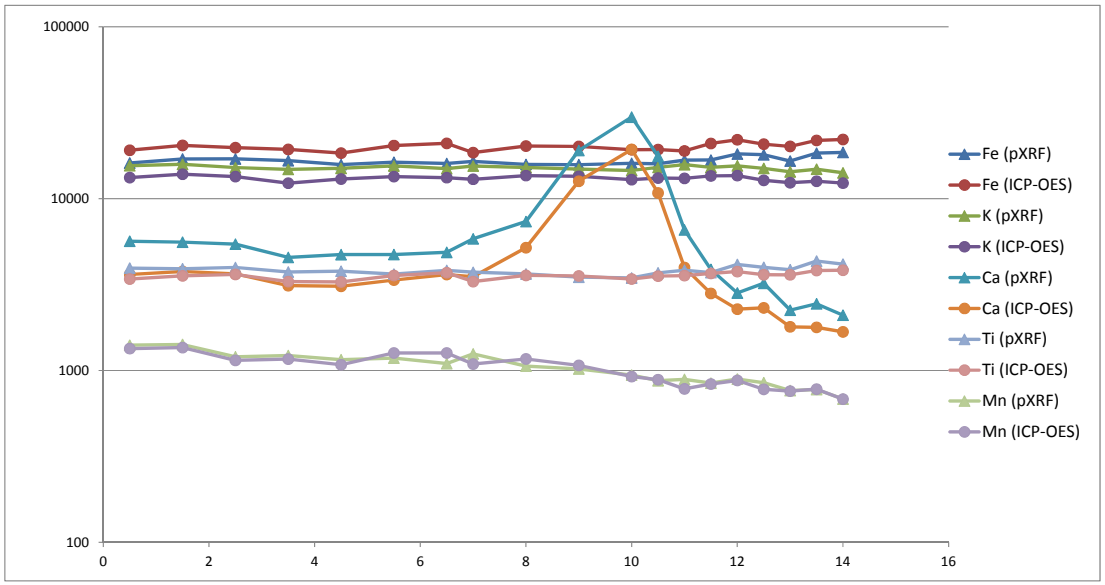

Figure 6-24: Comparative graphics showing the results of the major elements analised by pXRF and ICP-OES.

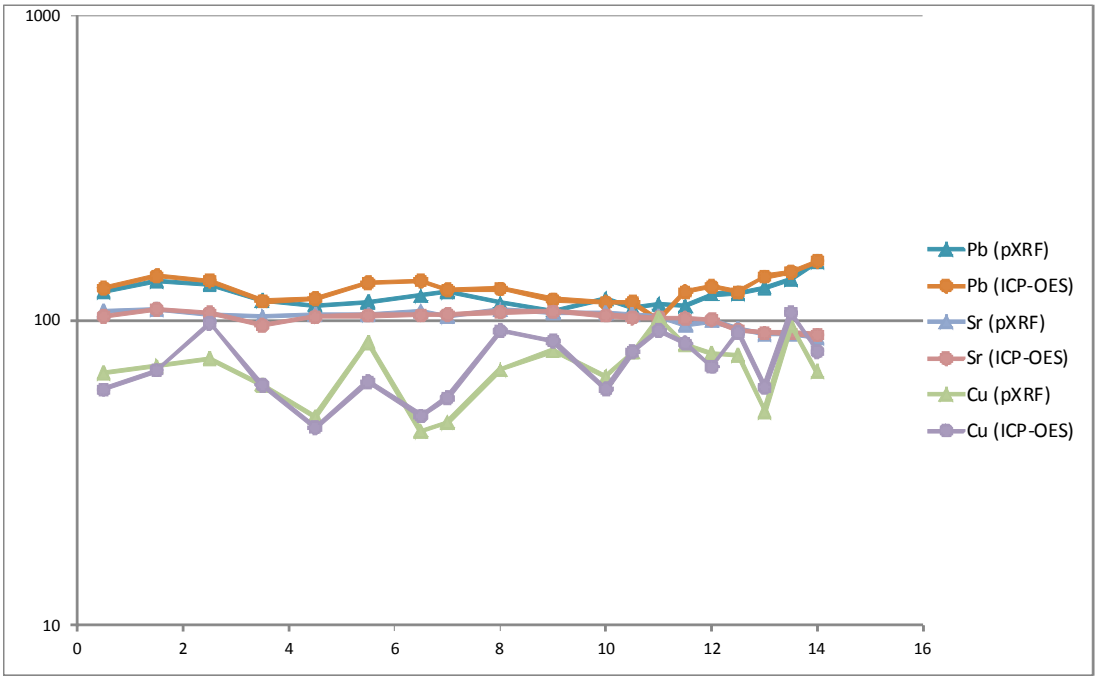

Figure 6-25: Comparative graphics showing the results of the major and trace elements analised by pXRF and ICP-OES.

6.4. General Discussion

The earth resistance survey provided the most informative results revealing a series of sub-circular high resistance anomalies that may be delineating unknown circular structures at the site. These anomalies were not apparent in the magnetic data perhaps because of the weak magnetic contrast against the surrounding host soil as well as the effect of the magnetic disturbance created by the debris at the north end of the survey area. The soil's clay content affected the penetration of the high frequency GPR survey, but the low frequency overcame the attenuation effect.

Some of the high resistance circular anomalies seem to match the circular patch of vegetation visible in the aerial views (Figure 6-2). Therefore, the patch of vegetation appears to have developed *over* the buried remains. Accordingly, the resistance circular anomaly correlates with higher organic content values and a subtle increase in magnetic susceptibility. Both enhancements appear to have been produced by the patches of vegetation that indirectly denoted the targeted anomaly rather than by the buried structure itself.

Mn depletion shows the location of the targeted feature. Accoding to the existing literature (Lovley *et al*. 1991; Magen *et al.* 2011) this chemical anomaly seems to be related to the high organic matter content (vegetation patch) and associated moisture retention. Other enrichments in Pb and Cu may be associated with the organic matter soil fraction and CEC (Wilson *et al.* 2007).

Outside the targeted resistance anomaly, there was a distinctive anomalous Ca concentration. This anomaly may be related to an alkali concentration, (*e.g* lime or mortar) probably related to the activities carried out at the site when the Outer Ward was used as a work-camp for the construction of the stone castle documented during the 14th century. The variation in moisture content related to this element may be associated with low resistance and the strong GPR reflections.

Chapter 7

Surveying on Arable Brown Soils: The Ditched Enclosure of the Prehistoric Ritual Complex at Forteviot (Perthshire)

7.1. Introduction

A group of cropmarks at Forteviot are the only remaining traces of an extensive early prehistoric ceremonial landscape built of earth and timber and one of the most important Pictish royal centres of Scotland. The site is located in Strathearn in southern Perthshire, one of the most agriculturally fertile regions in central Scotland. The cropmarks revealing the prehistoric ritual complex were first identified by aerial photography in the mid-1970s and successive overflights photographed further cropmarks related to an early medieval cemetery in the vicinity.

The Strathearn Environs and Royal Forteviot research project (SERF) began in 2006 as a long-term research project and was the in-house archaeological field school of the University of Glasgow. Its aim was to explore the factors involved in the creation of such an significant centre of ceremony at Forteviot in the third millennium BC and its later reuse as royal centre during the Pictish period (Driscoll *et al.* 2010). Two key objectives of the SERF project were to characterise the cropmarks complex at Forteviot by targeted archaeological excavations and monitor past and present agricultural impacts and land-use patterns on the archaeology of the study area.

7.1.1. Research Problem

Prior to excavations by SERF initial gradiometer and earth resistance surveys were carried out. In general, the results were disappointing by comparison with the aerial photographs in that they yielded little beyond confirming the cropmarks. The gradiometer data, acquired at 1m or 0.5m traverse spacing in zig-zag mode, was characterised by very faint and negative responses indicating

the ditches. The performance of earth resistance survey (1m x 1m sampling interval) was similarly rather poor. Therefore, what are the reasons behind the poor results of the geophysical surveys at Forteviot? And are there other routine prospecting techniques that can provide better results?

The poor geophysical results of an *a priori* fairly suitable survey environment characterised by freely-drained brown earth soils and sedimentary geology, the confident location of the archaeological targets and the prospects for soil sampling and ground-truthing within the SERF project framework all contributed to the decision to integrate the site at Forteviot into this PhD. The case study focuses on the results of the geophysical survey and the geochemical soil analysis over the cropmark of a ditch enclosure at Forteviot. The study aimed to implement integrated geophysical and geochemical methods to assess the detection potential of routine prospecting techniques and to understand the causes of the poor result of the magnetic and earth resistance responses in such a remarkable archaeological site. The investigation also aimed to contribute towards the general archaeological understanding of the ditched enclosure in order to contribute to the aims of the SERF project.

7.1.2. Location

Forteviot is a village located in south-east Perthshire at the eastern end of the fertile Strathearn valley (Figure 7-1). It is situated 11km south-west of Perth and 5km north-east of Dunning. The village stands south of the River Earn, on a levelled terrace to the right bank of the Water of May and it is 18.28m above sea-level.

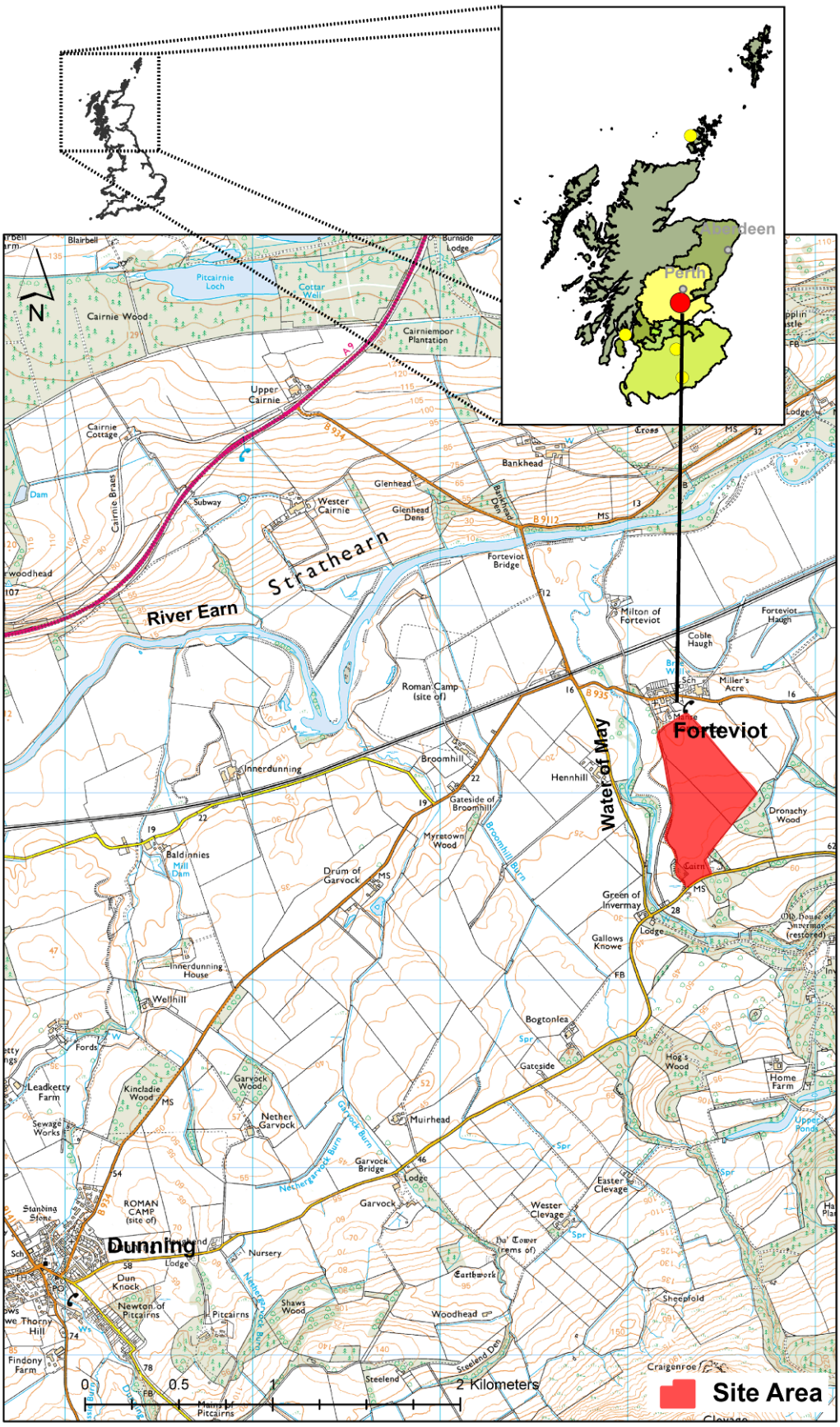

Figure 7-1: Location map (top right) of Forteviot (red dot) in Perth and Kinross district (Central Scotland) and in relation to the other case study sites (yellow dots). In bottom map, the area of the cropmarks complex is in red, immediately to the south of Forteviot village (based on © Crown Copyright/database right 2012. An Ordnance Survey/EDINA supplied).

Forteviot and its environs are characterised by rich agricultural land including pasture, stubble, autumn sown cereal or fodder crops, and ploughed fields (Figure 7-2). The cropmarks site lies in the arable fields immediately south of Forteviot village and occupies an area of approximately 26 hectares (Figure 7-2). The area is generally flat except on its southernmost end where it gently rises as a field terrace.

Figure 7-2: Location of the prehistoric cropmarks (in yellow, top, © Google). The oblique aerial photograph (bottom) shows the cropmark of the targeted monument (yellow arrow) as a single ditch enclosure during an overflight by John Dewar (© RCAHMS).

Beyond the cropmarks site, the terrain drops significantly near the Water of May, a stream which runs along the western edge of the area (Figure 7-1). The stream was canalised to its current course, but in the past it was very active and it carved a steep scarp in the east as it approaches Forteviot and the site (Alcock and Alcock 1992).

There are two areas of cropmark: the northernmost area contains the early medieval cemetery (NGR NO 0537 1739) while the prehistoric ritual complex (NGR NO0524 1701) lies to the south-east. This case study focussed on the investigation of a ditch enclosure located in the NW of the ritual complex (Figure 7-2).

7.1.3. Geology, Soils & Land Cover

7.1.3.1. **General Bedrock & Drift Deposits**

The underlying bedrock in Forteviot is within the Strathmore basin, an elongate trough that extends along the Midland Valley of Scotland and dates from the Lower Devonian (*c*. 410 mya). It corresponds to the Old Red Sandstone formation (Browne *et al.* 2002) and is mainly composed of sandstones, with successions of conglomerates, shales, mudstones and volcanic rocks (Figure 7-3 and Figure 7-4). The lithostratigraphical classification is in the Arbuthnott-Garvock Group (Figure 7-3) and it is 2400-4000m thick (Browne *et al.* 2002). This group is characterised by sandstones, principally from the Scone Sandstone Formation. It can also contain some clast-supported conglomerates, siltstones and calcareous mudstones. Pebbles of metasedimentary and volcanic rock are also present (Browne *et al.* 2002).

The superficial deposits in the area of Forteviot, shown in Figure 7-4, are composed of fluvioglacial sand and gravel deposits associated with large melt-water rivers that drained Highland areas during the last period of retreat of the glacial ice.

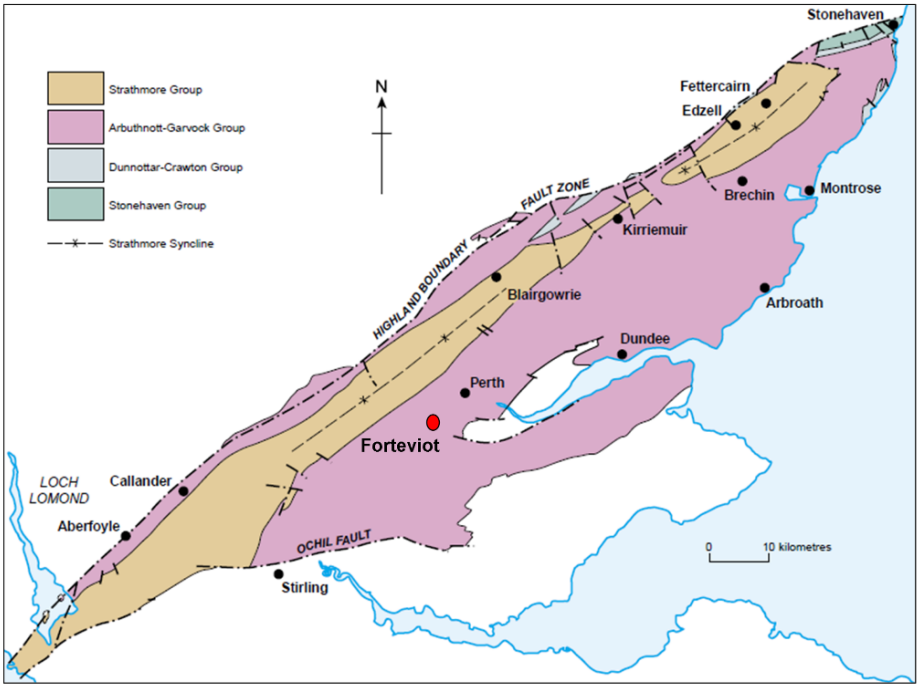

Figure 7-3: Map showing the distribution of the Old Red Sandstone groups (Lower Devonian) in the Middle Valley of Scotland (Browne *et al.* 2002). The figure shows the location of Forteviot within the Arbuthnott-Garvock Group area.

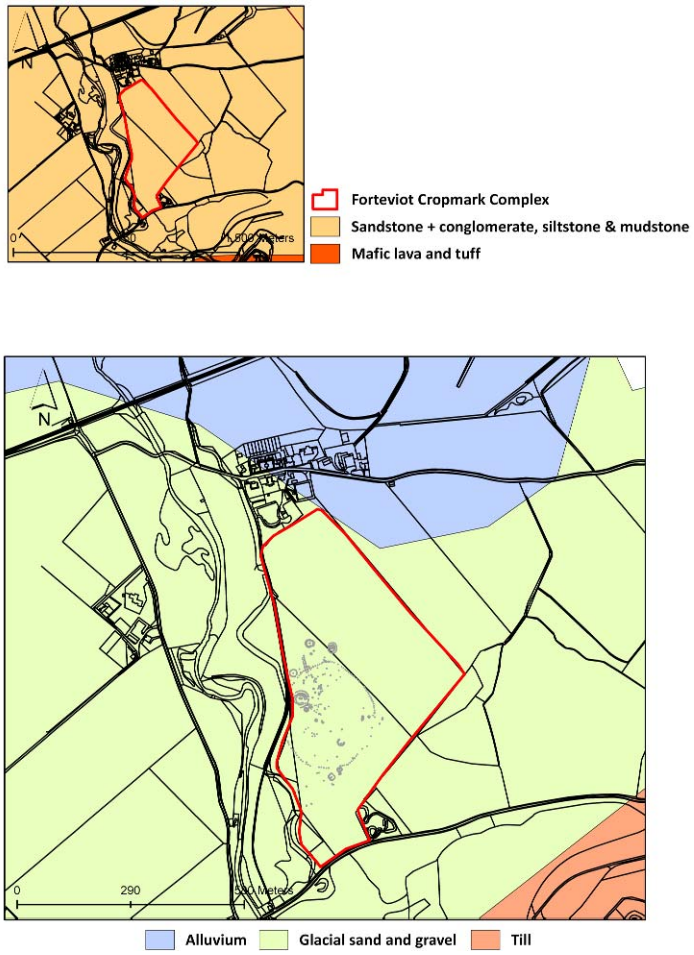

Figure 7-4: The underlying solid geology (top) and superficial deposits (bottom) at Forteviot. The transcription of the cropmarks recorded aerial photographs are shown in grey (bottom) (based on Geological Map Data ©NERC 2012).

7.1.3.2. **Soils**

Following the Scottish Soils classification of the Macaulay Institute, Forteviot soils are in the Gleneagles series. These soils are brown earths which are well drained reddish soils with bright colours and mineral topsoil, which is generally sandy. The general soil profile recorded in the area by SIFSS is shown on Figure 7-5. The first horizon is a ploughed topsoil (Ap) *c.* 0.30m deep. The subsoil (B) is 0.30m and it may contain a sesquioxides horizon (Bs) characterized by Fe and Al enrichment. The C horizon generally appears at 0.65m depth.

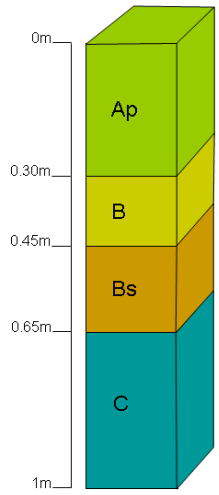

Figure 7-5: Soil horizons and depths of the brown earths (Gleneagles series) at the Forteviot site described by the Soil Indicators for Scottish Soils (SIFSS) database (Macaulay Land Use Research Institute 2011).

7.1.3.3. **Land Cover**

The site area has been intensively cultivated and deep ploughed for a variety of crops in the recent past. The harvested crops are potatoes, wheat, carrots and barley. The field with the prehistoric ritual cropmarks was under barley when the survey commenced.

7.1.4. Archaeological Background

The prehistoric ceremonial complex was discovered by aerial photography (St Joseph 1976). The cropmarks gave evidence of a concentration of hengiform monuments dating from the Neolithic to the Bronze Age (Alcock and Alcock 1992). These included a massive palisaded enclosure containing an earth henge monument with a timber circle. Outside the palisaded enclosure another

enclosure was identified, with a potential barrow and a double ditch enclosure that was the target for this PhD project (Figure 7-2).

The SERF project dedicated two fieldwork seasons (2008-2009) to the investigation of two monuments close to the double ditch enclosure; the palisaded enclosure entrance (Noble and Brophy 2007) and the henge within this enclosure (Noble and Brophy 2008). The excavation of the palisaded enclosure entrance showed a good match between cropmark and archaeological remains as well as the truncation of shallow features by ploughing.

Since their discovery, the cropmarks have been continuously flown over and photographed if visible. The archive of these aerial photographs is kept at the Royal Commission on the Ancient and Historical Monuments of Scotland (RCAHMS). The aerial photographs taken by the RCAHMS in 1977 show a single ditched enclosure while one taken in 1982 shows two concentric ditches. In 2010, the ditch enclosure was targeted for excavation by SERF. The monument had been initially interpreted as a 'hengiform' monument or a possible round-house. The excavation aimed to expose the enclosure complex in plan in order to define its character and extent (James and Gondek 2010). Prior to excavation, the ditched enclosure was targeted with a multi-technique geophysical survey and surface soil sampling for geochemical analysis as part of this PhD research. Further geochemical exploration of the ditched enclosure was carried out by soil sampling during its excavation.

7.2. The Geophysical Survey

7.2.1. Aims & Objectives

The aims of the survey were to detect the outer and inner ditches of the enclosure and other potential features of interest by using gradiometry, earth resistance, GPR and FDEM in order to assess the results obtained from the different techniques. The objectives of the survey were:

- Comparison of different resolutions with the gradiometer survey to assess the effectiveness of standard traverse spacing (i.e. 0.5m) in this type of survey environment.

- Repetition of the geophysical surveys (sequential survey) after removal of topsoil to explore how the topsoil impacts on the results of these techniques.
- Exploration of the effects of increased ground soil moisture content carrying out sequential survey over the baulks left during excavation.

7.2.2. Survey Area & Data Collection

The survey grids were located over the approximate area where the cropmarks of the ditch enclosure were expected using the aerial cropmark transcriptions as a reference. The location of the different survey grids is on Figure 7-6.

Firstly, four grids (20m x 20m) were surveyed with the gradiometer. Then this area was re-defined in light of the results of this survey and a single grid of 25m x 23m was surveyed with earth resistance and FDEM (EM38). Prior to the GPR survey the dried barley of the survey area was flattened with a garden roller to allow better dragging of the antennae. The high and low frequency antennae were tested at the site. Since the high frequency antennae (450MHz) penetrated to the depth of the targeted ditches, this frequency was used for the high-resolution survey and single GPR traverses (GPR 1 & 2 in Figure 7-6) in order to obtain the highest horizontal and vertical resolution. The high-resolution survey focused on an area (23m x 7m) to the N of the ditch enclosure and a total of 39 GPR traverses were collected to create time-slices. After stripping of the topsoil to reveal the cropmarks before the excavation began in August, the gradiometer and EM38 surveys were repeated to assess the effect of the topsoil. The earth resistance survey was not repeated because of potential disturbance of the archaeology by inserting the mobile probes. A series of single GPR transects (lines 3 and 5 in Figure 7-6) were collected immediately after the topsoil stripping in order to explore the effect of the topsoil on the GPR data.

The survey dates and parameters are shown in Table 7-1**.** The surveys were carried out by two experienced operators and a pool of volunteers (students from the University of Glasgow). The general weather conditions during the survey were variable as usual for the Scottish climate but generally dry.

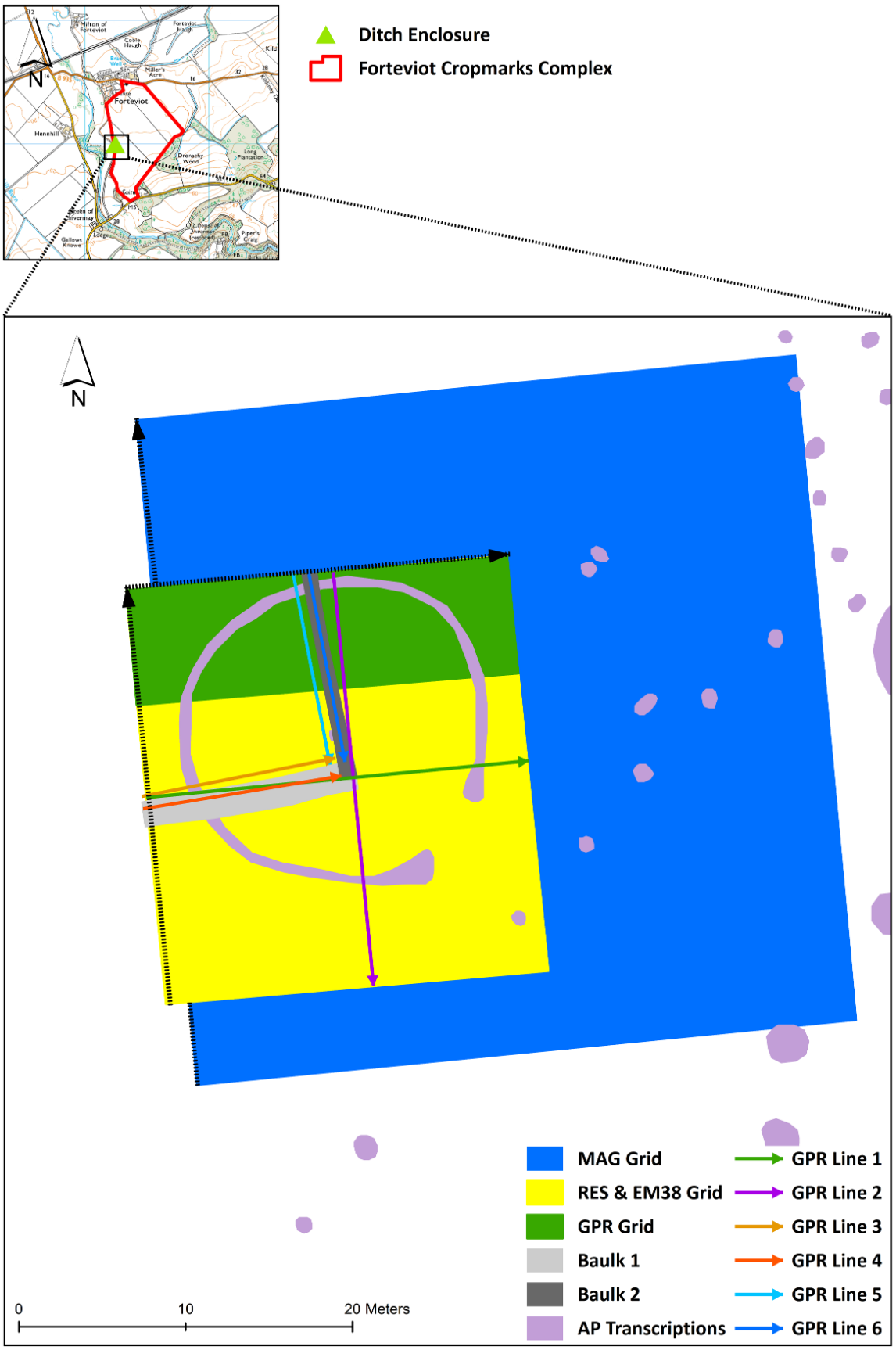

Figure 7-6: Grid location of the multi-technique geophysical survey carried out at Forteviot. The black dashed arrows indicate the origin and direction of the first traverse of the high resolution GPR survey (GPR Grid) and other surveys (gradiometry-MAG, earth resistance-RES and FDEM-EM38).

Technique	Date	Instrument	Traverse Spacing	Sampling Interval	Survey Mode	Other
Gradiometry (a)	30/05/2010	Bartington Grad 601-2 &1	0.5m	0.125m	Parallel (uni-directional) traverses & lower sensor c. 20cm above the surface & 0.03nT/m (resolution).	The survey was carried before the stripping of the topsoil.
Gradiometry (b)	14/06/2010		0.25	0.125		The survey was carried out before the stripping of the topsoil.
Gradiometry (c)	26/07/2010					The survey was carried out after the stripping of the topsoil.
Earth Resistance	22/07/2010	Geoscan RM15 & (MPX15)	0.5m	0.5m	Zig-zag traverses	0.5m and 1m probe spacing / x1 range (sensitivity range).
GPR-450 MHz	25 and 26/06/2010 - 17and 19/07/2010	Sensors & Software PulseEKKO 1000	0.25	0.05m	Parallel (uni-directional) traverses, continuous mode, time window=150ns, stacks=16, samples=200ps, average velocity used during collection= 0.1m/ns.	The survey was carried before the stripping of the topsoil.
Single GPR-450 MHz	27/07/2010					The survey was carried out during a sunny and dry day, over the baulks and over the immediately stripped area.
Single GPR-450 MHz	11/08/2010					The survey was carried out after a day of torrential rain, over the baulks and over the immediately stripped area.
FDEM (a)	22/07/2010	Geonics EM 38	1m	1m	Parallel (uni-directional) traverses, vertical mode & in-phase and quadrature components logged. The instrument was connected to a GPS (RTK).	The survey was carried out before the stripping of the topsoil.
FDEM (b)	26/07/2010					The survey was carried out after the stripping of the topsoil.

Table 7-1: Instrument settings used during the multi-technique geophysical survey at Forteviot.

7.2.3. Gradiometry Results

7.2.3.1. **Gradiometer Survey (a)**

The first gradiometer survey carried out over the ditch enclosure used a 0.5m traverse spacing resolution. The raw and processed data results are plotted in Figure 7-7 and Figure 7-8 respectively. The range of the unclipped raw data was fairly high (100 to -100nT) and affected by a strong response at the NW edge of the corner. The range of background readings in less noisy areas were *c*.-18nT to 21nT.

A standard processing flow (Table 7-2) was applied to correct the effect of the strong response and to remove the banding effects within the grids. After data processing, the general gradient range was -55nT to 31nT. The results are characterised by the strong magnetic response at the NW of the grid and a weaker strong response to the SW of the grid. Other circular negative magnetic responses appeared on the data along with linear and thin negative anomalies with a general NE-SW direction. The results did not shown any coherent anomaly in the area where the ditch enclosure was expected.

Function	**Parameters**
Clip	Min -20, Max 20
Despike	1 (X/Y Radii), 3 (Threshold), Mean (Replacement)
Zero Mean Traverse	All (Grid), On (Less Mean Fit), Not applied (Threshold)
Low Pass Filter	1 (X & Y), Gaussian (Weighting)
Interpolate	X & Y (Direction), Expand, SinX/X

Table 7-2: Data processing (Geoplot 3.0 software) applied to the data acquired during the gradiometer survey (a) at Forteviot.

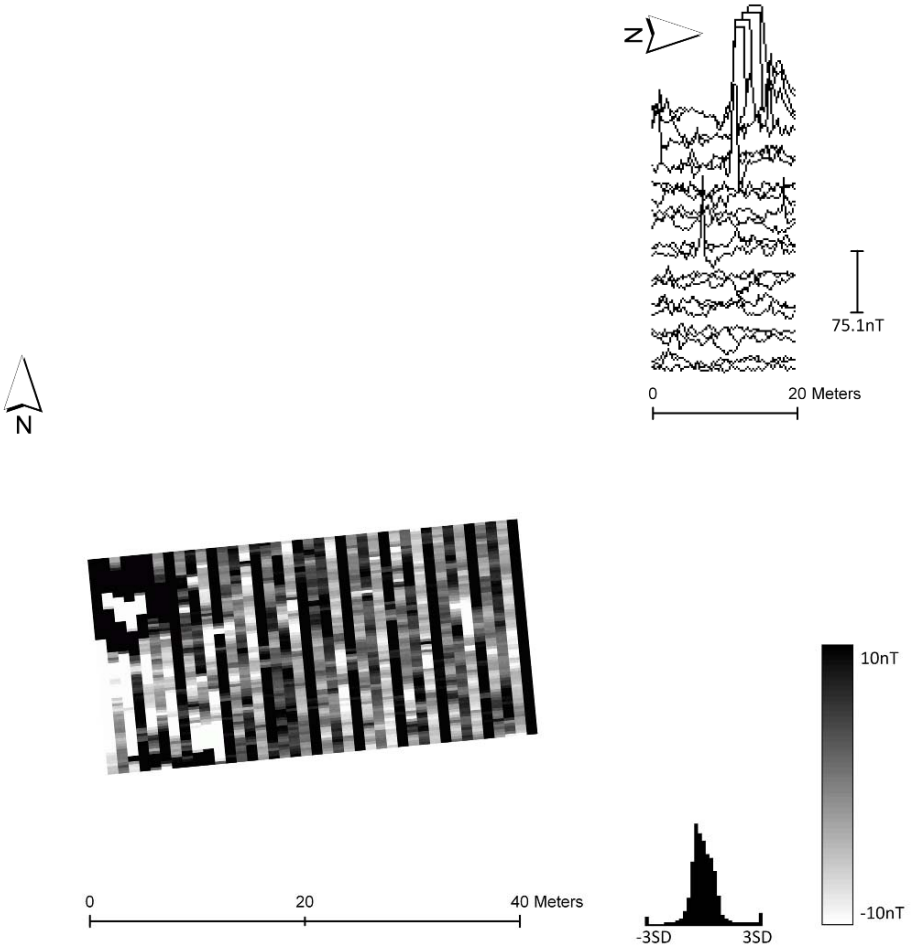

Figure 7-7: Shade (bottom left) and trace plot (top right) of the raw data of the gradiometer survey (a) at Forteviot (before topsoil stripping). The data was plotted at -10/10 Absolute units, contrast 1 and using the Geoplot grey99 palette.

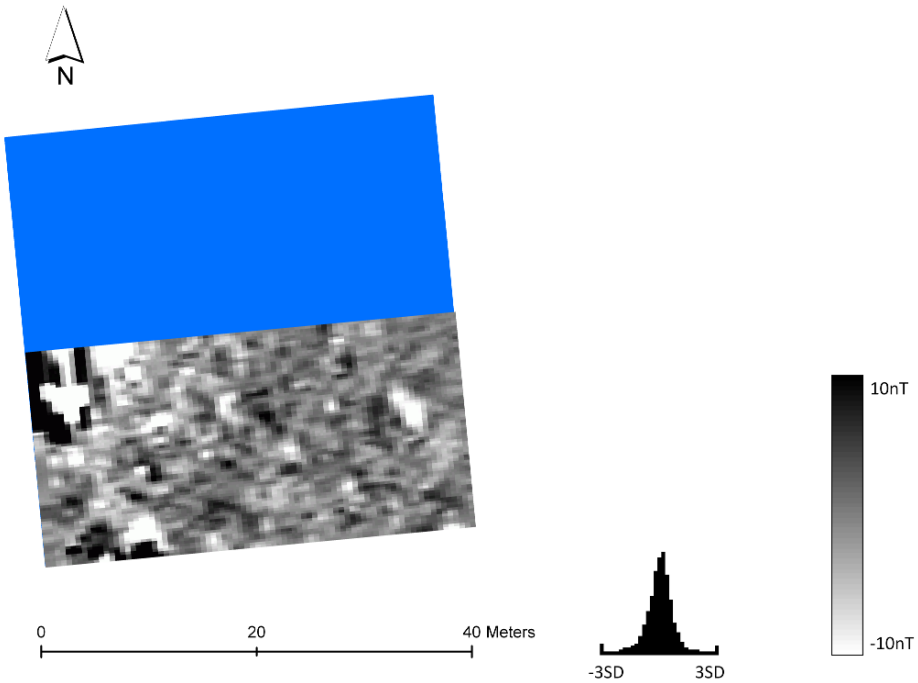

Figure 7-8: Shade plot of the processed data results of the gradiometer survey (a) at Forteviot (before topsoil stripping). The data was plotted at -10/10 Absolute units, contrast 1 and using the Geoplot grey99 palette.

7.2.3.2. **Gradiometer Survey (b)**

The raw and processed data results of this survey are plotted in Figure 7-9 and Figure 7-10 respectively. The high range of the unclipped raw data was also affected by the strong magnetic W edge of the grid. The range of background readings in less noisy areas was *c.*-11 to 29nT.

The closer traverse interval of 0.25m adopted for this survey successfully detected the target enclosure as two circular, weak negative magnetic anomalies. The raw data reveals areas of magnetic enhancement with a NE-SW direction *c.* 4m wide and the other anomalies detected by the previous survey (a). Further discrete dipoles and pit-like positive magnetic anomalies were detected inside and outside the enclosure. The processing flow is detailed in Table 7.3. The effect of the igneous response was solved here by applying a high pass filter on the area affected by this anomaly. The application of this filter preceded the banding correction (using zero mean traverse) which avoided the graphic looking blurred.

Function	Parameters
Clip	Min -20, Max 20
Despike	1 (X/Y Radii), 3 (Threshold), Mean (Replacement)
Destagger	1 (Grid), -2 (Shift), 12-27-34-45-46-47-59-61 (Line)
Zero Mean Traverse	All (Grid), On (Less Mean Fit), Not applied (Threshold)
Low Pass Filter	1 (X & Y), Gaussian (Weighting)
High Pass Filter	11 (X & Y), Uniform (Weighting), Block on (igneous response)
Interpolate	X & Y (Direction), Expand, SinX/X

Table 7-3: Data processing (Geoplot 3.0 software) applied to the data acquired during the gradiometer survey (b) at Forteviot.

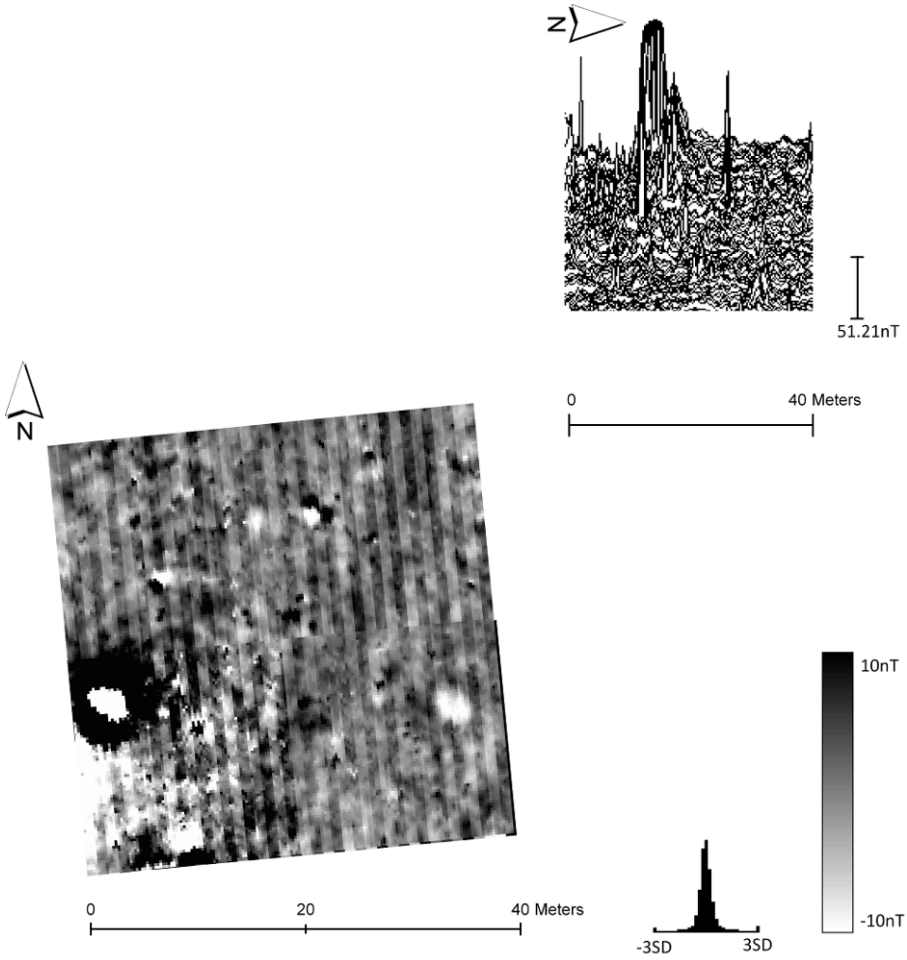

Figure 7-9: Shade (left) and trace plot (right) of the raw data results of the gradiometer survey (b) at Forteviot (before topsoil stripping). The data was plotted at -10/10 Absolute units, contrast 1 and using the Geoplot grey99 palette.

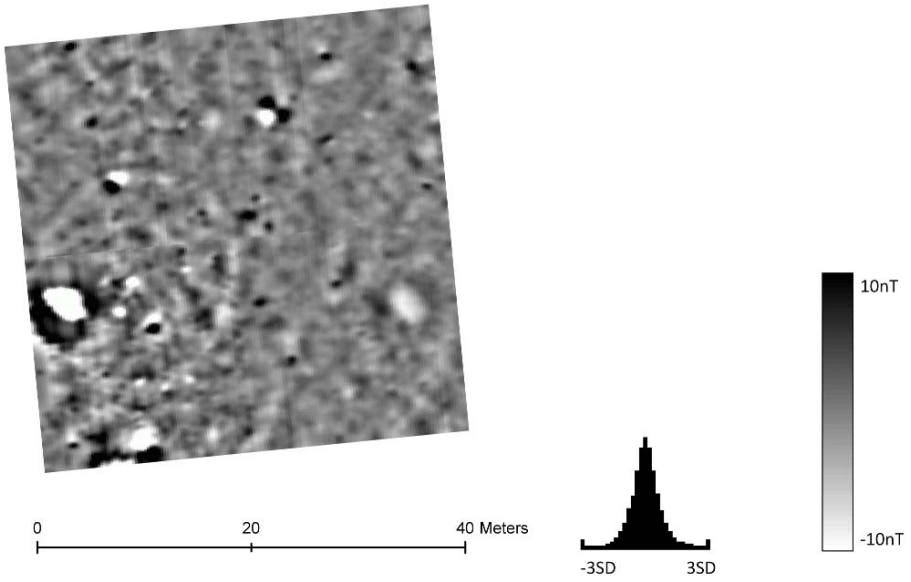

Figure 7-10: Shade plot of the processed data results of the gradiometer survey (b) at Forteviot (before topsoil stripping). The data was plotted at -10/10 Absolute units, contrast 1 and using the Geoplot grey99 palette.

7.2.3.3. **Gradiometer Survey (c)**

Once the topsoil was stripped in preparation for excavation, the gradiometer survey was repeated over the re-defined excavation area (RES and EM38 grid in Figure 7-6). The processing flow is summarised in Table 7-4 and the raw and processed data results of this survey are plotted in Figure 7-11 and Figure 7-12 respectively. The range of background readings in less noisy areas was *c.*-21 to 33nT. Sharper circular negative magnetic anomalies showing the targeted ditches and more defined pit-like positive magnetic anomalies were detected inside the enclosure. A semi-circular positive magnetic anomaly was also detected north of the outer ditch. The proximity to the surface of the buried igneous feature affected strongly the results in the west of the survey area.

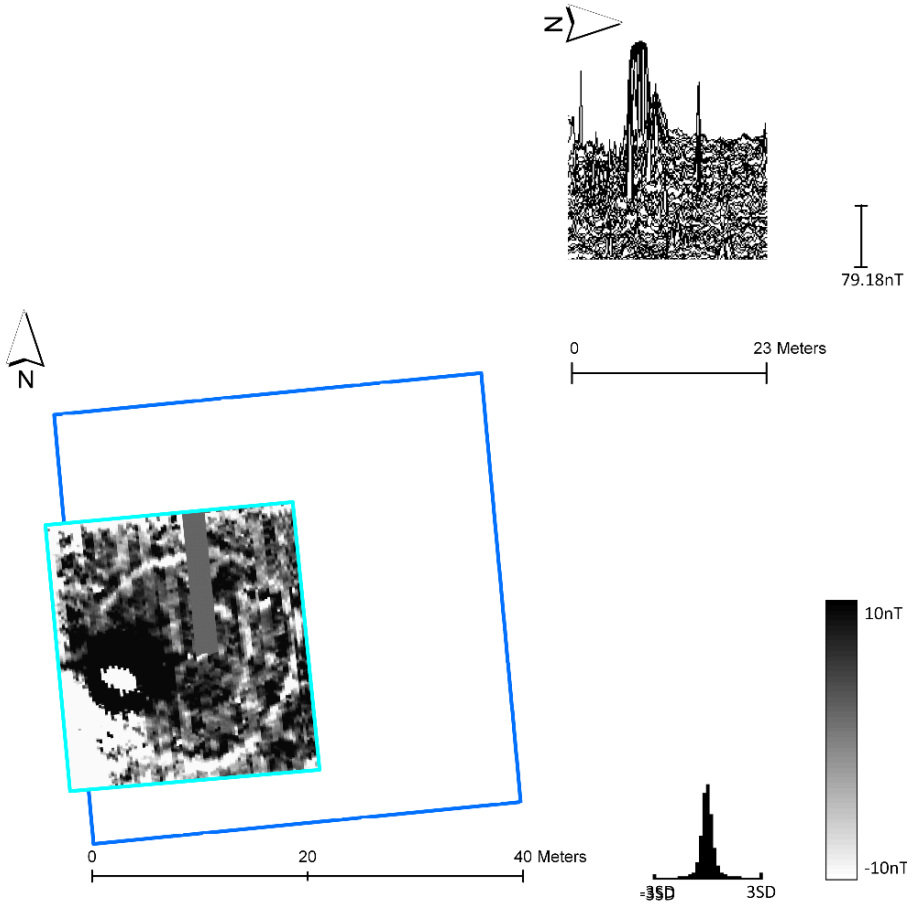

Figure 7-11: Shade (left) and trace plot (right) of the raw data results of the gradiometer survey (c) at Forteviot (after topsoil stripping). The data was plotted at -10/10 Absolute units, contrast 1 and using the Geoplot grey99 palette.

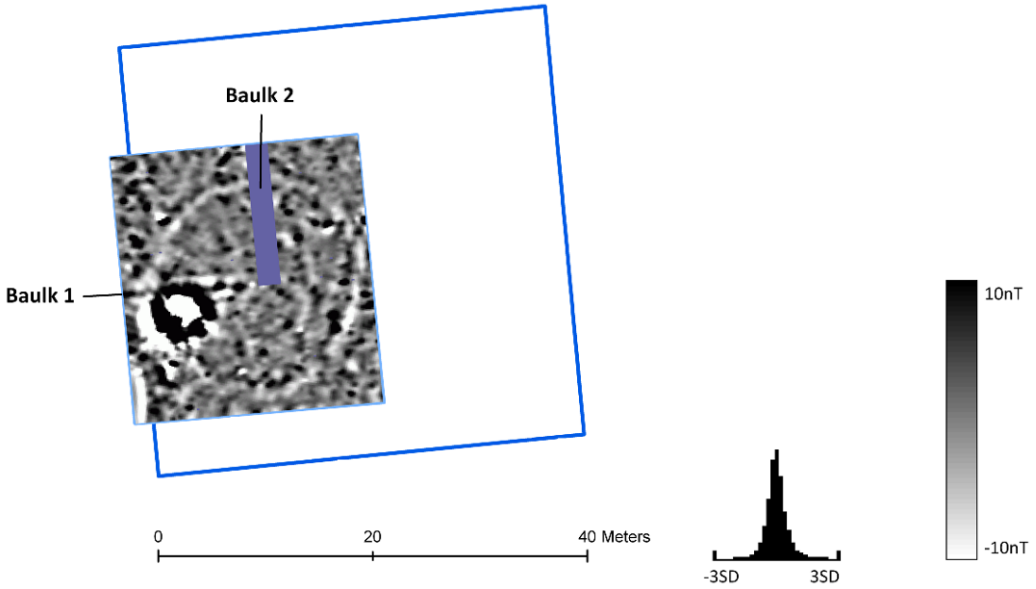

Figure 7-12: Shade plot of the processed data results of the gradiometer survey (c) at Forteviot (after topsoil stripping). The data was plotted at -10/10 Absolute units, contrast 1 and using the Geoplot grey99 palette.

Function	Parameters
Clip	Min -20, Max 20
Despike	1 (X/Y Radii), 3 (Threshold), Mean (Replacement)
Zero Mean Traverse	All (Grid), On (Less Mean Fit), Not applied (Threshold)
Low Pass Filter	1 (X & Y), Gaussian (Weighting)
High Pass Filter	11 (X & Y), Uniform (Weighting), Block on (igneous response)
Interpolate	X & Y (Direction), Expand, SinX/X

Table 7-4: Data processing (Geoplot 3.0 software) applied to the data acquired during the gradiometer survey (c) at Forteviot.

7.2.4. Earth Resistance Results

The raw and processed results are plotted in Figure 7-13 and the processing is summarised in (Table 7-5). The survey was finally accomplished (Table 7-1) after two previous attempts failed because of the high stone content and free-draining character of the soils. The results from both probe separations (0.5m and 1m) were fairly similar, though the 0.5m probe separation data produced better defined results. The survey successfully revealed the targeted feature but this time as a single circular low resistance anomaly with a large central low resistance pit-like anomaly (*c.* 2.5m diameter). A curvilinear area and a trend of high resistance were detected in the NNW of the survey grid. At right angle to the latter anomaly a longitudinal area of high resistance with a W-E projection

was revealed. The survey also detected areas of high and low resistance with a general NW-SE direction.

Function	Parameters
Despike	2 (X/Y Radii), 2 (Threshold), Mean (Replacement)
Interpolate	X & Y (Direction), Expand, SinX/X

Table 7-5: Data processing (Geoplot 3.0 software) applied to the data acquired during the earth resistance survey at Forteviot.

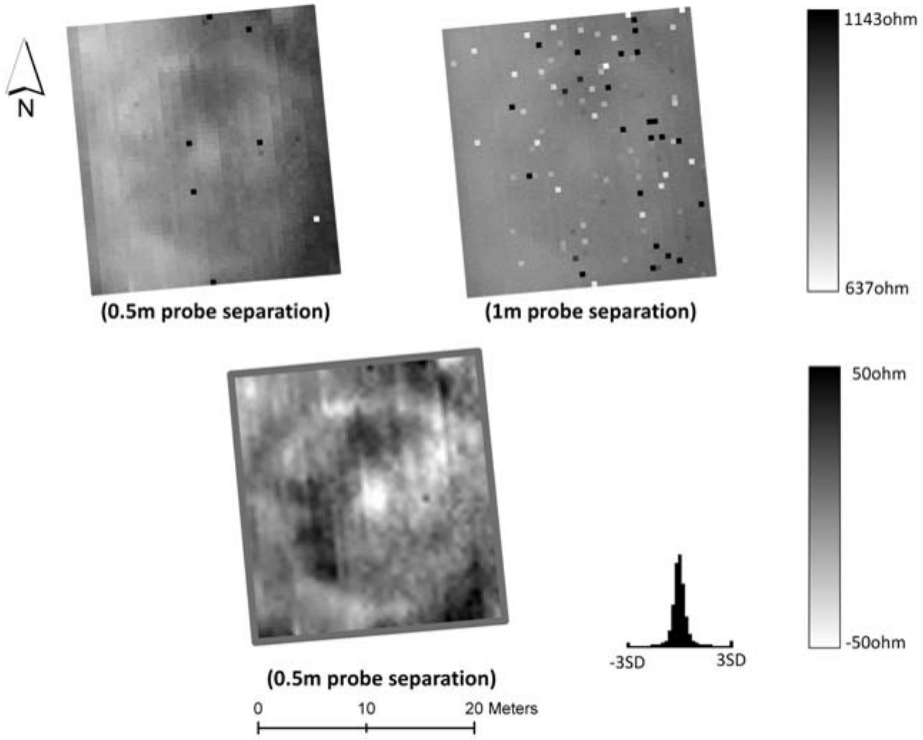

Figure 7-13: Shade plot of the raw (top) and processed (bottom) data results of the earth resistance survey over the ditch enclosure at Forteviot (before topsoil stripping). The data was plotted at -1/1 SD units, contrast 1 and using the Geoplot grey99 palette.

7.2.5. FDEM Results

7.2.5.1. **FDEM Survey (a)**

Figure 7-14 shows the raw results of the EM survey. The data sets were characterised by severe striping in traverse orientation both in the quadrature and in-phase responses. The quadrature component presented a W-E gradient from high to low conductivity that may explain the fairly wide range of readings

(18 to -24mS/m). The in-phase survey recorded a few extra lines to the west of the survey area and showed a narrower range in values (3.8 to 1.3ppt).

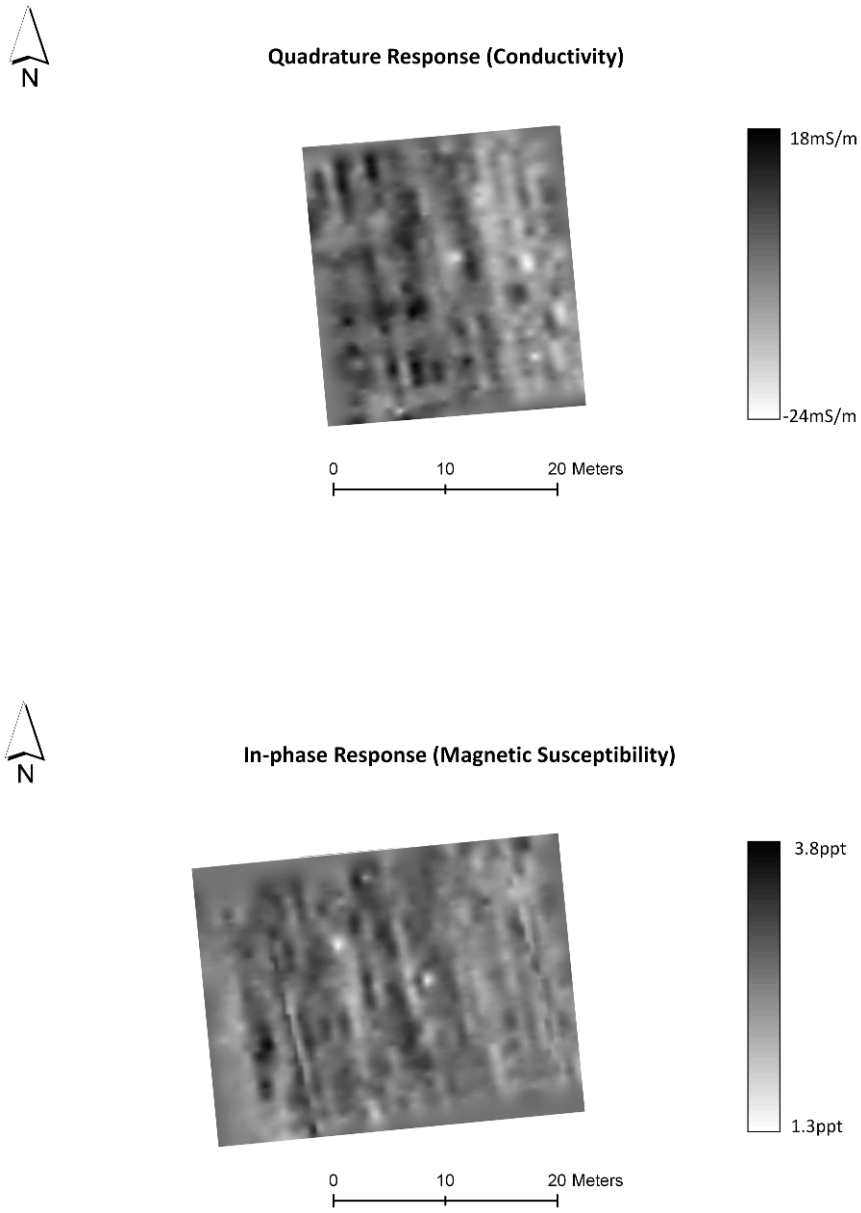

Figure 7-14: Image plot of the raw data results of the FDEM survey (a) over the ditch enclosure at Forteviot (before topsoil stripping). The images show the vertical quadrature (top) and vertical in-phase response (bottom). The data was plotted using Surfer 8 software.

Despite no obvious anomalies in the data relating to the targeted enclosure were identified, a closer look to the results of the quadrature and in-phase components revealed a very weak circular conductivity and MS trend around a central pit-like anomaly of low conductivity and MS. Other curvilinear anomalies unrelated to the targeted feature were also detected.

7.2.5.2. **FDEM Survey (b)**

The raw EM data results are plotted in Figure 7-15. The range of readings of the in-phase component was wider than that of the quadrature data. The EM data showed the two baulks left after the topsoil stripping. The outer ditch of the enclosure was detected as a well-defined lower MS anomaly, slightly weak in the SW. Some segments of the inner ditch were also distinguishable as curvilinear trends of lower MS. A very weak conductivity trend was barely visible in the quadrature component data. However, the two baulks left after the topsoil stripping were fairly distinct in the in-phase data and there was a circular high and low conductive anomaly in the location where the igneous response was detected in the gradiometer data. The anomalies caused by the baulks and the igneous feature were also noticiable in the in-phase data.

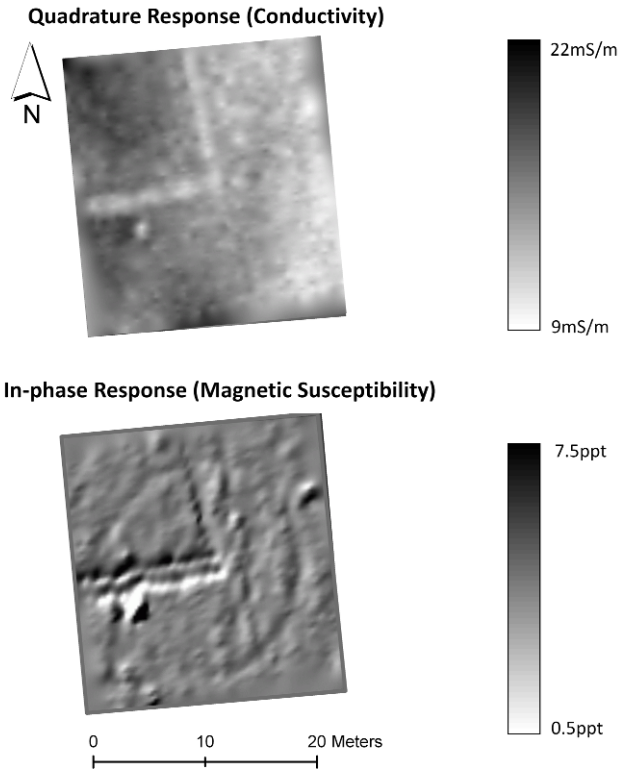

Figure 7-15: Image plot (top) and shade plot (bottom) of the raw data of the FDEM survey (b) over the ditch enclosure at Forteviot (after topsoil stripping). The images show the vertical quadrature (top) and vertical in-phase response (bottom). The data was plotted using Surfer 8 software.

7.2.6. GPR Results

Figure 7-16 shows the results of the processing flow applied to the GPR data and Table 7-6 summarises the processing steps used. The approximate time window for each time-slice is detailed in the figures and the velocity used to estimate their depth was 0.098 m/ns. The signal penetration reached the first 30ns (*c*.1.80m) with the 450MHz survey, deep enough to characterise the targeted ditches.

Function
Subtract-mean (dewow)
Time zero Correction
Background Removal
Manual gain (y)
Time cut
Migration (FD Migration)
Velocity analysis (hyperbolic velocity analysis)
Time-depth conversion

Table 7-6: Data processing (ReflexW v.5.6 software) applied to the GPR data acquired with the 450 MHz shielded antenna at Forteviot.

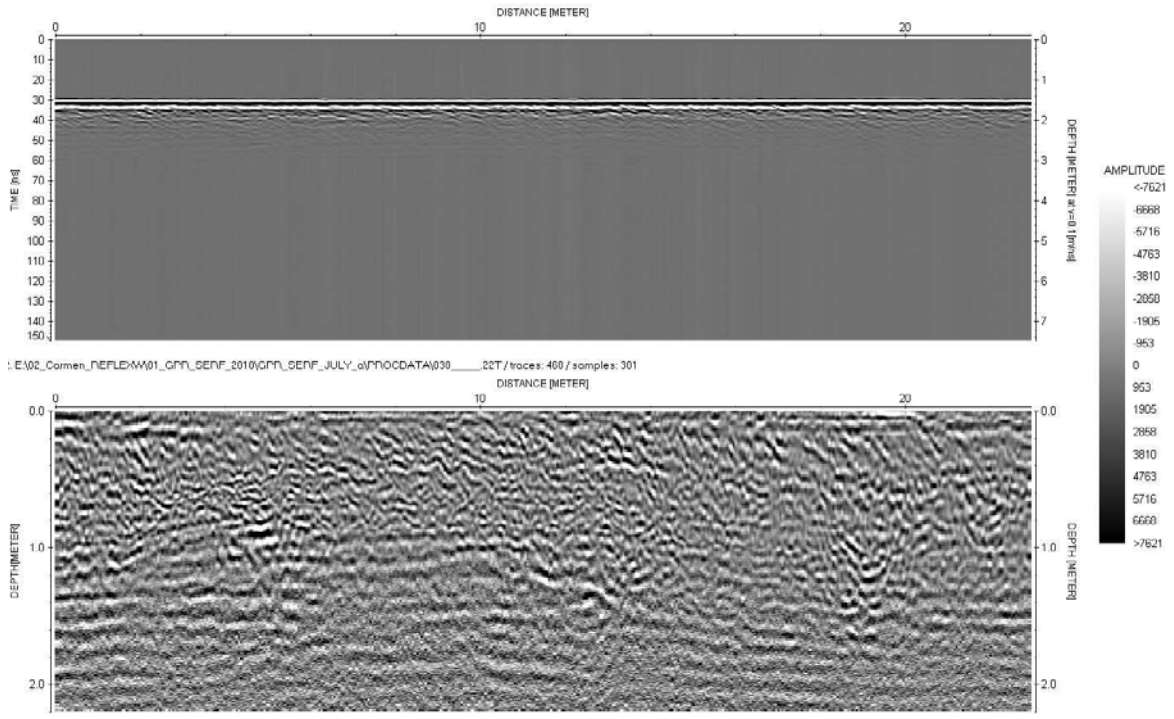

Figure 7-16: Radargram from the 450 MHz high resolution GPR survey (Figure 7-6) over the ditch enclosure at Forteviot (before topsoil stripping) showing the raw (top) and processed (bottom) results of line 30 (y=7m).

Strong reflections were visible in the radargrams where the targeted ditches were expected. These reflections were accentuated in the GPR lines that were collected after topsoil stripping (GPR Line 3 in Figure 7-17). In the lines collected over the baulks after a day of torrential rain (GPR Line 4 in Figure 7-17) reflections from the ditches were detetcted and the signal penetration was not affected despite the higher ground moisture content. GPR Line 6 presented some dipping air-wave reflections produced by the bad coupling of the antenna over the narrow baulks. In despite of these spurious signals, the reflections produced by the ditches were also confirmed.

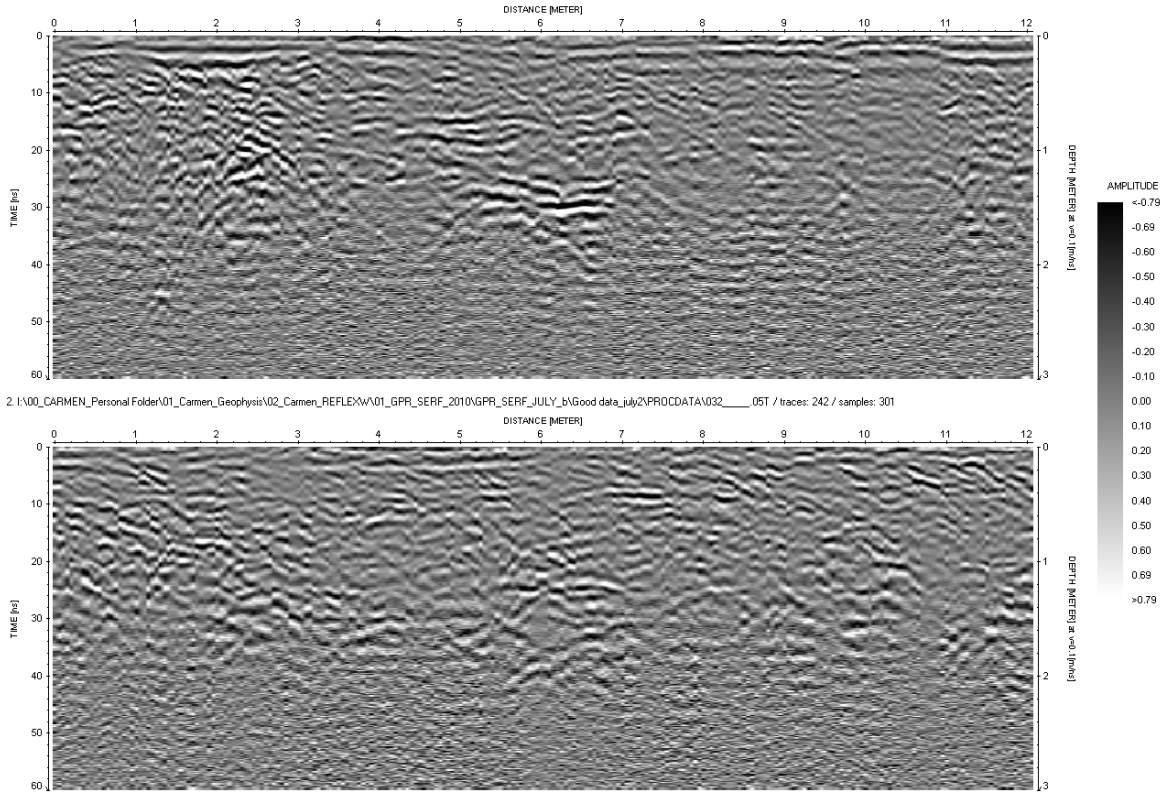

Figure 7-17: Results of GPR Line 3 (top) and GPR Line 4 (bottom) radargrams from the 450MHz frequency survey at Forteviot.

The high resolution survey detected two high amplitude curvilinear anomalies associated to the outer and inner ditches of the enclosure. The time-slices show these anomalies to start at 12ns or *c*.0.40m (1 in Figure 7-18) and be clearly defined at 24ns or *c*.1m (2 in Figure 7-18). The time-slices also showed a semi-circular high amplitude anomaly, connected to the north of the outer ditch. This anomaly seems to correlate with the results of the gradiometer survey in Figures 7-11 and 7-12.

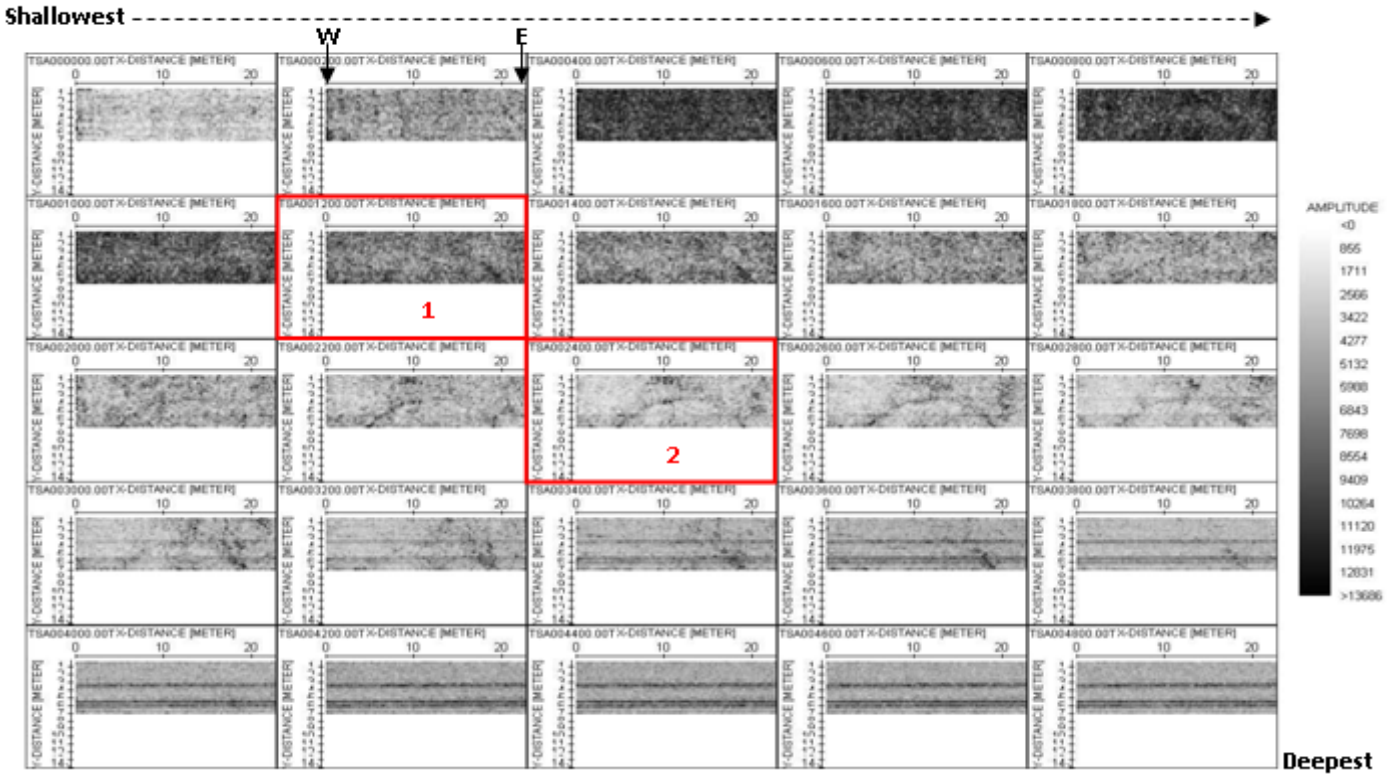

Figure 7-18: Time slices showing the results of the high resolution GPR survey (450 MHz) over the ditch enclosure at Forteviot (before topsoil stripping). The time-slices in red mark the examples described in the main text.

7.2.7. Gradiometry Interpretation

Gradiometer survey (a) (Figure 7-19) did not succeed in identifying the targeted ditch enclosure. Only the strong response of a potential igneous feature was detected at the NW edge of the survey area. The results also revealed agricultural marks detected as negative magnetic anomalies with a general NE-SW direction.

Gradiometer survey (b) revealed the targeted feature as a double ditch enclosure, characterised by a coherent but faded circular negative magnetic anomaly (outer ditch) and segments of a second negative magnetic anomaly (inner ditch) (Figure 7-20). The outer ditch presented two breaks on its southern edge (1 and 2 in Figure 7-20) which may represent two entrances to the monument that were previously recorded by aerial photography. Of special interest was the magnetic dipole located in the middle of the enclosure (3 in Figure 7-20). The readings of this anomaly were around 12nT and its position in the centre of the enclosure suggested an archaeological significance. The anomaly was tested during the excavation in August 2010 and an unusual triple cist burial was found. The strong igneous response was also detected in this survey and found on excavation to be a large glacial erratic of dolerite/gabbro, interpreted as a standing stone related to the enclosure. Other strong dipoles (4 and 5 in Figure 7-20) gave readings of c.80nT-90nT which were interpreted as ferrous surface objects. Some of the pit-like positive magnetic anomalies were excavated and interpreted as a post-hole (6 in Figure 7-20) and a possible corn-drying kiln (7 in Figure 7-20) (James and Gondek 2010).

The magnetically enhanced areas visible in the raw data did not appear in the processed data probably due to the effect of the high pass filter. These enhanced areas may be evidence of historical-period cultivation practices such as rig and furrow (Figure 7-20).

After the topsoil stripping the general background readings of the magnetic data were higher than in the gradiometer survey (b). The outer ditch anomaly appears sharper and with more contrasting readings between the ditches and soil matrix (e.g. in the order of *c*.7nT of difference instead of *c*.2 or 3nT in the previous survey). The results of this survey were similar to the previous one and

no further interpretation was undertaken for this research, although other anomalies of potential archaeological interest were detected inside and outside the targeted enclosure (e.g. the semi-circular positive magnetic anomaly at the north of the outer ditch).

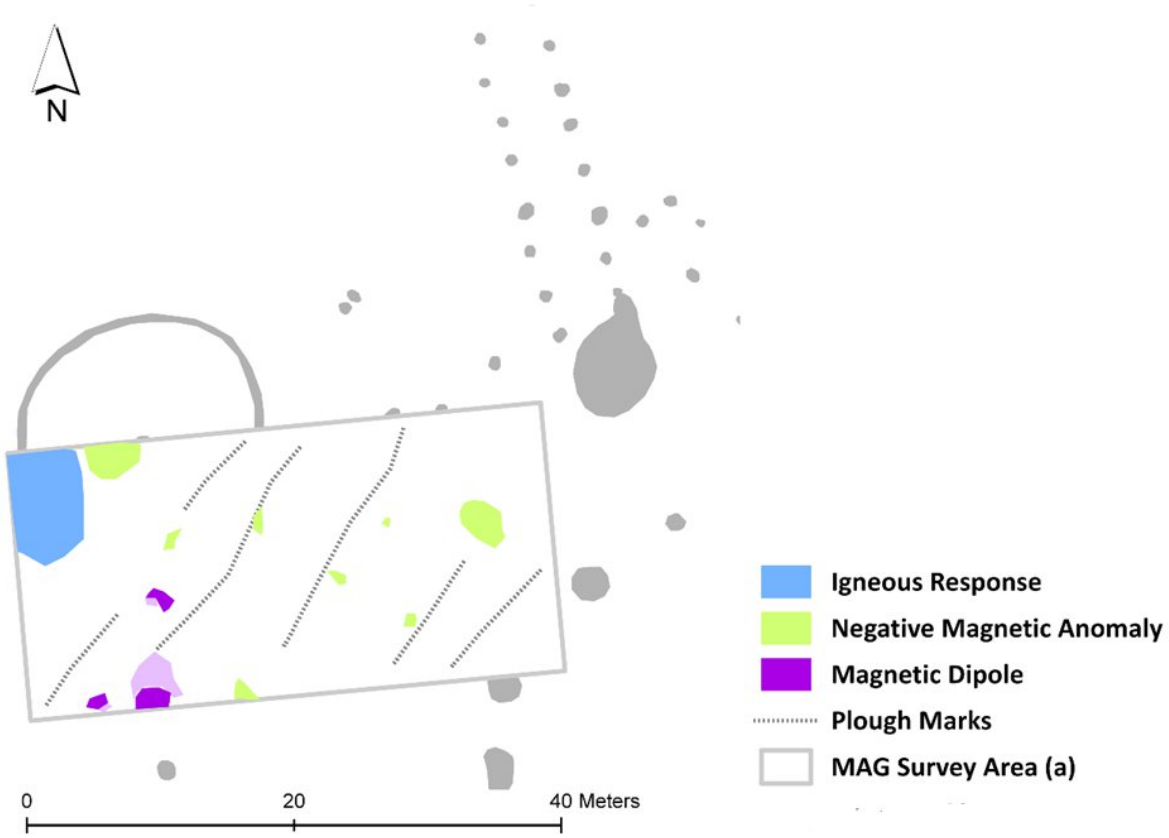

Figure 7-19: Anomaly extraction and interpretation plot of the gradiometer results (a) over the ditch enclosure at Forteviot (before topsoil stripping). The grey colours indicate the aerial photograph transcriptions of the archaeological cropmarks to show the approximate location where potential anomalies relating to the ditch enclosure were expected.

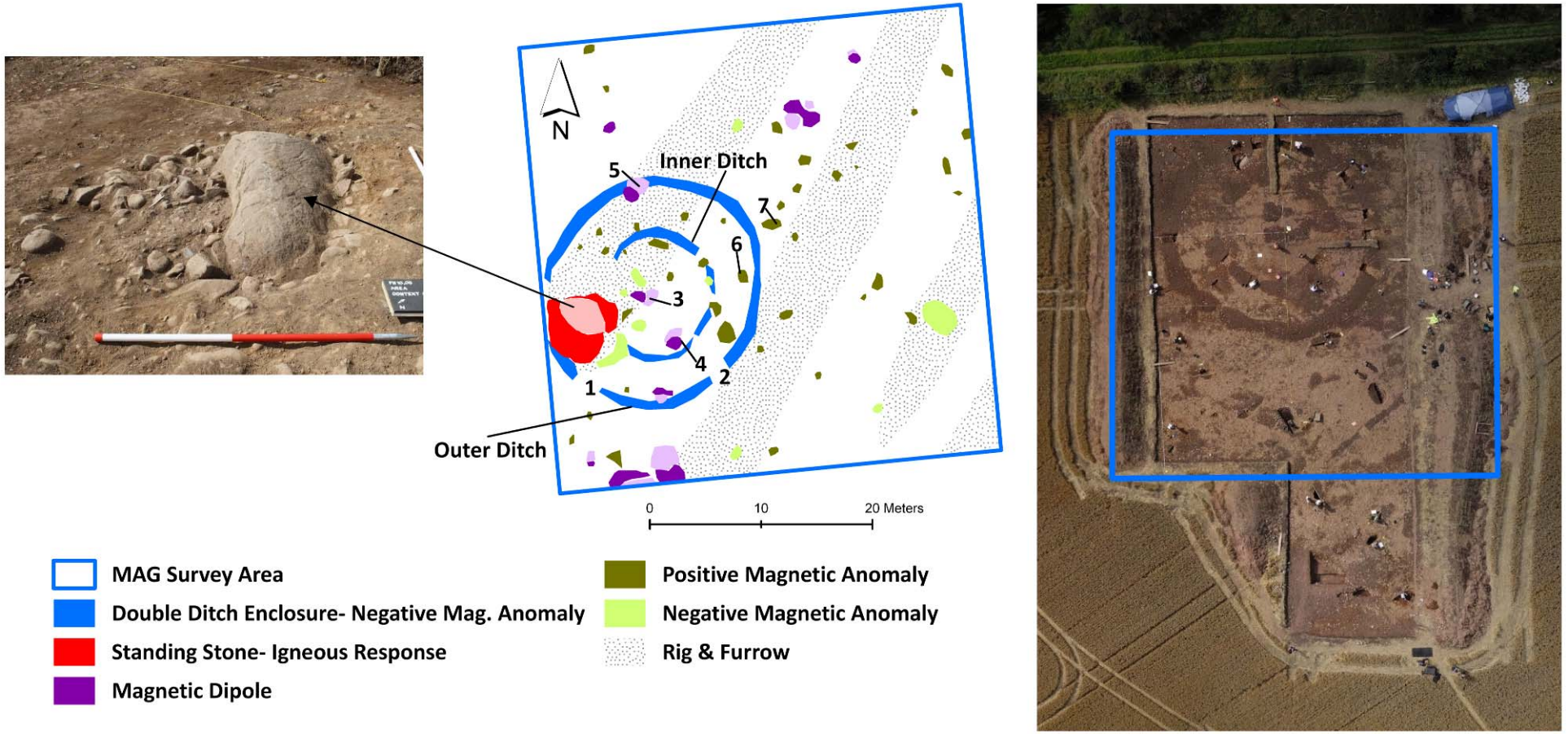

Figure 7-20: Anomaly extraction and interpretation plot (centre) of the gradiometer results (b) over the ditch enclosure at Forteviot (before topsoil stripping). The numbers (1-5) mark the anomalies discussed in the main text. The figure shows the outer and inner ditches (right) and the glacial erratic (standing stone) (left) exposed during the excavation.

7.2.8. Earth Resistance Interpretation

The earth resistance results in Figure 7-21 reveal a single and low resistance ditch anomaly with a central and large pit. This central pit turned out to be the triple cist burial. The detection of the targeted enclosure as a single ditch (instead of two, as with the gradiometer data) coincides with most of the aerial photography evidence (see Figure 7-2). The curvilinear anomaly and trend (2 in Figure 7-21) may indicate the truncated remains of a possible bank associated with the ditch enclosure, and anomaly 3 (Figure 7-21) may be the access area to the monument. The adjacent standing stone detected with the gradiometer survey may be associated with this entrance. The areas of low and high resistance seem to follow the same orientation as the rig and furrow evidence detected with the gradiometer survey.

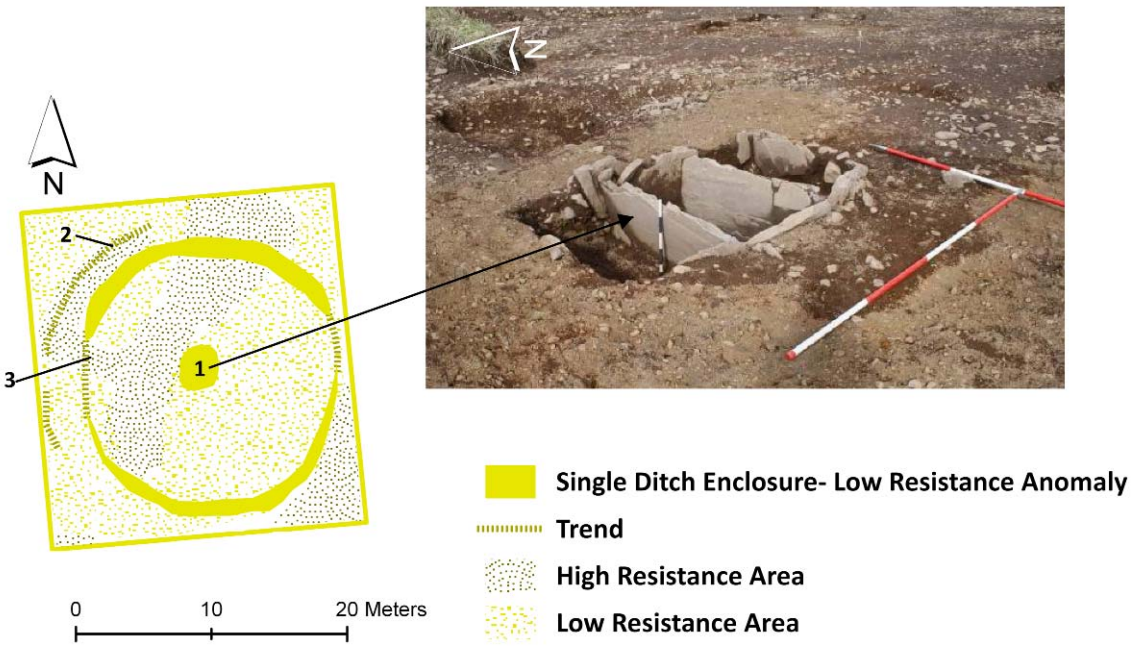

Figure 7-21: Anomaly extraction and interpretation plot of the earth resistance results (left) over the ditch enclosure at Forteviot (before topsoil stripping). The numbers (1-3) mark the anomalies discussed in the main text. The figure shows the triple cist burial (anomaly 1) found duing the excavation (right).

7.2.9. FDEM Interpretation

The EM survey before topsoil stripping (Figure 7-22) detected subtle conductivity and MS trends that correlate with the outer ditch of the enclosure. The pit-like anomaly, corresponding to the area where the triple cist burial occurs, was recorded as a lower conductivity and MS response. The lower values in conductivity may be caused by the higher resistance produced by the stone content of the cist burial. Since the base of the triple cist burial was reached at *c*.1m depth, the lower values of the in-phase data may be related to the negative response of positive magnetic anomalies that the instrument can give in vertical mode at depths greater than 0.6m (see section3.4.2).

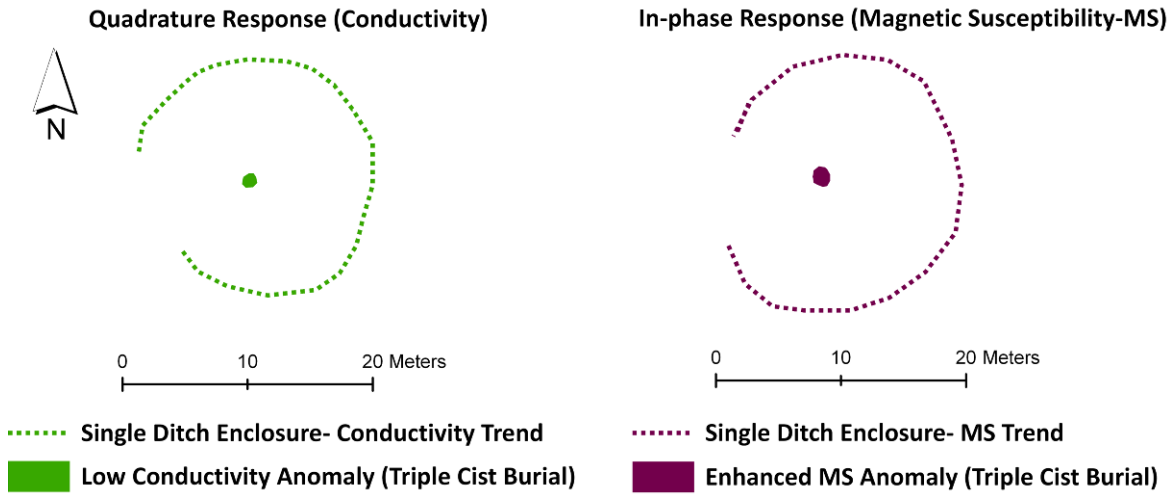

Figure 7-22: Anomaly extraction and interpretation plot of the FDEM (a) results over the ditch enclosure at Forteviot (before topsoil stripping).

After stripping the topsoil, the in-phase component of the EM survey over the ditch enclosure easily detected the outer ditch and weak segments of the inner ditch (Figure 7-23). The quadrature component failed to confirm the targeted ditches as the barely perceptible conductivity trend would have not been capable of identification without the baulk references. However, the quadrature detected the igneous standing stone (anomaly 1 in Figure 7-23), which is slightly surprising since FDEM are usually more successful in resolving conductive anomalies rather than impervious ones. Since the standing stone was of igneous origin, and taking into account that FDEM instruments can be affected by the presence of metal objects, the detection of this resistive feature may be related to its highly magnetic nature.

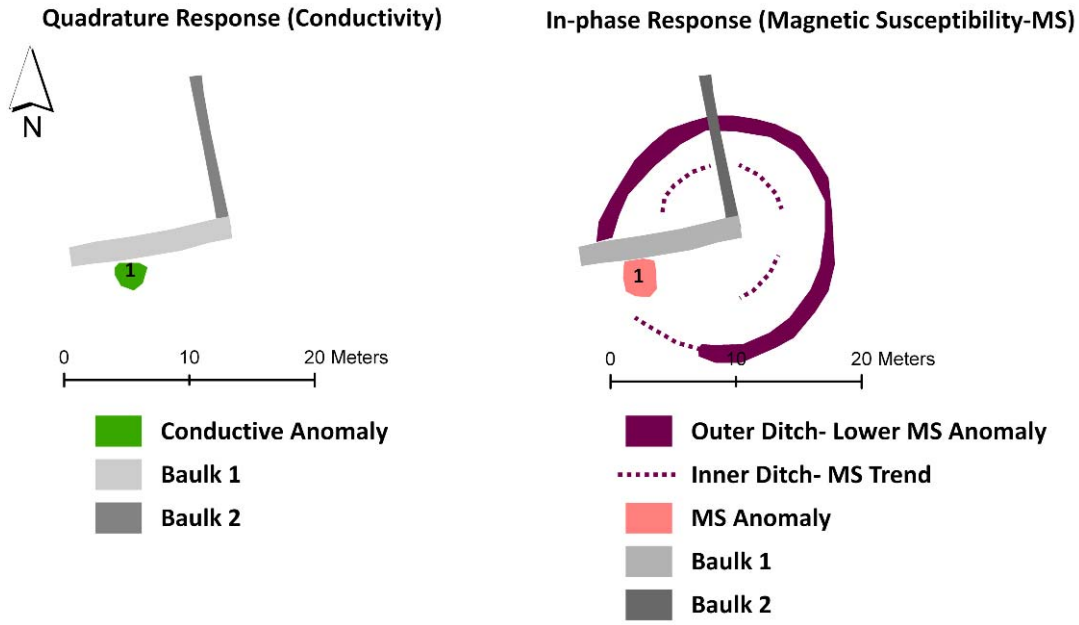

Figure 7-23: Anomaly extraction and interpretation plot of the FDEM (b) results over the ditch enclosure at Forteviot (after topsoil stripping).

7.2.10. GPR Interpretation

The high resolution GPR surveys succeeded in detecting the outer and inner ditches of the targeted feature as two curvilinear high amplitude anomalies. Other reflections of potential archaeological interest were revealed in the time-slices such as a semi-circular anomaly at the north of the outer ditch (1 in Figure 7-24), which confirmed the positive magnetic anomaly detected after topsoil stripping (Figures 7-11 and 7-12).

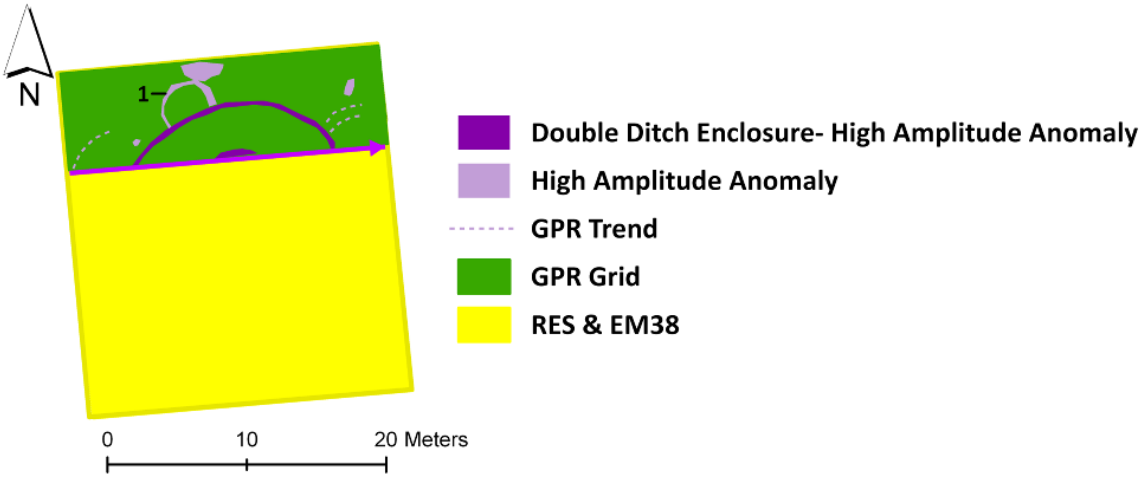

Figure 7-24: Anomaly extraction and interpretation of the high resolution GPR survey over the ditch enclosure at Forteviot (before topsoil stripping). The time slice used for the extractions was 24-26 ns (twt) (*c.*1m depth). The purple arrow shows the location of the last GPR line collected during the high resolution survey at 7m.

This anomaly could be associated with a deeper feature either of geological or of archaeological significance. The latter interpretation would point to a feature pre-dating the enclosure. Since this anomaly was slightly deeper, not visible after the topsoil stripping and slightly outside the main excavation area, it was not ground-truthed.

Whilst the time-slicing produced very distinctive anomalies, the radargrams were slightly more difficult to interpret although it helped that fiducial marks were introduced during the survey marking the location of the outer and inner ditch (Figure 7-25).

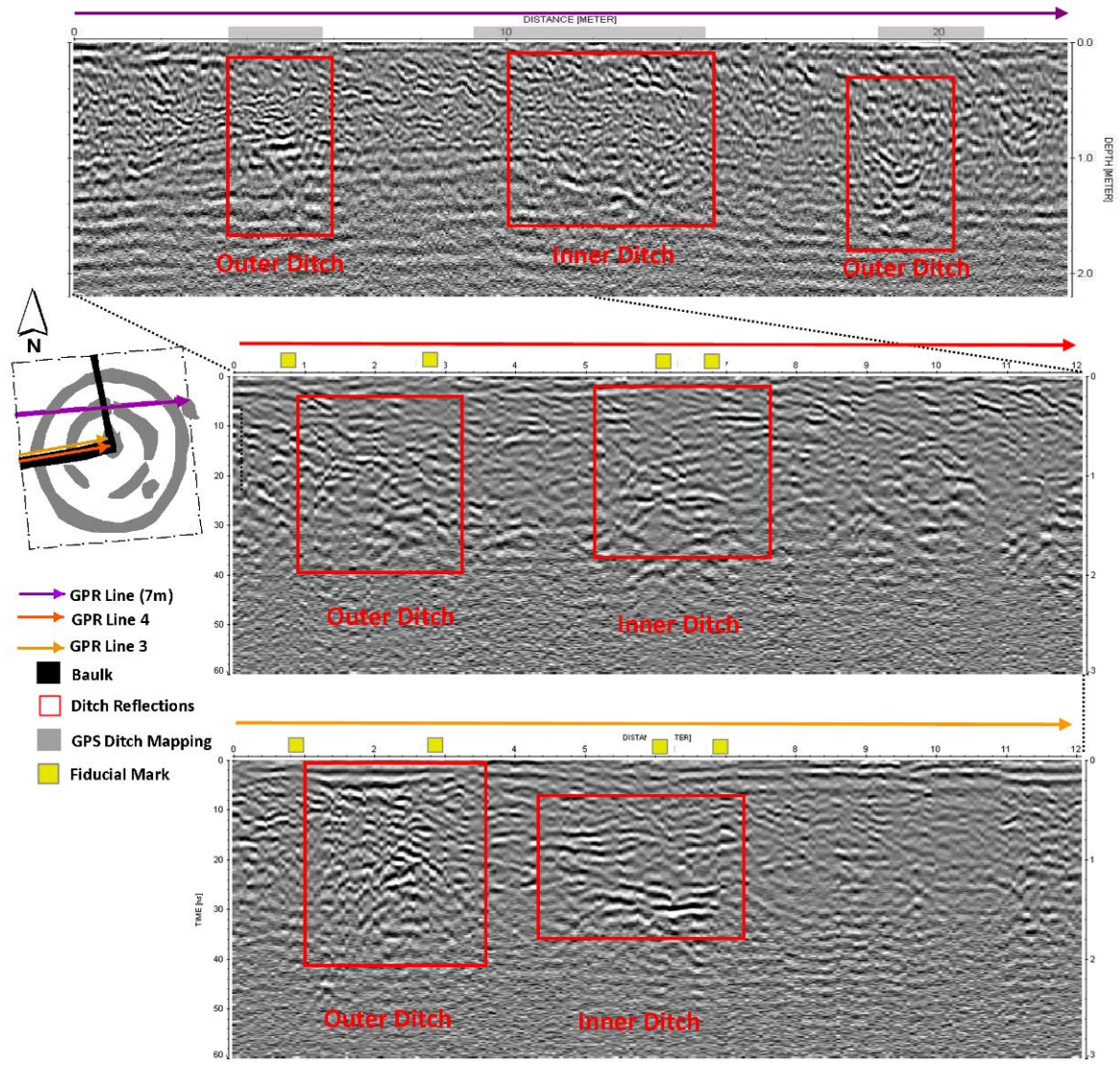

Figure 7-25: Radargrams showing the interpretation of the GPR single line 7m (see Figure 7-25), and single lines 4 and 3 (450 MHz frequency survey) over the ditch enclosure at Forteviot. The fiducial marks were introduced in the GPR data during the survey and show the location of the outer and inner ditch. The grey bar in GPR Line 7m shows the locations of the exposed ditches mapped with the differential GPS after topsoil stripping.

The outer ditch was visible in the time-slices as high amplitude reflections and as strong hyperbolic and linear reflections in the radargrams. The inner ditch was fairly distinctive in the radargrams collected at the north of the survey area (GPR single line 7m, top in Figure 7-25). The data recorded at the west also showed strong reflections for the inner ditch. Taking into account that the depths shown in the radargrams are an approximation, these reflections were detected deeper (GPR Line 3 in Figure 7-23) than the base of the excavated sections of the inner ditch at this area (*c*.0.55m deep at the west) which may indicate an earlier phase of the inner ditch or areas where the ditch was re-excavated.

7.2.11. Conclusions

Figure 7-26 gives a composite interpretation of all the techniques used over the ditched enclosure before topsoil stripping. The outer and inner ditch were detected by the GPR survey, providing the most defined results at the site as well as an approximation to the depth of the ditches. This technique revealed two concentric high amplitude anomalies both visible in the radargrams and time-slices. Some radargrams showed reflections relating to the inner ditch to a greater depth than those recorded during its excavation. This suggests earlier phases or re-excavation of the inner ditch in some areas, hence explaining its segmented character. The gradiometer survey detected the targeted enclosure only when the survey resolution was reduced to a 0.25m traverse interval. This made the survey fairly slow in comparison with the area coverage that can be achieved with the standard traverse resolution (0.5m) which failed to detect the enclosure at this site. This technique revealed the feature as two concentric negative magnetic anomalies: an outer and a segmented inner ditch (Figure 7-26). It also detected a magnetic dipole in the area where a triple cist burial was found and other positive magnetic pit-like anomalies associated with a post-hole feature and a possible corn-dryining kiln revealed during the archaeological excavation (Figure 7-26).

The earth resistance survey, although the slowest, revealed a different type of anomaly: a single concentric low resistance anomaly (the outer ditch) and central pit-like low resistance anomaly (the triple cist burial area). These features were the widest and deepest features of the enclosure; its inner ditch

was not detected. The higher moisture content retained in the outer and triple cist burial may be related to their relatively higher capacity to retain moisture in comparison with the surrounding soil. Since the inner ditch was fairly segmented and less consistent in depth, this may have affected its capacity to retain moisture and so to be detected.

The quadrature response of the EM38 survey produced a similar anomaly as the earth resistance technique: a subtle single concentric conductivity trend (the outer ditch). The higher ground moisture content after the heavy rain before the survey could have increased the contrast between the outer ditch and surrounding soil in the same manner as in the earth resistance survey. Therefore, earth resistance and conductivity surveys in environments such as at Forteviot may give better results when the moisture contrast has ben enhanced. The in-phase response was also very weak and the trend again showed a single circular anomaly. Although the responses of both components were fairly weak, the vertical mode of the EM38 demonstrated potential in identifying archaeological features at an expected depth of *c.* 0.5-1m, as the noise created by the plough layer was out of the instrument's maximum sensitivity range (section 2.4.3.3). The EM38 instrument attached to the differential GPS provided the quickest area coverage. A closer traverse spacing (0.5m instead of 1m) could have improved the definition of the weak trends. Therefore, this technique, used in vertical mode, shows potential at a site such as Forteviot in identifying features. It is also a rapid technique, which may be very convenient to use as a first approach in more extensive surveys.

After the topsoil stripping, the gradiometer survey revealed the same anomaly: a double ditch enclosure characterised by low magnetic readings. In this case the ditches were sharper due to the higher contrast between the anomalies and the surrounding soil, slightly masked before by the effect of the topsoil. This survey revealed better defined pit-like anomalies of archaeological interest than the previous gradiometer survey and also detected the semi-circular anomaly shown in the GPR time-slices. By carrying out gradiometer surveys after topsoil stripping and before excavation, further and deeper features not exposed on the surface can be detected, increasing the effectiveness and enhancing the findings of archaeological excavations.

The quadrature component failed to detect the enclosure after topsoil stripping. The instrument's lower sensitivity to near-surface features in vertical mode and the generally drier conditions during this survey (less contrast between the ditches and surrounding soil) may explain its unsuccessful outcome. However, the quadrature response revealed the standing stone buried at the west of the survey area owing to its high resistance and strong magnetic character. The double ditch enclosure appeared fairly well in the in-phase response in spite of using the vertical mode. The ditches presented positive but lower magnetic susceptibility values. Overall the in-phase response demonstrated potential in detecting near-surface anomalies in vertical mode.

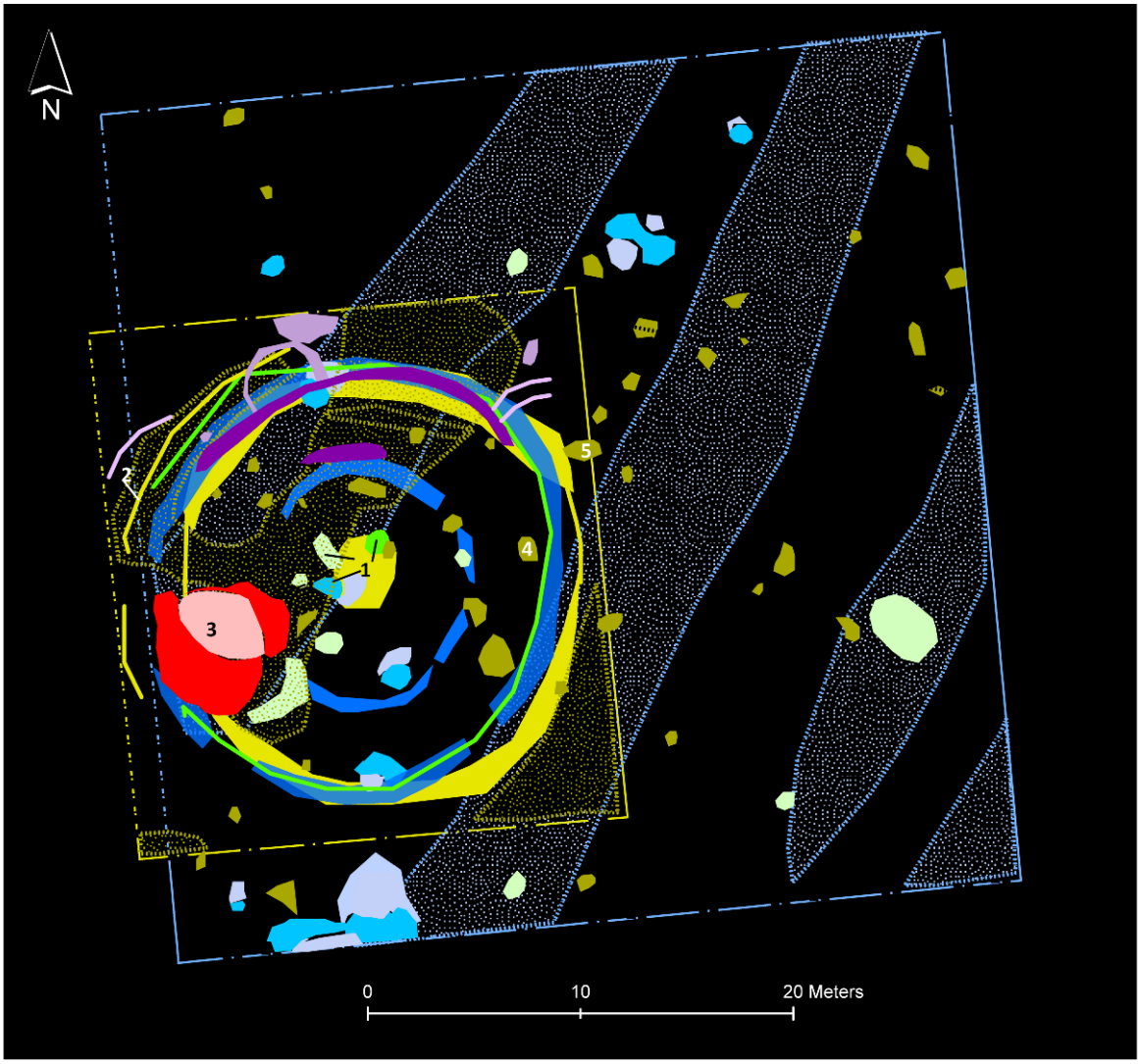

Targeted Feature

- Double Ditch Enclosure- Negative Mag. Anomaly
- Double Ditch Enclosure- High Amplitude Anomaly
- Single Ditch Enclosure- Low Resistance Anomaly
- Single Ditch Enclosure- Enhanced Conductivity Trend

Other Features

- Triple Cist Burial- Low Conductivity Anomaly (1)
- Possible Truncated Bank- RES Trend (2)
- Standing Stone- Very Strong Mag. Dipole (3)
- Posthole- Positive Mag. Anomaly (4)
- Possible Corn-drying Kiln - Positive Mag. Anomaly (5)
- Rig & Furrow- Magnetically Enhanced Area
- Rig & Furrow- Hig Resistance Area

- MAG Grid
- RES & EM38 Grid

Figure 7-26: Integrated anomaly extraction and interpretation from all the geophysical techniques used over the ditch enclosure at Forteviot.

7.3. Soil Analysis

7.3.1. Aims

The main aim of the soil analysis was to characterise the physical and chemical composition of surface soil samples taken across the ditched enclosure and from exposed sections to assess the effectiveness of the pXRF, ICP-OES, MS and phosphate analysis in detecting the enclosure. A secondary aim was to characterise the soil surface and vertical (in open sections) response of the ditches in terms of the total photon counts in the blue (BLSL) wavelengths using a portable OSL reader (pOSL) (section 3.5.2) to test if this technique can detect and characterise the targeted ditches.

The objectives of the soil analysis at Forteviot included: the identification of enhancements or depletions of chemical elements (including MS and total photon counts) associated with the outer and inner ditches; and experimentation with sequential sampling strategies (before and after topsoil striping) to assess the effect of the topsoil on the results.

7.3.2. Sampling Strategy

The samples were taken at 0.10m-0.15m from the surface and 0.5m intervals along two perpendicular lines across the targeted ditch enclosure (Figure 7-27). Once the topsoil had been stripped (by a JCB excavator) (Figure 7-28) the lines were immediately re-sampled. Further details about the length, resolution and specific numbers of samples collected are summarised in Table 7-7.Three control samples were collected outside the survey area (Figure 7-28).

During the excavation of the monument, 20 samples were collected from four sections (Figure 7-27), using a RTK GPS Leica 1200 system to accurately map their location.

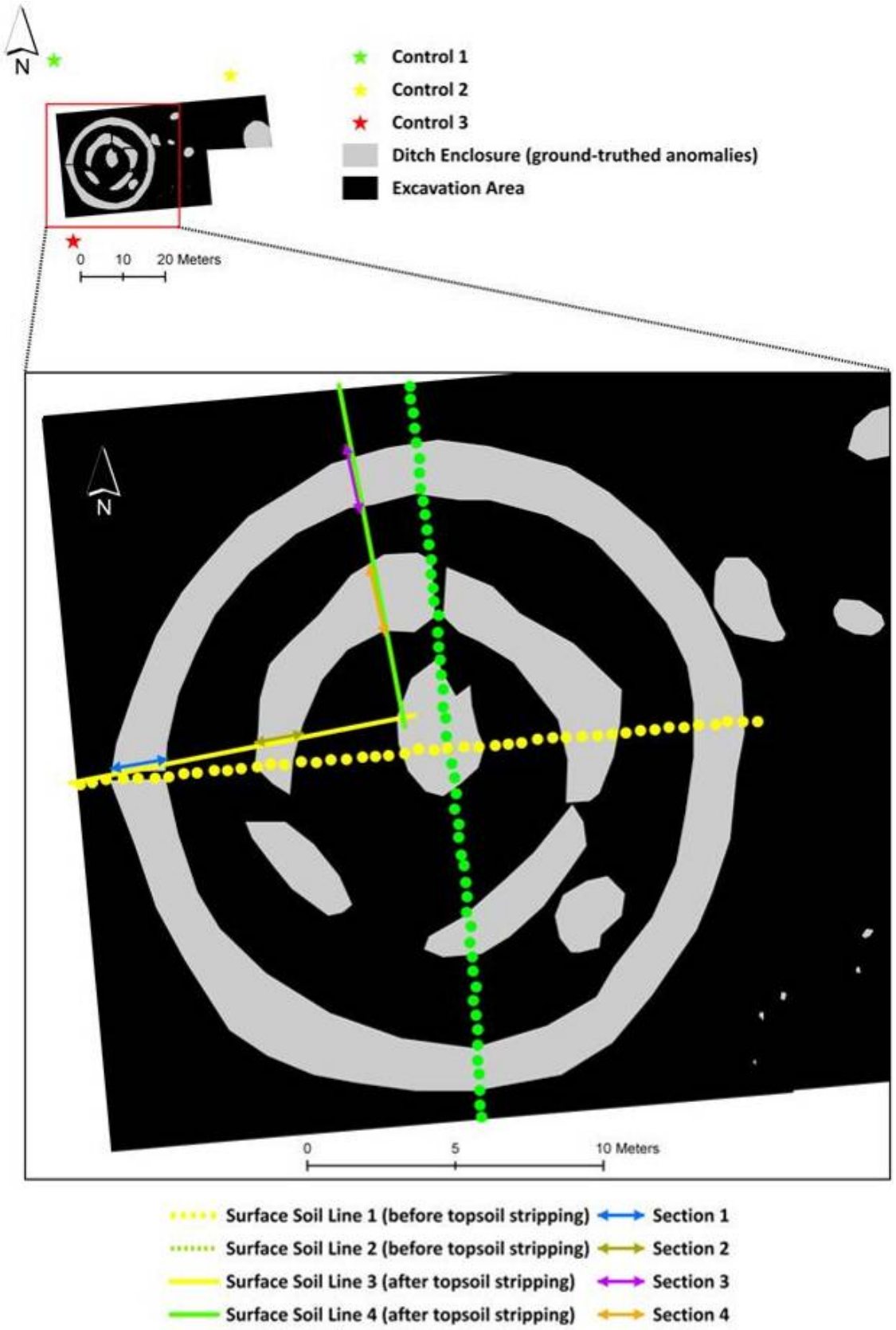

Figure 7-27: Location of the surface soil sampling lines (1-4), sampling sections (1-4) and controls (see top plan) for the physical and chemical analysis of the ditch enclosure at Forteviot.

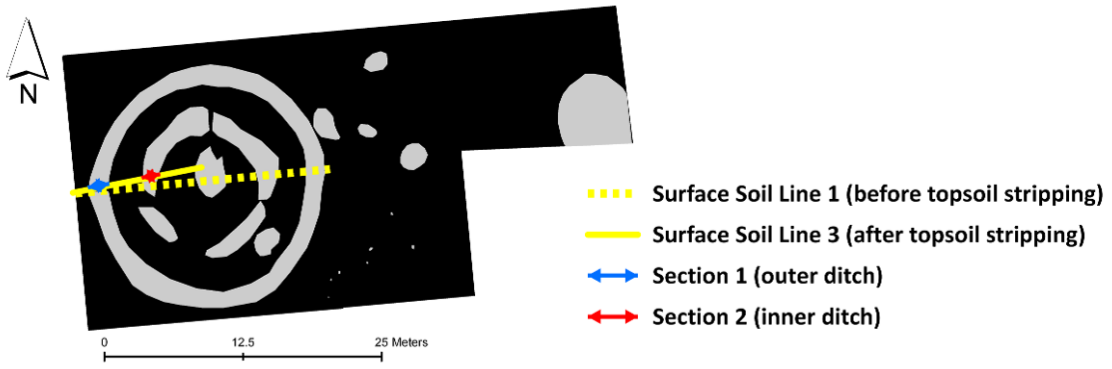

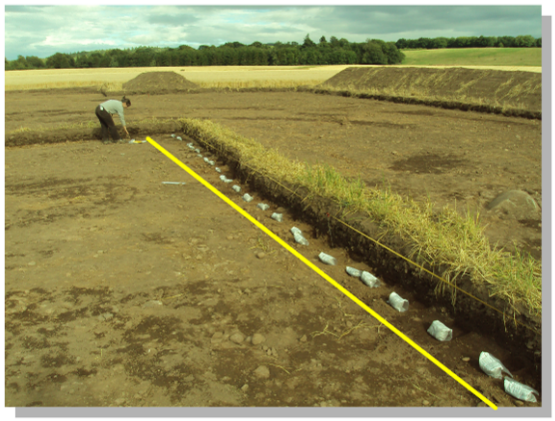

Figure 7-28: Sequential soil sampling carried out prior to, and during the excavation of the ditch enclosure at Forteviot. The white tags (bottom) show the location of the vertical and horizontal samples collected during the excavation of the outer (bottom-left) and inner (bottom-right) ditch enclosure.

Sample	Orientation	Sample spacing	Length/Depth	N°	Notes
Surface Soil Line 1	W-E	0.5m	23 long	47	Before topsoil stripping
Surface Soil Line 2	N-S	0.5m	23 long	51	
Surface Soil Line 3	W-E	0.5m (or less over the ditch)	12 long	28	After topsoil stripping
Surface Soil Line 4	N-S		12 long	31	
Section 1	N facing section	*c.* 0.10-0.20m	1.70 wide x 1.10m deph	15	Excavationg of the outer ditch
Section 2			0.30 wide x 0.30 depth	4	Excavation of the inner ditch
Section 3	W facing section		1.9 wide x 0.80 depth	5	Excavationg of the outer ditch
Section 4			0.50 wide x 0.40 depth	4	Excavation of the inner ditch
Total				**185**	

Table 7-7: Summary of the soil samples collected over and inside the ditch enclosure at Forteviot.

7.3.3. Physical & Chemical Results & Discussion

7.3.3.1. **Soil texture (Figure 7-29 and Table 7-8)**

The dark brownish loamy sand topsoil contained many small gravels and some sub-angular stones. These gravels and stones are derived from the underlying glacial deposits (sand and gravels) and may have added some magnetic noise to the gradiometer data collected before the plough soil was removed. This deposit overlay the truncated ditches of the enclosure and had deeper roots and bioturbation in the area over the outer ditch. This horizon was sampled at *c.* 0.10-0.15m depth before stripping. The features cut into the subsoil and parent material (B/C horizons respectively) were reddish brown loamy sands and presented very abundant gravels. The subsoil contained fewer roots and dried very quickly when wet. After the topsoil stripping this horizon was sampled as well as the exposed ditch features. The fresh exposed features were fairly

obvious after the stripping as they contrasted very well against the subsoil by their darker, smooth and shiny character (deposit 1 in Figure 7-29). This suggests a higher concentration of organic matter, clay and silt in the interface between the ploughsoil, subsoil and the truncated ditches, therefore a higher moisture content retention. However, this contrast completely faded away after a few minutes of exposure, and when dried they were very difficult to distinguish from the surrounding soil. The higher organic matter and clay content in this interface deposit indicated a higher CEC and moisture retention that would explain the ability of the outer ditch to retain moisture and be detected as a low resistance anomaly. This interface would also have caused the uppermost and linear strong reflections of the other ditch detected by GPR after topsoil stripping (GPR Line 3 in Figure 7-25). The very quick drainage capacity of the sandy and stony subsoil and topsoil explains the need for ground moisture saturation in order to complete the earth resistance survey.

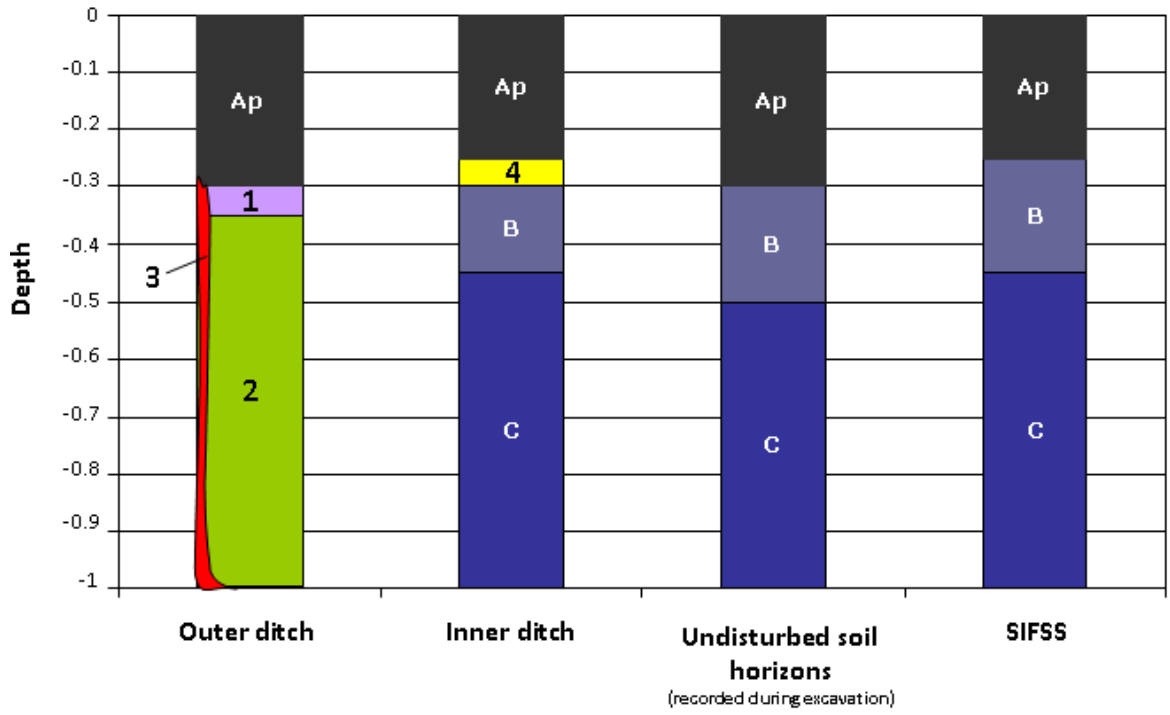

Figure 7-29: Diagram showing the main soil horizons and ditch deposits (1-4) identified during the excavation of the ditch enclosure at Forteviot. The figure also shows the main soil horizons described by the SIFSS database (Macaulay Land Use Research Institute 2011).

	Depth (m)	H	Colour Munsell	Texture	Structure	Consistency	Stoniness	Bioturb.	Notes
Mineral Horizons	0 to 30/38	Ap	2.5Y_2.5/1	Medium loamy sand.	Moderate, medium to fine & sub-angular blocky.	Slightly moist, firm and slightly plastic/slightly sticky. Hard when dry.	Many small/medium sub-rounded (gravels) & few medium angular stones.	Many & fine fibrous roots.	Ploughsoil overlaying all the features. Bioturbation and rooting in outer ditches.
	0.30/ 0.35 to 0.60-0.65	B	5YR_4/4		Moderate medium to fine size & sub-angular blocky.	Moist, very firm, slightly-sticky when wet. Hard to very hard when dry.	Many to very abundant small to medium rounded and sub-rounded stones.	Common, fine & fibrous roots.	General deposits in the trench where most of the fetaures are cut into. The deposits were very stony and dried quickly.
	0.60/0.65 to 1.10	C	5YR_4/5	Medium/coarse silt loam.	Weak coarse & granular.	Moist, not-plastic & not-sticky. Very friable when moist & loose when dry.	Very abundant small to medium rounded and sub-rounded stones (silts and gravels).	None.	Mineral horizon of unconsolidate material (silts and gravels).
		Cb	2.5YR_8/4	Clay.	Very fine platy.	Very moist, plastic & very sticky. Firm when moist & slightly hard when dry.	None.	None.	Natural lenses of thin layers of clay outwith the silts and gravels.
Section 1 & 3 (outer ditch)	0.35 to 1	1	5YR_4/3	Medium loamy sand.	Moderate medium to fine size & sub-angular blocky.	Moist, firm, sticky when wet. Soft when dry.	Few small rounded stones.	Common, fine & fibrous roots.	Top fill of the outer ditch. This deposit was very shinny when wet but difficult to distinguish when dry.
		2	5YR_4/4			Moist, firm, slightly-sticky when wet. Hard when dry.	Many to very abundant small to medium rounded and medium sub-rounded and angular stones.		General fill of the outer ditch. This ditch is deeper than the inner ditch. Charcoal fragments were found in section 3 (burned posts of a palisaded enclosure?).
		3	5YR_4/5			Moderately induration.	Very abundant small to medium rounded and sub-rounded stones.		Deposit created by the excavationof the outer ditch (higher deegree of slope in this side of the feature cut). The induration of the gravels seems to have been caused by the pression of the back fill of the ditch against this side (charcoal of possible posts=palisade?)
Section 2 & 4 (inner ditch)	0.26/0.30 to 0.40	4	5YR_4/6	Medium loamy sand.	Moderate medium to fine size & sub-angular blocky.	Moist, firm, slightly-sticky when wet. Hard when dry.	few small to medium rounded and medium sub-rounded and angular stones.	Common, fine & fibrous roots.	Fill of inner ditch.

Table 7-8: Description of the major soil horizons and deposits recorded in the excavation of the four sections (Figure 7-28) of the ditch enclosure at Forteviot.

The backfill deposits of the outer ditch (2 and 3 in Figure 7-29) suggest a high energy event instead of a slow filling up of this feature. Evidence of wooden stakes was found suggesting that the ditch was a palisade. If this is the case, this should have contributed to a magnetic susceptibility enhancement of the outer ditch and the detection of a positive instead of a negative magnetic anomaly. The inner ditch was very difficult to see in the sampled sections. Only samples from very shallow deposits (4 in Figure 7-29) were described and sampled. The segmented and truncated charater of the inner ditch and its different depths documented by the GPR survey and archaeological records made this feature slightly more difficult to analyse than the outer ditch.

7.3.3.2. **Soil Surface Sampling (before topsoil stripping)**

7.3.3.2.1. ***MS, Total P, OSL, LOI, EC and pH (Figure** 7-30 **and Table 7-9)***

The results of the MS, total phosphate and OSL analysis were fairly variable along the survey line and did not show any obvious response that correlates with the location of the targeted features. However, superimposing the excavated archaeological features, surveyed with a RTK-GPS system, onto the soil data (see coloured bars in Figure 7-30**)** allows some correlations between the approximate location of the archaeological features and the soil samples to be observed.

Depleted total P values correlated with the location of the westernmost outer and inner ditch and the cist burial (Figure 7-30). The mean of the total P values inside the ditch was 222 µg/kg whilst the mean immediately outside the ditch were 253 µg/kg. The mean of the inner ditch was 235 against the adjacent 263 µg/kg. The correlation of these low total P values with the targeted features seemed consistent with the steady and linear P results in the areas between these features. However, the results of the easternmost outer and inner ditches were less consistent as the P values here showed higher variability. The MS and OSL results did not show any consistent correlation with the location of the features.

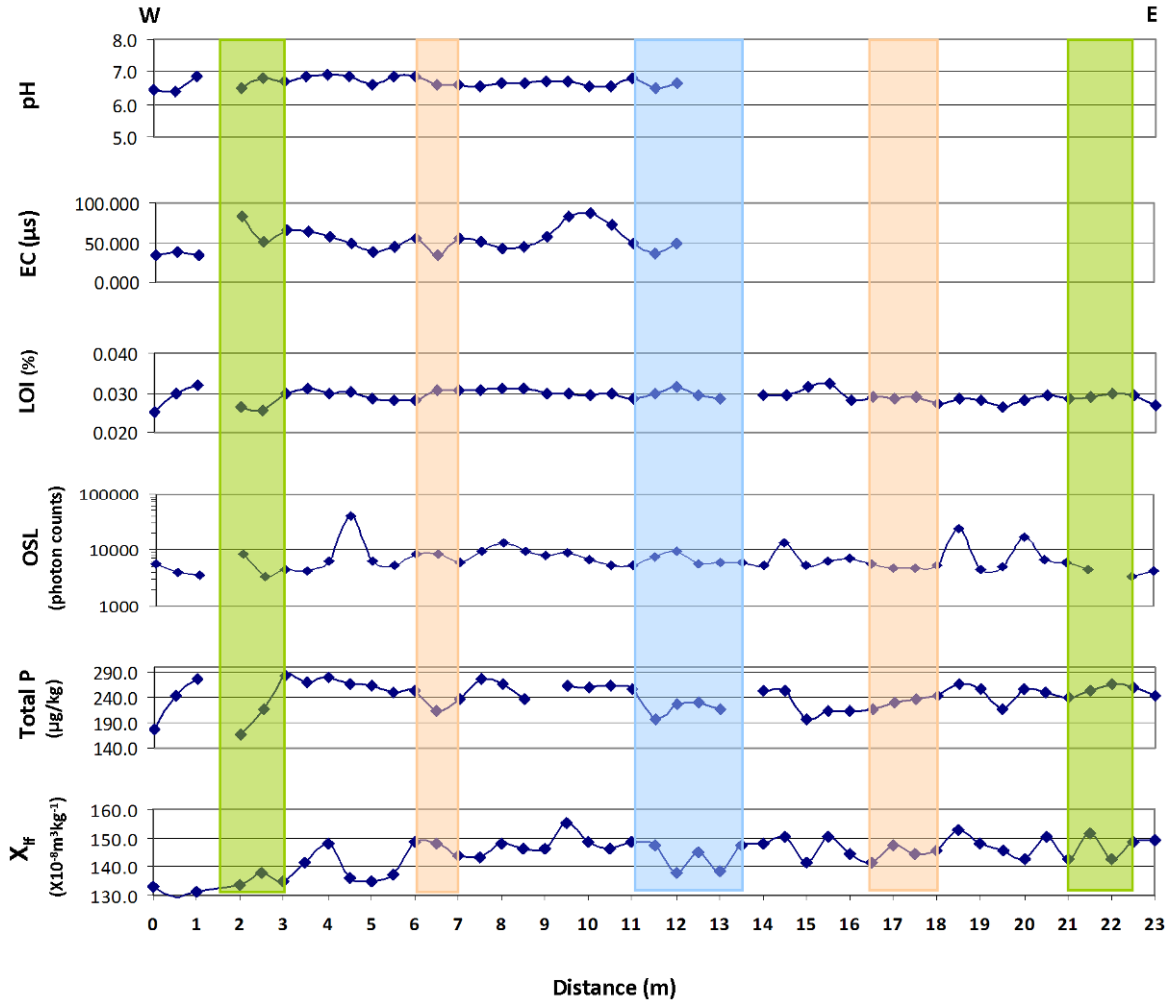

Figure 7-30: Surface distribution of magnetic susceptibility (χlf), total phosphate (Total P), luminescence signal (OSL-BLSL=blue light), loss on ignition (LOI), conductivity (EC) and pH of the samples collected over the ditch enclosure at Forteviot (Line 1, before topsoil stripping). The green (outer ditch), salmon pink (inner ditch) and blue (central pit) colours mark the approximate location of the targeted anomalies.

Distance (m)	χ_{lf} ($10^{-8}m^3kg^{-1}$)	Total P (µg/kg)	OSL (BLSL) (Photon counts)	LOI (%)	EC (µs)	pH
0	133	176	5611	0.025		6
0.5	130	243	4066	0.030	38	6
1	131	277	3510	0.032	34	7
1.5	*	*	*	*	*	*
2	134	165	8256	0.026	84	6
2.5	138	216	3399	0.025	52	7
3	135	284	4356	0.030	65	7
3.5	141	270	4250	0.031	63	7
4	148	280	6211	0.030	58	7
4.5	136	267	39120	0.030	48	7
5	135	263	6183	0.028	38	7
5.5	137	250	5373	0.028	45	7
6	149	253	8201	0.028	56	7
6.5	148	215	8273	0.031	35	7
7	144	237	6093	0.031	56	7
7.5	143	276	9226	0.031	52	7
8	148	266	13334	0.031	42	7
8.5	146	237	9296	0.031	44	7
9	146	*	8122	0.030	57	7
9.5	156	263	9167	0.030	82	7
10	148	260	6589	0.029	87	7
10.5	147	263	5308	0.030	73	7
11	149	257	5441	0.029	48	7
11.5	148	196	7527	0.030	36	7
12	138	228	9263	0.032	48	7
12.5	145	231	5761	0.029	*	*
13	138	218	5834	0.028	*	*
13.5	147	*	5977	*	*	*
14	148	253	5320	0.029	*	*
14.5	150	253	13102	0.029	*	*
15	142	196	5240	0.031	*	*
15.5	150	215	6181	0.032	*	*
16	144	215	7223	0.028	*	*
16.5	142	218	5743	0.029	*	*
17	147	231	4639	0.029	*	*
17.5	144	237	4671	0.029	*	*
18	146	245	5236	0.027	*	*
18.5	153	266	23291	0.029	*	*
19	148	257	4433	0.028	*	*
19.5	145	217	5111	0.026	*	*
20	143	257	16671	0.028	*	*
20.5	151	251	6707	0.029	*	*
21	143	237	6000	0.028	*	*
21.5	152	254	4400	0.029	*	*
22	142	266	*	0.030	*	*
22.5	149	260	3427	0.029	*	*
23	150	245	4239	0.027	*	*
Mean	144	242	7675	0.029	54	7
S.D	6	27	6028	0.002	16	0
C.V.	4	11	79	6	29	2
Control 1	143	272	4551	0.028	*	*
Control 2	141	*	4515	*	*	*
Control 3	155	269	4514	0.029	*	*

Outer ditch

Inner ditch

Central pit (cist burial)

* Not analysed

Table 7-9: Magnetic susceptibility (χ_{lf}), total phosphate (Total P), luminescence signal (OSL-BLSL= blue light), loss on ignition (LOI), conductivity (EC) and pH results of the surface soil Line 1 over the ditch enclosure at Forteviot (before topsoil stripping). The green (outer ditch), salmon pink (inner ditch) and blue (central pit) colours mark the approximate location of the targeted anomalies. The samples marked (*) were not analysed.

7.3.3.2.2. *pXRF (Figure 7-31 and Table 7-10)*

The results were characterised by high concentrations of Fe, K, Ca and Ti. The concentrations of K, Ca and Ti showed a consistent response along the survey line (depletion/enrichment/depletion) over the targeted ditches with a general anomalous response. These elements had the following statistically significant correlations (A and A-2 in Appendix F): K/Ti (Spearman's correlation= s-r: 0.90), K/Ca (s-r: 0.75) and Ca/Ti (s-r: 0.0.64) which indicate that these elements have a common distribution. Fe/Mn show a similar response along the survey line and also a strong correlation coefficient (s-r: 0.77 in A-Appendix F). The common variation in these elements' response over the ditches could be the effect of ploughed ditch deposits on the soil surface mineralogy. The more pronounced variation of the inner ditch in comparison to the outer ditch may be due to the effect of shallower deposits relating to the inner ditch at the sampling positions (Figure 7-29). The Mn concentration reaches a peak between the inner ditch and the central pit.

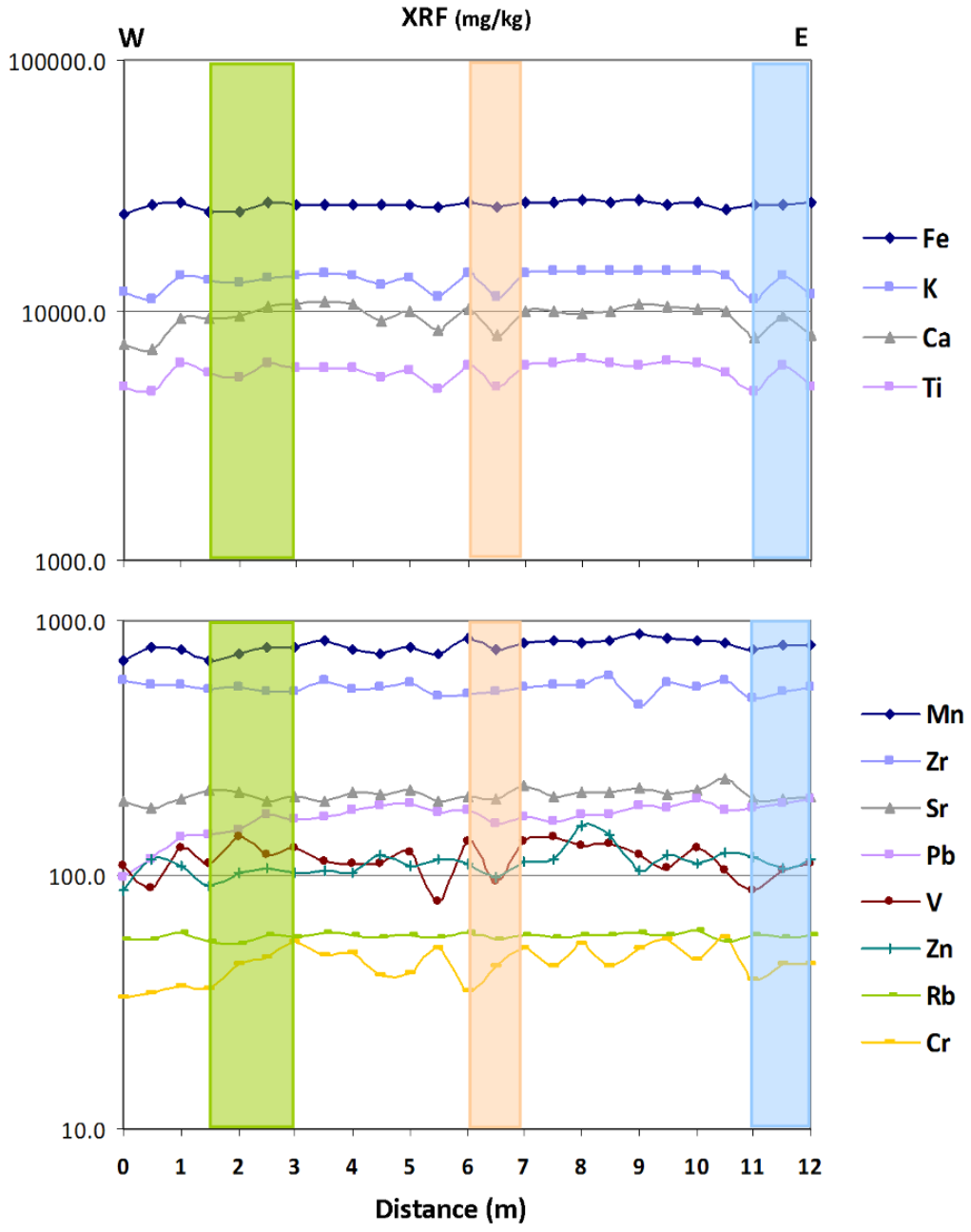

Figure 7-31: Surface distribution of soil element concentrations (pXRF data) over the ditch enclosure at Forteviot (Line 1, before topsoil stripping). The green (outer ditch), salmon pink (inner ditch) and blue (central pit) colours mark the approximate location of the targeted anomalies.

Distance (m)	Fe	K	Ca	Ti	Mn	Zr	Sr	Pb	Cu	V	Zn	Rb	Cr
0	24214	11886	7360	4900	698	577	194	97	48	107	87	56	33
0.5	26143	10956	6927	4727	781	553	182	116	146	88	115	56	35
1	27037	13766	9300	6083	767	552	200	141	112	127	108	59	37
1.5	24510	13012	9263	5595	702	538	216	143	55	111	90	54	36
2	24956	12890	9488	5349	746	550	210	150	44	142	101	53	45
2.5	26996	13510	10421	6065	788	529	195	173	117	121	107	58	47
3	26443	13691	10498	5822	792	525	201	166	70	126	101	57	54
3.5	26585	14086	10849	5830	828	575	194	168	94	112	103	60	48
4	26331	13672	10641	5873	762	534	210	181	76	110	101	58	49
4.5	26282	12524	8982	5415	741	551	207	186	159	110	119	56	40
5	26578	13313	9816	5745	779	569	215	189	107	122	109	58	41
5.5	25742	11281	8308	4853	744	501	196	177	125	79	115	56	52
6	27220	13928	10092	6029	851	514	203	179	93	137	111	60	35
6.5	26004	11207	7925	4927	763	526	200	158	90	95	98	56	44
7	27064	14064	9830	5940	814	548	224	169	155	136	112	58	52
7.5	27172	14254	9852	6135	826	559	203	164	114	142	116	57	44
8	27512	14354	9583	6440	812	559	212	172	346	131	156	58	54
8.5	27015	14234	9909	6086	830	605	212	174	326	132	143	58	43
9	27702	14301	10668	5947	877	460	219	188	57	120	104	59	52
9.5	26690	14458	10285	6248	850	563	209	182	159	106	120	58	56
10	27120	14373	10078	6115	832	541	218	197	68	127	111	60	46
10.5	25378	13700	9922	5555	812	583	237	180	243	105	123	55	57
11	26453	11071	7819	4723	776	494	200	182	138	87	117	58	39
11.5	26492	13599	9569	5959	803	521	200	189	86	105	105	57	45
12	26762	11603	8027	4955	802	550	202	199	128	112	114	58	45
Mean	26416	13189	9416	5653	791	543	206	169	126	116	112	57	45
S.D.	884	1175	1092	524	45	31	11	24	77	17	15	2	7
C.V	3	9	12	9	6	6	6	14	61	15	13	3	16
Control 1	26112	10740	7890	4569	743	517	201	85	44	86	100	56	32
Control 2	25212	13198	7949	5496	727	67	186	193	54	104	95	56	38
Control 3	26719	13887	9713	5943	778	484	193	241	66	125	114	59	42

Outer ditch **Inner ditch** **Central pit (triple cist burial)**

Table 7-10: pXRF results of the surface soil Line 1 over the ditch enclosure at Forteviot (before topsoil stripping). The element concentrations are expressed in mg/kg (=ppm). The green, salmon pink and blue colours mark the approximate location of the targeted anomalies. The location of the controls is shown in Figure 7-27 (top).

7.3.3.2.3. *ICP-OES (Figure 7-32 and Table 7-11)*

The ICP-OES results were similar to those of XRF. The strongest correlations (C and C-1 in Appendix F) were Al/Fe (s-r: 0.84), Al/K (s-r: 0.82), Fe/Mg (s-r: 0.87), Mg/P (s-r: 0.88). Also, K/Ti had a statistically significant correlation value (s-r: 0.66) this is a low value in agreement with the XRF data. The correlation between distance and Mn was also significant in the ICP-OES data (s-r=0.68, D in Appendix F) indicating an increase in Mn as the centre of the ditch enclosure is reached. Similarly, Ni showed a good correlation with distance (s-c=0.66). Furthermore, the strongest relationship was Mn/Ni (0.82). These two elements may be related to the presence of the enclosure. The correlation between

distance and Mn was significant in the ICP-OES data (s-r=0.68, D in Appendix F). The positive relationship between these two variables (D-1 in Appendix F) may indicate an increase in Mn concentration levels as the centre of the ditch enclosure is reached. Similarly, Ni showed a good correlation with distance (s-c=0.66). Furthermore, the strongest relationship was between Mn/Ni (0.82). These two elements may be related to the presence of the enclosure.

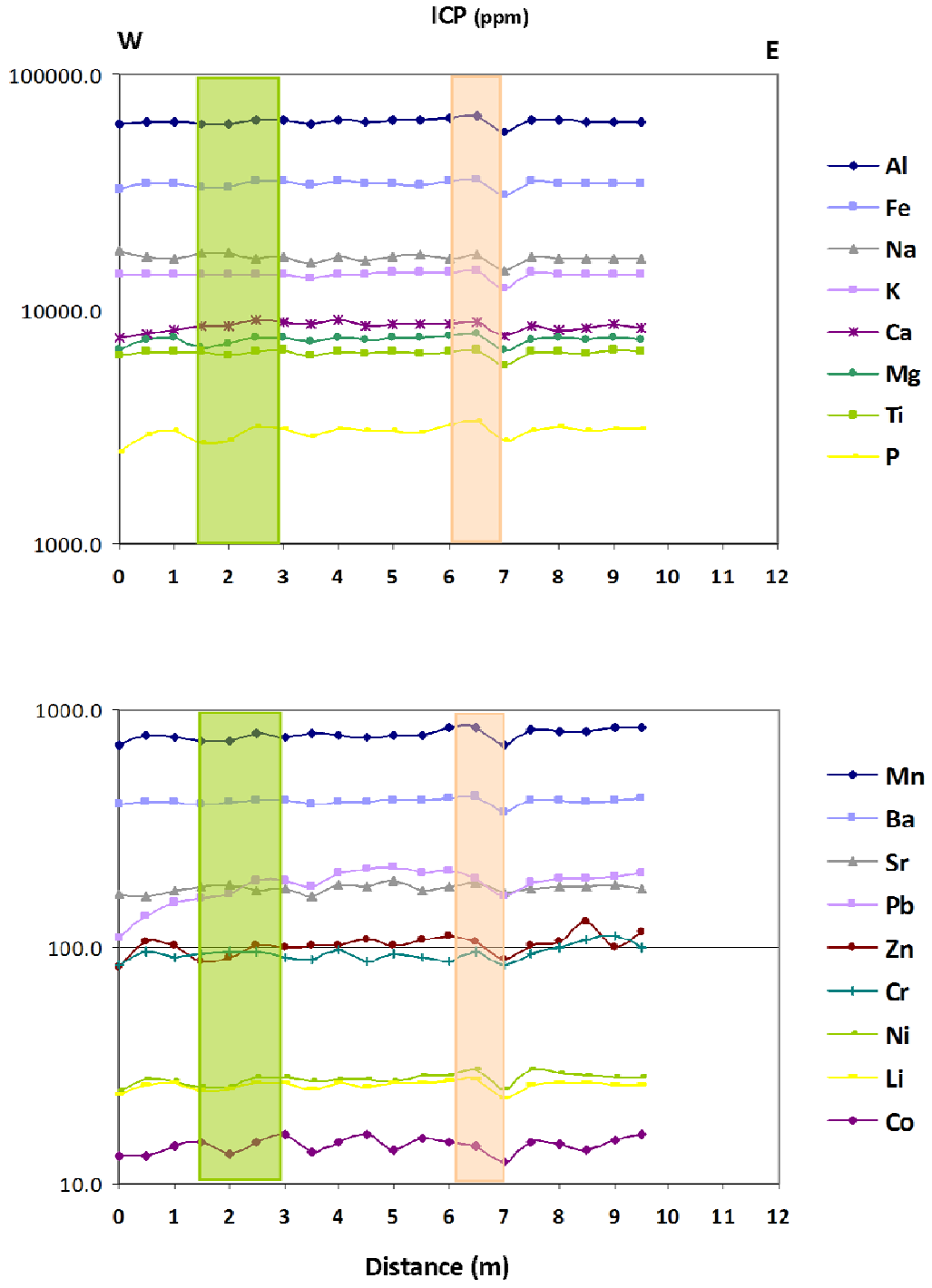

Figure 7-32: Surface distribution of soil element concentrations (ICP-OES) over the ditch enclosure at Forteviot (Line 1, before topsoil stripping). The green and salmon pink colours mark the approximate location of the targeted anomalies.

Distance (m)	Al	Fe	Na	K	Ca	Mg	Ti	P	Mn	Ba	Sr	Pb	Cu	Zn	Cr	Ni	Li	Co
0	60959	32096	17628	14005	7540	6688	6388	2465	704	398	165	109	60	82	84	25	24	13
0.5	62861	34201	16636	14120	7854	7378	6601	2933	781	410	164	134	142	105	95	27	26	13
1	63251	34310	16491	13997	8212	7479	6614	3056	769	405	172	154	117	101	89	27	26	14
1.5	*	*	*	*	*	*	*	*	*	*	*	*	*	*	*	*	*	*
2	61358	32812	17282	13956	8400	6904	6527	2718	733	401	181	161	72	87	94	25	25	15
2.5	62048	32824	17566	13959	8471	7059	6359	2757	740	406	183	167	57	90	96	26	25	13
3	64024	34686	16472	13983	8988	7553	6533	3131	790	413	173	188	95	101	96	28	26	15
3.5	63879	34941	16704	14159	8889	7538	6665	3101	767	411	176	189	66	99	90	28	27	16
4	61247	33591	15789	13537	8614	7245	6358	2866	791	397	164	179	112	100	89	27	25	14
4.5	63612	34916	16697	14082	9002	7595	6589	3067	787	410	184	203	86	100	96	28	26	15
5	62618	34118	16066	13957	8457	7367	6484	3017	770	407	178	213	148	106	87	27	26	16
5.5	63825	34464	16795	14378	8708	7478	6561	3034	786	419	189	219	81	100	93	27	26	14
6	64116	33954	17007	14234	8668	7480	6483	2966	780	414	173	205	141	107	90	28	26	16
6.5	65403	35222	16480	14413	8587	7692	6562	3216	844	424	179	210	80	111	87	29	27	15
7	65892	35692	16923	14493	8730	7815	6675	3344	843	429	186	194	107	105	95	31	27	14
7.5	57215	30550	14596	12351	7655	6723	5721	2723	715	369	168	163	89	88	83	25	23	12
8	63802	35020	16833	14271	8398	7469	6646	3012	818	418	175	186	128	101	94	30	26	15
8.5	63715	34516	16326	14129	8217	7579	6566	3176	814	418	179	194	119	105	99	29	27	15
9	63179	34142	16533	13957	8384	7371	6517	3050	806	409	180	192	343	126	108	29	26	14
9.5	63337	34665	16308	14182	8643	7506	6682	3116	838	417	184	199	63	99	110	28	26	15
10	63314	34322	16534	14156	8389	7347	6612	3073	839	420	176	205	185	115	99	28	26	16
10.5	*	*	*	*	*	*	*	*	*	*	*	*	*	*	*	*	*	*
11	*	*	*	*	*	*	*	*	*	*	*	*	*	*	*	*	*	*
11.5	*	*	*	*	*	*	*	*	*	*	*	*	*	*	*	*	*	*
12	*	*	*	*	*	*	*	*	*	*	*	*	*	*	*	*	*	*
Mean	62983	34052	16583	14016	8440	7363	6507	2991	786	410	177	183	115	101	94	28	26	15
S.D.	1838	1197	649	444	398	302	209	202	41	13	7	28	64	10	7	2	1	1
C.V.	3	4	4	3	5	4	3	7	5	3	4	15	56	10	8	6	4	7

Outer ditch **Inner ditch** **Central pit (triple cist** * **Not analysed**

Table 7-11: ICP-OES results of the surface soil sampling Line 1 (Figures 7-27 and 7-28) over the ditch enclosure at Forteviot (before topsoil stripping). The element concentrations are expressed in ppm (=mg/kg). The green, salmon pink and blue colours mark the approximate locations of the targeted anomalies.

7.3.3.3. **Soil Surface Sampling (after topsoil stripping)**

7.3.3.3.1. ***MS, Total P, OSL, LOI, EC and pH (Figure 7-33 and Table 7-12)***

The results of the MS, total P and OSL analysis showed depleted values over the outer ditch after the stripping of the first 30-40 cm of topsoil. The response of these techniques over the inner ditch was less clear. After topsoil stripping, the exposed deposits sampled from the inner ditch were far too shallow and unclear because of the truncation and different depths of this feature and sothe inner ditch was rejected for further analysis.

The average MS values inside the outer ditch were 84 10^{-6} m^3kg^{-1} and 170 10^{-6} m^3kg^{-1} outside the ditch. The difference between the susceptibilities of the targeted feature and the surrounding soil matrix correlates with the negative magnetic anomalies detected by the gradiometer survey. However, since the backfill of the outer ditch was in origin the same type of deposit as the surrounding soil matrix, it is possible that other soil processes are behind these low MS values.

The luminescence blue light (BLSL) signal produced a distinctive response over the outer ditch after light stimulation using the pOSL reader. The OSL results showed depleted luminescence values over the outer ditch (mean= 12356 total photon counts) and a higher luminescence dose outside the feature (mean= 68484 photon counts). The higher values of the soil matrix show the expected higher dose rate of 'old' sedimentary deposits that absorb radiation doses in their grains through time (Muñoz-Salinas *et al.* 2011). The low dose values of the samples over the outer ditch indicate their bleaching of luminescence by the disturbance of the natural stratigraphy and the exposure of the feature to light. The cut and backfill would have fully or partially bleached of luminescence before and during re-deposition, hence contrasting with the higher dose of the subsoil. There was a statistically significant correlation of OSL/MS (s-r: 0.61, e and E-2 in Appendix F). Since the MS of a soil is mainly determined by the amount and type of soil iron oxides (Kattenberg 2008) and the luminescence dose rates are related to the amount of quartz, feldspar and natural radio-elements contained in their grains and their size (Rhodes 2011), the mineralogical relationship may have produced this correlation.

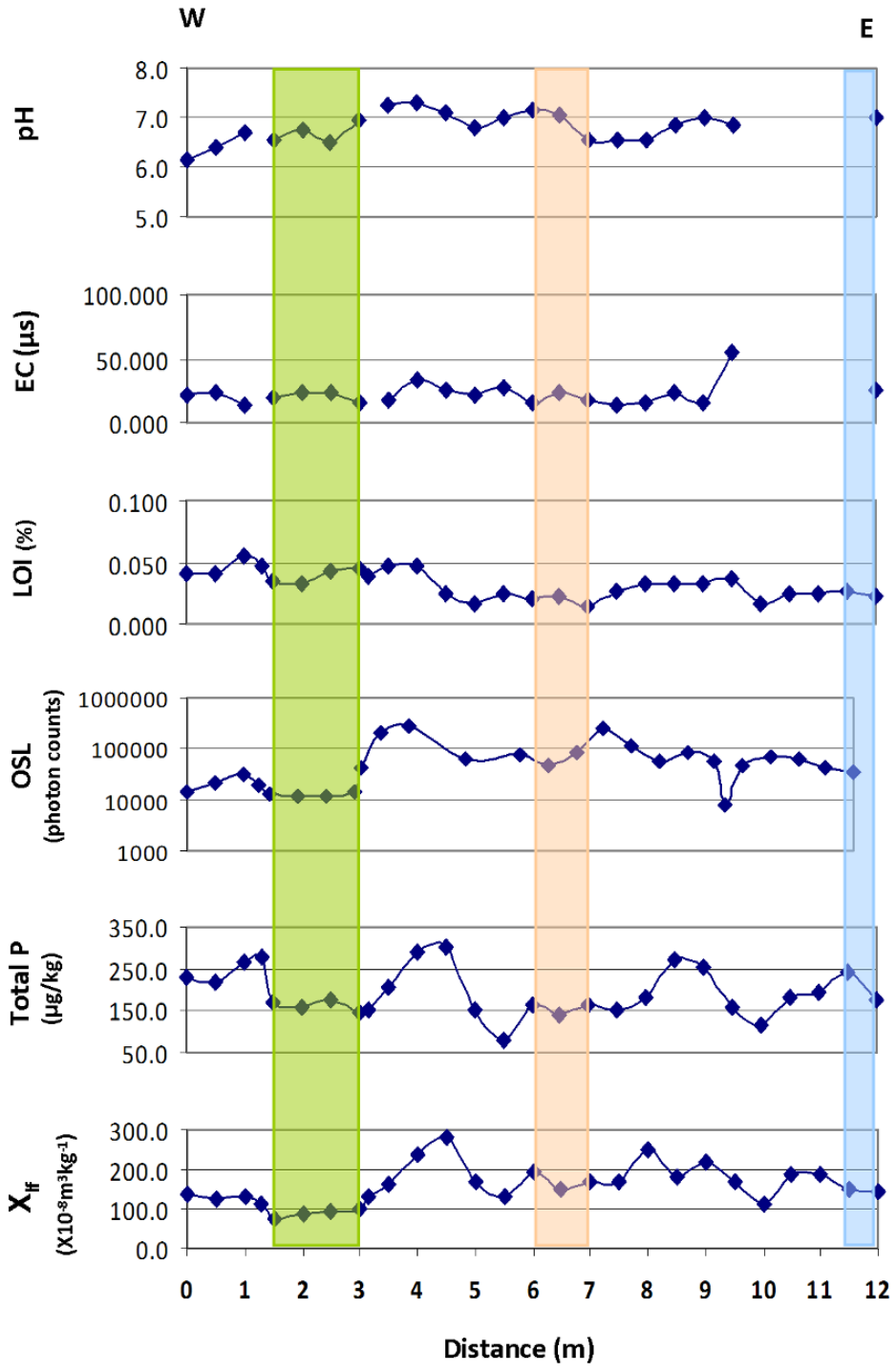

Figure 7-33: Surface distribution of magnetic susceptibility (χ_{lf}), total phosphate (Total P), luminescence signal (OSL-BLSL=blue light), loss on ignition (LOI), conductivity (EC) and pH of the samples collected over the ditch enclosure at Forteviot (Line 3 in Figure 7-27 and 7-28, after topsoil stripping). The green, salmon pink and blue colours mark the soil samples that were collected over the targeted anomalies.

Distance (m)	χ_{lf} ($10^{-8}m^3kg^{-1}$)	Total P (µg/kg)	OSL (BLSL) (Photon counts)	LOI (%)	EC (µs)	pH
0	136	230	14735	0.040	22	6
0.5	127	220	21779	0.042	24	6
1	134	266	31505	0.055	13	7
1.3	111	277	18648	0.047	*	*
1.5	74	171	13323	0.034	20	7
2	86	159	12319	0.032	24	7
2.5	93	178	11427	0.043	24	6
3	98	147	15084	0.046	16	7
3.15	134	152	42070	0.040	*	*
3.5	162	208	202058	0.047	18	7
4	240	291	274311	0.046	33	7
4.5	283	300	*	0.024	25	7
5	172	153	64095	0.017	22	7
5.5	132	83	75469	0.025	27	7
6	194	165	47141	0.021	16	7
6.5	152	141	84362	0.022	23	7
7	167	165	260849	0.015	18	7
7.5	168	150	112377	0.026	13	7
8	247	181	55388	0.033	16	7
8.5	181	272	82411	0.032	24	7
9	222	257	55657	0.032	16	7
9.5	169	159	8140	0.036	54	7
10	114	115	44692	0.016	*	*
10.5	186	182	69374	0.025	*	*
11	189	196	66259	0.024	*	*
11.5	153	243	42202	0.027	*	*
12	147	176	33285	0.023	25	7
Mean	158	194	67652	0.032	23	7
S.D.	50	56	71691	0.011	9	0
C.V	32	29	106	34	39	4

Outer ditch

Inner ditch

Central pit (cist burial)

* Not analysed

Table 7-12: Magnetic susceptibility (χ_{lf}), total phosphate (Total P), luminescence signal (OSL-BLSL=blue light), loss on ignition (LOI), conductivity (EC) and pH results of the surface soil Line 3 (Figure 7-27 and 7-28) over the ditch enclosure at Forteviot (after topsoil stripping). The green, salmon pink and blue colours mark the soil samples that were collected over the targeted anomalies.

7.3.3.3.2. *pXRF (Figure 7-34 and Table 7-13)*

The results of the pXRF analysis were characterised by a generally high variability of elemental concentrations and high concentrations of Fe, K and Ca. In spite of the variability, these elements presented very weak depletions over the outer ditch except Ti which was slightly enriched. The variation of other elements was too high and no statistically significant correlation was identified in this dataset.

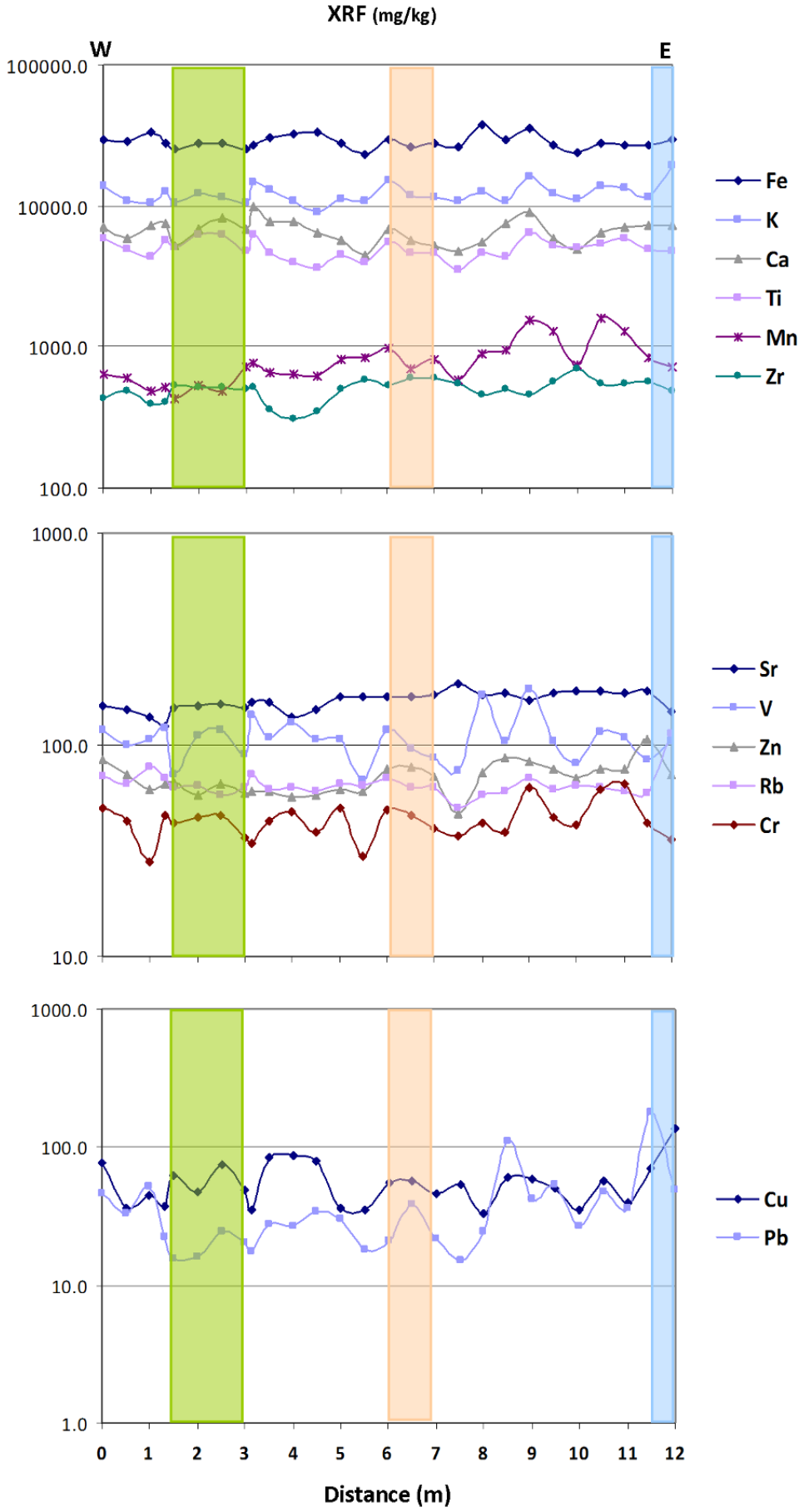

Figure 7-34: Surface distribution of soil element concentrations (pXRF data) over the ditch enclosure at Forteviot (Line 3 in Figure 7-27 and 7-28, after topsoil stripping). The green, salmon pink and blue colours mark the soil samples that were collected over the targeted anomalies.

Distance (m)	Fe	K	Ca	Ti	Mn	Zr	Sr	V	Zn	Rb	Cu	Cr	Pb
0	29704	13950	7086	5857	634	437	152	118	85	71	78	50	46
0.5	28811	10936	5854	4960	599	481	146	101	72	66	37	44	33
1	33400	10482	7219	4349	485	390	135	107	62	79	44	28	51
1.3	28254	12448	7639	5667	515	408	123	121	66	70	37	46	23
1.5	25249	10596	5188	5088	431	535	150	73	67	63	61	43	15
2	27691	12290	6791	6215	533	522	154	110	58	65	48	46	16
2.5	27931	11628	8176	6242	483	511	156	119	65	57	74	46	25
3	25067	10381	6768	4741	725	497	150	90	59	62	49	37	20
3.15	26987	14746	9778	6349	778	520	160	138	60	72	35	34	18
3.5	30167	13073	7852	4558	666	358	160	108	60	62	84	43	27
4	32211	10713	7727	3926	645	308	134	127	57	63	88	49	27
4.5	33317	9061	6397	3623	626	345	146	107	58	61	78	39	34
5	27709	11219	5754	4436	820	496	168	107	62	66	36	50	30
5.5	22918	11009	4450	4023	854	579	170	68	61	64	36	30	18
6	29258	14937	6953	5616	979	533	169	118	76	69	55	50	21
6.5	26604	11927	5798	4606	699	595	169	96	78	63	56	47	39
7	27749	11679	5193	4682	818	608	174	87	71	63	47	40	22
7.5	26386	10851	4733	3503	578	550	195	75	48	51	54	37	15
8	37450	12467	5531	4614	901	459	172	173	74	58	33	43	24
8.5	29296	10742	7616	4301	950	504	176	103	86	60	60	39	111
9	35620	16064	9018	6379	1536	458	162	183	84	70	59	63	42
9.5	27001	12145	5925	5222	1300	563	177	104	77	62	50	46	54
10	24227	11063	4890	5086	739	692	178	82	70	64	35	42	27
10.5	27558	13844	6563	5329	1599	542	179	116	77	63	57	61	48
11	27218	13481	7024	5817	1281	545	175	110	78	61	40	65	36
11.5	26832	11501	7413	4902	851	558	181	85	106	59	69	43	180
12	29470	19298	7294	4778	733	490	144	105	72	112	136	36	48
Mean	28670	12316	6690	4995	806	499	161	109	70	66	57	44	39
S.D.	3336	2135	1299	817	306	86	17	26	12	11	23	9	34
C.V.	12	17	19	16	38	17	10	24	17	16	40	20	88

Outer ditch **Inner ditch** **Central pit (triple cist burial)**

Table 7-13: pXRF results of the surface soil Line 3 (Figure 7-27 and 7-28) over the ditch enclosure at Forteviot (after topsoil stripping). The element concentrations are expressed in mg/kg (=ppm). The green, salmon pink and blue colours mark the soil samples that were collected over the targeted anomalies.

7.3.3.3.3. *ICP-OES (Figure 7-35 and Table 7-14)*

The ICP-OES gave similar results to that of the pXRF and a similar response over the outer ditch. P depletion also confirmed the Total P results over the outer ditch. P and Mg were notably correlated. Further depletion of trace elements such as Ni and Co also charaterised the exposed ditch deposits.

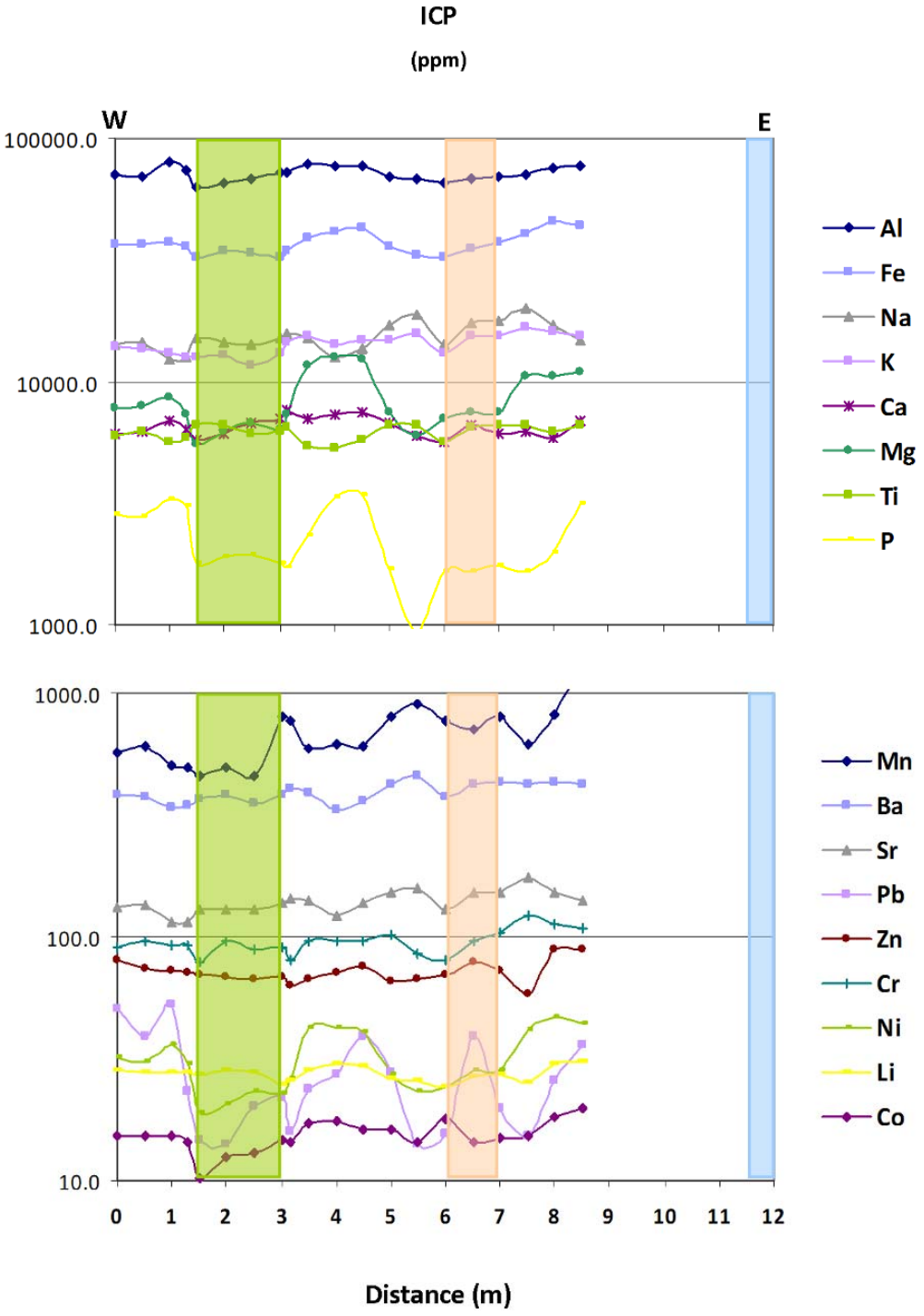

Figure 7-35: Surface distribution of soil element concentrations (ICP-OES data) over the ditch enclosure at Forteviot (Line 3 in Figure 7-27 and 7-28, after topsoil stripping). The green and salmon pink colours mark the soil samples that were collected over the targeted anomalies.

Distance (m)	Al	Fe	Na	K	Ca	Mg	Ti	P	Mn	Ba	Sr	Pb	Cu	Zn	Cr	Ni	Li	Co
0	71665	36935	14284	13937	6125	7831	5929	2874	574	381	132	51	66	80	91	32	28	15
0.5	70234	36373	14508	13593	6254	7861	6194	2767	605	377	134	39	48	73	96	31	28	15
1	79559	37661	12443	12988	6894	8653	5587	3296	503	340	114	53	35	72	93	36	28	15
1.3	74150	35921	12558	12620	6312	7322	5841	3098	493	346	115	23	63	72	92	30	28	14
1.5	62919	32294	15163	12689	5726	5549	6671	1792	461	370	131	15	88	70	79	19	27	10
2	66071	34597	14437	12916	6157	6175	6655	1903	494	379	131	14	42	68	96	21	29	12
2.5	67974	33815	14230	11723	6763	6746	6078	1926	454	350	129	20	63	67	88	23	28	13
3	72022	32428	15237	13090	7055	6391	6248	1775	798	385	137	22	84	68	90	23	25	15
3.15	72893	34406	15808	14385	7613	7267	6484	1730	764	405	143	16	28	63	80	26	26	14
3.5	78497	38473	14953	15378	6995	11667	5450	2328	595	387	140	23	91	66	96	42	28	17
4	77322	41473	12539	14270	7250	12505	5272	3319	624	334	122	27	117	71	96	42	30	17
4.5	77107	43250	13777	14759	7533	12432	5749	3377	609	363	139	39	105	75	96	41	30	16
5	70061	35793	17037	14911	6747	7526	6638	1696	808	424	151	28	36	66	102	27	26	16
5.5	68429	32916	18918	15745	5984	5991	6564	936	909	462	158	14	32	68	86	23	26	14
6	65589	32564	14362	13078	5639	7011	5682	1641	766	373	129	16	40	70	81	24	24	18
6.5	68745	35338	17357	15276	6645	7433	6469	1644	707	421	151	39	72	78	96	28	26	14
7	69673	37212	17860	15520	6062	7513	6655	1755	802	428	153	20	53	73	103	28	27	15
7.5	70500	40197	20055	16699	6289	10543	6639	1651	623	420	176	15	45	58	122	41	25	15
8	75442	45511	17081	16108	5850	10599	6208	1984	824	433	154	26	38	88	112	47	30	18
8.5	77565	43883	14769	15503	6907	10989	6556	3156	1367	421	141	36	78	89	108	44	30	20
9	*	*	*	*	*	*	*	*	*	*	*	*	*	*	*	*	*	*
9.5	*	*	*	*	*	*	*	*	*	*	*	*	*	*	*	*	*	*
10	*	*	*	*	*	*	*	*	*	*	*	*	*	*	*	*	*	*
10.5	*	*	*	*	*	*	*	*	*	*	*	*	*	*	*	*	*	*
11	*	*	*	*	*	*	*	*	*	*	*	*	*	*	*	*	*	*
11.5	*	*	*	*	*	*	*	*	*	*	*	*	*	*	*	*	*	*
12	*	*	*	*	*	*	*	*	*	*	*	*	*	*	*	*	*	*
Mean	71821	37052	15369	14259	6540	8400	6178	2232	689	390	139	27	61	72	95	32	27	15
S.D.	4669	3971	2094	1377	584	2214	454	728	210	35	15	12	26	8	11	9	2	2
C.V.	7	11	14	10	9	26	7	33	31	9	11	45	42	11	11	28	6	14

Outer ditch **Inner ditch** **Central pit** * **Not analysed**

Table 7-14**: ICP-OES results of the surface soil Line 3 (Figure 7-27 and 7-28) over the ditch enclosure at Forteviot (after topsoil stripping). The element concentrations are expressed in ppm (=mg/kg). The green and salmon pink colours mark the soil samples that were collected over the targeted anomalies.**

7.3.3.4. **Section Sampling (outer ditch)**

7.3.3.4.1. *MS, Total P, OSL, LOI, EC and pH (Figure 7-36 and Table 7-15)*

Depleted MS and total P values were found over the outer ditch confirming the surface results. Inside the outer ditch the LOI results showed a peak in its uppermost deposit (deposit 1 in Figure 7-29). This was a layer of slightly darker and more clayey and siltier sandy loam which contrasted fairly well with the reddish glacial subsoil exposed during the stripping of the topsoil. This contrast faded away as this deposit dried but was revealed again if moistened. The concentration of organic matter here, possibly, produced by the increased biomass of deeper roots from the crops, may be linked with the higher capacity of this deposit to retain moisture.

The OSL results were expected: an increase dose rate with depth towards earlier sedimentary deposits. The samples from deposit 2 (Figure 7-29) of the outer ditch gave similar values suggesting the rapid infill of the ditch enclosure, rather than a slow silting process. Interestingly, the uppermost sample (1 in Figure 7-29) and the lowest sample (3 in Figure 7-29) both gave lower values than the baulk ditch deposit 2. These lower values could be related to: a higher degree of bleaching of the luminescence signal because of the exposure of the subsoil and parent material to daylight (Rhodes 2011) during the ditch construction (3 in Figure 7-29); the attenuation of part of the ionizing radiation by water content (Aitken 1985) which may explain the lower values from the uppermost sample (1 in Figure 7-29), correlating with the LOI peak and water moisture retention observed in the texture analysis.

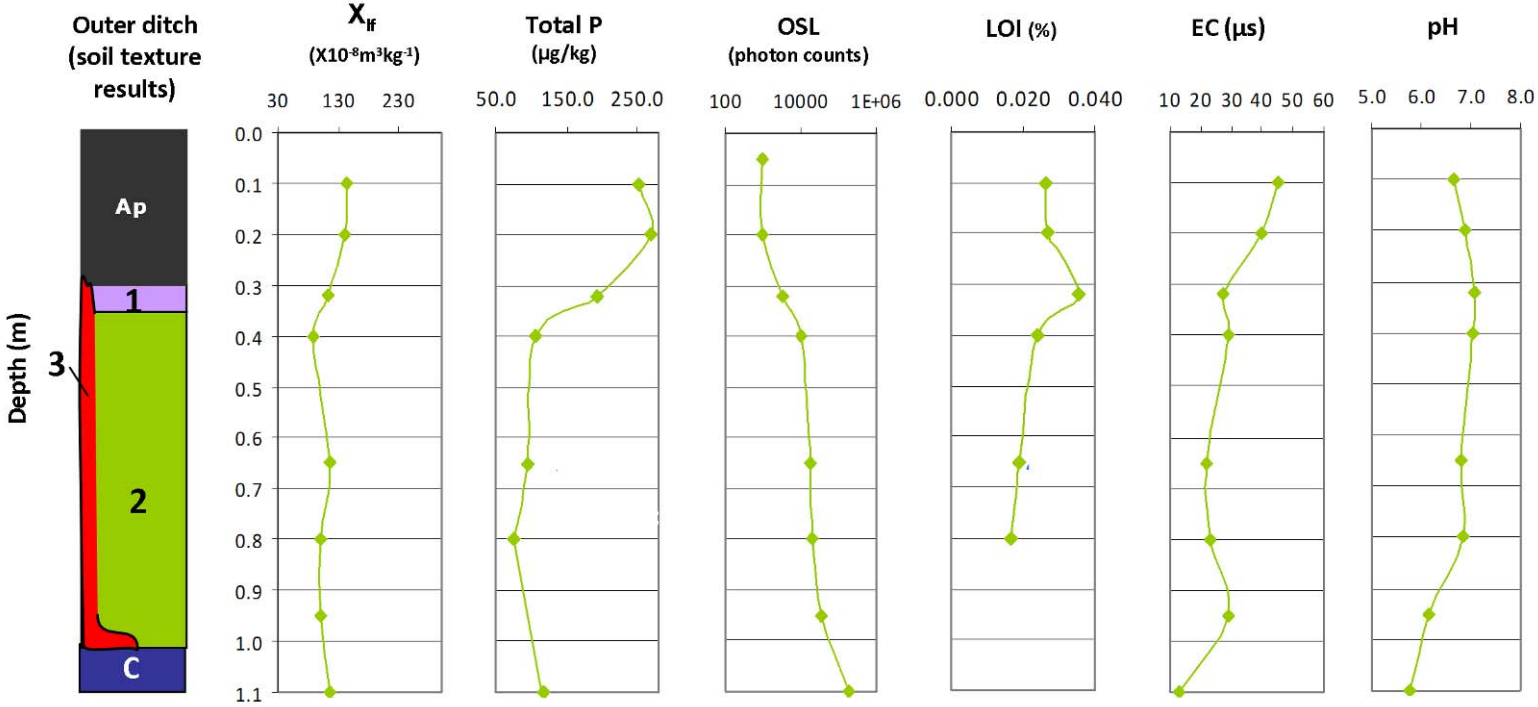

Figure 7-36: Soil texture, magnetic susceptibility (χ_{lf}), total phosphate (Total P), luminescence signal (OSL-BLSL=blue light), loss on ignition (LOI), conductivity (EC) and pH values versus depth for the samples collected during the excavation of the outer ditch (section 1) at Forteviot. The soil samples 3 to 7 were collected inside the ditch. Table 7-8 describes the major soil horizons and deposits identified in the soil texture analysis.

	Depth (m)	χ_{lf} ($10^{-8}m^3kg^{-1}$)	Total P µg/kg	OSL (BLSL) (Photon counts)	LOI (%)	EC µs	pH
Section 1	0.10	144	252	979	0.027	45	7
	0.20	139	268	939	0.027	40	7
	0.32	112	194	3257	0.036	27	7
	0.40	89	105	10333	0.024	29	7
	0.65	116	96	17898	0.019	22	7
	0.80	102	76	19593	0.016	23	7
	0.95	101	*	34656	*	29	6
	1.10	116	118	187039	*	13	6
	Mean	115	158	34337	0.025	29	7
	S.D	19	79	62765	0.007	10	0
	C.V	16	50	183	27	36	7

Table 7-15: Magnetic susceptibility (χlf), total phosphate (Total P), luminescence signal (OSL-BLSL=blue light), loss on ignition (LOI), conductivity (EC) and pH results of the vertical samples collected during the excavation of the outer ditch (Section 1).

7.3.3.4.2. *pXRF (Figure 7-37 and Table 7-16)*

The ditches were enhanced in Mn and, to a lesser extent in Ti, in accordance with the superficial results. There was a characterict trough showing a depletion of Mn in the sample that gave a LOI peak (Figure 7-36). Since Mn oxides are more reactive to organic compounds than Fe oxides, depletions in Mn can occur in environments where Mn is abundant (Lovley *et al*. 1991). The enhancement of Mn inside the ditch could be related to the remains of the palisade of large timber posts (at least *c*.0.30 Ø) which may have supported the outer ditch (James and Gondek 2010). Whilst the excavators suggested that the posts were deliberately removed rather than left to rot *in situ*, charcoal fragments were noted during excavation of the fills of these post-holes indicating a burning event. It is noteworthy that Mn has been reported in association with burning (Wilson *et al.* 2008). There was no enrichment of other common anthropogenic trace elements in the ditch deposits, nor other major vertical differences in the concentration of major elements.

Taking into account: the enrichment in Mn inside the outer ditch, possibly associated with burning which may have led to a MS enhancement; the similar Fe content of topsoil and ditch deposits; and the almost identical soil texture of subsoil/parent material and the baulk ditch deposit (2 in Figure 7-29 and Table 7-8), it is intriguing to observe the lower MS in the ditch deposits and higher values in the topsoil and subsoil.

According to Weston (2002, 213), prolonged waterlogged conditions could impede the transformation of the iron oxides/hydroxides into highly ferrimagnetic dehydrated forms affecting the MS of initially enhanced soils. Also, Fe can change from ferric (Fe(III)) to ferrous (Fe(II)) forms which are more soluble and once in solution, can be redistributed within the profile or leached out.

Whist the soils at Forteviot are characterised by a high drainage capacity, the higher capacity of the outer ditch to retain moisture, seen in the depletion of Mn in deposit 1 (Figure 7-37) and in the LOI peak (Figure 7-36), may have contributed to mineralogical changes in Fe-oxides and thereby, the lower susceptibilities. Further mineralogical changes inside the outer ditch may be suggested by the enrichment in Ti.

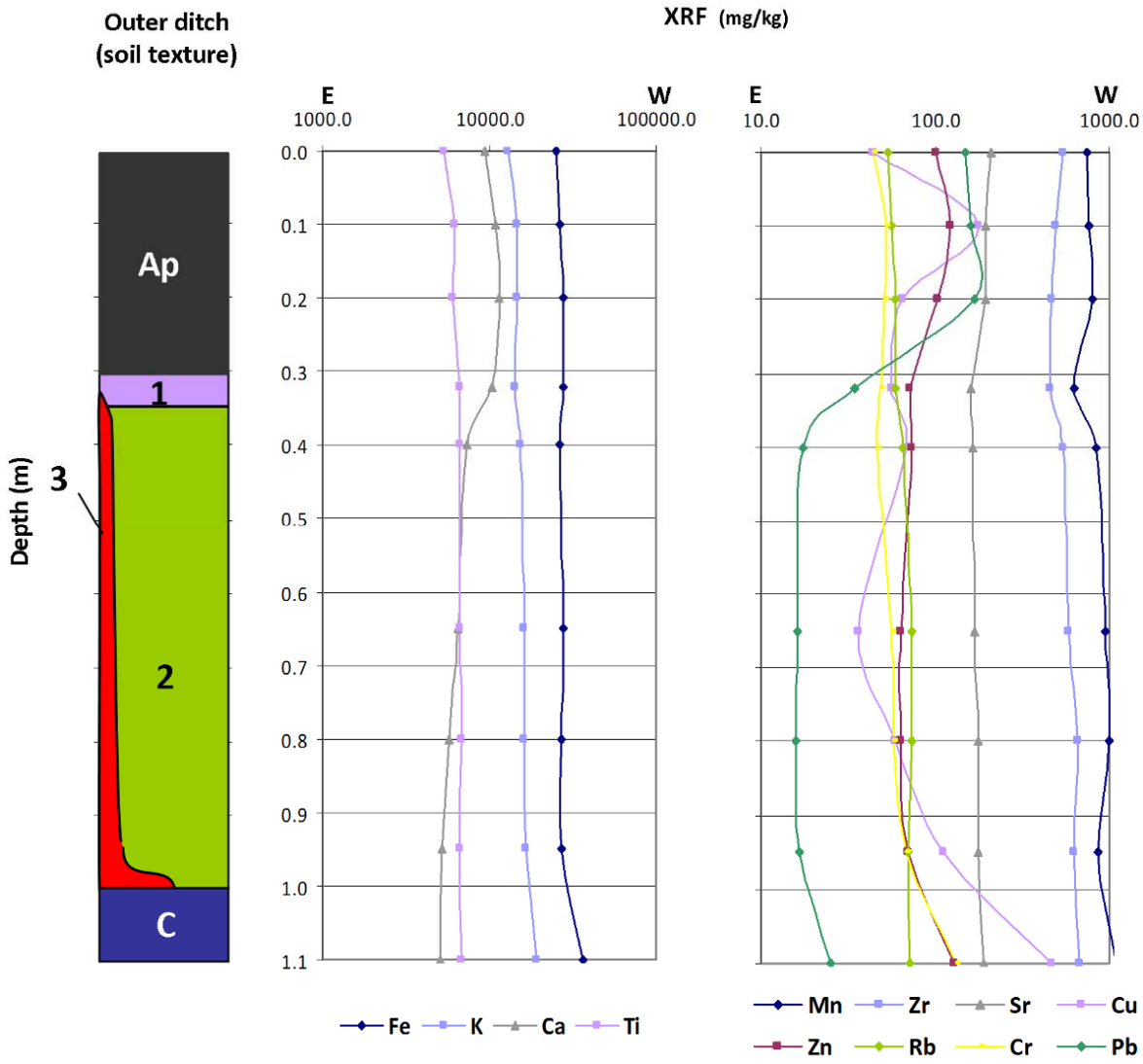

Figure 7-37: Soil texture and distribution of element concentrations (pXRF data) versus depth for the samples collected during the excavation of the outer ditch (Section 1 in Figure 7-28) at Forteviot.

	Distance (m)	Fe	K	Ca	Ti	Mn	Zr	Sr	V	Cu	Zn	Rb	Cr	Pb
Section 1	0.10	26366	14789	10967	6205	770	497	194	112	177	123	56	53	161
	0.20	27941	14756	11487	6105	797	474	195	134	66	103	59	51	170
	0.32	27814	14121	10422	6598	628	458	161	130	57	72	59	48	34
	0.40	26265	15347	7287	6580	841	541	166	128	68	74	65	46	18
	0.65	27962	16209	6458	6675	944	590	169	123	36	64	74	57	16
	0.80	27020	16271	5785	6837	1002	660	176	121	60	64	74	58	16
	0.95	27291	16677	5222	6689	856	635	179	140	113	70	71	68	17
	1.10	36104	19184	5137	6855	1114	670	191	168	468	130	71	133	25
	Mean	28346	15919	7846	6568	869	566	179	132	131	87	66	64	57
	S.D.	3205	1587	2682	275	150	85	13	17	143	27	7	28	67
	C.V.	11	10	34	4	17	15	7	13	110	31	11	44	118

Table 7-16: pXRF results of the vertical samples of the outer ditch (Section 1) at Forteviot. The element concentrations are expressed in mg/kg (=ppm).

The samples collected across the exposed section of the outer ditch (horizontal samples in Figure 7-38) showed a greater variation in elemental composition (Figure 7-38). Viewed in section, the 'collapse' of material from the steep cut of the outer ditch (3 in Figure 7-29; see also Figure 7-38) had collected at its base and inner most cut. The sands and gravels at this interface (Deposit 3) were also well-cemented. The change in soil texture (cementation) may have related to mineralogical changes at Deposit 3 and showed high variability of the chemical concentrations at this place. This cut was at a greater angle than the outermost cut (Figure 7-39). Deposit 2 (Figure 7-29) was fairly similar in colour and texture to the subsoil and parent material (B and C in Figure 7-29).The RDP contrast between the subsoil and these more cemented gravels may have caused the strong reflections seen towards the innermost side and base of the outer ditch (Figure 7-25). The shape of the wider angle of the outermost side of the ditch was also distinguishable in some radargrams (GPR Line 4 and 3 in Figure 7-25).

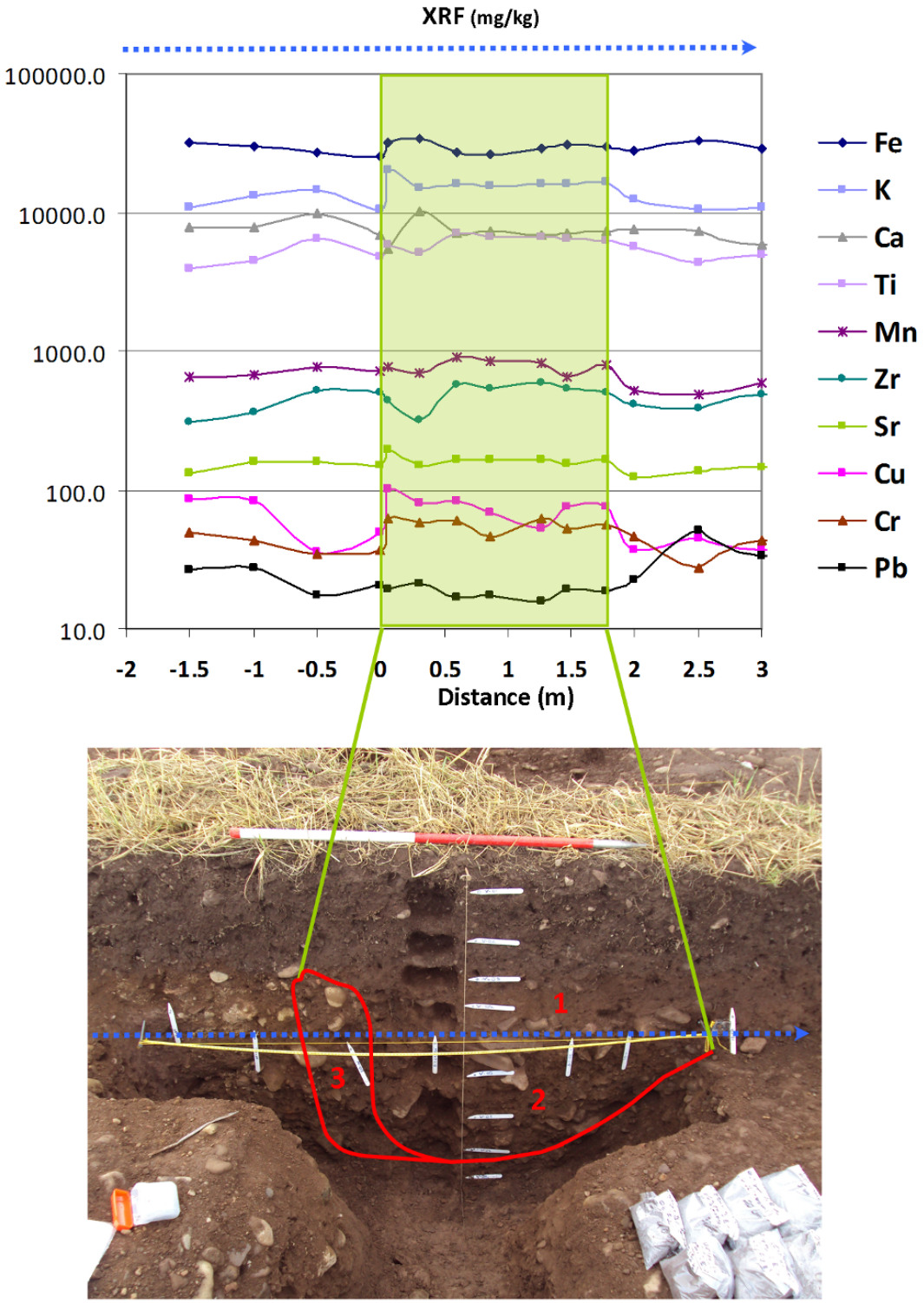

Figure 7-38: Distribution of soil element concentrations (pXRF data) versus distance for the horizontal samples collected during the excavation of the outer ditch at Forteviot. The samples collected inside the outer ditch are highlighted in green. The cross-section of the outer ditch and its deposits (1-4) are shown in red, and described in Table 7-8.

7.3.3.4.3. *ICP-OES (Figure 7-39 and Table 7-17)*

The results of the ICP-OES analysis confirmed the XRF findings. Furthermore, the strong depletion in P and Mg inside the ditch correlated with the total P. The fixation of P in soils is related to the presence of organic matter and influenced by land management (e.g. P content in fertilisers and therefore its high concentration in the topsoil). Whilst the P levels seem to increase in the C horizon (Figure 7-39) rather than by leaching of P through the ditch deposits, the depletion may have been produced by plant (crops) uptake. P and Mg are important plant macronutrients and their uptake by plants can be increased with increased moisture content (He *et al.* 2002). Therefore, P and Mg depletion inside the ditch would indicate the higher water content of the ditch deposits.

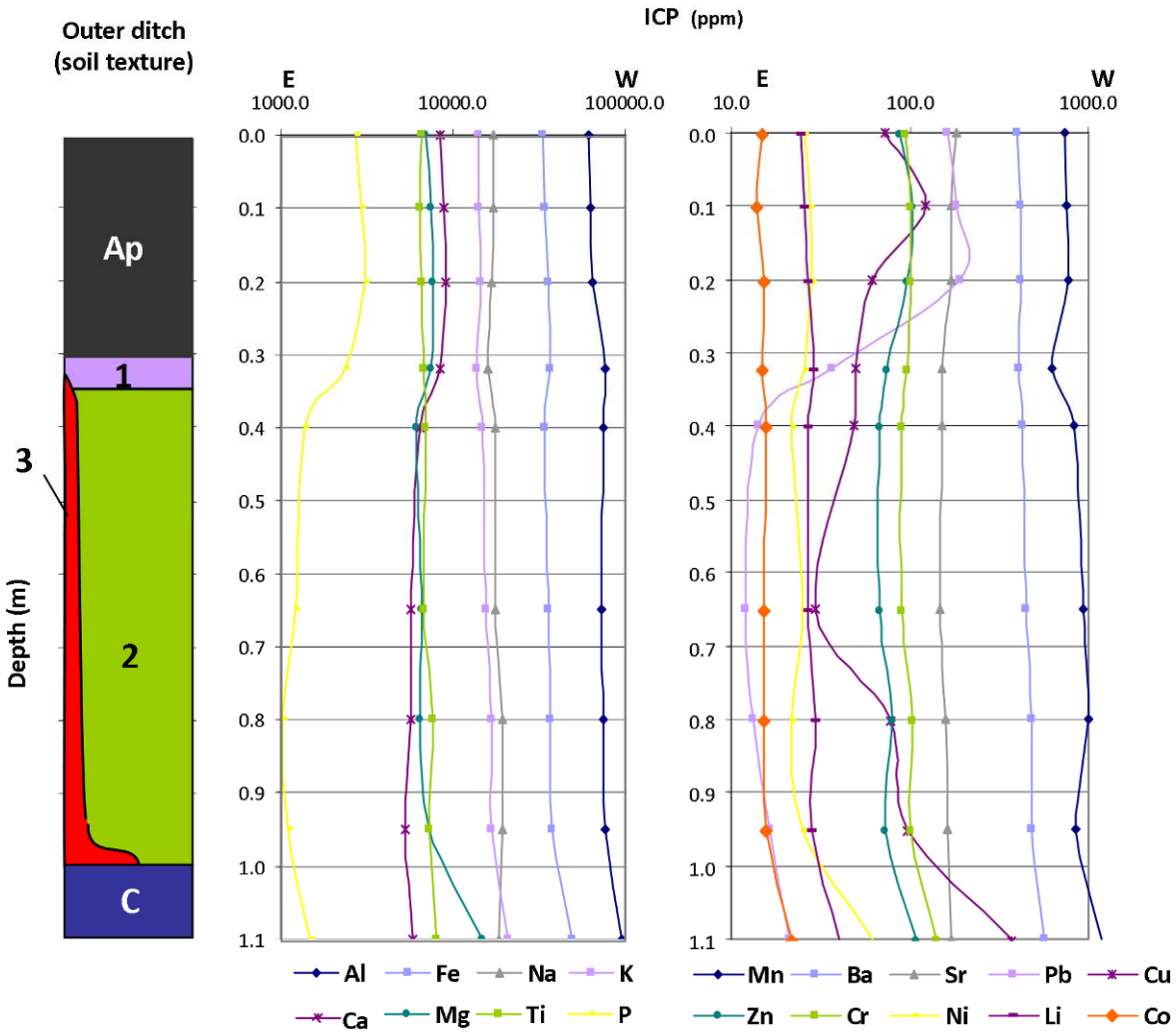

Figure 7-39: Soil texture and distribution of element concentrations (ICP-OES data) versus depth for the samples collected during the excavation of the outer ditch (Section 1) at Forteviot.

	Depth (m)	Al	Fe	Na	K	Ca	Mg	Ti	P	Mn	Ba	Sr	Pb	Cu	Zn	Cr	Ni	Li	Co
Section 1	0.00	61358	32812	17282	13956	8400	6904	6527	2718	733	401	181	161	72	87	94	25	25	15
	0.10	62980	34099	16961	14008	8819	7506	6490	2942	751	418	170	183	122	105	102	28	26	14
	0.20	64935	35559	16892	14405	9001	7667	6563	3081	774	416	171	193	62	97	101	28	27	15
	0.32	76620	36949	16046	13797	8384	7370	6719	2352	621	403	151	37	49	75	98	26	29	15
	0.40	73730	34412	17755	14780	6441	6075	6948	1364	833	430	152	14	49	68	90	22	27	16
	0.65	72787	36143	17470	15415	5760	6632	6832	1221	928	448	149	12	30	68	89	25	27	15
	0.80	74929	36703	19376	16747	5756	6444	7648	1032	1006	486	160	13	79	79	102	22	29	15
	0.95	76313	37264	19314	16821	5237	7218	7311	1100	854	484	163	16	98	72	101	25	28	16
	1.10	94619	48886	18451	20660	5881	14845	8018	1489	1180	567	172	21	367	110	141	61	40	22
	Mean	73141	36981	17728	15621	7075	7851	7006	1922	853	450	163	72	103	85	102	29	29	16
	S.D.	9978	4702	1126	2209	1537	2675	541	841	166	54	11	81	103	16	16	12	5	2
	C.V.	14	13	6	14	22	34	8	44	19	12	7	112	100	19	15	42	16	14

Table 7-17: ICP-OES results of the vertical samples of the outer ditch (Section 1) at Forteviot. The element concentrations are expressed in ppm (=mg/kg).

7.3.4. Conclusions

The general Mn enhancement of topsoil samples indicated the presence of the enclosure before the topsoil stripping. The OSL did not show any coherent enhancement or depletion indicating the enclosure nor the outer ditch. However, it produced a clear depletion over the outer ditch when the topsoil was stripped, confirming the total P and MS results from these samples. Therefore, by using coring techniques, archaeological features such as the outer ditch may possibly be detected by these proxy means.

According to the surface results before stripping, the outer ditch showed Mn enhancement after stripping the topsoil and from the excavated ditch sections. No other trace element was enriched inside the outer ditch. This confirmed Mn enhancement of the topsoil to be related to the outer ditch and possibly a product of ploughed material from inside the ditches of the enclosure.

The outer ditch was characterised by a lower MS than the topsoil or subsoil/parent material (Table 7-18). However, the Fe content of the ditch deposits was, on average, close to the surrounding soil matrix (Table 7-19 and Table 7-20), indicating that the change in MS may be caused by changes in mineralogy. The higher organic content identified in the uppermost deposit of the outer ditch (Table 7-18) and consequent higher moisture retention at this place, may be associated with possible redox reactions product of water retention and possible transformations of ferric material to less magnetic ferrous

forms (Weston 2002). This effect may have contributed to the lower MS detected from the outer ditches.

The strong correlation between the results from the ICP-OES and pXRF analysis confirmed the elemental characterisation of the soil samples at Forteviot.

Sampling			χ_{lf} ($10^{-8}m^3kg^{-1}$)	Total P (µg/kg)	OSL (Photon counts)	LOI (%)	EC (µs)	pH
Mean	Pre-Stripping	On-site	144	242	7675	0.029	53	7
	Post-Stripping	On-site	158	194	67652	0.032	23	7
	Outer Ditch	On-site	107	158	34337	0.047	29	7
	Controls	Off-site	151	271	4527	0.028	*	*
S.D	Pre-Stripping	On-site	6	27	6028	0.002	16	0
	Post-Stripping	On-site	50	56	71691	0.011	9	0
	Outer Ditch	On-site	23	79	62765	0.060	10	0
	Controls	Off-site	8	2	21	0.000	*	*
CV	Pre-Stripping	On-site	4	11	79	5.5	30	2
	Post-Stripping	On-site	32	29	106	33.8	39	4
	Outer Ditch	On-site	22	50	183	127.1	36	7
	Controls	Off-site	5	1	0	1	*	*

Table 7-18: Descriptive statistics of the magnetic susceptibility (χ_{lf}), total phosphate (Total P), luminescence signal (OSL- BLSL=blue light), loss on ignition (LOI), conductivity (EC) and pH results of the horizontal samples collected at the ditch enclosure (Forteviot).

Sampling/XRF			Fe	K	Ca	Ti	Mn	Zr	Sr	Pb	Cu	V	Zn	Rb	Cr
Mean	Pre-Stripping	On-site	26416	13189	9416	5653	791	543	206	169	126	116	112	57	45
	Post-Stripping	On-site	28670	12316	6690	4995	806	499	161	39	57	109	70	66	44
	Outer Ditch	On-site	28346	15919	7846	6568	869	566	179	57	131	132	87	66	64
	Cist	On-site	30681	15110	8297	5665	1028	520	187	76	81	134	93	57	65
	Controls	Off-site	26014	12608	8517	5336	749	356	193	173	55	105	103	57	37
S.D	Pre-Stripping	On-site	884	1175	1092	524	45	31	11	24	77	17	15	2	7
	Post-Stripping	On-site	3336	2135	1299	817	306	86	17	34	23	26	12	11	9
	Outer Ditch	On-site	3205	1587	2682	275	150	85	13	67	143	17	27	7	28
	Cist	On-site	6101	370	1769	709	313	145	9	92	24	16	22	5	20
	Controls	Off-site	759	1654	1036	701	26	251	7	80	11	20	10	1	5
CV	Pre-Stripping	On-site	3	9	12	9	6	6	6	14	61	15	13	3	16
	Post-Stripping	On-site	12	17	19	16	38	17	10	88	40	24	17	16	20
	Outer Ditch	On-site	11	10	34	4	17	15	7	118	110	13	31	11	44
	Cist	On-site	20	2	21	13	30	28	5	121	30	12	23	9	31
	Controls	Off-site	3	13	12	13	3	70	4	46	21	19	10	3	14

Table 7-19: Mean, standard deviation (S.D) and coefficient of variation (C.V) of the pXRF results of the samples collected at the ditch enclosure (Forteviot).

Sampling/ICP		Al	Fe	Na	K	Ca	Mg	Ti	P	Mn	Ba	Sr	Pb	Cu	Zn	Cr	Ni	Li	Co
Mean	Pre-Stripping	62983	34052	16583	14016	8440	7363	6507	2991	786	410	177	183	115	101	94	28	26	15
	Post-Stripping	71821	37052	15369	14259	6540	8400	6178	2232	689	390	139	27	61	72	95	32	27	15
	Outer Ditch	74614	37502	17783	15829	6910	7970	7066	1822	868	457	161	61	107	84	103	30	29	16
	Cist	78560	39952	17739	16445	6226	6969	7227	1745	843	465	151	14	31	80	96	24	29	15
S.D	Pre-Stripping	1838	1197	649	444	398	302	209	202	41	13	7	28	64	10	7	2	1	1
	Post-Stripping	4669	3971	2094	1377	584	2214	454	728	210	35	15	12	26	8	11	9	2	2
	Outer Ditch	9565	4741	1190	2265	1555	2834	545	841	171	54	10	79	109	17	16	13	5	2
	Cist	6701	2487	1243	534	945	1108	477	686	102	28	7	2	14	3	1	5	0	1
CV	Pre-Stripping	3	4	4	3	5	4	3	7	5	3	4	15	56	10	8	6	4	7
	Post-Stripping	7	11	14	10	9	26	7	33	31	9	11	45	42	11	11	28	6	14
	Outer Ditch	13	13	7	14	23	36	8	46	20	12	6	129	102	20	16	44	16	15
	Cist	9	6	7	3	15	16	7	39	12	6	4	12	44	3	1	21	0	8

Table 7-20: Mean, standard deviation (S.D) and coefficient of variation (C.V) of the ICP-OES results of the samples collected at the ditch enclosure (Forteviot).

7.4. General Discussion

The poor results of the initial gradiometer surveys at Forteviot were caused by the effect of the topsoil and an inadequate survey resolution. The topsoil contained highly magnetic soil and stone derived, by intense ploughing, from the underlying glacial parent material which contributed to the noisy datasets obscuring the contrast between the ditch deposits and surrounding soil. The technique resolved the enclosure by reducing the traverse spacing from the generally recommended 0.5m (English Heritage 2008) to 0.25m.

There was no MS enhancement or enrichment in the common anthropogenic trace elements in the outer ditch deposits. This partially explains the characteristic negative magnetic response instead of the more usual positive response. The working hypothesis is that the ditches at Forteviot are associated with a ritual site and not a settlement and so the ditch deposits were not exposed to a continuous magnetic susceptibility or anthropogenic elemental enhancement as at settlement sites; this factor was also contributing to their negative magnetic responses.

The ditches presented slight depletions in major elements (e.g. Fe), as well as a Mn and Ti enrichment. This indicates mineralogical changes of Fe/Ti-oxides inside the ditch caused by inter-mixed processes involving land management (e.g. ploughing), accumulation of organic matter (e.g. increased root biomass derived from the cropmarks), increased moisture retention and redox reactions. These effects are involved in the relatively low magnetic susceptibility values of the ditch deposits vs. the higher magnetic susceptibility of the topsoil and the even higher magnetic susceptibility of the subsoil (Table 7-18). Therefore, changes in the mineralogical composition of the ditch deposits and their inexistent anthropogenic enhancement are the causes behind the negative magnetic contrast revealed by the ditch features at Forteviot.

The successive failures to complete the earth resistance survey at Forteviot were caused by the stony topsoil (i.e. bad contact of the mobile probes into the ground), as well as its high drainage capacity and close to neutral pH (affecting the current flow into the ground). Ground saturation conditions after a day of

heavy rain were necessary to complete the survey and the detection of a low resistance anomalies revealing a triple cist burial and surrounding ditch. The less truncated character of the outer ditch (in comparison to the inner ditch) and the higher organic matter content measured in its deposits (Table 7-18) explain its higher capacity to retain moisture in comparison to the surrounding soil, hence its detection as a low resistance feature. The results from the 0.5m probe spacing using a 0.5m traverse spacing resolved sharper ditch anomalies than wider geometries. Although the sampling strategy and the necessary moist ground conditions made the survey fairly slow and tedious, the anomalies detected were very informative and greatly complement the gradiometer results.

The GPR survey produced the most informative result as it allowed depth estimation, high resolution mapping and an approximation to the truncation level of the ditches of the targeted enclosure. The correlation of these results and the soil physical and chemical analyses provided key information about the character of the ditch deposits.

The EM38 instrument attached to the GPS provided the most rapid survey. The quadrature component in vertical dipole of the EM38 instrument demonstrates its potential in identifying archaeological features expected at *c.* 0.5-1m, such as at Forteviot, since the noise created by the plough layer was outside the maximum sensitivity range of the instrument. Therefore, this survey may be the best first option to use in more extensive and exploratory surveys at sites such as Forteviot. However, the FDEM results produced the least defined anomalies. A closer traverse spacing (0.5m instead of 1m) could have improved the definition of the weak trends detected.

Repeating geophysical surveys after stripping of the topsoil in preparation for excavation allowed the detection of further and deeper features. This can be used to increase the effectiveness of archaeological excavation by showing potential targets that are not exposed on the stripped surface.

The study also allowed the assessment of the capacities of other geochemical techniques to detect the ditched enclosure. A general Mn enhancement of topsoil samples indicating the location of the enclosure was a useful outcome of

the geochemical survey. Anomalous Mn concentrations associated with burials have been reported in other studies (Oonk *et al.* 2009a). The pOSL showed its potential to detect the outer ditch in samples collected beneath the topsoil and characterise the ditch deposits, thereby validating the information suggested by other analysis (i.e. high energy backfill ditch deposit and reductive conditions in the uppermost ditch deposit).

Chapter 8

Surveying over Clay Soils: the Cropmarks at Chesterhall Parks Farm (South Lanarkshire)

8.1. Introduction

A group of prehistoric ring-ditch enclosures have been recorded on aerial photographs as positive cropmarks at two pasture fields at Chesterhall Parks Farm. The cropmarks have only appeared once or twice in 30 years of continuous aerial reconnaissance at the area (Aqdus *et al.* 2012). In 2000, the site was investigated by the Upper Clyde Valley Landscape Project (UCVLP), a five year research project into the evolution of archaeological landscape in the region. As part of the UCVLP investigation, a series of geophysical surveys and trial excavations were undertaken using gradiometry and earth resistance techniques. The geophysical results were fairly poor and inconclusive in terms of resolving the ditches revealed by the cropmark evidence (Sharpe 2004, 181).

8.1.1. Research Problem

The UCVLP excavation recorded poorly drained clay topsoil and subsoil at the site, although the area is mapped as containing freely drained brown soil (Macaulay Institute for Soil Research 1984). It is commonly known that clay deposits and associated waterlogged soil conditions can present challenges for geophysical surveying (English Heritage 2008, 16-17). For example, the high conductivity of clay soils may affect the earth resistance surveys by the blanketing effect of moisture saturation of archaeological features and soil matrix. Some types of clay soil may drastically attenuate the penetration and reflection of the GPR signal, hence preventing the detection of archaeological features. Therefore, are geophysical techniques of any use at a clay site such as Chesterhall Parks Farm? Further to the research undertaken by Sharpe (2004), this case study aimed to test other routine geophysical and geochemical techniques to detect the enclosures and assess their usefulness in such a clay survey environment.

8.1.2. Location

Chesterhall Parks Farm is located in south Lanarkshire, between Wiston and Biggar (Figure 8-1), and stands at the south side of the main A73 Ayr to Edinburgh road. The farm is owned by the Maxwell-Stuarts of Lamington and tenanted by Mr William McGregor.

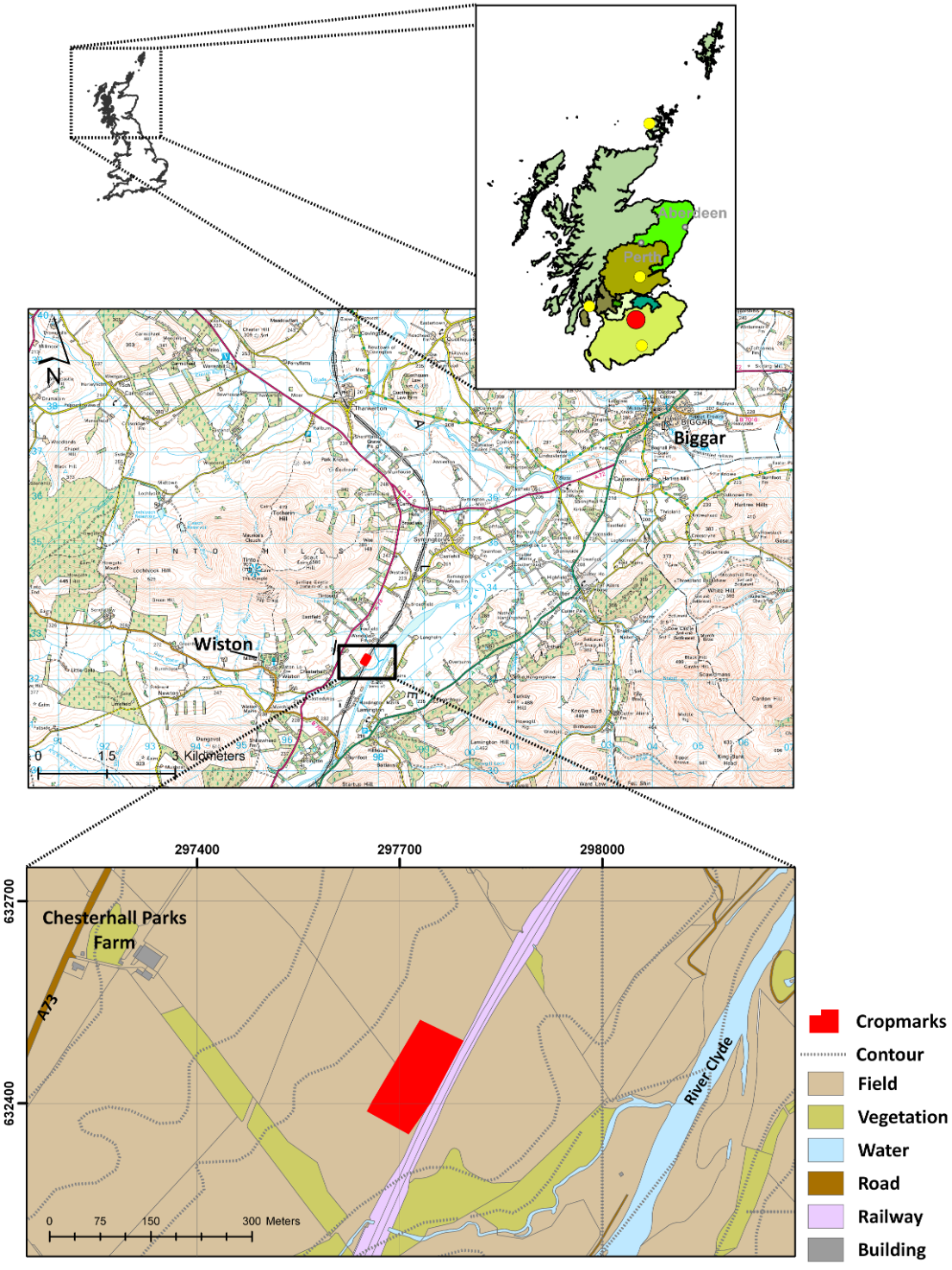

Figure 8-1: Location (top) of Chesterhall Parks Farm in relation to the other case study sites (yellow dots). The middle map shows the location of the farm and the cropmarks site between Wiston and Biggar. In the bottom map, the position of the cropmarks area is shown in red (based on © Crown Copyright/database right 2012. An Ordnance Survey/EDINA supplied).

The cropmark site lies near Tinto Hill, in a terrace above the present river Clyde flood plain. The two fields containing the cropmarks (Figure 8-2) are centred at NGR NS 977 324, to the south east of the farm buildings. At the NW of the site the land rises quite steeply up to a second terrace (Figure 8-3).

Figure 8-2: Oblique photograph of the cropmarks at Chesterhall Park farm (in red) showing five interlocking enclosures. To the east there is a wide-ditched oval settlement enclosure (Hardington Mains) (© W.S. Hanson, 1989).

Figure 8-3: NW (a) and SE (b) view of the site area showing Tinto hill in the background (a) and the rail way embankment (b) (based on L. Sharpe photographic archive).

An area at the west of the cropmarks and the southernmost area of the site get continuously waterlogged showing the poor drainage conditions of the soil. The main railway line linking Scotland and England runs along the SE edge of the cropmarks fields, in a quite steep embankment. The embankment position suggests that the enclosures may have been partly destroyed during the railway construction. The land gently rises up onto a small rounded hillock around 100m to the south of the enclosures. From here a small burn, the Garf Water, passes beneath the railway, and runs past another enclosure at Hardington Mains which lies to the east of the railway line (Figure 8-2).

8.1.3. Geology, Soils & Land Cover

8.1.3.1. **Bedrock & Superficial Deposits**

The underlying geology at the site is the Wiston Grey Volcaniclastic Sandstone Member of the Auchtitench Sandstone Formation (Old Red Sandstone super-group) (British Geological Survey 2012c). These are fine-to coarse-grained volcaniclastic sandstones of greenish grey ashy colour, *c.*1000m thick and of early Devonian age (Browne *et al.* 2002). They are composed of angular to sub-angular basaltic, andesitic and occasionally, dacitic volcanic rock fragments (Phillips 2007). The superficial deposits at the site consist of Clyde Valley fluvioglacial deposits (gravels, sands and silts) of the Quaternary period.

8.1.3.2. **Soils**

The soil at the site consists of deep and poorly drained heavy clay which generates frequent waterlogged conditions. However, the Scottish Soil Maps of the Macaulay Institute classified the soils here as sandy and well drained sandy brown earths (Symington series). Sharpe (2004, 179) noted the heavy clay topsoil with a thick clay subsoil layer.

8.1.3.3. **Land Cover**

The site area is used as a pasture field and it has been very occasionally ploughed. Since the land is continuously waterlogged, much drainage work has been undertaken (Sharpe 2004, 179) and one drainage exit was observed at the SW of the site.

8.1.4. Archaeological Background

The enclosures (NMRS NS93SE 34) are all circular, varying in size and in the number of ditches that surround them, with the smaller enclosures tending to have fewer ditches (Figure 8-4). The geophysical survey carried out by the UCVLP recorded a total of 22 survey grids (each 20m x 20m) using gradiometry and earth resistance and 1m traverse spacing resolution. The two or three positive cropmarks revealing the ditches of enclosure 1 (Figure 8-5) were not resolved by geophysical means (Figure 8-6). Only a series of dipolar magnetic anomalies were detected in the interior of enclosure 1 (Figure 8-5) which Sharpe (2004, 183) noted as "*typical magnetic response from habitation sites in Clydesdale*" (Figure 8-7). The outer ditch of the double ditched enclosure (2 in Figure 8-5) was detected as two large patches of low resistance to the west and a smaller low-resistance anomaly to the east. The single ditch of enclosure 3 (Figure 8-5) was not detected at all by geophysical means. Other single ditches (such as enclosure 4 and 5 in Figure 8-5) were revealed aerially as positive single ditch cropmarks with associated dipolar magnetic anomaly.

The archaeological trial excavation focussed on enclosures 1, 2 and 4 (Figure 8-5). During the excavation, the poor drainage capacity of the heavy clay soil resulted in the regular waterlogging of the trenches: "*up to a metre of water after overnight rain*" (Sharpe 2004, 179). The excavation confirmed the positive cropmarks of these enclosures to be due to deep ditches (Figure 8-8). The finds included large amounts of cremated bone from the floor layer in enclosure 2 (Figure 8-5) and metal working or smelting evidence within enclosure 4 (Figure 8-5) including lead slag and ore, in-situ burning with some burnt wood remaining in section (Sharpe 2004, 186). These finds showed that the random noise of a dipolar nature were indicating habitation areas and, in combination with the morphology of the enclosures, a probable Iron Age date was established for the site (Sharpe 2004, 186).

Bulk soil samples were collected from each context during the excavation of enclosure 2 (Figure 8-5) to analyse chemical concentrations. The ditches showed enrichment of Zn, S, Ca and P and depletions in many other elements. There was also a Ca enrichment inside the enclosure which probably was consequence of

the incorporation of large quantities of burnt bone in the floor (Figure 8-5) (Sharpe 2004, 302).

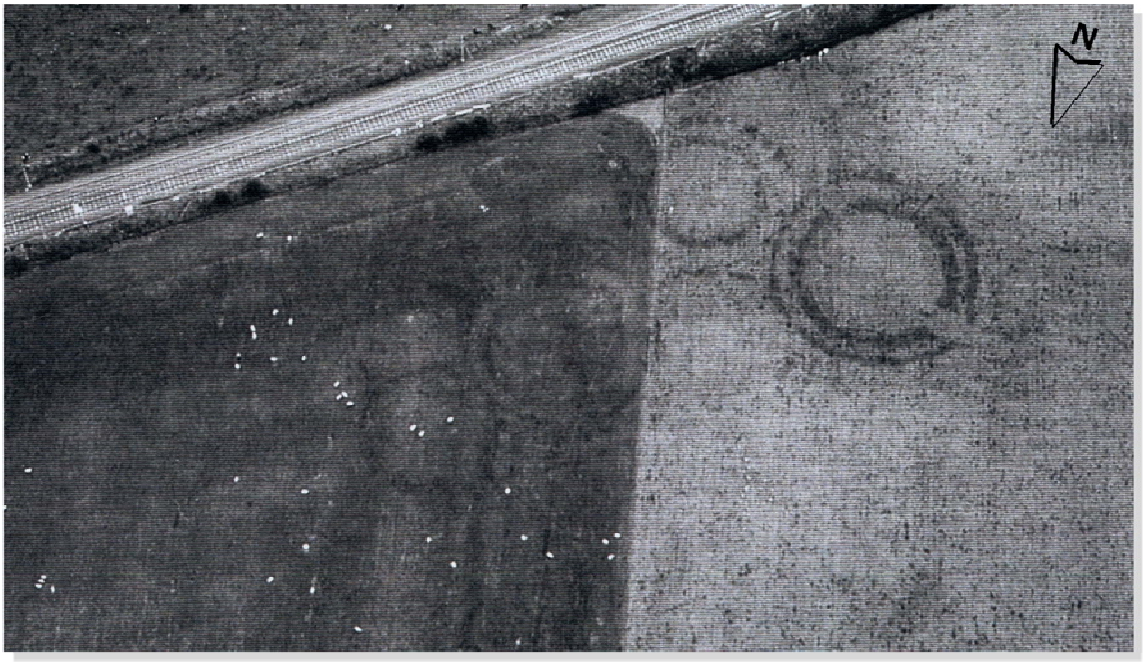

Figure 8-4: Aerial photograph showing the positive cropmarks related to the ditches of the enclosures at Chesterhall Parks Farm (© W.S. Hanson).

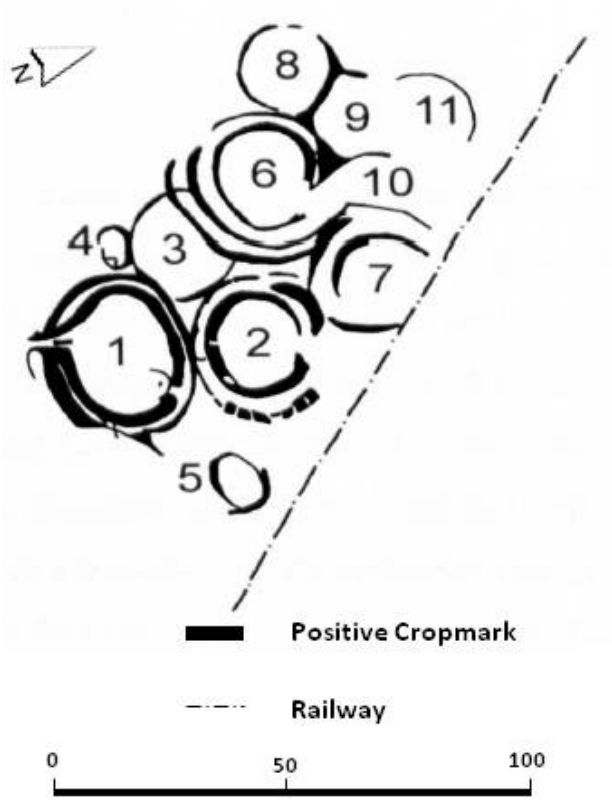

Figure 8-5: Cropmarks transcription taken from aerial photographs showing the numbers assigned to the enclosures at Chesterhall Parks Farm (Sharpe 2004, 180).

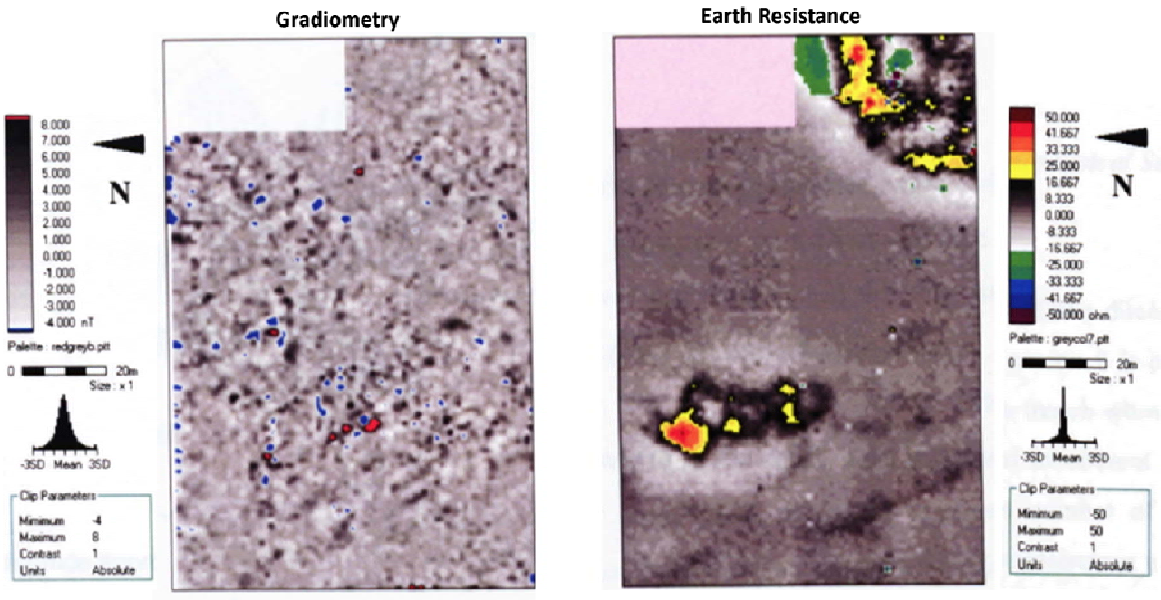

Figure 8-6: Results of the gradiometer and earth resistance survey by the UCVLP at Chesterhall Parks Farm in 2000 (Sharpe 2004, 182).

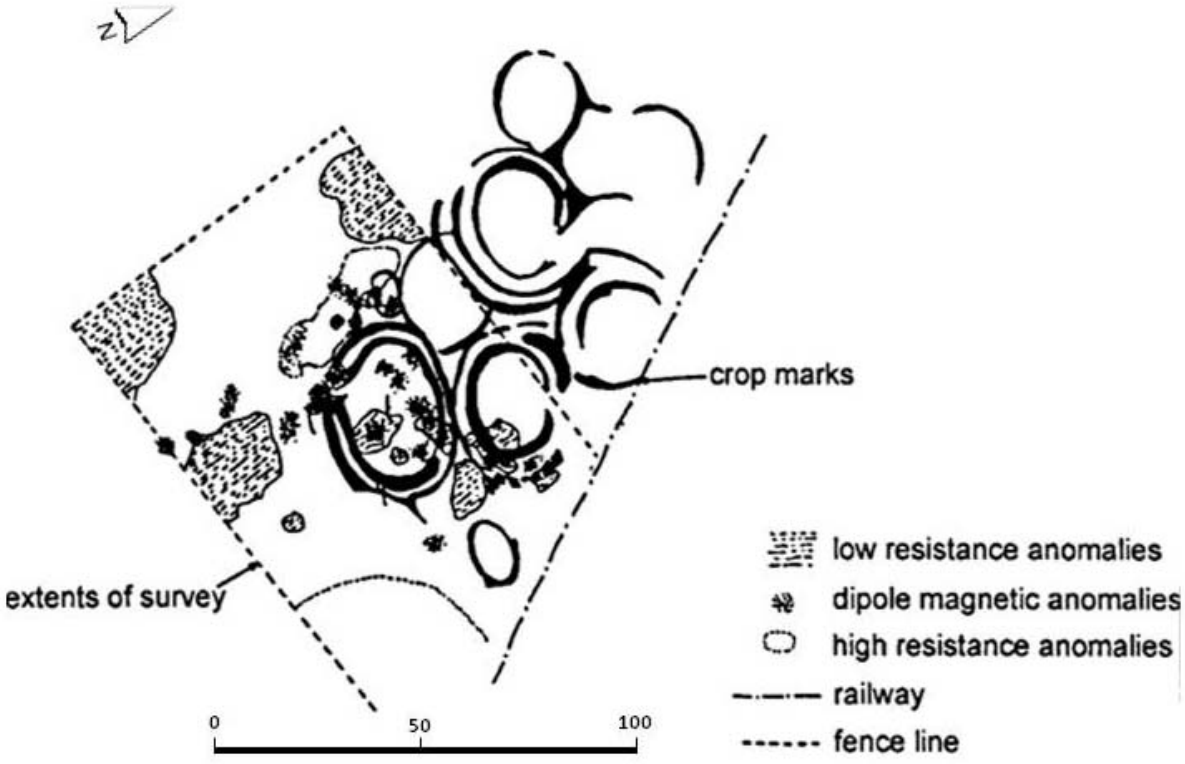

Figure 8-7: Interpretation of the geophysical surveys by the UCVLP at Chesterhall Parks Farm in 2000 (Sharpe 2004, 183).

Figure 8-8: Ditch exposed (enclosure 2) and heavy clay soil (inset) at Chesterhall Parks Farm (based on L. Sharpe photographic archive).

8.2. Geophysical Survey

8.2.1. Aim & Objectives

The aim of the survey was to detect the enclosures (1, 2, 3 and 4 in Figure 8-5) using a multi-technique approach (gradiometry, earth resistance, FDEM and GPR). The objectives were to assess the results of FDEM and GPR surveys at a

clay survey environment, and to repeat gradiometry and earth resistance surveys using a finer sampling strategy than in 2000.

8.2.2. Survey Area & Data Collection

Prior to the geophysical survey, the field containing the westernmost group of cropmarks was surveyed with the GPS Leica 1200 system. The aim was to map several topographical features of interest such as the continuously waterlogged areas, the hillock near the embankment and other small rises of the ground.

A total of nine 20m x 20m grids were surveyed with the gradiometer (Figure 8-9). The data was collected in a parallel mode and using a 0.5m traverse spacing. After the extensive gradiometer survey, four grids were surveyed again with the earth resistance meter and EM38 instrument (Figure 8-9). The earth resistance had to be postponed several times because of very wet weather. Eventually, the grids were surveyed using 0.5m traverse spacing (Table 8-1) during a sunny day and superficial dry soil conditions. The background readings were fairly low (*c*.24 ohm) and constantly drifted. This temperamental behaviour may have been produced by topsoil saturation since the previous day the fieldwork had been, again, cancelled due to heavy rain. The FDEM survey was carried out during a wet day and using a 0.5m traverse spacing. Several single GPR lines were recorded (Figure 8-9) in order to detect the ditches of the enclosures 1, 2 and 3 (Figure 8-5) and to test the penetration of the signal. A pilot GPR survey was carried out over the ditches of enclosure 1 and 2 (Figure 8-5). Further details about the survey parameters used at the site are summarised in Table 8-1.

The surveys were carried out during eight days between April and September (2010), in generally wet to variable weather conditions. The mean minimum/maximum temperatures for April and September 2010 recorded at the Eskdalemuir weather station were 1.6/11.7 and 7.8/15.9°C respectively. The total rain fall was of 74.5mm in April and 151.6mm in September (Met Office 2012).The almost daily sporadic showers experienced at the site in May and September, even when it was sunny elsewhere, may have been caused by the proximity of Tinto Hill (711m) which makes of this area a fairly wet place.

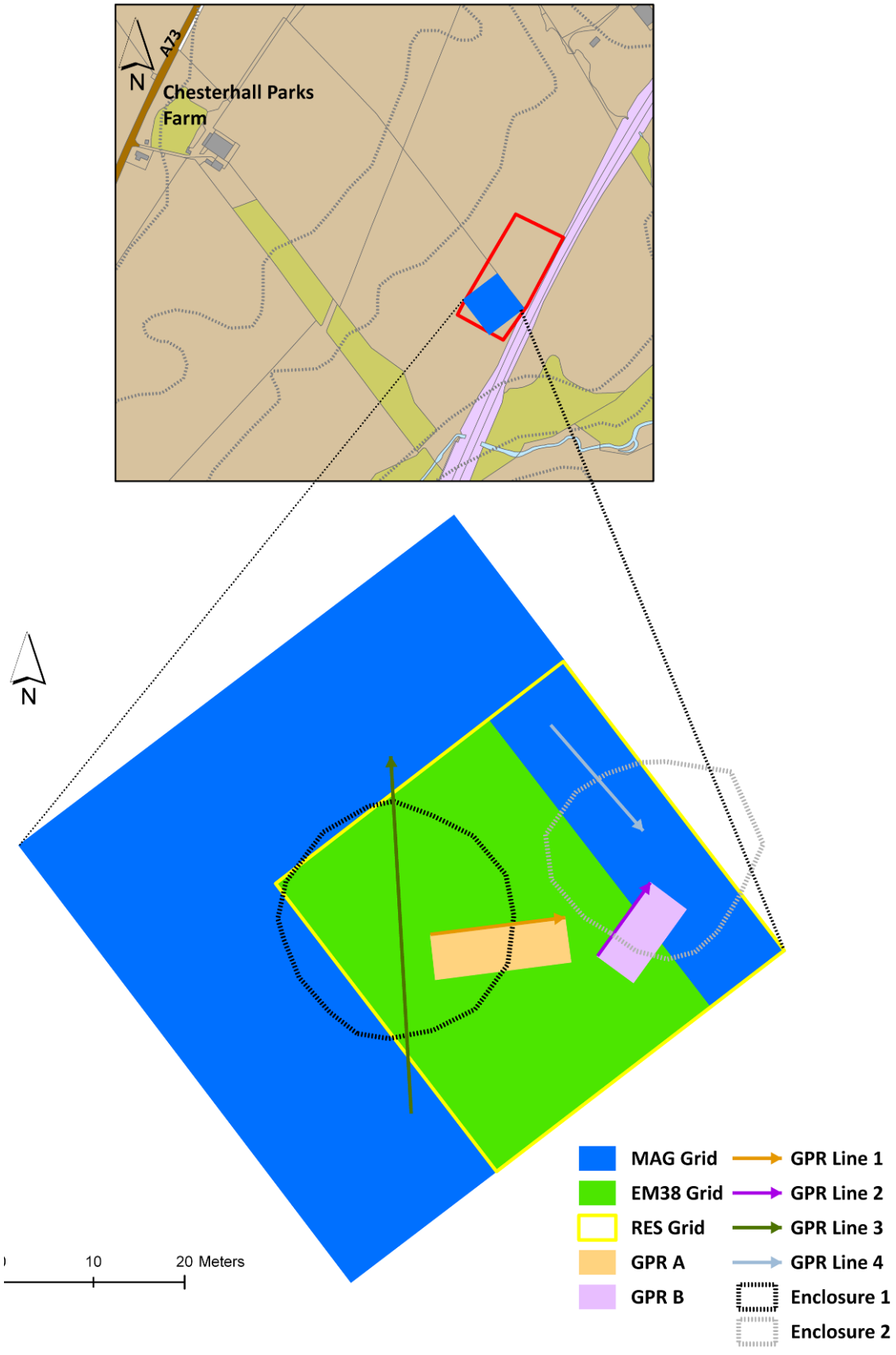

Figure 8-9: Grid location of the geophysical surveys carried out at Chesterhall Parks Farm.

Technique	Date	Instrument	Traverse Spacing	Sampling Interval	Survey Mode	Other
Gradiometry	28-29/04/2010	Bartington Grad 601-2	0.5m	0.125m	Parallel traverses.	Lower sensor *c* . 20cm above the surface & 0.03nT/m (resolution).
Earth Resistance	14 and 23/09/2010	Geoscan RM15 (0.5 mobile probe spacing)	0.5m	0.5m	Zig-zag traverses.	x1 range (sensitivity range).
GPR-450 MHz	21/09/2010	Sensors & Software PulseEKKO 1000	Single traverses	0.05m	Continuous mode, time window=60ns, stacks=16, samples=200ps.	An average velocity used during collection for real-time data visualisation= 0.08m/ns.
GPR-225 MHz	21/09/2010			0.10m	Continuous mode, time window= 100ns, stacks=16, samples=400ps.	
3D GPR-450 MHz (GPR A & B)	22-23-24/09/2010		0.25 (GPR A)/0.5 (GPR A & B)	0.05m	Continuous mode, time window=60ns, stacks=16, samples=200ps.	
GPR-225 MHz (GPR A)	23/09/2010		0.5m	0.10m	Continuous mode, time window= 100ns, stacks=16, samples=400ps.	
EM 38	22/09/2010	Geonics EM 38	1m		Parallel traverses, vertical mode & in-phase and quadrature components logged.	The instrument was connected to a GPS (RTK).

Table 8-1: Instrument settings used during the multi-technique geophysical survey at Chesterhall Parks Farm.

8.2.3. Gradiometry Results

The raw and processed data of the gradiometer survey are plotted in Figure 8-10 and Figure 8-11 respectively. The high range of the unclipped raw data (100nT to -100nT) was caused by superficial ferrous objects. The easternmost area of the grid was not surveyed to avoid the interference of a metallic fence. Once the data processing was done (Table 8-2) the general gradient range was -10nT to 13nT. The results of the gradiometer survey were characterised by some magnetically noisy areas to the N and E of the grid and a less noisy area to the W-SW. A group of fragmented and concentric weak positive magnetic anomalies

revealed the targeted cropmarks in a fragmented manner. Other areas relating to the enclosures showed a certain degree of magnetic enhancement.

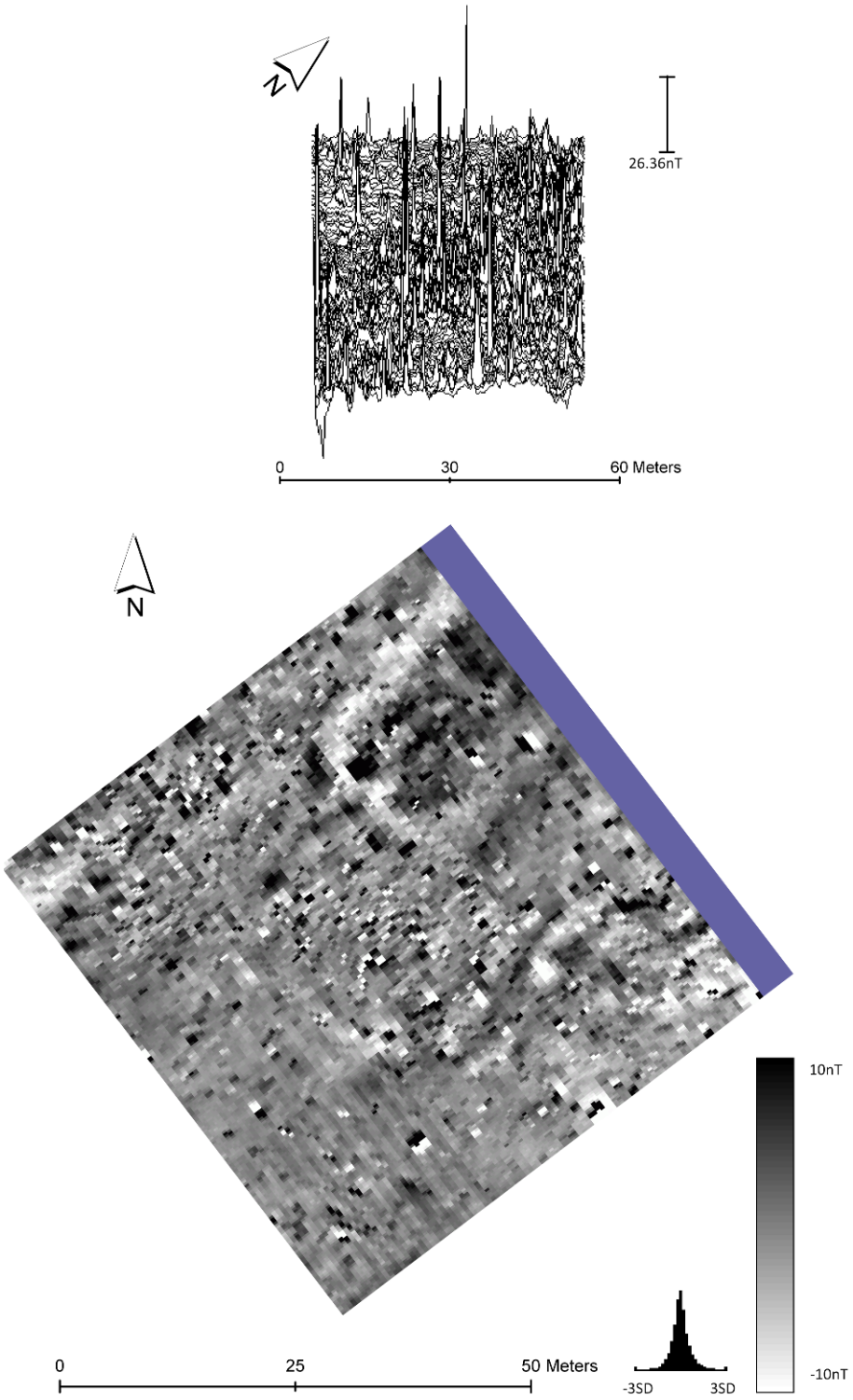

Figure 8-10: Shade (bottom-left) and trace plot (top-right) of the raw data results of the gradiometer survey at Chesterhall Parks Farm. The data was plotted at -10/10 Absolute units, contrast 1 and using the Geoplot grey99 palette.

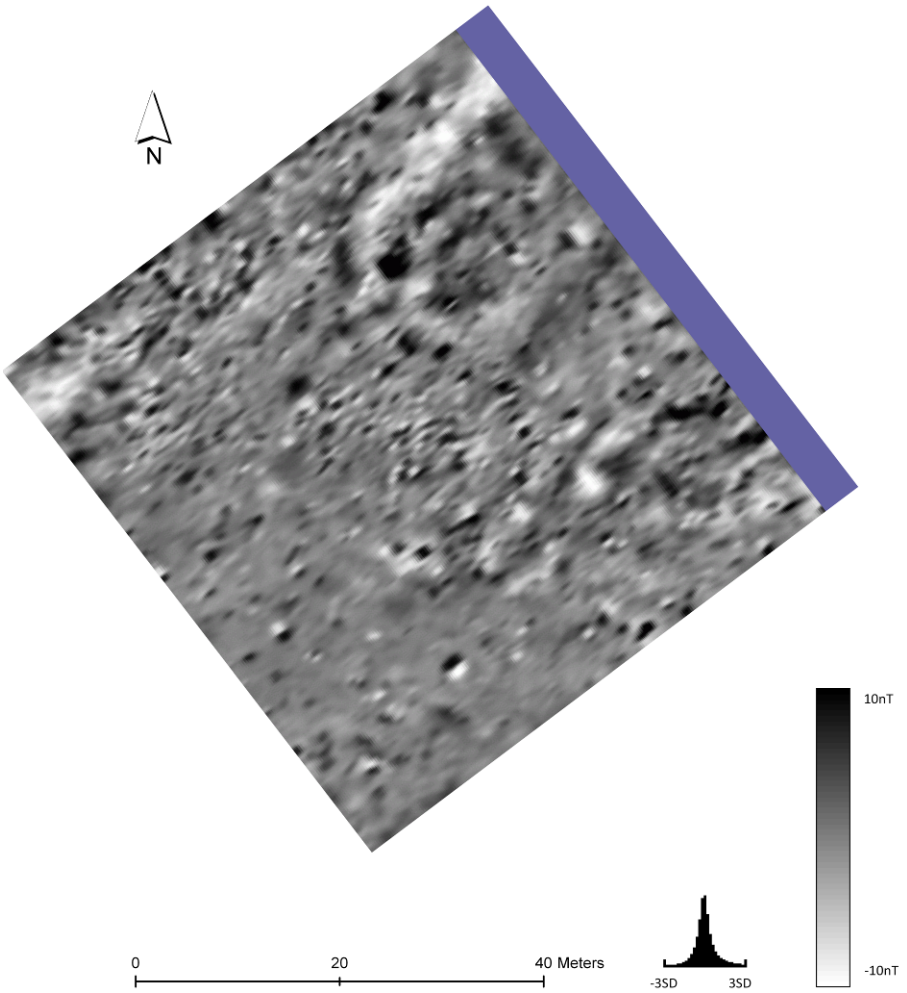

Figure 8-11: Shade plot of the processed data results of the gradiometer survey at Chesterhall Parks Farm. The data was plotted at -10/10 Absolute units, contrast 1 and using the Geoplot grey99 palette.

Function	Parameters
Clip	Min -20, Max 20
Despike	2 (X/Y Radii), 3 (Threshold), Mean (Replacement)
Zero Mean Grid	.5 (Threshold)
Zero Mean Traverse	All (Grid), On (Less Mean Fit), Not applied (Threshold)
Low Pass Filter	2 (X & Y), Gaussian (Weighting)
Interpolate	X & Y (Direction), Expand, SinX/X

Table 8-2: Processing (Geoplot 3.0 software) applied to the magnetic data collected over the cropmarks at Chesterhall Parks Farm.

8.2.4. Earth Resistance Results

The earth resistance survey did not produce good results. The results of the raw and processed data are shown in Figure 8-12 and 8-13 respectively. Little was achieved by processing the data (Table 8-3). The mean value of the raw data

was very low (23.89 ohm). There was a general gradient in the resistance data from low resistance readings in the easternmost grids to higher resistance values towards the west of the survey area that match with the order in which the grids were surveyed. A few curvilinear trends of high resistance seem to match with the approximate locations of enclosure 1 (Figure 8-5).

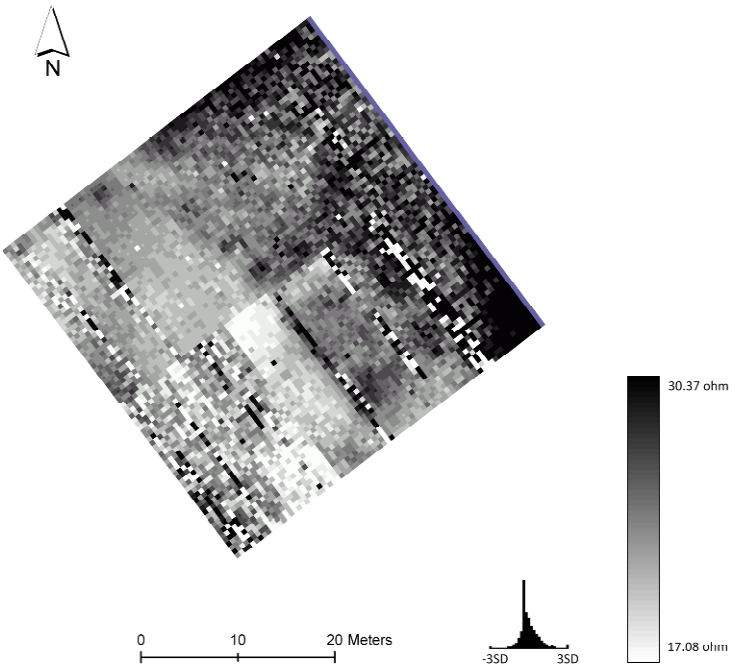

Figure 8-12: Shade plot of the raw data results of the earth resistance survey at Chesterhall Parks Farm. The data was plotted at -1/1 SD units, contrast 1 and using the Geoplot grey99 palette.

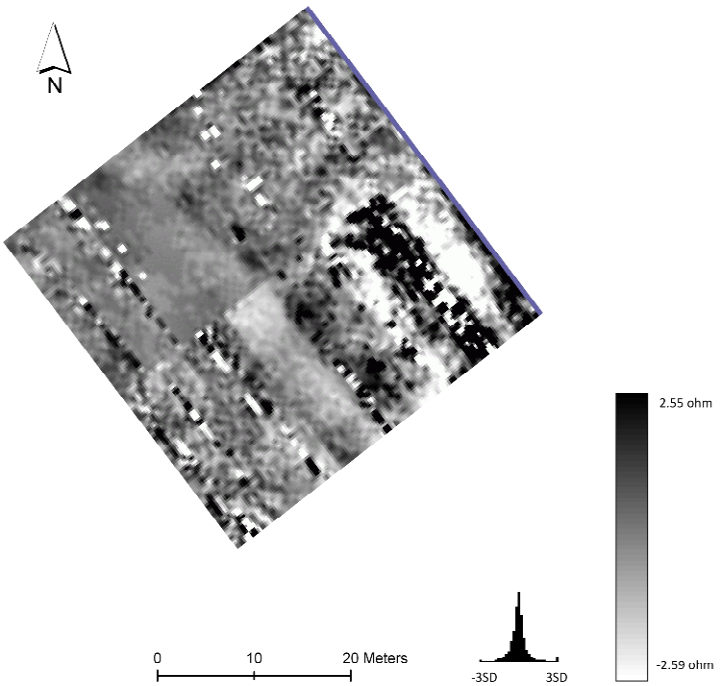

Figure 8-13: Shade plot of the processed data results of the earth resistance survey at Chesterhall Parks Farm. The data was plotted at -1/1 SD units, contrast 1 and using the Geoplot grey99 palette.

Function	Parameters
Despike	1 (X/Y Radii), 3 (Threshold), Mean (Replacement)
High Pass Filter	10 (X & Y), Uniform (Weighting)
Low Pass Filter	1 (X & Y), Gaussian (Weighting)
Interpolate	X & Y (Direction), Expand, SinX/X

Table 8-3: Processing (Geoplot 3.0 software) applied to the electrical data collected at Chesterhall Parks Farm.

8.2.5. FDEM Results

The quadrature results (Figure 8-14) showed curvilinear conductive trends that correlate with the location of the ditches and other features relating enclosure 1 (Figure 8-5). The in-phase response (Figure 8-15) did not reveal any coherent anomaly associated with the targeted enclosures.

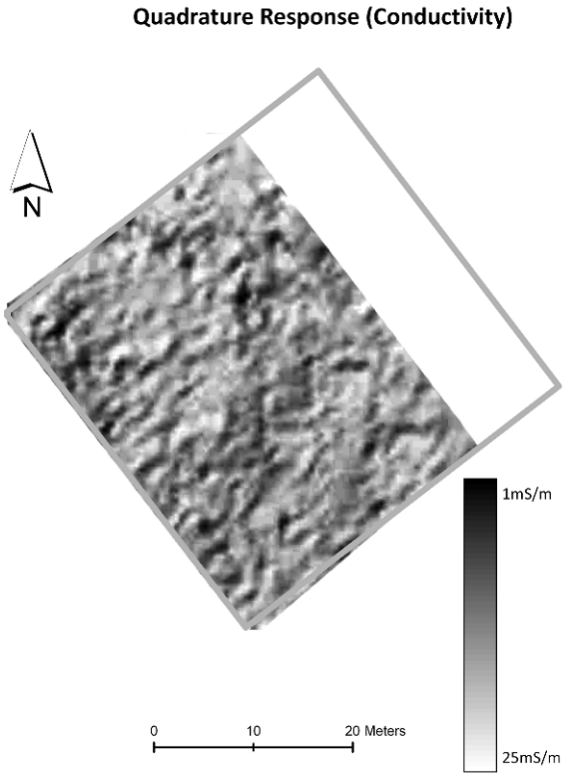

Figure 8-14: Image plot of the raw data results of the FDEM survey (vertical mode, quadrature component) at Chesterhall Park Farm. The data was plotted using Surfer 8 software.

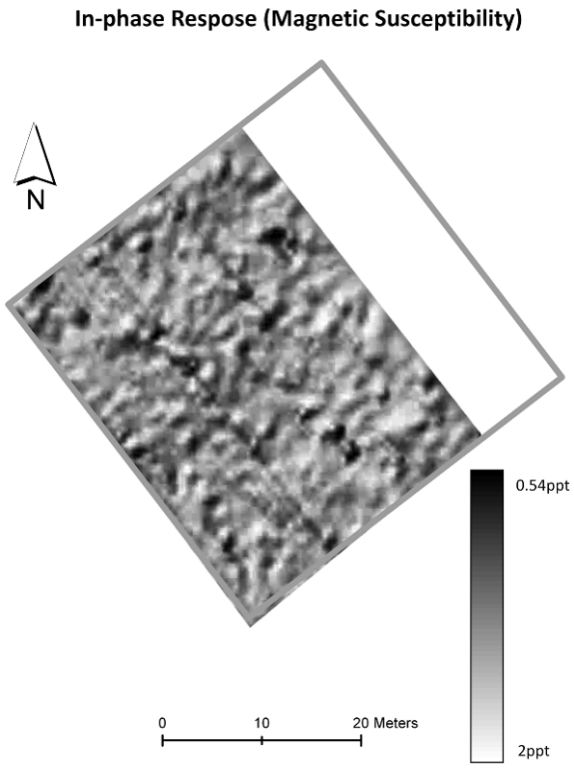

Figure 8-15: Image plot of the raw data results of the FDEM survey (vertical mode, in-phase component) at Chesterhall Park Farm. The data was plotted using Surfer 8 software.

8.2.6. GPR Results

Figure 8-16 shows the results of the processing flow applied to the GPR data and Figure 8-17 shows the results of the 225MHz survey. Table 8-4 summarises the steps used in data processing. The velocity used to estimate depth was 0.08 m/ns (by hyperbola adaptation). The signal penetration reached the first 18ns (*c*.0.60m) with the 450MHz survey possibly due to the attenuation produced by the clay soil. However, the signal penetration improved with the 225MHz survey (*c*.60ns or 2.2m) in which strong reflections were visible in the radargrams at the locations where the targeted ditches were expected. The reflections from the ditches the 225MHz surveys showed at approximately 0.6m to 1.20m (225MHz) and at 0.25m from the surface (450 MHz survey). The time-slices also showed amplitude trends in association with the targeted ditch features at the same depth as shown by the radargrams.

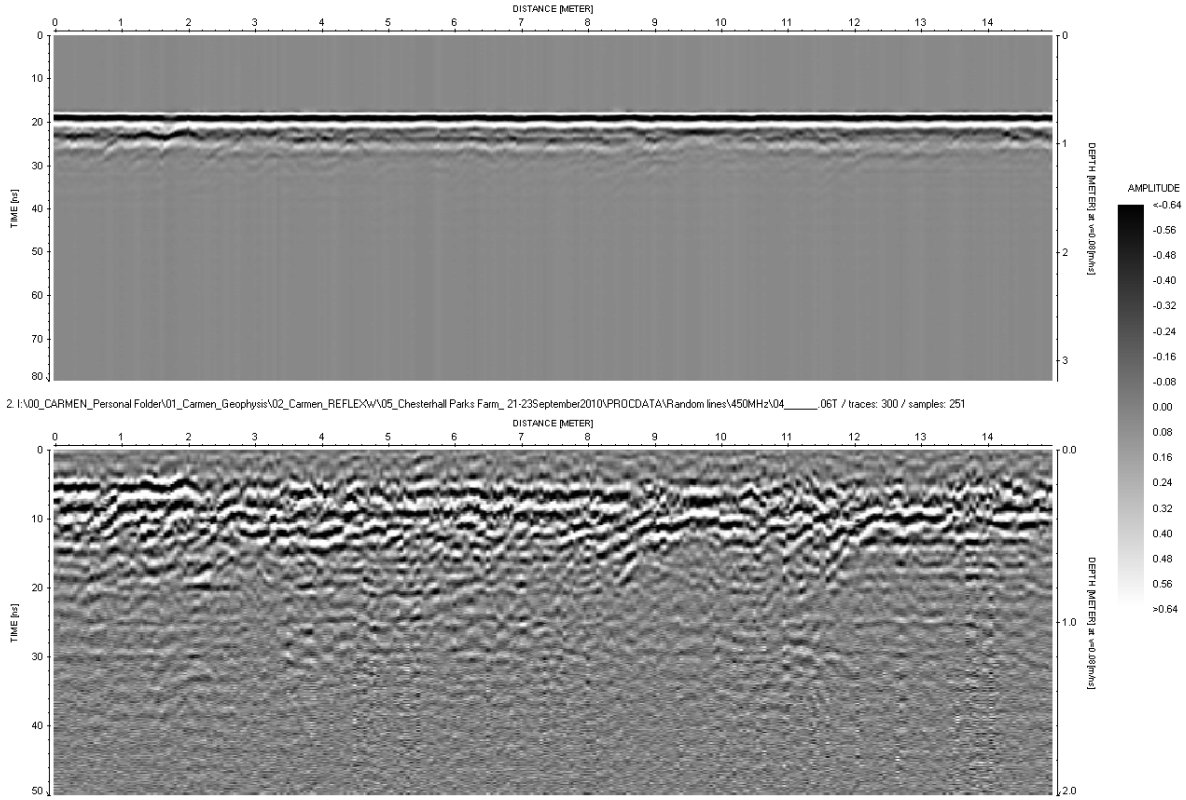

Figure 8-16: Radargram from the 450MHz survey over enclosure 1 (Figure 8-5) at Chesterhall Parks Farm showing the raw (top) and processed (bottom) results of GPR Line 1 (Figure 8-9).

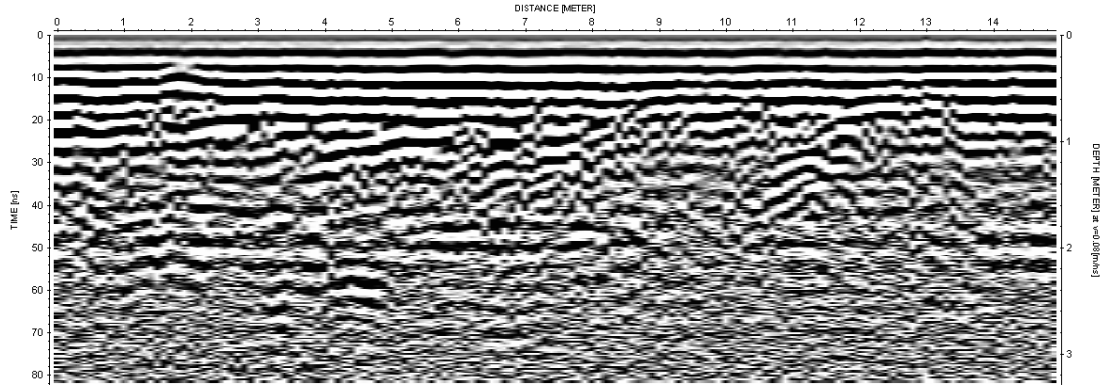

Figure 8-17: Radargram from the 225MHz survey over enclosure 1 (Figure 8-5) at Chesterhall Parks Farm showing the processed results of GPR Line 1 (Figure 8-9).

Function
Subtract-mean (dewow)
Time zero Correction
Background Removal
Manual gain (y)

Table 8-4: Processing (ReflexW v.5.6 software) applied to the GPR data collected at Chesterhall Parks Farm.

8.2.7. Gradiometry Interpretation

The gradiometer survey detected the targeted enclosures as concentric weak positive magnetic anomalies showing magnetically enhanced ditches. The enclosure 1 was fully detected in the form of two ring-like anomalies (ditches) with two possible entrances on it south and west. There was an area of magnetic enhancement in the S entrance (1 in Figure 8-18). Fragmented trends surrounding the outermost ditch may suggest the remains of a possible third ditch or palisade. The interior of the enclosure had an area of noise (2 in Figure 8-18) that may be related to the function of the enclosure. A series of linear weak positive magnetic trends inside the enclosure (3 in Figure 8-18) may reveal an internal structure. Three fragmented and concentric positive magnetic anomalies showed enclosure 2. Also, three fragmented ditches were detected relating to enclosure 3 as well as an area of magnetic enhancement (4 in Figure 8-18) at its centre.

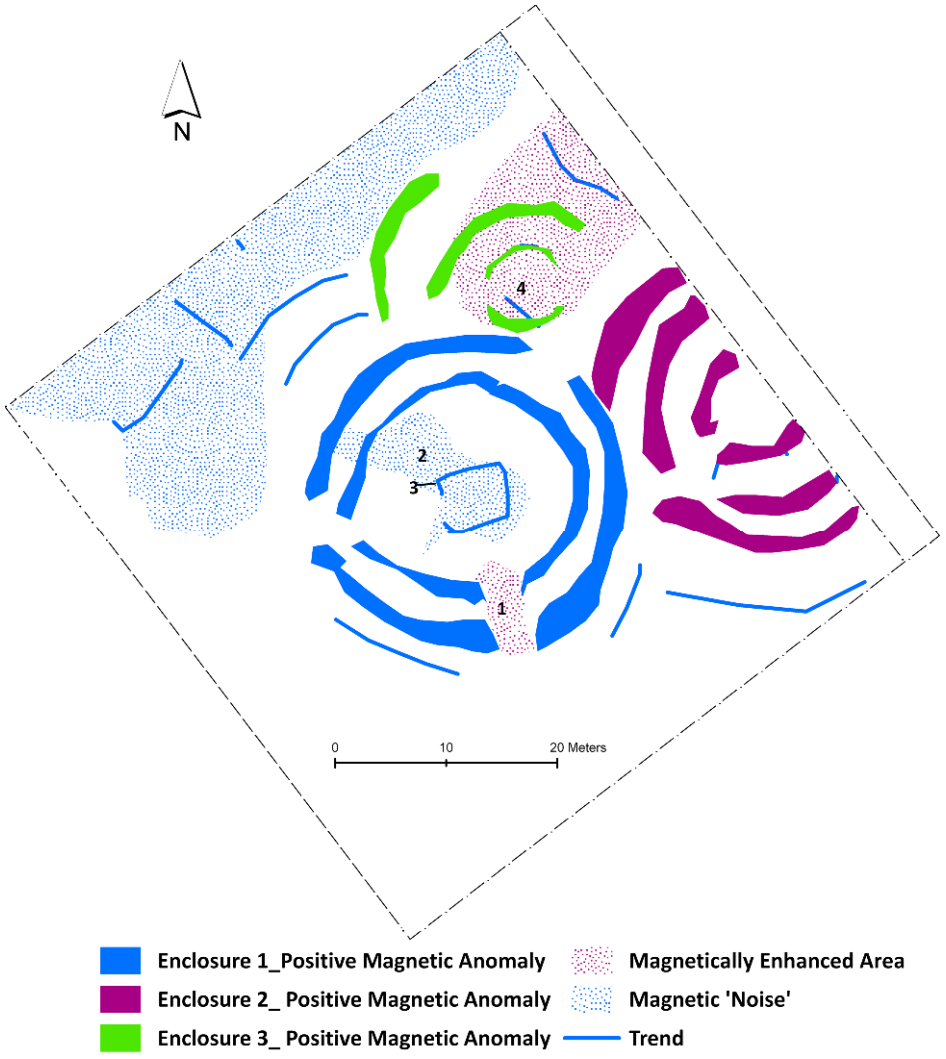

Figure 8-18: Anomaly interpretation plot of the gradiometer results over the enclosures at Chesterhall Parks Farm. The numbers (1-4) mark the anomalies discussed in the main text.

8.2.8. Earth Resistance Interpretation

High resistance trends seemed to correlate with the location of the ditches (Figure 8-19). Other high resistance values at the SE of the survey area were associated with a slight topographic rise, perhaps relating to a change in the underlying geology or drainage conditions.

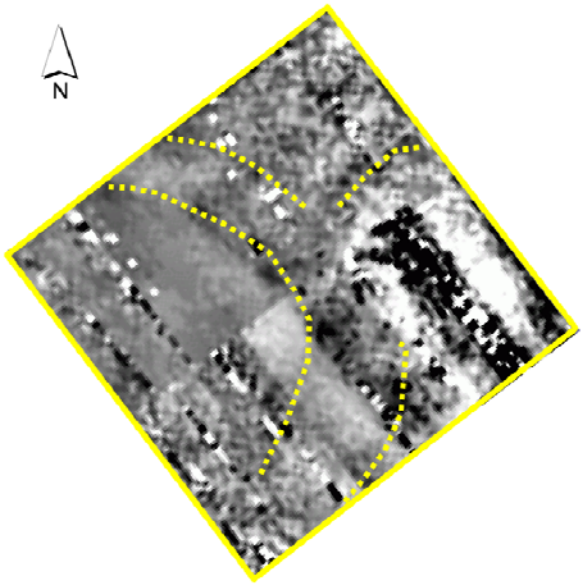

Figure 8-19: Anomaly interpretation plot of the earth resistance results at Chesterhall Parks Farm. The high resistance trends relating the targeted features are mark in yellow (dotted line).

8.2.9. FDEM Interpretation

Conductive trends (Figure 8-20) were detected in association with the targeted ditches, also confirming the earth resistance results.

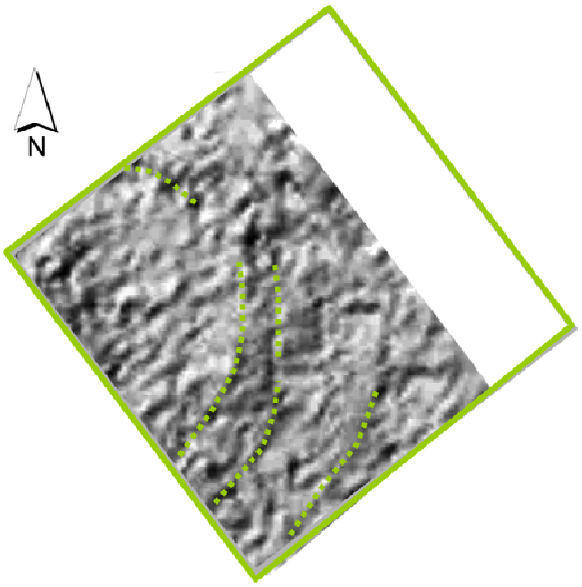

Figure 8-20: Anomaly interpretation of the FDEM (conductivity) results at Chesterhall Park Farm. The conductivity trends relating the targeted features are mark in green (dotted line).

8.2.10. GPR Interpretation

Figure 8-21 shows some of the results of the GPR survey. The ditches were fairly deep and they were bottomed with the low frequency survey (225MHz) at *c.*1.20m. The uppermost reflections were recorded at 0.25m (450MHz survey) from the topsoil.

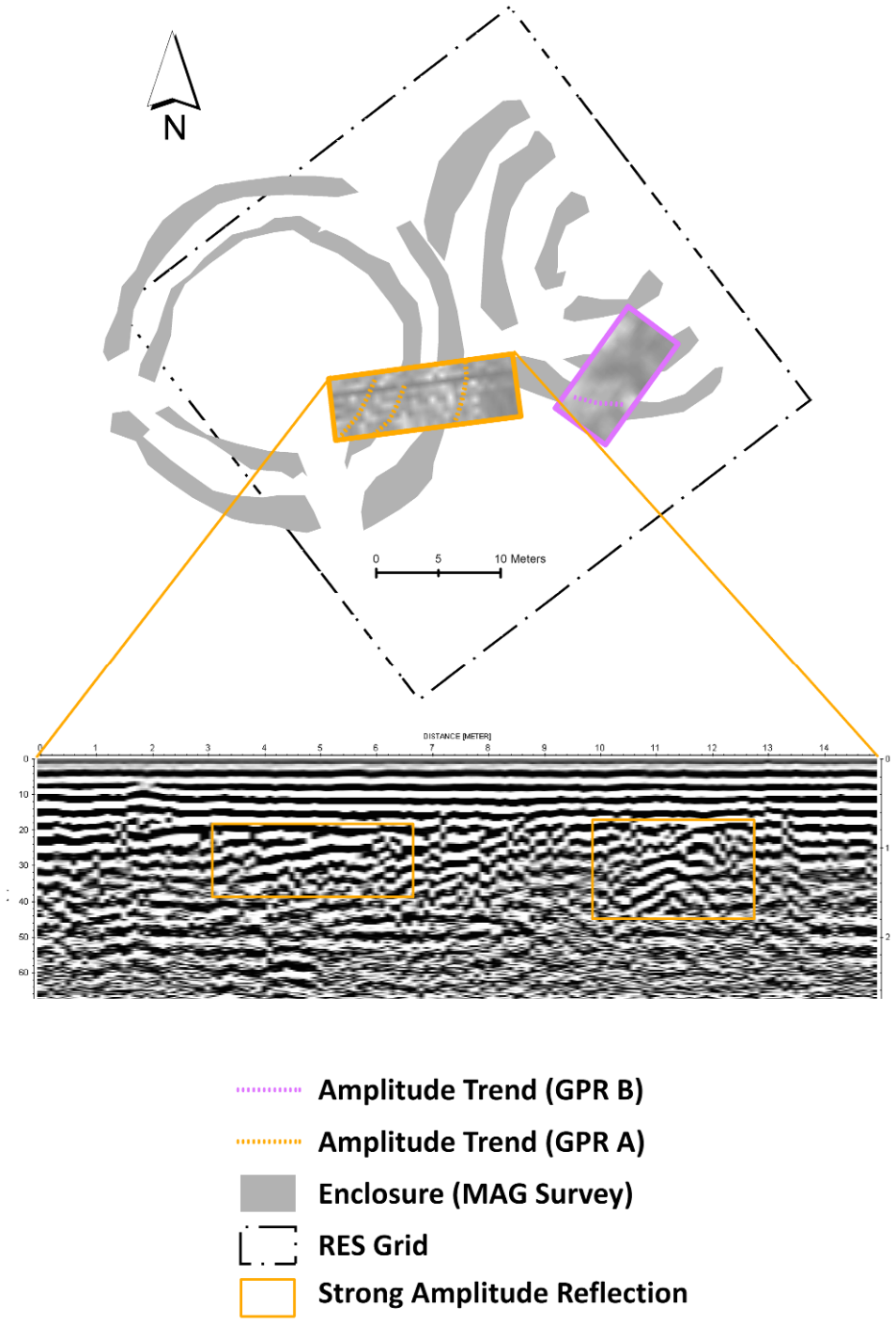

Figure 8-21: Time-slices (*c.* 1m depth, GPR A) and radargram (GPR 1, 225MHz survey) showing the reflections produced by the ditches of enclosure 1. The time-slice (c.1m depth, GPR B) shows other high amplitude anomalies related to enclosure 2.

8.2.11. Conclusions

A higher survey resolution (0.5m instead of 1m) was necessary to resolve satisfactorily the enclosures using gradiometry at Chesterhall Parks Farm. This survey also revealed other internal anomalies that may be related to habitation or functional areas within the enclosures. In spite of the clay soil and frequent waterlogged conditions, the electromagnetic methods proved able to detect the targeted ditches. The GPR gave useful information relating to the deep ditches of the enclosures and the reflections were particularly good in the data collected with the low frequency survey. The quadrature component of the FDEM survey in vertical dipole showed potential to detect the ditches. Whist the ditches were exposed at a very low depth during the excavation (Figure 8-8) they were also fairly deep. The depth of these features may be related to their detection by the FDEM in vertical mode.

8.3. Soil Analysis

8.3.1. Aim

The aim was to characterise the soil surface response of the ditches of enclosure 1 (Figure 8-5) in terms of its physical and chemical composition in order to assess the effectiveness of portable XRF, magnetic susceptibility and phosphate analysis in detecting the targeted ditches and overall enclosure.

8.3.2. Sampling Strategy

Soil samples were collected along GPR Line 1 each 0.5cm and *c*.0.10cm from the surface. The line was extended to reach part of enclosure 2 (Figure 8-22).

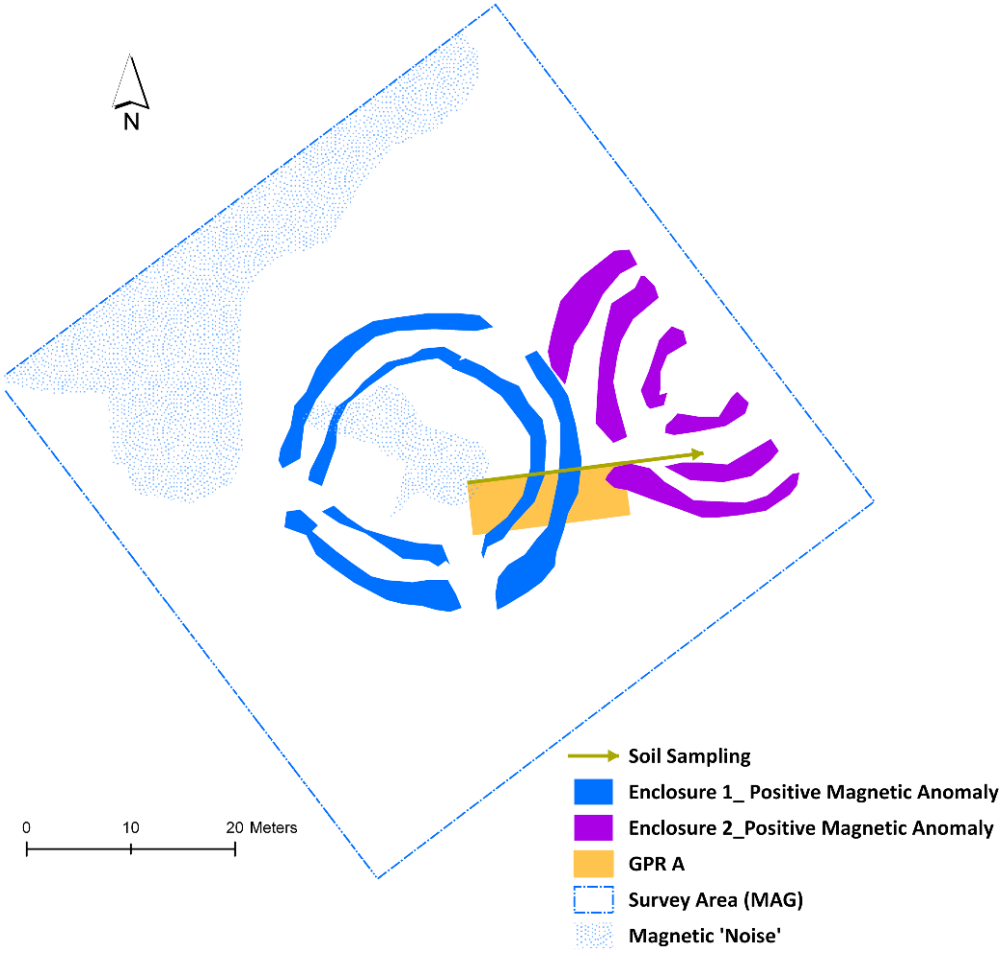

Figure 8-22: Surface soil sampling carried out over enclosure 1 and 2 (**Figure 6-17**) at Chesterhall Parks Farm**. The arrow shows the direction of the soil sampling.**

8.3.3. Physical and Chemical Results & Discussion

8.3.3.1. **MS, Total P, LOI, EC and pH**

The general results of the different analysis are shown in Table 8-5. The MS results showed a general and gradual increase over enclosure 2 (Figure 8-22) that might be related with its function. There was an area of greater MS variability at *c*.4m to 6m (Figure 8-23) that may indicate a shallower innermost ditch of enclosure 1 (Figure 8-22). Other results indicate acidic (pH 6) and fairly conductive soil conditions (96.8µs) in the results shown in Table 8-5.

Distance (m)	χ_{lf}	Total P µg/kg	LOI (%)	EC µs	pH	Distance (m)	χ_{lf}	Total P µg/kg	LOI (%)	EC µs	pH
0.0	20	58	0.016	65	6	13.5	20	108	0.030	*	*
1.0	19	78	0.021	*	*	14.0	20	111	0.028	*	*
2.0	19	78	0.019	*	*	14.5	20	74	0.041	*	*
3.0	20	110	0.022	*	*	15.0	21	99	0.034	94	6
3.5	21	110	0.022	*	*	15.5	21	86	0.040	*	*
4.0	20	81	0.021	*	*	16.0	22	120	0.044	*	*
4.5	21	104	0.023	*	*	16.5	23	114	0.039	*	*
5.0	19	100	0.025	79	6	17.0	22	86	0.030	*	*
5.5	21	130	0.026	*	*	17.5	23	105	0.031	*	*
6.0	20	94	0.026	*	*	18.0	23	145	0.033	*	*
6.5	21	94	0.026	*	*	18.5	23	80	0.029	*	*
7.0	19	107	0.029	*	*	19.0	22	77	0.031	*	*
7.5	19	107	0.030	*	*	19.5	23	80	0.038	*	*
8.0	20	126	0.029	*	*	20.0	22	86	0.034	90	6
8.5	20	143	0.033	*	*	20.5	23	99	0.032	*	*
9.0	19	115	0.038	*	*	21.0	22	70	0.032	*	*
9.5	20	109	0.039	*	*	22.0	24	80	0.037	*	*
10.0	20	94	0.043	156	6	23.0	24	80	0.029	*	*
10.5	21	103	0.039	*	*	**Mean**	**21**	**99**	**0.031**	**97**	**6**
11.0	19	96	0.034	*	*	**S.D**	**1**	**19**	**0.007**	**35**	**0**
11.5	19	117	0.038	*	*	**C.V**	**7**	**19**	**23**	**36**	**3**
12.0	21	93	0.047	*	*	Control 1	63	198	0.040	126	6
12.5	21	108	0.033	*	*	Control 2	58	75	0.026	107	5
13.0	20	102	0.037	*	*	Control 3	23	104	0.027	*	*

Ditch (Enclosure 1) Enclosure 2 * Not measured

Table 8-5: Magnetic susceptibility (χ_{lf}), total phosphate (P), loss on ignition (LOI), conductivity (EC) and pH results of the surface soil samples collected at Chesterhall Parks Farm. The green and blue colours mark the location of the targeted features (Figure 8-22).

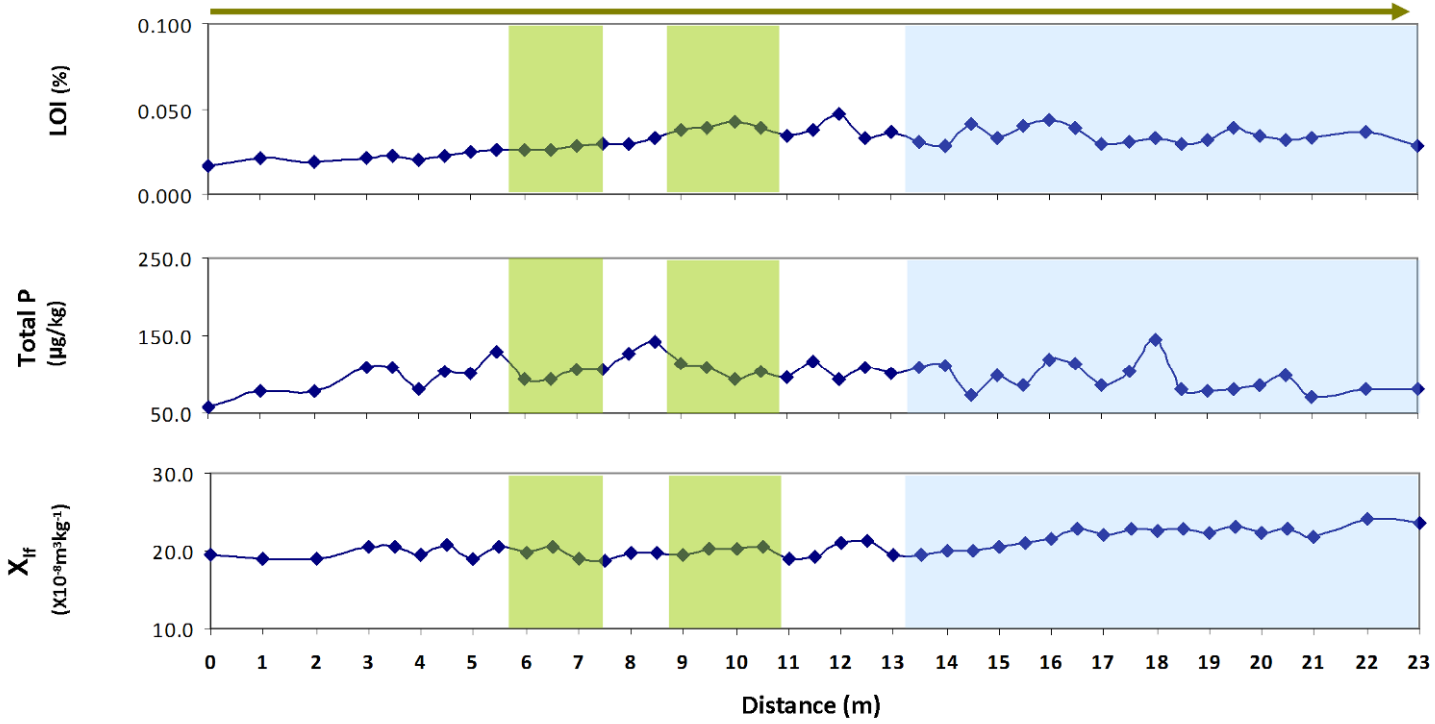

Figure 8-23: Surface distribution of magnetic susceptibility (χ_{lf}), total phosphate (Total P) and loss on ignition (LOI) of the soil samples collected at Chesterhall Parks Farm. The colours mark the location of the ditch anomalies relating enclosure 1 (in green) and enclosure 2 (in blue).

8.3.3.2. **pXRF Results**

The results of the pXRF analysis are summarized in Table 8-6 and Figure 8-24. The main observations from this analysis were general Fe enrichment towards the centres of the enclosures and K depletion and Pb enhancement over the ditches of enclosure 1 (Figure 8-24).

Distance (m)	Fe	K	Ca	Ti	Zr	Mn	Sr	V	Zn	Cu	Rb	Cr	Pb
0	28327	12731	6993	4996	352	307	177	154	81	113	55	52	19
1	25025	10138	7128	4867	340	292	180	127	81	59	45	61	25
2	27416	11512	7084	4941	346	283	179	171	72	30	52	56	24
3	25064	10483	7276	4997	337	286	184	150	81	26	46	67	30
3.5	24707	11456	8662	5355	353	345	179	155	78	53	46	64	28
4	25153	10970	7252	4994	349	268	180	136	76	24	50	53	32
4.5	23754	9646	7220	4979	316	285	177	146	81	43	43	94	35
5	24410	9573	7606	5074	321	271	179	127	81	31	44	63	48
5.5	23107	9726	7728	4954	332	298	176	146	88	74	41	62	50
6	24558	9420	7567	5031	325	267	184	132	85	66	43	56	46
6.5	23262	8891	7709	4751	316	297	174	143	87	97	39	48	61
7	22848	8934	7899	4791	319	246	180	124	83	44	40	62	43
7.5	22351	8659	7693	4641	299	264	169	133	93	87	39	84	41
8	23499	8726	8448	4975	282	280	177	156	94	51	40	73	47
8.5	21827	8967	8647	4916	318	267	171	153	85	43	43	78	42
9	22251	9366	8121	4901	302	251	172	151	87	30	46	79	43
9.5	24009	9480	8276	4894	295	352	170	163	85	24	47	66	44
10	27713	10000	7730	4927	331	340	187	142	111	64	54	75	46
10.5	22233	10652	7963	4942	320	272	174	138	84	49	50	75	35
11	21943	11026	8228	5088	339	262	179	166	84	57	54	87	31
11.5	20750	10830	7827	4753	273	300	160	136	84	49	49	89	34
12	22806	10302	7583	4686	297	279	173	154	84	30	51	64	34
12.5	22230	10992	7618	4898	339	311	165	144	84	37	53	62	33
13	23369	10384	7479	4921	309	311	174	138	92	44	52	64	36
13.5	21567	10210	7701	5042	312	309	171	152	85	51	46	61	37
14	23219	10843	7546	4946	292	287	174	146	85	76	52	74	35
14.5	22504	10953	7500	4950	294	290	176	138	86	41	52	78	32
15	21189	10418	7445	4992	295	304	171	151	89	60	48	72	34
15.5	24158	9688	7855	4761	337	303	206	144	140	349	52	60	39
16	22816	9472	7414	4946	314	296	173	144	84	48	43	70	39
17	23644	9189	7168	4985	266	316	169	144	83	67	42	64	39
17.5	23786	9831	7342	5099	283	290	172	141	89	94	44	59	36
18	22758	10173	7742	4951	342	294	178	127	91	132	43	63	33
18.5	25352	10004	7167	4891	286	263	173	172	79	49	45	50	35
19	25235	10619	7037	4890	311	250	175	135	70	53	45	48	28
20	26952	10627	6965	5084	256	281	166	142	72	63	49	59	50
20.5	26314	10044	6976	4955	271	266	167	151	86	138	45	49	28
21	24454	9562	7466	5024	306	254	176	162	67	26	42	65	27
22	26279	10252	7325	4976	329	267	178	143	70	46	47	54	29
23	26966	10585	6536	4995	283	260	176	133	70	28	51	51	28
Mean	**23995**	**10133**	**7573**	**4944**	**312**	**287**	**175**	**145**	**85**	**64**	**47**	**65**	**36**
S.D	**1870**	**852**	**468**	**124**	**26**	**25**	**7**	**12**	**12**	**54**	**5**	**12**	**9**
C.V	**8**	**8**	**6**	**3**	**8**	**9**	**4**	**8**	**14**	**85**	**10**	**18**	**23**
Control 1	23737	13251	6309	4618	314	621	146	136	97	87	70	56	36
Control 2	24128	15157	3646	4504	254	515	124	130	78	34	81	58	24
Control 3	18681	9227	5813	5119	266	300	158	114	76	106	46	74	30

Ditch (Enclosure 1) Enclosure 2

Table 8-6: pXRF results of the surface soil samples collected at Chesterhall Parks Farm. The element concentrations are expressed in mg/kg (=ppm). The green and blue colours mark the location of the targeted features (Figure 8-22).

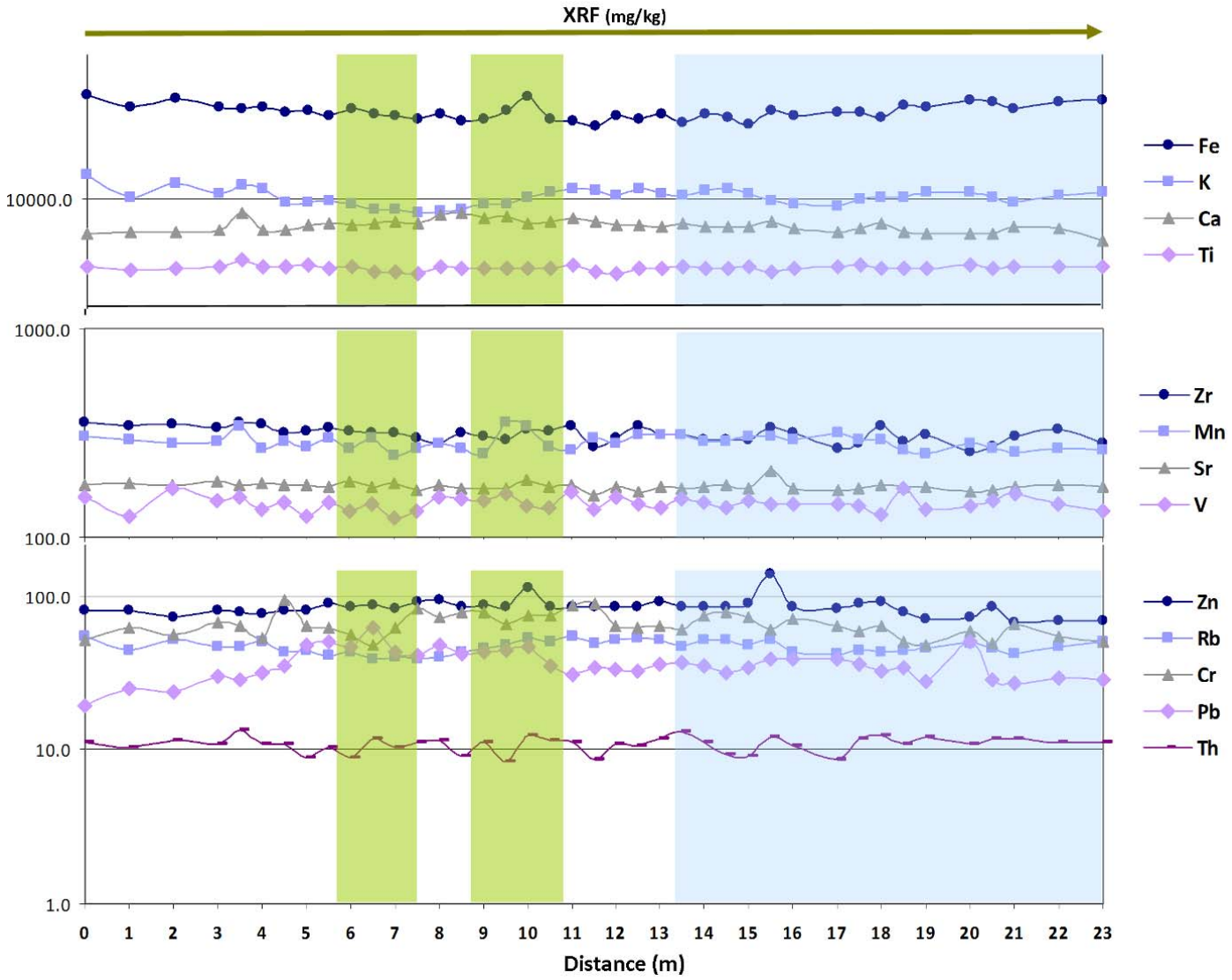

Figure 8-24: Surface distribution of elements (pXRF data) of the soil samples collected at Chesterhall Parks Farm.

8.3.3.3. **ICP-OES Results**

The results (Table 8-7 and Figure 8-25) focused on the ditches from enclosure 1. There was a general high variation of many elements over the ditches and a more steady response outside the ditch areas. This type of anomalous response is characterised by a high variation in element concentration. There was also a general depletion of K over the ditches and as well as P enhancement.

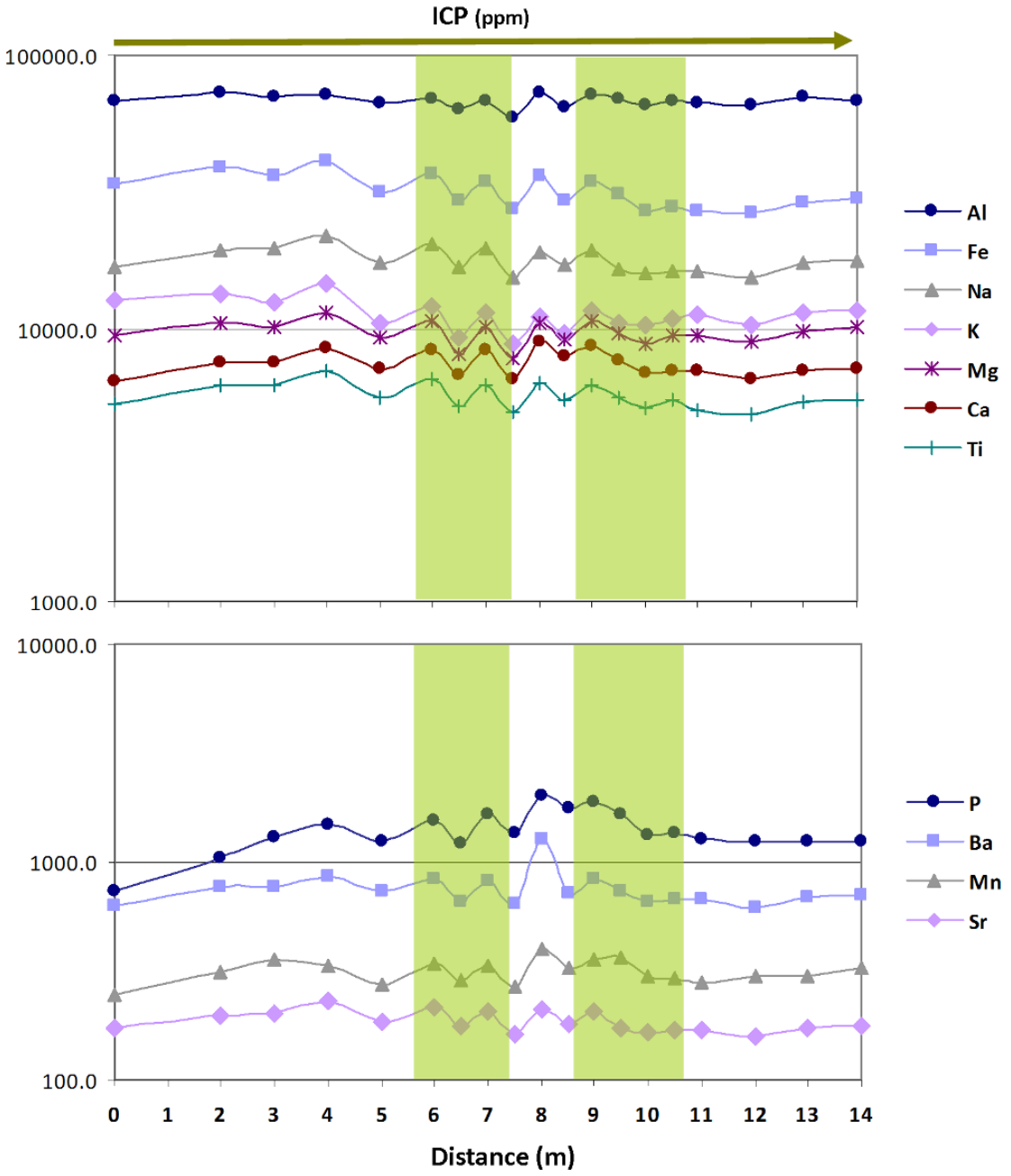

Figure 8-25: Surface distribution of elements (ICP-OES data) of the soil samples collected at Chesterhall Parks Farm. The locations of the two targeted ditches of enclosure 1 are marked in green.

Distance (m)	Al	Fe	Na	K	Mg	Ca	Ti	P	Ba	Mn	Sr	Cr	Zn	Cu	Pb	Li	Ni	Co
0	67665	33497	16821	12626	9430	6441	5271	735	636	248	173	86	65	83	18	31	35	11
2	73394	38981	19220	13316	10360	7461	6179	1046	775	311	199	106	83	43	28	39	42	15
3	70109	36204	19485	12363	10086	7516	6188	1301	776	353	203	105	87	50	34	39	44	16
4	71801	41126	21711	14506	11418	8507	6951	1499	855	334	229	133	93	37	43	40	50	16
5	66549	31756	17429	10492	9317	7104	5604	1243	731	277	184	90	75	38	52	37	38	13
6	69526	36973	20417	11927	10568	8308	6495	1551	841	339	215	111	98	104	60	43	46	13
6.5	63698	29123	16714	9296	8071	6741	5160	1217	654	289	176	85	76	98	68	34	36	11
7	67590	34076	19646	11324	10094	8346	6214	1662	829	331	207	108	93	57	60	43	44	12
7.5	58808	27515	15489	8752	7781	6495	4905	1358	641	270	163	80	77	112	46	34	32	9
8	72534	35970	18934	10964	10507	8956	6296	2029	1271	399	211	112	104	81	61	48	45	15
8.5	64992	29456	17096	9583	9134	7958	5440	1783	727	323	181	98	87	51	53	41	38	11
9	72123	34515	19139	11618	10586	8602	6157	1887	843	354	206	110	93	43	59	48	45	15
9.5	69120	30716	16463	10491	9647	7641	5552	1644	733	364	173	100	89	36	48	42	39	11
10	65753	26784	15864	10331	8785	6848	5115	1332	652	298	165	90	76	61	40	39	36	10
10.5	68532	28043	16274	10906	9363	7022	5419	1349	679	291	168	98	79	42	39	41	39	10
11	67375	26712	16304	11157	9432	6960	5049	1267	671	279	168	96	73	53	33	40	36	10
12	65195	26306	15433	10329	8869	6473	4842	1235	611	302	159	87	67	40	37	38	37	10
13	70760	28908	17280	11376	9732	6998	5391	1242	683	299	174	104	74	45	35	42	40	11
14	68211	29855	17670	11525	10007	7126	5504	1250	703	324	176	110	82	104	40	40	41	12
Mean	**68091**	**31922**	**17757**	**11204**	**9641**	**7448**	**5670**	**1402**	**753**	**315**	**186**	**100**	**83**	**62**	**45**	**40**	**40**	**12**
S.D	**3533**	**4453**	**1788**	**1385**	**898**	**787**	**596**	**305**	**147**	**37**	**21**	**13**	**11**	**26**	**13**	**4**	**5**	**2**
C.V	**5**	**14**	**10**	**12**	**9**	**11**	**11**	**22**	**20**	**12**	**11**	**12**	**13**	**42**	**29**	**10**	**11**	**19**
Control 2	73966	31144	14045	15232	13286	3146	5358	971	352	544	120	101	77	41	25	20	39	12

Table 8-7: ICP-OES results of the surface soil samples collected at Chesterhall Parks Farm. The element concentrations are expressed in ppm (=mg/kg). The location of the ditches of enclosure 1 (Figure 8-22) are marked in green.

8.3.4. Conclusions

Taking into account that the soils at the cropmark site are infrequently ploughed and kept for pasture, there were few enhancements and depletions of interest relating to the location of the enclosures and the ditches. First of all, the MS enrichment over enclosure 2 as well as the higher Fe concentration over the middle of the two enclosures targeted here seems to show the centre of the enclosures. The ditches were characterised by K depletion and enhancement of Pb and P. The latter element was also enhanced in the bulk samples collected from inside the ditches during their excavations by the by the UCVLP in 2000. However, there was not a significant enhancement in other elements such as Zn or the general Ca enrichment over enclosure 2 produced by large quantities of burnt bone in the floor the enclosure (Sharpe 2004, 302). Finally, the ditches also produced a high variation (anomalous response) in the multi-element results (especially the ICP-OES data) and MS (inner ditch of enclosure 1). This type of high variation response, in association to a specific feature, has been observed before and it will be further discussed in Chapter 9.

8.4. General Discussion

In spite of the results of the previous gradiometer survey carried out at the site (Sharpe 2004, 182), the magnetic response produced by the presence of the enclosures at Chesterhall Parks Farm clearly improved by increasing the density of the surveyed traverses. The weak contrast detected between the ditch infill and surrounding subsoil may have been an effect of the general low MS of the clayey topsoil (21 $10^{-6}m^3kg^{-1}$ in Table 8-5), and areas of increased magnetic enhancement possibly influenced by the local volcaniclastic sandstones of the area. The slopes of Tinto Hill are mantled by frost-weathered detritus that has been extensively soliflucted (Ballantyne 1993). Therefore, the magnetic noise distinguishable in the northern area of the survey area may be caused by soliflucted material from Tinto Hill.

Whilst the anomalies showing the ditches were weak because of the mixed effects explained above, they confirmed the sporadically observed cropmarks at the site. Furthermore, other magnetic anomalies such as the internal dipole anomalies provided important information relating to the enclosures and their

function, hence contributing to their archaeological interpretation. However, taking into account the interlocked or truncated character of these magnetic anomalies indicating the enclosures, it may be possible that their function changes over time.

The internal magnetic anomalies correlate with Fe and MS enhancements inside the enclosures which, along with the Pb and P enrichment of the samples collected over the ditches, points towards habitation activities such as metal working (e.g.slag and ore and cremated floor materials which were found during the trial excavation at the site in 2000). These enhancements have also been reported at other metal smelting sites (Oonk *et al.* 2009a). However, other enhancements identified by Sharpe (2004, 302), such as the Ca enrichment on the floor deposits of enclosure 2 were not observed on the multi-element analysis of the topsoil samples. Since ploughing is a seldom practice this field, deeper archaeological deposits may remain undisturbed. This may be the reason behind the lack of the element enhancements that Sharpe (2004, 301) reported from her analysis in comparison to this study.

In spite of the clay soils and low resistance values at the site (23.89 ohm), the GPR survey produced some useful results. The high frequency GPR survey did not penetrate enough to reach the ditches because of the highly conductive soil, but the signal penetration was improved with the low frequency survey. Therefore, the *c*.0.95m deep ditches of enclosure 1 were characterised by strong reflections in the radargrams. The depth of these ditches may explain their detection by the quadrature (conductivity) component of the FDEM survey using a vertical mode. Whilst electromagnetic methods demonstrated their potential to detect the targeted features at the site despite of the high conductive nature of the clay soil, more extensive surveys may be necessary to assess shallower ditches from other enclosures at the site. The high rainfall regime that characterises the weather at this area may also affect the electromagnetic results in future surveys.

Part III: Discussion & Conclusion

Chapter 9

Discussion & Conclusions

9.1. Introduction

This chapter focuses on answering the research questions formulated in Chapter 1 and discusses other general remarks. It dedicates a critique of the overall PhD project and its impact. The chapter concludes by proposing a series of integrated survey strategies which could be used in future surveys, combining the geophysical and geochemical methods tested in this project. This final section ends with some recommendations for further research.

9.2. Addressing the Research Questions

9.2.1. Which soil factors have an impact on the detection of archaeological anomalies by geophysical means at the five case study sites?

This section is structured as an assessment of some of the soil factors introduced in section 2.2 taking into consideration the results of the geochemical characterisation of the samples collected at the five sites and on-site observations such as specific ground surface conditions during the surveys.

9.2.1.1. **Soil Parent Material**

Most of the sites surveyed for this research lie over sedimentary rock (Figure 2-4) belonging to different groups of the Old Red Sandstone (ORS) formation, some containing volcanic and meta-sedimentary components such as at Forteviot (Chapter 7) and Chesterhall Parks Farm (Chapter 8) or meta-igneous elements like the Ophiolite complex at Scalpsie Bay (Chapter 4). The presence of the different igneous, meta-igneous and meta-sedimentary extrusive and intrusive rocks within the general sedimentary formation shows the great diversity that characterises the geology in Scotland.

In spite of the igneous content of the bedrock at some of the sites, its direct effect on the results of the case studies in this investigation was minimal and basically affects only the gradiometer data, for example the possible meta-igneous serpentinite band at Scalpsie Bay (Chapter 4). This deposit did not affect the detection of the targeted feature, and the geological noise introduced into the data was easily corrected using high pass filters. However, other areas with igneous bedrock may be more problematic. For example, the complex geology of the Shetlands with numerous faults, fold axes and combined metamorphic, igneous and sedimentary formations, can present challenges to the gradiometer technique (Ovenden 2010). Also the volcanic isle of Skye, with much of the isle composed of basaltic lava flows, gabbro and granite hills and numerous dykes and sills (Birch *et al.* 2005). Most of the examples mentioned produced results of interest for archaeological prospection despite the high thermo-remanent magnetic noise. Other surveys carried out on igneous islands such as St Kilda (Carruthers *et al.* 2004), Mull and in metamorphic areas such as in Balivanich in the Western Isles (Hale 2010) have also produced good results, even with the gradiometer.

The potential problems associated with igneous geology and its impact on geophysical survey may only affect one technique (i.e. gradiometry). Other geophysical techniques, less dependent on the general magnetic background of the survey environment, can be effective. Therefore, general assumptions on the impact of the solid geology on geophysical methods are not very useful in Scottish environments. This is because the particular setting of a site in an area of great geodiversity, such as Scotland, depends upon many other factors which must be assessed in detail, taking into account, not only the high variability in bedrock but also other aspects such as the depth of subsoils/parent material, soils, type of archaeology and land surface conditions.

9.2.1.1.1. *Glacial Drift Deposits*

The glacial past influenced the composition of the superficial deposits at most of the case studies (Figure 2-5) which are characterised by glacial till and fluvioglacial sand and gravel deposits (Table 3.1). For example, the till deposits that form the subsoil at the easternmost area at Scalpsie Bay (Chapter 4) are unsorted and unstratified deposits where the soil particles and stone fragments

vary in size from finely ground flour to large boulders. These unsorted till deposits filled up many valleys and their plains, as they were dumped by the ice or by episodic melt waters from the glacier. On the other hand, sorted fluvioglacial deposits are the product of the relatively steady melt waters from glaciers and the ice-sheet. Here, a great deal of rock and soil debris has been carried downstream and gradually deposited in river valleys by melt water, in this case in a stratified manner. These deposits are therefore composed of sorted sands and gravels as at Forteviot (Chapter 7).

Drift superficial deposits often form the soil matrix in which archaeological features are buried in Scotland (generally within the first metre of soil), hence they characterise many soil survey environments. These very heterogeneous deposits may contain a great variety of rock debris (*e.g.*volcaniclastic deposits at Chesterhall Parks Farm) that may add some background noise to the geophysical datasets, especially from magnetic surveys. Till and fluvioglacial deposits are often found together, adding complexity to the background signature of the survey environment as it may vary very rapidly (e.g the NE area of Scalpsie Bay where the noisy magnetic area could be due to the more heterogeneous till deposits). Their characterisation is important in understanding the potential background variability of datasets and to the responses detected by geophysical means (*e.g.* higher MS of the subsoil and its effect on the detection of negative and weak magnetic anomalies at Forteviot).

The glacial past also influences the geomorphology of the sites surveyed in the form of outwash terraces (Forteviot and Lochmaben) and hillslope processes (Chesterhall Parks Farm) reshaped by fluvial processes and isostatic rebound (raised beach of Scalspie Bay). These landforms may affect the results of the surveys by introducing noise and high background variability in the datasets. Geomorphological features associated with glacier landscapes, such as kames, eskers, drumlins, ice wedges, may be taken into consideration when surveying and interpreting Scottish sites since geophysical surveys may also detect these formations.

9.2.1.2. **Soil Type**

Although most of the soils at sites studied in this research are developed from fairly thick Quaternary glacial or post-glacial parent materials (Figure 2-6 and Table 3-1) there are some other soil types that derive directly from in-situ parent material. Examples are rankers and lithosols developed over non-calcareous rocks within 30cm or 10cm depth respectively, or redzinas which are confined to areas of calcareous rock. These shallow soils are generally very stony and present an organo-mineral surface horizon but generally lack subsoil. Rankers are developed in mountainous or hilly terrain or on glacially eroded rocky terrain, directly reflecting the nature of the bedrock. Therefore, the results of geophysical surveys at sites characterised by shallow soils can be problematic in Scotland as the results could be directly affected by the strong thermo-remanence of hard rock igneous geology where present. Examples of thin soil environments covering areas of archaeological potential include ranker soils developed in mountains where Iron Age hillforts are located or peaty rankers covering other prehistoric sites in the Highlands and Islands or hillslopes in the Southern uplands. Therefore, the assessment of the specific soil type at Scottish sites can be fundamental in planning an appropriate survey strategy using geophysical techniques.

Three of the five sites of this research featured cropmarks (Forteviot) or grassmarks (Lochmaben Castle and Chesterhall Parks Farm), and they all concentrate in low-lying south/eastern areas. This reflects the impact of aerial photography in the discovery of archaeological sites in Scotland. Flights by the RCAHMS have flown and over-flown 'honey-pot' areas for cropmark development which are focused in principal valleys, on free draining and arable soils in south-east Scotland (Cowley 2002). Whilst aerial photography has played an important role in archaeological prospection, it has also introduced a bias in the number of sites discovered and recorded in Scotland. Some of the aerial photographs used in this research were taken over soils unsuited to develop cropmark evidence such as the poorly drained site at Chesterhall Parks Farm. These conditions may be similar to other areas that are not covered by aerial photography or where cropmarks do not always develop. Hence, geophysical methods can have an important role in discovering new sites and prospecting archaeology over these

areas. Furthermore, geophysical prospection may be fundamental in monitoring and assessing the conservation of cropmark sites.

9.2.1.3. **Soil Materials & Properties**

Table 9-1 shows a summary of the results of some of the soil surface analyses carried out at the five sites. Most of these soils were developed from generally reddish and coarse sands and gravels with variable amounts of sands, silts and clay. The general reddish colour of these materials reflects the Fe content of their original rocks. For example, the ORS formation, widespread in Scotland, contains hematite as the main Fe-oxide with minor goethite also being present (Wilson 1971). Whilst goethite FeOOH is antiferromagnetic, hematite Fe_2O_3 is weakly ferromagnetic or antiferromagnetic (Cornell and Schwertmann 2007, 5) and gives the ORS deposits their characteristic red colour. The diversity of igneous and metamorphic rock components that ORS formations may contain also contributes to the high variability in MS of the parent material from which soil develops in different areas of Scotland. From the means taken at the case study sites, the MS values ranged from 55 at Lochmaben Castle to 151 at Forteviot (Table 9-1). The general soil textures and pH also denote the generally coarse and acidic character of Scottish soils.

Exceptions to these coarse and freely draining superficial deposits were the clay soil at Chesterhall Parks Farm and the alkaline soils at the Bay of Skaill, both of which were characterised by fairly low MS values (Table 9-1). This shows that simple soil analysis can give a rapid and cheap assessment of the survey environment that may be of great help where there is neither preliminary information nor a database to consult.

	Scalpsie Bay (Isle of Bute)		Bay of Skaill (Orkney)		Lochmaben Castle (Dumfriesshire)		Forteviot (Perthshire)		Chesterhall Parks Farm (South Lanarkshire)	
Site Type	Burial Cairn (positive feature)		Viking Settlement (positive feature)		Outer Ward (cropmark)		Prehistoric Enclosure (cropmark)		Prehistoric Enclosure (cropmark)	
Soil	Humus-iron podzol		Calcareous regosol		Mixed brown earth		Brown earth		Clay	
Soil Texture (A Horizon)	Medium-coarsed loamy sand with some gravels		Fine-grained sands with some fragments of shells		Medium-grained sandy loam		Stony sandy loam		Clay with some gravels	
In/off- site	In	Off	In	Off	In	Off	In	Off	In	Off
LOI *(%)*	0.031	0.025	0.061	*	0.057	0.075	0.029	0.028	0.031	0.031
Total P *(µg/kg)*	238	206	155	*	291	287	243	271	99	125
EC *(µs)*	*	*	100	*	118	122	54	*	97	117
pH (Figure 3-13)	Very strong acidity (4-4.5, from SIFSS database)		Strong alkalinity 9	*	Strong/very strong acidity 5	4	Very slight acidity 6.5	*	Medium acidity 6	5
MS *(10^{-8} m^3 kg^{-1})*	87	78	7	*	64	55	144	151	21	48
pXRF *(mg/kg)*										
Fe	33250	26196	11933	*	17512	16508	26416	26015	23995	22182
Mn	1460	1079	308	*	1003	735	791	749	287	478
Ti	6302	5969	1456	*	3876	3985	5653	5336	4944	4747
K	19294	17048	13955	*	15732	15044	13189	12608	10133	12545
Ca	3610	5544	148313	*	7382	2480	9416	8518	7573	5256

Table 9-1: Summary of the mean results of the physical and chemical analysis of the topsoil samples collected at the five case study sites. Most of the results show the in-site and off-site (controls) values. The * signifies not analysed.

9.2.1.3.1. *Soil Texture*

Coarse sandy soils drain water more quickly than finer clayey soils. Arable coarse soils with neutral pH and a thin litter layer, overlying a freely draining sand and gravel subsoil, can produce very high resistance values which may hamper earth resistance surveys in the Scottish summer time, as was the case at Forteviot. Here the rapid drainage capacity of the soils along with the stony nature of the topsoil impeded the completion of the earth resistance survey. On-site observation of soil texture suggested that the relatively high clay content of the topsoil (in the absence of a well developed organic layer) could retain some moisture for a while. The survey was repeated after a day of heavy rain and successfully completed. Sandy soils also may give clues about the nature of the soil survey environment as they often develop leaching processes and podzolic conditions which may have an impact on geophysical survey. These aspects are discussed in the section on soil post-deposition processes.

The higher number of micropores in clay soils cause retention of water, whilst the lack of macropores limit water infiltration rates, causing waterlogged conditions such as those seen in the clay soil at Chesterhall Parks Farm. Although such conditions can saturate and mask soil resistance contrast, the earth resistance survey nevertheless provided some results at the site. The GPR also provided useful results, especially with the low frequency survey (225MHz), as did the FDEM (quadrature in vertical mode). Despite the clay soil environment at Chesterhall Parks Farm, the targeted ditched enclosures were substantial (0.95m deep) and shallow buried. These aspects contributed to their detection by these techniques.

9.2.1.3.2. *Soil pH*

The pH characterisation of the soil samples taken at the five sites revealed their general acidic nature and defined the strong alkalinity of the wind-blown sands at the Bay of Skaill (Table 9-1). pH analysis of soil samples at Forteviot contributed to understanding the consecutive failures of the earth resistance survey. According to Pozdnyakov and Pozdnyakova (2002), the basic source of mobile electrical charges in humid areas is from soil cation exchange capacity (CEC, the soil's ability to absorb and exchange cations) and retention capacity. This may have contributed to the problems experienced with this survey. In spite

of the acidic nature (hence higher conductivity and mobilisation of charge particles) of the parent material from which the topsoil at Forteviot developed, the topsoil pH was close to neutral (Table 9-1).

pH neutralization of acidic topsoils can decrease the exchange capacity, hence reducing soil conductivity. This effect may be the consequence of agricultural practices used to control the pH to improve water retention of the naturally acidic soils at Forteviot. The electrical survey was completed after a day of heavy rain, demonstrating the benefits of temporal water availability to mobilize electrical charges in soils in survey environments characterised by coarse soil texture, neutral pH and low CEC such as at Forteviot. The increase in water availability after heavy rainfall could have triggered a temporary decrease in soil pH (increasing acidity), higher CEC and mobilisation of the electrical charges within the soil. This would have contributed to reduce the high soil resistivity, allowing the completion of the electrical survey. The sources of these electrical charges or ions are diverse and depend on many soil chemical properties, such as humus content, CEC, soil mineral composition and the amount of soluble salts.

9.2.1.3.3. *Major Soil Elements & MS*

Determination of the iron content in soil, if combined with MS analysis, may give an idea of magnetic background and state of the Fe-oxides present at the survey environment. Table 9-1 clearly shows the relatively high Fe concentrations in topsoil samples at the case study sites showing the impact of the acidic parent material from which most of these soils develop. However, high Fe concentration in soil does not always correlate with high MS; at Chesterhall Parks Farm, despite high Fe contents, the MS values are fairly low owing to the frequently waterlogged conditions at this site.

But more important is the determination of Fe and MS of topsoil, subsoil and archaeological deposits because this elucidates the complex factors of contrast and detection of archaeological features at the sites. For example, these analyses were fundamental in understanding the magnetic reversal of the ditches detected at Forteviot (Chapter 7).

9.2.1.4. **Soil Processes**

9.2.1.4.1. *Additions*

Archaeologically-rich coastal areas in Scotland are often characterised by sites concealed under high energy deposits of fine-grained sands developed by aeolian processes. These sites may present a series of challenges for geophysical survey as seen at the Viking site in the Bay of Skaill (Chapter 5). The sands at this site have a high concentration of Ca (Table 9-1) due to the calcium carbonate of the shells from which they were partially derived and the general MS values measured in the sands were fairly low. These low MS values are due to the main constituents of the sands, silica (SiO_2) in the form of quartz, and calcium carbonate ($CaCO_3$) which are diamagnetic materials. Cut features presenting enhanced MS fill deposits may be detected, for example, by gradiometer survey. However, these deposits can be fairly deep and the detection of archaeological features by gradiometry or earth resistance masked. The case study demonstrates the potential of GPR and FDEM survey to detect structural features in deep wind-blown sands. Although the gradiometer did not detect any structural feature at the site, it proved useful in identifying the midden deposits located near the Viking settlement. Whilst natural mounds may show homogenous and magnetically quiet sand deposits, anthropogenic mounds may be expected to be magnetically noisy. Therefore, this technique can still be useful in exploring mounds of potential archaeological importance by identifying magnetically noisy areas associated with anthropogenic deposits and so revealing former human occupation.

9.2.1.4.2. *Translocation*

Soil processes may develop localised hill/terrace slope deposits, such as the soliflucted fine-grained clays and colluvial volcaniclastic material at Chesterhall Parks Farm (Chapter 8), that may not correspond to the deposits indicated in soil maps. These deposits are the result of the gradual accumulation of fine weathered material that moved slowly downslope from the nearby Tinto Hill, induced by gravitational forces on saturated sediments and as a result of Periglacial/Postglacial conditions. The deep clay at this site explains the frequent waterlogged conditions at a site mapped as freely draining brown earth. Despite the high conductivity of clay soils and the magnetic noise introduced by the igneous material, the targeted enclosures at the site were

detected, to a relative degree, by geophysical means. The cut features showing the deep ditches at Chesterhall Parks Farm were detectable due to the shallowness of the overlying clay topsoil.

9.2.1.4.3. *Transformation*

Although the chemical analytical techniques used in this investigation (pXRF and ICP-OES) did not identify chemical forms, they allow an estimate of soil mineralogical transformations involved in the contrast and type of geophysical response detected at several sites.

For example, depletions of Mn occurring as a result of reductive dissolution of Mn oxides due to the decomposition of organic matter were observed at Scalpsie Bay (Chapter 4), Lochmaben Castle (Chapter 6) and Forteviot (Chapter 7). This transformation is the result of Mn oxides acting as electron acceptors for decomposing organic matter (Lovley *et al.* 1991). In environments where Mn is abundant, Mn reduction can be the main way to decompose organic matter (Magen *et al.* 2011). Mn and MS depletions correlated with the negative magnetic anomalies at Scalpsie Bay and Forteviot. Furthermore, Mn depletions were associated with increased biomass occurring as vegetation patches where potential structures were detected by the earth resistance and GPR surveys at Lochmaben. Similarly, the cropmark site at Forteviot showed Mn depletion and LOI enhancement in the uppermost fill deposit of the targeted ditched enclosure.

Other transformations related to redox processes are or can be triggered by organic matter accumulation. For example, increased water retention and transformation of ferric material to less magnetic ferrous forms (Weston 2002) may also have been involved in the detection of the targeted ditch enclosure at Forteviot. The reduction of iron to a lower magnetic form may have contributed to the lower MS of the outer ditch and the negative magnetic contrast.

The variations in water retention caused by the presence of organic matter inside the ditch at Forteviot seems to have given rise to contrasts in dielectric and conductivity properties, and their detection with the GPR and FDEM survey. However, soil textural variations in the cementation of the sands and gravels of the innermost cut of the ditch also led to electromagnetic wave impedance

contrast (section 7.3.3). The strong GPR reflections identified in the radargrams correlate with the location of the cemented sands and gravels as well as with the high variability of the chemical compositions here.

Topsoil samples at Chesterhall Parks Farm (Chapter 8) presented the characteristic mottling produced by waterlogging and reduction conditions (gleying). The frequent waterlogged conditions of the clay soils may have weakened the magnetic contrast produced by the ditch deposits of the targeted enclosures at this site, hence the weak anomalies. The generally low MS topsoil values and high Fe concentration (Table 9-1) support this observation.

9.2.1.4.4. *Loss of material*

Sandy soils in areas of high rainfall often develop podzols and the leaching processes associated with this type of soil may affect the distribution of chemical elements as seen in Scalpsie Bay (Chapter 4). Localized weak magnetic anomalies may be produced by leaching of Fe/Al as the ground-truthing of some anomalies suggested in Scalpsie Bay. Intense and localised magnetic responses have been reported to be presumably triggered by iron panning (Cole 1995). However, the magnetic intensity of the deposits reported by Cole's survey was higher than the anomalies ground-truthed at Scalpsie bay. The intensity or type of magnetism of the 'spurious' magnetic anomalies was not fully explored in this investigation. Given the profusion of podzols in Scotland, the potential occurrence of such 'spurious' anomalies may have to be taken into account during data interpretation.

9.2.1.5. **Ground Surface Conditions**

Land management practices have an impact on soils and, therefore, an effect on geophysical survey. For example, soil acidity management and fertiliser addition may explain the lower MS values of the topsoil at Forteviot. For example, the concentration of Ca of the topsoil at Forteviot (Table 9-1) seems to be higher than regional backgrounds (*c.*4439 mg/kg Ca) (Paterson 2011). Ca^{+2} is the dominant cation in the exchange complex in many soils, and its high value reflects the influence of farming where the addition of lime is a prerequisite for the growth of many arable crops. Therefore, the intense ploughing regime at

Forteviot in association with a leaching process and redox reactions explains the lower MS values and negative magnetic anomalies detected at this site.

9.2.2. Can a geophysical anomaly be explained chemically?

Soil chemical composition have an indirect effect on the detection of geophysical anomalies and contributed to understanding particular geophysical responses as explained in section 9.2.1, for example, Mn depletion (triggered by higher soil organic matter content) in association with negative magnetic anomalies. The suite of elements identified in the deposits sampled within the kerbed-wall at the site at Skaill (section 9.2.3) was associated with organic deposits related to the targeted wall structure. The high CEC and water retention of these deposits led to their detection as a conductive anomaly detected in the FDEM survey. Therefore, the causes of detection of geophysical anomalies at the sites studied in this thesis point to many inter-related soil factors, as the results from Forteviot (Chapter 7) clearly demonstrate. From the conclusions reported in this investigation there was no demonstrable direct effect of the concentration of a particular element, or suite of elements, on the respective geophysical response.

9.2.3. Can geophysical survey contribute to the understanding of geochemical anomalies of archaeological interest?

Yes. Anomalous geochemical compositions associated with the geophysical response of archaeological features have been observed in this investigation. For example, the area showing Ca enhancement and related to the work-camp activity (perhaps mortar/lime accumulation) in the outer ward of Lochmaben Castle (section 6.3.3) correlated with strong GPR reflections and an area of low resistance. Also, enhancement of MS, total phosphate and K, Fe, Ti, Mn, P, Rb, Ba, Cr, Li and Pb were identified in the deposits sampled within the kerbed-wall at the site at the Bay of Skaill (section 5.3.3) in association with a conductive anomaly detected in the FDEM survey.

Geochemical enhancements or depletions associated with the targeted features can be very complex. They may not always be the product of a direct

anthropogenic input, but can be caused by post-depositional processes developed inside archaeological features. An example is Mn, a reported anthropogenic element (section 2.3.6) which has shown depletion in association with higher water retention and organic matter accumulation at Scalpsie Bay (section 4.4) and Lochmaben (section 6.3.3).

Depletion of macronutrients (*e.g.* P, Mg and Ca) associated with the geophysical response of cropmarks or grassmarks evidence has also been observed at Lochmaben (section 6.3.3) and Forteviot (section 7.3.3). Again, whilst these depletions seem to be due to the uptake of such macronutrients by plants, there are also indirect indications of archaeological features.

Another characteristic geochemical response associated with near-surface ditch features was the high surface variation of many element concentrations in the topsoil samples. At Forteviot (section 7.3.3) the effect of ploughed ditch deposits on the soil surface mineralogy may have had an effect on the topsoil distribution of K, Ti and Ca. Similarly, many elements showed a high variation over the ditches at Chesterhall Parks Farm (section 8.3.3) in comparison with the more steady response outside the ditch areas. The more distinctive response at this site, in comparison with Forteviot, may have been a consequence of the rare ploughing in this field. The high variability of the chemical concentrations was also seen in the horizontal samples taken from the excavated sections at Forteviot (section 7.3.3).

9.2.4. What are the potential advantages of integrating geophysical and geochemical techniques?

The findings obtained from the five sites have demonstrated that the integration of geochemical and geophysical techniques can provide important information regarding particular causes of contrast and detection of archaeological anomalies (micro-scale) and other more general aspects about the impact of the site environment on the techniques (macro-scale). The micro-scale contributions can enhance the interpretation of particular geophysical and geochemical anomalies in the following ways:

- From a geophysical point of view, the geochemical analysis of soil samples from targeted archaeological features may help explain particular geophysical responses. Examples are the detection of weak magnetic negative responses from cut features at Forteviot (Chapter 7) or the detection of a conductive anomaly related to impervious feature in the FDEM survey as at the Bay of Skaill (Chapter 5). This is because soil post-depositional processes developed inside archaeological features can be fundamental to understand soil contrast dynamics (section 9.2.1). Also, the correlation of geophysical and geochemical datasets may help to confirm geophysical anomalies. At Scalpsie Bay (Chapter 4) the correlation of an uncertain negative magnetic anomaly with a set of elements suggested that the anomaly was the product of soil contrast and probably related to a subsurface feature rather than an effect of magnetic halos.

- The issue of whether a geochemical anomaly is anthropogenic or not can be better understood by its correlation with the corresponding geophysical response (*e.g.* 'anthropogenic' Mn depletions). Potential new types of geochemical response can be identified, for example, depletions in major elements in association with cropmark evidence, and these responses will in turn be usefully added to existing knowledge (section 9.2.3).

On a macro-scale, the integrated research strategy used in this thesis has proved useful to understand how local geological and soil conditions may affect the results of routine geophysical surveys. This information is fundamental to enable archaeological geophysicists to be more reflective about the potential influences on their results, such as the initial 'poor' results from Forteviot (Chapter 7), and to reconsider methods and approaches to survey. The physical and chemical characterisation of the survey environment before and during the surveys has demonstrated its importance in this study. These analyses may provide site-specific information, for example, at Chesterhall Parks Farm (Chapter 8) by characterising the poorly drained nature and fairly low MS of the topsoil. Such characterisation can be important in planning the most appropriate survey strategy at a new site. Soil characterisation and comparison with other sites (Table 9-1) allowed some important observations such as the effect of highly variable glacial drift deposits in gradiometer surveys carried out in Scottish

environments. Therefore, the general soil characterisation achievable with this integrated methodology may contribute to future efforts to evaluate the potential of geophysical surveys in other regions.

9.2.5. General Remarks

The aim (section 1.3) was to explore the combination of geophysical and geochemical techniques in order to improve the existing understanding of the factors involved in the genesis of contrast, in other words, how archaeological anomalies reveal themselves. The integrated survey strategy used at the five sites demonstrated that the results obtained from geophysical and geochemical methods can be better understood when they are combined because of the complementary information they provide.

The research leads to three general findings relating to the factors of contrast involved in the detection of geophysical and geochemical anomalies:

1. Soil settings and post-depositional processes are fundamental in understanding the detection of geophysical anomalies and this research demonstrates how soil factors and dynamics can be directly or indirectly identified by the integration of soil geochemical analysis (section 9.2.1).

2. The detection of geophysical and geochemical anomalies often depends upon inter-related and case specific variables (section 9.2.2) involving: soil type and geochemical dynamics; ground surface conditions and temporal climatic variations; and type and depth of burial of archaeological features.

3. The identity of chemical anomalies as either anthropogenic or natural (geogenetic) can be better understood if they are compared with the geophysical results (section 9.2.3).

Light has also been shed on the more general issue of the potential of geophysical techniques to survey archaeological sites in Scotland. The results presented in this thesis indicate that archaeological geophysical surveying does work in Scotland and can be a powerful tool to prospect and study sites in a non-destructive manner. The remarkable Scottish geodiversity (section 2.3), concentrated in a relatively small area, provides a high variability of survey

environments with the result that surveys based on a single technique may not be successful.

The advantages of using multi-technique surveys are well known among practitioners of archaeological geophysics because of the complementary information each dataset provides. However, it needs to be emphasised that for those who commission surveys or are end users of the results of surveys this multi-technique approach is necessary at archaeological sites in Scotland. This is because of the influence of the glacial past on the variability of the soil survey environment, along with equally variable weather conditions and types of archaeological feature.

The observations relating the effects of soil setting and processes on the detection of archaeological anomalies considered in this research may also be relevant to other northern European countries with similar geological, pedological and climatic characteristics. However, the strategies recommended in section 9.6, to plan and carry out cost-effective surveys using non-destructive techniques, can be applied worldwide, irrespective of environmental conditions.

9.3. Assessing the Success of the PhD Project

The aim and objectives of this project were successfully achieved. The characterisation of the geophysical response of archaeological features *vs*. soil matrix in terms of chemical composition and other soil properties provided invaluable results that led to a better understanding of the factors involved in the detection of archaeological anomalies. The findings were considered in the general conclusions of each case study site and they are further discussed in section 9.2.

The integrated survey strategy developed for this research combining geophysical and geochemical techniques was carefully planned (section 3.2) and was systematically applied at the five case study sites. Each of the case studies and archaeological targets posed a particular challenge for archaeological prospection and satisfied other criteria established in section 3.3.1. Since there were some difficulties in finding sites available to sample/ground-truth due to site regulations (section 9.4), the confirmation and soil sampling of the

archaeological targets by excavation was only possible at the Bay of Skaill (Chapter 5) and Forteviot (Chapter 7) and topsoil samples were taken at the remainder of sites (Chapters 4, 6 and 8). A qualitative assessment of the results of each technique and general suggestions relating to improvements in survey methodology were provided in the conclusion of each case study. The results of the survey strategy used in this thesis proved that the combination of geophysical and geochemical techniques can greatly contribute to answering archaeological questions. A drawback was the lack of time for extending the surveys but recommendations were given for future and more extensive survey at each case study site. Finally, section 9.6 focuses on the integrated strategies recommended for future surveys at archaeological sites as a result of this investigation.

9.4. Critique of the Study

The reasons behind the selection of the sites used in this project are explained in section 3.3.1. An important aspect in their selection was that the sites should be suitable for trial excavation in order to collect soil samples from inside and outside the targeted features as well as from the topsoil. However, permission for ground-truthing was rather difficult and eventually, it was only possible at two sites: Forteviot (Chapter 7) and the site at bay of Skaill (Chapter 5). At these sites, the possibility of comparing the geochemical results from topsoil samples, section samples and the geophysical response produced a wealth of information that was key to understanding the geophysical anomalies and topsoil geochemical concentrations.

Excavation at Scalpsie (Chapter 4), Lochmaben Castle (Chapter 6) and Chesterhall Parks Farm (Chapter 8) was not possible due to farming activities and scheduled monument restrictions. At these sites the geochemical analyses were done on topsoil samples and compared with the geophysical anomalies but there was not a direct geochemical characterisation of the targeted features. However, topsoil geochemical analysis provided useful information on general ground conditions and also characterised some archaeological features (*e.g.* Ca enrichment relating to the work-camp area at Lochmaben or the general high variation of elements over ditch features in Chesterhall Park and Forteviot).

Since the surveys carried out at the case studies focused on targeted features, rather small data sets were collected. The promising results of some of the techniques used would have required more extensive surveys in order to solve emerging questions relating to the archaeology (e.g. extending the GPR and FDEM survey at Skaill to search for the projection of the targeted kerbed-wall in relation to the long-house). The time-constraints of the fieldwork within the program of this research did not allow further extensive surveys, however recommendations for future surveys are given in the conclusions of each case study site.

Similarly, this research focused on targeted geochemical exploration rather than on chemical surveys for activity area determination. Nonetheless, several enhancements were observed in the sites of this investigation, such as Ca enrichment over the cairn at Scalpsie Bay (section 4.3.2) and over a work-camp area at Lochmaben Castle (section 6.3.3) as well as Mn enhancement over the targeted enclosure at Forteviot (section 7.3.3). These concentrations seem to be derived from ploughing activity, bringing up enhanced deposits from buried features and enhancing the sampled topsoils. More extensive geochemical surveys would have been of interest to confirm the extent of these geochemical concentrations but were impossible to undertake within the scope and time-limits of this PhD.

Establishing the minimum representative number of soil samples was difficult to determine before the field-work due to the multiple soil variables to be analysed and the lack of standard procedures in the relevant literature. Advice was sought at the Department of Statistics (University of Glasgow) and the Macaulay Land Use Research Institute. In general, a 0.5m sampling interval was used for topsoil sampling, decreasing the sampling interval over the targeted features (if known). The strategy adopted in sampling the exposed sections of features was to sample sufficiently densely to characterise all the deposits relating to the targeted feature and surrounding soil matrix. Since archaeological features often contain high-energy deposits (few deposits from a single event), such as at Forteviot (Chapter 7), rather than low-energy ones (layering), the sample size needed to characterise these deposits would appear to be lower. However, the experience from this investigation is that even high-energy archaeological features can be fairly complex and contain many micro-deposits which are key in

understanding the contrast they produce against the natural soil. Therefore, a systematic and high sampling density at several depths of all features containing many or only a few contexts is highly recommended, rather than increasing the number of samples in particular deposits. This is because during the sampling, details of the deposits can be missed, especially at those sites where the backfill material and subsoil are almost identical.

9.5. Impact of the Project

A new integrated approach: This project is the first systematic study to integrate geophysical and geochemical tools to survey archaeological features in order to understand the reasons behind their detection. Rather than comparing the results of the surveys and giving an independent interpretation of the structures (geophysical input) and possible activity carried out inside/outside the structure (geochemical input), this project is the first to focus on specific archaeological features to understand the soil dynamics involved in the detection of geophysical and geochemical anomalies. By focusing on single features and assessing their geophysical and geochemical relationships, this thesis has demonstrated that soil formation processes involved in the 'history' of buried archaeological features are of importance, the reasons behind the detection of anomalies can be better understood by using both geophysical and geochemical tools, and an enhanced interpretion of the site can therefore be provided.

Challenging and archaeologically 'rich' survey environments: This investigation is based on the results of a series of archaeological sites in environmental settings that may present a challenge for archaeological prospecting. Some of these survey environments are archaeologically 'rich', for example the aeolian coastal sediments in Chapter 5. The systematic multi-technique approach used in this project allowed a comprehensive assessment of its geophysical and geochemical potential with which to devise guidelines and recommendations for future prospection.

Developing cost-effective/affordable survey strategies: Cutting-edge geophysical and geochemical instruments are expensive and generally not affordable within the budget of most archaeological investigations. The use of

such new instruments in routine archaeological evaluations is also rare. Whilst most of the research has focused on technological advances, which is vital for developing the archaeological geophysics and geochemistry disciplines, reappraisals relating to the use of routine techniques (e.g. how to use them or combine them in specific site settings) are uncommon. Guidelines and standardised strategies relating to prospection methods are seldom published, with some exceptions, such as those published by English Heritage (2008) relating the use of geophysical prospection to archaeological field evaluations. Therefore, this project contributes by providing integrated strategies to assess sites prior to and during surveys in order to improve the cost-effectiveness of non-destructive techniques in archaeological investigation. The recommendations formulated in this project, based on the results of the different surveys carried out and challenges tackled in each case study site, also contribute to existing and future guidelines in archaeological prospection.

Assessing the potential of geophysical surveys in Scotland: This research was carried out during a period of review of the contribution of archaeological science to cultural resource management in Scotland, including the role of geophysical techniques (Milek and Jones 2012). For many years the ‘myth’ that 'geophysics did not work in Scotland' has been held amongst archaeologists working in Scotland, where archaeological geophysics has been regarded as unnecessary and a waste of money, despite the increasing use of these techniques (Ovenden 2010). Whilst geophysical techniques are mentioned in the Scottish national guidelines in the PAN 42 (Scottish Office 1994), their integration as routine techniques into the recommendations given by planning officers to developers has not been that successful. In 2003, the contributions of geophysical surveys carried out in Scottish archaeology was reviewed at the conference ‘Going over Old Ground’ (Jones and Sharpe 2006). A second effort to promote the potential of archaeological geophysics in archaeological field evaluation was made in 2010 with the ALGAO (Association of Local Government Archaeological Officers) and the IfA's GeoSIG Seminar in Geophysics 2010. The growing number of surveys undertaken throughout Scotland, the proliferation of geophysical commercial companies, and the number of archaeological community projects based on geophysical surveys show that the view on the role of geophysical survey in Scottish archaeology is changing. Taking into account

that challenging survey environments were deliberately selected in this research, the results and general recommendations obtained from the case study sites will assist with this change of perspective by providing guidance and tools in evaluating the potential of geophysical survey at Scottish sites.

9.6. Recommendations

This section suggests a series of strategies, distilled from the experience of this research, that integrate the use of soil geochemical analysis with geophysical surveying in order to aid in the design of *ad hoc* surveys and enhance data interpretation. The general assessment and recommendations of the different geophysical and geochemical techniques used in this research is detailed in the conclusions of each case study site.

Table 9-2 details how geochemical soil analysis used in this investigation can be applied to the planning and implementation of geophysical surveys at archaeological sites. Whist some of this analysis can be done on-site, Figure 3-11 shows how it can be organised in a more controlled laboratory/on-site laboratory environment. Bulk soil samples (B in Table 9-2) from the topsoil, subsoil and archaeological deposits can be collected as described in section 3.4.3. Coring or augering (C-A in Table 9-2) techniques can also be used. Corers or intact blocks (IB in Table 9-2), such as kubiena tins, are generally preferred since these techniques usually provide undisturbed samples. Direct analysis of exposed sections (ES in Table 9-2) of excavated features can be carried out by some techniques. Table 9-2 lists other relevant studies which combine geophysical surveys and soil analysis, where further information relating to the use of specific techniques can be consulted.

Ideally, the soil sampling should be organised at different stages of the geophysical surveys which include: site assessment, multi-technique survey and, when possible, ground-truthing of the geophysical results.

First, the pre-survey site assessment (SA in Table 9-2) involves the compilation of all the existing information relating to the site as explained in section 3.3.2. At this stage, a site visit and initial soil exploration (topsoil and subsoil if possible at several locations) may provide useful information about the survey

environment to help design the best strategy. Aspects such as confirmation of soil type, ground conditions, topsoil depth, type of parent material, exploring topsoil/subsoil magnetic susceptibilities and major element compositions, soil pH and general ground conductivity can give a rounded view of general ground conditions. Visual assessments to take into account include landforms as they can also provide clues about soil formation processes that may characterise the survey environment. Whilst temporal effects of climatic parameters may affect the results of geophysical surveys, these are difficult to control especially in a country such as Scotland. However, regional local weather records can give an insight into possible ground survey conditions to expect and the potential effect on the techniques.

Second, the survey (S in Table 9-2) should be planned according to the findings of the site assessment and the selection and prioritisation of geophysical techniques upon time and resources (*e.g.* budget). The order of use of techniques ideally should start with those that can provide rapid area coverage in order to explore the site. Next come higher resolution surveys or other techniques that require more time in the field. Soil sampling can be useful to monitor soil conditions during the course of the fieldwork and to assist data interpretation (Table 9-2).

Third, and in the case of excavations or ground-truthing (E-GT in Table 9-2) following the geophysical survey, further surveys should be organised, encompassing soil sampling as the excavation develops. Excavations naturally provide invaluable opportunities to confirm the interpretations and explore the factors behind the detection of geophysical anomalies, as the investigations at Forteviot (Chapter 7) and the Bay of Skaill (Chapter 5) illustrate. Ground-truthing of specific geophysical anomalies using augering/coring techniques can also be quickly assessed by carrying out on-site pXRF analysis. This type of portable instrument offers great potential not only in the (in-situ) interpretation of geophysical anomalies but also in providing a quick assessment of the soil survey environment.

The adoption of these integrated strategies (section 9.2.4) may be most applicable in a research environment, where the techniques, time and interdisciplinary teams are likely to be available. The extra effort in acquiring

and analysing the geochemical data that is required in this integrated approach must be taken into account. However, their incorporation into a commercial environment must also be considered and understood. For example, the dual approach can help to resolve geophysical anomalies in evidence and to contribute to their interpretation using less invasive geochemical analyses as the ones presented in Table 9-2. Planning cost-effective survey strategies requires a deep understanding of the survey environment, and so the analytical tools used in the site assessment stage presented in Table 9-2 will help in selecting the most appropriate suite of techniques to successfully prospect a site. Site visits, familiarisation with pre-existing information and minimal soil exploration can be a real mitigation strategy to avoid disappointments and improve cost-effectiveness of commercial surveys. Where a site visit is impossible, every effort should be made to consult pre-existing databases, such as the ones summarised in Table 3.2 for Scotland. Furthermore, augering-coring of particular geophysical anomalies in order to enhance geophysical data interpretation using portable instruments (*e.g.* pXRF) in combination with other cheap and quick soil analysis (*e.g.* MS) can add a new dimension to commercial geophysical surveys for archaeological evaluation.

Of course, this would require some effort on the part of commercial contractors and organisations such as the IfA in order, for example, to develop opportunities (*e.g.* CPD schemes) to train operators in soil geochemical analysis and instrument handling. Whilst these efforts initially require time, the advantages achievable in the long term can be many. Taking into account the increasing number of commercial geophysical companies not only in Scotland but elsewhere, archaeological geophysicists from academic and commercial environments must have a good understanding of the physics behind the techniques and technological developments, as well as an understanding of soil geochemistry.

Soil Analysis	Survey Stages	Sample Type	Application	On-site	Lab	Cost-effective	References
Texture	SA, E-GT	B, C-A	To identify macro-soil properties of site soil environments or archaeological deposits. Texture analysis can give clues on the water retention regime of the soils and other related soil processes that may have an effect on geophysical surveys.		✓	✓	Here (Chapter 3)
pH & EC	SA, S, E-GT	B, C-A	To characterise the degree of acidity or alkalinity of the survey soil environments or archaeological deposits. pH determination can contribute to understand soil water retention dynamics and their effect in the movements of electrical charges that may have an effect in soil conductivity.	✓	✓	✓	Here (Chapter 3)
LOI	SA, S, E-GT	B, C-A	To estimate the organic matter content at the survey soil environments or archaeological deposits. Organic matter can determine the water retention of soils and affect their drainage. This may have an effect on geophysical surveys.		✓	✓	Here (as part of Total P analysis, Chapter 3)
Total P	SA, S, E-GT	B, C-A	To identify possible land management practices affecting geochemistry of topsoil/subsoil/archaeological deposits. To identify Total P anomalies (in correlation with potential geophysical responses) to enhance the interpretation of the geophysical anomalies.		✓	✓	Here (Chapter 3)
ICP-OES	E-GT	B, C-A	To assist pXRF analysis as a control technique in order to test the concentration of common elements in a number of soil samples. If time and resources are available, to accurately identify anthropogenic trace elements (in correlation with potential geophysical responses) to enhance the interpretation of the geophysical anomalies.		✓	Costly, high accuracy (lighter elements)	Here & Armstrong 2010 (peat soil samples from archaeological sites)
pXRF	SA, S, E-GT	B, C-A, IB, ES	To determine the concentrations of major/minor elements to obtain general information about soil mineralogy that may have an impact on geophysical results. For example, Fe characterisation may contribute an understanding of the magnetic background and state of the Fe-oxides present in the survey soil environments or archaeological deposits (better if combined with MS analysis). Fe-oxides can also have an effect on the water retention capacity of soils. Finally, pXRF can be used to identify anthropogenic trace elements (in correlation with potential geophysical responses) to enhance the interpretation of geophysical anomalies.	✓	✓	✓	Here (Chapter 3)
MS	SA, S, E-GT	B, C-A, IB, ES	To measure the χhf, χlf and χfd of soil samples: to characterise the MS of topsoil, subsoil and archaeological deposits to identify anthropogenic sediments in correlation with potential geophysical responses; also to obtain mineralogical information especially relating the geochemistry of Fe (better if combined with pXRF analysis) that may have an impact on geophysical results. MS analysis can also help to establish the natural or anthropogenic origin of element concentrations by assessing the χfd values of the soil samples (*e.g* . high χfd and χlf in correlation to enhanced Mn, indicating burning).	✓	✓	✓	Here (Chapter 3), Dearing *et al.* 1996, Kattenberg 2008 & Armstrong 2010 (peat soil)

Site Assessment (**SA)** Survey (**S**) Excavation/Ground-truthing (**E-GT**) / Bulk samples (**B**) Core-auger (**C-A**) Intact block (**IB**) Exposed section (**ES**)

Table 9-2: Summary of soil geochemical analyses used in this research and their possible application to archaeological geophysics.

9.7. Further Work & Research Opportunities

9.7.1. Effects on Sample Homogeneity

Further to the sampling strategies and analyses suggested in section 9.6, I would suggest a formal pXRF study comparing the elemental composition of fresh augered or bulk soil samples versus air-dried samples analysed in the laboratory. This comparison would be useful to assess the effect of possible deviations in pXRF results due to inhomogeneous fresh samples (matrix effects in section 3.5.1.3.3).

9.7.2. Testing Additional Techniques

Other portable instruments could also be tested for mineralogical determination of ground-truthed archaeological anomalies such as portable X-ray Diffraction (pXRD). pXRD is a direct analytical method for determining the presence of mineral species in a sample (Nakai and Abe 2011). In combination with pXRF, this may provide a quick and accurate analysis of the soil mineralogy directly involved in the detection of geophysical anomalies and contribute to their interpretation.

Another technique to consider is time-domain reflectometry (TDR). TDR is widely used to measure the water content of soils and is based on the relationship between propagation velocity, dielectric permittivity and volumetric water content determination (Topp *et al.*1980). It has also been used to determine the velocity of radar waves in archaeological deposits (Leckebusch 2000; Verdonck *et al*. 2009) as well as identifying differences in relative permittivity between deposits to assess the causes of GPR reflections in archaeological deposits (Verdonck *et al*. 2009) and Fe-oxide deposits (Van Dam *et al*. 2002). While TDR has proven useful in understanding GPR reflections (Van Dam 2001, 98), direct correlations between TDR measurements and GPR reflections have not yet been demonstrated.

A pOSL instrument (section 3.5.2.3) was tested at Forteviot (section 7.3.3) by analysing topsoil and bulk samples collected over the targeted ditch. Further studies with increased numbers of soil samples analysed, taken over different

soil types, plough regimes (e.g. recently ploughed fields) and more controlled sampling conditions would be necessary to properly assess its potential. While the pOSL results of topsoil samples did not show any coherent enhancement or depletion indicating the enclosure, the analysis of the bulk samples taken inside the ditch showed clear depletions in luminescence which is potentially interesting for two reasons. Firstly, pOSL can be used for quick detection of archaeological features by coring/augering, especially at those sites where the backfill of cut features is similar to the surrounding soil, as was the case at Forteviot (Chapter 7). Secondly, since the excavation of ditches for the construction of prehistoric enclosures seems to have bleached significantly their natural luminescence dose, as the depleted values of ditch samples show, anomalous radiation doses of natural radioactive elements such as K, Th and U, remotely detected by instruments such as a gamma ray spectrometer, may be indicative of near-surface archaeological features. This opens a relatively unexplored new area of research (Ruffell and Wilson 1998; Moussa 2001) in which radiometrics could be used for archaeological prospection.

9.7.3. Testing & Modelling Responses

Further research on the study of geophysical and geochemical responses of common archaeological features should focus on sites where the archaeological and geophysical evidence is well-understood, and where the archaeological targets can be ground-truthed and sampled for soil analyses. This strategy has demonstrate in this thesis to provide more conclusive results since it allows a more complete assessment of geochemical techniques against well-known targets. Such sites can be understood as test-sites where particular hypotheses relating to the detection of geophysical or geochemical anomalies at archaeological sites can be addressed in future investigations.

Whilst test-sites may be difficult to find and organised for ground-truthing in the time-span of a research project, an alternative for future hypothesis-testing approaches can be through the development of response modelling via 3D physical models (e.g. sand test-box, 3D printing replicas of soil and archaeological features) or synthetic forward modelling. However, the limits of these approaches have also to be understood as the recreated medium (physical or synthetic) is not the same as the real field conditions (test-site). Therefore,

test-site studies followed by response modelling may be the ideal approach for future hypothesis oriented investigations.

9.7.4. Final Thoughts

Whilst the integrated strategies used in this thesis and those recommended in section 9.6 can improve the planning and understanding of the results of surveys, prediction can only be provided by forward modelling and general mapping of the geochemical/geophysical properties and their potential for survey. The experience and findings from this investigation may contribute towards future efforts in these developments.

In the variety and dynamics of soil systems, there is neither a single factor that can explain the diverse processes that allow the detection of geophysical or geochemical anomalies of archaeological significance, nor a “magic” method able to detect them regardless of the soil environment. Soil properties and post-burial soil formation processes are inherently related to archaeological features and their proxy detection, and they have to be considered simultaneously to enable a deeper understanding of the data. Therefore it is crucial to develop and use survey strategies based on various sources of proxy data which, when combined, can provide a better understanding of the datasets. A closer cooperation between soil science, archaeological geophysics and geochemical survey has provided, in this thesis, new insights and opened up new ways for the fascinating discipline of archaeological prospection to progress.

References

Adderley, W.P., Alberts, I.L., Simpson, I.A., Wess, T.J., 2004. Calcium–iron–phosphate features in archaeological sediments: characterization through microfocus synchrotron X-ray scattering analyses. *Journal of Archaeological Science* 31, 1215–1224.

Aitken, M.J., 1985. *Thermoluminescence Dating*. Academic Press, London.

Aitken, M.J., 1998. *An introduction to optical dating: the dating of Quaternary sediments by the use of photon-stimulated luminiscence*. Oxford University Press: New York.

Alcock, L. & Alcock, E.A., 1992. Reconnaissance excavations on early historic fortifications and other royal sites in Scotland, 1974-84; excavations and other fieldwork at Forteviot, Perthshire, 1981; excavations at Urquhart Castle, Inverness-shire, 1983; excavations at Dunnottar, Kincardineshire. *Proceedings of the Society of Antiquaries of Scotland* 122, 215–287.

Annan, A.P., 2001. Ground Penetrating Radar. Workshop notes. Sensors & Software. Ontario, Canada.

Annan, A.P., 2009. Electromagnetic principles of ground penetrating radar, in: Jol, H.M. (Ed.), *Ground Penetrating Radar: Theory and Applications*, 3–40. Elsevier, Oxford.

Aqdus, S.A., Hanson, W.S., Drummond, J., 2012. The potential of hyperspectral and multi-spectral imagery to enhance archaeological cropmark detection: a comparative study. J*ournal of Archaeological Science* 39, 1915–1924.

Arcone, S., Grant, S., Boitnott, G., Bostick, B., 2008. Complex permittivity and clay mineralogy of grain-size fractions in a wet silt soil. *Geophysics* 73, J1–J13.

Armstrong, K., 2010. *Archaeological Geophysical Prospection in Peatland Environments*. PhD thesis. Bournemouth University.

Aspinall, A., Gaffney, C., Schmidt, A., 2008. *Magnetometry for Archaeologists.* AltaMira Press, Lanham, Maryland.

Aston, M., Martin, M.H., Jackson, A.W., 1998a. The use of heavy metal soil analysis for archaeological surveying. *Chemosphere* 37, 465–477.

Aston, M.A., Martin, M.H., Jackson, A.W., 1998b. The potential for heavy metal soil analysis on low status archaeological sites at Shapwick, Somerset. *Antiquity* 72, 838–847.

Atkinson, R.J.C., 1953. *Field Archaeology,* (second edition). Methuen, London.

Baker, G.S. & Jol, H.M., 2007. *Stratigraphic Analyses using GPR*. Geological Society of America.

Baker, G.S., Jordan, T.E., Pardy, J., 2007. An introduction to Ground Penetrating Radar (GPR), in: Baker, G.S., Jol, H.M. (Eds.), *Stratigraphic Analyses Using GPR*. Geological Society of American Special Publication 432.

Ballantyne, C.K., 1993. Tinto hill, in: Gordon, J.E., Sutherland, D.G. (Eds.), *Quaternary of Scotland,* 554–556. Chapman & Hall.

Bartington Instruments, 1993. Operation manual for Grad601 magnetic gradiometer. Witney, Oxford.

Bartington Instruments, 2008. Operation Manual for MS2 Magnetic Susceptibility System. Oxford, United Kingdom.

Barton, K., Stenvik, L., Birgisdottir, B., 2009. A chieftain' s hall or a grave: ground penetrating radar in an archaeological geophysics survey to target the excavation of a cropmark near Stiklestad, Nord-Trondelag. *5th International Workshop on Advance Ground Penetrating Radar IWAGPR2009* 5–10.

Becker, H. & Fassbinder, J.W.E., 2001. *Magnetic Prospecting in Archaeological Sites*, Paris: ICOMOS.

Benech, C. & Marmet, E., 1999. Optimum depth of investigation and conductivity response rejection of the different electromagnetic devices measuring apparent magnetic susceptibility. *Archaeological Prospection* 6, 31–45.

Bevan, B.W., 2000. An early geophysical survey at Williamsburg, USA. *Archaeological Prospection* 58, 51–58.

Bibby, J.S., 1984. *Soil Survey of Scotland, Firth of Clyde. Sheet 63, 1:50 000 Provisional Soil Map*. The Macaulay Institute for Soil Research. Aberdeen.

Bintliff, J., Gaffney, C., Waters, A., Davies, B., Snodgrass, A., 1990. Trace metal accumulation in soils on and around ancient settlements in Greece, in: Bottema, S., Entjes-Nieborg, G., van Zeist, W. (Eds.), *Man's Role in Shaping of the Eastern Mediterranean Landscape,* 159–172. Balkema, Rotterdam.

Birch, S., Wildgoose, M., Kozikovski, G., 2005. Uamh an Ard Achadh (High Pasture Cave). Strath, Isle of Skye 2004. Data Structure Report.

Bluck, B.J., 2010. The Highland Boundary Fault and the Highland Border Complex. *Scottish Journal of Geology* 46, 113–124.

Breiner, S., 1999. Applications Manual for Portable Magnetometer. Geometrics. California.

Bristow, C.S., 2009. Ground penetrating radar in aeolian dune sands, in: Jol, H.M. (Ed.), *Ground Penetrating Radar: Theory and Applications*. Elsevier Science.

Bristow, C.S. & Jol, H.M., 2003. An introduction to ground penetrating radar in sediments, in: *Ground Penetrating Radar in Sediments,* 1–7. The Geological Society, London.

British Geological Survey, 2012a. Corncockle Sandstone Formation. BGS on-line lexicon of rock units, (http://www.bgs.ac.uk/lexicon/lexicon.cfm?pub=CCK, accessed 31 May 2012).

British Geological Survey, 2012b. Kilblane Formation. BGS on-line lexicon of rock units, (http://www.bgs.ac.uk/lexicon/lexicon.cfm?pub=KBSG, accessed 13 June 2012).

British Geological Survey, 2012c. Wiston Grey Volcaniclastic Sandstone Member, BGS on-line lexicon of rock units, (http://www.bgs.ac.uk/lexicon/lexicon.cfm?pub=WGVS, accessed 10 June 2012).

Brito-Schimmel P. & Carreras, C., 2010. Metodología para la prospección geofísica en Arqueología: apuntes a partir de los trabajos de Iesso, Can Tacó, Molins Nous y el Goleró. *Lucentum* 29, 9–22.

Brown, J.F., 1975. Potassium-argon evidence of a Permian age for the camptonite dykes: Orkney. *Scottish Journal of Geology* 11, 259–262.

Browne, M., Smith, R., Aitken, A.M., 2002. Stratigraphical framework for the Devonian (Old Red Sandstone) rocks of Scotland south of a line from Fort William to Aberdeen. British Geological Survey.

Bryce, T.H., 1904. On the cairns and tumuli of the Island of Bute. A record of explorations during the season of 1903. *Proceedings of the Society of Antiquaries of Scotland* 38, 52–57.

Campana, S. & Piro, S., 2009. *Seeing the Unseen. Geophysics and Landscape Archaeology*. London: Taylor & Francis.

Carruthers, M., Lelong, O., Maguire, D., Shearer, I., 2004. The Village, Hirta, St Kilda (Harris parish), souterrain; 19th-century crofting village. *Discovery Excavation Scotland*, 5, 136.

Cassidy, N.J., 2008a. Introduction to GPR. Pre-conference Workshops. *12th International Conference on Ground Penetrating Radar (GPR'08)*. Birmingham, UK.

Cassidy, N.J., 2008b. GPR attenuation and scattering in a mature hydrocarbon spill: a modeling study. *Vadose Zone Journal* 7, 140.

Cassidy, N.J., 2009a. Electrical and magnetic properties of rocks, soils and fluids, in: Jol, H.M. (Ed.), *Ground Penetrating Radar: Theory and Applications*, 41–72. Elsevier, Oxford.

Cassidy, N.J., 2009b. Ground penetrating radar data processing, modelling and analysis, in: Jol, H.M. (Ed.), *Ground Penetrating Radar: Theory and Applications*, 141–176. Elsevier, Amsterdam..

Cassidy, N.J., Eddies, R., Dods, S., 2011. Void detection beneath reinforced concrete sections: the practical application of ground-penetrating radar and ultrasonic techniques. *Journal of Applied Geophysics* 74, 263–276.

CEN, 2005. Determination of pH in soil, sewage sludge and biowaste. European Commission and the European Free Trade Association. European Committee for Standardization (CEN).

Chiesi, L., Kejik, P., Janossy, B., Popovic, R.S., 2000. CMOS planar 2D micro-fluxgate sensor. *Sensors and Actuators A: Physical* 82, 174–180.

Childe, V.G., 1931a. Skara Brae: a "Stone Age" village in Orkney. *Antiquity* 5, 47–60.

Childe, V.G., 1931b. *Skara Brae, A Pictish village in Orkney*. London.

Christensen, B.T. & Malmros, P.A., 2012. Loss-on-ignition and carbon content in a beech forest soil profile. *Oikos* 5, 376–380.

Clark, A., 1990. *Seeing Beneath the Soil. Prospecting Methods in Archaeology.* Routledge, London.

Clarke, C.M., Utsi, E., Utsi, V., 1999. Ground penetrating radar investigations at North Ballachulish Moss, Highland, Scotland. *Archaeological Prospection* 6, 107–121.

Clarke, D.V., 2003. Once upon a time Skara Brae was unique, in: Armit, I., Murphy, E., Nelis, E., D, S. (Eds.), *Neolithic Settlement in Ireland and Western Britain,* 84–92. Oxbow Books, Oxford.

Cole, M.A., 1995. Baston Drove, Thurlby, Lincolnshire. Report on Geophysical Survey. The English Heritage Geophysical Survey Database, 55/95, (http://www.eng-h.gov.uk/reports/thurlby, accessed 1 August 2012).

Conyers, L.B., 2004. *Ground-Penetrating Radar for Archaeology*. AltaMira Press, Oxford.

Conyers, L.B., Ernenwein, E.G., Grealy, M., Lowe, K.M., 2008b. Electromagnetic conductivity mapping for site prediction in meandering river floodplains. Archaeological Prospection 15, 81–91.

Cook, M., Rankin, D., Ellis, C., Cowie, R., Sheridan, A., Mcsweeney, K., 1999. Excavation of two cairns, a cist and associated features at Sanaigmhor Warren, Islay, Argyll and Bute. *Proceedings of the Society of Antiquaries of Scotland* 129, 251–279.

Cook, S.R., Clarke, a. S., Fulford, M.G., 2005. Soil geochemistry and detection of early Roman precious metal and copper alloy working at the Roman town of Calleva Atrebatum (Silchester, Hampshire, UK). *Journal of Archaeological Science* 32, 805–812.

Cornell, R.M. & Schwertmann, U., 2007. *The iron oxides: structure, properties, reactions, occurences and uses*. WILEY-VCH Verlag GmbH & Co, Weinheim.

Cowley, D.C., 2002. A case study in the analysis of patterns of aerial reconnaissance in a lowland area of Southwest Scotland. *Archaeological Prospection* 9, 255–265.

Cuenca-García, C., 2010. The interface of geophysical and geochemical survey: towards an understanding of geophysical data quality in challenging archaeological sites, in: The Geological Society (Ed.), Near Surface Geophysics Group (NSGG) Day Meeting: Recent Work in Archaeological Geophysics, 44. The Burlington House, London, (poster available at: http://glasgow.academia.edu/CarmenCuencaGarcia/Papers).

Cuenca-García, C., 2011. Geophysical survey at Scalpsie Bay (Isle of Bute). *Discovery and Excavation in Scotland* 12, 53-54.

Cuenca-García, C. & Jones, R.E., 2011. The Geophysical Equipment Facility Project 912 Scientific Report: the interface of geophysical & geochemical survey in archaeological prospection. *The Geophysical Equipment Facility (GEF), NERC*. Edinburgh.

Cuenca-García, C. & Poller, T., 2011. SERF: Forteviot cropmark complex geophysics. *Discovery and Excavation in Scotland* 12, 149-150.

Cuenca-García, C., 2013. The burial cairn at Scalpsie Bay: an integrated geophysical survey, in: Duffy, P. (Ed.), *One Island, Many Voices: Bute, Archaeology and the Discover Bute Landscape Partnership Scheme*, 50-51. Society of Antiquaries of Scotland, Edinburgh.

Cuenca-García, C., Jones, R.E., Hall, A.J., Poller, T., 2013. From the air to the atomic level of a ditch: integrating geophysical and geochemical techniques at the cropmark complex of Forteviot (Perthshire, Scotland). In *10th International Conference on Archaeological Prospection (AP2013)*. Universität Wien, Austrian Academy of Sciences, Vienna.

Cuenca-García, C. & Jones, R.E., (*in preparation*). Gradiometer survey at the industrial limekiln site of Craigend (Milngavie, Scotland). Archaeology, School of Humanities, University of Glasgow, Scotland.

Dalan, R.A., 2006. Magnetic Susceptibility, in: Johnson, J.K.. (Ed.), *Remote Sensing in Archaeology: an explicitly North American perspective.* University of Alabama Press, Tuscaloosa, Alabama.

Dalan, R.A., 2008. A review of the role of magnetic susceptibility in archaeogeophysical studies in the USA: recent developments and prospects. *Archaeological Prospection* 31, 1–31.

David, A., 2005. The role and practice of archaeological prospection, in: Brothwell, D.R., Pollar, A.M. (Eds.), *Handbook of Archaeological Science,* 521–527. Wiley, Chichester.

DBLPS, 2011. Discover Bute Landscape Partnership Scheme (DBLPS), (http://www.discoverbute.com, accessed 1 August 2012).

DCLG, 2012. *PPS5: Planning for the Historic Environment.* Department for Communities and Local Government. London.

Dearing, J.A., Hay, K.L., Baban, S.M.J., Huddleston, A.S., Wellington, E.M.H., 1996. Magnetic susceptibility of soils: an evaluation of conflicting theories using national data set. *Geophysical Journal International* 127, 728-743.

Dearing, J.A., 1999. Environmental magnetic susceptibility using the Bartington MS2 system, (second edition). Chi Publishing, England.

Delaune, R.D. & Reddy, K.R., 2005. Redox potential, in: Hillel, D. (Ed.), *Encyclopedia of Soils in the Environment*, 366–371. Academic Press.

Dixon, J.B. & Schulze, D.G., 2002. *Soil Mineralogy with Environmental Applications*. Soil Science Society of America. Book Series 7.

Driscoll, S., Brophy, K., Noble, G., 2010. The Strathearn Environs and Royal Forteviot Project (SERF), (http://antiquity.ac.uk/projgall/driscoll323, accessed 1 August 2012).

Eckel, W.P., Rabinowitz, M.B., Foster, G.D., 2002. Investigation of unrecognized former secondary lead smelting sites: confirmation by historical sources and elemental ratios in soil. *Environmental Pollution* 117, 273–279.

English Heritage, 2008. *Geophysical Survey in Archaeological Field Evaluation,* (second edition). English Heritage Publishing, Swindon.

Entwistle, J.A., Abrahams, P.W., Dodgshon, R.A., 1998. Multi-element analysis of soils from scottish historical sites. Interpreting land-use history through the physical and geochemical analysis of soil. *Journal of Archaeological Science* 25, 53–68.

Entwistle, J.A., Abrahams, P.W., Dodgshon, R.A., 2000a. The geoarchaeological significance and spatial variability of a range of physical and chemical soil properties from a former habitation site, Isle of Skye. *Journal of Archaeological Science* 27, 287–303.

Entwistle, J.A., Abrahams, P.W., Dodgshon, R.A., 2000b. An investigation of former land-use activity through the physical and chemical analysis of soils from the Isle of Lewis, Outer Hebrides. *Archaeological Prospection* 188, 171-188.

Entwistle, J.A., Mccaffrey, K.J.W., Dodgshon, R.A., 2007. Analysis of soils to interpret land-use history in the Hebrides, Scotland. *Geoarchaeology* 22, 391–415.

Entwistle, J.A. & Wilson, C.A., 2007. A comparison of XRF and nitric-extraction/ICP-AES for differentiating and interpreting soils from an abandoned rural township in Perthshire. Scotland, *Society of Archaeological Science*. SAS Bulletin 30, 10–12.

EPA, 2007. Method 6200: Field portable X-ray fluorescence spectrometry for the determinations of elemental concentrations in soils and sediments. Environmental Protection Agency (EPA). US.

Esu, I. E., 2010. *Soil Characterisation, Classification and Survey.* African Books Collective, HEBN Publishers Plc, Ibadan, Nigeria.

Fassbinder, J.W.E. & Stanjek, H., 1993. Occurrence of bacterial magnetite in soils from archaeological sites. *Archaeologia Polona* 31, 117–128.

Fassbinder, J.W.E., Stanjek, H., Vali, H., 1990. Occurence of magnetic bacteria in soil. *Nature* 343, 161–163.

Fitzpatrick, E.A., 1963. Deeply weathered rock in Scotland, its occurrence, age, and contribution to the soils. *Journal of Soil Science* 14, 33–43.

Frahm, E. & Doonan, R.C.P., 2013. The technological versus methodological revolution of portable XRF in archaeology. *Journal of Archaeological Science*, 40, 1425–1434.

Gaffney, C.F. & Gater, J., 2003. *Revealing the Buried Past: Geophysics for Archaeologists.* Tempus, Stroud.

Gaffney, C., 2008. Detecting trends in the prediction of the buried past: a review of geophysical techniques in archaeology. *Archaeometry*, 50 (2), 313–336.

Gardiner, D.T. & Miller, R.W., 2004. *Soils in Our Environment*, 10th ed. Pearson Education, Upper Saddle River, New Jersey.

Geoscan Research, 2004. Geoplot (Data processing). Instruction Manual. Bradford.

Gill, R. & Ramsey, M.H., 1997. What a geochemical analysis means, in: R. Gill (Ed.) (Ed.), *Modern Analytical Geochemistry: an Introduction to Quantitative Chemical Analysis Techniques for Earth, Environmental and Materials Scientists*, 1–11. Addison Wesley Longman, Essex, UK.

Goodman, D., Hongo, H., Higashi, N., Inaoka, H., Nishimura, Y., 2007. GPR surveying over burial mounds: correcting for topography and the tilt of the GPR antenna. *Near Surface Geophysics* 383–388.

Gordon, J.E., Lees, R.G., Leys, K.F., Macfadyen, C.C.J., Puri, G., Threadgould, R., Kirkbride, V., 2002. Natutal Heritage Zones: Earth Sciences. Scottish Natural Heritage.

Griffiths, D., 2006. Birsay and Skaill Orkney, Landscape Survey 2003–04, in: Jones, R., Sharpe, L. (Eds.), *Going over Old Ground, Perspectives on Archaeological Geophysical and Geochemical Survey in Scotland,* 213–224. British Series 416, Oxford.

Griffiths, D., 2007. Birsay-Skaill Landscape Archaeology Project. Data Structure Report 2007 (Phase VIII). University of Oxford.

Griffiths, D. & Ashmore, P., 2011. *Aeolian Archaeology: The Archaeology of Sand Landscapes in Scotland,* 9–24. Society of Antiquaries of Scotland, Historic Scotland, Council for British Archaeology.

Griffiths, D. & Harrison, J., 2011. Settlement under the sand. *Current Archaeology* 253, 12–19.

Guttmann, E.B., Simpson, I.A., Davidson, D.A., Dockrill, S.J., 2006. The management of arable land from prehistory to the present: case studies from the northern isles of Scotland. *Geoarchaeology* 21, 61–92.

Hale, D., 2010. Geophysical evaluation in Scotland and beyond: some case studies, in: *ALGAO Seminar on Geophysics.* ALGAO Scotland (GeoSIG) & the IFA. Edinburgh.

Hammon III, W.S., McMechan, G.A., Zeng, X., 2000. Forensic GPR: finite-difference simulations of responses from buried human remains. *Journal of Applied Geophysics* 45, 171–186.

Haslam, R. & Tibbett, M., 2004. Sampling and analyzing metals in soils for archaeological prospection: a critique. *Geoarchaeology* 19, 731–751.

Hawkes, H.E., 1957. *Principles of Geochemical Prospecting*. Geological Survey Bulletin 1000-F, Washington D.C.

He, Y.Q., Zhu, Y.G., Smith, S.E., Smith, F.A., 2002. Interactions between soil moisture content and phosphorus supply in spring wheat plants grown in pot culture. *Journal of Plant Nutrition* 25, 913–925.

Heron, C., 2001. Geochemical Prospecting, in: Brothwell, D.R., Pollard, A.M. (Eds.), *Handbook of Archaeological Science,* 565–573. Wiley: Chichester.

Hesse, A., 1980. La prospection des vestiges préhistoriques en milieu proche-oriental: une douzaine d'années d'expériences géophysiques. *Paléorient* 6, 45–54.

Historic Scotland, 2012. Lochmaben Castle, (http://www.historic-scotland.gov.uk/propertyresults/propertydetail.htm?PropID=PL_203&PropName=Lochmaben Castle, accessed 1 August 2012).

Holliday, V.T., Gartner, W.G., 2007. Methods of soil P analysis in archaeology. *Journal of Archaeological Science* 34, 301–333.

ISO/10390, 2003. Soil Quality: Determination of pH. ISO International Standard.

James, H. & Gondek, M., 2010. Forteviot double enclosure complex excavations 2010. Data Structure Report for the Strathearn Environs and Royal Forteviot (SERF), University of Glasgow. Archaeology, School of Humanities, University of Glasgow.

Jansen, J., Haddad, B., Fassbender, W., Jurcek, P., 1992. Frequency domain induction sounding survey for landfill site characterisation. *Ground Water Monitoring Review* 12, 103–109.

Jol, H.M. (Ed.), 2009. *Ground Penetrating Radar: Theory and Applications*. Elsevier, Oxford.

Jones, R.E. & Sharpe, L., 2006. *Going over old ground. Perspectives on archaeological geophysical and geochemical survey in Scotland. Proceedings of a conference held at the Department of Archaeology, University of Glasgow, Scotland, August 2003*. British Archaeological Report 416, Oxford.

Jones, R.E., O'Grady, O., Malcolm, J., 2009. A preliminary report to the Hunter Trust on the geophysical survey in 2009 in the environs south of Lochmaben Castle, Dumfriesshire. Archaeology, School of Humanities, University of Glasgow.

Jones, R.E., Challands, A., French, C., Card, N., Downes, J., Richards, C., 2010. Exploring the location and function of a Late Neolithic house at Crossiecrown, Orkney by geophysical, geochemical and soil micromorphological methods. *Archaeological Prospection* 17, 29–47.

Jones, R.E., Cuenca-García, C., O'Grady, O., 2010. Geophysical survey in the environs of Lochmaben Castle, Dumfriesshire: a report to the Hunter Trust. Archaeology, School of Humanities, University of Glasgow.

Jordan, D., 2009. How effective is geophysical survey? A regional review. *Archaeological Prospection* 16, 77–90.

Kabata-Pendias, A. & Mukherjee, A.B., 2007. *Trace Elements from Soil to Human*. Springer, New York.

Kalnicky, D.J.& Singhvi, R., 2001. Field portable XRF analysis of environmental samples. *Journal of Hazardous Materials* 83, 93–122.

Karathanasis, A.D., 2006. Soil mineralogy, in: UNESCO (Ed.), *Land Use and Land Cover*, from *Encyclopedia of Life Support Systems* (EOLSS). EOLSS Publishers, Oxford, United Kingdom.

Kattenberg, A.E., 2008. *The Application of Magnetic Methods for Dutch Archaeological Resource Management*. Institute of Geoarchaeological and Bioarchaeological Studies. Faculty of Earth and Life Sciences. PhD Thesis. Vrije Universiteit. Amsterdam.

Kattenberg, A.E. & Aalbersberg, G., 2004. Archaeological prospection of the Dutch perimarine landscape by means of magnetic methods. *Archaeological Prospection* 11, 227–235.

Krzic, M., Sanborn, P., Watson, K., Bomke, A.A., Crowley, C., Doree, A., Dyanatkar, S., 2008. Soil Formation and Soil Processes. University of Northern British Columbia (Vancouver) and Thompson Rivers University (Kamloops), (http://soilweb.landfood.ubc.ca/processes, accessed 1 August 2012).

Kumpiene, J., Lagerkvist, A., Maurice, C., 2008. Stabilization of As, Cr, Cu, Pb and Zn in soil using amendments: a review. *Waste Management* 28, 215–225.

Kvamme, K.L., 2003. Geophysical surveys as landscape archaeology. *American Antiquity*, 68(3), 435–457.

Lambeck, K., 1991. Glacial rebound and sea-level change in the British-Isles. *Terra Nova* 3, 379–389.

Leckebusch, R.G., 2000. Two- and three-dimensional ground-penetrating radar surveys across a medieval choir: a case study in archaeology. *Archaeological Prospection* 7, 189–200.

Leica Geo Office, 2004. Leica Geosystems. Leica Geo Office. Online Help, (http://www.surveyequipment.com/PDFs/LGO_80_Help_en.pdf, accessed 1 August 2012).

Leica Geosystems, 2009. Leica GPS1200 Series High performance GNSS System, (http://www.leica-geosystems.co.uk/downloads123/zz/gps/general/brochures/GPS1200_brochure_en.pdf, accessed 1 August 2012).

Leucci, G., 2008. Ground penetrating radar: the electromagnetic signal attenuation and maximum penetration depth. *Scholarly Research Exchange*, 2008, 1–7.

Lilly, A., Bell, J.S., Hudson, G., Nolan, A.J., Towers, W., 2010. National soil inventory of Scotland (1978-1988): Soil location, sampling and profile description protocols. Technical Bulletin, Macaulay Institute.

Linderholm, J., 2007. Soil chemical surveying: a path to a deeper understanding of prehistoric sites and societies in Sweden. *Geoarchaeology* 22, 417–438.

Lovley, D.R., Holmes, D.E., Nevin, K.P., 1991. Dissimilatory Fe(III) and Mn(IV) reduction. *Advances in Microbial Physiology* 49, 219–86.

Macaulay Institute for Soil Research, 1984. *Soil Survey of Scotland: Systematic Soil Survey. Soil map of Hamilton (Sheet 23)*. Aberdeen.

Macaulay Land Use Research Institute, 2010a. Soil Associations- Exploring Scotland, (http://www.macaulay.ac.uk/explorescotland, accessed 1 August 2012).

Macaulay Land Use Research Institute, 2010b. Soil Parent Material. Exploring Scotland, (http://www.macaulay.ac.uk/explorescotland/soil_pm.html, accessed 1 August 2012).

Macaulay Land Use Research Institute, 2011. Soil Indicators for Scottish Soils (SIFSS), (http://sifss.macaulay.ac.uk, accessed 1 August 2012).

Macaulay Land Use Research Institute, 2012. The soil beneath your feet- Where does it come from? (http://www.macaulay.ac.uk/soilquality, accessed 31 May 2012).

Macdonald, A.D.S. & Laing, L.R., 1977. Excavations at Lochmaben Castle, Dumfriesshire. *Proceedings of the Society of Antiquaries of Scotland* 106, 124–57.

Magen, C., Mucci, A., Sundby, B., 2011. Reduction rates of sedimentary Mn and Fe oxides: an incubation experiment with Arctic ocean sediments. *Aquatic Geochemistry* 17, 629–643.

Marshall, D.N. & Taylor, I.D., 1971. The excavation of the chambered cairn at Glenvoidean, Isle of Bute. *Proceedings of the Society of Antiquaries of Scotlan* 108, 1-39.

McCauley, A., Jones, C., Jacobsen, J., 2005. Basic soil properties. Montana State University.

McMillan, A.A., Merritt, J.W., Auton, C.A., Golledge, N.R., 2011. The Quaternary Geology of the Solway. Geology and Landscape (Scotland) Programme. Research Report RR/11/04. British Geological Survey.

McNeill, J.D., 1980. Electromagnetic terrain conductivity measurements at low induction numbers. Technical Note TN-6. Geonics Ltd., Ontario, Canada.

McNeill, J.D., 1986. Geonics EM38 ground conductivity meter: Operating instructions and survey interpretation techniques. Technical Note TN-21, Geonics Limited. In Mississauga, Ontario, Canada.

McNeill, J.D., 1997. The application of electromagnetic techniques to environmental geophysical surveys, in: McCann, D.M., Eddleston, M., Fenning, P.J., Reeves, G.M. (Eds.), *Modern Geophysics in Engineering Geology,* 103–112*.* The Geological Society, London.

McQueen, K.G., 2008. Identifying geochemical anomalies, in: Garnett, D., Govett, G., Worrall, L. (Eds.), *A Guide for Mineral Exploration Through the Regolith of the Central Gawler Craton, South Australia*. Cooperative Research Centre for Landscape Environments and Mineral Exploration (CRC LEME).

Met Office, 2012. Historic Station Data, (http://www.metoffice.gov.uk/climate/uk/stationdata, accessed 1 August 2012).

Middleton, W.D. & Price, D.T., 1996. Identification of activity areas by multielement characterization of sediments from modern and archaeological house floors using inductively coupled plasma-atomic emission spectroscopy. *Journal of Archaeological Science* 23, 673–687.

Middleton, W.D., 2004. Identifying chemical activity residues on prehistoric house floors: a methodology and rationale for multi-elemental characterization of a mild acid extract of anthropogenic sediments. *Archaeometry* 46, 47–65.

Milek, K.B. & Jones, R.E., 2012. *Scottish Archaeological Research Framework (ScARF). Science in Scottish Archaeology: ScARF Panel Report,*

(http://www.scottishheritagehub.com/sites/default/files/u12/ScARF%20Science%20June%202012.pdf, accessed 1 August 2012).

Milek, K.B. & Roberts, H.M., 2012. Integrated geoarchaeological methods for the determination of site activity areas: a study of a Viking Age house in Reykjavik, Iceland. *Journal of Archaeological Science* 40, 1845-185.

Møller, I. & Anthony, D., 2003. A GPR study of sedimentary structures within a transgressive coastal barrier along the Danish North Sea coast. In C. S. Bristow & H. M. Jol, eds. *Ground Penetrating Radar in Sediments*. Geological Society, London, 55–65.

Moskowitz, B.M., 1991. Hitchhiker's guide to magnetism. Environmental Magnetism Workshop. University of Minnesota.

Moussa, M., 2001. Gamma-ray spectrometry: a new tool for exploring archaeological sites; a case study from East Sinai, Egypt. J*ournal of Applied Geophysics* 48, 137–142.

Muchingami, I., Hlatywayo, D.J., Nel, J.M., Chuma, C. 2012. Electrical resistivity survey for groundwater investigations and shallow subsurface evaluation of the basaltic-greenstone formation of the urban Bulawayo aquifer. *Physics and Chemistry of the Earth*, 50-52, 44–51.

Mullins, C.E., 1977. Magnetic susceptibility of the soil and its significance in soil science: a review. *Journal of Soil Science* 28, 223–246.

Muñoz-Salinas, E., Bishop, P., Sanderson, D.C.W., Zamorano, J., 2011. Interpreting luminescence data from a portable OSL reader: three case studies in fluvial settings. *Earth Surface Processes and Landforms* 36, 651–660.

Nakai, I. & Abe, Y., 2011. Portable X-ray powder diffractometer for the analysis of art and archaeological materials. *Applied Physics A*, 106 (2), 279–293.

Neubauer, W., 2001. Images of the invisible-prospection methods for the documentation of threatened archaeological sites. *Naturwissenschaften*, 88 (1), 13–24.

Noble, G. & Brophy, K., 2007. Forteviot, Perthshire: excavations at the entrance avenue of the Neolithic palisaded enclosure 2007. Data Structure Report for the Strathearn Environs and Royal Forteviot (SERF), Archaeology, School of Humanities, University of Glasgow.

Noble, G. & Brophy, K., 2008. Forteviot, Perthshire: excavations of a henge monument and timber circle. Data Structure Report for the Strathearn Environs and Royal Forteviot (SERF), Archaeology, School of Humanities University of Glasgow.

Novo, A., Lorenzo, H., Rial, F.I., Pereira, M., Solla, M., 2008. Ultra-dense grid strategies for 3D GPR in Archaeology. 12th *International Conference on Ground Penetrating Radar.* June 16-19, Birmingham, UK.

Novo, A., Lorenzo, H., Rial, F.I., Solla, M., 2010. Three-dimensional ground-penetratingradar strategies over an indoor archaeological site: Convent of Santo Domingo (Lugo,Spain). *Archaeological Prospection* 17, 213-222.

Novo, A., Dabas, M., Morelli, G., 2012. The STREAM X multichannel GPR system: first test at Vieil-Evreux (France) and comparison with other geophysical data. *Archaeological Prospection 19, 179-189.*

Nuzzo, L., Leucci, G., Negri, S., Carrozzo, M., Quarta, T., 2002. Applications of 3D visualization techniques in the analysis of GPR data for archaeology. *Annals of Geophysics* 45, 321–337.

Oonk, S., 2009. *The Application of Geochemical Prospection for Dutch Archaeological Resource Management*. Institure for Geo-Bioarchaeology. PhD Thesis. Faculty of Earth and Life Sciences. VU University of Amsterdam.

Oonk, S., Slomp, C.P., Huisman, D.J., 2009a. Geochemistry as an aid in archaeological prospection and site interpretation: Current issues and research directions. *Archaeological Prospection* 16, 35–51.

Oonk, S., Slomp, C.P., Huisman, D.J., Vriend, S.P., 2009b. Effects of site lithology on geochemical signatures of human occupation in archaeological house plans in the Netherlands. *Journal of Archaeological Science* 36, 1215–1228.

Oonk, S., Slomp, C.P., Huisman, D.J., Vriend, S.P., 2009c. Geochemical and mineralogical investigation of domestic archaeological soil features at the Tiel-Passewaaij site, The Netherlands. *Journal of Geochemical Exploration* 101, 155–165.

Ordnance Survey, 1893. *OS Name Book*, Buteshire.

Ovenden, S., 2010. Geophysics: a waste of time and money? The use of geophysics in archaeological planning control in the Northern Isles. *Seminar on Geophysics*. ALGAO Scotland & GeoSIG (IFA). Edinburgh.

Pallat, N. & Thornley, D., 1990. The role of bound water and capillary water in the evaluation of porosity in reservoir rocks. *Society of Core Analysis Symposium (EUROCAS I)*. London, 223–238.

Parnell, J.J., Terry, R.E., Nelson, Z., 2002. Soil chemical analysis applied as an interpretive tool for ancient human activities in Piedras Negras, Guatemala. *Journal of Archaeological Science* 29, 379–404.

Paterson, E., 2011. *Geochemical Atlas for Scottish Topsoils*. The Macaulay Land Use Research Institute, Aberdeen.

Pavageau, M., Morin, A., Seby, F., Guimon, C., Krupp, E., Pécheyran, C., Poulleau, J., Donard, O.F.X., 2004. Partitioning of metal species during an enriched fuel combustion experiment. Speciation in the gaseous and particulate phases. *Environmental Science & Technology* 38, 2252–63.

Petrie, G., 1867. Notice of ruins of ancient dellings at Skara, Bay of Skaill, in the parish of Sandwick, Orkney, recently excavated. *Proceedings of the Society of Antiquaries of Scotland* 7, 201–19.

Peña, J.A., 2010. Estudios geofísicos en yacimientos arqueológicos andaluces 1985-2010. *Primer Congreso de Prehistoria de Andalucía*. Antequera, 22-25 September, Málaga, Spain.

Phillips, E., 2007. Petrology and provenance of the Siluro-Devonian (Old Red Sandstone facies). Sedimentary rocks of the Midland Valley, Scotland. Geology and Landscape Northern Britain Programme, Internal Report IR/07/040. British Geological Survey. Keyworth, Nottingham.

Pomfret, J., 2006. Ground-penetrating radar profile spacing and orientation for subsurface resolution of linear features. *Archaeological Prospection* 13, 151–153.

Powlesland, D. & Lyall, J., 1996. The application of high resolution fluxgate gradiometry as an aid to excavation planning and strategy formulation. *Internet Archaeology 1*, (http://intarch.ac.uk/journal/issue1/lyall_index.html, accessed 20 December 2012).

Pozdnyakov, A. & Pozdnyakova, L., 2002. Electrical fields and soil properties, in: *17th World Congress of Soil Science* Symp. Bangkok, Thailand. Landvise, LLC.

Prescott, J.R. & Hutton, J. T., 1994. Cosmic ray contributions to dose-rates for luminescence and ESR dating: large depths and long-term variations. *Radiation Measurements* 23, 497-500.

Prescott, J.R. & Clay, R.W., 2000. Cosmic ray dose for luminiscence and ESR dating: measured with a scillation counter. *Ancient TL* 18, 11–14.

Reimann, C., Filzmoser, P., Garrett, R.G., 2005. Background and threshold: critical comparison of methods of determination. *The Science of the Total Environment* 346, 1–16.

Rhodes, E.J., 2011. Optically stimulated luminescence dating of sediments over the past 200,000 years. *Annual Review of Earth and Planetary Sciences* 39, 461–488.

Richards, C., 1990. Skara Brae: Revisiting a Neolithic village in Orkney, in: Hanson, W.S., Slater, E.A. (Eds.), *Scottish Archaeology. New Perceptions*. Aberdeen, 24–43.

Ritchie, G., 1997. Early settlement in Argyll, in: Graham Ritchie (Ed.), *The Archaeology of Argyll.* RCAHMS Edinburgh University Press, Edinburgh, 38–66.

Rotherham, I.D., 2007. Wild Gorse: History, Conservation, and Management. *Farming and Wildlife Advisory Group Scotland (FWAG Scotland)* 7, 17–21.

Ruffell, A. & Wilson, J., 1998. Near-surface investigation of ground chemistry using radiometric measurements and spectral Gamma-ray data. *Archaeological Prospection* 5, 203-215.

Sala, J. & Linford, N., 2010. Processing stepped frequency continuous wave GPR systems to obtain maximum value from archaeological data sets, in: *13th International Conferencein Ground Penetrating Radar*, 1–6. IEEE Explore, Lecce, Italy.

Samouëlian, A. Cousin, I., Tabbagh, A., Bruand, A., Richard, G., 2005. Electrical resistivity survey in soil science: a review. *Soil and Tillage Research*, 83 (2), 173–193.

Sanderson, D.C.W. & Murphy, S., 2010. Using simple portable OSL measurements and laboratory characterisation to help understand complex and heterogeneous sediment sequences for luminescence dating. *Quaternary Geochronology* 5, 299–305.

Sandmeier, K.J., 1998. ReflexW. Version 6.1. Manual. Windows™ 9x/NT/2000/XP/7-program for the processing of seismic, acoustic or electromagnetic reflection, refraction and transmission data. Karlsruhe, Germany.

Sarris, A. & Jones, R., 2000. Geophysical and related techniques applied to archaeological survey in the Mediterranean: a review. *Journal of Mediterranean Archaeology* 13, 3–75.

Schaetz, R.J. & Anderson, A.S., 2005. *Soils: Genesis and Geomorphology*. Cambridge: Cambridge University Press.

Schlezinger, D.R. & Howes, B.L., 2000. Organic phosphorus and elemental ratios as indicators of prehistoric human occupation. *Journal of Archaeological Science* 27, 479–492.

Schmidt, A., 2009. Electrical and magnetic methods in archaeological prospection, in: Campana, S., Piro, S. (Eds.), *Seeing the Unseen. Geophysics and Landscape Archaeology,* 67–81. Taylor & Francis, London.

Schmidt, A., 2013. *Earth Resistance for Archaeology.* AltaMira Press, U.S.

Scollar, I., 1962. Electromagnetic Prospecting Methods in Archaeology. *Archaeometry* 5, 146–153.

Scollar, I., Tabbagh, A., Hesse, A., Herzog, I., 1990. *Archaeological Prospecting and Remote Sensing*. Cambridge University Press, Cambridge.

Scottish Office, 1994. PAN42_Planning Advice Note. Archaeology. The Planning Process and Scheduled Monument Procedures.

Sharma, P.V., 1997. *Environmental and Engineering Geophysics*. Cambridge University Press, Cambridge.

Sharpe, L., 2004. *Geophysical, geochemical and arable crop responses to archaeological sites in the Upper Clyde Valley, Scotland*. Department of Archaeology. PhD thesis. University of Glasgow.

Sheriff, R.E., 1989. Principles of electromagnetic induction in ground conductivity measurements, in: *Geophysical Methods*, 210–240. Prentice Hall.

Sheriff, R.E., 2001. Understanding the Fresnel Zone. *Search and Discovery,* (http://www.searchanddiscovery.com/documents/geophysical/sheriff, accessed 20 December 2012).

Simpson, D., Lehouck, A., Van, M., Bourgeois, J., Thoen, E., Vervloet, J., 2008. Geoarchaeological prospection of a medieval manor in the Dutch polders using an electromagnetic induction augerings. *Geoarchaeology* 23, 305–319.

Simpson, D., 2009. *Geoarchaeological prospection with multi-coil electromagnetic induction sensors*. Department of Archaeology and Ancient History of Europe. PhD Thesis. Ghent University.

Simpson, I.A., Dockrill, S.J., Bull, I.D., Evershed, R.P., 1998. Early anthropogenic soil formation at Tofts Ness, Sanday, Orkney. *Journal of Archaeological Science* 729–746.

Simpson, I.A., Barrett, J.H., Milek, K.B., 2005. Interpreting the Viking Age to medieval period transition in Norse Orkney through cultural soil and sediment analyses. *Geoarchaeology* 20, 355–377.

Solla, M., Lorenzo, H., Rial, F.I., Novo, A., 2012. Ground-penetrating radar for the structural evaluation of masonry bridges: results and interpretational tools. *Construction and Building Materials* 29, 458–465.

St Joseph, J.K.S., 1976. Air Reconnaissance: Recent Results. *Antiquity* 40, 55–57.

Tabbagh, A., 1986. Applications and advantages of the slingram electromagnetic method for archaeological prospecting. *Geophysics* 51, 576–584.

Terry, R.E., Fernández, F.G., Parnell, J.J., Inomata, T., 2004. The story in the floors: chemical signatures of ancient and modern Maya activities at Aguateca, Guatemala. *Journal of Archaeological Science* 31, 1237–1250.

Topp, C., Davis, J.L., Annan, A.P., 1980. Electromagnetic determination of soil water content: Measurements in coaxial transmission lines. *Water Resources Research* 16, 574–582.

Trinks, I., Johansson, B., Gustafsson, J., Emilsson, J., Friborg, J., Gustafsson, C., Nissen, J., Hinterleitner, A., 2010. Efficient, large-scale archaeological prospection using a true three-dimensional ground-penetrating radar array system. *Archaeological Prospection* 186, 175–186.

Tzanis, A. & Kafetsis, G., 2004. A freeware package for the analysis and interpretation of common-offset ground probing radar data, in: *Proceedings*

of the 10th International Congress, 1347–1354. Geological Society of Greece, Thessaloniki.

Utsi, E., 2004. Ground-penetrating radar time-slices from North Ballachulish Moss. *Archaeological Prospection* 11, 65–75.

Van Dam, R.L., 2001. *Causes of ground-penetrating radar reflections in sediment*. PhD Thesis. Vrije Universiteit Amsterdam, Netherlands.

Van Dam, R.L., Schlager, W., Dekkers, M.J., Huisman, J.A., 2002. Iron oxides as a cause of GPR reflections. *Geophysics* 67, 536.

Van Dam, R.L., Harrison, J.B.J., Hirschfeld, D.A., Meglich, T.M., Li, Y., North, R.E., 2008. Mineralogy and magnetic properties of basaltic substrate soils: Kaho'olawe and Big Island, Hawaii. *Soil Science Society of America Journal* 72, 244.

Van der Kruk, J. & Slob, E.C., 2004. Reduction of reflections from above surface objects in GPR data. *Journal of Applied Geophysics*, 55 (3-4), 271–278.

Verdonck, L., Simpson, D., Cornelis, W.M., Plyson, A., Bourgeois, J., Docter, R., Van Meirvenne, M., 2009. Ground-penetrating radar survey over Bronze Age circular monuments on a sandy soil, complemented with electromagnetic induction and fluxgate gradiometer data. *Archaeological Prospection* 16, 193–202.

Viberg, A., Trinks, I., Liden, K., 2011. A review of the use of geophysical archaeological prospection in Sweden. *Archaeological Prospection* 18, 43–56.

Watts, P. & Howe, P., 2010. Strontium and strontium compounds. *Concise International Chemical Assessment Document* 77. World Health Organization.

Wells, E.C., 2004. Investigating activity patterns in Prehispanic plazas: weak acid-extraction ICP/AES analysis of anthrosols at Classic period El Coyote, northwest Honduras. *Archaeometry* 1, 67–84.

Weston, D.G., 2002. Soil and susceptibility: aspects of thermally induced magnetism within the dynamic pedological system. *Archaeological Prospection* 9, 207–215.

Weymouth, J.W., 1986. Geophysical methods of archaeological site surveying, in: Schiffer, M.B. (Ed.), *Advances in Archaeological Method and Theory,* Vol. 9, 311–395. Academic Press, Orlando, Florida.

Wightman, W.E., Jalinoos, F., Sirles, P., Hanna, K., 2003. *Application of Geophysical Methods to Highway Related Problems*. Lakewood, Colorado.

Wilson, C.A., Davidson, D.A., Cresser, M.S., 2005. An evaluation of multielement analysis of historic soil contamination to differentiate space use and former function in and around abandoned farms. *The Holocene* 15, 1094–1099.

Wilson, C.A., Cresser, M.S., Davidson, D.A., 2006. Sequential element extraction of soils from abandoned farms: an investigation of the partitioning of anthropogenic element inputs from historic land use. *Journal of Environmental Monitoring* 8, 439–44.

Wilson, C.A., Davidson, D.A., Cresser, M.S., 2007. Evaluating the use of multi-element soil analysis in archaeology: a study of a post-medieval croft (Olligarth) in Shetland. *Atti della Società Toscana di Scienze Naturali* 112, 69–78.

Wilson, C.A., Davidson, D.A., Cresser, M.S., 2008. Multi-element soil analysis: an assessment of its potential as an aid to archaeological interpretation. *Journal of Archaeological Science* 35, 412–424.

Wilson, C.A., Davidson, D.A., Cresser, M.S., 2009. An evaluation of the site specificity of soil elemental signatures for identifying and interpreting former functional areas. *Journal of Archaeological Science* 36, 2327–2334.

Wilson, M.J., 1971. Clay mineralogy of the Old Red Sandstone (Devonian) of Scotland. *Journal of Sedimentary Petrology* 41, 995–1007.

Wilson, M.J., Bain, D.C., Duthie, M.L., 1984. The soil clays of Great Britain: II Scotland. *Clay Minerals* 19, 709–735.

Witten, A.J., 2006. *Geophysics and Archaeology*. Equinox, London.

Wynn, J.C., 1986. A review of geophysical methods used in Archaeology. *Geoarchaeology*, 1 (3), 245–257.

Zhang, K. & Li, D., 2007. *Electromagnetic Theory for Microwaves and Optoelectronics*, Springer.

Zhdanov, M.S., 2009. *Geophysical Electromagnetic Theory and Methods*. Elsevier, Oxford, United Kingdom.